# MECHANISMS OF NEURONAL RECOVERY IN THE CENTRAL NERVOUS SYSTEM

EDITED BY: Luis B. Tovar-y-Romo, Alicia Guemez-Gamboa and João M. N. Duarte
PUBLISHED IN: Frontiers in Cell and Developmental Biology and Frontiers in Cellular Neuroscience

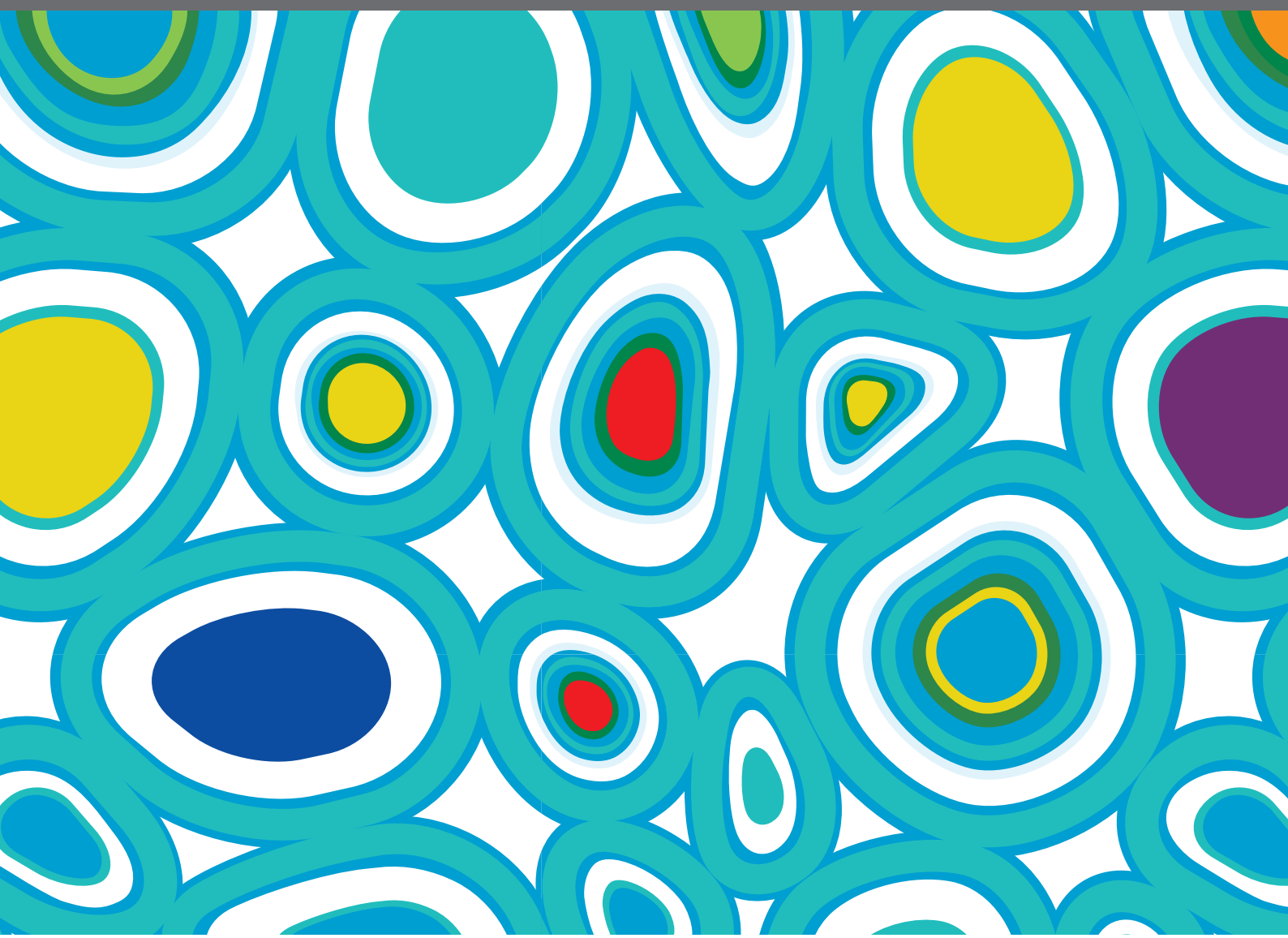

frontiers Research Topics

ISSN 1664-8714
ISBN 978-2-88971-470-4
DOI 10.3389/978-2-88971-470-4

## About Frontiers

Frontiers is more than just an open-access publisher of scholarly articles: it is a pioneering approach to the world of academia, radically improving the way scholarly research is managed. The grand vision of Frontiers is a world where all people have an equal opportunity to seek, share and generate knowledge. Frontiers provides immediate and permanent online open access to all its publications, but this alone is not enough to realize our grand goals.

## Frontiers Journal Series

The Frontiers Journal Series is a multi-tier and interdisciplinary set of open-access, online journals, promising a paradigm shift from the current review, selection and dissemination processes in academic publishing. All Frontiers journals are driven by researchers for researchers; therefore, they constitute a service to the scholarly community. At the same time, the Frontiers Journal Series operates on a revolutionary invention, the tiered publishing system, initially addressing specific communities of scholars, and gradually climbing up to broader public understanding, thus serving the interests of the lay society, too.

## Dedication to Quality

Each Frontiers article is a landmark of the highest quality, thanks to genuinely collaborative interactions between authors and review editors, who include some of the world's best academicians. Research must be certified by peers before entering a stream of knowledge that may eventually reach the public - and shape society; therefore, Frontiers only applies the most rigorous and unbiased reviews.
Frontiers revolutionizes research publishing by freely delivering the most outstanding research, evaluated with no bias from both the academic and social point of view. By applying the most advanced information technologies, Frontiers is catapulting scholarly publishing into a new generation.

## What are Frontiers Research Topics?

Frontiers Research Topics are very popular trademarks of the Frontiers Journals Series: they are collections of at least ten articles, all centered on a particular subject. With their unique mix of varied contributions from Original Research to Review Articles, Frontiers Research Topics unify the most influential researchers, the latest key findings and historical advances in a hot research area! Find out more on how to host your own Frontiers Research Topic or contribute to one as an author by contacting the Frontiers Editorial Office: frontiersin.org/about/contact

# MECHANISMS OF NEURONAL RECOVERY IN THE CENTRAL NERVOUS SYSTEM

Topic Editors:
**Luis B. Tovar-y-Romo,** University of Mexico, Mexico
**Alicia Guemez-Gamboa,** Northwestern University, United States
**João M. N. Duarte,** Lund University, Sweden

**Citation:** Tovar-y-Romo, L. B., Guemez-Gamboa, A., Duarte, J. M. N., eds. (2021). Mechanisms of Neuronal Recovery in the Central Nervous System. Lausanne: Frontiers Media SA. doi: 10.3389/978-2-88971-470-4

# Table of Contents

frontiers in Cell and Developmental Biology

EDITORIAL
published: 20 August 2021
doi: 10.3389/fcell.2021.733066

# Editorial: Mechanisms of Neuronal Recovery in the Central Nervous System

*Luis B. Tovar-y-Romo*[1]*, *Alicia Guemez-Gamboa*[2]* and *João M. N. Duarte*[3]*

[1] Institute of Cellular Physiology, Universidad Nacional Autónoma de México, Mexico City, Mexico, [2] Department of Neuroscience, Feinberg School of Medicine, Northwestern University, Chicago, IL, United States, [3] Wallenberg Centre for Molecular Medicine, Faculty of Medicine, Lund University, Lund, Sweden

**Keywords: neuronal death mechanisms, neuronal recovery, neuroinflammation, transcriptome, axon regeneration, CNS injury and repair, autophagy, neurorestoration**

## Editorial on the Research Topic

## Mechanisms of Neuronal Recovery in the Central Nervous System

The central nervous system (CNS) is highly plastic, allowing for the integration of new neuronal circuits and vascular networks. This capacity to dynamically change brain structures upon external stimuli lays the groundwork for the adaptive transformations that help shape the many brain functions. However, the mammalian brain and spinal cord have minimal capacity for self-renewal, notably lacking robust mechanisms of adaptation to injury and reduced flexibility in terms of tissue repair and healing.

In this Research Topic published across Frontiers in Cell and Developmental Biology and Frontiers in Cellular Neuroscience, a collection of articles describing the most recent findings into the mechanisms that drive the physiological adaptation to neuronal injury draw a general picture of the current understanding of cellular and molecular processes involved in neuronal injury, neuronal regeneration, and restoration of brain functions.

Animal species better suited for investigating neural plasticity help us understand some of the primary mechanisms for neuronal regrowth. In this collection, two articles describe molecular processes for regeneration in zebrafish. First, Demirci et al. made a comprehensive description of transcriptional changes in the recovery phase of telencephalon damage; this comparative transcriptome analysis of the reorganizing telencephalon provides biological targets for assessing traumatic brain injuries in humans. Then, Shimizu et al. explored radial glia proliferation in neurogenic niches by performing histological analyses that revealed increased isolectin B4-positive macrophages before radial glia proliferation and identified IL6/Stat3 signaling as a trigger of radial glia activation during tectum regeneration.

Understanding the transcriptional profile of these processes is also relevant in mammalian systems. Here, Chohan puts into perspective how interventions based on the endogenously coded machinery for adult neurogenesis could provide a means to develop therapies. These therapies include the transplantation of gene-edited neuronal precursors for achieving neural repair in CNS injury and disease. Approaches like these enhance our understanding of the overall impact of directed therapies to recover function, as shown by Jermakowicz et al., who tested whether low-frequency electrical stimulation of the rat nucleus raphe magnus after incomplete spinal cord injury reversed damage. In this setting, the non-specific serotonin 5-$HT_7$ receptor antagonist pimozide alleviated the initial transcriptional response of the injured spinal cord by stimulating the raphe magnus.

Besides transcriptional regulation, the control of the metabolic process is also a relevant mechanism to protect the brain from different types of insults where autophagy might play a key



***Edited and reviewed by:***
*Timothy W. Corson, Indiana University Bloomington, United States*

***Correspondence:**
*Luis B. Tovar-y-Romo*
*ltovar@ifc.unam.mx*
*Alicia Guemez-Gamboa*
*alicia.guemez@northwestern.edu*
*João M. N. Duarte*
*joao.duarte@med.lu.se*

***Specialty section:***
*This article was submitted to Molecular and Cellular Pathology, a section of the journal Frontiers in Cell and Developmental Biology*

***Received:*** *29 June 2021*
***Accepted:*** *02 July 2021*
***Published:*** *20 August 2021*

***Citation:***
*Tovar-y-Romo LB, Guemez-Gamboa A and Duarte JMN (2021) Editorial: Mechanisms of Neuronal Recovery in the Central Nervous System. Front. Cell Dev. Biol. 9:733066. doi: 10.3389/fcell.2021.733066*

role. Torres-Esquivel et al. proved that alternative energetic substrates to glucose, such as the ketone body β-hydroxybutyrate, mechanistically help the brain engage the autophagic flux to prevent neuronal death by modulating the AMPK pathway. In another study using cultured spinal cord motor neurons as a model, Chen et al. described that autophagy inhibition increases the injury caused by oxygen and glucose deprivation. Both studies indicate that the proper activation of autophagy is needed to prevent the neuronal death elicited by metabolic stress.

The regulation of metabolic signaling can also improve neurological functions after damage. Bader et al. tested the treatment potential of glucagon-like peptide 1 (GLP-1) and glucose-dependent insulinotropic polypeptide (GIP) mimetics in a murine model of traumatic brain injury. They found that both a GLP-1 analog and a dual agonist of GLP-1 and GIP receptors improved cognitive deficiencies, neurodegeneration, and neuroinflammation, which were mechanistically mediated through the regulation of the PKA pathway.

The classical mechanisms of regulation of neural damage and recovery have also been explored in detail in this Research Topic, with new insights into the role of mitochondrial regulation of neuronal death. Benítez-Rangel et al. characterized the molecular responses of caspase-3 activation under different death inducers in a model of cerebellar granule neurons. They showed that voltage-gated $Ca^{2+}$ channels in the endoplasmic reticulum are critical to maintaining mitochondrial membrane polarization.

As well, axon regeneration, regulation of vascularization, and neuroinflammation were given extensive consideration. Chung et al. reviewed the literature on the role of growth-associated protein-43 and brain acid-soluble protein 1 in neurodegenerative diseases. Both proteins present with alterations in their expression and phosphorylation profiles, highlighting both their involvement in neural injury response and regeneration, and their therapeutic potential to compensate for neuron loss. Jara et al. reviewed how CNS circuit connectivity after damage is enhanced by electrical stimulation by activating genetic neuroplasticity programs, revealing its therapeutic potential to enhance neuronal repair and recovery. Sutherland and Geoffroy summarize the evidence of axon growth decline with aging and evaluate how the cumulative alterations in astrocytes and microglia contribute to the impaired axonal repair with age. Sobrido-Cameán et al. examined the effect of inhibiting gamma-secretase on axonal regeneration after spinal cord injury in the sea lamprey. The authors used two different transcriptomic assessments with two related-drug applications targeting GABA receptors, suggesting gamma-secretase targeting as an effective axonal repair approach.

Regulation of brain perfusion is crucial for matching neuronal energetic demands. Regarding cerebrovascular regulation, Filchenko et al. explored the critical role of caveolin in the evolution of edema in stroke and its relation to the expression of aquaporin-4. The authors showed that loss of caveolin-1 results in decreased aquaporin-4 expression and contributes to brain swelling. Hierro-Bujalance et al. demonstrated that erythropoietin administration in a model of germinal matrix-intraventricular hemorrhage reduced long-term brain atrophy and malfunction. Vanherle et al. made a case for linking cardiovascular disease to cognitive impairment and dementia, where the diminished cerebral blood flow potentially induces neuronal death, especially in hypertension, heart failure, and stroke.

Finally, on the regulation of neuroinflammation, Jung and colleagues critically discussed the literature on the role of TNF-α-mediated neuroinflammatory processes and the potential of immunomodulatory imide drugs targeting the 3'UTR of TNF-α to reduce inflammation-associated neurodegenerative processes. The authors situate these compounds as potential inductors to alleviate symptoms and slow down the progression of neurodegenerative disease. Hu et al. investigated the regulatory effects of miR34a on the expression of major histocompatibility complex class I in hippocampal neurons and its involvement in shaping the neural morphology during development.

Despite not providing an exhaustive overview of the mechanisms that can be used for neuronal repair upon injury, this Research Topic collects original research articles and literature reviews that are representative of highly active research domains within the overall purpose of regenerating and/or repairing neurons for reestablishing adequate neuronal function.

## AUTHOR CONTRIBUTIONS

All authors contributed to editing the Research Topic and prepared the Editorial piece.

## ACKNOWLEDGMENTS

LT-y-R's work was financed by Programa de Apoyo a Proyectos de Investigación e Innovación Tecnológica (IN207020) and Consejo Nacional de Ciencia y Tecnología (A1-S-13219). AG-G was supported by National Institutes of Health grant R00 NS089943. The Knut and Alice Wallenberg Foundation, the Medical Faculty at Lund University and Region Skåne are acknowledged for generous financial support to JD.

**Conflict of Interest:** The authors declare that the research was conducted in the absence of any commercial or financial relationships that could be construed as a potential conflict of interest.

**Publisher's Note:** All claims expressed in this article are solely those of the authors and do not necessarily represent those of their affiliated organizations, or those of the publisher, the editors and the reviewers. Any product that may be evaluated in this article, or claim that may be made by its manufacturer, is not guaranteed or endorsed by the publisher.

frontiers in Cellular Neuroscience

ORIGINAL RESEARCH
published: 19 November 2019
doi: 10.3389/fncel.2019.00510

# Brainstem-Evoked Transcription of Defensive Genes After Spinal Cord Injury

*Walter J. Jermakowicz†, Melissa M. Carballosa-Gautam, Alberto A. Vitores and Ian D. Hentall**

*The Miami Project to Cure Paralysis, Department of Neurological Surgery, University of Miami, Miami, FL, United States*

The spinal cord after injury shows altered transcription in numerous genes. We tested in a pilot study whether the nucleus raphé magnus, a descending serotonergic brainstem region whose stimulation improves recovery after incomplete spinal cord injury (SCI), can influence these transcriptional changes. Rats received 2 h of low-frequency electrical stimulation in the raphé magnus 3 days after an impact contusion at segment T8. Comparison groups lacked injuries or activated stimulators or both. Immediately following stimulation, spinal cords were extracted, their RNA transcriptome sequenced, and differential gene expression quantified. Confirming many previous studies, injury primarily increased inflammatory and immune transcripts and decreased those related to lipid and cholesterol synthesis and neuronal signaling. Stimulation plus injury, contrasted with injury alone, caused significant changes in 43 transcripts (39 increases, 4 decreases), all protein-coding. Injury itself decreased only four of these 43 transcripts, all reversed by stimulation, and increased none of them. The non-specific 5-HT7 receptor antagonist pimozide reversed 25 of the 43 changes. Stimulation in intact rats principally caused decreases in transcripts related to oxidative phosphorylation, none of which were altered by stimulation in injury. Gene ontology (biological process) annotations comparing stimulation with either no stimulation or pimozide treatment in injured rats highlighted defense responses to lipopolysaccharides and microorganisms, and also erythrocyte development and oxygen transport (possibly yielding cellular oxidant detoxification). Connectivity maps of human orthologous genes generated in the CLUE database of perturbagen-response transcriptional signatures showed that drug classes whose effects in injured rats most closely resembled stimulation without pimozide include peroxisome proliferator-activated receptor agonists and angiotensin receptor blockers, which are reportedly beneficial in SCI. Thus the initial transcriptional response of the injured spinal cord to raphé magnus stimulation is upregulation of genes that in various ways are mostly protective, some probably located in recently arrived myeloid cells.

**Keywords: spinal cord injury, mRNA, raphe magnus nucleus, electrical stimulation, rat (Brown Norway)**

OPEN ACCESS

***Edited by:***
*Luis B. Tovar-y-Romo, National Autonomous University of Mexico, Mexico*

***Reviewed by:***
*Michele R. Brumley, Idaho State University, United States*
*Eibar Ernesto Cabrera-Aldana, National Autonomous University of Mexico, Mexico*

***Correspondence:**
*Ian D. Hentall*
*IanHentall@gmail.com*

***†Present address:***
*Walter J. Jermakowicz, Department of Neurological Surgery, Vanderbilt University Medical Center, Nashville, TN, United States*

***Specialty section:***
*This article was submitted to Cellular Neuropathology, a section of the journal Frontiers in Cellular Neuroscience*

***Received:*** *09 July 2019*
***Accepted:*** *29 October 2019*
***Published:*** *19 November 2019*

***Citation:***
*Jermakowicz WJ, Carballosa-Gautam MM, Vitores AA and Hentall ID (2019) Brainstem-Evoked Transcription of Defensive Genes After Spinal Cord Injury. Front. Cell. Neurosci. 13:510. doi: 10.3389/fncel.2019.00510*

**Abbreviations:** cAMP, cyclic adenosine monophosphate; DAVID, Database for Annotation, Visualization and Integrated Discovery; DBS, deep brain stimulation; DGE, differential gene expression; EPO, erythropoietin; FC, fold change; MS, multiple sclerosis; NCBI, National Center for Biotechnology Information; NRM, nucleus raphé magnus; pCREB, phosphorylated cAMP response binding element; pim, pimozide; PPAR, peroxisome proliferator-activated receptor; pPKA, phosphorylated protein kinase A; SCI, spinal cord injury; st, stimulation; TBI, traumatic brain injury.

## INTRODUCTION

Mechanical SCI causes numerous molecular, cellular and structural changes that vary in duration and onset, both at the site of injury and beyond (Dulin et al., 2015; O'Shea et al., 2017). These include changes in gene transcription that collectively and individually could influence recovery via protein synthesis and downstream molecules. It is therefore of interest to find ways to modify influential transcriptional changes by enhancing or opposing them according to their benefit or harm. Here we explore whether activity in a raphé nucleus of the hindbrain, the NRM, regulates transcription after SCI. The NRM is one of several ventral medullary nuclei that send overlapping serotonergic projections (as well as non-serotonergic projections) directly to the dorsal and ventral spinal cord, others being the nucleus raphe obscurus, nucleus raphe pallidus and the laterally adjacent paragigantocellularis and gigantocellularis nuclei (Kwiat and Basbaum, 1992; Gautier et al., 2017).

Previously, we showed that prolonged electrical stimulation of the NRM (for several days to weeks) significantly enhanced recovery from various autonomic, sensory, and motor deficits of contusional cervical or thoracic SCI in rats, while improving myelination and serotonergic innervation near the lesion (Hentall and Burns, 2009; Hentall and Gonzalez, 2012; Vitores et al., 2018). A shorter period of NRM stimulation (2 h) was found to restore injury-depleted levels in the spinal cord of cAMP and its downstream targets, phosphorylated cAMP response element-binding protein, and pPKA (Carballosa-Gonzalez et al., 2014), which cause neurotrophic effects via alterations in gene expression (Hannila and Filbin, 2008; Carballosa-Gonzalez et al., 2014; Batty et al., 2017). Stimulation of the midbrain's median and dorsal raphé, which send ascending projections throughout the forebrain, analogously yielded partial restoration of anatomic and functional deficits following TBI in rats, as well as normalizing cAMP levels, thus establishing the generality of the idea that raphé nuclei provide central links for restorative feedback. In mice, prolonged NRM stimulation attenuated signs of experimental autoimmune encephalomyelitis, a model of MS, including cellular pathology and cytokine upregulation (Madsen et al., 2017), which further supports this idea. Our general aim in the studies cited above has been to achieve lasting, clinically significant recovery with a period of prolonged electrical DBS by evoking neurotrophic or protective effects from activated neuronal systems. In contrast, most studies of DBS for neurodegenerative conditions such as SCI, TBI, and MS have focused on the acute reversal of overt problematic signs or symptoms (e.g., pain, paralysis, altered mental status), without necessarily remedying the underlying pathology (Roy and Aziz, 2014; Shin et al., 2014; Chari et al., 2017).

Here, we examine transcriptional changes produced by NRM stimulation in rats with thoracic (T8) SCI. Stimulation was applied for 2 h to the NRM on the third day after a weight-drop SCI at segment T8. At this post-injury stage, many molecular pathways that promote plasticity and inflammation are near their peak (David and Kroner, 2011; Mao et al., 2016). The relatively brief period of stimulation, lasting just long enough for initial transcriptional effects to emerge, was followed by immediate extraction of various portions of the spinal cord and standard processing for RNA sequence analysis. Both injured and non-injured controls were studied with and without stimulation ($n \geq 3$). Additional injured rats ($n = 2$) received stimulation after being pretreated with the non-specific 5-HT7 antagonist pimozide, to assess possible participation of serotonin release from the axon terminals of NRM neurons. The results proved surprising. Our working hypothesis was that stimulation in injured rats would induce neurotrophic transcriptional effects and predominantly reverse injury-produced changes. Instead it altered a small number of genes that are mostly concerned with inflammation and erythrocyte formation, very few of which were altered by injury alone. These findings shed new light on the brainstem's descending modulatory influence on endogenous processes in healthy and injured spinal cord, and also identified molecules with potential for improving outcomes after SCI.

## MATERIALS AND METHODS

### Animal Surgical Procedures and Treatments

All experiments were performed in accordance with the guidelines of the NIH Guide for the Care and Use of Laboratory Animals, and were approved by the University of Miami Miller School of Medicine Institutional Animal Care and Use Committee. Female young-adult Sprague-Dawley rats (220–240 g, 10–12 weeks old), obtained from Harlan Sprague-Dawley, Inc. (Indianapolis, IN, United States), were anesthetized with intraperitoneal ketamine (50 mg/kg) plus xylazine (10 mg/kg) and mounted in a stereotaxic head holder. Following a midline back incision and lateral dissection of the spinous musculature, a T8 laminectomy was performed and a moderate bilateral contusion injury was caused with a NYU-MASCIS Impactor, which applied a force by letting a 10 g rod of 2 mm diameter drop 12.5 mm centered on the midline of the spinal cord (Kearney et al., 1988). Some control animals received a laminectomy without the contusion injury. Dissected muscle layers were sutured and the skin was closed with wound clips. Animals recovered on a 37°C heating blanket. The opioid buprenorphine (0.01 mg/kg bid, subcutaneous) was given daily for analgesia and the antibiotic gentamycin (0.01 mg/kg bid, subcutaneous) to prevent infection. Bladder volume was checked daily and manually emptied.

At 72 h after the injury or sham injury, the animals were anesthetized with isoflurane (1.2% in oxygen) by face mask after induction in a glass chamber and mounted in a stereotaxic holder. A single monopolar stimulating microelectrode was placed in the brainstem by making a linear skin incision and drilling a 1.8 mm craniostomy on the midline, 2.2 mm caudal to the interaural line. To apply stimulation, a tungsten microelectrode (AC impedance 0.5 megohm, diameter 0.13 mm) was inserted into the midline NRM at the stereotaxic coordinates 2.2 mm caudal and 10 mm ventral to the interaural line (flat-skull orientation). Accuracy was confirmed by observing bilateral facial

twitching 1.2–1.5 mm above the target, which disappeared once the electrode reached the NRM. This localization method was validated histologically in a previously published study (Hentall and Gonzalez, 2012). Monopolar stimulation, consisting of 8-Hz trains of cathodal pulses (30 μA, 1 ms), was given for 2 h in a 5 min, 50% duty cycle, ending in the stimulation phase. Electrodes were also placed in sham and injured control animals that did not receive the 2 h of stimulation. One injured group received pimozide by intraperitoneal injection of 1 mg/kg, 1 h prior to stimulation onset. Immediately after the stimulation period, the subdural spinal cord (including pia-arachnoid) was rapidly dissected and transversely sectioned into three 0.5 cm blocks encompassing the C4–C6, T7–T9, and L1–L3 spinal segments. The blocks were immediately placed in liquid nitrogen and stored at −80°C. Animals were euthanized by isoflurane overdose. No adverse effects of stimulation or other treatment were seen.

## RNAseq Sample Preparation

Cervical, thoracic and lumbar regions were combined for RNA analysis. Preparation and sequencing of RNA libraries was carried out by personnel of the John P. Hussman Institute for Human Genomics at the Center for Genome Technology, University of Miami Miller School of Medicine. RNA isolated from rat spinal cords was extracted using Trizol and purified using the QIAGEN (Venlo, Netherlands) RNeasy kit, by following the kit's standard protocol. Samples were analyzed with an Agilent Bioanalyzer (Santa Clara, CA, United States). All analyzed samples passed minimum quality and quantity threshold required for RNA sequencing, including RNA integrity score above 7.0. Mean concentration of total RNA were 0.43 μg/μl (*SD*: 0.15); the mean purity (260/280 ratio) was 2.06 (*SD*: 0.041) and was > 2.02 in all individuals. From each sample, 500 ng of total RNA was provided to an Illumina TruSeq Stranded Total RNA Library Prep Kit with Ribo-Zero (San Diego, CA, United States) to create ribosomal RNA-depleted sequencing libraries with a unique barcode. Sequencing was performed to >25 million raw reads in a single-end 75 bp sequencing run on the Illumina NextSeq500.

## Production of RNAseq Data

Raw sequence data was processed by the on-instrument Real Time Analysis software (v.2.7.7) transferred to de-multiplexed FASTQ files with the Illumina-supplied scripts in BCL2FASTQ software (v2.17). The quality of the reads was determined with FASTQC software[1] for per base sequence quality, duplication rates, and overrepresented k-mers. Illumina sequencing adapters were trimmed from the ends of the reads using the Trim Galore! Package[2], then aligned for *Rattus norvegicus* (Rnor_5.0) with the STAR aligner (v2.5.0a) (Dobin et al., 2013). Gene count quantification for aligned reads was performed using the GeneCounts function within STAR against the Ensembl gene build pipeline (release 79).

## Data Analysis

Experimental groups, to which rats were assigned in random order, were as follows: group A, sham injury and sham stimulation; group B, SCI and sham stimulation; group C, SCI and stimulation; group D, SCI with stimulation and pimozide; group E, sham injury with stimulation. Many subjects had also provided material for a previously published assay of cAMP, cAMP response element-binding protein and protein kinase A (Carballosa-Gonzalez et al., 2014); exceptions were one subject in group E and both subjects in group D, whose samples were contemporaneous with the rest but had not previously been assayed for publication. Within 5 experimental groups, there were 10 possible contrasts, of which 6 were analyzed (**Table 1**). These contrasts are named in the text by the positively changed

[1]http://www.bioinformatics.babraham.ac.uk/projects/fastqc/

[2]www.bioinformatics.babraham.ac.uk/projects/trim_galore

**TABLE 1 |** Groups and contrasts analyzed.

| Contrast: name, ratio | Group | Injury | Stimulation | Pimozide | Number flagged (up/down) | SD (difference) |
|---|---|---|---|---|---|---|
| ±SCI(0), B/A | B, *n* = 3 | Yes | No | No | 982 (922/60) | 1047 |
| | A, *n* = 4 | No | No | No | | |
| ±st(SCI), C/B | C, *n* = 3 | Yes | Yes | No | 43 (39/4) | 327 |
| | B, *n* = 3 | Yes | No | No | | |
| ±pim(st/SCI), D/C | D, *n* = 2 | Yes | Yes | Yes | 81 (52/29) | 601 |
| | C, *n* = 3 | Yes | Yes | No | | |
| ±st(0), E/A | E, *n* = 5 | No | Yes | No | 28 (20/8) | 226 |
| | A, *n* = 4 | No | No | No | | |
| ±st/SCI(0), C/A | C, *n* = 3 | Yes | Yes | No | 1150 (1084/66) | 854 |
| | A, *n* = 4 | No | No | No | | |
| ±SCI(st), C/E | C, *n* = 3 | Yes | Yes | No | 1374 (1205/168) | 911 |
| | E, *n* = 5 | No | Yes | No | | |

*The last column shows the numbers of significant differences in individual genes that were flagged by EdgeR software, according to the joint criteria FDR < 0.05 and abs($log_2$(FC)) > 1. The condition in the first row provided the numerator for FC, the second row provided the denominator. Increases [$log_2$(FC) > 1] and decreases [0 < $log_2$(FC) < 1] are consistently thus defined in this paper. The standard deviation (SD) was calculated from the differences in count taken over all genes. Underlining specifies the parameter(s) varied in the given contrast.*

factor followed in parentheses by the constant background. Thus, ±st(SCI) refers to the contrast of stimulation (st) with no stimulation in injured rats, ±SCI(st) contrasts injury with no injury in stimulated rats, ±pim(st/SCI) contrasts pimozide's presence with its absence in stimulated, injured rats; ±st(0), ±SCI(0), and ±st/SCI(0) respectively contrast stimulation, injury or both with their absence (in rats with no other interventions).

Differential gene expression analysis was performed on the gene count data with edgeR software (Robinson et al., 2010). Gene counts were normalized against total aligned reads to generate counts-per-million for each gene in each sample. Given the relatively small sample sizes per group, the exact test implemented in EdgeR was used to determine differential expression, producing a false discovery rate (FDR) *p*-value. Significant differential expression was decided by EdgeR with joint criteria of FDR $< 0.05$ and a greater than 100% change: $\text{abs}(\log_2(\text{FC})) > 1$, where FC is FC. For comparison, output from two other DGE software packages, DESeq2 and baySeq, was also examined (Hardcastle and Kelly, 2010; Love et al., 2014). Numbers of significant increases and decreases obtained in different contrasts were analyzed in $2 \times 2$ contingency tables with the two-tailed Chi-square test.

Pathway and network analyses were performed with Ingenuity Pathway Analysis (QIAGEN), using as input the lists of genes with FDR $< 0.05$, as determined by EdgeR. Gene ontology (biological process) analysis was performed for each set of genes meeting EdgeR cutoff criteria of $\text{abs}(\log_2(\text{FC})) > 1$ and FDR $< 0.05$ with the DAVID[3]. Statistical overrepresentation was determined with the default settings in DAVID. Gene names used in tables were official gene symbols given by DAVID, supplemented by Gene from the United States' NCBI.

Human orthologs of rat genes flagged in the various EdgeR contrasts were obtained from the Ensembl 2018 website (Zerbino et al., 2018). The resulting human gene list was applied to the L1000 gene expression database of the CLUE software platform (Subramanian et al., 2017). This platform produced a connectivity map that was analyzed with the Query tool to find classes of perturbagens (drugs) whose expression signatures most closely resembled those yielded by the experiments.

## Data Availability

The high-throughput sequence data is available from the GEO repository of the NCBI, accession number GSE133093. Other data relevant to the study's conclusions are available on request from the corresponding author.

# RESULTS

## Numbers Flagged as Upregulated or Downregulated

A total of 32,494 transcripts with unique rat gene identification (Ensembl) numbers were analyzed. These included 1,563 micro RNAs, 1,471 small RNAs, and 22,019 experimentally confirmed protein-coding RNAs; further details are given in the **Supplementary Figure 1**. For all six contrasts, the DGE software applications EdgeR and DESEq2 were of roughly equal leniency, and showed mean overlap of 75% for selected transcripts. The baySeq application was considerably more stringent, flagging on average 45% of those flagged by the other two software applications (**Supplementary Figure 1**). The following presentation is limited to results obtained with EdgeR. In the key contrasts ±st(SCI) and ±st(0), neither DESeq2 nor baySeq found any significant genes that were not flagged by edgeR.

The contrasts ±SCI(0), ±st/SCI(0) and ±SCI(st), all of which pair intact rats with rats injured 3 days previously, revealed a large number of differentially expressed transcripts. These numbers differed significantly (pairwise Chi-squared contingency tables, $p < 0.0001$). Contrast ±SCI(0) showed fewer differentially transcribed genes ($n = 982$) than ±st/SCI(0) ($n = 1150$), and ±SCI(st) showed the most differentially expressed transcripts ($n = 1374$). The relatively brief interventions of 2 h of stimulation or 3 h of pimozide's presence caused far fewer significant alterations in transcription. The numbers of genes affected in the contrast ±pim(st/SCI) ($n = 81$) was significantly different ($p = 0.0009$) from the numbers for ±st(SCI) ($n = 43$), but the latter was not significantly different ($p = 0.10$) from the contrast ±st(0) ($n = 28$). With the brief interventions, there was also less variation in the difference between counts for the paired conditions, as reflected in their standard deviations (**Table 1**). All three interventions (injury, stimulation, pimozide) consistently produced more increases than decreases in transcript counts (**Table 1**): pimozide [contrast ±pim(st/SCI)] revealed 64% increases, injury alone [contrast ±SCI(0)] revealed 94% increases and stimulation after injury [contrast ±st(SCI)] revealed 91% increases. Differing kinetics of decay and synthesis may in some cases have contributed to this imbalance (see section "Discussion").

## Genes Affected by Stimulation: Responses to Injury Alone

The contrast showing the effect of stimulation in injury, contrast ±st(SCI), was of greatest importance for the goals of this study. It found that 43 transcripts, all protein-coding, had changed significantly (**Table 2**). When one of these 43 transcripts was flagged in another contrast involving injury, the direction of the effect was consistent: for example, in the opposite direction of the effects from injury alone [contrast ±SCI(0)] and in the same direction as the effect of injury plus stimulation compared with untreated rats [±st/SCI(0)] and as the effect of injury versus sham on stimulated rats [±SCI(st)] (**Table 2**). However, it was notable that only 9% of injury-produced transcriptional changes [contrast ±SCI(0)], all downregulation, were reversed by NRM stimulation [contrast ±st(SCI)].

The effect of stimulation on injury could also be shown less directly, by comparing genes flagged as altered by stimulation plus injury, in contrast ±st/SCI(0), with those flagged by injury alone, in contrast ±SCI(0). Some genes ($n = 315$) showed altered transcription after stimulation plus injury, in

[3]https://david.ncifcrf.gov/tools.jsp

**TABLE 2 |** Genes altered by stimulation in injured animals, selected by contrast ±st(SCI).

| Protein (gene) | ±SCI(0) | ±st(SCI) | ±pim(st/SCI) | ±st/SCI(0) | ±SCI(st) |
|---|---|---|---|---|---|
| *Similar to 60S ribosomal protein L12 (*RGD1564883*) | −6.63 | 7.12 | −10.44 | | |
| *Cathepsin G (*Ctsg*) | | 3.90 | −2.26 | | 2.55 |
| *Carbonic anhydrase I (*Car1*) | | 3.78 | −2.49 | | |
| *Defensin NP-4 precursor (*Np4*) | | 3.69 | −2.85 | | 2.35 |
| *Matrix metallopeptidase 13 (*Mmp13*) | −1.85 | 3.55 | −3.17 | 1.70 | 2.41 |
| *Defensin alpha 5 (*Defa5*) | | 3.31 | −3.36 | 1.83 | 2.45 |
| Rh-associated glycoprotein (*Rhag*) | | 3.18 | | | 2.86 |
| Pro-platelet basic protein (*Ppbp*) | | 2.92 | −4.08 | 2.14 | 4.13 |
| *Myeloperoxidase (*Mpo*) | | 2.86 | −2.42 | 1.71 | 2.72 |
| *Hemogen (*Hemgn*) | | 2.63 | −2.65 | | 2.23 |
| *Neutrophilic granule protein (*Ngp*) | | 2.60 | −1.62 | 1.57 | |
| Rh blood group, D antigen (*Rhd*) | | 2.54 | −2.49 | 1.84 | 1.95 |
| *Defensin RatNP-3 precursor (*RatNP-3b*) | | 2.50 | −2.99 | | 2.70 |
| *S100 calcium binding protein A8 (*S100a8*) | | 2.37 | −2.22 | 2.10 | 1.74 |
| *Solute carrier family 4, member 1 (*Slc4a1*) | | 2.36 | −1.93 | | 2.26 |
| Elastase, neutrophil expressed (*Elane*) | | 2.35 | −3.00 | | 2.93 |
| *S100 calcium binding protein A9 (*S100a9*) | | 2.35 | −1.86 | 1.83 | 1.57 |
| Eosinophil peroxidase (*Epx*) | | 2.30 | | | |
| *Alpha hemoglobin stabilizing protein (*Ahsp*) | | 2.29 | −2.48 | | 2.05 |
| Multimerin 1 (*Mmrn1*) | | 2.24 | | | 1.90 |
| *Cathelicidin antimicrobial peptide (*Camp*) | | 2.16 | | 1.36 | 1.75 |
| Erythroblast membrane-associated protein (*Ermap*) | | 2.10 | | | 2.08 |
| ATP binding cassette subfam. A member 13 (*Abca13*) | | 2.04 | | | 1.66 |
| Kell blood group, metallo-endopeptidase (*Kel*) | | 2.00 | | | 2.47 |
| Kruppel like factor 1 (*Klf1*) | | 2.00 | | 1.52 | 1.75 |
| Interleukin-23 receptor-like (*LOC103690079*) | | 1.92 | −2.74 | | |
| Nuclear factor, erythroid 2 (*Nfe2*) | | 1.87 | | | 1.99 |
| Roundabout homolog 1 *(Robo-1)* | | 1.82 | | 2.13 | 2.09 |
| 5′-aminolevulinate synthase 2 (*Alas2*) | | 1.75 | −1.99 | | 1.53 |
| T-cell Ig and mucin domain containing 2 (*Timd2*) | | 1.71 | | 3.25 | 3.08 |
| Hemoglobin, alpha 2 (*Hba2*) | | 1.68 | −2.03 | | 1.28 |
| Ficolin B (*Fcnb*) | | 1.65 | | 2.71 | 2.70 |
| Hemoglobin, alpha 1 (*Hba1*) | −1.11 | 1.61 | −1.89 | | 1.17 |
| Beta globin minor gene (*LOC100134871*) | | 1.58 | −1.66 | | 1.06 |
| Aquaporin 1 (*Aqp1*) | | 1.54 | | | 1.57 |
| Hemoglobin subunit beta (*Hbb*) | −1.14 | 1.49 | −1.66 | | |
| Erythrocyte membrane protein band 4.2 (*Epb42*) | | 1.45 | | | 1.31 |
| Hemoglobin, beta adult major chain (*Hbb-b1*) | | 1.30 | −1.89 | | 1.20 |
| Integrin subunit alpha 2b (*Itga2b*) | | 1.12 | | | 1.23 |
| AABR07043748.1 (unmapped) | | −1.47 | | | |
| Solute carrier family 17 member 7 (*Slc17a7, Vglut1*) | | −2.16 | | −2.57 | −2.97 |
| Guanylate binding protein family member 6 (*Gbp6*) | | −4.50 | 5.56 | −3.73 | −4.31 |
| AABR07043200.1 (uncharacterized) | | −6.33 | | −6.47 | −6.22 |

*Also listed are those additionally selected by other contrasts involving injured animals: ±SCI(0), ±pim(st/SCI), ±st/SCI(0) and ±SCI(st). Quantities are $\log_2$(FC). Selection was made with edgeR analysis according to the criteria abs($\log_2$(FC)) > 1 and FDR < 0.05. Genes marked by * meet the stricter criterion FDR < 0.00001. Positive numbers indicate relative upregulation by injury, stimulation, pimozide or stimulation plus injury; negative numbers represent relative downregulation.*

contrast ±st/SCI(0), but were not affected by injury alone, in contrast ±SCI(0). Most genes ($n$ = 835) were flagged by both contrasts, and some ($n$ = 147) were flagged by ±SCI(0) but not ±st/SCI(0). As seen in **Table 2**, of the 43 genes selected by contrast ±st(SCI), 15 were flagged by ±st/SCI(0) but not by ±SCI(0), 3 were flagged by ±SCI(0) but not by ±st/SCI(0) and one gene (*Mmmp13*) was flagged by both contrasts. This numerical imbalance confirms that stimulation caused changes in transcription mainly in genes that were unaffected by injury alone.

## Effect of Pimozide on the Response to Stimulation

Pimozide significantly altered 58% of the genes affected by stimulation after injury. Despite the possibility of bias for

increases over decreases described above and the low sample number ($n$ = 2 rats), genes flagged in contrast ±pim(st/SCI) showed a consistent direction of effect on genes flagged in contrast ±st(SCI) (**Table 2**). That is, upregulation was reversed in 24 genes and downregulation was reversed in one gene.

## Effect of Injury on the Response to Stimulation

Among rats that received stimulation, comparison of injured with intact groups, in contrast ±SCI(st), yielded further insight. A large number ($n$ = 1374) of genes was flagged by ±SCI(st), most of which (36 of 43) were also flagged by contrasting stimulation with no stimulation, ±st(SCI) (**Table 2**). Injury thus profoundly alters the response to stimulation. Confirming this conclusion, the transcriptional response of intact rats to stimulation, as determined by contrast ±st(0), yielded a list of 28 flagged genes (**Table 3**), none of which was among those significantly affected by stimulation in injured rats [±st(SCI)]. Many genes flagged by ±st(0) were not protein-coding: 10 were genes for small RNAs. Unlike in injured rats, significant effects of stimulation in intact rats were in the same direction as the effects (when present) of injury and pimozide (**Table 3**).

## Genes of Interest

Individual genes of greatest interest for understanding the effect of NRM stimulation on SCI are those flagged by all of the three contrasts that involved stimulation (without pimozide) in injury: ±st(SCI), ±SCI(st) and ±st/SCI(0). Twelve of these genes were increased by stimulation: *Mmp13*, *Defa5*, *Ppbp*, *Mpo*, *Rhd*, *S100a8*, *S100a9*, *Camp*, *Klf1*, *Robo-1*, *Timd2,* and *Fcnb*. Of these 12 genes, 7 also passed the considerably more restrictive filtering criterion of FDR < 0.00001, and all except one of these (*Camp*) was reversed by pimozide (**Table 2**). Three genes that were flagged in these three contrasts were decreased by stimulation: *Slc17a7*, *Gbp6* and the uncharacterized *AABR07043200.1*, of which only the decrease in *Gbp6* was reversed by pimozide. **Figure 1** shows the normalized counts for all 5 experimental conditions of the key characterized genes that were upregulated or down-regulated.

Few sRNA and miRNA genes underwent significantly altered transcription under any experimental condition. *Mir100* was down-regulated in the contrasts ±SCI(0) and ±SCI(st). *Mir3593* was down-regulated in the contrast ±SCI(st). Finally *Mir6326*, *Mir675,* and *Mir21* were up-regulated in the contrast ±SCI(st).

**TABLE 3 |** Genes selected by contrast ±st(0) (effect of stimulation in non-injured rats).

| Gene name | Transcript type | ±st(0) | ±pim(st/SCI) | ±SCI(0) |
|---|---|---|---|---|
| AABR07007730.1 (unmapped) | Processed_pseudogene | 6.01 | | 6.87 |
| Kallikrein B1 (*Klkb1*) | Protein_coding | 5.73 | | 6.22 |
| Rn50_X_0694.1 (unmapped) | Processed_pseudogene | 5.70 | | |
| Similar to Tpi1 protein (*RGD1563601*) | Processed_pseudogene | 3.77 | | |
| AABR07021745.1 (unmapped) | Small nuclear RNA | 2.05 | 3.87 | |
| Prothymosin alpha (*Ptma*) | Protein_coding | 1.99 | | |
| AC127784.3 (unmapped) | Small nucleolar RNA | 1.79 | 1.94 | |
| Neutrophil immunoglobulin-like receptor 1 (*Nilr1*) | Protein_coding | 1.77 | | 3.45 |
| AC129753.3 (unmapped) | Small nucleolar RNA | 1.73 | 2.84 | |
| Leukocyte immunoglobulin-like receptor (*Lilrb3*l) | Protein coding | 1.71 | | 2.99 |
| AABR07067449.1 (unmapped) | Small nucleolar RNA | 1.51 | | |
| AC118113.1 (unmapped) | Small nucleolar RNA | 1.46 | | |
| AC112093.1 (unmapped) | Small nucleolar RNA | 1.25 | | |
| AC097575.3 (unmapped) | Small nuclear RNA | 1.24 | 1.58 | |
| AABR07005613.1 (unmapped) | Miscellaneous_RNA | 1.22 | | |
| AABR07050379.1 (unmapped) | Small nuclear RNA | 1.22 | 2.02 | |
| AABR07072283.4 (unmapped) | Small Cajal body-specific RNA | 1.18 | | |
| Flavin containing monooxygenase 3 (*Fmo3*) | Protein coding | 1.15 | | |
| Ribosomal_L22 domain containing protein (*RGD1359290*) | Protein coding | 1.10 | | |
| AABR07036645.1 (unmapped) | Small nucleolar RNA | 1.08 | 1.39 | |
| AC094643.2 (unmapped) | Protein coding | −1.02 | | |
| ATPase subunit 8 (*mt-Atp8*) | Protein coding | −1.04 | | |
| Early growth response 1 (*Egr1*) | Protein coding | −1.07 | | |
| Cytochrome b (*mt-Cyb*) | Protein coding | −1.12 | | |
| NADH dehydrogenase subunit 2 (*mt-Nd2*) | Protein coding | −1.20 | | |
| NADH dehydrogenase subunit 4L (*mt-Nd4l*) | Protein coding | −1.52 | | |
| TNF receptor superfamily member 14 (*Tnfrsf14*) | Protein coding | −2.03 | | |
| Major intrinsic protein of lens fiber (*Mip*) | Protein coding | −3.01 | | |

*Their transcript type is also listed shown. Quantities shown are $log_2$(FC), as in* ***Table 2****. Genes that additionally showed significant effects of pimozide [±pim(st/SCI)] or untreated injury [±SCI(0)] are indicated in the adjacent columns.*

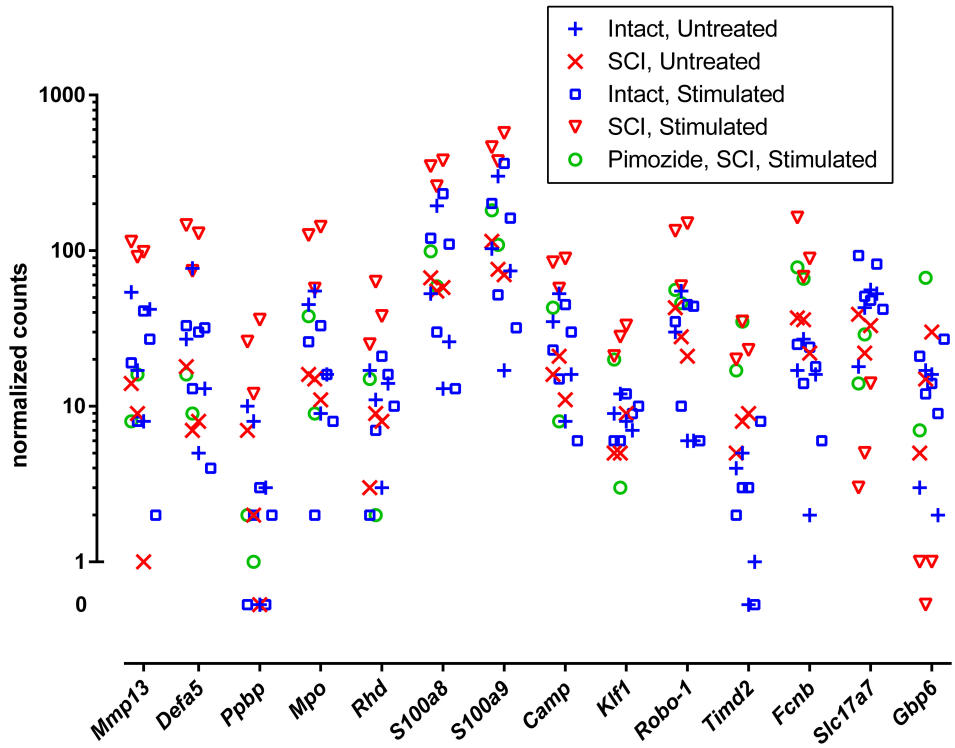


**FIGURE 1 |** Normalized RNA molecular counts from individual rats for 14 characterized genes identified as prominently up-regulated ($n$ = 12) or down-regulated ($n$ = 2) by stimulation. The included genes were those flagged by all three contrasts ±st(SCI), ±SCI(st) and ±st/SCI(0), as listed in **Table 2**. The vertical axis is scaled logarithmically and log zero values (equal to $-\infty$) are presented separately off-scale.

## Inferred Pathways and Biological Processes

Injury primarily increased inflammatory and immune transcripts and decreased those related to lipid and cholesterol synthesis and neuronal signaling, confirming previous reports (Bareyre and Schwab, 2003; Chamankhah et al., 2013; Shi et al., 2017). This was seen in the top canonical pathways determined with Ingenuity Pathway Analysis (**Table 4**) and in DAVID gene ontologies (biological process) for the contrast ±SCI(0) (some of which are listed in **Table 5**). Stimulation after injury had a major effect on pathways concerned with defense responses to lipopolysaccharides and various microorganisms (fungi, bacteria, yeast, viruses) and related inflammatory and immune responses (**Tables 4**, **5**). Many of these same pathways were among the principal targets of pimozide. Also prominent among the pathways affected by stimulation in injury were erythrocyte development, oxygen transport and heme biosynthesis (**Tables 4**, **5**). On the other hand, stimulation without injury, contrast ±st(0), had its largest effects on the canonical pathways for oxidative phosphorylation and mitochondrial dysfunction, with little influence on inflammatory and immune processes (**Table 4**). The DAVID gene ontologies (biological process) for contrast ±st(0) found that only two terms reached (weak) significance: "response to hyperoxia" and "regulation of apoptotic process."

## Resemblances of Expression Patterns to Perturbation With Drug Classes

The L1000 gene expression database of the CLUE software platform (clue.io) (Subramanian et al., 2017) was used to ascertain drug classes whose actions on cell cultures resembled to some quantifiable degree the effect of NRM stimulation on SCI. Human orthologs of the rat genes flagged in the two EdgeR contrasts ±st(SCI) and ±pim(st/SCI) were obtained from the Ensembl 2018 website (Zerbino et al., 2018). From the contrast ±st(SCI), which had flagged 43 rat genes, 37 human orthologous genes could be identified, and from the contrast ±pim(st/SCI), which originally yielded 81 rat genes, 65 human orthologous genes were identified (**Supplementary Table 1**). These two human gene lists were input to the CLUE Query tool to probe the database connectivity map, constructed from genetic changes in various human cell culture lines in response to diverse drugs. The classes of perturbagens (drugs) whose expression signatures most closely resembled those obtained in the experiments are listed in **Table 6**. The similarity score for the ±pim(st/SCI) contrast was reversed so that the absence of the drug pimozide was designated as the positive effect. High similarity (>98%) was reached in both contrasts by four perturbagen classes: PPAR agonists, angiotensin receptor antagonists, glucocorticoid receptor agonists, and nucleoporin loss of function (LOF).

**TABLE 4 |** Top canonical pathways indicated by IPA for the effects of injury alone [±SCI(0)], of stimulation after injury [±st(SCI)], stimulation on intact rats [±st(0)], and of pimozide on injured, stimulated rats [±pim(st/SCI)].

| Pathway | *p*-Value | Overlap |
|---|---|---|
| **±SCI(0) up-regulated** | | |
| EIF2 signaling | 4.59E−27 | 35.3% 78/221 |
| TREM1 signaling | 1.98E−16 | 45.3% 34/75 |
| Role of macrophages, fibroblasts, and endothelial cells in rheumatoid arthritis | 1.90E−14 | 23.6% 73/309 |
| Fc receptor-mediated phagocytosis in macrophages and monocytes | 7.15E−14 | 37.6% 35/93 |
| Role of pattern recognition receptors in recognition of bacteria and viruses | 1.75E−13 | 31.4% 43/137 |
| **±SCI(0) down-regulated** | | |
| Superpathway of cholesterol biosynthesis | 9.06E−18 | 60.7% 17/28 |
| Cholesterol biosynthesis I | 1.56E−12 | 76.9% 10/13 |
| Cholesterol biosynthesis II (via 24,25-dihydrolanosterol) 1.56E−12 | 1.56E−12 | 76.9% 10/13 |
| Cholesterol biosynthesis III (via desmosterol) | 1.56E−12 | 76.9% 10/13 |
| Synaptic long term depression | 1.43E−09 | 16.4% 24/146 |
| **±st(SCI)** | | |
| Role of IL-17A in psoriasis | 2.13E−04 | 15.4% 2/13 |
| Osteoarthritis pathway | 5.34E−03 | 1.4% 3/211 |
| Tetrapyrrole biosynthesis II | 8.40E−03 | 20.0% 1/5 |
| Heme biosynthesis II | 1.51E−02 | 11.1% 1/9 |
| Atherosclerosis signaling | 1.94E−02 | 1.6% 2/127 |
| **±st(0)** | **±st(SCI)** | **±st(SCI)** |
| Oxidative phosphorylation | 1.21E−11 | 7.3% 8/109 |
| Mitochondrial dysfunction | 4.54E−10 | 4.7% 8/171 |
| Sirtuin signaling pathway | 9.91E−06 | 2.1% 6/291 |
| Glycine degradation (creatine biosynthesis) | 3.46E−03 | 50.0% 1/2 |
| MSP-RON signaling pathway | 6.92E−03 | 2.8% 2/72 |
| **±pim(st/SCI)** | | |
| Role of IL-17A in psoriasis | 2.38E−04 | 15.4% 2/13 |
| G protein signaling mediated by tubby | 1.48E−03 | 6.2% 2/32 |
| Tec kinase signaling | 3.41E−03 | 1.8% 3/170 |
| RhoGDI signaling | 3.82E−03 | 1.7% 3/177 |
| Agranulocyte adhesion and diapedesis | 4.72E−03 | 1.6% 3/191 |

# DISCUSSION

## General Observations and Technical Considerations

The effect of the NRM, or indeed of any brainstem system, on transcription in the spinal cord has not previously been reported. Here we show that transcriptional changes occurred in the first 2 h of NRM stimulation in a small fraction of the total genome. A longer period of stimulation probably could have produced more changes, as seen with the 3-day injury period and even with the 3-h presence of pimozide. The effect of the NRM stimulation differed completely between injured and normal spinal cord. The changes due to stimulation were for the most part not reversals (or enhancements) of those caused by injury alone, and thus implicate a distinct set of genes. In SCI, stimulation affected primarily transcription in genes with defensive immune functions. Other notable changes were in genes involved in erythrocyte development, such as constituent molecules of hemoglobin. There was a paucity of neuron-specific effects. These general findings lead to a somewhat revised and more complex model of the NRM's repair effect, with defensive and protective processes preceding (and perhaps permitting or evoking) the regenerative benefits of stimulation.

The validity of the findings and their interpretation must take into account the low numbers in each group. Low numbers are not uncommon in RNAseq studies, typically imposed by costs and by other external factors. A study of biological replicate numbers with various DGE software applications (Schurch et al., 2016), found that EdgeR, DESeq2, and baySeq can all produce satisfactory and mutually consistent conclusions with as few as three replicates, given a $< 5\%$ false discovery rate and a fold change of $\pm 50\%$ [or abs(log2(FC)) $> 0.58$]. Here, we applied a more restrictive criterion for fold change of $\pm 100\%$ [abs($\log_2$(FC)) $> 1$] along with the $< 5\%$ false positive rate, and all groups except pimozide treatment consisted of $> = 3$ rats. Further strengthening the conclusions, the core list of altered genes (**Figure 1**, see section "Genes of Interest") was derived from three paired contrasts that utilized all but two of the studied animals ($n = 15$). Thus the early changes in gene transcription found with NRM stimulation in injured animals can be specified with reasonable certainty. However, the findings strictly apply to female rats only, under conditions of treatment with buprenorphine, gentamycin and halothane, and the possibility remains of different genes emerging from contrasts made under other conditions or in other types of subject.

Pimozide is an antipsychotic drug that acts as an antagonist with a high affinity for both 5-HT7 receptors and for dopamine D2 subtype receptors (Roth et al., 1994). In the two subjects tested with pimozide, the drug consistently blocked and never enhanced the effects of stimulation in injury on individual genes. The descending pathways from the NRM are strongly serotonergic whereas dopaminergic projections are not prominent in the spinal cord and their cell bodies are distant to the site of stimulation (van Dijken et al., 1996). Thus the results with pimozide suggest that the effect of NRM stimulation after SCI was mediated in many genes by serotonin release, while a role for dopamine release is unlikely. The relatively rapid effect of pimozide in reversing gene expression induced by 2 h of NRM stimulation in SCI is likely to have occurred at the level of post-synaptic 5-HT7 receptors in the spinal cord. These receptors have been implicated in anti-inflammation, repair, and neuroplasticity at various CNS sites including the spinal cord (Kvachnina et al., 2005; de las Casas-Engel et al., 2013; Carballosa-Gonzalez et al., 2014; Di Pilato et al., 2014; Volpicelli et al., 2014; Fields and Mitchell, 2015). However, an action of pimozide at other CNS sites or other organs, which then indirectly causes a block of the influence of NRM stimulation on RNA synthesis in the spinal cord appears unlikely.

Measurements made after the 2 h time window of stimulation or after 3 days of injury represent snapshots of dynamic processes, which may include transient or long-lasting or even multiphasic changes in messenger RNA level. Changes in transcription rate are thought to determine the direction of most effects,

**TABLE 5 |** Gene Ontology terms (biological process, GOTERM_BP_DIRECT) found to be enriched in by stimulation after injury [±st(SCI)] or its modification by pimozide [±pim(st/SCI)].

| Term | GO number | ±st(SCI) | ±pim(st/SCI) | ±SCI(0) |
|---|---|---|---|---|
| Defense response to fungus | 0050832 | 6.52E−08 | 6.74E−08 | |
| Erythrocyte development | 0048821 | 1.60E−07 | 5.81E−04 | |
| Oxygen transport | 0015671 | 4.25E−06 | 6.20E−06 | |
| Leukocyte migration involved in inflammatory response | 0002523 | 2.02E−04 | 1.86E−04 | |
| Defense response to bacterium | 0042742 | 3.44E−04 | 3.83E−03 | 1.62E−02 |
| Negative regulation of growth of symbiont in host | 0044130 | 3.59E−04 | 1.33E−02 | |
| Hydrogen peroxide catabolic process | 0042744 | 3.61E−04 | 3.31E−04 | |
| Killing of cells of other organism | 0031640 | 4.36E−04 | 5.04E−04 | |
| Ammonium transport | 0015696 | 2.69E−03 | | |
| Ammonium transmembrane transport | 0072488 | 4.14E−03 | | |
| Response to lipopolysaccharide | 0032496 | 6.48E−03 | 7.80E−04 | 1.98E−09 |
| Chronic inflammatory response | 0002544 | 7.43E−03 | | |
| Cellular oxidant detoxification | 0098869 | 8.26E−03 | 8.18E−03 | |
| Response to yeast | 0001878 | 8.55E−03 | | |
| Response to hydrogen peroxide | 0042542 | 1.02E−02 | 1.08E−02 | |
| Defense response to Gram-positive bacterium | 0050830 | 1.55E−02 | | 2.67E−07 |
| Innate immune response | 0045087 | 3.20E−02 | 9.36E−05 | 1.86E−13 |
| Antibacterial humoral response | 0019731 | 3.23E−02 | | |
| Response to virus | 0009615 | | 7.13E−04 | 4.20E−04 |
| Defense response to virus | 0051607 | | 3.64E−03 | 1.07E−08 |

*Terms were obtained with DAVID 6.8. Those additionally enriched by injury in untreated rats [±SCI(0)] are also listed. The input data for DAVID came from gene lists containing both up-regulated and down-regulated genes that met the EdgeR criteria abs($log_2$(FC)) > 1 and FDR < 0.05. Values shown are Benjamini probabilities, which were applied to the enrichment criterion p < 0.05.*

because degradation rates and post-transcriptional processing are constant for most individual genes (Rabani et al., 2011, 2014), although inflammatory and immune signaling genes and targets of NFκB signaling are more likely to show modulated degradation (Rabani et al., 2011). The half-life of decay is typically slower than the transcription rate, which suggests the possibility of bias in favor of detecting increases over decreases. The half-life of messenger RNA in mammalian cell cultures averages 7–9 h, with a lower median, e.g., 4–6 h, and regulators of transcription and signal transduction tend to have shorter half-lives (Friedel et al., 2009; Schwanhausser et al., 2011). Therefore, given typical half-lives, the finding that 94% of changes were increases after the 3 day post-injury period probably reflects true differences in the direction of transcription rates. However, the finding that 91% of changes after the 2 h stimulation window were increases is alternatively explained by the slowness of decay.

## Background Studies

This work is part of a series exploring the central control of endogenous repair mechanisms. It is proposed that the various brainstem raphé nuclei, including the NRM, form the central links of feedback loops controlling repair. In our model, raphé neurons receive sensory, chemical and central-state signals indicative of recent injury (e.g., pain, vestibular input, hypothermia, circulating cytokines). Their evoked electrical activity then causes axonal release of serotonin and co-release of neuropeptide transmitters from terminals that, collectively, innervate almost the entire CNS (Molliver, 1987; Hornung, 2003). Trophic and protective cellular effects can be produced by these various neuropeptides: thyrotropin releasing hormone (Daimon et al., 2013), substance P (Jiang et al., 2012; Kim et al., 2015), galanin (Hobson et al., 2008), met-enkephalin (Narita et al., 2006; Campbell et al., 2012) as well as by serotonin (Azmitia, 2007; Trakhtenberg and Goldberg, 2012), all acting through non-synaptic volume transmission (Ridet et al., 1993; Agnati et al., 1995; Borroto-Escuela et al., 2015). As in the response to infection which is frequently concurrent with injury, an endogenous repair system from the perspective of natural selection should promiscuously exploit (facilitate or depress) multiple molecular and cellular mechanisms.

The main experimental evidence for this model is that some days or weeks of stimulation in a raphé nucleus starting in the first days following incomplete contusional SCI or fluid-pressure TBI or induction of MS-like signs was found to improve behavioral signs over several weeks (Hentall and Gonzalez, 2012; Carballosa Gonzalez et al., 2013; Madsen et al., 2017). Concomitant histological changes seen at chronic endpoints following stimulation include increased myelination and serotonergic innervation around the injury after T8 SCI (Hentall and Gonzalez, 2012), increased calcitonin gene related peptide after C5 SCI (Vitores et al., 2018), restored volume loss in neocortex after TBI (Carballosa Gonzalez et al., 2013), and lessened cellular pathology and cytokine production in experimental autoimmune encephalomyelitis (Madsen et al., 2017).

The mechanisms leading to these long-term changes are likely to involve complexly interwoven cellular and molecular processes. To better understand the proximate causes of

**TABLE 6 |** Perturbagens (pharmacologic and genetic) whose expression signatures most closely resemble the effect of stimulation after injury and its modification by pimozide.

| Drug class | % similarity ±st(SCI) | −(% similarity) ±pim(st/SCI) |
|---|---|---|
| PPAR receptor agonist | 99.78 | 99.97 |
| Nucleoporin LOF | 99.59 | 99.73 |
| Phospholipases GOF | 99.46 | 81.78 |
| Structural maintenance of chromosomes proteins LOF | 99.40 | <80% |
| Angiotensin receptor antagonist | 99.02 | 99.22 |
| Wnt family GOF | 98.55 | 96.27 |
| SRC inhibitor | 98.53 | <80% |
| Potassium channel blocker | 98.37 | <80% |
| Glucocorticoid receptor agonist | 98.24 | 98.48 |
| Imidazoline ligand | 97.9 | <80% |
| Bacterial DNA gyrase inhibitor | 97.87 | <80% |
| SRY LOF | 97.61 | 93.55 |
| NFkB pathway inhibitor | 97.14 | 87.87 |
| HMGCR inhibitor | 96.44 | <80% |
| FOS transcription factor family GOF | 96.18 | 99.8 |
| Heat shock 70 kDa proteins LOF | 95.71 | <80% |
| Proteasome pathway LOF | 95.30 | <80% |
| NKL subclass homeoboxes and pseudogenes LOF | 94.86 | <80% |
| Serine proteases GOF | 94.59 | 98.28 |
| Na-K-Cl transporter inhibitor | 94.5 | 88.32 |

*The genes flagged as affected by stimulation in injury [contrast ±st(SCI)], as listed in* ***Table 2****, were converted to their human equivalents, if known, and fed to the Query function of the CLUE software platform (clue.io) (Subramanian et al., 2017). The genes flagged as affected by pimozide in rats that were both stimulated and injured [contrast ±pim(st/SCI)] were similarly processed, but their effects were reversed (i.e., similarity scores were multiplied by −1). GOF, genetic gain of function; LOF, genetic loss of function.*

improved recovery with NRM stimulation, this and some other studies have focused on more acute, post-injury endpoints and shorter stimulation periods. An immunostaining study of 3-day C5 injury after 2 days of NRM stimulation showed changes in numbers of inflammatory cell types and a transition from neural precursors to radial glia that facilitate differentiation (Jermakowicz et al., 2019). In rats with 3-day T8 contusions, 2 h of NRM stimulation, as in the present protocol, restored normal levels of injury-depleted cAMP, phosphorylated cAMP response binding element (pCREB), and pPKA (Carballosa-Gonzalez et al., 2014). The same study showed that NRM stimulation had no significant effects on levels of cAMP, pPKA or pCREB in intact animals, but pimozide in intact animals with or without stimulation lowered cAMP to injured levels. Reversal of cAMP depletion has also been shown in the neocortex and hippocampus of rats with 3-day old TBI following 3 days of electrical stimulation in the median raphé nucleus (Carballosa Gonzalez et al., 2013).

## Interpretation of Main Findings

Cyclic AMP can promote axonal regeneration following SCI via elevated pPKA and pCREB, which subsequently increases expression of various trophic genes, although a non-genetic route via pPKA can also have beneficial effects on the cytoskeleton via the small G protein, Rho (Lehmann et al., 1999; Hannila and Filbin, 2008). Given the previously demonstrated NRM-evoked recovery of cAMP after T8 SCI (Carballosa-Gonzalez et al., 2014), it was unsurprising that transcriptional effects of stimulation were seen. However, it was not expected that the main increases would be in defensive and pro-inflammatory genes, for example, *Ctsg*, *Np4*, *RatNP-3b*, *Defa5*, *Elane*, *Mpo*, *S100a8*, *S100a9,* and *Ppbp*. The proteins S100A8 and S100A9 are frequently combined as the antimicrobial dimer calprotectin (Striz and Trebichavsky, 2004). They probably arrive in the injured spinal cord as constituents of myeloid cells, particularly neutrophils (Fleming et al., 2006; Mitchell et al., 2008), which are thought to be deleterious to recovery (McCreedy et al., 2018), although S100A8 and S100A9 can also be induced in macrophages and microglia by neuropathic states (Abe et al., 1999). While there is some indirect evidence that S100A9 promotes recovery from SCI (Roet et al., 2013), but pro-inflammatory effects are more likely the dominant initial action.

Other genes upregulated by stimulation in SCI may also have deleterious effects. *Mpo* has been shown by gene knockout to exacerbate secondary injury after SCI (Kubota et al., 2012). *Ctsg* is a pronociceptive mediator in the spinal cord (Liu et al., 2015), as is carbonic anhydrases (gene *Car1*) (Asiedu et al., 2010). Neutrophil elastase, which is released by activated neutrophils, is reported to be a key mediator of secondary pathogenesis in SCI (Semple et al., 2015). On the other hand, matrix metalloproteinase 13 is a matrix-degrading enzyme released from monocytes that is important in functional recovery after SCI (Shechter et al., 2011). Of the several microRNAs tagged in these studies, *Mir21*, which was upregulated in the contrast ±SCI(st), is of greatest interest. *Mir21* is increased by exercise after SCI and improves recovery in rats, probably by regulating the pro-regenerative PTEN/mTOR pathway, since it lowers PTEN messenger RNA and raises mTOR messenger RNA (Liu et al., 2012). Few of the genes affected by stimulation after SCI (**Table 2**) are particularly associated with the CNS. One exception was the downregulated solute carrier family 17 member 7 (*Slc17a7*), also known as *Vglut1*, whose protein transports glutamate into synaptic vesicles (Shigeri et al., 2004); its levels in the spinal cord are reported to be decreased after peripheral nerve damage (Rotterman et al., 2014; Wang et al., 2016). Acute decreases in *Vglut1* (*Slc17a7*) with stimulation, as observed here, could lead to lower net glutamate release, which is likely to reduce damage due to over-stimulation of neurons (Krzyzanowska et al., 2014), although recovery ultimately requires restoration of *Vglut1* (Burnside et al., 2018). A second exception was *Robo-1*, which was increased by stimulation, whose protein product an important player in pioneer longitudinal axon guidance (Kim et al., 2011).

Another interesting group of genes unexpectedly upregulated by stimulation in injury is related to erythrocyte development and oxygen transport: *Klf1*, *Rhd*, *Rhag*, *Hbb*, *Hba*, *Hba2*, *Hbb-b1*. The last four produce components of hemoglobin, which is constitutively expressed in the brain and spinal cord (Biagioli et al., 2009; Richter et al., 2009; Russo et al., 2013), and may

act protectively by sequestering oxygen and free radicals (Xie and Yang, 2016). Indeed, "cellular oxidant detoxification" also featured among biological processes enriched by stimulation after SCI (**Table 5**). The key regulator of erythropoiesis, erythropoietin (EPO), is known to promote recovery and regeneration in SCI (Gassmann et al., 2003; Matis and Birbilis, 2009). There were no significant changes in expression of the *Epo* gene in this study, but it is possible that the increase in erythropoietic genes was due to increased erythropoiten release (Hasselblatt et al., 2006). Both the protein and *Epo* messenger RNA are reported to be increased by serotonin in the mouse hippocampus (Choi and Son, 2013). Further study of how erythropoiten synthesis and release responds at different time points post-injury and during NRM stimulation appears to be warranted.

The prevalence of altered transcription in exogenous cells of the injured spinal cord requires further experimental investigation. Among various possibilities to test, arriving myeloid cells such as neutrophils could be more attracted to the spinal cord's injury site after they have been altered in some way by NRM stimulation. Alternatively, transcription in exogenous cells, once arrived, could be influenced (perhaps toward a pro-regeneration phenotype) by the NRM stimulation or by local sequelae of that stimulation. Classic synapses are not necessary for the effects of the NRM stimulation, since both serotonin and co-released neuropeptides participate in non-synaptic volume transmission in the spinal cord (Ridet et al., 1993). A growing body of evidence implicates serotonin in both neural and humoral aspects of immune control. Serotonin and its receptors are present on numerous cells of the adaptive and innate immune systems and have been implicated in macrophage activation (Jiang et al., 2009; Krabbe et al., 2012; Baganz and Blakely, 2013).

## CONCLUSION

The present study adds important new details to the general concept that the raphé system senses and alleviates stress or injury. The effects of NRM stimulation on gene transcription were very different in injured and intact animals, mirroring our prior study of the effects of NRM stimulation on levels of cAMP, PKA, and CREB (Carballosa-Gonzalez et al., 2014). The earliest changes in gene transcription brought about by NRM stimulation were seen to be confined mainly to defensive and erythropoietic functions. Whereas a week or more of NRM stimulation facilitates repair (Hentall and Burns, 2009; Hentall and Gonzalez, 2012; Madsen et al., 2017; Vitores et al., 2018), the shorter 2-h period used here intensified transcription of predominantly inflammatory genes. Although the products of these genes are often assumed to be harmful, immune responses cannot necessarily be simply parsed into harmful and beneficial processes (Doty et al., 2015; Li et al., 2018). Conceivably, the inflammatory effects of substances such as S100A8 and S100A9, however harmful they may be initially, are necessary preliminaries with net benefits to the overall repair process, and lead later to neural-specific effects. Consistent with these ideas, three of the four top perturbagen classes that resembled the effect of 2 h of stimulation (**Table 6**) are known to produce improvements in SCI: PPARs agonists (Park et al., 2007), angiotensin receptor antagonists (Guler et al., 2010) and glucocorticoid receptor agonists, although this last group's benefits in SCI are more controversial (Akhtar et al., 2009). Furthermore, all three classes inactivate inflammatory pathways, such as those controlled by NF-κB (Bekhbat et al., 2017; Labandeira-Garcia et al., 2017; Villapol, 2018). The present study thus tends to confirm the therapeutic promise of these drug classes. The study also provides further support for interim DBS of the NRM or, more practically from the surgical standpoint, of its midbrain periaqueductal gray input, as a therapy for SCI that may ultimately be superior to single or combined drugs in its simplicity and safety of application and the range of signs and symptoms improved (Chari et al., 2017).

## DATA AVAILABILITY STATEMENT

The datasets generated for this study can be found in the National Center for Biotechnology Information (NCBI), GEO Accession Number GSE133093.

## ETHICS STATEMENT

The animal study was reviewed and approved by the Institutional Animal Care and Use Committee of the University of Miami, Miller School of Medicine.

## AUTHOR CONTRIBUTIONS

IH designed the experiments and wrote the manuscript. WJ managed the RNA sequencing and analysis. MC-G and AV performed animal surgery, stimulation, and tissue extraction.

## FUNDING

This work was funded in part by Robert J. Kleberg, Jr. and Helen C. Kleberg Foundation.

## ACKNOWLEDGMENTS

We thank Dr. Anthony J. Griswold for valuable help with the high-throughput sequencing and for advice on its analysis.

## SUPPLEMENTARY MATERIAL

The Supplementary Material for this article can be found online at: https://www.frontiersin.org/articles/10.3389/fncel.2019.00510/full#supplementary-material

## REFERENCES


Abe, M., Umehara, F., Kubota, R., Moritoyo, T., Izumo, S., and Osame, M. (1999). Activation of macrophages/microglia with the calcium-binding proteins MRP14 and MRP8 is related to the lesional activities in the spinal cord of HTLV-I associated myelopathy. *J. Neurol.* 246, 358–364. doi: 10.1007/s004150050363

Agnati, L. F., Bjelke, B., and Fuxe, K. (1995). Volume versus wiring transmission in the brain: a new theoretical frame for neuropsychopharmacology. *Med. Res. Rev.* 15, 33–45. doi: 10.1002/med.2610150104

Akhtar, A. Z., Pippin, J. J., and Sandusky, C. B. (2009). Animal studies in spinal cord injury: a systematic review of methylprednisolone. *Altern. Lab. Anim.* 37, 43–62. doi: 10.1177/026119290903700108

Asiedu, M., Ossipov, M. H., Kaila, K., and Price, T. J. (2010). Acetazolamide and midazolam act synergistically to inhibit neuropathic pain. *Pain* 148, 302–308. doi: 10.1016/j.pain.2009.11.015

Azmitia, E. C. (2007). Serotonin and brain: evolution, neuroplasticity, and homeostasis. *Int. Rev. Neurobiol.* 77, 31–56. doi: 10.1016/S0074-7742(06)77002-7

Baganz, N. L., and Blakely, R. D. (2013). A dialogue between the immune system and brain, spoken in the language of serotonin. *ACS Chem. Neurosci.* 4, 48–63. doi: 10.1021/cn300186b

Bareyre, F. M., and Schwab, M. E. (2003). Inflammation, degeneration and regeneration in the injured spinal cord: insights from DNA microarrays. *Trends Neurosci.* 26, 555–563. doi: 10.1016/j.tins.2003.08.004

Batty, N. J., Fenrich, K. K., and Fouad, K. (2017). The role of cAMP and its downstream targets in neurite growth in the adult nervous system. *Neurosci. Lett.* 652, 56–63. doi: 10.1016/j.neulet.2016.12.033

Bekhbat, M., Rowson, S. A., and Neigh, G. N. (2017). Checks and balances: the glucocorticoid receptor and NFkB in good times and bad. *Front. Neuroendocrinol.* 46:15–31. doi: 10.1016/j.yfrne.2017.05.001

Biagioli, M., Pinto, M., Cesselli, D., Zaninello, M., Lazarevic, D., Roncaglia, P., et al. (2009). Unexpected expression of alpha- and beta-globin in mesencephalic dopaminergic neurons and glial cells. *Proc. Natl. Acad. Sci. U.S.A.* 106, 15454–15459. doi: 10.1073/pnas.0813216106

Borroto-Escuela, D. O., Agnati, L. F., Bechter, K., Jansson, A., Tarakanov, A. O., and Fuxe, K. (2015). The role of transmitter diffusion and flow versus extracellular vesicles in volume transmission in the brain neural-glial networks. *Philos. Trans. R. Soc. Lond. B Biol. Sci.* 370:20140183. doi: 10.1098/rstb.2014.0183

Burnside, E. R., De Winter, F., Didangelos, A., James, N. D., Andreica, E. C., Layard-Horsfall, H., et al. (2018). Immune-evasive gene switch enables regulated delivery of chondroitinase after spinal cord injury. *Brain* 141, 2362–2381. doi: 10.1093/brain/awy158

Campbell, A. M., Zagon, I. S., and McLaughlin, P. J. (2012). Opioid growth factor arrests the progression of clinical disease and spinal cord pathology in established experimental autoimmune encephalomyelitis. *Brain Res.* 1472, 138–148. doi: 10.1016/j.brainres.2012.07.006

Carballosa Gonzalez, M. M., Blaya, M. O., Alonso, O. F., Bramlett, H. M., and Hentall, I. D. (2013). Midbrain raphe stimulation improves behavioral and anatomical recovery from fluid-percussion brain injury. *J. Neurotrauma.* 30, 119–130. doi: 10.1089/neu.2012.2499

Carballosa-Gonzalez, M. M., Vitores, A., and Hentall, I. D. (2014). Hindbrain raphe stimulation boosts cyclic adenosine monophosphate and signaling proteins in the injured spinal cord. *Brain Res.* 1543, 165–172. doi: 10.1016/j.brainres.2013.11.013

Chamankhah, M., Eftekharpour, E., Karimi-Abdolrezaee, S., Boutros, P. C., San-Marina, S., and Fehlings, M. G. (2013). Genome-wide gene expression profiling of stress response in a spinal cord clip compression injury model. *BMC Genomics* 14:583. doi: 10.1186/1471-2164-14-583

Chari, A., Hentall, I. D., Papadopoulos, M. C., and Pereira, E. A. (2017). Surgical neurostimulation for spinal cord injury. *Brain Sci.* 7:E18. doi: 10.3390/brainsci7020018

Choi, M., and Son, H. (2013). Effects of serotonin on erythropoietin expression in mouse hippocampus. *Exp. Neurobiol.* 22, 45–50. doi: 10.5607/en.2013.22.1.45

Daimon, C. M., Chirdon, P., Maudsley, S., and Martin, B. (2013). The role of Thyrotropin Releasing Hormone in aging and neurodegenerative diseases. *Am. J. Alzheimers Dis.* 1. doi: 10.7726/ajad.2013.1003

David, S., and Kroner, A. (2011). Repertoire of microglial and macrophage responses after spinal cord injury. *Nat. Rev. Neurosci.* 12, 388–399. doi: 10.1038/nrn3053

de las Casas-Engel, M., Dominguez-Soto, A., Sierra-Filardi, E., Bragado, R., Nieto, C., Puig-Kroger, A., et al. (2013). Serotonin skews human macrophage polarization through HTR2B and HTR7. *J. Immunol.* 190, 2301–2310. doi: 10.4049/jimmunol.1201133

Di Pilato, P., Niso, M., Adriani, W., Romano, E., Travaglini, D., Berardi, F., et al. (2014). Selective agonists for serotonin 7 (5-HT7) receptor and their applications in preclinical models: an overview. *Rev. Neurosci.* 25, 401–415. doi: 10.1515/revneuro-2014-0009

Dobin, A., Davis, C. A., Schlesinger, F., Drenkow, J., Zaleski, C., Jha, S., et al. (2013). STAR: ultrafast universal RNA-seq aligner. *Bioinformatics* 29, 15–21. doi: 10.1093/bioinformatics/bts635

Doty, K. R., Guillot-Sestier, M. V., and Town, T. (2015). The role of the immune system in neurodegenerative disorders: adaptive or maladaptive? *Brain Res.* 1617, 155–173. doi: 10.1016/j.brainres.2014.09.008

Dulin, J. N., Antunes-Martins, A., Chandran, V., Costigan, M., Lerch, J. K., Willis, D. E., et al. (2015). Transcriptomic approaches to neural repair. *J. Neurosci.* 35, 13860–13867. doi: 10.1523/JNEUROSCI.2599-15.2015

Fields, D. P., and Mitchell, G. S. (2015). Spinal metaplasticity in respiratory motor control. *Front. Neural. Circuits* 9:2. doi: 10.3389/fncir.2015.00002

Fleming, J. C., Norenberg, M. D., Ramsay, D. A., Dekaban, G. A., Marcillo, A. E., Saenz, A. D., et al. (2006). The cellular inflammatory response in human spinal cords after injury. *Brain* 129(Pt 12), 3249–3269. doi: 10.1093/brain/awl296

Friedel, C. C., Dolken, L., Ruzsics, Z., Koszinowski, U. H., and Zimmer, R. (2009). Conserved principles of mammalian transcriptional regulation revealed by RNA half-life. *Nucleic Acids Res.* 37:e115. doi: 10.1093/nar/gkp542

Gassmann, M., Heinicke, K., Soliz, J., and Ogunshola, O. O. (2003). Non-erythroid functions of erythropoietin. *Adv. Exp. Med. Biol.* 543, 323–330. doi: 10.1007/978-1-4419-8997-0_22

Gautier, A., Geny, D., Bourgoin, S., Bernard, J. F., and Hamon, M. (2017). Differential innervation of superficial versus deep laminae of the dorsal horn by bulbo-spinal serotonergic pathways in the rat. *IBRO Rep.* 2, 72–80. doi: 10.1016/j.ibror.2017.04.001

Guler, A., Sahin, M. A., Ucak, A., Onan, B., Inan, K., Oztas, E., et al. (2010). Protective effects of angiotensin II type-1 receptor blockade with olmesartan on spinal cord ischemia-reperfusion injury: an experimental study on rats. *Ann. Vasc. Surg.* 24, 801–808. doi: 10.1016/j.avsg.2010.03.023

Hannila, S. S., and Filbin, M. T. (2008). The role of cyclic AMP signaling in promoting axonal regeneration after spinal cord injury. *Exp. Neurol.* 209, 321–332. doi: 10.1016/j.expneurol.2007.06.020

Hardcastle, T. J., and Kelly, K. A. (2010). baySeq: empirical Bayesian methods for identifying differential expression in sequence count data. *BMC Bioinformatics* 11:422. doi: 10.1186/1471-2105-11-422

Hasselblatt, M., Ehrenreich, H., and Siren, A. L. (2006). The brain erythropoietin system and its potential for therapeutic exploitation in brain disease. *J. Neurosurg. Anesthesiol.* 18, 132–138. doi: 10.1097/00008506-200604000-00007

Hentall, I. D., and Burns, S. B. (2009). Restorative effects of stimulating medullary raphe after spinal cord injury. *J. Rehabil. Res. Dev.* 46, 109–122.

Hentall, I. D., and Gonzalez, M. M. (2012). Promotion of recovery from thoracic spinal cord contusion in rats by stimulation of medullary raphe or its midbrain input. *Neurorehabil. Neural. Repair.* 26, 374–384. doi: 10.1177/1545968311425178

Hobson, S. A., Bacon, A., Elliot-Hunt, C. R., Holmes, F. E., Kerr, N. C., Pope, R., et al. (2008). Galanin acts as a trophic factor to the central and peripheral nervous systems. *Cell. Mol. Life Sci.* 65, 1806–1812. doi: 10.1007/s00018-008-8154-7

Hornung, J. P. (2003). The human raphe nuclei and the serotonergic system. *J. Chem. Neuroanat.* 26, 331–343. doi: 10.1016/j.jchemneu.2003.10.002

Jermakowicz, W. J., Sloley, S. S., Dan, L., Vitores, A., Carballosa-Gautam, M. M., and Hentall, I. D. (2019). Cellular changes in injured rat spinal cord following electrical brainstem stimulation. *Brain Sci.* 9:E124. doi: 10.3390/brainsci9060124

Jiang, M. H., Chung, E., Chi, G. F., Ahn, W., Lim, J. E., Hong, H. S., et al. (2012). Substance P induces M2-type macrophages after spinal cord injury. *Neuroreport* 23, 786–792. doi: 10.1097/WNR.0b013e3283572206

Jiang, X., Wang, J., Luo, T., and Li, Q. (2009). Impaired hypothalamic-pituitary-adrenal axis and its feedback regulation in serotonin transporter knockout mice. *Psychoneuroendocrinology* 34, 317–331. doi: 10.1016/j.psyneuen.2008.09.011

Kearney, P. A., Ridella, S. A., Viano, D. C., and Anderson, T. E. (1988). Interaction of contact velocity and cord compression in determining the severity of spinal cord injury. *J. Neurotrauma.* 5, 187–208. doi: 10.1089/neu.1988.5.187

Kim, K. T., Kim, H. J., Cho, D. C., Bae, J. S., and Park, S. W. (2015). Substance P stimulates proliferation of spinal neural stem cells in spinal cord injury via the mitogen-activated protein kinase signaling pathway. *Spine J.* 15, 2055–2065. doi: 10.1016/j.spinee.2015.04.032

Kim, M., Roesener, A. P., Mendonca, P. R., and Mastick, G. S. (2011). Robo1 and Robo2 have distinct roles in pioneer longitudinal axon guidance. *Dev. Biol.* 358, 181–188. doi: 10.1016/j.ydbio.2011.07.025

Krabbe, G., Matyash, V., Pannasch, U., Mamer, L., Boddeke, H. W., and Kettenmann, H. (2012). Activation of serotonin receptors promotes microglial injury-induced motility but attenuates phagocytic activity. *Brain Behav. Immun.* 26, 419–428. doi: 10.1016/j.bbi.2011.12.002

Krzyzanowska, W., Pomierny, B., Filip, M., and Pera, J. (2014). Glutamate transporters in brain ischemia: to modulate or not? *Acta Pharmacol. Sin.* 35, 444–462. doi: 10.1038/aps.2014.1

Kubota, K., Saiwai, H., Kumamaru, H., Maeda, T., Ohkawa, Y., Aratani, Y., et al. (2012). Myeloperoxidase exacerbates secondary injury by generating highly reactive oxygen species and mediating neutrophil recruitment in experimental spinal cord injury. *Spine* 37, 1363–1369. doi: 10.1097/BRS.0b013e31824b9e77

Kvachnina, E., Liu, G., Dityatev, A., Renner, U., Dumuis, A., Richter, D. W., et al. (2005). 5-HT7 receptor is coupled to G alpha subunits of heterotrimeric G12-protein to regulate gene transcription and neuronal morphology. *J. Neurosci.* 25, 7821–7830. doi: 10.1523/JNEUROSCI.1790-05.2005

Kwiat, G. C., and Basbaum, A. I. (1992). The origin of brainstem noradrenergic and serotonergic projections to the spinal cord dorsal horn in the rat. *Somatosens Mot. Res.* 9, 157–173. doi: 10.3109/08990229209144768

Labandeira-Garcia, J. L., Rodriguez-Perez, A. I., Garrido-Gil, P., Rodriguez-Pallares, J., Lanciego, J. L., and Guerra, M. J. (2017). Brain renin-angiotensin system and microglial polarization: implications for aging and neurodegeneration. *Front. Aging Neurosci.* 9:129. doi: 10.3389/fnagi.2017.00129

Lehmann, M., Fournier, A., Selles-Navarro, I., Dergham, P., Sebok, A., Leclerc, N., et al. (1999). Inactivation of Rho signaling pathway promotes CNS axon regeneration. *J. Neurosci.* 19, 7537–7547. doi: 10.1523/jneurosci.19-17-07537.1999

Li, T., Peng, M., Yang, Z., Zhou, X., Deng, Y., Jiang, C., et al. (2018). 3D-printed IFN-gamma-loading calcium silicate-beta-tricalcium phosphate scaffold sequentially activates M1 and M2 polarization of macrophages to promote vascularization of tissue engineering bone. *Acta Biomater.* 71, 96–107. doi: 10.1016/j.actbio.2018.03.012

Liu, G., Detloff, M. R., Miller, K. N., Santi, L., and Houle, J. D. (2012). Exercise modulates microRNAs that affect the PTEN/mTOR pathway in rats after spinal cord injury. *Exp. Neurol.* 233, 447–456. doi: 10.1016/j.expneurol.2011.11.018

Liu, X., Tian, Y., Meng, Z., Chen, Y., Ho, I. H., Choy, K. W., et al. (2015). Up-regulation of cathepsin G in the development of chronic postsurgical pain: an experimental and clinical genetic study. *Anesthesiology* 123, 838–850. doi: 10.1097/ALN.0000000000000828

Love, M. I., Huber, W., and Anders, S. (2014). Moderated estimation of fold change and dispersion for RNA-seq data with DESeq2. *Genome Biol.* 15:550. doi: 10.1186/s13059-014-0550-8

Madsen, P. M., Sloley, S. S., Vitores, A. A., Carballosa-Gautam, M. M., Brambilla, R., and Hentall, I. D. (2017). Prolonged stimulation of a brainstem raphe region attenuates experimental autoimmune encephalomyelitis. *Neuroscience* 346, 395–402. doi: 10.1016/j.neuroscience.2017.01.037

Mao, Y., Mathews, K., and Gorrie, C. A. (2016). Temporal response of endogenous neural progenitor cells following injury to the adult rat spinal cord. *Front. Cell Neurosci.* 10:58. doi: 10.3389/fncel.2016.00058

Matis, G. K., and Birbilis, T. A. (2009). Erythropoietin in spinal cord injury. *Eur. Spine J.* 18, 314–323. doi: 10.1007/s00586-008-0829-0

McCreedy, D. A., Lee, S., Sontag, C. J., Weinstein, P., Olivas, A. D., Martinez, A. F., et al. (2018). Early targeting of L-selectin on leukocytes promotes recovery after spinal cord injury, implicating novel mechanisms of pathogenesis. *eNeuro* 5:ENEURO.0101-18.2018. doi: 10.1523/ENEURO.0101-18.2018

Mitchell, K., Yang, H. Y., Tessier, P. A., Muhly, W. T., Swaim, W. D., Szalayova, I., et al. (2008). Localization of S100A8 and S100A9 expressing neutrophils to spinal cord during peripheral tissue inflammation. *Pain* 134, 216–231. doi: 10.1016/j.pain.2007.10.024

Molliver, M. E. (1987). Serotonergic neuronal systems: what their anatomic organization tells us about function. *J. Clin. Psychopharmacol.* 7(6 Suppl.), 3S–23S.

Narita, M., Kuzumaki, N., Miyatake, M., Sato, F., Wachi, H., Seyama, Y., et al. (2006). Role of delta-opioid receptor function in neurogenesis and neuroprotection. *J. Neurochem.* 97, 1494–1505. doi: 10.1111/j.1471-4159.2006.03849.x

O'Shea, T. M., Burda, J. E., and Sofroniew, M. V. (2017). Cell biology of spinal cord injury and repair. *J. Clin. Invest.* 127, 3259–3270. doi: 10.1172/JCI90608

Park, S. W., Yi, J. H., Miranpuri, G., Satriotomo, I., Bowen, K., Resnick, D. K., et al. (2007). Thiazolidinedione class of peroxisome proliferator-activated receptor gamma agonists prevents neuronal damage, motor dysfunction, myelin loss, neuropathic pain, and inflammation after spinal cord injury in adult rats. *J. Pharmacol. Exp. Ther.* 320, 1002–1012. doi: 10.1124/jpet.106.113472

Rabani, M., Levin, J. Z., Fan, L., Adiconis, X., Raychowdhury, R., Garber, M., et al. (2011). Metabolic labeling of RNA uncovers principles of RNA production and degradation dynamics in mammalian cells. *Nat. Biotechnol.* 29, 436–442. doi: 10.1038/nbt.1861

Rabani, M., Raychowdhury, R., Jovanovic, M., Rooney, M., Stumpo, D. J., Pauli, A., et al. (2014). High-resolution sequencing and modeling identifies distinct dynamic RNA regulatory strategies. *Cell* 159, 1698–1710. doi: 10.1016/j.cell.2014.11.015

Richter, F., Meurers, B. H., Zhu, C., Medvedeva, V. P., and Chesselet, M. F. (2009). Neurons express hemoglobin alpha- and beta-chains in rat and human brains. *J. Comp. Neurol.* 515, 538–547. doi: 10.1002/cne.22062

Ridet, J. L., Rajaofetra, N., Teilhac, J. R., Geffard, M., and Privat, A. (1993). Evidence for nonsynaptic serotonergic and noradrenergic innervation of the rat dorsal horn and possible involvement of neuron-glia interactions. *Neuroscience* 52, 143–157. doi: 10.1016/0306-4522(93)90189-m

Robinson, M. D., McCarthy, D. J., and Smyth, G. K. (2010). edgeR: a bioconductor package for differential expression analysis of digital gene expression data. *Bioinformatics* 26, 139–140. doi: 10.1093/bioinformatics/btp616

Roet, K. C., Franssen, E. H., de Bree, F. M., Essing, A. H., Zijlstra, S. J., Fagoe, N. D., et al. (2013). A multilevel screening strategy defines a molecular fingerprint of proregenerative olfactory ensheathing cells and identifies SCARB2, a protein that improves regenerative sprouting of injured sensory spinal axons. *J. Neurosci.* 33, 11116–11135. doi: 10.1523/JNEUROSCI.1002-13.2013

Roth, B. L., Craigo, S. C., Choudhary, M. S., Uluer, A., Monsma, F. J. Jr., Shen, Y., et al. (1994). Binding of typical and atypical antipsychotic agents to 5-hydroxytryptamine-6 and 5-hydroxytryptamine-7 receptors. *J. Pharmacol. Exp. Ther.* 268, 1403–1410.

Rotterman, T. M., Nardelli, P., Cope, T. C., and Alvarez, F. J. (2014). Normal distribution of VGLUT1 synapses on spinal motoneuron dendrites and their reorganization after nerve injury. *J. Neurosci.* 34, 3475–3492. doi: 10.1523/JNEUROSCI.4768-13.2014

Roy, H. A., and Aziz, T. Z. (2014). Deep brain stimulation and multiple sclerosis: therapeutic applications. *Mult. Scler. Relat. Disord.* 3, 431–439. doi: 10.1016/j.msard.2014.02.003

Russo, R., Zucchelli, S., Codrich, M., Marcuzzi, F., Verde, C., and Gustincich, S. (2013). Hemoglobin is present as a canonical alpha2beta2 tetramer in dopaminergic neurons. *Biochim. Biophys. Acta* 1834, 1939–1943. doi: 10.1016/j.bbapap.2013.05.005

Schurch, N. J., Schofield, P., Gierlinski, M., Cole, C., Sherstnev, A., Singh, V., et al. (2016). How many biological replicates are needed in an RNA-seq experiment and which differential expression tool should you use? *RNA* 22, 839–851. doi: 10.1261/rna.053959.115

Schwanhausser, B., Busse, D., Li, N., Dittmar, G., Schuchhardt, J., Wolf, J., et al. (2011). Global quantification of mammalian gene expression control. *Nature* 473, 337–342. doi: 10.1038/nature10098

Semple, B. D., Trivedi, A., Gimlin, K., and Noble-Haeusslein, L. J. (2015). Neutrophil elastase mediates acute pathogenesis and is a determinant of long-term behavioral recovery after traumatic injury to the immature brain. *Neurobiol. Dis.* 74, 263–280. doi: 10.1016/j.nbd.2014.12.003

Shechter, R., Raposo, C., London, A., Sagi, I., and Schwartz, M. (2011). The glial scar-monocyte interplay: a pivotal resolution phase in spinal cord repair. *PLoS One* 6:e27969. doi: 10.1371/journal.pone.0027969

Shi, L. L., Zhang, N., Xie, X. M., Chen, Y. J., Wang, R., Shen, L., et al. (2017). Transcriptome profile of rat genes in injured spinal cord at different stages by RNA-sequencing. *BMC Genomics* 18:173. doi: 10.1186/s12864-017-3532-x

Shigeri, Y., Seal, R. P., and Shimamoto, K. (2004). Molecular pharmacology of glutamate transporters, EAATs and VGLUTs. *Brain Res. Brain Res. Rev.* 45, 250–265. doi: 10.1016/j.brainresrev.2004.04.004

Shin, S. S., Dixon, C. E., Okonkwo, D. O., and Richardson, R. M. (2014). Neurostimulation for traumatic brain injury. *J. Neurosurg.* 121, 1219–1231. doi: 10.3171/2014.7.JNS131826

Striz, I., and Trebichavsky, I. (2004). Calprotectin - a pleiotropic molecule in acute and chronic inflammation. *Physiol. Res.* 53, 245–253.

Subramanian, A., Narayan, R., Corsello, S. M., Peck, D. D., Natoli, T. E., Lu, X., et al. (2017). A next generation connectivity map: L1000 platform and the first 1,000,000 profiles. *Cell* 171, 1437–1452.e17. doi: 10.1016/j.cell.2017.10.049

Trakhtenberg, E. F., and Goldberg, J. L. (2012). The role of serotonin in axon and dendrite growth. *Int. Rev. Neurobiol.* 106, 105–126. doi: 10.1016/B978-0-12-407178-0.00005-3

van Dijken, H., Dijk, J., Voom, P., and Holstege, J. C. (1996). Localization of dopamine D2 receptor in rat spinal cord identified with immunocytochemistry and in situ hybridization. *Eur. J. Neurosci.* 8, 621–628. doi: 10.1111/j.1460-9568.1996.tb01247.x

Villapol, S. (2018). Roles of peroxisome proliferator-activated receptor gamma on brain and peripheral inflammation. *Cell. Mol. Neurobiol.* 38, 121–132. doi: 10.1007/s10571-017-0554-5

Vitores, A. A., Sloley, S. S., Martinez, C., Carballosa-Gautam, M. M., and Hentall, I. D. (2018). Some autonomic deficits of acute or chronic cervical spinal contusion reversed by interim brainstem stimulation. *J. Neurotrauma.* 35, 560–572. doi: 10.1089/neu.2017.5123

Volpicelli, F., Speranza, L., di Porzio, U., Crispino, M., and Perrone-Capano, C. (2014). The serotonin receptor 7 and the structural plasticity of brain circuits. *Front. Behav. Neurosci.* 8:318. doi: 10.3389/fnbeh.2014.00318

Wang, H. S., Yu, G., Wang, Z. T., Yi, S. P., Su, R. B., and Gong, Z. H. (2016). Changes in VGLUT1 and VGLUT2 expression in rat dorsal root ganglia and spinal cord following spared nerve injury. *Neurochem. Int.* 99, 9–15. doi: 10.1016/j.neuint.2016.05.008

Xie, L. K., and Yang, S. H. (2016). Brain globins in physiology and pathology. *Med. Gas Res.* 6, 154–163. doi: 10.4103/2045-9912.191361

Zerbino, D. R., Achuthan, P., Akanni, W., Amode, M. R., Barrell, D., Bhai, J., et al. (2018). Ensembl 2018. *Nucleic Acids Res.* 46, D754–D761. doi: 10.1093/nar/gkx1098

**Conflict of Interest:** The authors declare that the research was conducted in the absence of any commercial or financial relationships that could be construed as a potential conflict of interest.

frontiers in Cell and Developmental Biology

REVIEW
published: 04 December 2019
doi: 10.3389/fcell.2019.00313

# Neuroinflammation as a Factor of Neurodegenerative Disease: Thalidomide Analogs as Treatments

*Yoo Jin Jung*, David Tweedie, Michael T. Scerba and Nigel H. Greig**

*Drug Design & Development Section, Translational Gerontology Branch, Intramural Research Program, National Institute on Aging, National Institutes of Health, Baltimore, MD, United States*

Neuroinflammation is initiated when glial cells, mainly microglia, are activated by threats to the neural environment, such as pathogen infiltration or neuronal injury. Although neuroinflammation serves to combat these threats and reinstate brain homeostasis, chronic inflammation can result in excessive cytokine production and cell death if the cause of inflammation remains. Overexpression of tumor necrosis factor-α (TNF-α), a proinflammatory cytokine with a central role in microglial activation, has been associated with neuronal excitotoxicity, synapse loss, and propagation of the inflammatory state. Thalidomide and its derivatives, termed immunomodulatory imide drugs (IMiDs), are a class of drugs that target the 3′-untranslated region (3′-UTR) of TNF-α mRNA, inhibiting TNF-α production. Due to their multi-potent effects, several IMiDs, including thalidomide, lenalidomide, and pomalidomide, have been repurposed as drug treatments for diseases such as multiple myeloma and psoriatic arthritis. Preclinical studies of currently marketed IMiDs, as well as novel IMiDs such as 3,6′-dithiothalidomide and adamantyl thalidomide derivatives, support the development of IMiDs as therapeutics for neurological disease. IMiDs have a competitive edge compared to similar anti-inflammatory drugs due to their blood-brain barrier permeability and high bioavailability, with the potential to alleviate symptoms of neurodegenerative disease and slow disease progression. In this review, we evaluate the role of neuroinflammation in neurodegenerative diseases, focusing specifically on the role of TNF-α in neuroinflammation, as well as appraise current research on the potential of IMiDs as treatments for neurological disorders.

**Keywords: neuroinflammation, tumor necrosis factor-α (TNF-α), neurodegeneration, thalidomide, lenalidomide, pomalidomide, apremilast, immunomodulatory imide drugs (IMiDs)**

OPEN ACCESS

***Edited by:***
*Alicia Guemez-Gamboa, Northwestern University, United States*

***Reviewed by:***
*Deepak Kumar Kaushik, University of Calgary, Canada*
*Sultan Darvesh, Dalhousie University, Canada*

****Correspondence:***
*Yoo Jin Jung*
*YooJin.Jung@nih.gov;*
*yjung1@alumni.nd.edu*
*Nigel H. Greig*
*Greign@grc.nia.nih.gov*

***Specialty section:***
*This article was submitted to Molecular Medicine, a section of the journal Frontiers in Cell and Developmental Biology*

***Received:*** *13 September 2019*
***Accepted:*** *18 November 2019*
***Published:*** *04 December 2019*

***Citation:***
*Jung YJ, Tweedie D, Scerba MT and Greig NH (2019) Neuroinflammation as a Factor of Neurodegenerative Disease: Thalidomide Analogs as Treatments. Front. Cell Dev. Biol. 7:313. doi: 10.3389/fcell.2019.00313*

## INTRODUCTION

Inflammation is initiated as the body's immune cells activate inflammatory cascades to prevent tissue damage from injury or infiltrating antigens. When successful, the inflammatory response eradicates pathogens, instigates the processes of wound healing and angiogenesis, and then subsides. Contrary to this protective homeostatic action, inflammation has been observed in a multitude of diseases, and its impact on neurological disorders has been proposed as a leading cause of disease progression in recent years. Within the CNS, microglia, known as 'the brain's immune cells,' interact with astrocytes and neurons by assuming phagocytic phenotypes and releasing inflammatory cytokines. This can cause neurodegeneration, phagocytosis of synapses, diminished neural function, microglial activation, inflammatory cytokine release, and further microglial activation until threat to the neural

environment abates. Activation of astrocytes, termed astrogliosis, also occurs as part of the inflammatory process. When acute, this neuroinflammatory response is necessary and even beneficial to the neural environment in eliminating pathogens or aiding brain repair. However, when extreme threats to the neural environment such as protein aggregates (i.e., lewy bodies, neurofibrillary tangles) accumulate in the brain and protractedly sustain inflammation, continuous gliosis and apoptosis can occur as a result of unregulated inflammatory cytokine release. Continuity of this activated state results in chronic inflammation, which is implicated in virtually all neurological disorders, including AD, PD, and ALS.

The majority of neurodegenerative diseases affect the aging population, which is growing at an exponential rate due to medical advancements that have prolonged lifespan (He et al., 2015). For example, AD is projected to affect an estimated 13.8 million people over the age of 65 in the U.S. alone during the next few decades (Alzheimer's Association, 2019), while the number of PD patients is expected to rise to 1.24 million people in the next decade (Marras et al., 2018). Despite considerable effort and resources, drug developments to combat these neurodegenerative disorders have resulted in a mere handful of drugs that mitigate symptoms rather than slow disease progression (Mehta et al., 2017). There are numerous reasons why clinical trials have thus far largely failed, including the recruitment of patients too far into disease progression. However, the greatest reason for failure may be the selection of the disease target, exemplified by the predominant focus on inhibiting amyloid or tau aggregation for reversing AD and reducing α-synuclein to treat PD. There is a great need to expand target mechanisms to encompass prevention of chronic neuroinflammation, which has been elucidated as a key factor driving neurological disease progression through multiple cascades that include processes impacting the classical targets of amyloid, tau and α-synuclein.

## MECHANISM AND SIGNALING EVENTS OF NEUROINFLAMMATION IN CNS NEURODEGENERATIVE DISEASES

In response to deleterious stimuli such as injury or dysregulation in the CNS, proinflammatory cytokines and in particular, TNF-α, are released by brain endothelial cells, neurons, infiltrating immune cells, and resident glial cells (Sébire et al., 1993; Gadient and Otten, 1994; Ringheim et al., 1995; Reyes et al., 1999). This leads to activation of transcription factors by MAPKs, namely ERK, JNK, and p38, causing the upregulation of oxidative stress inducers and TNF-α, and the activation of microglia, astrocytes, and the NF-κB pathway (von Bernhardi et al., 2015). The NF-κB pathway can be canonically or non-canonically activated. Canonical activation involves direct NF-κB activation by TNF-α or proinflammatory triggers, such as ROS, and leads to increased proinflammatory gene expression. Canonical activation is necessary for a fast and acute response to both peripheral and central threats and injuries. In contrast, non-canonical activation occurs in response to various stimuli such as lymphotoxin and is slower, with specific, long-term effects. Lymphotoxin is a proinflammatory cytokine that activates the NF-κB pathway, initiating changes in gene expression crucial for not only inflammation, but also for processes such as lymph node development and gastrointestinal immune homeostasis (Bauer et al., 2012). Although most NF-κB activation is canonical, non-canonical activation has been implicated in neural stem cell pluripotency and possibly differentiation (Yang et al., 2010; Zhang and Hu, 2012; Xiao et al., 2018).

Whereas an inflammatory response is fundamental to successfully fight off disease and reestablish homeostasis in response to injury, an acute inflammation can become chronic and exacerbate disease when inflammatory pathways are mis-regulated. Neuronal NF-κB activation generally promotes cell survival and can mediate glial cell activation, proliferation, and inflammation (Tansey and Goldberg, 2010). When the PI3K/AKT/mTOR pathway is activated, the NF-κB sequestering protein IKB is released and NF-κB proinflammatory target genes are expressed, further stimulating the inflammatory pathway (Lokensgard et al., 2000; Kaltschmidt et al., 2005; Mémet, 2006). Proinflammatory cytokines can induce the expression of iNOS or COX-2 and lead to ROS production (Hirsch and Hunot, 2009). ROS cause oxidative damage that, in turn, can cause DNA damage, shortening of telomeres, increased apoptosis, and aging. A rise in ROS can lead to increased autophagy, which is consistent with the increased Aβ autophagy and dysfunctional mitochondria observed in AD patients (Cui et al., 2012). Oxidative damage results in an increase in ROS, which leads to yet further oxidative damage and feeds this self-propagating cycle (Cui et al., 2012). ROS may also trigger protein misfolding, potentially leading to protein aggregation, which is a classical hallmark of neurodegenerative diseases such as AD and PD (Narhi et al., 1999; Virmani et al., 2013). When cytokines, PAMPs, and DAMPs stimulate receptors such as TLR to canonically activate the NF-κB pathway, genes expressing proinflammatory cytokines are triggered, activating the nervous system's immune response (Jana et al., 2008; Baker et al., 2011; Clark and Vissel, 2018). This leads to inflammation of the CNS, which is maintained until the brain environment reaches conditions to trigger deactivation of the immune response.

The presence of proinflammatory cytokines can also cause a shift or polarization of resting microglia to adopt their activated states. Microglial activation is routinely divided into two main phenotypes, M1 and M2, albeit that microglia can lie

**Abbreviations:** Aβ, Beta-amyloid; Ach, acetylcholine; AD, Alzheimer's disease; ALS, amyotrophic lateral sclerosis; APP, amyloid precursor protein; ARE, AU-rich element; BBB, blood–brain barrier; CCI, controlled cortical impact; COX-2, cyclooxygenase-2; ChEI, cholinesterase inhibitor; CNS, central nervous system; CSF, cerebrospinal fluid; DA, dopaminergic; DAMP, damage-associated molecular pattern; HD, Huntington's disease; IFN, interferon; IL, interleukin; IMiD, immunomodulatory imide drug; iNOS, inducible nitric oxide synthase; LPS, lipopolysaccharide; LTD, long-term depression; LTP, long-term potentiation; MAPK, mitogen-activated protein kinases; MS, multiple sclerosis; mTBI, mild traumatic brain injury; NF-κB, nuclear factor kappa-light-chain-enhancer of activated B cells; PAMP, pathogen-associated molecular pattern; PD, Parkinson's disease; PNS, peripheral nervous system; PPARγ, peroxisome proliferator-activated receptor gamma; pTau, phosphorylated tau; ROS, reactive oxygen species; TBI, traumatic brain injury; TBM, tuberculous meningitis; TGF-β, transforming growth factor beta; TLRs, toll-like receptors; TNF-α, tumor necrosis factor alpha; UTR, untranslated region.

anywhere within the broad spectrum between these states (Town et al., 2005; Mosser and Edwards, 2008). M1 macrophages are activated by IFN-γ, IL-6, ROS, iNOS, and TNF-α in what is referred to as classical activation. Classical activation results in proinflammatory cytokine release, lymphocyte recruitment, and a strengthened immune response. M2 macrophage activation, also referred to as alternative activation, has neurotrophic and anti-inflammatory effects and leads to tissue repair. Alternative activation occurs as a result of stimulation by IL-4/10/13, and TGF-β. The M1:M2 phenotypic ratio is greater in times of injury, and higher ratios have been associated with chronic inflammation (Colton et al., 2006; Baker et al., 2011; Tang and Le, 2016).

Whereas mild levels of TNF-α and oxidative species may be neuroprotective and anti-apoptotic, excessive or prolonged neuroinflammation can be detrimental to brain health (Arends et al., 2000; Lee et al., 2010; Wenzel and Klegeris, 2018). In this regard, inflammation may be either protective or harmful depending on factors that include the activation cause, intensity, target, duration, transcriptional changes, and resulting intercellular activities (Scherbel et al., 1999; Gabbita et al., 2012). Additional elements such as increased blood-brain barrier (BBB) permeability along with CNS recruitment of peripheral lymphocytes can exacerbate chronic inflammation and cause a prolonged autoimmune-like response to injury (Hirsch and Hunot, 2009; Van Eldik et al., 2016). Continuous dysregulation of cytokine production can result in neurotoxicity and disrupt neural function (Hanisch, 2002).

As excessive neuroinflammation can impair neural function and induce neurotoxicity, regulating cytokines and restoring the brain microenvironment to pre-inflammatory conditions is crucial for reestablishing brain health following neural injury. Lowering and inhibiting proinflammatory cytokines, enhancing the activity of anti-inflammatory cytokines, effective phagocytic cell clearance, and selective inactivation of NF-κB can constrain inflammation and limit neuronal dysfunction and demise in neurodegenerative models (Baker et al., 2011; Song and Suk, 2017; Kabba et al., 2018).

## THE ROLE OF INFLAMMATION AND TNF-α IN NEURODEGENERATIVE DISEASE (FIGURE 1)

TNF-α is a proinflammatory cytokine produced by monocytes in the periphery and microglia, neurons, and astrocytes in the CNS (Clark et al., 2010). As a key player in inflammation, TNF-α acts as a major regulator of acute phase inflammation, initiating inflammatory cytokine signaling cascades (Parameswaran and Patial, 2010). Outside of the context of injury and inflammation, a lower level of constitutively expressed TNF-α is suggested to have physiological roles affecting fetal development, cardiovascular health, and various components of the immune system, including hematopoietic cell regeneration, affecting development and homeostasis of peripheral systems (Haider and Knöfler, 2009; Mizrahi and Askenasy, 2014; Urschel and Cicha, 2015). In the neural environment, constitutive physiological levels of TNF-α regulate synaptic plasticity, both in the context of injury (Liu Y. et al., 2017; Rizzo et al., 2018), development, and homeostasis (Gilmore et al., 2004; Lewitus et al., 2016; Liu Y. et al., 2017). TNF-α modulates dendritic maturation, pruning, and synaptic connectivity to respond to alterations in sensory stimuli to maintain homeostatic plasticity (Kaneko et al., 2008; Lewitus et al., 2016; Yee et al., 2017). One key mechanism regulating this is the cell-surface expression of AMPA receptors, a type of glutamate receptor regulating the influx of $Ca^{2+}$ and $Na^{+}$ in action potential initiation. AMPA receptors, whose trafficking is regulated by TNF-α, are key players in excitatory neurotransmission and long-term potentiation (LTP). Specifically, glial TNF-α has been shown to improve synaptic efficacy by increasing the cell-surface expression of AMPA receptors. Conversely, blocking TNF-α-mediated signaling has the opposite action. Notably, whereas TNF-α can adjust AMPA receptor cell surface expression, LTP and LTD are unaffected by TNF-α, but are regulated by physiological levels of the proinflammatory cytokine IL-1β. In contrast, TNF-α continuously adjusts synaptic scaling to keep the postsynaptic balance of excitatory synapses around a firing rate set point for optimal efficiency. In this manner, synaptic scaling provides a homeostatic form of synaptic plasticity, elicited to globally diminish (downscaling) or elevate (upscaling) the excitatory drive during chronic inactivity or hyperactivity, respectively, to maintain optimal neuronal performance (Liu Y. et al., 2017; Rizzo et al., 2018).

In response to injury, TNF-α functions to restore brain homeostasis during acute inflammation, acting as a defensive guard to protect against CNS injury, infection, neurodegeneration, and neurotoxicity. As with excessive production of other proinflammatory cytokines, unregulated TNF-α expression contributes to chronic inflammation, glutamatergic toxicity, synaptic loss, and excessive gliosis. Chronic TNF-α expression is observed in MS, ALS, PD, ischemia, HIV-associated dementia, and AD (Decourt et al., 2016; Hu et al., 2019).

All neurodegenerative diseases possess a neuroinflammatory component (Lee et al., 2010). A rise in brain TNF-α, for example, has been described across neurodegenerative disorders and may play a role in not only disease pathology and progression, but also the advancement of some of these diseases into others. An injury to the CNS in the event of a TBI can, for instance, lead to chronic inflammation that fuels Aβ misfolding and an increased risk for AD, as observed in post-mortem studies of TBI patients (Roberts et al., 1994; Ikonomovic et al., 2004; DeKosky et al., 2007). As a prolonged or chronic inflammatory response can induce an environment that is susceptible to dysfunction, TNF-α may be an ideal drug target as a treatment strategy to mitigate neurodegenerative diseases (Ramos-Cejudo et al., 2018).

### Traumatic Brain Injury

In response to TBI, cell death in the meninges, blood vasculature, and parenchyma is observed in the immediate impact area (DeWitt and Prough, 2003; Roth et al., 2014). Following primary injury, secondary injury is propagated by the resulting increase in ROS (Hall et al., 1994), glutamatergic toxicity (Bullock et al., 1995), and inflammation (Shi et al., 2019).

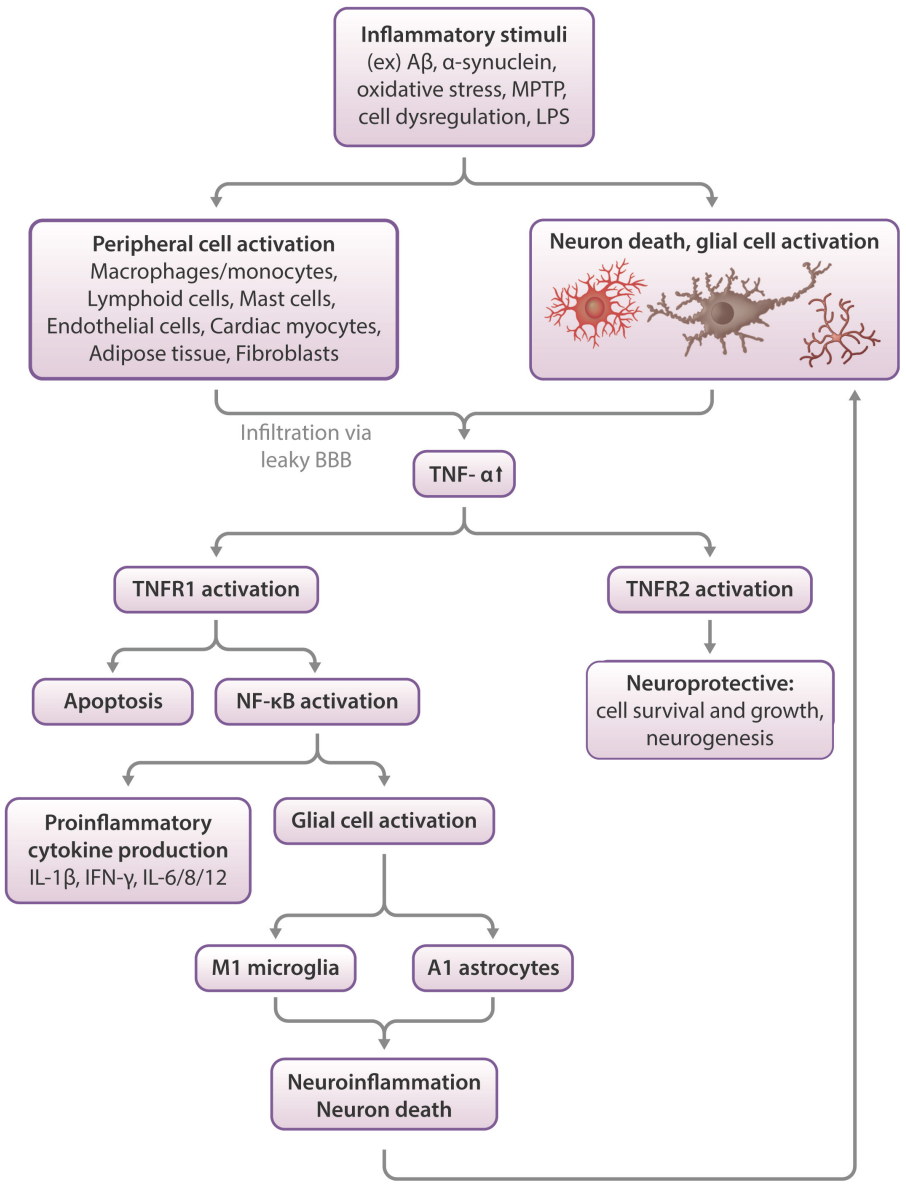


**FIGURE 1 |** Effects of TNF-α in the CNS. Inflammatory stimuli such as Aβ, α-synuclein or oxidative stress can cause neuronal death and glial cell activation, which leads to the release of inflammatory cytokines such as TNF-α. In severe cases, peripheral macrophages can infiltrate the compromised blood-brain barrier to propagate an immune response in the CNS. TNF-α activates two types of receptors- TNFR1 and TNFR2. These function differentially, with TNFR1 promoting apoptosis and activating NF-κB, which leads to proinflammatory cytokine production and glial activation, which leads to neuroinflammation and neuronal death. More glial cell activation occurs in response to this pathway, feeding the positive feedback loop of increased neuroinflammation leading to increased cell death and vice versa. On the other hand, TNFR2 activation appears largely to be neuroprotective, stimulating neurogenesis and promoting cell survival and growth (Chen and Palmer, 2013; Longhi et al., 2013).

Weakening of the BBB in response to injury can lead to CNS infiltration of peripheral monocytes and subsequent transformation into macrophages, as described in a study of controlled cortical impact (CCI) murine models (Hsieh et al., 2013).

Inflammation allows the CNS to respond to challenges such as TBI, and in ideal situations, reinstate neural function. To elucidate the role of TNF-α in TBI, TNF-α was knocked out in mice, after which cognitive performance was measured. Results showed that in the acute post-injury phase, TNF-α (−/−) mice performed better, but later, these same animals functioned worse than wildtype mice, with the TNF-α (−/−) mice exhibiting no cognitive recovery and a greater cortical injury volume (Scherbel et al., 1999; Longhi et al., 2013). The TNF-α receptor (TNFR) has two different subtypes, TNFR1 and TNFR2, which produce different effects when activated. Activation of neuronal/microglial TNFR1 contributes to neuroinflammation and degeneration, while activation of

TNFR2 largely protects against the consequences of CNS injury, such as toxic accumulation of ROS/$Ca^{2+}$, via the NF-κB pathway (Barger et al., 1995; Fontaine et al., 2002; Chen and Palmer, 2013; Longhi et al., 2013). TNFR1/2 KO mice exhibit increased vulnerability to ischemia and seizure-induced neuron damage (Bruce et al., 1996), indicating the need to selectively activate TNFR2 and deactivate TNFR1 at specific timepoints following injury to promote recovery.

## Alzheimer's Disease

Alzheimer's disease is an age-related neurodegenerative disease characterized by Aβ plaque and neurofibrillary tangle formation. Aβ aggregation is initiated in the frontal neocortex, including the orbitofrontal and transentorhinal cortices (Braak and Braak, 1991; Thal et al., 2002), and accumulates between neurons, resulting in synaptotoxicity (Dubnovitsky et al., 2013; Nieweg et al., 2015). As Aβ plaques can form more than a decade prior to cognitive symptom appearance in AD patients, numerous studies report tau pathology to correlate better with cognitive decline (Bejanin et al., 2017; Mielke et al., 2017). Similar to Aβ aggregation, tau tangles begin formation in the entorhinal cortex and manifest in areas of the brain controlling higher order cognitive processes such as memory formation and decision making (Pooler et al., 2013). Recent evidence suggests Aβ aggregates propagate tau tangle formation and the combined pathology of Aβ and tau aggregates lead to cognitive decline (Hanseeuw et al., 2019).

Multiple genetic and environmental factors contribute to AD risk. Some of these factors enhance neuroinflammation and hasten disease progression (Duyckaerts et al., 2009). APOE-ε4, a genetic risk factor for AD, intensifies brain atrophy. Rodents with the APOE-ε4 allele have higher proinflammatory cytokine release in response to LPS stimulation (Fernandez et al., 2019), indicating microglial hypersensitivity associated with the presence of APOE-ε4. Deactivation of another gene that aids in AD prevention, PIN1, leads to pTau accumulation and an increase in neuroinflammation (Clark and Vissel, 2018). Furthermore, activated glial cells have been widely found in post-mortem brains of AD patients (Heneka et al., 2015), indicating the presence of inflammation in late term AD brains.

Inflammation is also observed throughout AD progression and directly contributes to AD pathology. Early neuronal changes in AD pathology include increased production of prostaglandins, which stimulate inflammation at injury sites. Microglial activation is observed prior to cerebral neurodegeneration and astrocyte activation (Cagnin et al., 2001; Vehmas et al., 2003), and brain inflammation occurs early in preclinical AD patients (Monson et al., 2014). In middle to late stages of the disease, Aβ and pTau accumulate and astrocyte activation ensues (Vehmas et al., 2003). Neuroinflammation and cytokine production continue to increase as a result (Hoozemans et al., 2006). NF-κB has been shown to regulate the transcription of BACE1, an enzyme with an essential role in APP cleavage, due to the proximity of the BACE1 promoter to several NF-κB binding sites (Sambamurti et al., 2004). Upregulation of BACE1 leads to increased γ-secretase-mediated cleavage of APP, which leads to the generation and accumulation of Aβ (reviewed in Cole and Vassar, 2008), which in turn leads to increased inflammation, to yield a positive feedback loop of increased pathology (Combs et al., 2001; Kinney et al., 2018). There are also several signal transduction pathways linking cytokines such as TNF-α, IL-1, and IFN-γ with APP processing and subsequent Aβ plaque formation, as well as tau tangle formation (Griffin et al., 2006; Yamamoto et al., 2007; Shaftel et al., 2008). Due to the complex and broad impact that inflammatory processes can have in AD, theories such as the 'damage signals hypothesis' have arisen. This hypothesis theorizes that accumulation of cell stress from oxidative stress or neural injury results in long-term innate immune system activation/chronic neuroinflammation that instigates neurodegeneration, and ultimately leads to AD (Maccioni et al., 2009). It thereby provides a unifying mechanism to account for the diversity of risk factors that over long periods of time can bring different individuals into common pathways leading to AD.

To date, Aβ and pTau have been the most popular targets in AD drug development and research. However, emerging views of neural Aβ and pTau accumulation as disease hallmarks rather than the initial causes of AD, as well as the lack of success in AD drug development using these targets have led to a search for new drug targets. *In vivo* positron emission and single-photon emission computed tomography (PET and SPECT) scans of AD patients and AD transgenic mouse studies have pointed to neuroinflammation as a biomarker for disease progression and severity, allowing for the possibility of more accurate prediction of cognitive decline in preclinical or early AD patients (Hamelin et al., 2018; Focke et al., 2019). This suggests the need to look into factors of inflammation as potential therapeutic targets for AD. TNF-α, a key and initiating element in neuroinflammation, is known to activate various parts of the amyloid pathway, which underpins a key component of AD pathology. Hence targeting TNF-α, which appears to be both involved throughout both early and late stages of the cascades that trigger Aβ accumulation, may lead to a viable treatment for AD (Sriram and O'Callaghan, 2007; Clark et al., 2010; Clark and Vissel, 2018).

Recent research showing the positive effects of physical exercise, IL-6 supplementation, and anti-inflammatory medications to reduce TNF-α in AD models supports the premise that lowering TNF-α may mitigate or prevent AD pathology (Decourt et al., 2016). In addition, the increasing number and sophistication of ligands that permit time-dependent *in vivo* imaging of microglial and astrocyte activation, whether by PET or SPECT (for review see Edison et al., 2018), together with exosome technology to quantitatively follow inflammatory proteins enriched from brain derived exosomes available in the plasma (Pulliam et al., 2019) have the potential to serve for early diagnosis of AD, to monitor disease progression and to test the efficacy and the most effective time window for potential anti-inflammatory treatment strategies.

## Amyotrophic Lateral Sclerosis

Amyotrophic lateral sclerosis, a disease characterized by a loss of motor neurons in motor cortex, brainstem, and spinal cord, also demonstrates aspects of inflammation that may drive disease progression. Although the mechanisms through which ALS

progresses remain to be more fully elucidated, mutations in ALS-associated genes such as C9orf72 or SOD1, which may activate microglia, increase risk of ALS (Brettschneider et al., 2012; Lall and Baloh, 2017). Activated microglia, astrocytes, and T cells have been found in all sites of motor neuron injury in ALS brains. ALS patients often generate immune responses to autoantigens, implying dysregulation of the immune system (Lall and Baloh, 2017). In addition, the over-activation of NF-κB and resulting inflammation leads to motor neuron degeneration in ALS disease models (Akizuki et al., 2013; Palotas et al., 2017).

Based on familial studies of ALS, C9orf72 mutations are the most common genetic cause of ALS, accounting for approximately 40% of familial ALS and 5–10% of sporadic ALS cases (DeJesus-Hernandez et al., 2011; Renton et al., 2011). C9orf72 is a protein thought to regulate endosomal trafficking (Farg et al., 2014), and its mutation was the first genetic link to frontotemporal dementia and ALS pathology. Some ALS cases have shown cognitive decline driven by TDP-43, a major source of ALS and FTD proteinopathy, and microglial activation in frontotemporal regions of the brain (Brettschneider et al., 2012). Rodent studies have shown links between reduced expression of C9orf72 and upregulation of TREM2, a protein expressed solely in microglia within the CNS and associated with increased phagocytosis of cell debris and pathogens (Lall and Baloh, 2017; Gratuze et al., 2018), leading to increased microglial activation and inflammation in the spinal cord (Fellner et al., 2017). Factors in CSF from ALS patients activate rat astroglial and microglial cultures, upregulating inflammatory cytokines, downregulating neuroprotective factors, and causing neurodegeneration in cocultures containing motor neurons (Mishra et al., 2016, 2017).

There is also substantial evidence behind the role for TNF-α in ALS. TNF- α is reported to be upregulated in the blood and CSF of ALS patients (Babu et al., 2008; Cereda et al., 2008), and TNFR1 and TNF-α have been found to be upregulated in the spinal cord of SOD1 mutant mice (Veglianese et al., 2006; Brambilla et al., 2016). According to genomic sequencing data, TNF-α is a major differentially expressed gene affecting protein interactions in ALS patients with C9orf72 mutations, making TNF-α a promising target for ALS treatment (Kotni et al., 2016). RNA sequencing data also points to TNF-α as a major regulator of upregulated inflammatory pathways in ALS patients' spinal cords (Brohawn et al., 2016). Astrocyte and motor neuron cocultures from mice with mutations in genes linked to ALS, such as FUS or SOD1, demonstrate an increased release of TNF-α, leading to excitotoxicity-induced neurodegeneration. This degeneration can be blocked with TNF-α antibodies or synthesis inhibitors, such as thalidomide (Tortarolo et al., 2015; Kia et al., 2018).

## Parkinson's Disease

Parkinson's disease, an age-related neurodegenerative disorder, is distinguished by a progressive motor phenotype that encompasses tremors, rigidity, and bradykinesia. Neuropathologically, PD is characterized by the presence of Lewy bodies- intracellular proteinaceous inclusions that are chiefly comprised of insoluble α-synuclein aggregates. These aggregates induce deterioration of DA neurons in the *substantia nigra pars compacta* (SN) and fibers within the striatum (Polymeropoulos et al., 1997; Miller et al., 2004), as well as BBB dysfunction from increased production of inflammatory cytokines such as TNF-α and IL-6 (Dohgu et al., 2019). Neuroinflammation is implicated in PD as seen through results of post-mortem autopsies and molecular findings. Large numbers of activated microglia are universally observed in PD patient brains post-mortem, and PD brains and CSF have elevated levels of inflammatory factors such as TNF-α, IL-1β, IL-6, and IFN-γ. Furthermore, the densest population of microglia in the brain appears to lie in the midbrain with DA neurons, which are particularly sensitive to cytokines and oxidative stress. Astrocyte exposure to α-synuclein results in astrogliosis and sensitization of the inflammatory pathway, which ultimately leads to neuronal death in neuron and astrocyte cocultures (Chavarría et al., 2018; Hughes et al., 2019).

Neuroinflammation intensifies with disease progression (Mccoy et al., 2006; Hirsch and Hunot, 2009), and there is a multitude of research suggesting inflammation can trigger PD pathology. Some of this research revolves around associations of immune function-related genes [i.e., LRRK-2, HLA-DR, Nurr1 (Gardet et al., 2010; Hamza et al., 2010; Decressac et al., 2013)] and high levels of phosphorylated α-synuclein proteins with higher risk and incidence of PD. Other theories revolve around the possibility of α-synuclein aggregating in the olfactory bulb or gut lumen due to inflammatory processes and being spread to the striatum via the olfactory tract, vagus nerve, or spinal cord through a prion-like propagation (Hawkes et al., 2007; Greene, 2011). There is also evidence of greater α-synuclein aggregation in response to oxidative stress, which induces inflammation (Myöhänen et al., 2012; Scudamore and Ciossek, 2018). In this regard, PD patients may be more sensitive to chronic inflammation, as it may promote α-synuclein aggregation (Brundin et al., 2008; Hirsch and Hunot, 2009; Lema Tomé et al., 2013).

Several treatments focused to mitigate neuroinflammation have been shown to positively impact PD models. Early treatment with NSAIDs or other anti-inflammatory drugs has been shown to delay or prevent PD onset (Tansey and Goldberg, 2010). TNF-α inhibitors have been shown to block neurotoxin-induced nigral DA neuron loss by 50% (Mccoy et al., 2006) and attenuate reductions in striatal dopamine in MPTP rodent models (Boireau et al., 1997; Ferger et al., 2004), highlighting the potential use of these agents as treatments for PD.

## Multiple Sclerosis

Multiple sclerosis is a neurological demyelinating disorder in which immune cells from the periphery infiltrate boundaries of the CNS and attack the myelin sheath coating axons, leading to myelin, axonal, and neuronal degeneration (Shechter et al., 2013). The pathological basis of disease initiation remains an area of critical investigation, and it is unclear as to whether MS originates in the CNS, where degeneration of oligodendrocytes triggers activation and infiltration of peripheral immune cells, or if MS is initiated by autoimmune mechanisms within the periphery (Stys et al., 2012; Ghasemi et al., 2017).

Microglial activation takes part in the prevention and repair of MS in its early stages, but also acts to exacerbate disease

by releasing inflammatory cytokines to increase peripheral immune cell recruitment and induce demyelination (Rawji and Yong, 2013). Of the inflammatory cytokines involved in MS progression, TNF-α has been at the forefront of MS pathology, with autopsy results showing elevated TNF-α levels in areas of active lesion formation (Hofman et al., 1989). An increase in TNF-α levels in the CSF of patients with chronic progressive MS, as compared to those with stable MS, has also been observed, indicating a link between heightened TNF-α levels and MS progression (Sharief and Hentges, 1991). Reductions in proinflammatory cytokines, including TNF-α, have been shown to decrease demyelination and immune cell infiltration into the CNS in models of experimental autoimmune encephalomyelitis (EAE), one of the primary models of MS in preclinical research (Nomura et al., 2011; Haghmorad et al., 2019).

Although TNF-α blockers have shown promising results in EAE models, clinical trials of TNF-α-targeting drugs have proven to be ineffective and even detrimental in MS patients (Van Oosten et al., 1996). There have even been reports of MS onset in TNF-α-blocker therapy for treatment of other diseases (Titelbaum et al., 2005; Al Saieg and Luzar, 2006; Pfueller et al., 2008; Bradshaw et al., 2016), pointing to the sensitivity of MS to levels of systemic TNF-α. These detrimental effects could be due to the non-selective inhibition of TNF-α (Williams et al., 2014; Steeland et al., 2017; Pegoretti et al., 2018; Sanadgol et al., 2018; Valentin-Torres et al., 2018; Fischer et al., 2019), pointing to the need for research that elucidates the subtype and time-dependent roles of TNF-α and inflammation in pathways relating to myelination.

## HISTORY AND MECHANISM OF THALIDOMIDE (FIGURE 2)

Thalidomide (α-phthalimidoglutarimide) was first marketed by Chemie-Grunenthal in 1957 under the drug name "Contergan." It was advertised as a safe, multipotent drug capable of treating symptoms ranging from anxiety to hyperthyroidism (Lenz, 1988; Vargesson, 2015). It was prescribed to pregnant women in Europe as a well-tolerated morning sickness treatment. However, after 4 years and approximately 10,000 babies born with congenital limb deficiencies, thalidomide was taken off of the market due to its teratogenic effects (McBride, 1961; Vargesson, 2015).

Repurposing of the drug began more than 50 years ago as a serendipitous treatment for erythema nodosum leprosum (ENL), a skin disorder caused by leprosy (Sheskin, 1965). Since then, thalidomide has been discovered to have anti-angiogenic and anti-inflammatory properties, with the potential to treat a multitude of diseases, such as AIDS, certain cancers, and rheumatoid arthritis. Currently, it is being used to treat multiple myeloma, refractory anemia and Crohn's disease (Wilhelm et al., 2006; Kurtin and List, 2009).

In 1991, thalidomide was discovered to inhibit TNF-α synthesis (Sampaio et al., 1991) and as a consequence, novel analogs, often referred to as IMiDs, have been synthesized and evaluated in the hope of enhancing drug potency and decreasing side effects. Thalidomide and analogs have been found to possess a broad range of actions, including anti-angiogenic, anti-proliferative, and anti-inflammatory effects (Zeldis et al., 2011; **Figure 3**).

In the periphery, thalidomide has anti-angiogenic and anti-proliferative properties (Arrieta et al., 2002), making it a potential drug for treatment of diseases such as cancer (D'Amato et al., 1994). Thalidomide was FDA approved to treat refractory multiple myeloma in 2013 due to its induction of apoptosis of myeloma cells and ability to inhibit bone marrow support to myeloma cells by impairing cell adhesion (Mitsiades et al., 2002; Vallet et al., 2008). Thalidomide also has analgesic properties shown in models of neuropathic pain, attributed to its ability to attenuate TNFR expression (Andrade et al., 2012).

Within the CNS, thalidomide has been shown to reduce the generation and secretion of inflammatory cytokines such as IL-1, IL-6, IL-8, IL-12, GM-CSF and TNF-α (Vallet et al., 2008; Majumder et al., 2012). The drug downregulates NF-κB in activated B cells (Keifer et al., 2001; Yagyu et al., 2005; Paul et al., 2006; Li et al., 2009) and degrades TNF-α mRNA by altering it at its 3′-UTR (untranslated region) to destabilize the cytokine post-transcriptionally, ultimately shortening its half-life (Moreira, 1993; Zhu et al., 2003; **Figure 3**). With lower TNF-α levels, proinflammatory cytokine production is inhibited, and neuroinflammation is reduced. Thalidomide has also been shown to have anti-oxidative and anti-apoptotic effects in stroke and TBI models (Farfán et al., 2015; Tsai et al., 2018).

Although thalidomide derivatives have varying properties and potencies, they all appear to lower TNF-α. A breakthrough in understanding potential mechanisms underpinning thalidomide and related IMiDs is that some appear to bind to cereblon, a critical component of an E3 ubiquitin ligase complex with an intermediary role in immunomodulation (Mendy et al., 2012; **Figure 4**). In the context of multiple myeloma, thalidomide analogs cause cereblon to interact with associated factors to form a ligase that breaks down Ikaros (IKZF1) and Aiolos (IKZF3), two members of the Ikaros family of zinc finger transcription factors important in B-cell development (Krönke et al., 2014). The protein degradation abilities of thalidomide via its interactions with cereblon have been an emerging topic of interest in the field of drug development (Winter et al., 2015; An and Fu, 2018). However, the implications and detailed mechanism of cereblon interactions with thalidomide's anti-inflammatory response remain unclear (Millrine and Kishimoto, 2017). It is quite possible that IMiDs have both cereblon-dependent and independent mechanisms that impact TNF-α and its multiple associated proteins in neuroinflammation, as not all IMiDs with TNF-α inhibiting properties have cereblon binding potential (Min et al., 2016; Millrine and Kishimoto, 2017). It is clear, however, that cereblon and IKZF1/3 are expressed within the brain and are associated with learning and memory, with mutations in cereblon posing a risk for intellectual disabilities (Higgins et al., 2004; Chang and Keith Stewart, 2011). Interestingly, in an integrated multi-cohort transcriptional meta-analysis of neurodegenerative diseases in which genes associated with M1-polarized macrophages/microglia and reactive astrocytes were strongly enriched, IKZFI was identified across all of the neurodegenerative disorders evaluated

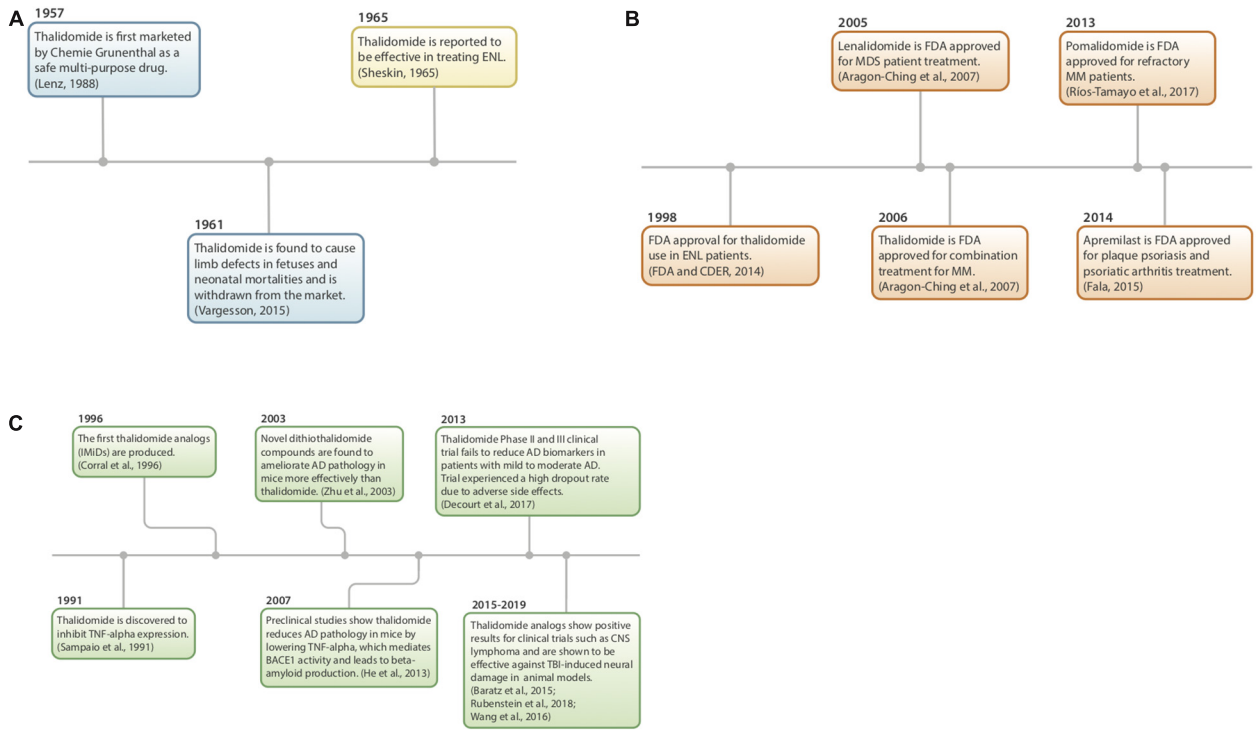


**FIGURE 2 | (A–C)** History of thalidomide and IMiDs. **(A)** Thalidomide discovery, market withdrawal, and repurposing (Sheskin, 1965; Lenz, 1988; Vargesson, 2015). **(B)** FDA approval of IMiDs (Aragon-Ching et al., 2007; FDA and CDER, 2014; Fala, 2015; Ríos-Tamayo et al., 2017). **(C)** Preclinical studies using IMiDs (Sampaio et al., 1991; Corral et al., 1996; Zhu et al., 2003; Baratz et al., 2015; Wang et al., 2016b; Decourt et al., 2017; Liu T. et al., 2017; Rubenstein et al., 2018).

(Li et al., 2014). Thalidomide has also shown anticonvulsant actions in seizure models of mice, possibly through the inhibition of iNOS (Payandemehr et al., 2014), which, likewise, has a role in inflammation (Mansouri et al., 2018).

## CLINICAL TRIALS OF THALIDOMIDE AND ITS ANALOGS IN NEURODEGENERATIVE DISEASE

Thalidomide and its analogs have and are continuing to be evaluated in clinical trials that have led to the repurposing of IMiDs for diseases such as multiple myeloma. Thus far, the majority of research and clinical trials performed on novel thalidomide derivatives have related to peripheral diseases. The few trials that have had CNS disease targets (**Table 1**) have focused on the anti-angiogenic properties of IMiDs. For instance, NCT02415153 is a phase I trial in which the tolerability and best dose of pomalidomide in treating younger patients with persistent tumors of the brain or spine are being studied. NCT01553149 is a phase II trial that compares the effects of low and high doses of lenalidomide in treating younger patients with juvenile pilocytic astrocytomas or recurrent, refractory, or progressive optic nerve pathway gliomas.

However, these drugs have yet to be evaluated systematically in subjects of neurodegenerative disease. Thus far, thalidomide has been tested in ALS patients in 2 studies. One study (NCT00231140) was terminated prematurely due to safety concerns regarding a common sinus bradycardia effect in the patients (Meyer et al., 2008). Another study (NCT00140452) observed primarily adverse effects and no improvement in treated subjects (Stommel et al., 2009). Thalidomide has also been tested in AD patients, but no differences in BACE1, a genetic measure of AD severity, were observed and 14 out of 25 patients dropped out of the trial due to adverse drug effects (Decourt et al., 2017), preventing the trial from administering the necessary dose to see an efficacious response (NCT01094340). Although thalidomide trials of neurological diseases have been unsuccessful to date, forthcoming trials should be focused on more potent new generation IMiDs in treating neurological diseases as, clearly, improvements over thalidomide need to be made in new analogs before they can be used to effectively treat neuroinflammation. Drug dose adjustment to mitigate toxicity and enhance potency via an increased understanding of drug-to-target attraction and bioavailability should be made for future clinical studies. As an example of the latter, lenalidomide distribution into brain is surprisingly low, in contrast to thalidomide (Rozewski et al., 2012). Whereas the structure and lipophilicity of lenalidomide and thalidomide are similar, a recent study suggests that the former is a substrate of the efflux transporter, *P*-glycoprotein (Hofmeister et al., 2011), which actively removes select compounds from the brain as part of the BBB (Erickson et al., 2012). Future research focused on separating the anti-inflammatory from the primary

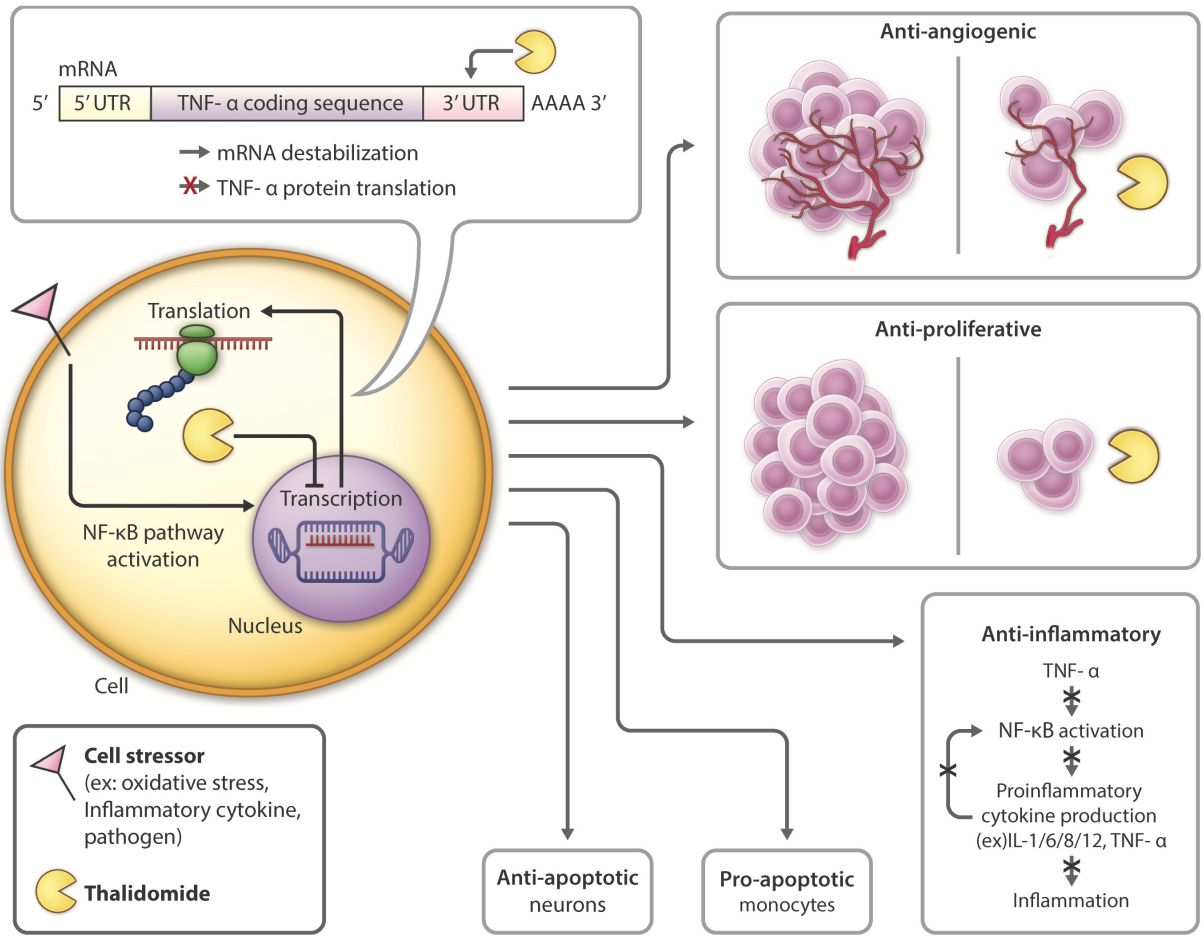


**FIGURE 3 |** Thalidomide mechanism of action and pleiotropic effects: Following introduction of cell stressors such as inflammatory cytokines or pathogens, the NF-kB transcription factor is activated, leading to increased transcription and translation of TNF-α. Thalidomide binds to the 3′-UTR of TNF-α mRNA, leading to mRNA destabilization and inhibiting TNF-α cytokine production. Thalidomide has anti-angiogenic (D'Amato et al., 1994; Zeldis et al., 2011) and anti-proliferative (Arrieta et al., 2002; Zeldis et al., 2011; Mendy et al., 2012) properties, inhibiting tumor growth, and making it a promising candidate for cancer treatment. Thalidomide also possesses anti-inflammatory (Sampaio et al., 1991; Zeldis et al., 2011; Farfán et al., 2015) properties, which have the potential to be used in inhibiting inflammation contributing to neurological disease. Thalidomide has differential roles in the periphery versus the CNS, activating anti-apoptotic (Baratz et al., 2015; Farfán et al., 2015; Tsai et al., 2018) pathways in neurons and pro-apoptotic (Mitsiades et al., 2002; Gockel et al., 2014) in monocytes.

adverse effects of IMiDs could potentially lead to repurposing of thalidomide analogs as treatments for neurodegenerative diseases such as AD, PD, ALS, or TBI.

## ADVANTAGES OF THALIDOMIDE DERIVATIVES OVER OTHER DRUGS

Thalidomide analogs such as lenalidomide and pomalidomide are the lead IMiDs being tested in clinical trials (Bartlett et al., 2004a). One advantage of thalidomide is its high bioavailability (90% after oral dosing) and distribution to the brain (brain/plasma ratio 0.89 in rodent studies (Huang et al., 2005), CSF/plasma ratio 0.42 in non-human primates (Muscal et al., 2012). As noted, a key mechanism by which thalidomide inhibits TNF-α production is post-transcriptionally via mRNA degradation (Moreira, 1993; Rowland et al., 1999). TNF-α levels, like other proteins, are regulated both transcriptionally and post-transcriptionally. However, under healthy control conditions the translation of TNF-α mRNA into protein is highly repressed via RNA-binding proteins and miRNAs that interact with AREs within the 3′-UTR of TNF-α (Mazumder et al., 2010). This translational control provides a tactical benefit for cells, such as microglia, that generate and release proteins that have a physiological role (at routine low levels) and an immune role (at high concentrations), allowing a rapid change in roles through the use of pre-existing mRNAs to sidestep the lengthy nuclear control mechanisms (i.e., transcription, splicing, and transport). Simultaneously, it affords the equally rapid reversibility through modifications (e.g., reversible phosphorylation) of the regulatory intermediates. Collectively, this permits rapid activation or cessation of synthesis of a specific protein required for inflammation. Hence, in response to LPS or a similar challenge, a 3 to 4 log (1000 to 10,000-fold) increase in TNF-α protein

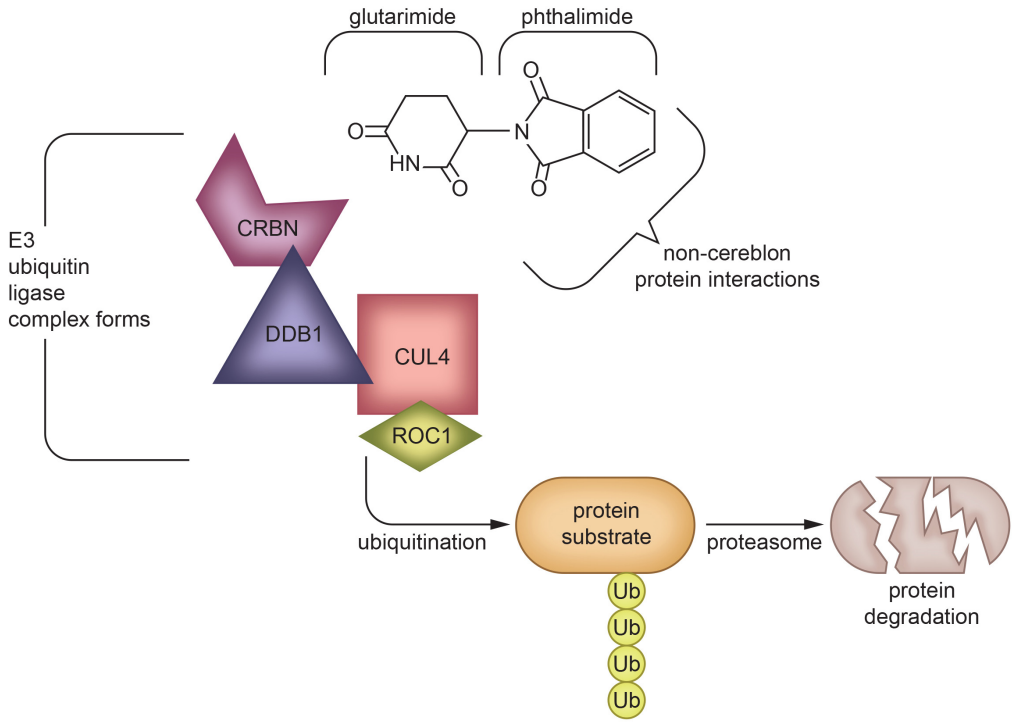


**FIGURE 4 |** Protein degradation mechanism of Thalidomide via cereblon-binding: Thalidomide is composed of glutarimide and phthalimide moieties, which interact differentially with various targets. The glutarimide ring binds cereblon to create an E3 ubiquitin ligase complex (Mendy et al., 2012), while phthalimide targets non-cereblon proteins (Noguchi et al., 2004). The formation of an E3 ubiquitin ligase complex leads to protein degradation (Winter et al., 2015; An and Fu, 2018), which underlies the ability of IMiDs to treat multiple myeloma (Krönke et al., 2014) and potentially other diseases in which protein aggregation or malfunction play a role. The exact mechanism of TNF-α inhibition by IMiDs is yet to be elucidated, but is likely to be a combination of effects of both glutarimide and phthalimide moieties (Schett et al., 2010; Millrine and Kishimoto, 2017; Chelucci et al., 2019). CRBN, Cereblon; DDB1, DNA damage-binding protein 1; CUL4, Cullin-4; ROC1, Regulator of Cullins-1.

secretion can be swiftly delivered by removal of the translational blockade and concurrent activation of transcription. A group of RNA-binding proteins are recruited to the ARE within the 3′-UTR of TNF-α that, collectively, stringently regulate translation. These include the RNA stabilizing protein HuR, heterogeneous nuclear ribonucleoprotein (hnRNP)-A1, T cell intracellular Ag (TIA)-1, TIA-1–related protein, AUF1 and tristetraprolin (TTP). For example, hnRNP-A1 binding to the ARE element represses TNF-α mRNA basal translation, and subsequent phosphorylation of hnRNP-A1 by Mnk, a kinase downstream of p38 MAPK, lowers its affinity for the ARE and, thereby, restores TNF-α translation (Mazumder et al., 2010). Likewise, TTP and AUF1 both destabilize TNF-α mRNA and thus reduce its translation into protein (Zhang et al., 2002; Lai et al., 2015). Both these RNA-binding proteins appear to be regulated by p38 MAPK, and p38 MAPK has been shown to be inhibited by thalidomide (Noman et al., 2009) – providing one of likely several mechanisms via which thalidomide and similar IMiDs regulate TNF-α levels. As TNF-α expression has been shown to be upregulated in models of neurological disease (Colton et al., 2006; Brohawn et al., 2016; Lindenau et al., 2017), supporting the need to target TNF-α to decrease neuroinflammation accompanying neurodegeneration, the high brain penetrance of thalidomide and analogs together with an ability to repress TNF-α at the level of its synthesis, provides a promising approach to mitigate neuroinflammation.

Support of TNF-α as a drug target for neurodegenerative disorders is provided by etanercept (Enbrel®) and infliximab (Remicade®). These TNF-α specific monoclonal antibodies and recombinant fusion proteins are widely used TNF-α modulators that have proven to be highly effective against a broad number of inflammatory-mediated diseases, including rheumatoid arthritis, Crohn's disease, ulcerative colitis, psoriatic arthritis, plaque psoriasis and ankylosing spondylitis (for review see Sedger and McDermott, 2014; Monaco et al., 2015), and have been applied to neurological disorders. By acting as a false target and binding to soluble and membrane-bound TNF-α, these biologicals prevent TNF-α from interacting with its receptors, thereby precluding ligand triggered TNFR signaling. The application of the anti-TNF-α antibody chimeric monoclonal antibody approach to neurodegenerative disorders was pioneered by Tobinick (2010, 2018). In a 6-month open AD trial, etanercept administration demonstrated significant improvements in dementia patients (Tobinick et al., 2006), whereas infliximab has been reported to improve cognition in an AD case study (Shi et al., 2011), providing positive preliminary data that warrants support to follow up in a double blind study. Notably for systemic disorders like rheumatoid arthritis, both etanercept and infliximab require

**TABLE 1 |** Clinical trials of Thalidomide and its FDA approved analogs relating to neurological disorders.

| Candidate | Condition | ClinicalTrials.gov Identifier(s) | Clinical phase | Results |
|---|---|---|---|---|
| Thalidomide | Amyotrophic Lateral Sclerosis (ALS) | NCT00231140, NCT00140452 | Pilot, Phase II | Study was terminated due to bradycardia occurrence as a common adverse effect (Meyer et al., 2008); no significant improvement in function or cytokine profile following 9 months of treatment (Stommel et al., 2009). |
| Thalidomide | Arachnoiditis | NCT00284505 | Phase II | Unavailable |
| Thalidomide | Epilepsy | NCT01061866 | Phase I, II | The mean number of seizures in the patients tested decreased from 27 ± 4 to 7 ± 1 seizures per month, showing a high therapeutic potential for thalidomide on refractory seizures (Palencia et al., 2010). |
| Thalidomide | CNS tumor and metastases | NCT00049361, NCT00527657, NCT00039468, NCT00179881, NCT00098865, NCT00006358, NCT00079092, NCT00014443, NCT00112502, NCT00047281, NCT00047294 | Phase I, II, III | No beneficial effect of thalidomide on CNS metastases was observed. In a trial with thalidomide treatment combined with radiation therapy (NCT00049361), nearly half of the thalidomide treatment group discontinued treatment due to side effects (Knisely et al., 2008). When given in conjunction with radiation therapy and temozolomide, efficacy was low (Atkins et al., 2008; Penas-Prado et al., 2015) (NCT00112502). Some trials are ongoing (NCT00179881) or have no reported results. |
| Thalidomide | Adrenoleuko-dystrophy | NCT00004450 | Orphan study | Immunosuppressive drugs combinations had no beneficial effect on patients (Berger and Gärtner, 2006). |
| Thalidomide | Alzheimer's Disease | NCT01094340 | Phase II, III | Thalidomide was poorly tolerated by trial participants, preventing patients from reaching the target dose of thalidomide and causing patients to drop out of the study prematurely (Decourt et al., 2017). |
| Lenalidomide | CNS tumor | NCT00036894, NCT03050450, NCT01553149, NCT00100880, NCT0370316, NCT03558750 | Phase I, II | Lenalidomide proved to be well tolerated in CNS tumor patients (Fine et al., 2007) (NCT00036894), and was found to have antitumor activity in pediatric CNS tumor patients (Warren et al., 2010) (NCT00100880). Some trials are ongoing (NCT01553149, NCT03703167) or have no reported results. |
| Lenalidomide | POEMS Syndrome | NCT00971685, NCT01816620, NCT02193698, NCT02921893 | Phase II | Lenalidomide treatment in conjunction with dexamethasone significantly relieved symptoms of POEMS, such as extravascular volume overload, organomegaly, and pulmonary hypertension (Li et al., 2018) (NCT01816620). NCT02921893 is ongoing, but preliminary data suggests ixazomib, dexamethasone, and lenalidomide combination therapy is effective at treating POEMS syndrome (Dispenzieri et al., 2019). |
| Lenalidomide | Neuropathy | NCT00665652 | Phase II | Trial was terminated due to unexpected paraproteinemia side effect (Connolly et al., 2010). |
| Pomalidomide | CNS tumor | NCT02415153, NCT03257631, NCT03798314 | Phase I, II | Pomalidomide treatment of children with CNS tumors failed to meet clinical significance (Fangusaro et al., 2019). NCT03798314 is ongoing. |

intravenous or subcutaneous injection for routine administration as they are biologicals that possess a low bioavailability and are subject to degradation if taken orally. As protein therapeutics, they have strictly limited BBB penetration, and are hence best administered by perispinal injection paired with Trendelenburg positioning- a head-down tilt placing to attempt to facilitate drug delivery into the CSF following their distribution into the cerebrospinal venous system (Tweedie et al., 2007; Tobinick, 2010, 2018; Sumbria et al., 2017; Clark and Vissel, 2018).

In contrast and as noted, thalidomide, is orally active, has a high bioavailability and readily permeates the BBB, allowing for its easy and less invasive administration. Studies comparing etanercept, infliximab, and thalidomide treatments are rare, but a preclinical one exists in a STZ-induced dementia rat model that demonstrated the efficacy of all three treatments to mitigate neurodegeneration. Thalidomide was favored as the treatment group by the studies' authors as it demonstrated a trend for lowest neuritic plaque formation (Kübra Elçioğlu et al., 2015).

A promising feature of the above approaches is their pleiotropic nature, as TNF-α is tied into multiple signaling pathways that impact key mediators on inflammation. Unfortunately, TNF-α lowering agents are not a magic bullet for all inflammatory disorders. Adverse events can be severe in some patients. For anti-TNF-α antibodies, infections can develop, up to 20% of subjects do not initially respond to therapy, and immunogenicity can occur that leads to a lack of response in up to 46% of patients over 12 months of treatment (Ben-Horin et al., 2014). In contrast, IMiDs are known to be teratogenic and therefore cannot be prescribed to women who are pregnant or who may become pregnant during therapy. Thalidomide is associated with neutropenia, leukopenia and lymphopenia at high doses as well as with peripheral neuropathy

and somnolence. Nevertheless, the repurposing or repositioning of a drug, if efficacious and tolerable, can be beneficial as it can lead to a rapid disease treatment with limited resources and/or a proof of mechanism study that, if positive, can then open up a new and focused drug development. The cost of clinical trials to demonstrate safety and efficacy of an original drug can take up to 15 years and $2.6 billion (DiMasi et al., 2016). In comparison, repurposing an existing drug provides an accelerated route in light of its known clinical safety and pharmacokinetic data – resulting in substantially lower costs [as low as $8.4 million and 3–12 years (Agrawal, 2015; Hernandez et al., 2017)] and a lower rate of attrition. As a pertinent example, thalidomide was successfully repurposed by Celgene for the treatment of a broad number of systemic inflammatory disorders and cancers. Thus far, however, the preclinical promise of thalidomide in animal models of neurodegeneration has not translated into clinical efficacy (Meyer et al., 2008; Stommel et al., 2009; Decourt et al., 2017) as sufficient CNS TNF-α and anti-inflammatory action appears unachievable in the absence of dose-limiting adverse effects. This, amongst other factors, provides a basis of evaluating both existing and new analogs that may pair higher potency with greater tolerability.

## CURRENT RESEARCH SURROUNDING THALIDOMIDE ANALOGS

Thalidomide has been modified to form several analogs, some of which have been widely tested for efficacy in treating various cancerous and immunological diseases. These new analogs have been generated to provide more TNF-α inhibition, a broader range of activities and, in some cases, a high BBB penetrance (Corral et al., 1996; Tweedie et al., 2007).

Not all thalidomide analogs have the same properties; for instance, analogs such as apremilast are PDE inhibitors, while others are not. While non-PDE inhibiting analogs stimulate T cells, IL-2, and IFN-γ production, PDE inhibiting analogs have little effect on peripheral T cells (Corral et al., 1999; Marriott et al., 1999).

### Thalidomide (THALOMID®) and First Generation of IMiDS (1996–1998; Figure 5)

Currently, thalidomide is used in the treatment of a broad number of inflammatory disorders such as Crohn's disease, arthritis, ulcerative colitis, ENL, multiple myeloma, and dermal conditions involved with Behcet's disease, as well as some types of cancers (Sheskin, 1965; Wettstein and Meagher, 1997; Haslett et al., 2005; FDA and CDER, 2014). Additionally, as already noted, due to its multipotent characteristics, thalidomide has been evaluated for repurposing across numerous neurological disorders.

In preclinical studies, both short-term and long-term thalidomide treatment of AD rodents led to decreases in overall disease pathology, neuroinflammation, and cognitive impairment (He et al., 2013; Kübra Elçioğlu et al., 2015). Thalidomide has also been shown to have anti-apoptotic effects in stroke models *in vitro* and *in vivo*. These effects are likely due to thalidomide's induction of phosphorylated Akt and activation of the pro-growth PI3K/Akt pathway, which potentially counter the apoptotic effects associated with AD and stroke. Thalidomide's protection against oxidative stress may also play a part in offsetting neuronal damage (Hyakkoku et al., 2009; Zhang et al., 2010; Farfán et al., 2015). Thalidomide has also shown promise in patients with blindness rising from TBM, with case studies of multiple patients being completely cured of blindness from a reduction of inflammation (Roberts et al., 2003; Schoeman et al., 2010). However, a pilot study of thalidomide treatment in children with TBM was terminated due to adverse effects (Schoeman, 2000).

To create the first generation of IMiDs, imide carbonyl groups of the thalidomide backbone were thionated in specific key positions. The resulting thiothalidomide analogs possess enhanced TNF-α inhibition, with di- and tri-thionated species demonstrating enhanced anti-TNF activity relative to standard thalidomide (Zhu et al., 2003). TNF-α lowering potency increased with the number of thions added to the glutarimide backbone, with trithiothalidomide decreasing TNF-α levels 30-fold more effectively than thalidomide (Greig et al., 2004; Tweedie et al., 2009).

3,6′-Dithiothalidomide (3,6′-DT), a compound developed and evaluated within our laboratory, demonstrated a decrease in microglial activation, TNF-α levels, and chronic inflammation in LPS-induced cell and rat models. In rats, treatment restored cognitive function and normalized plasticity-mediating gene expression in the hippocampus (Belarbi et al., 2012).

In mild TBI (mTBI) models, 3,6′-DT ameliorated all effects of injury in mice when treatment was administered from 1 to 12 h post-injury. These effects involved reversal of mTBI-induced decreases in cognitive function, increases in activated astrocytes, neuronal loss, increased TNF-α, and increased apoptosis in a mouse model of concussive injury (Baratz et al., 2011, 2015). These actions translated to a moderate to severe rat model of TBI in which 3,6′-DT significantly reduced contusion volume, neuronal degeneration, neuronal apoptosis and neurological deficits when administered within 5 h of injury, substantially lowering pro-inflammatory cytokines at the transcription and translation level, and suppressing neuronal markers of oxidative stress (Batsaikhan et al., 2019).

In AD mouse models of stereotaxic intracerebroventricular $A\beta_{1-42}$, 3,6′-DT ameliorated Aβ-induced neuroinflammation and microglial activation, prevented neurodegeneration, and improved memory (Russo et al., 2012). In 3xTg ($APP_{Swe}/PS1_{M146V}/tau_{P301L}$) AD mice, long term thalidomide or 3,6′-DT treatment stabilized TNF-α gene expression and protein levels to WT levels. However, thalidomide treatment failed to prevent cognitive decline in 3xTg mice's working memory, whereas 3,6′-DT treatment successfully achieved this. Furthermore, only 3,6′-DT treatment increased the ratio of resting and activated microglia, which is associated with neuroprotection (Gabbita et al., 2012). 3,6′-DT treatment of 3xTg AD mice also resulted in lower hippocampal Aβ levels, tau

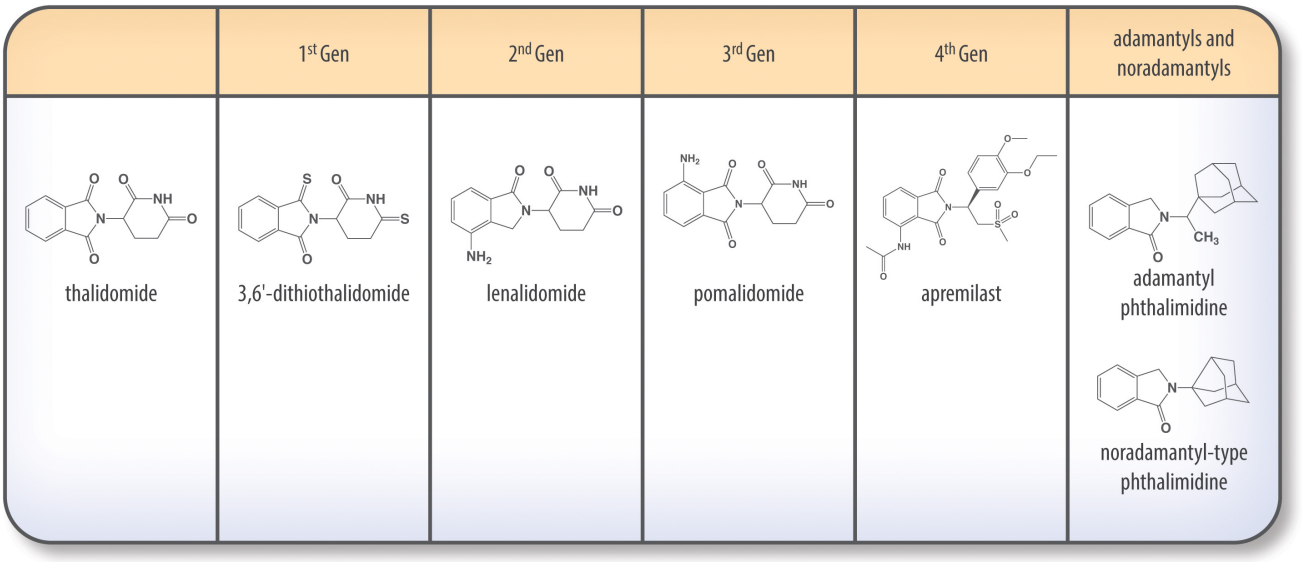


**FIGURE 5 |** Chemical structures of thalidomide and its analogs.

deposits, and improved cognition (Gabbita et al., 2012; Tweedie et al., 2012).

In focal ischemic stroke mouse models, 3,6′-DT proved to be efficacious when administered 1–3 h post-stroke to reduce neuronal loss, inhibit TNF-α, IL-1β, iNOS, and apoptosis, whereas thalidomide showed no significant effect. Notably, TNFR KO mice were not rescued with 3,6′-DT post-injury, consistent with a critical role for the suppression of TNF-α production and TNF-α signaling in the therapeutic action of 3,6′-DT, and the value of potent TNF-α suppressing agents to restrain microglial activation and inflammation (Yoon et al., 2013). In separate studies, 3,6′-DT treatment of mice post-hypoxia or blast injury attenuated injury-related increases in TNF-α and changes in synaptic transmission (Wall et al., 2015; Wang et al., 2018), thereby, cross-validating the suppression of TNF-α generation and release to mitigate inflammation-mediated neuronal damage across animal models of CNS injury. Finally, in a recent study, both 3,6′DT and thalidomide were demonstrated to mitigate the severity of L-dopa-induced dyskinesia in nigrostriatal-lesioned rat models of PD, suppressing both microgliosis and elevated TNF-α in the striatum and substantia nigra, and restoring IL-10 anti-inflammatory cytokine levels (Boi et al., 2019).

## Second Generation – Lenalidomide (REVLIMID®) (FDA Approved 2006; Figure 5)

Lenalidomide, marketed as Revlimid by Celgene, is an analog of thalidomide with an amino group on the C4 position of the benzene ring system. Cellular studies have shown lenalidomide to activate T cells, suppress angiogenesis, and modulate inflammation by decreasing cytokines (Melchert and List, 2007). The drug induces M2 polarization of macrophages by upregulating IL-10 and activating STAT3, acting against inflammation to promote survival in MS models (Weng et al., 2018). It also downregulates inflammation-related miRNA in astrocyte cultures stimulated with LPS and MRP8 (Omran et al., 2013). Lenalidomide has also been reported to be 2,000-fold more potent than thalidomide in inhibiting TNF-α secretion from monocytes (Vallet et al., 2008). Lenalidomide treatment of ALS transgenic mice resulted in enhanced motor performance, decreased motor neuron death, and increased life span (Kiaei, 2006). Lenalidomide and, in particular, combination therapy with ROS scavenger Nanoceria were shown to ameliorate cognitive decline, CNS myelin loss, ventricular volume enlargement, neuroinflammation, and white matter damage in a MS model in mice (Eitan et al., 2015). Thalidomide and lenalidomide have also been shown to reduce microgliosis and NF-κB activation, motor deficits, and excitotoxicity and DA fiber loss in the striatum of PD mouse models (Palencia et al., 2015; Valera et al., 2015), supporting the potential use of IMiDs as a treatment for PD.

Lenalidomide was approved by the FDA in May 2006 for combination treatment with dexamethasone for relapsed or refractory multiple myeloma, and has undergone clinical trials for an increasing number of solid tumor malignancies, including prostate cancer, melanoma, and glioma (Aragon-Ching et al., 2007). It was also approved to treat myelodysplastic syndromes in 2005 (List, 2006; Melchert and List, 2007). The drug is currently in a phase 2 trial for relapsed CNS myeloma treatment (Rubenstein et al., 2018), and appears to have fewer adverse effects compared to thalidomide in the treatment of multiple myeloma. Notably, thalidomide's often prominent side effects of constipation, peripheral neuropathy, and drowsiness, were not observed in lenalidomide clinical trials (Richardson et al., 2002), suggesting that these may not necessarily be drug-class dependent. Lenalidomide was determined to be safe in clinical trials for refractory melanoma, with T-cell stimulatory

effects in cancer patients (Bartlett et al., 2004b). However, its association with increased risk for stroke was recently observed in multiple myeloma patients (de Celis et al., 2018). Although lenalidomide is not associated with the level of neurotoxicity that accompanies thalidomide (where peripheral neuropathy is reported in up to 83% of myeloma patients, Dalla Torre et al., 2016), with the longer use of lenalidomide reports of neurotoxicity – albeit milder than thalidomide and sometimes subclinical – are appearing in the literature (Dalla Torre et al., 2016). In contrast, venous thromboembolism has emerged as lenalidomide's most common side effect (Bartlett et al., 2004a; Melchert and List, 2007), which may potentially be reduced when used in combination therapy with aspirin (Baz et al., 2005).

There is limited information in relation to the utility of lenalidomide in neurodegenerative disorders, but its evaluation in a PD α-synuclein mouse model demonstrated promising activity. It reduced motor behavioral deficits and mitigated DA fiber loss in the striatum. Microgliosis was decreased in both the striatum and hippocampus, and pro-inflammatory cytokines expression levels were decreased leading to a reduction in NF-κB activation (Valera et al., 2015).

## Third Generation – Pomalidomide (POMALYST®) (FDA Approved 2013; Figure 5)

Pomalidomide, marketed by Celgene under the name Actimid, is one of the most potent thalidomide derivatives to be discovered thus far. In a rat model of moderate to severe TBI, pomalidomide treatment ameliorated injury-induced neurodegeneration, apoptosis, cognitive decline, and proinflammatory cytokine upregulation when given up to 5 h post-injury. The same effects were observed in primary microglia and cortical cell cultures challenged with glutamate in a dose-dependent manner (Wang et al., 2016a). As shown in oxidative stress models, pomalidomide has neuroprotective and antioxidative effects mediated by Nrf2/SOD2/catalase pathways (Tsai et al., 2018). Finally, a recent study has demonstrated the activity of pomalidomide post-injury administration in a rat model of ischemic stroke, reducing the cerebral infarct volume and mitigating functional deficits (Tsai et al., 2019). A recent novel compound of interest, 3,6′-dithiopomalidomide (3,6′-DP), combines the advantages of thionation evident in 3,6′-DT on the thalidomide backbone into third generation pomalidomide. Preliminary studies demonstrate the potent action of 3,6′-DP in rodent TBI at one fifth of the efficacious dose of pomalidomide, and further results in other neuroinflammatory cellular and animal models are awaited with interest.

As noted earlier, recent studies have shown that IMiDs, excluding apremilast, bind to cereblon. Cereblon interacts with the DNA damage-binding protein-1 (DDB1), Cullin 4 (Cul4A or Cul4B), and regulator of Cullins 1 (RoC1) to create the functional E3 ubiquitin ligase complex. Within this ligase complex, cereblon acts as a substrate receptor to target select proteins for proteolysis via a ubiquitin-proteasome pathway (Shi and Chen, 2017). Cereblon appears to be one of many substrate receptor proteins that can be recruited into the E3 ubiquitin ligase complex to allow it to target different substrates. In this regard, IMiDs have been reported to form a molecular bridge between cereblon, within the E3 ubiquitin ligase complex, and its target protein to destine it for proteasome degradation. The glutarimide moiety of the IMiD binds cereblon, and the phthalimide moiety binds to the target proteins (Chamberlain et al., 2014; Fischer et al., 2014). Known targeted proteins, such as IKZF1/3, are predicted to possess a β-hairpin motif that comes into contact with the phthalimide structure (Petzold et al., 2016). Thalidomide, lenalidomide, or pomalidomide treatment hence leads to diminished levels of IKZF1/3, and likely other select proteins, which causes upregulation of IL-2 and activates T cells (Haslett et al., 2005; Gandhi et al., 2014). Pomalidomide appears to be the most potent with regards to T cell co-stimulation, but appears to have similar anti-angiogenic activity to that of lenalidomide (Bartlett et al., 2004b). Pomalidomide effectively modulates tumorigenesis and angiogenesis, making it a favorable drug for use in cancer treatment. It has been approved for use in multiple myeloma patients for whom lenalidomide and bortezomib have failed to prevent disease progression (Ríos-Tamayo et al., 2017).

## Fourth Generation – Apremilast (Otezla®) (FDA Approved 2014; Figure 5)

Apremilast was FDA approved to treat moderate to severe cases of plaque psoriasis and psoriatic arthritis in 2014 (Fala, 2015). Similar to other IMiDs, apremilast inhibits TNF-α protein synthesis. However, as noted previously, the drug acts via PDE4 inhibition, upregulating cAMP and thereby reducing proinflammatory cytokine production. Although apremilast is effective in treating peripheral inflammation, it has poor brain penetrance, as shown in *in vivo* pharmacokinetic studies using radioactivity to measure drug levels in the brain (Committee for Medicinal Products for Human Use [CHMP], 2014). LogP values of apremilast and other thalidomide analogs indicate apremilast has higher lipophilicity than other IMiDs, and its molecular size (460.5 Da) and general features are within the range of molecules that can cross the BBB (**Table 2**). However, *in vitro* confirmation of apremilast as a P-glycoprotein substrate, the low CNS MPO Score of apremilast in comparison to other IMiDs (**Table 2**), and its low brain/plasma concentration ratio of $\leq$0.1 in pharmacokinetic studies (Committee for Medicinal Products for Human Use [CHMP], 2014) support its lack of potential as an active drug for CNS disorders. There do not currently appear to be any literature reports of apremilast evaluation in animal models of neurodegeneration.

## Adamantyl and Noradamantyl Phthalimidines (Luo et al., 2018; Figure 5)

Adamantyl groups can be added to drugs to increase lipophilicity, drug stability, and plasma half-life (Liu J. et al., 2011). Adamantyl groups also strengthen molecule interactions with CNS targets, allowing development of more efficient drugs. For instance, iron chelator Desferrioxamine B (DFOB), which was seen to be effective in PD cell and animal models, was conjugated with adamantane and increased 66-fold in efficacy (Liddell et al., 2013). Likewise, many neuroprotective drugs such as

**TABLE 2 |** Factors of drug pharmacokinetics at physiological conditions.

| Drug name | Molecular weight (g/mol) | cLogP | cLogD (pH7.4) | Number of Hydrogen bond donors | Number of Hydrogen bond acceptors | Topological polar surface area (Å$^2$) | Strongest basic p$K_a$ calculation | CNS MPO Score |
|---|---|---|---|---|---|---|---|---|
| Thalidomide | 258.2 | 0.02 | 0.02 | 1 | 4 | 83.55 | 11.59* | 4.8 |
| 3,6′-Dithiothalidomide | 290.4 | 1.80 | 1.79 | 1 | 2 | 49.41 | 9.8* | 4.9 |
| Lenalidomide | 259.3 | −0.71 | −0.71 | 2 | 4 | 92.50 | 2.31 | 5.4 |
| Pomalidomide | 273.2 | −0.16 | −0.16 | 2 | 5 | 109.57 | 1.56 | 4.8 |
| 3,6′-Dithiopomalidomide | 305.4 | 0.97 | 0.96 | 2 | 3 | 75.43 | 2.33 | 5.5 |
| Apremilast | 460.5 | 1.31 | 1.31 | 1 | 7 | 119.08 | 12.98* | 3.1 |
| Adamantyl phthalimidine | 295.4 | 3.86 | 3.86 | 0 | 1 | 20.31 | −1.04 | 3.7 |
| Noradamantyl phthalimidine | 253.3 | 2.75 | 2.75 | 0 | 1 | 20.31 | −0.85 | 4.7 |

*Molecular weight, cLogP/D value, number of Hydrogen bond donors/acceptors, topological polar surface area, and p$K_a$ were generated using Chemicalize for several IMiDs, including a recent pomalidomide derivative of interest- 3,6′-dithiopomalidomide (3,6′-DP). IMiDs generally follow the Lipinski rule of five, which predicts the likelihood of a drug being delivered to its target in human physiological conditions based on its physical properties (Banks and Greig, 2019). A CNS MPO Score, which predicts drug BBB permeability, was calculated using parameters and functions described by Wager et al. (2010). Higher CNS MPO Score correlates with greater drug BBB permeability. *Indicates the calculated strongest acidic p$K_a$ value used to calculate CNS MPO Score when the calculated strongest basic p$K_a$ value was not provided in Chemicalize calculations. Calculated acidity values are not necessarily representative of the neutral parent compound and may instead reflect the p$K_a$ of a corresponding protonated species.*

memantine, one of the only drugs approved to treat AD, and amantadine, which is used to treat Parkinson disease, contain adamantyl groups (Rascol et al., 2011; Salomone et al., 2012). Another adamantyl derivative, *N*-adamantyl-4-methylthiazol-2-amine (KHG26693), suppresses oxidative damage caused by Aβ and LPS-induced increases in proinflammatory cytokines by suppressing NF-κB (Cho et al., 2015; Kim et al., 2017).

Our laboratory synthesized 15 novel IMiDs featuring adamantyl and noradamantyl phthalimidines. As noted earlier, the glutarimide and phthalimide moieties of thalidomide and analogs interact with cereblon and its targeted proteins, respectively, and modifications in these moieties could potentially influence the affinity and selection of targeted proteins (Yu et al., 2019). These 15 compounds have been shown to have nitrite and TNF-α lowering activity. The degree of nitration of adamantyl phthalimidines has also been shown to affect drug efficacy, with higher nitration yielding greater anti-nitrite activity (Luo et al., 2018). Interestingly, in a broader series of novel IMiDs likewise synthesized within our laboratory in which both small and substantial modifications were introduced into the glutarimide and phthalimide moieties, the resulting agents demonstrated a range of pharmacological actions (Beedie et al., 2016). Cohorts of compounds expressed anti-angiogenic properties, others anti-inflammatory properties and some exhibited both, thereby, allowing the separation of these and likely other actions. Compounds from these series are now being evaluated in animal models of neurodegeneration, and results are awaited with interest.

## CONSIDERATIONS PRIOR TO IMiD CLINICAL TRIALS FOR NEURODEGENERATIVE DISEASE

Although thalidomide analogs are promising, there are still negative findings and drug adverse effects that must be addressed prior to its use for targeting inflammation in neurodegenerative disease.

First, thalidomide appears to be a pleiotropic drug, affecting multiple biological pathways upon entering the circulatory system. Although the multipotency of thalidomide gives the drug potential to treat a multitude of symptoms via many positive pathways, it also increases the risk for drug side effects. For instance, thalidomide has been very effective in healing orogenital ulceration via its anti-inflammatory effects while simultaneously inducing or exacerbating erythema nodosum via its T-cell costimulatory effects in Behcet syndrome patients (Hamuryudan et al., 1998). Thalidomide's co-stimulation of T-cells has also been observed in a clinical trial of thalidomide in HIV patients (Corral et al., 1999; Vergara et al., 2017), pointing to the possibility of thalidomide inducing inflammation in immunocompromised individuals. The mechanisms underlying other adverse actions, such as the teratogenic effect, have yet to be fully characterized but are postulated to consist of a combination of thalidomide/metabolite interactions with the bodily environment, including thalidomide binding with cereblon, which yields angiogenesis inhibition (Vargesson, 2015). Additionally, recent research reveals that thalidomide interacts with cereblon to target and repress SALL4, a key transcription factor of the Spalt-like family with a critical role in embryonic limb development (Donovan et al., 2018; Matyskiela et al., 2018; Vargesson, 2019). Interestingly, nitric oxide has been shown to diminish thalidomide-induced teratogenicity by 80–94% (Siamwala et al., 2012), shedding light on the possibility of interventions that can be used to potentially mitigate adverse effects of IMiDs.

Another factor to consider is the multifaceted nature of neuroinflammation. Neuroinflammation sometimes promotes recovery from injury and is necessary at certain time points. For example, 50% of mTBI patients experience meningeal vascular injury from which they recover via actions of inflammatory myeloid cells. Subduing inflammation post-injury may potentially prevent positive effects of inflammation

(Russo et al., 2018). As the inflammatory response is time-dependent and multi-faceted, IMiDs, which target both TNFR1 and TNFR2 activation, must be administered at timepoints corresponding to the detrimental effects of inflammation when treating various neurological diseases.

After the most efficacious thalidomide analogs are chosen for clinical studies following preclinical research, phase I trials to evaluate their safety and efficacy in humans with neurodegenerative diseases must be designed and conducted. As thalidomide analogs prevent and mitigate inflammation, clinical trials should be focused on AD patients that demonstrate elevated biomarkers associated with increased neuroinflammation.

Testing the efficacy of thalidomide analogs in conjunction with other drugs targeting different aspects of inflammation (i.e., RXR/PPARγ agonists) or neurodegeneration to enhance neuroprotective effects could also be taken into consideration. Furthermore, as enhancing oral bioavailability of the drug has been an issue due to low drug solubility, finding ways to enhance drug solubility while maintaining its oral delivery method is also critical. Delivering lower doses of thalidomide and analogs via solid dispersions is a potential alternative that can increase bioavailability (Barea et al., 2017), especially for patients with diminished drug absorption abilities.

## SUMMARY

Repurposing drugs already on the market and modifying existing pharmacologic structures could yield therapeutic interventions capable of meeting pressing needs for neurological disease. Among drugs already on the market, thalidomide has shown great success despite its controversial history, yielding several analogs that have been approved for the treatment of diseases ranging from multiple myeloma to arthritis. Recent clinical studies of thalidomide have demonstrated that its preclinical promise in animal models of neurodegeneration does not translate to human disease consequent to dose-limiting adverse actions. Translational studies of second, third and fourth generation drugs have yet to be undertaken, and there is recent promising preclinical data on pomalidomide that, if cross-validated, may be supportive of human trials. Small, open label clinical trials of the anti-TNF-α antibody strategy involving perispinal injection suggest that targeting TNF-α is a reasonable approach to potentially treat a range of neurodegenerative disorders. Recent medicinal chemistry studies on the backbone of the classical glutarimide and phthalimide moieties that are common to thalidomide, lenalidomide, and pomalidomide indicate that we can separate pharmacological actions from one another. By altering the chemical structure of thalidomide and its analogs, we may be able to increase potency and bioavailability of IMiDs, and reduce their adverse action, possibly expanding their use to target neuroinflammation to ameliorate symptoms of neurological disease and even slow their progression.

Preclinical studies on TNF-α inhibition using thalidomide and IMiDs in models of diseases such as ALS, PD, AD, and TBI have shown promise, indicating the potential for the advancement of select members of this drug class from the bench to clinical trials and eventually, to the bedside of patients of neurological disease in need of treatment.

## AUTHOR CONTRIBUTIONS

YJ wrote the manuscript and designed the figures. NG provided input and revised the manuscript. DT and MS provided input and direction in structuring of the manuscript. MS provided the chemical structures of the IMiDs.

## FUNDING

This research was supported by the Intramural Research Program of the National Institute on Aging, National Institutes of Health, Baltimore, MD, United States.

## ACKNOWLEDGMENTS

We would like to thank Marc Raley and Lauren Brick of the Visual Media core at the National Institute on Drug Abuse for the graphic design of the figures used throughout the article.

## REFERENCES

Agrawal, P. (2015). Advantages and challenges in drug re-profiling. *J. Pharmacovigil.* 2, 2–3. doi: 10.4172/2329-6887.S2-e002

Akizuki, M., Yamashita, H., Uemura, K., Maruyama, H., Kawakami, H., Ito, H., et al. (2013). Optineurin suppression causes neuronal cell death via NF-kB pathway. *J. Neurochem.* 126, 699–704. doi: 10.1111/jnc.12326

Al Saieg, N., and Luzar, M. J. (2006). Etanercept induced multiple sclerosis and transverse myelitis. *J Rheumatol.* 33, 1202–1204.

Alzheimer's Association, (2019). *2019 ALZHEIMER'S DISEASE FACTS AND FIGURES Includes a Special Report on Alzheimer's Detection in the Primary Care Setting: Connecting Patients and Physicians*. Available at: https://alz.org/media/Documents/alzheimers-facts-and-figures-2019-r.pdf (accessed July 9, 2019).

An, S., and Fu, L. (2018). Small-molecule PROTACs: an emerging and promising approach for the development of targeted therapy drugs. *EBioMedicine* 36, 553–562. doi: 10.1016/j.ebiom.2018.09.005

Andrade, P., Visser-Vandewalle, V., Rosario, J. S. Del, Daemen, M. A., Buurman, W. A., Steinbusch, H. W., et al. (2012). The thalidomide analgesic effect is associated with differential TNF-α receptor expression in the dorsal horn of the spinal cord as studied in a rat model of neuropathic pain. *Brain Res.* 1450, 24–32. doi: 10.1016/j.brainres.2012.02.033

Aragon-Ching, J. B., Li, H., Gardner, E. R., and Figg, W. D. (2007). Thalidomide analogues as anticancer drugs. *Recent Pat. Anticancer Drug Discov.* 2, 167–174. doi: 10.2174/157489207780832478

Arends, Y. M., Duyckaerts, C., Rozemuller, J. M., Eikelenboom, P., and Hauw, J. J. (2000). Microglia, amyloid and dementia in Alzheimer disease: a correlative study. *Neurobiol. Aging* 21, 39–47. doi: 10.1016/S0197-4580(00)00094-4

Arrieta, O., Guevara, P., Tamariz, J., Rembao, D., Rivera, E., and Sotelo, J. (2002). Antiproliferative effect of thalidomide alone and combined with carmustine against C6 rat glioma. *Int. J. Exp. Pathol.* 83, 99–104. doi: 10.1046/j.1365-2613.2002.00219.x

Atkins, M. B., Sosman, J. A., Agarwala, S., Logan, T., Clark, J. I., Ernstoff, M. S., et al. (2008). Temozolomide, thalidomide, and whole brain radiation therapy for

patients with brain metastasis from metastatic melanoma: a phase II cytokine working group study. *Cancer* 113, 2139–2145. doi: 10.1002/cncr.23805

Babu, G. N., Kumar, A., Chandra, R., Puri, S. K., Kalita, J., and Misra, U. K. (2008). Elevated inflammatory markers in a group of amyotrophic lateral sclerosis patients from northern India. *Neurochem. Res.* 33, 1145–1149. doi: 10.1007/s11064-007-9564-x

Baker, R. G., Hayden, M. S., and Ghosh, S. (2011). NF-κB, inflammation, and metabolic disease. *Cell Metab.* 13, 11–22. doi: 10.1016/j.cmet.2010.12.008

Banks, W. A., and Greig, N. H. (2019). Small molecules as central nervous system therapeutics: old challenges, new directions, and a philosophic divide. *Future Med. Chem.* 11, 489–493. doi: 10.4155/fmc-2018-0436

Baratz, R., Tweedie, D., Rubovitch, V., Luo, W., Yoon, J. S., Hoffer, B. J., et al. (2011). Tumor necrosis factor-α synthesis inhibitor, 3,6′- dithiothalidomide, reverses behavioral impairments induced by minimal traumatic brain injury in mice. *J. Neurochem.* 118, 1032–1042. doi: 10.1111/j.1471-4159.2011.07377.x

Baratz, R., Tweedie, D., Wang, J. Y., Rubovitch, V., Luo, W., Hoffer, B. J., et al. (2015). Transiently lowering tumor necrosis factor-α synthesis ameliorates neuronal cell loss and cognitive impairments induced by minimal traumatic brain injury in mice. *J. Neuroinflam.* 12:45. doi: 10.1186/s12974-015-0237-4

Barea, S. A., Mattos, C. B., Cruz, A. C. C., Chaves, V. C., Pereira, R. N., Simões, C. M. O., et al. (2017). Solid dispersions enhance solubility, dissolution, and permeability of thalidomide. *Drug Dev. Ind. Pharm.* 43, 511–518. doi: 10.1080/03639045.2016.1268152

Barger, S. W., Horster, D., Furukawa, K., Goodman, Y., Krieglstein, J., and Mattson, M. P. (1995). Tumor necrosis factors alpha and beta protect neurons against amyloid beta-peptide toxicity: evidence for involvement of a kappa B-binding factor and attenuation of peroxide and Ca2+ accumulation. *Proc. Natl. Acad. Sci. U.S. A.* 92, 9328–9332. doi: 10.1073/pnas.92.20.9328

Bartlett, J. B., Dredge, K., and Dalgleish, A. G. (2004a). The evolution of thalidomide and its IMiD derivatives as anticancer agents. *Nat. Rev. Cancer* 4, 314–322. doi: 10.1038/nrc1323

Bartlett, J. B., Michael, A., Clarke, I. A., Dredge, K., Nicholson, S., Kristeleit, H., et al. (2004b). Phase I study to determine the safety, tolerability and immunostimulatory activity of thalidomide analogue CC-5013 in patients with metastatic malignant melanoma and other advanced cancers. *Br. J. Cancer* 90, 955–961. doi: 10.1038/sj.bjc.6601579

Batsaikhan, B., Wang, J. Y., Scerba, M. T., Tweedie, D., Greig, N. H., Miller, J. P., et al. (2019). Post-injury neuroprotective effects of the thalidomide analog 3,6′-dithiothalidomide on traumatic brain injury. *Int. J. Mol. Sci.* 20:E520. doi: 10.3390/ijms20030502

Bauer, J., Namineni, S., Reisinger, F., Zller, J., Yuan, D., and Heikenwlder, M. (2012). Lymphotoxin. NF-κB, and cancer: the dark side of cytokines. *Dig. Dis.* 30, 453–468. doi: 10.1159/000341690

Baz, R., Li, L., Kottke-Marchant, K., Srkalovic, G., McGowan, B., Yiannaki, E., et al. (2005). The Role of Aspirin in the prevention of thrombotic complications of thalidomide and anthracycline-based chemotherapy for multiple Myeloma. *Mayo Clin. Proc.* 80, 1568–1574. doi: 10.4065/80.12.1568

Beedie, S. L., Rore, H. M., Barnett, S., Chau, C. H., Luo, W., Greig, N. H., et al. (2016). *In vivo* screening and discovery of novel candidate thalidomide analogs in the zebrafish embryo and chicken embryo model systems. *Oncotarget* 7, 33237–33245. doi: 10.18632/oncotarget.8909

Bejanin, A., Schonhaut, D. R., La Joie, R., Kramer, J. H., Baker, S. L., Sosa, N., et al. (2017). Tau pathology and neurodegeneration contribute to cognitive impairment in Alzheimer's disease. *Brain* 140, 3286–3300. doi: 10.1093/brain/awx243

Belarbi, K., Jopson, T., Tweedie, D., Arellano, C., Luo, W., Greig, N. H., et al. (2012). TNF-a protein synthesis inhibitor restores neuronal function and reverses cognitive deficits induced by chronic neuroinflammation. *J. Neuroinflam.* 9:23. doi: 10.1186/1742-2094-9-23

Ben-Horin, S., Kopylov, U., and Chowers, Y. (2014). Optimizing anti-TNF treatments in inflammatory bowel disease. *Autoimmun. Rev.* 13, 24–30. doi: 10.1016/j.autrev.2013.06.002

Berger, J., and Gärtner, J. (2006). X-linked adrenoleukodystrophy: clinical, biochemical and pathogenetic aspects. *Biochim. Biophys. Acta Mol. Cell Res.* 1763, 1721–1732. doi: 10.1016/j.bbamcr.2006.07.010

Boi, L., Pisanu, A., Greig, N., Scerba, M. T., Tweedie, D., Mulas, G., et al. (2019). Immunomodulatory drugs alleviate L-dopa-induced dyskinesia in a rat model of Parkinson's disease. *Mov. Disord* doi: 10.1002/mds.27799 [Epub ahead of print].

Boireau, A., Bordier, F., Dubédat, P., Pény, C., and Impérato, A. (1997). Thalidomide reduces MPTP-induced decrease in striatal dopamine levels in mice. *Neurosci. Lett.* 234, 123–126. doi: 10.1016/S0304-3940(97)00685-X

Braak, H., and Braak, E. (1991). Neuropathological stageing of Alzheimer-related changes. *Acta Neuropathol.* 82, 239–259. doi: 10.1007/BF00308809

Bradshaw, M. J., Mobley, B. C., Zwerner, J. P., and Sriram, S. (2016). Autopsy-proven demyelination associated with infliximab treatment. *Neurol. Neuroimmunol. Neuroinflam.* 3:e205. doi: 10.1212/NXI.0000000000000205

Brambilla, L., Guidotti, G., Martorana, F., Iyer, A. M., Aronica, E., Valori, C. F., et al. (2016). Disruption of the astrocytic TNFR1-GDNF axis accelerates motor neuron degeneration and disease progression in amyotrophic lateral sclerosis. *Hum. Mol. Genet.* 25, 3080–3095. doi: 10.1093/hmg/ddw161

Brettschneider, J., Libon, D. J., Toledo, J. B., Xie, S. X., McCluskey, L., Elman, L., et al. (2012). Microglial activation and TDP-43 pathology correlate with executive dysfunction in amyotrophic lateral sclerosis. *Acta Neuropathol.* 123, 395–407. doi: 10.1007/s00401-011-0932-x

Brohawn, D. G., O'Brien, L. C., and Bennett, J. P. (2016). RNAseq analyses identify tumor necrosis factor-mediated inflammation as a major abnormality in ALS spinal cord. *PLoS One* 11:e0160520 doi: 10.1371/journal.pone.0160520

Bruce, A. J., Boling, W., Kindy, M. S., Peschon, J., Kraemer, P. J., Carpenter, M. K., et al. (1996). Altered neuronal and microglial responses to excitotoxic and ischemic brain injury in mice lacking TNF receptors. *Nat. Med.* 2, 788–794. doi: 10.1038/nm0796-788

Brundin, P., Li, J.-Y., Holton, J. L., Lindvall, O., and Revesz, T. (2008). Research in motion: the enigma of PD pathology spread. *Nat. Rev. Neurosci.* 9, 741–745. doi: 10.1038/nrn2477

Bullock, R., Zauner, A., Myseros, J. S., Marmarou, A., Woodward, J. J., and Young, H. F. (1995). Evidence for prolonged release of excitatory amino acids in severe human head trauma. Relationship to clinical events. *Ann. N. Y. Acad. Sci.* 765, 290–297. doi: 10.1111/j.1749-6632.1995.tb16586.x

Cagnin, A., Brooks, D. J., Kennedy, A. M., Gunn, R. N., Myers, R., Turkheimer, F. E., et al. (2001). In-vivo measurement of activated microglia in dementia. *Lancet* 358, 461–467. doi: 10.1016/S0140-6736(01)05625-2

Cereda, C., Baiocchi, C., Bongioanni, P., Cova, E., Guareschi, S., Metelli, M. R., et al. (2008). TNF and sTNFR1/2 plasma levels in ALS patients. *J. Neuroimmunol.* 194, 123–131. doi: 10.1016/j.jneuroim.2007.10.028

Chamberlain, P. P., Lopez-Girona, A., Miller, K., Carmel, G., Pagarigan, B., Chie-Leon, B., et al. (2014). Structure of the human Cereblon-DDB1-lenalidomide complex reveals basis for responsiveness to thalidomide analogs. *Nat. Struct. Mol. Biol.* 21, 803–809. doi: 10.1038/nsmb.2874

Chang, X. B., and Keith Stewart, A. (2011). What is the functional role of the thalidomide binding protein cereblon? *Int. J. Biochem. Mol. Biol.* 2, 287–294

Chavarría, C., Rodríguez-Bottero, S., Quijano, C., Cassina, P., and Souza, J. M. (2018). Impact of monomeric, oligomeric and fibrillar alpha-synuclein on astrocyte reactivity and toxicity to neurons. *Biochem. J.* 475, 3153–3169. doi: 10.1042/bcj20180297

Chelucci, R. C., de Oliveira, I. J., Barbieri, K. P., Lopes-Pires, M. E., Polesi, M. C., Chiba, D. E., et al. (2019). Antiplatelet activity and TNF-α release inhibition of phthalimide derivatives useful to treat sickle cell anemia. *Med. Chem. Res.* 28, 1264–1271. doi: 10.1007/s00044-019-02371-z

Chen, Z., and Palmer, T. D. (2013). Differential roles of TNFR1 and TNFR2 signaling in adult hippocampal neurogenesis. *Brain Behav. Immun.* 30, 45–53. doi: 10.1016/j.bbi.2013.01.083

Cho, C. H., Kim, J., Ahn, J.-Y., Hahn, H.-G., and Cho, S.-W. (2015). N-adamantyl-4-methylthiazol-2-amine suppresses lipopolysaccharide-induced brain inflammation by regulating NF-κB signaling in mice. *J. Neuroimmunol.* 289, 98–104. doi: 10.1016/j.jneuroim.2015.10.016

Clark, I. A., Alleva, L. M., and Vissel, B. (2010). The roles of TNF in brain dysfunction and disease. *Pharmacol. Ther.* 128, 519–548. doi: 10.1016/j.pharmthera.2010.08.007

Clark, I. A., and Vissel, B. (2018). Therapeutic implications of how TNF links APOE. P-tau, α-synuclein, β-amyloid, and insulin resistance in neurodegenerative diseases. *Br. J. Pharmacol.* 175, 3859–3875. doi: 10.1111/bph.14471

Cole, S. L., and Vassar, R. (2008). The role of amyloid precursor protein processing by BACE1, the β-secretase, in Alzheimer disease pathophysiology. *J. Biol. Chem.* 283, 29621–29625. doi: 10.1074/jbc.R800015200

Colton, C. A., Mott, R. T., Sharpe, H., Xu, Q., Van Nostrand, W. E., and Vitek, M. P. (2006). Expression profiles for macrophage alternative activation genes in AD and in mouse models of AD. *J. Neuroinflam.* 3:27. doi: 10.1186/1742-2094-3-27

Combs, C. K., Karlo, J. C., Kao, S.-C., and Landreth, G. E. (2001). β-Amyloid stimulation of microglia and monocytes results in TNFα-dependent expression of inducible nitric oxide synthase and neuronal apoptosis. *J. Neurosci.* 21, 1179–1188. doi: 10.1523/jneurosci.21-04-01179.2001

Committee for Medicinal Products for Human Use [CHMP], (2014). *Assessment Report : Otezla*. Available at: http://www.ema.europa.eu/docs/en_GB/document_library/EPAR_-_Public_assessment_report/human/003746/WC500182629.pdf (accessed November 15, 2019).

Connolly, S. J., Ezekowitz, M. D., Yusuf, S., Reilly, P. A., and Wallentin, L. (2010). Newly Identified Events in the RE-LY Trial. *N. Engl. J. Med.* 363, 1875–1876. doi: 10.1056/NEJMc1007378

Corral, L. G., Haslett, P. A., Muller, G. W., Chen, R., Wong, L. M., Ocampo, C. J., et al. (1999). Differential cytokine modulation and T cell activation by two distinct classes of thalidomide analogues that are potent inhibitors of TNF-alpha. *J. Immunol.* 163, 380–386.

Corral, L. G., Muller, G. W., Moreira, A. L., Chen, Y., Wu, M., Stirling, D., et al. (1996). Selection of novel analogs of thalidomide with enhanced tumor necrosis factor alpha inhibitory activity. *Mol. Med.* 2, 506–515 doi: 10.1007/bf03401909

Cui, H., Kong, Y., and Zhang, H. (2012). Oxidative stress, mitochondrial dysfunction, and aging. *J. Signal Transduct.* 2012:646354. doi: 10.1155/2012/646354

Dalla Torre, C., Zambello, R., Cacciavillani, M., Campagnolo, M., Berno, T., Salvalaggio, A., et al. (2016). Lenalidomide long-term neurotoxicity: clinical and neurophysiologic prospective study. *Neurology* 87, 1161–1166. doi: 10.1212/wnl.0000000000003093

D'Amato, R. J., Loughnan, M. S., Flynn, E., and Folkman, J. (1994). Thalidomide is an inhibitor of angiogenesis. *Proc. Natl. Acad. Sci. U.S.A.* 91, 4082–4085. doi: 10.1073/pnas.91.9.4082

de Celis, E., Alonso, de Leciñana, M., Rodríguez-Pardo, J., Fuentes, B., and Díez-Tejedor, E. (2018). Increased risk of ischemic stroke in multiple Myeloma associated with lenalidomide Treatment. *Clin. Neuropharmacol.* 41, 232–235. doi: 10.1097/WNF.0000000000000310

Decourt, B., Drumm-Gurnee, D., Wilson, J., Jacobson, S., Belden, C., Sirrel, S., et al. (2017). Poor safety and tolerability hamper reaching a potentially therapeutic dose in the use of thalidomide for alzheimer's disease: results from a double-blind, placebo-controlled trial. *Curr. Alzheimer Res.* 14, 1–1. doi: 10.2174/1567205014666170117141330

Decourt, B., Lahiri, D. K., and Sabbagh, M. N. (2016). Targeting Tumor Necrosis Factor Alpha for Alzheimer's Disease. *Curr. Alzheimer Res.* 14, 412–425. doi: 10.2174/1567205013666160930

Decressac, M., Volakakis, N., Björklund, A., and Perlmann, T. (2013). NURR1 in Parkinson disease—from pathogenesis to therapeutic potential. *Nat. Rev. Neurol.* 9:629. doi: 10.1038/nrneurol.2013.209

DeJesus-Hernandez, M., Mackenzie, I. R., Boeve, B. F., Boxer, A. L., Baker, M., Rutherford, N. J., et al. (2011). Expanded GGGGCC hexanucleotide repeat in noncoding region of C9ORF72 causes chromosome 9p-Linked FTD and ALS. *Neuron* 72, 245–256. doi: 10.1016/j.neuron.2011.09.011

DeKosky, S. T., Abrahamson, E. E., Ciallella, J. R., Paljug, W. R., Wisniewski, S. R., Clark, R. S. B., et al. (2007). Association of increased cortical soluble Aβ42 levels with diffuse plaques after severe brain injury in humans. *Arch. Neurol.* 64:541. doi: 10.1001/archneur.64.4.541

DeWitt, D. S., and Prough, D. S. (2003). Traumatic cerebral vascular injury: the effects of concussive brain injury on the cerebral vasculature. *J. Neurotrauma.* 20, 795–825. doi: 10.1089/089771503322385755

DiMasi, J. A., Grabowski, H. G., and Hansen, R. W. (2016). Innovation in the pharmaceutical industry: new estimates of R&D costs. *J. Health Econ.* 47, 20–33. doi: 10.1016/j.jhealeco.2016.01.012

Dispenzieri, A., Lacy, M., Mauermann, M., LaPlant, B., Go, R. S., Kapoor, P., et al. (2019). Ixazomib, lenalidomide, and dexamethasone for patients with POEMS syndrome. *J. Clin. Oncol.* 37:8019. doi: 10.1200/JCO.2019.37.15_suppl.8019

Dohgu, S., Takata, F., Matsumoto, J., Kimura, I., Yamauchi, A., and Kataoka, Y. (2019). Monomeric α-synuclein induces blood–brain barrier dysfunction through activated brain pericytes releasing inflammatory mediators in vitro. *Microvasc. Res.* 124, 61–66. doi: 10.1016/j.mvr.2019.03.005

Donovan, K. A., An, J., Nowak, R. P., Yuan, J. C., Fink, E. C., Berry, B. C., et al. (2018). Thalidomide promotes degradation of SALL4, a transcription factor implicated in Duane radial ray syndrome. *eLife* 7, 1–25. doi: 10.7554/eLife.38430

Dubnovitsky, A., Sandberg, A., Rahman, M. M., Benilova, I., Lendel, C., and Härd, T. (2013). Amyloid-β protofibrils: size. Morphology and synaptotoxicity of an engineered mimic. *PLoS One* 8:e0066101. doi: 10.1371/journal.pone.0066101

Duyckaerts, C., Delatour, B., and Potier, M. C. (2009). Classification and basic pathology of Alzheimer disease. *Acta Neuropathol.* 118, 5–36. doi: 10.1007/s00401-009-0532-1

Edison, P., Donat, C. K., and Sastre, M. (2018). In vivo imaging of glial activation in alzheimer's disease. *Front. Neurol.* 9:625. doi: 10.3389/fneur.2018.00625

Eitan, E., Hutchison, E. R., Greig, N. H., Tweedie, D., Celik, H., Ghosh, S., et al. (2015). Combination therapy with lenalidomide and nanoceria ameliorates CNS autoimmunity. *Exp. Neurol.* 273, 151–160. doi: 10.1016/j.expneurol.2015.08.008

Erickson, M. A., Dohi, K., and Banks, W. A. (2012). Neuroinflammation: a common pathway in CNS diseases as mediated at the blood-brain barrier. *Neuroimmunomodulation* 19, 121–130. doi: 10.1159/000330247

Fala, L. (2015). Otezla (Apremilast), an Oral PDE-4 inhibitor. Receives FDA approval for the treatment of patients with active psoriatic arthritis and plaque psoriasis. *Am. Heal. Drug Benefits* 8, 105–110.

Fangusaro, J. R., Locatelli, F., Garré, M. L., Marshall, L. V., Massimino, M., Benettaib, B., et al. (2019). A phase II clinical study of pomalidomide (CC-4047) monotherapy for children and young adults with recurrent or progressive primary brain tumors. *J. Clin. Oncol.* 37, 10035–10035. doi: 10.1200/JCO.2019.37.15_suppl.10035

Farfán, D. J., Trejo-Solís, C., Medrano, J. Á, Ortiz-Plata, A., Sotelo, J., Palencia, G., et al. (2015). Anti-apoptotic, anti-oxidant, and anti-inflammatory effects of thalidomide on cerebral ischemia/reperfusion injury in rats. *J. Neurol. Sci.* 351, 78–87. doi: 10.1016/j.jns.2015.02.043

Farg, M. A., Sundaramoorthy, V., Sultana, J. M., Yang, S., Atkinson, R. A. K., Levina, V., et al. (2014). C9ORF72, implicated in amytrophic lateral sclerosis and frontotemporal dementia, regulates endosomal trafficking. *Hum. Mol. Genet.* 23, 3579–3595. doi: 10.1093/hmg/ddu068

FDA, and CDER, (2014). *Reference ID : 3528190*. Available at: www.celgeneriskmanagement.com (accessed April 1, 2019).

Fellner, A., Barhum, Y., Angel, A., Perets, N., Steiner, I., Offen, D., et al. (2017). Toll-Like receptor-4 inhibitor TAK-242 attenuates motor dysfunction and spinal cord pathology in an amyotrophic lateral sclerosis mouse model. *Int. J. Mol. Sci.* 18:1666. doi: 10.3390/ijms18081666

Ferger, B., Leng, A., Mura, A., Hengerer, B., and Feldon, J. (2004). Genetic ablation of tumor necrosis factor-alpha (TNF-α) and pharmacological inhibition of TNF-synthesis attenuates MPTP toxicity in mouse striatum. *J. Neurochem.* 89, 822–833. doi: 10.1111/j.1471-4159.2004.02399.x

Fernandez, C. G., Hamby, M. E., McReynolds, M. L., and Ray, W. J. (2019). The role of apoE4 in disrupting the homeostatic functions of astrocytes and microglia in aging and Alzheimer's disease. *Front. Aging Neurosci.* 10:14. doi: 10.3389/fnagi.2019.00014

Fine, H. A., Kim, L., Albert, P. S., Duic, J. P., Ma, H., Zhang, W., et al. (2007). A phase I trial of lenalidomide in patients with recurrent primary central nervous system tumors. *Clin. Cancer Res.* 13, 7101–7106. doi: 10.1158/1078-0432.CCR-07-1546

Fischer, E. S., Böhm, K., Lydeard, J. R., Yang, H., Stadler, M. B., Cavadini, S., et al. (2014). Structure of the DDB1–CRBN E3 ubiquitin ligase in complex with thalidomide. *Nature* 512:49. doi: 10.1038/nature13527

Fischer, R., Padutsch, T., Bracchi-Ricard, V., Murphy, K. L., Martinez, G. F., Delguercio, N., et al. (2019). Exogenous activation of tumor necrosis factor receptor 2 promotes recovery from sensory and motor disease in a model of multiple sclerosis. *Brain Behav. Immun.* 81, 247–259. doi: 10.1016/j.bbi.2019.06.021

Focke, C., Blume, T., Zott, B., Shi, Y., Deussing, M., Peters, F., et al. (2019). Early and longitudinal microglial activation but not amyloid accumulation predicts

cognitive outcome in PS2APP mice. *J. Nucl. Med.* 60, 548–554. doi: 10.2967/jnumed.118.217703

Fontaine, V., Mohand-Said, S., Hanoteau, N., Fuchs, C., Pfizenmaier, K., and Eisel, U. (2002). Neurodegenerative and neuroprotective effects of tumor Necrosis factor (TNF) in retinal ischemia: opposite roles of TNF receptor 1 and TNF receptor 2. *J. Neurosci.* 22:RC216.

Gabbita, S. P., Srivastava, M. K., Eslami, P., Johnson, M. F., Kobritz, N. K., Tweedie, D., et al. (2012). Early intervention with a small molecule inhibitor for tumor nefosis factor-α prevents cognitive deficits in a triple transgenic mouse model of Alzheimer's disease. *J. Neuroinflam.* 9:99. doi: 10.1186/1742-2094-9-99

Gadient, R. A., and Otten, U. (1994). Identification of interleukin-6 (IL-6)-expressing neurons in the cerebellum and hippocampus of normal adult rats. *Neurosci. Lett.* 182, 243–246. doi: 10.1016/0304-3940(94)90807-9

Gandhi, A. K., Kang, J., Havens, C. G., Conklin, T., Ning, Y., Wu, L., et al. (2014). Immunomodulatory agents lenalidomide and pomalidomide co-stimulate T cells by inducing degradation of T cell repressors Ikaros and Aiolos via modulation of the E3 ubiquitin ligase complex CRL4CRBN. *Br. J. Haematol.* 164, 811–821. doi: 10.1111/bjh.12708

Gardet, A., Benita, Y., Li, C., Sands, B. E., Ballester, I., Stevens, C., et al. (2010). LRRK2 is involved in the IFN-γ response and host response to pathogens. *J. Immunol.* 185, 5577–5585. doi: 10.4049/jimmunol.1000548

Ghasemi, N., Razavi, S., and Nikzad, E. (2017). Multiple sclerosis: pathogenesis. Symptoms, diagnoses and cell-based therapy. *Cell J.* 19, 1–10. doi: 10.22074/cellj.2016.4867

Gilmore, J. H., Jarskog, L. F., Vadlamudi, S., and Lauder, J. M. (2004). Prenatal infection and risk for schizophrenia: IL-1β. IL-6, and TNFα inhibit cortical neuron dendrite development. *Neuropsychopharmacology* 29, 1221–1229. doi: 10.1038/sj.npp.1300446

Gockel, H. R., Lugering, A., Heidemann, J., Schmidt, M., Domschke, W., Kucharzik, T., et al. (2014). Thalidomide induces Apoptosis in human monocytes by using a cytochrome c-dependent pathway. *J. Immunol.* 172, 5103–5109. doi: 10.4049/jimmunol.172.8.5103

Gratuze, M., Leyns, C. E. G., and Holtzman, D. M. (2018). New insights into the role of TREM2 in Alzheimer's disease. *Mol. Neurodegener.* 13:66. doi: 10.1186/s13024-018-0298-9

Greene, J. G. (2011). Animal models of gastrointestinal problems in Parkinson's disease. *J. Parkinsons. Dis.* 1, 137–149. doi: 10.3233/JPD-2011-11033

Greig, N. H., Giordano, T., Zhu, X., Yu, Q., Perry, T. A., Holloway, H. W., et al. (2004). Thalidomide-based TNF-alpha inhibitors for neurodegenerative diseases. *Acta Neurobiol. Exp.* 64, 1–9.

Griffin, W. S. T., Liu, L., Li, Y., Mrak, R. E., and Barger, S. W. (2006). Interleukin-1 mediates Alzheimer and Lewy body pathologies. *J. Neuroinflam.* 3:5. doi: 10.1186/1742-2094-3-5

Haghmorad, D., Yazdanpanah, E., Jadid Tavaf, M., Zargarani, S., Soltanmohammadi, A., Mahmoudi, M. B., et al. (2019). Prevention and treatment of experimental autoimmune encephalomyelitis induced mice with 1, 25-dihydroxyvitamin D 3. *Neurol. Res.* 41, 943–957. doi: 10.1080/01616412.2019.1650218

Haider, S., and Knöfler, M. (2009). Human tumour necrosis factor: physiological and pathological roles in placenta and endometrium. *Placenta* 30, 111–123. doi: 10.1016/j.placenta.2008.10.012

Hall, E. D., Hall, E. D., Andrus, P. K., Andrus, P. K., Yonkers, P. A., Yonkers, P. A., et al. (1994). Generation and detection of hydroxyl radical following experimental head injury. *Ann. N. Y. Acad. Sci.* 738, 15–24. doi: 10.1111/j.1749-6632.1994.tb21785.x

Hamelin, L., Lagarde, J., Dorothée, G., Potier, M. C., Corlier, F., Kuhnast, B., et al. (2018). Distinct dynamic profiles of microglial activation are associated with progression of Alzheimer's disease. *Brain* 141, 1855–1870. doi: 10.1093/brain/awy079

Hamuryudan, V., Mat, C., Saip, S., Ozyazgan, Y., Siva, A., Yurdakul, S., et al. (1998). Thalidomide in the treatment of the mucocutaneous lesions of the Behcet syndrome. A randomized, double-blind, placebo-controlled trial. *Ann. Intern. Med.* 128, 443–450. doi: 10.7326/0003-4819-128-6-199803150-00004

Hamza, T. H., Zabetian, C. P., Tenesa, A., Laederach, A., Montimurro, J., Yearout, D., et al. (2010). Common genetic variation in the HLA region is associated with late-onset sporadic Parkinson's disease. *Nat. Genet.* 42, 781–785. doi: 10.1038/ng.642

Hanisch, U. K. (2002). Microglia as a source and target of cytokines. *Glia* 40, 140–155. doi: 10.1002/glia.10161

Hanseeuw, B. J., Betensky, R. A., Jacobs, H. I. L., Schultz, A. P., Sepulcre, J., Becker, J. A., et al. (2019). Association of amyloid and tau with cognition in preclinical alzheimer disease: a longitudinal study. *JAMA Neurol.* 02114, 915–924. doi: 10.1001/jamaneurol.2019.1424

Haslett, P. A., Roche, P., Ruth Butlin, C., Macdonald, M., Shrestha, N., Manandhar, R., et al. (2005). Effective treatment of Erythema Nodosum Leprosum with thalidomide is associated with immune stimulation. *J. Infect. Dis.* 192, 2045–2053. doi: 10.1086/498216

Hawkes, C. H., Del Tredici, K., and Braak, H. (2007). Parkinson's disease: a dual-hit hypothesis. *Neuropathol. Appl. Neurobiol.* 33, 599–614. doi: 10.1111/j.1365-2990.2007.00874.x

He, P., Cheng, X., Staufenbiel, M., Li, R., and Shen, Y. (2013). Long-term treatment of thalidomide ameliorates amyloid-like pathology through inhibition of β-Secretase in a mouse model of Alzheimer's disease. *PLoS One* 8:e0055091. doi: 10.1371/journal.pone.0055091

He, W., Goodkind, D., and Kowa, P. (2015). *An Aging World: 2015 International Population Reports*. Suitland, MA: United States Census Bureau, doi: 10.1007/978-3-642-19335-4_63

Heneka, M. T., Carson, M. J., Khoury, J. El, Landreth, G. E., Brosseron, F., Feinstein, D. L., et al. (2015). Neuroinflammation in Alzheimer's disease. *Lancet Neurol.* 14, 388–405. doi: 10.1016/S1474-4422(15)70016-5

Hernandez, J. J., Pryszlak, M., Smith, L., Yanchus, C., Kurji, N., Shahani, V. M., et al. (2017). Giving drugs a second chance: overcoming regulatory and financial hurdles in repurposing approved drugs as cancer therapeutics. *Front. Oncol.* 7:273. doi: 10.3389/fonc.2017.00273

Higgins, J. J., Pucilowska, J., Lombardi, R. Q., and Rooney, J. P. (2004). A mutation in a novel ATP-dependent Lon protease gene in a kindred with mild mental retardation. *Neurology* 63, 1927–1931. doi: 10.1212/01.WNL.0000146196.01316.A2

Hirsch, E. C., and Hunot, S. (2009). Neuroinflammation in Parkinson's disease: a target for neuroprotection? *Lancet Neurol.* 8, 382–397. doi: 10.1016/S1474-4422(09)70062-6

Hofman, F. M., Hinton, D. R., Johnson, K., and Merrill, J. E. (1989). Tumor necrosis factor identified in multiple sclerosis brain. *J. Exp. Med.* 170, 607–612. doi: 10.1084/jem.170.2.607

Hofmeister, C. C., Yang, X., Pichiorri, F., Chen, P., Rozewski, D. M., Johnson, A. J., et al. (2011). Phase I Trial of Lenalidomide and CCI-779 in patients with relapsed multiple myeloma: evidence for Lenalidomide–CCI-779 Interaction via P-Glycoprotein. *J. Clin. Oncol.* 29, 3427–3434. doi: 10.1200/JCO.2010.32.4962

Hoozemans, J. J. M., Veerhuis, R., Rozemuller, J. M., and Eikelenboom, P. (2006). Neuroinflammation and regeneration in the early stages of Alzheimer's disease pathology. *Int. J. Dev. Neurosci.* 24, 157–165. doi: 10.1016/j.ijdevneu.2005.11.001

Hsieh, C. L., Kim, C. C., Ryba, B. E., Niemi, E. C., Bando, J. K., Locksley, R. M., et al. (2013). Traumatic brain injury induces macrophage subsets in the brain. *Eur. J. Immunol.* 43, 2010–2022. doi: 10.1002/eji.201243084

Hu, W. T., Howell, J. C., Ozturk, T., Gangishetti, U., Kollhoff, A. L., Hatcher-Martin, J. M., et al. (2019). CSF cytokines in aging, multiple sclerosis, and dementia. *Front. Immunol.* 10:480. doi: 10.3389/fimmu.2019.00480

Huang, Y. J., Liao, J. F., and Tsai, T. H. (2005). Concurrent determination of thalidomide in rat blood, brain and bile using multiple microdialysis coupled to liquid chromatography. *Biomed. Chromatogr.* 19, 488–493. doi: 10.1002/bmc.466

Hughes, C. D., Choi, M. L., Ryten, M., Hopkins, L., Drews, A., Botía, J. A., et al. (2019). Picomolar concentrations of oligomeric alpha-synuclein sensitizes TLR4 to play an initiating role in Parkinson's disease pathogenesis. *Acta Neuropathol.* 137, 103–120. doi: 10.1007/s00401-018-1907-y

Hyakkoku, K., Nakajima, Y., Izuta, H., Shimazawa, M., Yamamoto, T., Shibata, N., et al. (2009). Thalidomide protects against ischemic neuronal damage induced by focal cerebral ischemia in mice. *Neuroscience* 159, 760–769. doi: 10.1016/j.neuroscience.2008.12.043

Ikonomovic, M. D., Uryu, K., Abrahamson, E. E., Ciallella, J. R., Trojanowski, J. Q., Lee, V. M. Y., et al. (2004). Alzheimer's pathology in human temporal cortex surgically excised after severe brain injury. *Exp. Neurol.* 190, 192–203. doi: 10.1016/j.expneurol.2004.06.011

Jana, M., Palencia, C. A., and Pahan, K. (2008). Fibrillar Amyloid-β peptides activate microglia via TLR2: implications for Alzheimer's disease 1. *J. Immunol.* 181, 7254–7262. doi: 10.4049/jimmunol.181.10.7254

Kabba, J. A., Xu, Y., Christian, H., Ruan, W., Chenai, K., Xiang, Y., et al. (2018). Microglia: housekeeper of the central nervous system. *Cell. Mol. Neurobiol.* 38, 53–71. doi: 10.1007/s10571-017-0504-2

Kaltschmidt, B., Widera, D., and Kaltschmidt, C. (2005). Signaling via NF-κB in the nervous system. *Biochim. Biophys. Acta Mol. Cell Res.* 1745, 287–299. doi: 10.1016/j.bbamcr.2005.05.009

Kaneko, M., Stellwagen, D., Malenka, R. C., and Stryker, M. P. (2008). Tumor necrosis factor-α mediates one component of competitive, experience-dependent plasticity in developing visual cortex. *Neuron* 58, 673–680. doi: 10.1016/j.neuron.2008.04.023

Keifer, J. A., Guttridge, D. C., Ashburner, B. P., and Baldwin, A. S. (2001). Inhibition of NF-κB Activity by Thalidomide through suppression of IκB Kinase activity. *J. Biol. Chem.* 276, 22382–22387. doi: 10.1074/jbc.M100938200

Kia, A., McAvoy, K., Krishnamurthy, K., Trotti, D., and Pasinelli, P. (2018). Astrocytes expressing ALS-linked mutant FUS induce motor neuron death through release of tumor necrosis factor-alpha. *Glia* 66, 1016–1033. doi: 10.1002/glia.23298

Kiaei, M. (2006). Thalidomide and Lenalidomide Extend Survival in a Transgenic Mouse Model of Amyotrophic Lateral Sclerosis. *J. Neurosci.* 26, 2467–2473. doi: 10.1523/jneurosci.5253-05.2006

Kim, J., Cho, C. H., Hahn, H.-G., Choi, S.-Y., and Cho, S.-W. (2017). Neuroprotective effects of N-adamantyl-4-methylthiazol-2-amine against amyloid β-induced oxidative stress in mouse hippocampus. *Brain Res. Bull.* 128, 22–28. doi: 10.1016/j.brainresbull.2016.10.010

Kinney, J. W., Bemiller, S. M., Murtishaw, A. S., Leisgang, A. M., Salazar, A. M., and Lamb, B. T. (2018). Inflammation as a central mechanism in Alzheimer's disease. *Alzheimer's Dement. Transl. Res. Clin. Interv.* 4, 575–590. doi: 10.1016/j.trci.2018.06.014

Knisely, J. P. S., Berkey, B., Chakravarti, A., Yung, A. W. K., Curran, W. J., Robins, H. I., et al. (2008). A Phase III study of conventional radiation therapy plus thalidomide versus conventional radiation therapy for multiple brain metastases (RTOG 0118). *Int. J. Radiat. Oncol. Biol. Phys.* 71, 79–86. doi: 10.1016/j.ijrobp.2007.09.016

Kotni, M. K., Zhao, M., and Wei, D. Q. (2016). Gene expression profiles and protein-protein interaction networks in amyotrophic lateral sclerosis patients with C9orf72 mutation. *Orphanet J. Rare Dis.* 11, 1–9. doi: 10.1186/s13023-016-0531-y

Krönke, J., Udeshi, N. D., Narla, A., Grauman, P., Hurst, S. N., Mcconkey, M., et al. (2014). Lenalidomide causes selective degradation of IKZF1 and IKZF3 in multiple Myeloma cells. *Science* 343, 301–305. doi: 10.1126/science.1244851

Kübra Elçioğlu, H., Kabasakal, L., Tufan, F., Elçioğlu, ÖH., Solakoglu, S., Kotil, T., et al. (2015). Effects of systemic Thalidomide and intracerebroventricular Etanercept and Infliximab administration in a Streptozotocin induced dementia model in rats. *Acta Histochem.* 117, 176–181. doi: 10.1016/j.acthis.2014.12.002

Kurtin, S. E., and List, A. F. (2009). Durable long-term responses in patients with Myelodysplastic Syndromes treated with Lenalidomide. *Clin. Lymphoma Myeloma* 9, E10–E13. doi: 10.3816/CLM.2009.n.053

Lai, W. S., Carballo, E., Strum, J. R., Kennington, E. A., Phillips, R. S., and Blackshear, P. J. (2015). Evidence that Tristetraprolin binds to AU-rich elements and promotes the deadenylation and destabilization of tumor necrosis factor Alpha mRNA. *Mol Cell Biol.* 19, 4311–4323. doi: 10.1128/mcb.19.6.4311

Lall, D., and Baloh, R. H. (2017). Microglia and C9orf72 in neuroinflammation and ALS and frontotemporal dementia. *J. Clin. Invest.* 127, 3250–3258. doi: 10.1172/JCI90607

Lee, Y. J., Han, S. B., Nam, S. Y., Oh, K. W., and Hong, J. T. (2010). Inflammation and Alzheimer's disease. *Neurobiol. Aging* 21, 383–421. doi: 10.1007/s12272-010-1006-7

Lema Tomé, C. M., Tyson, T., Rey, N. L., Grathwohl, S., Britschgi, M., and Brundin, P. (2013). Inflammation and α-synuclein's prion-like behavior in Parkinson's disease–is there a link? *Mol. Neurobiol.* 47, 561–574. doi: 10.1007/s12035-012-8267-8

Lenz, W. (1988). A short history of thalidomide embryopathy. *Teratology* 38, 203–215. doi: 10.1002/tera.1420380303

Lewitus, G. M., Konefal, S. C., Greenhalgh, A. D., Pribiag, H., Augereau, K., and Stellwagen, D. (2016). Microglial TNF-α suppresses cocaine-induced plasticity and behavioral sensitization. *Neuron* 90, 483–491. doi: 10.1016/j.neuron.2016.03.030

Li, J., Huang, X. F., Cai, Q. Q., Wang, C., Cai, H., Zhao, H., et al. (2018). A prospective phase II study of low dose lenalidomide plus dexamethasone in patients with newly diagnosed polyneuropathy, organomegaly, endocrinopathy, monoclonal gammopathy, and skin changes (POEMS) syndrome. *Am. J. Hematol.* 93, 803–809. doi: 10.1002/ajh.25100

Li, M., Sun, W., Yang, Y. P., Xu, B., Yi, W. Y., Ma, Y. X., et al. (2009). In vitro anticancer property of a novel thalidomide analogue through inhibition of NF-kB activation in HL-60 cells. *Acta Pharmacol. Sin.* 30, 134–140. doi: 10.1038/aps.2008.13

Li, M. D., Burns, T. C., Morgan, A. A., and Khatri, P. (2014). Integrated multi-cohort transcriptional meta-analysis of neurodegenerative diseases. *Acta Neuropathol. Commun.* 2:93. doi: 10.1186/s40478-014-0093-y

Liddell, J. R., Obando, D., Liu, J., Ganio, G., Volitakis, I., Mok, S. S., et al. (2013). Lipophilic adamantyl- or deferasirox-based conjugates of desferrioxamine B have enhanced neuroprotective capacity_ implications for Parkinson disease. *Free Radic. Biol. Med.* 60, 147–156. doi: 10.1016/j.freeradbiomed.2013.01.027

Lindenau, J. D., Altmann, V., Schumacher-Schuh, A. F., Rieder, C. R., and Hutz, M. H. (2017). Tumor necrosis factor alpha polymorphisms are associated with Parkinson's disease age at onset. *Neurosci. Lett.* 658, 133–136. doi: 10.1016/j.neulet.2017.08.049

List, A. (2006). *Fda Approves Revlimid and Dacogen for the Treatment of Myelodysplastic Syndromes for Hematology Physicians Advocate Outcome of Growing*. Available at: http://www.hematology.org/Thehematologist/Features/6345.aspx#.XFoEtCz-k2A.mendeley (accessed February 5, 2019).

Liu, J., Obando, D., Liao, V., Lifa, T., and Codd, R. (2011). The many faces of the adamantyl group in drug design. *Eur. J. Med. Chem.* 46, 1949–1963. doi: 10.1016/j.ejmech.2011.01.047

Liu, T., Guo, F., Zhu, X., He, X., and Xie, L. (2017). Thalidomide and its analogues: a review of the potential for immunomodulation of fibrosis diseases and opthalmopathy. *Exp. Ther. Med.* 14, 5251–5257. doi: 10.3892/etm.2017.5209

Liu, Y., Zhou, L. J., Wang, J., Li, D., Ren, W. J., Peng, J., et al. (2017). TNF-α differentially regulates synaptic plasticity in the hippocampus and spinal cord by microglia-dependent mechanisms after peripheral nerve injury. *J. Neurosci.* 37, 871–881. doi: 10.1523/JNEUROSCI.2235-16.2016

Lokensgard, J. R., Hu, S., van Fenema, E. M., Sheng, W. S., and Peterson, P. K. (2000). Effect of thalidomide on chemokine production by human microglia. *J. Infect. Dis.* 182, 983–987. doi: 10.1086/315754

Longhi, L., Perego, C., Ortolano, F., Aresi, S., Fumagalli, S., Zanier, E. R., et al. (2013). Tumor necrosis factor in traumatic brain injury: effects of genetic deletion of p55 or p75 receptor. *J. Cereb. Blood Flow Metab.* 33, 1182–1189. doi: 10.1038/jcbfm.2013.65

Luo, W., Tweedie, D., Beedie, S. L., Vargesson, N., Figg, W. D., Greig, N. H., et al. (2018). Design, synthesis and biological assessment of N- adamantyl, substituted adamantyl and noradamantyl phthalimidines for nitrite, TNF-α and angiogenesis inhibitory activities. *Bioorg. Med. Chem.* 26, 1547–1559. doi: 10.1016/j.bmc.2018.01.032

Maccioni, R. B., Rojo, L. E., Fernández, J. A., and Kuljis, R. O. (2009). The role of neuroimmunomodulation in Alzheimer's disease. *Ann. N. Y. Acad. Sci.* 1153, 240–246. doi: 10.1111/j.1749-6632.2008.03972.x

Majumder, S., Sreedhara, S. R., Banerjee, S., and Chatterjee, S. (2012). TNF α signaling beholds thalidomide saga: a review of mechanistic role of TNF-α signaling under thalidomide. *Curr. Top. Med. Chem.* 12, 1456–1467. doi: 10.2174/156802612801784443

Mansouri, M. T., Naghizadeh, B., Ghorbanzadeh, B., Alboghobeish, S., Amirgholami, N., Houshmand, G., et al. (2018). Venlafaxine prevents morphine antinociceptive tolerance: the role of neuroinflammation and the l -arginine-nitric oxide pathway. *Exp. Neurol.* 303, 134–141. doi: 10.1016/j.expneurol.2018.02.009

Marras, C., Beck, J. C., Bower, J. H., Roberts, E., Ritz, B., Ross, G. W., et al. (2018). Prevalence of Parkinson's disease across North America. *NPJ Park. Dis.* 4:21. doi: 10.1038/s41531-018-0058-0

Marriott, J. B., Muller, G., and Dalgleish, A. G. (1999). Thalidomide as an emerging immunotherapeutic agent. *Immunol. Today* 20, 538–540. doi: 10.1016/S0167-5699(99)01531-5

Matyskiela, M. E., Couto, S., Zheng, X., Lu, G., Hui, J., Stamp, K., et al. (2018). SALL4 mediates teratogenicity as a thalidomide-dependent cereblon substrate. *Nat. Chem. Biol.* 14, 981–987. doi: 10.1038/s41589-018-0129-x

Mazumder, B., Li, X., and Barik, S. (2010). Translation control: a multifaceted regulator of inflammatory response. *J. Immunol.* 184, 3311–3319. doi: 10.4049/jimmunol.0903778

McBride, W. G. (1961). Thalidomide and congenital abnormalities. *Lancet* 281:1358. doi: 10.1016/S0140-6736(63)91347-3

Mccoy, M. K., Martinez, T. N., Ruhn, K. A., Szymkowski, D. E., Smith, C. G., Botterman, B. R., et al. (2006). Blocking soluble tumor necrosis factor signaling with dominant-negative tumor necrosis factor inhibitor attenuates loss of dopaminergic neurons in models of Parkinson's disease. *J. Neurosci.* 26, 9365–9375. doi: 10.1523/JNEUROSCI.1504-06.2006

Mehta, D., Jackson, R., Paul, G., Shi, J., and Sabbagh, M. (2017). Why do trials for Alzheimer's disease drugs keep failing? A discontinued drug perspective for 2010-2015. *Expert Opin. Investig. Drugs* 26, 735–739. doi: 10.1080/13543784.2017.1323868

Melchert, M., and List, A. (2007). The thalidomide saga. *Int. J. Biochem. Cell Biol.* 39, 1489–1499. doi: 10.1016/j.biocel.2007.01.022

Mémet, S. (2006). NF-κB functions in the nervous system: from development to disease. *Biochem. Pharmacol.* 72, 1180–1195. doi: 10.1016/j.bcp.2006.09.003

Mendy, D., Ito, T., Miller, K., Gandhi, A. K., Kang, J., Karasawa, S., et al. (2012). Cereblon is a direct protein target for immunomodulatory and antiproliferative activities of lenalidomide and pomalidomide A Lopez-Girona. *Leukemia* 26, 2326–2335. doi: 10.1038/leu.2012.119

Meyer, T., Maier, A., Borisow, N., Dullinger, J. S., Splettstößer, G., Ohlraun, S., et al. (2008). Thalidomide causes sinus bradycardia in ALS. *J. Neurol.* 255, 587–591. doi: 10.1007/s00415-008-0756-3

Mielke, M. M., Hagen, C. E., Wennberg, A. M. V., Airey, D. C., Savica, R., Knopman, D. S., et al. (2017). Association of plasma total tau level with cognitive decline and risk of mild cognitive impairment or dementia in the Mayo Clinic study on aging. *JAMA Neurol.* 74, 1073–1080. doi: 10.1001/jamaneurol.2017.1359

Miller, D. W., Hague, S. M., Clarimon, J., Baptista, M., Gwinn-Hardy, K., Cookson, M. R., et al. (2004). α-synuclein in blood and brain from familial Parkinson disease with SNCA locus triplication. *Neurology* 62, 1835–1838. doi: 10.1212/01.WNL.0000127517.33208.F4

Millrine, D., and Kishimoto, T. (2017). A brighter side to thalidomide: its potential use in immunological disorders. *Trends Mol. Med.* 23, 348–361. doi: 10.1016/j.molmed.2017.02.006

Min, Y., Wi, S. M., Kang, J. A., Yang, T., Park, C. S., Park, S. G., et al. (2016). Cereblon negatively regulates TLR4 signaling through the attenuation of ubiquitination of TRAF6. *Cell Death Dis.* 7:e2313. doi: 10.1038/cddis.2016.226

Mishra, P. S., Dhull, D. K., Nalini, A., Vijayalakshmi, K., Sathyaprabha, T. N., Alladi, P. A., et al. (2016). Astroglia acquires a toxic neuroinflammatory role in response to the cerebrospinal fluid from amyotrophic lateral sclerosis patients. *J. Neuroinflam.* 13:212. doi: 10.1186/s12974-016-0698-0

Mishra, P. S., Vijayalakshmi, K., Nalini, A., Sathyaprabha, T. N., Kramer, B. W., Alladi, P. A., et al. (2017). Etiogenic factors present in the cerebrospinal fluid from amyotrophic lateral sclerosis patients induce predominantly pro-inflammatory responses in microglia. *J. Neuroinflam.* 14:251. doi: 10.1186/s12974-017-1028-x

Mitsiades, N., Mitsiades, S., Poulaki, V., Chauhan, D., Richardson, P. G., Hideshima, T., et al. (2002). Apoptotic signaling induced by immunomodulatory thalidomide analogs in human multiple myeloma cells: therapeutic implications. *Blood* 99, 4525–4530. doi: 10.1182/blood.V99.12.4525

Mizrahi, K., and Askenasy, N. (2014). Physiological functions of TNF family receptor/ligand interactions in hematopoiesis and transplantation. *Blood* 124, 176–183. doi: 10.1182/blood-2014-03-559641

Monaco, C., Nanchahal, J., Taylor, P., and Feldmann, M. (2015). Anti-TNF therapy: past, present and future. *Int. Immunol.* 27, 55–62. doi: 10.1093/intimm/dxu102

Monson, N. L., Ireland, S. J., Ligocki, A. J., Chen, D., Rounds, W. H., Li, M., et al. (2014). Elevated CNS inflammation in patients with preclinical Alzheimer's disease. *J. Cereb. Blood Flow Metab.* 34, 30–33. doi: 10.1038/jcbfm.2013.183

Moreira, A. L. (1993). Thalidomide exerts its inhibitory action on tumor necrosis factor alpha by enhancing mRNA degradation. *J Exp Med.* 177, 1675–1680. doi: 10.1084/jem.177.6.1675

Mosser, D. M., and Edwards, J. P. (2008). Exploring the full spectrum of macrophage activation. *Nat. Rev. Immunol.* 8, 958–969. doi: 10.1038/nri2448

Muscal, J. A., Sun, Y., Nuchtern, J. G., Dauser, R. C., McGuffey, L. H., Gibson, B. W., et al. (2012). Plasma and cerebrospinal fluid pharmacokinetics of thalidomide and lenalidomide in nonhuman primates. *Cancer Chemother. Pharmacol.* 69, 943–947. doi: 10.1007/s00280-011-1781-y

Myöhänen, T. T., Hannula, M. J., Van Elzen, R., Gerard, M., Van Der Veken, P., García-Horsman, J. A., et al. (2012). A prolyl oligopeptidase inhibitor, KYP-2047, reduces α-synuclein protein levels and aggregates in cellular and animal models of Parkinson's disease. *Br. J. Pharmacol.* 166, 1097–1113. doi: 10.1111/j.1476-5381.2012.01846.x

Narhi, L., Wood, S. J., Steavenson, S., Jiang, Y., Wu, G. M., Anafi, D., et al. (1999). Both familial Parkinson's disease mutations accelerate α-synuclein aggregation. *J. Biol. Chem.* 274, 9843–9846. doi: 10.1074/jbc.274.14.9843

Nieweg, K., Andreyeva, A., Van Stegen, B., Tanriöver, G., and Gottmann, K. (2015). Alzheimer's disease-related amyloid-β induces synaptotoxicity in human iPS cell-derived neurons. *Cell Death Dis.* 6:e1709. doi: 10.1038/cddis.2015.72

Noguchi, T., Sano, H., Shimazawa, R., Tanatani, A., Miyachi, H., and Hashimoto, Y. (2004). Phenylhomophthalimide-type NOS inhibitors derived from thalidomide. *Bioorg. Med. Chem. Lett.* 14, 4141–4145. doi: 10.1016/j.bmcl.2004.06.026

Noman, A. S. M., Koide, N., Hassan, F., I-E-Khuda, I., Dagvadorj, J., Tumurkhuu, G., et al. (2009). Thalidomide inhibits lipopolysaccharide-induced tumor necrosis factor-α production via down-regulation of MyD88 expression. *Innate Immun.* 15, 33–41. doi: 10.1177/1753425908099317

Nomura, T., Abe, Y., Kamada, H., Shibata, H., Kayamuro, H., Inoue, M., et al. (2011). Therapeutic effect of PEGylated TNFR1-selective antagonistic mutant TNF in experimental autoimmune encephalomyelitis mice. *J. Control Release.* 149, 8–14. doi: 10.1016/j.jconrel.2009.12.015

Omran, A., Ashhab, M. U., Gan, N., Kong, H., Peng, J., and Yin, F. (2013). Effects of MRP8, LPS, and lenalidomide on the expressions of TNF-brain-enriched, and inflammation-related MicroRNAs in the primary astrocyte culture. *Sci. World J.* 2013, 208309. doi: 10.1155/2013/208309

Palencia, G., Garcia, E., Osorio-Rico, L., Trejo-Solís, C., Escamilla-Ramírez, A., and Sotelo, J. (2015). Neuroprotective effect of thalidomide on MPTP-induced toxicity. *Neurotoxicology* 47, 82–87. doi: 10.1016/j.neuro.2015.02.004

Palencia, G., Martinez-Juarez, I. E., Calderon, A., Artigas, C., and Sotelo, J. (2010). Thalidomide for treatment of refractory epilepsy. *Epilepsy Res.* 92, 253–257. doi: 10.1016/j.eplepsyres.2010.10.003

Palotas, A., Kallikourdis, M., Liu, J., and Wang, F. (2017). Role of neuroinflammation in Amyotrophic lateral Sclerosis: cellular mechanisms and therapeutic implications. *Front. Immunol* 8:1005. doi: 10.3389/fimmu.2017.01005

Parameswaran, N., and Patial, S. (2010). Tumor necrosis factor-a signaling in macrophages. *Crit. Rev. Eukaryot. Gene Expr.* 20, 87–103. doi: 10.1615/CritRevEukarGeneExpr.v20.i2.10

Paul, S. C., Lv, P., Xiao, Y. J., An, P., Liu, S. Q., and Luo, H. S. (2006). Thalidomide in rat liver cirrhosis: blockade of tumor necrosis factor-α via inhibition of degradation of an inhibitor of nuclear factor-κB. *Pathobiology* 73, 82–92. doi: 10.1159/000094492

Payandemehr, B., Rahimian, R., Gooshe, M., Bahremand, A., Gholizadeh, R., Berijani, S., et al. (2014). Nitric oxide mediates the anticonvulsant effects of thalidomide on pentylenetetrazole-induced clonic seizures in mice. *Epilepsy Behav.* 34, 99–104. doi: 10.1016/j.yebeh.2014.03.020

Pegoretti, V., Baron, W., Laman, J. D., and Eisel, U. L. M. (2018). Selective modulation of TNF-TNFRs signaling: Insights for multiple sclerosis treatment. *Front. Immunol.* 9:925. doi: 10.3389/fimmu.2018.00925

Penas-Prado, M., Hess, K. R., Fisch, M. J., Lagrone, L. W., Groves, M. D., Levin, V. A., et al. (2015). Randomized phase II adjuvant factorial study of dose-dense temozolomide alone and in combination with isotretinoin, celecoxib, and/or thalidomide for glioblastoma. *Neuro. Oncol.* 17, 266–273. doi: 10.1093/neuonc/nou155

Petzold, G., Fischer, E. S., and Thomä, N. H. (2016). Structural basis of lenalidomide-induced CK1α degradation by the CRL4CRBN ubiquitin ligase. *Nature* 532:127. doi: 10.1038/nature16979

Pfueller, C. F., Seipelt, E., Zipp, F., and Paul, F. (2008). Multiple sclerosis following etanercept treatment for ankylosing spondylitis. *Scand. J. Rheumatol.* 37, 397–399. doi: 10.1080/03009740802136164

Polymeropoulos, M. H., Lavedan, C., Leroy, E., Ide, S. E., Dehejia, A., Dutra, A., et al. (1997). Mutation in the α-synuclein gene identified in families with Parkinson's disease. *Science* 276, 2045–2047. doi: 10.1126/science.276.5321.2045

Pooler, A. M., Polydoro, M., Wegmann, S., Nicholls, S. B., Spires-Jones, T. L., and Hyman, B. T. (2013). Propagation of tau pathology in Alzheimer's disease: identification of novel therapeutic targets. *Alzheimers Res. Ther.* 5:49. doi: 10.1186/alzrt214

Pulliam, L., Sun, B., Mustapic, M., Chawla, S., and Kapogiannis, D. (2019). Plasma neuronal exosomes serve as biomarkers of cognitive impairment in HIV infection and Alzheimer's disease. *J. Neurovirol.* 25, 702–709. doi: 10.1007/s13365-018-0695-4

Ramos-Cejudo, J., Wisniewski, T., Marmar, C., Zetterberg, H., Blennow, K., De Leon, M. J., et al. (2018). Traumatic brain injury and Alzheimer's disease: the cerebrovascular link. *EBioMedicine* 28, 21–30. doi: 10.1016/j.ebiom.2018.01.021

Rascol, O., Lozano, A., Stern, M., and Poewe, W. (2011). Milestones in Parkinson's disease therapeutics. *Mov. Disord.* 26, 1072–1082. doi: 10.1002/mds.23714

Rawji, K. S., and Yong, V. W. (2013). The benefits and detriments of macrophages/microglia in models of multiple sclerosis. *Clin. Dev. Immunol.* 2013:13. doi: 10.1155/2013/948976

Renton, A. E., Majounie, E., Waite, A., Simón-Sánchez, J., Rollinson, S., Gibbs, J. R., et al. (2011). A hexanucleotide repeat expansion in C9ORF72 is the cause of chromosome 9p21-linked ALS-FTD. *Neuron* 72, 257–268. doi: 10.1016/j.neuron.2011.09.010

Reyes, T. M., Fabry, Z., and Coe, C. L. (1999). Brain endothelial cell production of a neuroprotective cytokine, interleukin-6, in response to noxious stimuli. *Brain Res.* 851, 215–220. doi: 10.1016/S0006-8993(99)02189-7

Richardson, P. G., Schlossman, R. L., Weller, E., Hideshima, T., Mitsiades, C., Davies, F., et al. (2002). Immunomodulatory drug CC-5013 overcomes drug resistance and is well tolerated in patients with relapsed multiple myeloma. *Blood* 100, 3063–3067. doi: 10.1182/blood-2002-03-0996

Ringheim, G. E., Burgher, K. L., and Heroux, J. A. (1995). Interleukin-6 mRNA expression by cortical neurons in culture: evidence for neuronal sources of interleukin-6 production in the brain. *J Neuroimmunol.* 63, 113–123. doi: 10.1016/0165-5728(95)00134-4

Ríos-Tamayo, R., Martín-García, A., Alarcón-Payer, C., Sánchez-Rodríguez, D., De La Guardia, A. M. D. V. D., Collado, C. G. G., et al. (2017). Pomalidomide in the treatment of multiple myeloma: design, development and place in therapy. *Drug Des. Devel. Ther.* 11, 2399–2408. doi: 10.2147/DDDT.S115456

Rizzo, F. R., Musella, A., De Vito, F., Fresegna, D., Bullitta, S., Vanni, V., et al. (2018). Tumor necrosis factor and interleukin-1β modulate synaptic plasticity during neuroinflammation. *Neural Plast.* 2018:8430123. doi: 10.1155/2018/8430123

Roberts, G. W., Gentleman, S. M., Lynch, A., Murray, L., Landon, M., and Graham, D. I. (1994). β3 Amyloid protein deposition in the brain after severe head injury: implications for the pathogenesis of Alzheimer's disease. *J. Neurol. Neurosurg. Psychiatry* 57, 419–425. doi: 10.1136/jnnp.57.4.419

Roberts, M. T. M., Mendelson, M., Meyer, P., Carmichael, A., and Lever, A. M. L. (2003). The use of thalidomide in the treatment of intracranial tuberculomas in adults: two case reports. *J. Infect.* 47, 251–255. doi: 10.1016/S0163-4453(03)00077-X

Roth, T. L., Nayak, D., Atanasijevic, T., Koretsky, A. P., Latour, L. L., and McGavern, D. B. (2014). Transcranial amelioration of inflammation and cell death after brain injury. *Nature* 505, 223–228. doi: 10.1038/nature12808

Rowland, T. L., Mchugh, S. M., Deighton, J., Ewan, P. W., Dearman, R. J., and Kimber, I. (1999). Selective down-regulation of T cell-and non-T cell-derived tumour necrosis factor a by thalidomide: comparisons with dexamethasone. *Immunol. Lett.* 68, 325–332. doi: 10.1016/s0165-2478(99)00055-3

Rozewski, D. M., Herman, S. E. M., Towns, W. H., Mahoney, E., Stefanovski, M. R., Shin, J. D., et al. (2012). Pharmacokinetics and tissue disposition of lenalidomide in mice. *AAPS J.* 14, 872–882. doi: 10.1208/s12248-012-9401-2

Rubenstein, J. L., Geng, H., Fraser, E. J., Formaker, P., Chen, L., Sharma, J., et al. (2018). Phase 1 investigation of lenalidomide/rituximab plus outcomes of lenalidomide maintenance in relapsed CNS lymphoma. *Blood Adv.* 2, 1595–1607. doi: 10.1182/bloodadvances.2017014845

Russo, I., Caracciolo, L., Tweedie, D., Choi, S.-H., Greig, N. H., Barlati, S., et al. (2012). 3,6′-Dithiothalidomide, a new TNF-α synthesis inhibitor, attenuates the effect of Aß1-42 intracerebroventricular injection on hippocampal neurogenesis and memory deficit. *Brain Physiol. Metab. Sect. Natl. Inst. Aging* 122, 1181–1192. doi: 10.1111/j.1471-4159.2012.07846.x

Russo, M. V., Latour, L. L., and Mcgavern, D. B. (2018). Distinct myeloid cell subsets promote meningeal remodeling and vascular repair after mild traumatic brain injury. *Nat. Immunol.* 19, 442–452. doi: 10.1038/s41590-018-0086-2

Salomone, S., Caraci, F., Leggio, G. M., Fedotova, J., and Drago, F. (2012). New pharmacological strategies for treatment of Alzheimer's disease: focus on disease modifying drugs. *Br. J. Clin. Pharmacol.* 73, 504–517. doi: 10.1111/j.1365-2125.2011.04134.x

Sambamurti, K., Kinsey, R., Maloney, B., Ge, Y. W., and Lahiri, D. K. (2004). Gene structure and organization of the human β-secretase (BACE) promoter. *FASEB J.* 18, 1034–1036. doi: 10.1096/fj.03-1378fje

Sampaio, E. P., Sarno, E. N., Galilly, R., Cohn, Z. A., and Kaplan, G. (1991). Thalidomide selectively inhibits tumor necrosis factor alpha production by stimulated human monocytes. *J. Exp. Med.* 173, 699–703. doi: 10.1084/jem.173.3.699

Sanadgol, N., Golab, F., Mostafaie, A., Mehdizadeh, M., Khalseh, R., Mahmoudi, M., et al. (2018). Low, but not high, dose triptolide controls neuroinflammation and improves behavioral deficits in toxic model of multiple sclerosis by dampening of NF-κB activation and acceleration of intrinsic myelin repair. *Toxicol. Appl. Pharmacol.* 342, 86–98. doi: 10.1016/j.taap.2018.01.023

Scherbel, U., Raghupathi, R., Nakamura, M., Saatman, K. E., Trojanowski, J. Q., Neugebauer, E., et al. (1999). Differential acute and chronic responses of tumor necrosis factor-deficient mice to experimental brain injury. *Proc. Natl. Acad. Sci. U.S.A.* 96, 8721–8726. doi: 10.1073/pnas.96.15.8721

Schett, G., Sloan, V. S., Stevens, R. M., and Schafer, P. (2010). Apremilast: a novel PDE4 inhibitor in the treatment of autoimmune and inflammatory diseases. *Ther. Adv. Musculoskelet. Dis.* 2, 271–278. doi: 10.1177/1759720X10381432

Schoeman, J. F. (2000). Thalidomide therapy in childhood *Tuberculous meningitis*. *J. Child Neurol.* 15:838. doi: 10.1177/088307380001501221

Schoeman, J. F., Andronikou, S., Stefan, D. C., Freeman, N., and Van Toorn, R. (2010). Tuberculous meningitis-related optic neuritis: recovery of vision with thalidomide in 4 consecutive cases. *J. Child Neurol.* 25, 822–828. doi: 10.1177/0883073809350507

Scudamore, O., and Ciossek, T. (2018). Increased oxidative stress exacerbates α-synuclein aggregation in vivo. *J. Neuropathol. Exp. Neurol.* 77, 443–453. doi: 10.1093/jnen/nly024

Sébire, G., Emilie, D., Wallon, C., Héry, C., Devergne, O., Delfraissy, J. F., et al. (1993). In vitro production of IL-6, IL-1 beta, and tumor necrosis factor-alpha by human embryonic microglial and neural cells. *J. Immunol.* 150, 1517–1523.

Sedger, L. M., and McDermott, M. F. (2014). TNF and TNF-receptors: from mediators of cell death and inflammation to therapeutic giants - past, present and future. *Cytokine Growth Factor Rev.* 25, 453–472. doi: 10.1016/j.cytogfr.2014.07.016

Shaftel, S. S., Griffin, W. S. T., and Kerry, K. M. (2008). The role of interleukin-1 in neuroinflammation and Alzheimer disease: an evolving perspective. *J. Neuroinflam.* 5:7. doi: 10.1186/1742-2094-5-7

Sharief, M. K., and Hentges, R. (1991). Association between tumor necrosis factor-α and disease progression in patients with multiple Sclerosis. *N. Engl. J. Med.* 325, 467–472. doi: 10.1056/NEJM199108153250704

Shechter, R., London, A., and Schwartz, M. (2013). Orchestrated leukocyte recruitment to immune-privileged sites: absolute barriers versus educational gates. *Nat. Rev. Immunol.* 13, 206–218. doi: 10.1038/nri3391

Sheskin, J. (1965). Thalidomide in the treatment of lepra reactions. *Clin. Pharmacol. Ther.* 6, 303–306. doi: 10.1002/cpt196563303

Shi, J. Q., Wang, B. R., Jiang, W. W., Chen, J., Zhu, Y. W., Zhong, L. L., et al. (2011). Cognitive improvement with intrathecal administration of infliximab in a woman with Alzheimer's disease. *J. Am. Geriatr. Soc.* 59, 1142–1144. doi: 10.1111/j.1532-5415.2011.03445.x

Shi, K., Zhang, J., Dong, J., and Shi, F.-D. (2019). Dissemination of brain inflammation in traumatic brain injury. *Cell. Mol. Immunol.* 16, 523–530. doi: 10.1038/s41423-019-0213-5

Shi, Q., and Chen, L. (2017). Cereblon: a protein crucial to the multiple functions of immunomodulatory drugs as well as cell metabolism and disease generation. *J. Immunol. Res.* 2017:9130608. doi: 10.1155/2017/9130608

Siamwala, J. H., Veeriah, V., Priya, M. K., Rajendran, S., Saran, U., Sinha, S., et al. (2012). Nitric oxide rescues thalidomide mediated teratogenicity. *Sci. Rep.* 2:679. doi: 10.1038/srep00679

Song, G. J., and Suk, K. (2017). Pharmacological modulation of functional phenotypes of microglia in Neurodegenerative diseases. *Front. Aging Neurosci* 9:139. doi: 10.3389/fnagi.2017.00139

Sriram, K., and O'Callaghan, J. P. (2007). Divergent roles for tumor necrosis factor-α in the brain. *J. Neuroimmune Pharmacol.* 2, 140–153. doi: 10.1007/s11481-007-9070-6

Steeland, S., Van Ryckeghem, S., Van Imschoot, G., De Rycke, R., Toussaint, W., Vanhoutte, L., et al. (2017). TNFR1 inhibition with a Nanobody protects against EAE development in mice. *Sci. Rep.* 7:13646. doi: 10.1038/s41598-017-13984-y

Stommel, E. W., Cohen, J. A., Fadul, C. E., Cogbill, C. H., Graber, D. J., Kingman, L., et al. (2009). Efficacy of thalidomide for the treatment of amyotrophic lateral sclerosis: a phase II open label clinical trial. *Amyotroph. Lateral. Scler.* 10, 393–404. doi: 10.3109/17482960802709416

Stys, P. K., Zamponi, G. W., Van Minnen, J., and Geurts, J. J. G. (2012). Will the real multiple sclerosis please stand up? *Nat. Rev. Neurosci.* 13, 507–514. doi: 10.1038/nrn3275

Sumbria, R., Chang, R., and Yee, K.-L. (2017). Tumor necrosis factor α inhibition for Alzheimer's disease. *J. Cent. Nerv. Syst. Dis.* 9:1177/1179573517709278. doi: 10.1177/1179573517709278

Tang, Y., and Le, W. (2016). Differential roles of M1 and M2 Microglia in Neurodegenerative diseases. *Mol. Neurobiol.* 53, 1181–1194. doi: 10.1007/s12035-014-9070-5

Tansey, M. G., and Goldberg, M. S. (2010). Neuroinflammation in Parkinson's disease: its role in neuronal death and implications for therapeutic intervention. *Neurobiol. Dis.* 37, 510–518. doi: 10.1016/j.nbd.2009.11.004

Thal, D. R., Rüb, U., Orantes, M., and Braak, H. (2002). Phases of Aβ-deposition in the human brain and its relevance for the development of AD. *Neurology* 58, 1791–1800. doi: 10.1212/WNL.58.12.1791

Titelbaum, D. S., Degenhardt, A., and Kinkel, R. P. (2005). Anti-tumor necrosis factor alpha-associated multiple sclerosis. *AJNR Am. J. Neuroradiol.* 26, 1548–1550.

Tobinick, E. (2010). Perispinal etanercept: a new therapeutic paradigm in neurology. *Expert Rev. Neurother.* 10, 985–1002. doi: 10.1586/ern.10.52

Tobinick, E. (2018). Perispinal etanercept advances as a neurotherapeutic. *Expert Rev. Neurother.* 18, 453–455. doi: 10.1080/14737175.2018.1468253

Tobinick, E., Gross, H., Weinberger, A., and Cohen, H. (2006). TNF-alpha modulation for treatment of Alzheimer's disease: a 6-month pilot study. *MedGenMed* 8:25.

Tortarolo, M., Vallarola, A., Lidonnici, D., Battaglia, E., Gensano, F., Spaltro, G., et al. (2015). Lack of TNF-alpha receptor type 2 protects motor neurons in a cellular model of amyotrophic lateral sclerosis and in mutant SOD1 mice but does not affect disease progression. *J. Neurochem.* 135, 109–124. doi: 10.1111/jnc.13154

Town, T., Nikolic, V., and Tan, J. (2005). The microglial "activation" continuum: from innate to adaptive responses. *J. Neuroinflam.* 2:24. doi: 10.1186/1742-2094-2-24

Tsai, Y. R., Chang, C. F., Lai, J. H., Wu, J. C. C., Chen, Y. H., Kang, S. J., et al. (2018). Pomalidomide ameliorates H2O2-induced oxidative stress injury and cell death in rat primary cortical neuronal cultures by inducing anti-oxidative and anti-apoptosis effects. *Int. J. Mol. Sci.* 19:3252. doi: 10.3390/ijms19103252

Tsai, Y.-R., Tweedie, D., Navas-Enamorado, I., Scerba, M. T., Chang, C.-F., Lai, J.-H., et al. (2019). Pomalidomide reduces ischemic brain injury in rodents. *Cell Transplant.* 28:096368971985007. doi: 10.1177/0963689719850078

Tweedie, D., Ferguson, R. A., Fishman, K., Frankola, K. A., Van Praag, H., Holloway, H. W., et al. (2012). Tumor necrosis factor-α synthesis inhibitor 3,6′-dithiothalidomide attenuates markers of inflammation, Alzheimer pathology and behavioral deficits in animal models of neuroinflammation and Alzheimer's disease. *J Neuroinflam.* 9:106. doi: 10.1186/1742-2094-9-106

Tweedie, D., Luo, W., Short, R. G., Brossi, A., Holloway, H. W., Li, Y., et al. (2009). A cellular model of inflammation for identifying TNF-α synthesis inhibitors. *J. Neurosci. Methods* 183, 182–187. doi: 10.1016/j.jneumeth.2009.06.034

Tweedie, D., Sambamurti, K., and Greig, N. H. (2007). TNF-alpha inhibition as a treatment strategy for neurodegenerative disorders: new drug candidates and targets. *Curr. Alzheimer Res.* 4, 378–385.

Urschel, K., and Cicha, I. (2015). TNF-α in the cardiovascular system: from physiology to therapy. *Int. J. Interf. Cytokine Mediat. Res.* 7, 9–25. doi: 10.2147/IJICMR.S64894

Valentin-Torres, A., Savarin, C., Barnett, J., and Bergmann, C. C. (2018). Blockade of sustained tumor necrosis factor in a transgenic model of progressive autoimmune encephalomyelitis limits oligodendrocyte apoptosis and promotes oligodendrocyte maturation. *J. Neuroinflam.* 15:121. doi: 10.1186/s12974-018-1164-y

Valera, E., Mante, M., Anderson, S., Rockenstein, E., and Masliah, E. (2015). Lenalidomide reduces microglial activation and behavioral deficits in a transgenic model of Parkinson's disease. *J. Neuroinflam.* 12:93. doi: 10.1186/s12974-015-0320-x

Vallet, S., Palumbo, A., Raje, N., Boccadoro, M., and Anderson, K. C. (2008). Thalidomide and lenalidomide: mechanism-based potential drug combinations. *Leuk. Lymphoma* 49, 1238–1245. doi: 10.1080/10428190802005191

Van Eldik, L. J., Carrillo, M. C., Cole, P. E., Feuerbach, D., Greenberg, B. D., Hendrix, J. A., et al. (2016). The roles of inflammation and immune mechanisms in Alzheimer's disease. Alzheimer's Dement. *Transl. Res. Clin. Interv.* 2, 99–109. doi: 10.1016/j.trci.2016.05.001

Van Oosten, B. W., Barkhof, F., Truyen, L., Boringa, J. B., Bertelsmann, F. W., Von Blomberg, B. M. E., et al. (1996). Increased MRI activity and immune activation in two multiple sclerosis patients treated with the monoclonal anti-tumor necrosis factor antibody cA2. *Neurology* 47, 1531–1534. doi: 10.1212/WNL.47.6.1531

Vargesson, N. (2015). Thalidomide-induced teratogenesis: history and mechanisms. *Birth Defects Res. Part C Embryo. Today Rev.* 105, 140–156. doi: 10.1002/bdrc.21096

Vargesson, N. (2019). The teratogenic effects of thalidomide on limbs. *J. Hand Surg. Eur. Vol.* 44, 88–95. doi: 10.1177/1753193418805249

Veglianese, P., Lo Coco, D., Bao Cutrona, M., Magnoni, R., Pennacchini, D., Pozzi, B., et al. (2006). Activation of the p38MAPK cascade is associated with upregulation of TNF alpha receptors in the spinal motor neurons of mouse models of familial ALS. *Mol. Cell. Neurosci.* 31, 218–231. doi: 10.1016/j.mcn.2005.09.009

Vehmas, A. K., Kawas, C. H., Stewart, W. F., and Troncoso, J. C. (2003). Immune reactive cells in senile plaques and cognitive decline in Alzheimer's disease. *Neurobiol. Aging.* 24, 321–331. doi: 10.1016/s0197-4580(02)00090-8

Vergara, T. R. C., Samer, S., Santos-Oliveira, J. R., Giron, L. B., Arif, M. S., Silva-Freitas, M. L., et al. (2017). Thalidomide is associated with increased T Cell activation and inflammation in antiretroviral-naive HIV-infected individuals in a randomised clinical trial of efficacy and safety. *EBioMedicine* 23, 59–67. doi: 10.1016/j.ebiom.2017.08.007

Virmani, A., Pinto, L., Binienda, Z., and Ali, S. (2013). Food, nutrigenomics, and neurodegeneration - Neuroprotection by what you eat!. *Mol. Neurobiol.* 48, 353–362. doi: 10.1007/s12035-013-8498-3

von Bernhardi, R., Cornejo, F., Parada, G. E., and Eugenín, J. (2015). Role of TGFβ signaling in the pathogenesis of Alzheimer's disease. *Front. Cell. Neurosci.* 9:28. doi: 10.3389/fncel.2015.00426

Wager, T. T., Hou, X., Verhoest, P. R., and Villalobos, A. (2010). Moving beyond rules: the development of a central nervous system multiparameter optimization (CNS MPO) approach to enable alignment of druglike properties. *ACS Chem. Neurosci.* 1, 435–449. doi: 10.1021/cn100008c

Wall, A. M., Mukandala, G., Greig, N. H., and O'Connor, J. J. (2015). Tumor necrosis factor-α potentiates long-term potentiation in the rat dentate gyrus after acute hypoxia. *J. Neurosci. Res.* 93, 815–829. doi: 10.1002/jnr.23540

Wang, J. Y., Huang, Y. N., Chiu, C. C., Tweedie, D., Luo, W., Pick, C. G., et al. (2016a). Erratum: pomalidomide mitigates neuronal loss, neuroinflammation, and behavioral impairments induced by traumatic brain injury in rat. *J Neuroinflam.* 12:168. doi: 10.1186/s12974-016-0668-6

Wang, J. Y., Huang, Y. N., Chiu, C. C., Tweedie, D., Luo, W., Pick, C. G., et al. (2016b). Pomalidomide mitigates neuronal loss, neuroinflammation, and behavioral impairments induced by traumatic brain injury in rat. *J. Neuroinflam.* 13:168. doi: 10.1186/s12974-016-0668-6

Wang, W., Zinsmaier, A. K., Firestone, E., Lin, R., Yatskievych, T. A., Yang, S., et al. (2018). Blocking tumor necrosis factor-alpha expression prevents blast-induced excitatory/inhibitory synaptic imbalance and parvalbumin-positive

interneuron loss in the hippocampus. *J. Neurotrauma* 35, 2306–2316. doi: 10.1089/neu.2018.5688

Warren, K. E., Goldman, S., Pollack, I. F., Fangusaro, J., Schaiquevich, P., Stewart, C. F., et al. (2010). Phase I trial of lenalidomide in pediatric patients with recurrent, refractory, or progressive primary CNS Tumors: pediatric brain tumor consortium study PBTC-018. *J. Clin. Oncol.* 29, 324–329. doi: 10.1200/JCO.2010.31.3601

Weng, Q., Wang, J., Wang, J., Wang, J., Sattar, F., Zhang, Z., et al. (2018). Lenalidomide regulates CNS autoimmunity by promoting M2 macrophages polarization article. *Cell Death Dis.* 9, 251. doi: 10.1038/s41419-018-0290-x

Wenzel, T. J., and Klegeris, A. (2018). Novel multi-target directed ligand-based strategies for reducing neuroinflammation in Alzheimer's disease. *Life Sci.* 207, 314–322. doi: 10.1016/j.lfs.2018.06.025

Wettstein, A. R., and Meagher, A. P. (1997). Thalidomide in Crohn's disease. *Gastroenterology* 126:A629.

Wilhelm, S. M., Taylor, J. D., Osiecki, L. L., and Kale-Pradhan, P. B. (2006). Novel therapies for Crohn's disease: focus on immunomodulators and antibiotics. *Ann. Pharmacother.* 40, 1804–1813. doi: 10.1345/aph.1H038

Williams, S. K., Maier, O., Fischer, R., Fairless, R., Hochmeister, S., Stojic, A., et al. (2014). Antibody-mediated inhibition of TNFR1 attenuates disease in a mouse model of multiple Sclerosis. *PLoS One* 9:e90117. doi: 10.1371/journal.pone.0090117

Winter, G. E., Buckley, D. L., Paulk, J., Roberts, J. M., Souza, A., Dhe-Paganon, S., et al. (2015). Phthalimide conjugation as a strategy for in vivo target protein degradation. *Science* 348, 1376–1381. doi: 10.1126/science.aab1433

Xiao, X., Putatunda, R., Zhang, Y., Soni, P. V., Li, F., Zhang, T., et al. (2018). Lymphotoxin β receptor-mediated NFκB signaling promotes glial lineage differentiation and inhibits neuronal lineage differentiation in mouse brain neural stem/progenitor cells. *J. Neuroinflam.* 15:49. doi: 10.1186/s12974-018-1074-z

Yagyu, T., Kobayashi, H., Matsuzaki, H., Wakahara, K., Kondo, T., Kurita, N., et al. (2005). Thalidomide inhibits tumor necrosis factor-α-induced interleukin-8 expression in endometriotic stromal cells, possibly through suppression of nuclear factor-κB activation. *J. Clin. Endocrinol. Metab.* 90, 3017–3021. doi: 10.1210/jc.2004-1946

Yamamoto, M., Kiyota, T., Horiba, M., Buescher, J. L., Walsh, S. M., Gendelman, H. E., et al. (2007). Interferon-and tumor necrosis factor-regulate amyloid-plaque deposition and-secretase expression in swedish mutant APP transgenic mice. *Am. J. Pathol.* 170, 680–692. doi: 10.2353/ajpath.2007.060378

Yang, C., Atkinson, S. P., Vilella, F., Lloret, M., Armstrong, L., Mann, D. A., et al. (2010). Opposing putative roles for canonical and noncanonical NFκB signaling on the survival, proliferation, and differentiation potential of human embryonic stem cells. *Stem Cells* 28, 1970–1980. doi: 10.1002/stem.528

Yee, A. X., Hsu, Y. T., and Chen, L. (2017). A metaplasticity view of the interaction between homeostatic and hebbian plasticity. *Philos. Trans. R. Soc. B Biol. Sci.* 372:20160155. doi: 10.1098/rstb.2016.0155

Yoon, J. S., Lee, J.-H., Tweedie, D., Mughal, M. R., Chigurupati, S., Greig, N. H., et al. (2013). 3,6′-Dithiothalidomide improves experimental stroke outcome by suppressing neuroinflammation HHS public access. *J. Neurosci. Res.* 91, 671–680. doi: 10.1002/jnr.23190

Yu, H. H., Reitsma, J. M., Sweredoski, M. J., Moradian, A., Hess, S., and Deshaies, R. J. (2019). Single subunit degradation of WIZ, a lenalidomide- and pomalidomide dependent substrate of E3 ubiquitin ligase CRL4CRBN. *bioRxiv* [Preprint]. doi: 10.1101/595389

Zeldis, J. B., Knight, R., Hussein, M., Chopra, R., and Muller, G. (2011). A review of the history, properties, and use of the immunomodulatory compound lenalidomide. *Ann. N. Y. Acad. Sci.* 1222, 76–82. doi: 10.1111/j.1749-6632.2011.05974.x

Zhang, L., Qu, Y., Tang, J., Chen, D., Fu, X., Mao, M., et al. (2010). PI3K/Akt signaling pathway is required for neuroprotection of thalidomide on hypoxic-ischemic cortical neurons in vitro. *Brain Res.* 1357, 157–165. doi: 10.1016/j.brainres.2010.08.007

Zhang, T., Kruys, V., Huez, G., and Gueydan, C. (2002). AU-rich element-mediated translational control: complexity and multiple activities of trans-activating factors. *Biochem. Soc. Trans.* 30, 952–958. doi: 10.1042/bst0300952

Zhang, Y., and Hu, W. (2012). NFκB signaling regulates embryonic and adult neurogenesis. *Front. Biol.* 7:277–291. doi: 10.1007/s11515-012-1233-z

Zhu, X., Giordano, T., Yu, Q. S., Holloway, H. W., Perry, T. A., Lahiri, D. K., et al. (2003). Thiothalidomides: novel isosteric analogues of thalidomide with enhanced TNF-α inhibitory activity. *J. Med. Chem.* 46, 5222–5229. doi: 10.1021/jm030152f

**Conflict of Interest:** NG and DT are named inventors on patents covering novel thalidomide analogs and have assigned all their rights to the National Institute on Aging, NIH.

The remaining authors declare that the research was conducted in the absence of any commercial or financial relationships that could be construed as a potential conflict of interest.

frontiers in Cell and Developmental Biology

ORIGINAL RESEARCH
published: 10 January 2020
doi: 10.3389/fcell.2019.00356

# Neuroprotective Effects and Treatment Potential of Incretin Mimetics in a Murine Model of Mild Traumatic Brain Injury

*Miaad Bader[1]*, Yazhou Li[2], David Tweedie[2], Nathan A. Shlobin[3], Adi Bernstein[1], Vardit Rubovitch[1], Luis B. Tovar-y-Romo[2,4], Richard D. DiMarchi[5], Barry J. Hoffer[6], Nigel H. Greig[2] and Chaim G. Pick[1,7,8]*

[1] Department of Anatomy and Anthropology, Sackler Faculty of Medicine, Tel Aviv University, Tel Aviv, Israel, [2] Translational Gerontology Branch, Intramural Research Program, National Institute on Aging, National Institutes of Health, Baltimore, MD, United States, [3] Feinberg School of Medicine, Northwestern University, Chicago, IL, United States, [4] Division of Neuroscience, Institute of Cellular Physiology, Universidad Nacional Autónoma de México, Mexico City, Mexico, [5] Department of Chemistry, Indiana University, Bloomington, IN, United States, [6] Department of Neurosurgery, Case Western Reserve University School of Medicine, Cleveland, OH, United States, [7] Sagol School of Neuroscience, Tel Aviv University, Tel Aviv, Israel, [8] Center for the Biology of Addictive Diseases, Tel Aviv University, Tel Aviv, Israel

OPEN ACCESS

**Edited by:**
*Adelaide Fernandes, University of Lisbon, Portugal*

**Reviewed by:**
*Victor Gault, Ulster University, United Kingdom*
*Mosharraf Sarker, Teesside University, United Kingdom*

***Correspondence:**
*Miaad Bader*
*miaad.bader@gmail.com*

**Specialty section:**
*This article was submitted to Molecular Medicine, a section of the journal Frontiers in Cell and Developmental Biology*

**Received:** *09 September 2019*
**Accepted:** *10 December 2019*
**Published:** *10 January 2020*

**Citation:**
*Bader M, Li Y, Tweedie D, Shlobin NA, Bernstein A, Rubovitch V, Tovar-y-Romo LB, DiMarchi RD, Hoffer BJ, Greig NH and Pick CG (2020) Neuroprotective Effects and Treatment Potential of Incretin Mimetics in a Murine Model of Mild Traumatic Brain Injury. Front. Cell Dev. Biol. 7:356. doi: 10.3389/fcell.2019.00356*

Traumatic brain injury (TBI) is a commonly occurring injury in sports, victims of motor vehicle accidents, and falls. TBI has become a pressing public health concern with no specific therapeutic treatment. Mild TBI (mTBI), which accounts for approximately 90% of all TBI cases, may frequently lead to long-lasting cognitive, behavioral, and emotional impairments. The incretins glucagon-like peptide-1 (GLP-1) and glucose-dependent insulinotropic polypeptide (GIP) are gastrointestinal hormones that induce glucose-dependent insulin secretion, promote β-cell proliferation, and enhance resistance to apoptosis. GLP-1 mimetics are marketed as treatments for type 2 diabetes mellitus (T2DM) and are well tolerated. Both GLP-1 and GIP mimetics have shown neuroprotective properties in animal models of Parkinson's and Alzheimer's disease. The aim of this study is to evaluate the potential neuroprotective effects of liraglutide, a GLP-1 analog, and twincretin, a dual GLP-1R/GIPR agonist, in a murine mTBI model. First, we subjected mice to mTBI using a weight-drop device and, thereafter, administered liraglutide or twincretin as a 7-day regimen of subcutaneous (s.c.) injections. We then investigated the effects of these drugs on mTBI-induced cognitive impairments, neurodegeneration, and neuroinflammation. Finally, we assessed their effects on neuroprotective proteins expression that are downstream to GLP-1R/GIPR activation; specifically, PI3K and PKA phosphorylation. Both drugs ameliorated mTBI-induced cognitive impairments evaluated by the novel object recognition (NOR) and the Y-maze paradigms in which neither anxiety nor locomotor activity were confounds, as the latter were unaffected by either mTBI or drugs. Additionally, both drugs significantly mitigated mTBI-induced neurodegeneration and neuroinflammation, as quantified by immunohistochemical staining with Fluoro-Jade/anti-NeuN and anti-Iba-1 antibodies, respectively. mTBI challenge significantly decreased PKA phosphorylation levels in

ipsilateral cortex, which was mitigated by both drugs. However, PI3K phosphorylation was not affected by mTBI. These findings offer a new potential therapeutic approach to treat mTBI, and support further investigation of the neuroprotective effects and mechanism of action of incretin-based therapies for neurological disorders.

### HIGHLIGHTS

- Liraglutide and twincretin ameliorate mTBI-induced cognitive deficits.
- Liraglutide and twincretin mitigate mTBI-induced neurodegeneration.
- Liraglutide and twincretin alleviate mTBI-induced elevation in microglial expression.
- mTBI challenge result in a decline in p-PKA levels in ipsilateral cortex.
- Liraglutide and twincretin attenuate mTBI-induced reduction in p-PKA expression.

**Keywords: glucagon-like peptide-1, glucose-dependent insulinotropic polypeptide, incretin, traumatic brain injury, concussive head injury, twincretin, liraglutide**

## INTRODUCTION

Traumatic brain injury (TBI) is a profound public health concern, affecting at least 1.7 million people in the United States alone each year and leading to diverse impairments, hospitalizations, and deaths (Faul et al., 2010). TBI has hence become a major economic burden, as the total annual cost of TBI in the United States including direct costs of medical treatments and deaths, as well as reduced productivity, was estimated to be 60.43 billion U.S. dollars, based on data from 2000 (Finkelstein et al., 2006). The major causes of TBI are falls, vehicle accidents, assaults, and sport injuries (Bruns and Hauser, 2003). These injuries are more frequent among men, especially adolescents and young adults, due to vehicle accidents and alcohol-related trauma, and the elderly due to a higher risk for falls (Moppett, 2007). Diagnosis of TBI relies mainly on clinical symptoms, including level of consciousness and amnesia, as well as CT findings evaluating morphological brain damage following exposure to injury (Tagliaferri et al., 2006; Maas et al., 2008). There is a growing body of evidence suggesting that TBI is a significant risk factor for the development of neurodegenerative diseases such as Parkinson's and Alzheimer's disease (Fleminger et al., 2003; Tweedie et al., 2013; Gardner and Yaffe, 2015).

Traumatic brain injury results in a myriad of pathophysiological changes that develop in two phases. Primary brain injury, which is a direct consequence of the external force exerted on the brain, consists of tissue distortion and destruction proximal to the injury and disruption of axons and small vessels, causing immediate necrotic neuronal cell death (Greve and Zink, 2009). Processes initiated during the primary phase lead to progressive and extended secondary damage, including neuroinflammation, oxidative stress, and glutamate excitotoxicity, which all contribute to neuronal apoptotic cell death (Werner and Engelhard, 2007; Greve and Zink, 2009).

Mild TBI (mTBI) accounts for approximately 80–90% of all TBI cases (Levin and Diaz-Arrastia, 2015). Although routine diagnostic evaluations of mTBI patients often fail to show clear structural brain damage, these patients frequently suffer short- and long-lasting cognitive, behavioral, and emotional impairments (Daneshvar et al., 2011). Such impairments include, among others, memory and concentration deficits, poor executive functions, depression, and anxiety-related disorders (Levin and Diaz-Arrastia, 2015). Continuation of these symptoms for 1–3 months post injury has been defined as "post-concussive syndrome" (PCS), whereas continuation for more than 3 months is defined as persistent PCS (PPCS). Some 50% of mTBI casualties suffer from PCS and 15% suffer PPCS for more than 1 year following the injury (Coronado et al., 2012); with a recent report suggesting yet higher rates (McInnes et al., 2017). Whereas clinical mTBI management generally includes assessment, observation, symptomatic treatment, and post-discharge follow-up, there remains a significant need to develop evidence-based interventions to mitigate long-term impairments and disabilities (Levin and Diaz-Arrastia, 2015).

The incretins, glucagon-like peptide-1 (GLP-1) and glucose-dependent insulinotropic polypeptide (GIP), are glucose-lowering, intestinal-derived peptides. Their receptors, GLP-1R and GIPR, are primarily localized to pancreatic islet cells and implicated in the treatment of type 2 diabetes mellitus (T2DM) (Lovshin and Drucker, 2009; Seino et al., 2010). However, both receptors are also present elsewhere and particularly throughout the nervous system, on the dendritic branches of neurons as well as on activated microglia and astrocytic cells (Hamilton and Holscher, 2009; Figueiredo et al., 2011). As incretins act protectively and trophically on β-cells (Trümper et al., 2001; Drucker, 2003; Li et al., 2003) and their receptors are coupled to the cAMP second messenger pathway whose upregulation is associated with neuroprotection and anti-inflammation (Tabuchi et al., 2002; Perry and Greig, 2003; Cui and So, 2004), the potential therapeutic benefit of incretin mimetics in brain pathologies is of growing interest. Our hypothesis is that incretin mimetics provide neurotrophic, protective, and anti-inflammatory processes, similar to their actions in

pancreas (Perry et al., 2002; Nyberg et al., 2005; Li et al., 2010b; Paratore et al., 2011).

In animal models, incretin analogs have been efficacious in preclinical models of: (i) Alzheimer's disease (Li et al., 2010a; McClean et al., 2011; Faivre and Holscher, 2013), (ii) Parkinson's disease (Bertilsson et al., 2008; Li et al., 2009, 2016), (iii) stroke and ischemia (Li et al., 2009; Hyun Lee et al., 2011), (iv) peripheral neuropathy (Perry et al., 2007), (v) amyotrophic lateral sclerosis (Li et al., 2012), (vi) Huntington's disease (Martin et al., 2009), and (vii) TBI (Rachmany et al., 2013; Li et al., 2015; Yu et al., 2016; Tamargo et al., 2017; Bader et al., 2019). Moreover, as marketed GLP-1 analogs to treat T2DM are well-tolerated and rarely cause hypoglycemia, clinical trials have been undertaken to investigate the therapeutic effects of exendin-4 or liraglutide on Alzheimer's disease (Egefjord et al., 2012; Gejl et al., 2016), and Parkinson's disease patients (Aviles-Olmos et al., 2013; Athauda et al., 2017), and continue to be evaluated.

Previous studies by our group characterized select neuroprotective actions of liraglutide, a GLP-1 analog, and twincretin, a dual GLP-1 and GIP analog. Both analogs augmented cell viability following exposure to oxidative stress and glutamate excitotoxicity in neuronal cell cultures. The cAMP/PKA/CREB pathway apparently played an important role in these neuroprotective actions. Moreover, both agents mitigated short-term cognitive impairments in a concussive mTBI rodent model (Li et al., 2015; Tamargo et al., 2017), indicating translational relevance from cellular studies to *in vivo* ones.

The present study sought to provide a more comprehensive assessment of the potential therapeutic benefits of these incretin-based therapies on the cognitive deficits and brain pathology that occur following mTBI using the same rodent model that mimics key post concussive symptoms in humans. Specifically, the aim of the present study was to evaluate whether liraglutide and twincretin administration of a clinically translatable dose could mitigate mTBI-induced cognitive deficits, neuronal degeneration, and neuroinflammation, and to appraise which downstream cascade of GLP-1R/GIPR activation was primarily responsible for these neuroprotective actions. A secondary aim was to compare these two incretin-related therapeutic approaches to determine whether a therapeutic advantage exists in activating both GLP-1R and GIPR by twincretin in comparison to only the GLP-1R by liraglutide with clinically relevant doses.

# MATERIALS AND METHODS

## Experimental Animals

Adult ICR mice (6–8 weeks), weighting 31–34 g, were kept five per cage with food and water *ad libitum*, at a constant temperature of 22 ± 5°C and under 12 h light/dark cycle. All experimental procedures were conducted during the light phase of the cycle. Each mouse was used in only one experiment and all efforts were made to minimize potential suffering. The Ethics Committee of the Sackler Faculty of Medicine approved the experimental protocol (M-14-050 and M-15-011), in compliance with the guidelines for animal experimentation of the National Institutes of Health (DHEW publication 85-23, revised, 1995).

## Mild Traumatic Brain Injury Model

Head injury was induced using a weight drop head trauma device, as previously described (Zohar et al., 2003; Milman et al., 2005). This device is composed of a metal tube (80 cm long, 13 cm inner diameter) and a sponge under the tube to support the head of the mice. The mice were lightly anesthetized by inhalation of isoflurane and put under the device. A metal weight (30 g) was then dropped from the top of the 80 cm tube to strike the head of the mouse on the right temporal side between the corner of the eye and the ear. Immediately following the injury, mice were put back in their original cages for recovery. Sham mice were treated similarly to mTBI challenged mice. They were anesthetized by isoflurane and aligned under the weight drop device, but not exposed to the injury. They were then returned to their cages for recovery. Sham and mTBI mice were indistinguishable following their recovery from the procedure. Body temperature has been shown to be maintained in our previous studies with this procedure, and the selection of animal number for individual studies (whether behavioral, immunohistochemical, or biochemical) was determined from the variance in the data of our prior studies.

## Drug Administration

246.7 μg/kg of liraglutide or 50 μg/kg twincretin prepared in isotonic saline was administered to mice once daily in a 7-day regimen of subcutaneous (s.c.) injections, with the first injection given 30 min following the injury. Liraglutide dose (246.7 μg/kg/day) is equivalent to the common human dose (20 μg/kg/day) normalized to body surface area across species based on FDA guidelines (U.S. Department of Health and Human Services et al., 2005). Twincretin dose (50 μg/kg/day) was chosen based on previous studies in mice diabetes model (Finan et al., 2013) and on the manufacturer's recommendation. Notably, twincretin and liraglutide are used in humans at the same dose; specifically, both at 1.8 mg daily by s.c. administration. Translation of this 1.8 mg dose in an 88.8 kg human across species is approximately 246.7 μg/kg in a mouse for each agent. However, in the current mouse study, the twincretin selected dose was fivefold lower; specifically 50 μg/kg. This dose was based on preliminary studies indicating that it was on the linear portion of the dose–response curve. Mice were randomly divided into four groups: a sham group, an mTBI group, a liraglutide following mTBI group, and a twincretin following mTBI group. Sham and mTBI mice were injected by saline in the same regimen as treatment groups.

## Experimental Procedures

The timeline of the experimental procedures following exposure to mTBI is shown in **Figure 1**. Mice were subjected to mTBI and 30 min later, a 7-day regimen of either liraglutide or twincretin treatment was initiated. The behavioral tests were performed at 7 or 30 days following the injury in separate groups of animals. Immunohistochemical staining assessments were performed on brains that were collected 72 h post injury.

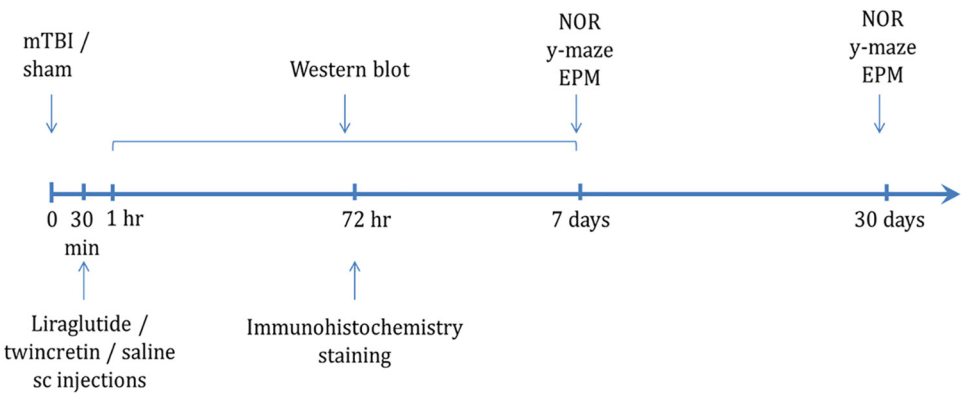


**FIGURE 1 |** Scheme of study design time line. Animals were exposed to sham/mTBI and 30 min later were given liraglutide (247.6 μg/kg), twincretin (50 μg/kg), or saline once daily via s.c. injections for 7 days {the human dose of liraglutide and twincretin is 1.8 mg s.c. daily that, for a 88.8 kg human [the mean weight of a male American (Yuan et al., 2017)], following normalization to body surface area across species in line with U.S. Department of Health and Human Services Food and Drug Administration guidelines (Han et al., 2016), translates to a mouse dose of approximately 247.6 μg/kg}. Behavioral tests to assess behavior and cognitive abilities were carried out 7 and 30 days following mTBI in separate cohorts of animals. Immunohistochemical staining to evaluate neurodegeneration and neuroinflammation was performed 72 h following mTBI challenge. Western blot analysis to assess changes in neuroprotective protein levels following mTBI and drug treatments was performed starting from 1 h to 1 week post mTBI. Each experimental time point was performed using a different group of mice (NOR: novel object recognition paradigm; EPM: elevated plus maze paradigm).

Western blot analysis was carried out on brain tissue collected from 1 h to 1 week post mTBI.

## Behavioral Tests

Behavioral assessments were conducted 7 or 30 days post mTBI. Each mouse was used for one time point only. Mouse behavior and cognition were assessed using the elevated plus maze, novel object recognition (NOR) and Y-maze paradigms. All equipment used for the behavioral tests was cleaned with 70% ethanol between sessions to minimize any olfactory influences on behavior.

### Elevated Plus Maze Paradigm

The elevated plus maze was used to evaluate anxiety-like behavior of the mice, as previously described (Zohar et al., 2011). This test relies on the preference of rodents to explore enclosed darkened environments rather than open, bright, and elevated environments. In addition, this test was used to evaluate locomotor activity of the mice. The apparatus consisted of a black, four-armed Pexiglass maze, in which two of the arms have low walls (open—30 × 5 × 1 cm) and the other two arms have high walls (closed—30 × 5 × 15 cm). Similar arms face each other, and all have no roof. Each mouse was put in the middle of the apparatus, facing one of the open arms, and was allowed to explore the arena for 5 min. The amount of time the mice spent in the open arms and the number of entries to the open/closed arms was recorded. Longer duration of time spent within the open arms has been associated with lower anxiety levels (Belzung and Griebel, 2001), while higher number of entries to the open/closed arms is indicative to higher locomotor activity.

### Novel Object Recognition Paradigm

The NOR task was chosen to assess the recognition and visual memory of the mice, as previously described (Edut et al., 2011). This paradigm relies on the tendency of rodents to investigate novel objects within their environment rather than known ones. This task is used to evaluate whether a mouse is able to discriminate between a familiar and a novel object. The arena consists of an open field black Plexiglass box (59 × 59 × 20 cm size); 48 h prior to the test, mice were individually put in the empty arena for habituation for 5 min. 24 h later, the mice were exposed to two identical objects within the arena for 5 min. On the test day, 24 h later, one of the familiar objects was replaced with a novel one, and mice were allowed to explore the arena again for 5 min, during which the time spent near the novel and the familiar object was measured. A preference index was calculated as follows: (time near novel object − time near familiar object)/(time near novel object + time near familiar object) (Dix and Aggleton, 1999).

### Y-Maze Paradigm

The Y-maze paradigm was used to evaluate spontaneous exploration, responsiveness to novel environments and spatial memory function, as previously described (Baratz et al., 2010). This test relies on the preference of rodents to explore new environments rather than familiar ones. The apparatus consists of three-armed black Plexiglass maze with arms separated by 120°. Each arm was identical (8 × 30 × 15 cm); however, different spatial cues were placed in each arm (i.e., a triangle, a square, or a circle). The start arm was chosen randomly. In the first session of the test, the mouse was put in the start arm of the arena and allowed to explore another arm while the third one was blocked for 5 min. The mouse was then returned to its home cage for 2 min. Meanwhile, the arena was cleaned with 70% ethanol. In the second session of the test after an interval of 2 min, all arms were open for exploration for 2 min. The time the mouse spent in the familiar arm and in the new arm was measured. A preference index was calculated as follows: (time in

new arm − time in familiar arm)/(time in new arm + time in familiar arm) (Dix and Aggleton, 1999).

## Immunohistochemical Staining

Immunohistochemistry studies were performed on mouse hippocampal (CA3 and dentate gyrus) and lateral cortical tissue sections obtained from animals euthanized on day 3 after injury; 72 h after injury and initiation of the various treatments, mice were anesthetized with a combination of ketamine (100 mg/kg) and xylazine (10 mg/kg) and perfused transcardially with 10 ml phosphate buffered saline (PBS) followed by 20 ml of 4% paraformaldehyde (PFA) in 0.1 M phosphate buffer, pH 7.4. Brains were removed, fixed overnight in 4% PFA, and then placed in 1% PFA. Prior to sectioning, brains were transferred to 30% sucrose for 48 h. Frozen coronal sections (30 μm) were cut on a cryostat and collected serially from bregma ∼ −1.28 mm to ∼ −2.4 mm. The sections were placed in a cryoprotectant solution containing phosphate buffer, ethylene glycol, and glycerin, and stored at −20°C. In all groups of mice, sections from both hemispheres were stained and analyzed. Random free-floating sections were blocked by 0.1% Triton X-100 in PBS (PBST) and 10% normal horse serum for 1 h at 25°C and incubated for 48 h at 4°C with appropriate primary antibodies specific to key features of interest in our studies. Controls consisted of omission of primary antibodies. Brain sections from multiple groups were reacted in the same well and evaluations were made by an observer blinded to the treatment groups.

### FJB and NeuN Immuno-Staining

To assess the neurodegeneration occurring at an early stage following mTBI, we performed double-staining using Fluoro Jade B (FJB), a marker of degenerating neurons, and neuronal nuclear antigen (NeuN), a marker of mature neurons. Sections were incubated for 48 h with a mouse primary antibody that detects NeuN (Millipore; MAB377, 1:50 in incubation buffer). After NeuN incubation, sections were washed and incubated with a Cy3 labeled anti-mouse secondary antibody (Jackson; 715-165-150, 1:300 incubation buffer). The probed sections were mounted onto 2% gelatin coated slides and stained with FJB (Millipore; AG310), as described by Schmued and Hopkins (2000). The brain sections were observed using a Zeiss Axiovert 200 fluorescence microscope (Zeiss), using a ×20 magnification. For each brain, three to four sections were used to capture six to eight images from the hippocampus (CA3 and dentate gyrus) and cortex. A ratio of the number of degenerating neurons (FJB positive cells) to the number of mature neurons (NeuN positive cells) was used as an index of trauma-induced neuronal degeneration. Images were taken from both sides of the brain, and subsequently, were quantitively analyzed using ImageJ 1.50i software to provide a mean value for each brain region.

### GFAP/Iba-1 Immuno-Staining

To assess changes in the expression of reactive astrocytes and activated microglia, sections were incubated for 48 h with rabbit glial fibrillary acidic protein (GFAP) primary antibody (Dako; Z0334, 1:500 in incubation buffer) or with rabbit ionized calcium-binding adapter molecule 1 (Iba-1) primary antibody (Wako; 019-19741, 1:500 in incubation buffer), respectively. The sections then were washed and incubated with donkey anti-rabbit secondary antibody (Abcam; Alexa Fluor® 594 ab150064, 1:300 in incubation buffer). After rinsing with PBST, sections were mounted onto 2% gelatin-coated slides. The brain sections were observed using a Leica SP5 confocal microscope (Leica, Germany), using a ×40 magnification. For each brain, three to four sections were used to capture six to eight images from the hippocampus (CA3 and dentate gyrus) and cortex. Images were taken from both sides of the brain, and subsequently, were quantitively analyzed using the Imaris software (Bitplane AG, Zurich, Switzerland) to provide a mean value for each brain region.

## Western Blotting

To assess the phosphorylated PI3K/PKA levels in mouse cortex and hippocampus, brains were collected following cervical translocation 1 h to 1 week following mTBI induction. Right/left cortex and right/left hippocampus were separated and frozen in liquid nitrogen, then stored in −80°C. Thereafter, brains were dissociated and homogenized in a buffer lysis (Tissue Protein extraction Reagent, Pierce) supplemented with a protease inhibitor cocktail (Halt Protease Inhibitor Cocktail, Sigma–Aldrich) using a Teflon pestle homogenizer. Homogenates were centrifuged for 15 min at 4°C and 14,000 r/min and the supernatant liquids were separated from the precipitates and stored at −80°C. Sample buffer was added to the samples and then stored at −20°C. Samples were heated to 90°C for 3 min; 30 μl of each sample was then loaded and run on 4–20% Mini-Protean TGX gels (Bio-Rad; 456-1094) followed by transfer onto nitrocellulose membranes (Bio-Rad; 1704159) by a transfer system (Trans-Blot Turbo, Bio-Rad). Afterward, blots were blocked for 1 h at room temperature, with Tris-buffered saline, containing 0.01% Tween-20 and 5% BSA or powdered milk. Membranes were then incubated overnight at 4°C with a rabbit primary phospho-PI3K antibody (Cell signaling; 4228, 1:1000) or a rabbit primary phospho-PKA antibody (Cell signaling; 5661, 1:900) followed by washings with TTBS. Membranes were then incubated at room temperature for 1 h with horseradish peroxidase-conjugated goat anti-rabbit antibody (Jackson; 111-035-003, 1:10,000). Bands were then visualized using enhanced chemiluminescence reagents for 1 min (enhanced chemiluminescence assay) (Millipore, Billerica, MA, United States) by Viber Fusion FX7 imaging system (Viber Lourmat, France). A densitometry analysis of the detected signal was made using ImageJ software. Uniform loading was verified by stripping and re-probing with a mouse primary α-tubulin antibody for 30 min in room temperature (Santa Cruz; sc-53030, 1:10,000), followed with conjugated goat anti-mouse secondary antibody (Jackson, 115-035-003, 1:10,000). The value of each sample was determined by the ratio of p-PI3K or p-PKA and α-tubulin. Averages of control values in each membrane were set to 1, and all other samples were calculated accordingly.

## Data Analysis

All results are presented as mean ± SEM and were analyzed by SPSS V 25 software. One-way ANOVA tests were performed for comparisons between multiple datasets, followed by Fisher's least significant difference (LSD) *post hoc* analysis, when found significant. Significant values between means are expressed as $^{*}p < 0.05$, $^{**}p < 0.01$, $^{***}p < 0.001$.

# RESULTS

## mTBI Exposure and Liraglutide/Twincretin Treatment Has No Effect on Anxiety and General Well-Being of the Mice

Following mTBI exposure and treatment with either liraglutide or twincretin, male ICR mice were evaluated using the elevated plus maze at 7 and 30 days post mTBI among separate cohorts. Specifically, two parameters were evaluated, the anxiety-like behavior and locomotor activity of the mice, by recording the time spent in the open arms of the maze and the total number of entrances to each arm of the maze, respectively.

As illustrated in **Figures 2A,B**, there were no differences in the time spent in the open arms between all groups at both time points tested, indicating that anxiety-like behavior of the mice was not affected either by the injury or by treatment with either liraglutide or twincretin.

Evaluation of the locomotor activity of the same animals revealed all groups had an approximately equal number of entrances to the arms of the maze and were not differentiated from one another at either 7 or 30 days post injury (**Figures 2C,D**), suggesting that the locomotor activity of the mice was unaffected by mTBI challenge or by liraglutide/twincretin treatment. Hence, mTBI and drug actions on anxiety and locomotor were not evident and cannot be considered caveats when evaluating actions on cognition.

## Liraglutide or Twincretin Treatment Reverses mTBI-Induced Cognitive Impairments in Mice

To assess the effects of liraglutide and twincretin treatment on post mTBI memory formation, the NOR and Y-maze paradigms were performed on mice at 7 and 30 days post injury, which received sham procedure, mTBI, or mTBI followed by either liraglutide or twincretin treatment. The time that mice spent investigating the novel/familiar object or arm was recorded, and a preference index was then calculated.

We have previously demonstrated that mice challenged with mTBI demonstrate cognitive impairments in visual and spatial memory, as evaluated by the NOR and Y-maze paradigms, respectively, and, notably, that liraglutide and twincretin ameliorate these impairments (Li et al., 2015; Tamargo et al., 2017). We show, herein, similar experiments with a direct comparison between the two drugs using doses relevant to clinical utilization of these agents [specifically, the selected liraglutide dose (246.7 μg/kg/day) translates across species to the human dose routinely used in T2DM; whereas the twincretin dose (50 μg/kg/day) translates to one-fifth of the dose used in humans]. There are two rationales for this approach. First is a cross validation with our previous work. Second, and particularly importantly, the immunohistochemical and molecular studies detailed below have not been previously undertaken for either liraglutide or twincretin, and were performed using brain tissue from a population of behaviorally evaluated animals.

The NOR test was used to examine visual recognition memory. mTBI-challenged mice suffered a significant visual memory deficit, evidenced by a reduced novel object exploration time compared to sham mice at both 7 and 30 days post injury ($p < 0.001$, **Figures 3A,B**). This deficit was substantially ameliorated by either liraglutide or twincretin treatment ($p < 0.01$). Importantly, at both 7 and 30 days post injury in separate cohorts of mice, liraglutide treatment demonstrated only partial recovery, as compared to controls, whereas twincretin resulted in full recovery. Notably, twincretin treated mTBI mice demonstrated significantly higher object discriminatory preference as compared to liraglutide treated mice ($p < 0.05$).

The Y-maze paradigm was implemented to evaluate the spatial memory. At both time points evaluated, mTBI-challenged mice experienced spatial memory impairment, as compared to sham mice ($p < 0.001$, **Figures 3C,D**); spending similar times exploring each arm of the maze. Treatment with either liraglutide or twincretin fully attenuated this impairment at both times tested ($p < 0.001$), with no observed superiority for one or the other treatments.

## Liraglutide or Twincretin Treatment Reduces mTBI-Induced Neuronal Degeneration

Assessment of degenerating neurons induced by mTBI was undertaken immunohistochemically using FJB staining and a NeuN antibody at 72 h following the injury. Three different brain areas were evaluated: the temporal cortex, CA3 region, and the dentate gyrus. FJB is widely used to label neurons that are undergoing degenerative processes, since it specifically binds to degenerating neurons. NeuN antibody is routinely used to detect mature neurons, as it specifically recognizes the DNA-binding neuron-specific protein NeuN. A ratio of the degenerating neurons in each area was determined as: number of cells undergoing degeneration/number of mature cells (FJB/NeuN). The larger this ratio, the greater the extent of the neuronal degeneration. mTBI challenge resulted in a significant elevation in degenerating neurons as compared to the sham procedure ($p < 0.001$, **Figure 4**). This cellular loss was diffuse and occurred throughout each of the three evaluated brain regions. Importantly, mTBI-induced neurodegeneration was both substantially and significantly mitigated by treatment with either liraglutide or twincretin ($p < 0.001$), and the FJB/NeuN ratios from drug-treated groups were similar to those of controls. There was no additional therapeutic benefit observed for twincretin compared to liraglutide treatment.

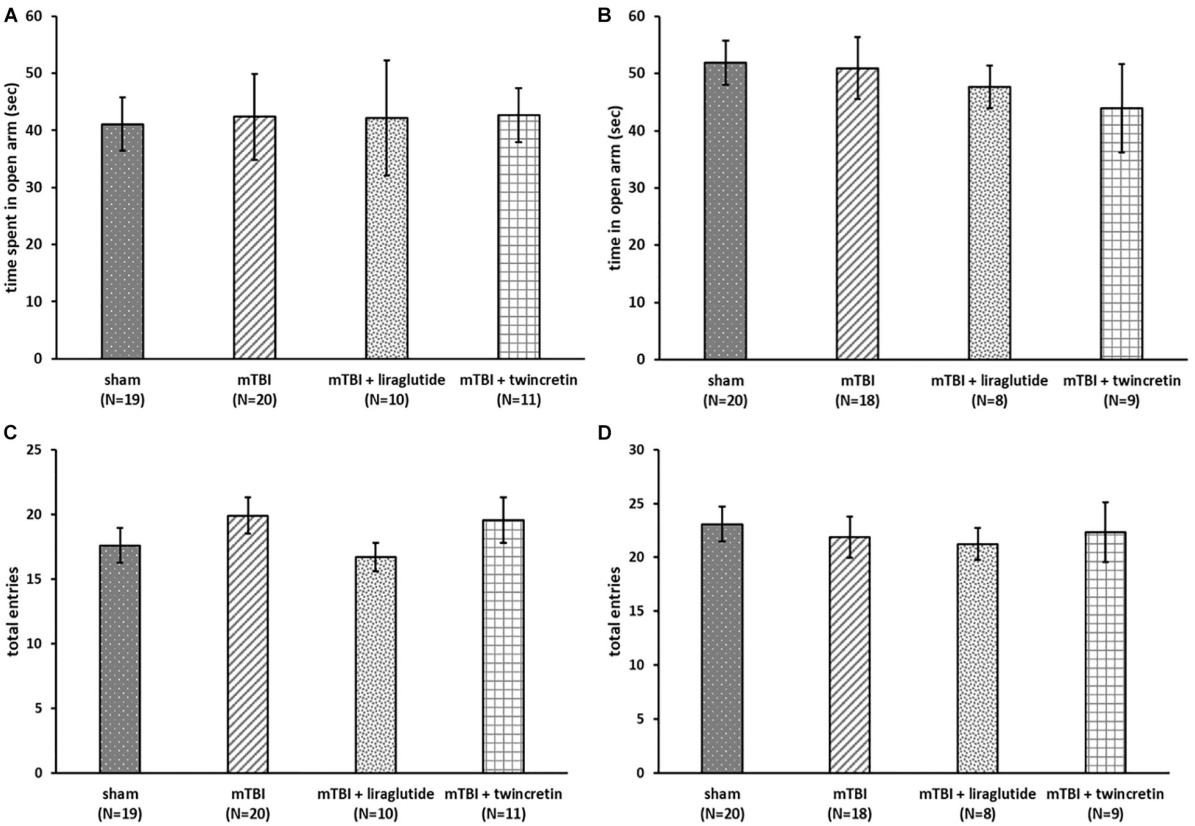


**FIGURE 2 |** mTBI exposure and liraglutide/twincretin treatment do not impact the overall condition of the mice, as assessed in the elevated plus maze at both 7 and 30 days post trauma. Anxiety-like behavior assessment at 7 **(A)** and 30 **(B)** days post injury. The time spent in open arms of the maze was recorded and compared between groups. One-way ANOVA analysis showed that there were no differences between groups and that all groups of mice spent equivalent times in the open arms at both 7 and 30 days post mTBI [**A:** $F(3,56) = 0.064$; NS and **B:** $F(3,51) = 0.374$; NS]. Values are mean ± SEM. Locomotor activity at 7 **(C)** and 30 **(D)** days post injury. The number of total entrances to the arms of the maze was recorded and compared between groups. One-way ANOVA analysis demonstrated that there were no differences between the groups and all groups of mice had an approximately equal number of entrances to the arms at both 7 and 30 days post mTBI [**C:** $F(3,56) = 0.830$; NS, and **D:** $F(3,51) = 0.218$; NS]. Values are mean ± SEM.

## Liraglutide/Twincretin Treatment Mitigates mTBI-Induced Neuroinflammation by Reducing Activated Microglial Expression, but Does Not Impact Astrogliosis

Evaluation of neuroinflammatory processes occurring subsequent to mTBI exposure was obtained by immunohistochemical staining using two different antibodies; GFAP labels reactive astrocytes and Iba-1 labels microglia. These were likewise studied across three different brain regions: temporal cortex, CA3 region, and the dentate gyrus, 72 h post injury. Increases in the expression and activation of astrocytes and microglia, together with acute upregulation of proinflammatory cytokines such as interleukin (IL)-1β, tumor necrosis factor (TNF)-α, and IL-6 (Patterson and Holahan, 2012), are key components in injury processes evident following mTBI. mTBI exposure induced a significant elevation in astrocyte and microglial reactivity within all three brain regions examined ($p < 0.01$ and $p < 0.05$, respectively, **Figures 5**, **6**). Treatment with neither liraglutide nor twincretin affected the mTBI-induced elevation in GFAP expression (**Figure 5**). However, both treatments equally reduced Iba-1 elevated immunoreactivity caused by mTBI challenge ($p < 0.05$, **Figure 6**).

## mTBI Induction Causes a Reduction in PKA Expression in the Ipsilateral Cortex but Does Not Affect PI3K Levels

To assess the effect of mTBI on the levels of neuroprotective proteins downstream to activation of GLP-1/GIP receptors, Western blot analysis was performed to quantify the levels of the phosphorylated form of PKA and PI3K in a time-dependent manner (1, 24, 48, and 72 h and 1 week post trauma) in four different brain regions: ipsilateral (right)/contralateral (left) cortex, and ipsilateral/contralateral hippocampus. Following activation of GLP-1R/GIPR, activated PKA is involved in the cAMP/PKA/CREB signaling pathway, whereas activated PI3K is involved in the PI3K/AKT pathway (Li et al., 2010b; Kim et al., 2017; Athauda and Foltynie, 2018). Both pathways promote cell

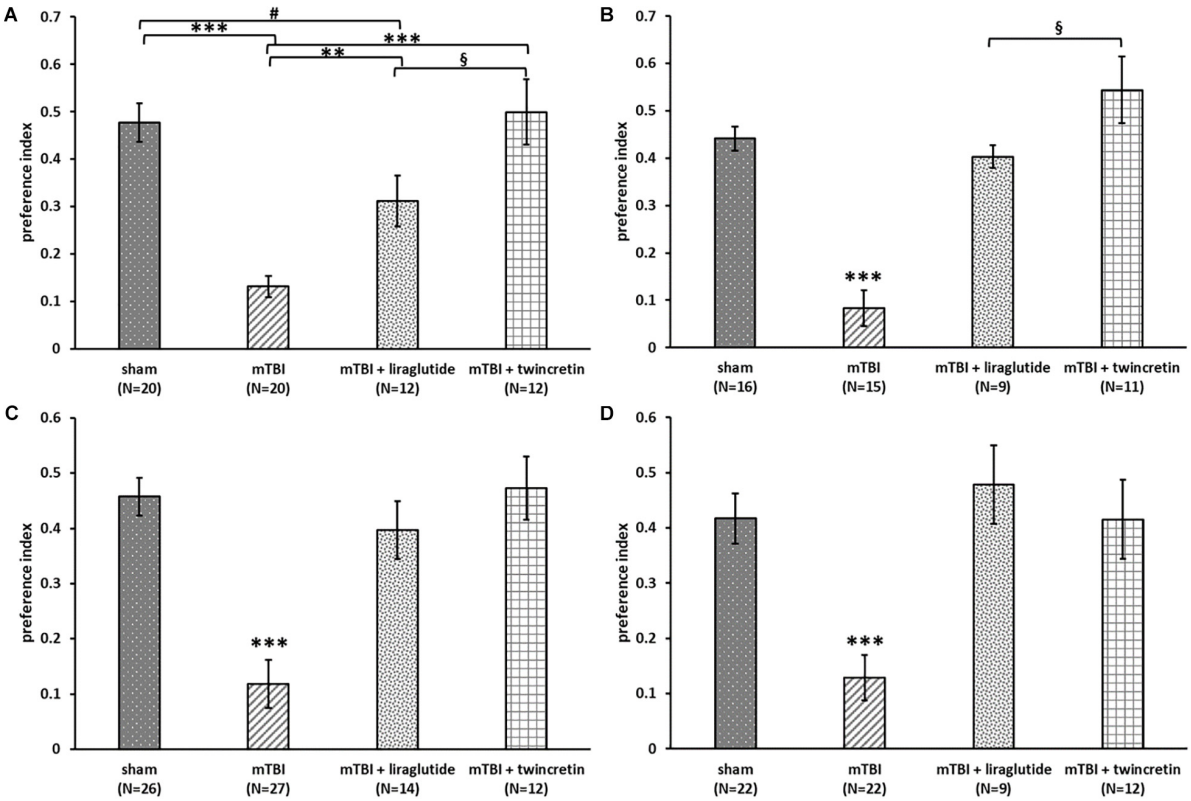


**FIGURE 3 |** Liraglutide and twincretin treatments lead to improvement in mTBI-induced cognitive impairments at both 7 and 30 days post trauma. Visual memory was assessed using the novel object recognition (NOR) paradigm at 7 days **(A)** and 30 days **(B)** post injury. Preference index was used to represent the relative time that animals spend exploring a novel object compared to a familiar one, which reflects visual memory. One-way ANOVA test followed by Fisher's LSD *post hoc* analysis revealed that the preference index of mTBI group was significantly lower than all other groups at both time points [**A:** $F(3,60) = 17.135$; $p < 0.001$ and **B:** $F(3,47) = 23.22$; $p < 0.001$, $^{**}p < 0.01$, $^{***}p < 0.001$). The preference index of the liraglutide treated group was significantly lower than sham and twincretin treated group at 7 days ($\#p < 0.05$ vs. sham and $\S p < 0.05$ vs. mTBI + liraglutide), while only lower than twincretin treated group at 30 days ($\S p < 0.05$ vs. mTBI + liraglutide). Values are mean ± SEM. Spatial memory was evaluated using the Y-maze paradigm at 7 **(C)** and 30 days **(D)** post injury. Preference index was used to represent the relative time that animals spent exploring a novel arm of the maze compared to a familiar one, reflecting spatial memory. One-way ANOVA followed by Fisher's LSD *post hoc* analysis revealed that the preference index of mTBI group was significantly lower than all other groups at both time points [**C:** $F(3,75) = 15.851$; $p < 0.001$ and **D:** $F(3,61) = 9.811$; $p < 0.001$, $^{***}p < 0.001$]. Treatment with either liraglutide or twincretin led to similar normalization. Values are mean ± SEM.

survival as well as neurite outgrowth, memory formation, and inhibition of apoptosis. mTBI challenge resulted in reduced levels of p-PKA in the ipsilateral cortex evident between 24 h to 1 week post mTBI (24–48 h: $p < 0.001$, 72 h–1 week: $p < 0.05$), whereas all other brain regions remained unaffected [**Figure 7** (please note that in **Figure 7F**, sample no. 2 of the original membrane was cropped from the image, as noted in the figure legend)]. In contrast, mTBI did not significantly alter PI3K phosphorylation levels across any of the brain regions (**Figure 8**).

## Liraglutide/Twincretin Treatment Attenuates mTBI-Induced Decline in p-PKA Expression in the Ipsilateral Cortex

As mTBI induced a significant change in expression of only p-PKA in ipsilateral cortex (**Figure 7A**), the effect of liraglutide or twincretin on p-PKA in this area was assessed at the most affected time point: 48 h. Treatment with either liraglutide or twincretin rescued the significant reduction in p-PKA expression 48 h following mTBI induction in the ipsilateral cortex ($p < 0.01$, **Figure 9**, please note that the order of the samples is not as in the original image of the membrane). Both treatments had similar efficacy.

# DISCUSSION

The present study proposes a potential therapeutic strategy to treat mTBI sequalae. Incretin analogs have successfully been used to treat T2DM for many years and are well tolerated. In addition to their insulinotropic actions, incretins promote pancreatic β-cell proliferation and inhibit apoptotic processes in these cells (Baggio and Drucker, 2007; Seino et al., 2010). These protective and trophic effects, along with enhanced memory formation, are evident in the brain (Perry et al., 2002; During et al., 2003;

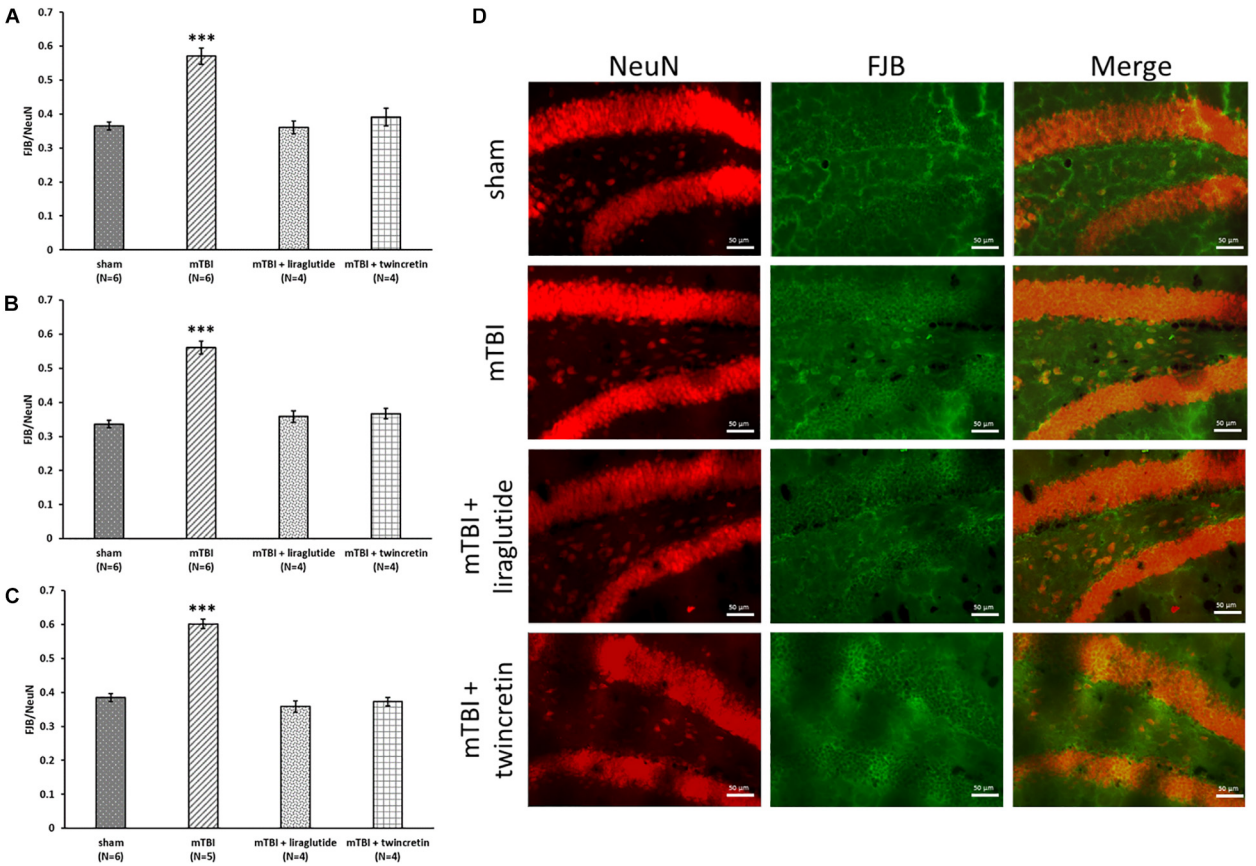


**FIGURE 4 |** Liraglutide and twincretin treatments mitigate mTBI-induced neurodegeneration, 72 h post trauma. Graphs showing the quantification of degenerating neurons as the ratio of FJB/NeuN in the temporal cortex **(A)**, CA3 region **(B)**, and the dentate gyrus **(C)**. One-way ANOVA test followed by Fisher's LSD *post hoc* analysis demonstrated that mTBI induction led to significant elevation in the ratio of degenerating neurons compared to sham tissues in all regions tested [**A:** $F(3,16) = 26.695$; $p < 0.001$, **B:** $F(3,16) = 48.130$; $p < 0.001$, and **C:** $F(3,15) = 73.021$; $p < 0.001$, $^{***}p < 0.001$]. Treatment with either liraglutide or twincretin caused a significantly lower FJB/NeuN ratio compared to mTBI ($^{***}p < 0.001$), suggesting a reduction in the development of neurodegeneration following the injury. Values are mean ± SEM. **(D)** Representative images of immunohistochemical staining in the dentate gyrus are presented. NeuN positive cells are shown in red and FJB positive cells are shown in green; merged images show the overlap of FJB/NeuN positive cells. The scale bars are 50 µm.

Nyberg et al., 2005; Li et al., 2009, 2010b; Paratore et al., 2011) since incretins cross the blood–brain barrier (BBB) and their receptors are expressed on neurons throughout the brain (Hamilton and Holscher, 2009; Figueiredo et al., 2011; Spielman et al., 2017). Numerous preclinical studies have emphasized the neuroprotective and neurotrophic actions of incretins and analogs in different rodent models of neurological disorders and neurodegenerative diseases, in which incretin mimetics enhanced memory and learning, promoted neuronal survival, induced neurogenesis, and inhibited neuroinflammation (Perry et al., 2007; Bertilsson et al., 2008; Li et al., 2009, 2016; Holscher and Li, 2010; McClean et al., 2011; Faivre and Holscher, 2013; Kim et al., 2017). Since findings from these preclinical studies were promising, GLP-1 analogs are now being investigated in humans in clinical trials for treatment of Alzheimer's disease (Egefjord et al., 2012; Gejl et al., 2016) and Parkinson's disease (Aviles-Olmos et al., 2013; Athauda et al., 2017, 2019). While several pharmacological treatments besides incretin analogs have been identified for these neurodegenerative diseases, TBI lacks any evidence-based treatment (Levin and Diaz-Arrastia, 2015). Therefore, investigation for a potential therapy that may alleviate the cognitive, behavioral, and emotional deficits occurring after TBI is important.

The pathophysiology of mTBI is complex and characterized especially by neuronal cell death and axonal damage induced primarily by the direct physical impact itself and secondarily by oxidative stress, neuroinflammation, mitochondrial dysfunction, DNA damage, and other pathological processes (Maas et al., 2008; Choe, 2016; McInnes et al., 2017). Since incretins have the capability to intervene in more than one of these pathological events (Perry et al., 2002; Nyberg et al., 2005; Iwai et al., 2006; Li et al., 2010b; Paratore et al., 2011; Yu et al., 2016; Verma et al., 2017), incretin mimetics have the potential to serve as neuroprotective agents following mTBI.

Our previous studies focused on the effects of several clinically relevant incretin analogs on mTBI-induced impairments in cellular and rodent mTBI models following administration of clinically translatable doses (Glotfelty et al., 2019). Specifically,

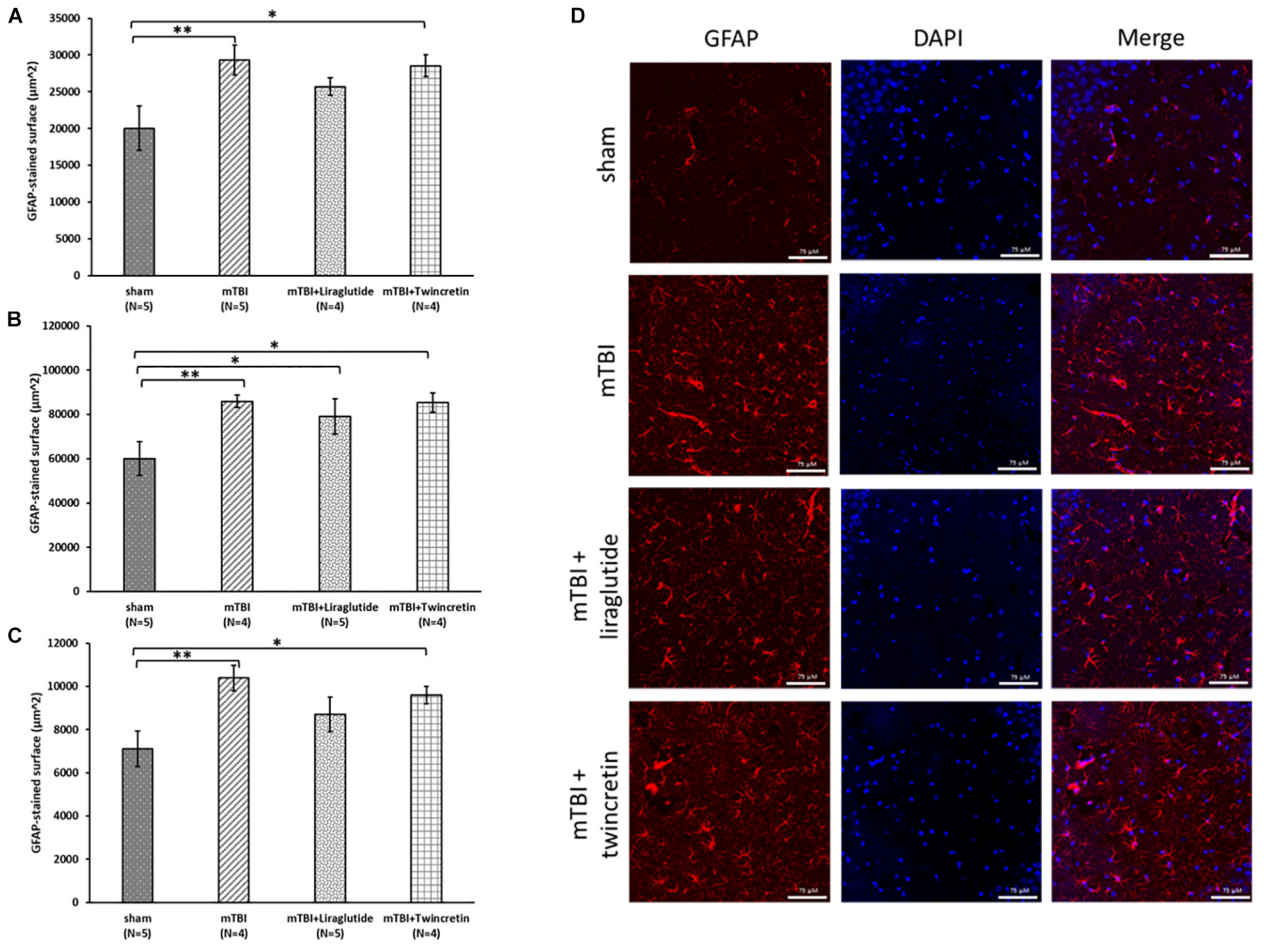


**FIGURE 5 |** Liraglutide and twincretin treatments do not affect the mTBI-induced elevation in reactive astrocyte expression, 72 h post trauma. Graphs presenting quantification of the total surface labeled with GFAP in the temporal cortex **(A)**, CA3 region **(B)**, and the dentate gyrus **(C)**. One-way ANOVA followed by Fisher's LSD *post hoc* analysis revealed that mTBI induction resulted in a significant elevation in GFAP expressing cells compared to sham tissues in all regions tested [**A:** $F(3,14) = 3.917$; $p < 0.05$, **B:** $F(3,15) = 3.785$; $p < 0.05$, and **C:** $F(3,15) = 4.178$; $p < 0.05$, $^{**}p < 0.01$]. Treatment with neither liraglutide nor twincretin affected this elevation as compared to mTBI. Liraglutide treatment following mTBI did not prevent the elevation in GFAP expression as compared to sham mice in the CA3 region ($^{*}p < 0.05$); GFAP expression in the twincretin treatment group was significantly higher than control in all three regions ($^{*}p < 0.05$). Values are mean ± SEM. **(D)** Representative images of immunohistochemical staining in the CA3 region are presented. GFAP positive cells are shown in red and DAPI positive cells are shown in blue. The scale bars are 75 μm.

we demonstrated the efficacy of exendin-4 (a GLP-1 analog), liraglutide (a long acting GLP-1 analog), twincretin (a dual GLP-1/GIP analog), and PT302 (a sustained release formulation of the GLP-1 analog Exanatide) to mitigate cellular damage associated with mTBI pathologies such as oxidative stress, glutamate induced toxicity, and apoptotic cell death. Moreover, these agents were successful in ameliorating the cognitive deficits evident following exposure to mTBI in mice (Rachmany et al., 2013; Li et al., 2015; Tamargo et al., 2017; Bader et al., 2019; Glotfelty et al., 2019) and other mTBI-induced brain pathologies such as neurodegeneration and neuroinflammation (Bader et al., 2019).

In the current study, we aimed for a more comprehensive and comparative evaluation of the potential benefit of enhancing incretin activity in the brain on mTBI-induced cognitive, cellular, and molecular impairments. To this end, we examined whether liraglutide and twincretin could be used as neuroprotective agents in a preclinical mTBI mouse model. In addition, we sought to assess whether there was a therapeutic advantage in jointly activating the two incretin receptors by twincretin vs. single GLP-1R activation by liraglutide. Liraglutide is an FDA approved treatment for T2DM, whereas twincretin is under investigation in ongoing clinical trials to treat T2DM (Finan et al., 2013; Frias et al., 2017; Portron et al., 2017; Schmitt et al., 2017).

Mice were exposed to mTBI using our well-characterized closed-head weight drop model that mimics key mTBI symptoms and pathologies in humans (Zohar et al., 2003; Milman et al., 2005), and post injury were administered either liraglutide at a translatable dose to humans [247.6 μg/kg: equivalent to a 1.8 mg dose in a human of approximately 88.8 kg weight (the mean weight of a male American (U.S. Department of Health and Human Services et al., 2016)], following normalization to body surface area across species in line with FDA guideline

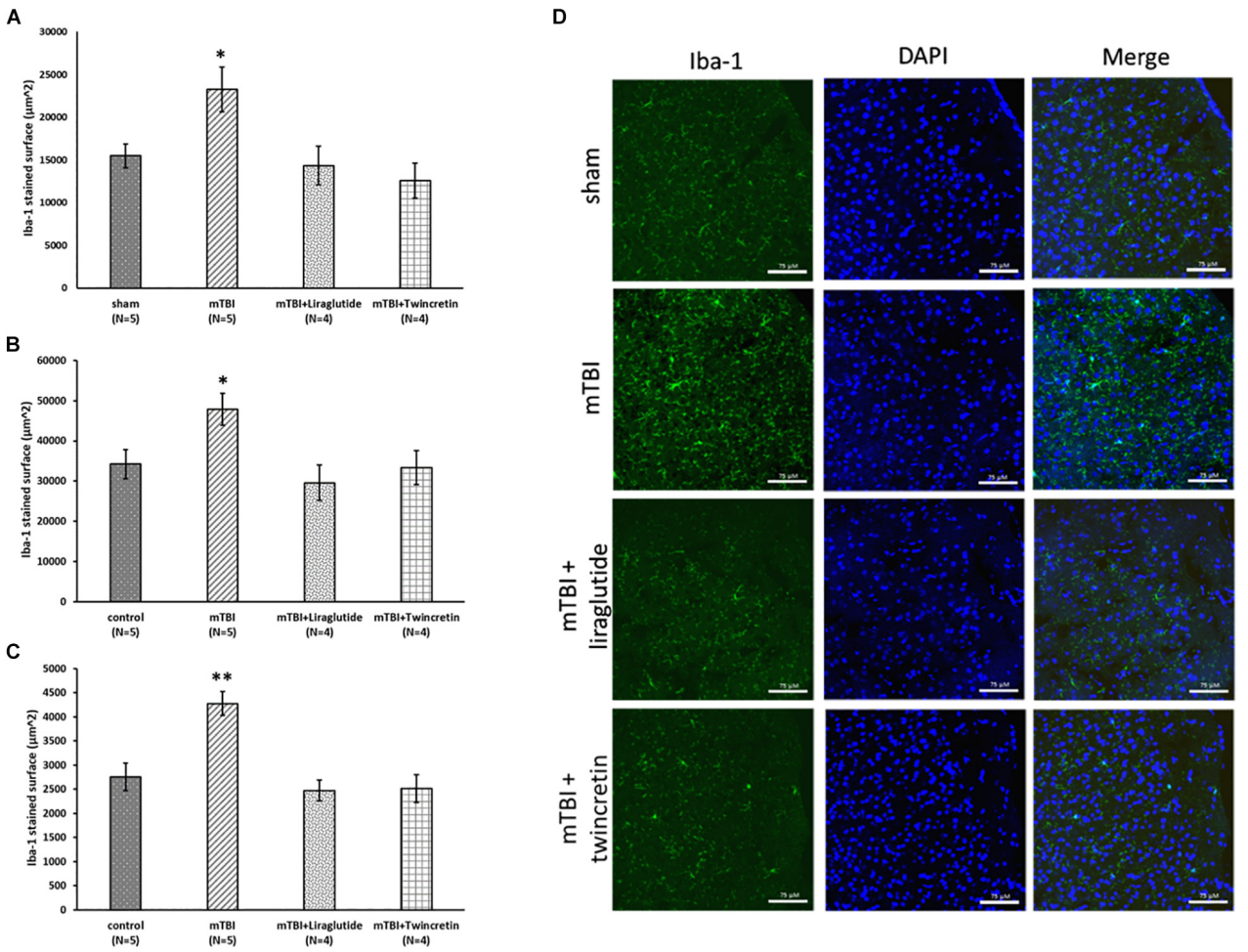


**FIGURE 6 |** Liraglutide and twincretin treatments reduce the mTBI-induced elevation in activated microglia expression, 72 h post trauma. Graphs presenting quantification of the total surface labeled with Iba-1 in the temporal cortex **(A)**, CA3 region **(B)**, and the dentate gyrus **(C)**. One-way ANOVA followed by Fisher's LSD *post hoc* analysis demonstrated that mTBI induction led to a significant elevation in Iba-1 expressing cells compared to sham tissues in all regions tested [**A:** $F(3,14) = 5.117$; $p < 0.05$, **B:** $F(3,14) = 4.060$; $p < 0.05$, and **C:** $F(3,14) = 11.102$; $p < 0.01$, $^{*}p < 0.05$ in the cortex and CA3 and $^{**}p < 0.01$ in the dentate gyrus]. Treatment with either liraglutide or twincretin following mTBI induction attenuated this elevation as compared to mTBI with no treatment. Values are mean ± SEM. **(D)** Representative images of immunohistochemical staining in the temporal cortex are presented. Iba-1 positive cells are shown in green and DAPI positive cells are shown in blue. The scale bars are 75 µm.

[U.S. Department of Health and Human Services Food and Drug Administration 2005 (U.S. Department of Health and Human Services et al., 2005)] or twincretin in a previously used efficacious dose in rodent models (50 µg/kg; Finan et al., 2013; Tamargo et al., 2017) by s.c. injections once a day for 7 consecutive days. Subsequently, mice were assessed behaviorally and cognitively, and brains of different mice cohorts were used for immunohistochemical staining and Western blot evaluations.

Mild TBI impairment in cognitive abilities was manifested in the NOR and Y-maze paradigms at both 7 and 30 days post mTBI (evaluated in separate cohorts of mice for each time point). Importantly, treatment with either liraglutide or twincretin protected against these short and longer term cognitive impairments, without impacting measures of anxiety or locomotor activity. Reports in the literature indicate that some TBI models can induce anxiety-like behavior (Washington et al., 2012), and there are accounts of anti-anxiety and antidepressant effects among GLP-1 and its analogs (Isacson et al., 2011; Anderberg et al., 2016). We avoided anxiety symptoms following the injury by using short-term anesthesia at the time of the TBI impact induction, to ensure that animals were unaware of the procedure. Hence, untoward actions on either anxiety or motor activity cannot be considered confounds when evaluating liraglutide and twincretin mitigation of mTBI-induced cognitive impairments, and these positive actions are in line with prior reports regarding the cognitive alleviation provided by incretin analogs following an mTBI challenge (Rachmany et al., 2013; Li et al., 2015; Tamargo et al., 2017; Bader et al., 2019; Glotfelty et al., 2019), as well as in Alzheimer's disease models (Faivre and Holscher, 2013; Shi et al., 2017; Batista et al., 2018; Glotfelty et al., 2019).

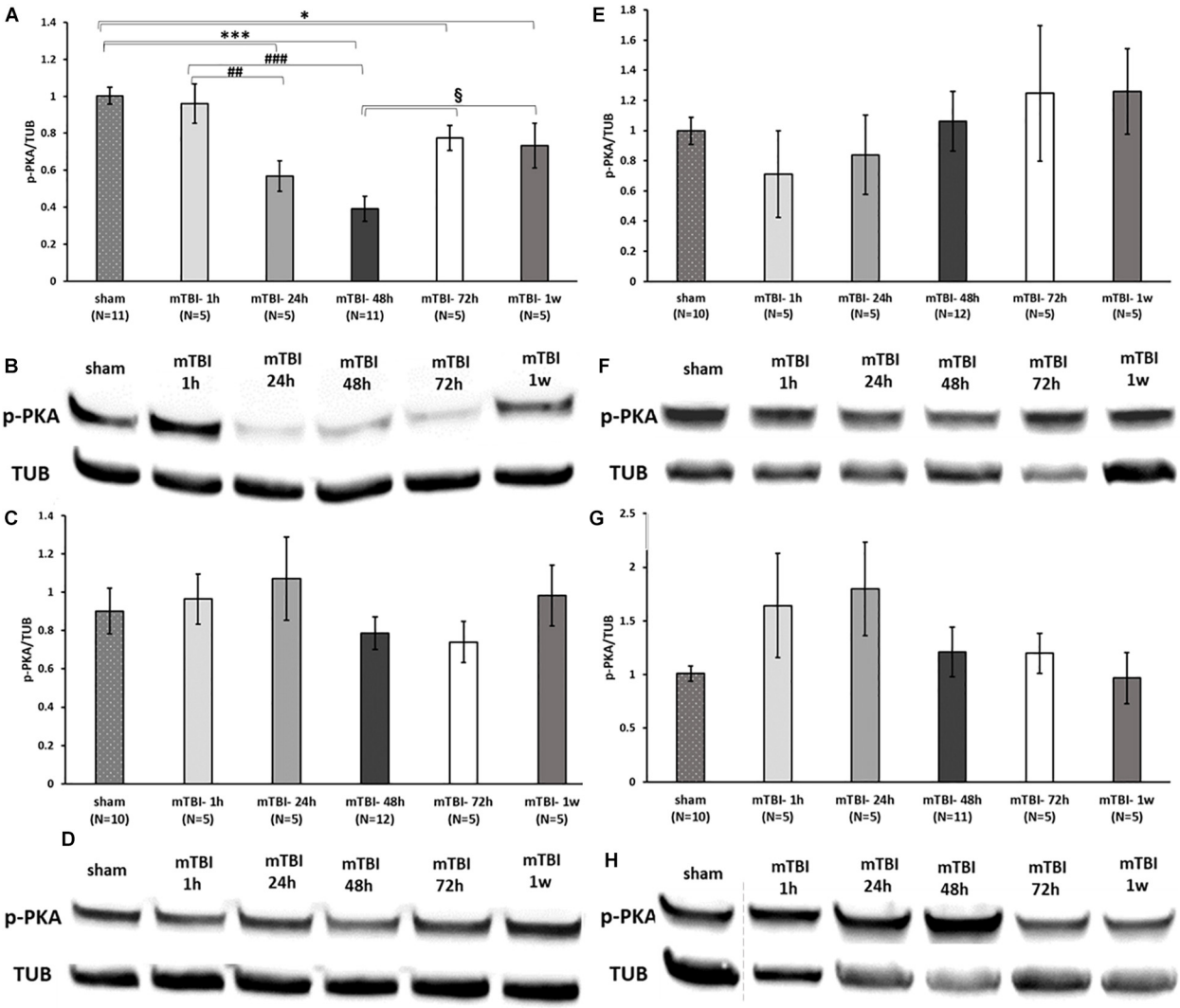


**FIGURE 7 |** mTBI results in a decline in p-PKA levels in ipsilateral cortex. Graphs presenting p-PKA expression in ipsilateral/right **(A)** and contralateral/left **(C)** cortex and ipsilateral **(E)** and contralateral **(G)** hippocampus in sham and 1 h to 1 week following mTBI. One-way ANOVA followed by Fisher's LSD *post hoc* analysis revealed a significant reduction in p-PKA expression in cortex right 24 h to 1 week following mTBI [**A:** $F(5,36) = 12.060$; $p < 0.001$, $^{***}p < 0.001$ sham vs. 24, 48 h and $^{*}p < 0.05$ sham vs. 72 h, 1 w], $^{\#\#}p < 0.01$, $^{\#\#\#}p < 0.001$ mTBI 1 h vs. mTBI 24 h and vs. 48 h, respectively, when the maximal reduction present in 48 h was followed by an elevation in the levels of PKA (72 h–1 week, §$p < 0.05$ vs. 48 h). Blots from all other regions remained unchanged by the injury [**C:** $F(5,36) = 0.809$; NS, **E:** $F(5,36) = 0.585$; NS, **G:** $F(5,35) = 1.373$; NS]. Values are mean ± SEM. **(B,D,F,H)** Representative images of gel electrophoresis followed by immunoblot analysis using antibodies against p-PKA and α-tubulin in ipsilateral cortex, contralateral cortex, ipsilateral hippocampus, and contralateral hippocampus, respectively. A crop of the original image was performed in 7F at loading site number 2 of the gel due to an abnormal value of a control sample that was therefore excluded from the statistical analysis.

In the NOR paradigm, treatment with twincretin, notably, resulted in significantly greater improvement in visual memory over that achieved by liraglutide, which likely is due to activation of both GLP-1R and GIPR, in contrast to liraglutide activation of GLP-1R alone. Several studies comparing the efficacy of dual GLP-1R/GIPR vs. a GLP-1R agonist across various pathologies, likewise, demonstrated a therapeutic advantage for the dual agonist. This was observed in diabetic (Finan et al., 2013), Parkinson's disease (Yuan et al., 2017), and ischemia (Han et al., 2016) models. In these prior studies, the same doses of the two substances were evaluated. In our study, however, the twincretin dose appraised (50 μg/kg) was, of note, some fivefold lower than liraglutide (247.6 μg/kg). Similarly, in the Y-maze paradigm in which an equal mitigation of mTBI-induced spatial memory loss was achieved with the two incretin mimetics, twincretin achieved this at one-fifth of the dose of liraglutide.

Our preliminary, dose-finding studies with twincretin in cellular and animal models demonstrated its greater potency over a single GLP-1R agonist at equimolar doses, and supported the evaluation of the selected twincretin 50 μg/kg dose (as opposed

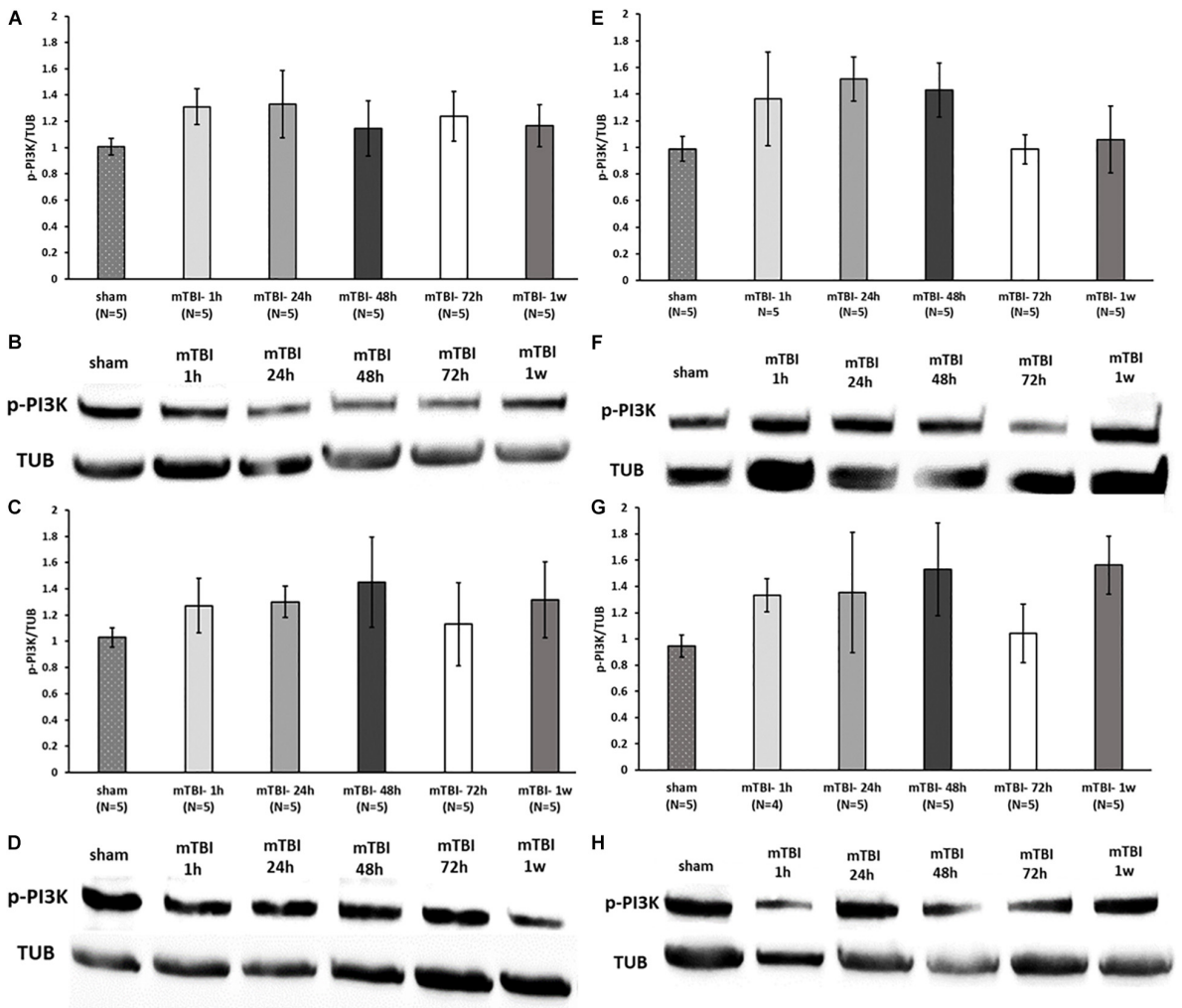


**FIGURE 8 |** mTBI challenge does not affect the p-PI3K levels in the cortex and hippocampus. Graphs showing p-PI3K expression in ipsilateral/right **(A)** and contralateral/left **(C)** cortex and ipsilateral **(E)** and contralateral **(G)** hippocampus in sham and 1 h to 1 week following mTBI. One-way ANOVA analysis showed no significant differences between the groups in all brain regions, indicating that mTBI induction does not affect the p-PI3K levels at the times tested [**A:** $F(5,24) = 0.538$; NS, **C:** $F(5,24) = 0.365$; NS, **E:** $F(5,24) = 1.236$; NS, **G:** $F(5,23) = 0.813$; NS]. Values are mean ± SEM. **(B,D,F,H)** Representative images of gel electrophoresis followed by immunoblot analysis using antibodies against p-PI3K and α-tubulin in ipsilateral cortex, contralateral cortex, ipsilateral hippocampus, and contralateral hippocampus, respectively.

to the 247.6 μg/kg dose), as the former appeared to be at the top end of the linear portion of the dose–response curve. In this context, twincretin provides a potential advantage in terms of potency over liraglutide, as in ongoing clinical trials twincretin (also known as RG7697 and NNC 0090-2746; Frias et al., 2017; Portron et al., 2017; Schmitt et al., 2017) is currently being evaluated at a dose of 1.8 mg, and appears to be well tolerated and efficacious. As noted, the clinically approved dose of liraglutide is also 1.8 mg in T2DM (i.e., 247.6 μg/kg in a mouse). Hence, in synopsis, a fivefold lower dose of twincretin provided similar or greater activity across outcome measures, as compared to a clinically translatable dose of liraglutide.

A caveat of our study is that we were unable to evaluate twincretin in comparison to a clinically translatable dose of a single GIPR agonist. Whereas single GIPR agonists are available as pharmacological tools and several are long-acting (Glotfelty et al., 2019), none have translated into humans and hence no information is available as to a clinically translatable dose to support a comparative evaluation. Our prior studies evaluating a constant infusion of GIP in moderate TBI to overcome its rapid disappearance, demonstrated its ability to mitigate impairments when plasma GIP levels were raised by 2.2-fold (Yu et al., 2016). This prior study suggests that a relatively modest elevation in the level of an incretin can provide a biologically relevant effect, which is important in the light of the relatively small but quantifiable amount that enters the brain following systemic administration of incretin mimetic: with CSF levels achieving some 2% of plasma levels (Bader et al., 2019).

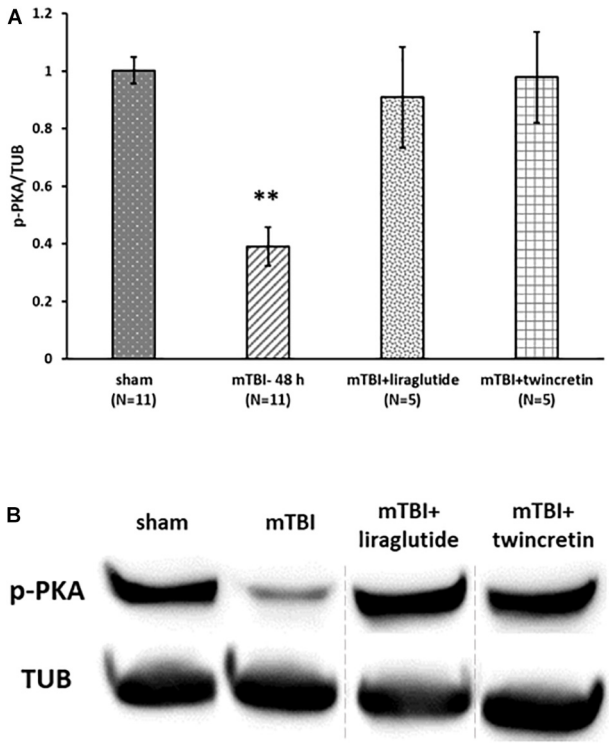


**FIGURE 9 |** Liraglutide and twincretin treatments block mTBI-induced reduction in p-PKA expression in the ipsilateral cortex. **(A)** Graph showing the p-PKA expression levels in ipsilateral/right cortex 48 h following mTBI. One-way ANOVA followed by Fisher's LSD *post hoc* analysis revealed a significant reduction in p-PKA expression in ipsilateral injured cortex 48 h following mTBI as compared to sham [$F(5,28) = 12.603$; $p < 0.001$, $^{**}p < 0.01$]. Treatment with either liraglutide or twincretin reduced the decline observed in mTBI affected brains ($^{**}p < 0.01$, respectively). Values are mean ± SEM. **(B)** Representative images of gel electrophoresis followed by immunoblot analysis using antibodies against p-PKA and α-tubulin in the ipsilateral cortex. A crop of the original image was performed, and sample number 3 was replaced by sample number 8, since the sample of mTBI + liraglutide was on loading site number 8 of the gel.

To gain a more thorough understanding of the causes of the cognitive impairments observed following mTBI, we examined select cellular changes in cortex and hippocampal regions associated with brain injury by performing immunohistochemical staining at 72 h post mTBI induction. This time point was chosen based on previous studies demonstrating that a number of biochemical changes are both evident and plateau at 72 h following mTBI (Tashlykov et al., 2007; Israelsson et al., 2009; Rubovitch et al., 2010). A significant elevation in neurodegenerative markers was observed across all regions evaluated. Treatment with each of the incretin analogs fully mitigated this. These results are in accord with elevations in neurodegenerative processes that occur following blast-mTBI and their amelioration by a clinically translatable dose of the GLP-1R agonist exendin-4 (Tweedie et al., 2016b). Moreover, a sustained-release formulation of exenatide (PT302) similarly prevented the elevation in neurodegenerative processes and prolonged neuronal loss following injury exposure in the same mTBI-model as in the present study (Bader et al., 2019).

We previously reported that our mTBI model, in line with other studies, induces key neuroinflammatory changes, including elevations in astrocyte and microglial expression, pro-inflammatory cytokine TNF-α levels, and expression of genes involved in inflammatory processes in several regions of the brain (Baratz et al., 2015; Tweedie et al., 2016a; Bader et al., 2019). In the current study, treatment with either liraglutide or twincretin reduced elevated microglial reactivity but failed to mitigate astrocyte changes, which is interesting in the light of recent studies suggesting that neurodegenerative processes triggered by neuroinflammation and the activation of microglia are mediated via A1 activated astrocytes (Liddelow et al., 2017; Yun et al., 2018). An increasing number of studies suggest that GLP-1R activation provides anti-inflammatory action, which our study supports. When evaluating these parameters at later time points, other studies have reported that incretin mimetics reduced elevated astrocyte expression in addition to microglial expression after 7–14 days of treatment (Yu et al., 2016; Barreto-Vianna et al., 2017; Yuan et al., 2017). One explanation for this difference, vs. our study, could be that the effect of these drugs on astrocytes occurs at a delayed time point compared to their effect on microglia, which was observed at 72 h following treatment initiation herein. Moreover, the GLP1R is highly expressed on microglia, in comparison to its expression on neurons and astrocytes (Iwai et al., 2006; Yun et al., 2018). Microglia have also been reported to generate and secrete GLP-1 (Kim et al., 2009; Kappe et al., 2012), and prior studies have demonstrated that GLP-1R agonists inhibit the activation of microglia in cellular studies following LPS stimulation and *in vivo* in response to numerous types of injury (Kim et al., 2009, 2017; Li et al., 2012; Gullo et al., 2017; Athauda and Foltynie, 2018; Wu et al., 2018; Yun et al., 2018). This results in a decline in the production of proinflammatory cytokines such as TNF-α and, as found in our study, a reduction in Iba-1 staining [as Iba-1 is a pan-microglial marker whose expression increases with microglial activation (Hopperton et al., 2018)].

Finally, to understand how our mTBI model and incretin analogs regulate neuroprotective protein expression, we examined the levels of PKA and PI3K phosphorylation in the cortex and hippocampus by Western blot. Contrary to the cellular pathways that incretins activate in the pancreas, those activated in brain remain to be fully characterized (Glotfelty et al., 2019). Multiple studies have proposed signaling pathways downstream to GLP-1R or GIPR activation in neurons (Perry and Greig, 2003; Li et al., 2010b; Holscher, 2014; McGrath et al., 2015; Kim et al., 2017; Athauda and Foltynie, 2018; Verma et al., 2018). In general, stimulation of either incretin receptors leads to the activation of the cAMP/PKA/CREB pathway that induces neuroprotection, inhibits apoptosis, regulates expression of genes that promote cell survival, and enhances memory formation (Glotfelty et al., 2019). This pathway also appears involved in GLP-1R mediated anti-inflammation (Wu et al., 2018). Agonist binding to the incretin receptors also activates the PI3K protein, which triggers several intracellular pathways involving the PKC, AKT/PKB, and MAPK proteins that ultimately promote cell

proliferation and regulate expression of genes interfering with apoptotic processes (Perry and Greig, 2003; Holscher, 2014; McGrath et al., 2015; Kim et al., 2017; Athauda and Foltynie, 2018; Verma et al., 2018).

In our model, mTBI induction did not affect p-PI3K levels. Previous studies investigating the effects of mTBI on proteins involved in the PI3K/AKT signaling pathway demonstrated inconsistent findings; some reports showed a decline in the activation of the PI3K/AKT pathway following mTBI (Chen et al., 2012; Shen et al., 2017); others showed an upregulation of this pathway (Rubovitch et al., 2010; Wang et al., 2017) and still others showed non-significant effects (Gao et al., 2016). Differences in the activation of this pathway following mTBI are apparently model-, time-, and region-dependent. However, p-PKA levels were decreased following mTBI exposure, which is consistent with previous findings showing downregulation in the cAMP/PKA/CREB pathway following mTBI (Atkins et al., 2009; Wang et al., 2018). Finally, treatment with each of liraglutide and twincretin resulted in attenuation in the mTBI-induced reduced expression of p-PKA. This likely contributes to the manifested neuroprotective effects of liraglutide and twincretin. Our previous work on neuronal cells *in vitro* demonstrated that incretin analogs activate adenylyl cyclase, increase production of cAMP, and also activate CREB (Li et al., 2010a,b, 2015; Tamargo et al., 2017; Glotfelty et al., 2019), with twincretin having a particularly potent action (Tamargo et al., 2017).

## CONCLUSION

Liraglutide and twincretin effectively prevented cognitive impairments and secondary damages induced by mTBI in mice. Although these two incretin mimetics similarly and fully inhibited these deficits in the majority of our evaluations, there appeared to be a potency advantage for twincretin, as similar or greater actions were achieved at a fivefold lower dose than liraglutide (50 and 247.6 μg/kg, respectively). By contrast, in humans, both drugs are administered at the same dose (1.8 mg) (Frias et al., 2017). Future studies within our collaborative group are focused to investigate the neuroprotective effects of liraglutide, twincretin and related analogs across a range of doses in order to obtain a dose–response analysis to allow a more comprehensive comparison between incretin mimetics and inform the optimal conditions for a human mTBI clinical trial. The consistent efficacy of clinically translatable doses of incretin mimetics mitigating neurodegenerative, neuroinflammatory, and behavioral outcome measures across preclinical TBI models (Glotfelty et al., 2019) is reinforced by the current study, and provides yet further support for the selection of an incretin mimetic to evaluate this treatment strategy in humans.

## DATA AVAILABILITY STATEMENT

The datasets generated for this study are included in the article/**Supplementary Material**. Requests to access the datasets should be directed to MB, miaad.bader@gmail.com.

## ETHICS STATEMENT

The animal study was reviewed and approved by the Ethics Committee of the Sackler Faculty of Medicine protocols M-14-050 and M-15-011.

## AUTHOR CONTRIBUTIONS

CP, MB, BH, RD, and NG conceived the study. MB, YL, DT, NS, AB, and VR performed the experiments. RD contributed essential materials. MB, LT-y-R, VR, YL, and DT analyzed the data. MB, BH, LT-y-R, and NG wrote the manuscript. MB and NG responded to reviewers' comments and revised the manuscript. All authors read and approved the final version of the manuscript.

## FUNDING

This research was supported in part by (i) the Ari and Regine Aprijaskis Fund, at Tel Aviv University, (ii) the Dr. Miriam and Sheldon G. Adelson Center for the Biology of Addictive Disease at Tel Aviv University, and (iii) the Intramural Research Program of the National Institute on Aging, National Institutes of Health, United States, and NIH grant R56AG057028.

## SUPPLEMENTARY MATERIAL

The Supplementary Material for this article can be found online at: https://www.frontiersin.org/articles/10.3389/fcell.2019.00356/full#supplementary-material

## REFERENCES

Anderberg, R. H., Richard, J. E., Hansson, C., Nissbrandt, H., Bergquist, F., and Skibicka, C. P. (2016). GLP-1 is both anxiogenic and antidepressant; divergent effects of acute and chronic GLP-1 on emotionality. *Psychoneuroendocrino* 65, 54–66. doi: 10.1016/j.psyneuen.2015.11.021

Athauda, D., and Foltynie, T. (2018). Protective effects of the GLP-1 mimetic exendin-4 in Parkinson's disease. *Neuropharmacology* 136(Pt B), 260–270. doi: 10.1016/j.neuropharm.2017.09.023

Athauda, D., Gulyani, S., Karnati, H., Li, Y., Tweedie, D., Mustapic, M., et al. (2019). Utility of neuronal-derived exosomes to examine molecular mechanisms that affect motor function in patients with parkinson disease: a secondary analysis of the exenatide-PD trial. *JAMA Neurol.* [Epub ahead of print]

Athauda, D., Maclagan, K., Skene, S. S., Bajwa-Joseph, M., Letchford, D., Chowdhury, K., et al. (2017). Exenatide once weekly versus placebo in Parkinson's disease: a randomised, double-blind, placebo-controlled trial. *Lancet* 390, 1664–1675. doi: 10.1016/S0140-6736(17)31585-4

Atkins, C. M., Falo, M. C., Alonso, O. F., Bramlett, H. M., and Dietrich, W. D. (2009). Deficits in ERK and CREB activation in the hippocampus after traumatic brain injury. *Neurosci. Lett.* 459, 52–56. doi: 10.1016/j.neulet.2009.04.064

Aviles-Olmos, I., Dickson, J., Kefalopoulou, Z., Djamshidian, A., Ell, P., Soderlund, T., et al. (2013). Exenatide and the treatment of patients with Parkinson's disease. *J. Clin. Invest.* 123, 2730–2736.

Bader, M., Li, Y., Lecca, D., Rubovitch, V., Tweedie, D., Glotfelty, E., et al. (2019). Pharmacokinetics and efficacy of PT302, a sustained-release Exenatide formulation, in a murine model of mild traumatic brain injury. *Neurobiol. Dis.* 124, 439–453. doi: 10.1016/j.nbd.2018.11.023

Baggio, L. L., and Drucker, D. J. (2007). Biology of incretins: GLP-1 and GIP. *Gastroenterology* 132, 2131–2157. doi: 10.1053/j.gastro.2007.03.054

Baratz, R., Rubovitch, V., Frenk, H., and Pick, C. G. (2010). The influence of alcohol on behavioral recovery after mTBI in mice. *J. Neuro.* 27, 555–563. doi: 10.1089/neu.2009.0891

Baratz, R., Tweedie, D., Wang, J. Y., Rubovitch, V., Luo, W., Hoffer, B. J., et al. (2015). Transiently lowering tumor necrosis factor-alpha synthesis ameliorates neuronal cell loss and cognitive impairments induced by minimal traumatic brain injury in mice. *J. Neuroinflamm.* 12:45. doi: 10.1186/s12974-015-0237-4

Barreto-Vianna, A. R. C., Aguila, M. B., and Mandarim-de-Lacerda, C. A. (2017). Beneficial effects of liraglutide (GLP1 analog) in the hippocampal inflammation. *Metab. Brain Dis.* 32, 1735–1745. doi: 10.1007/s11011-017-0059-4

Batista, A. F., Forny-Germano, L., Clarke, J. R., Lyra, E. S. N. M., Brito-Moreira, J., Boehnke, S. E., et al. (2018). The diabetes drug liraglutide reverses cognitive impairment in mice and attenuates insulin receptor and synaptic pathology in a non-human primate model of Alzheimer's disease. *J. Pathol.* 245, 85–100. doi: 10.1002/path.5056

Belzung, C., and Griebel, G. (2001). Measuring normal and pathological anxiety-like behaviour in mice: a review. *Behav. Brain Res.* 125, 141–149. doi: 10.1016/s0166-4328(01)00291-1

Bertilsson, G., Patrone, C., Zachrisson, O., Andersson, A., Dannaeus, K., Heidrich, J., et al. (2008). Peptide hormone exendin-4 stimulates subventricular zone neurogenesis in the adult rodent brain and induces recovery in an animal model of Parkinson's disease. *J. Neurosci. Res.* 86, 326–338. doi: 10.1002/jnr.21483

Bruns, J. Jr., and Hauser, W. A. (2003). The epidemiology of traumatic brain injury: a review. *Epilepsia* 44, 2–10. doi: 10.1046/j.1528-1157.44.s10.3.x

U.S. Department of Health and Human Services, Food and Drug Administration, Center for Drug Evaluation and Research, (2005). *Estimating the Safe Starting Dose in Clinical Trials for Therapeutics in Adult Healthy Volunteers, U.S. Food and Drug Administration (Rockville, MD, USA)*. Available at: https://www.fda.gov/media/72309/download (accessed September 14, 2019)

Chen, S. F., Tsai, H. J., Hung, T. H., Chen, C. C., Lee, C. Y., Wu, C. H., et al. (2012). Salidroside improves behavioral and histological outcomes and reduces apoptosis via PI3K/Akt signaling after experimental traumatic brain injury. *PLoS One* 7:e45763. doi: 10.1371/journal.pone.0045763

Choe, M. C. (2016). The pathophysiology of concussion. *Curr. Pain Headache Rep.* 20:42.

Coronado, V. G., McGuire, L. C., Faul, M., Sugerman, D. E., and Pearson, W. S. (2012). "Traumatic brain injury epidemiology and public health issues," in *Brain Injury Medicine: Principles and Practice*, eds N. D. Zasler, D. I. Katz, and R. D. Zafonte (New York, NY: Demos Medical), 84–100.

Cui, Q., and So, K. F. (2004). Involvement of cAMP in neuronal survival and axonal regeneration. *Anat. Sci. Int.* 79, 209–212. doi: 10.1111/j.1447-073x.2004.00089.x

Daneshvar, D. H., Riley, D. O., Nowinski, C. J., McKee, A. C., Stern, R. A., and Cantu, R. C. (2011). Long-term consequences: effects on normal development profile after concussion. *Phys. Med. Rehabil. Clin. N. Am.* 22, 683–700. doi: 10.1016/j.pmr.2011.08.009

Dix, S. L., and Aggleton, J. P. (1999). Extending the spontaneous preference test of recognition: evidence of object-location and object-context recognition. *Behav. Brain Res.* 99, 191–200. doi: 10.1016/s0166-4328(98)00079-5

Drucker, D. J. (2003). Glucagon-like peptides: regulators of cell proliferation, differentiation, and apoptosis. *Mol. Endocrinol.* 17, 161–171. doi: 10.1210/me.2002-0306

During, M. J., Cao, L., Zuzga, D. S., Francis, J. S., Fitzsimons, H. L., Jiao, X. Y., et al. (2003). Glucagon-like peptide-1 receptor is involved in learning and neuroprotection. *Nat. Med.* 9, 1173–1179. doi: 10.1038/nm919

Edut, S., Rubovitch, V., Schreiber, S., and Pick, C. G. (2011). The intriguing effects of ecstasy (MDMA) on cognitive function in mice subjected to a minimal traumatic brain injury (mTBI). *Psychopharmacology* 214, 877–889. doi: 10.1007/s00213-010-2098-y

Egefjord, L., Gejl, M., Moller, A., Braendgaard, H., Gottrup, H., Antropova, O., et al. (2012). Effects of liraglutide on neurodegeneration, blood flow and cognition in Alzheimer s disease - protocol for a controlled, randomized double-blinded trial. *Dan. Med. J.* 59:A4519.

Faivre, E., and Holscher, C. (2013). Neuroprotective effects of D-Ala(2)GIP on Alzheimer's disease biomarkers in an APP/PS1 mouse model. *Alzheimers Res. Ther.* 5:20. doi: 10.1186/alzrt174

Faul, M., Xu, L., Wald, M. M., Coronado, V., and Dellinger, A. M. (2010). Traumatic brain injury in the United States: national estimates of prevalence and incidence, 2002–2006. *Inj. Prev.* 16(Suppl. 1), A268–A268.

Figueiredo, C. P., Antunes, V. L. S., Moreira, E. L. G., de Mello, N., Medeiros, R., Di Giunta, G., et al. (2011). Glucose-dependent insulinotropic peptide receptor expression in the hippocampus and neocortex of mesial temporal lobe epilepsy patients and rats undergoing pilocarpine induced status epilepticus. *Peptides* 32, 781–789. doi: 10.1016/j.peptides.2010.12.010

Finan, B., Ma, T., Ottaway, N., Muller, T. D., Habegger, K. M., Heppner, K. M., et al. (2013). Unimolecular dual incretins maximize metabolic benefits in rodents, monkeys, and humans. *Sci. Transl. Med.* 5:209ra151. doi: 10.1126/scitranslmed.3007218

Finkelstein, E., Corso, P. S., and Miller, T. R. (2006). *The Incidence and Economic Burden of Injuries in the United States*. Oxford: Oxford University Press.

Fleminger, S., Oliver, D. L., Lovestone, S., Rabe-Hesketh, S., and Giora, A. (2003). Head injury as a risk factor for Alzheimer's disease: the evidence 10 years on; a partial replication. *J. Neurol. Neurosurg. Psychiatry* 74, 857–862. doi: 10.1136/jnnp.74.7.857

Frias, J. P., Bastyr, E. J. III, Vignati, L., Tschop, M. H., Schmitt, C., Owen, K., et al. (2017). The sustained effects of a dual GIP/GLP-1 receptor agonist, NNC0090-2746, in patients with Type 2 diabetes. *Cell Metab.* 26:e342. doi: 10.1016/j.cmet.2017.07.011

Gao, Y., Li, J., Wu, L., Zhou, C., Wang, Q., Li, X., et al. (2016). Tetrahydrocurcumin provides neuroprotection in rats after traumatic brain injury: autophagy and the PI3K/AKT pathways as a potential mechanism. *J. Surg. Res.* 206, 67–76. doi: 10.1016/j.jss.2016.07.014

Gardner, R. C., and Yaffe, K. (2015). Epidemiology of mild traumatic brain injury and neurodegenerative disease. *Mol. Cell. Neurosci.* 66, 75–80. doi: 10.1016/j.mcn.2015.03.001

Gejl, M., Gjedde, A., Egefjord, L., Moller, A., Hansen, S. B., Vang, K., et al. (2016). In Alzheimer's Disease, 6-month treatment with GLP-1 analog prevents decline of brain glucose metabolism: randomized, placebo-controlled, double-blind clinical trial. *Front. Aging Neurosci.* 8:108. doi: 10.3389/fnagi.2016.00108

Glotfelty, E. J., Delgado, T. E., Tovar-y-Romo, L. B., Luo, Y., Hoffer, B. J., Olson, L., et al. (2019). Incretin mimetics as rational candidates for the treatment of traumatic brain injury. *ACS Pharmacol. Transl. Sci.* 2, 66–91. doi: 10.1021/acsptsci.9b00003

Greve, M. W., and Zink, B. J. (2009). Pathophysiology of traumatic brain injury. *Mt. Sinai J. Med.* 76, 97–104. doi: 10.1002/msj.20104

Gullo, F., Ceriani, M., D'Aloia, A., Wanke, E., Constanti, A., Costa, B., et al. (2017). Plant polyphenols and exendin-4 prevent hyperactivity and TNF-α release in LPS-treated *in vitro* neuron/astrocyte/microglial networks. *Front. Neurosci.* 11:500. doi: 10.3389/fnins.2017.00500

Hamilton, A., and Holscher, C. (2009). Receptors for the incretin glucagon-like peptide-1 are expressed on neurons in the central nervous system. *Neuroreport* 20, 1161–1166. doi: 10.1097/WNR.0b013e32832fbf14

Han, L., Holscher, C., Xue, G. F., Li, G., and Li, D. (2016). A novel dual-glucagon-like peptide-1 and glucose-dependent insulinotropic polypeptide receptor agonist is neuroprotective in transient focal cerebral ischemia in the rat. *Neuroreport* 27, 23–32. doi: 10.1097/WNR.0000000000000490

Holscher, C. (2014). Central effects of GLP-1: new opportunities for treatments of neurodegenerative diseases. *J. Endocrinol.* 221, T31–T41. doi: 10.1530/JOE-13-0221

Holscher, C., and Li, L. (2010). New roles for insulin-like hormones in neuronal signalling and protection: new hopes for novel treatments of Alzheimer's disease? *Neurobiol. Aging* 31, 1495–1502. doi: 10.1016/j.neurobiolaging.2008.08.023

Hopperton, K. E., Mohammad, D., Trepanier, M. O., Giuliano, V., and Bazinet, R. P. (2018). Markers of microglia in post-mortem brain samples from patients

with Alzheimer's disease: a systematic review. *Mol. Psychiatry* 23:177. doi: 10.1038/mp.2017.246

Hyun Lee, C., Yan, B., Yoo, K. Y., Choi, J. H., Kwon, S. H., Her, S., et al. (2011). Ischemia-induced changes in glucagon-like peptide-1 receptor and neuroprotective effect of its agonist, exendin-4, in experimental transient cerebral ischemia. *J. Neurosci. Res.* 89, 1103–1113. doi: 10.1002/jnr.22596

Isacson, R., Nielsen, E., Dannaeus, K., Bertilsson, G., Patrone, C., Zachrisson, O., et al. (2011). The glucagon-like peptide 1 receptor agonist exendin-4 improves reference memory performance and decreases immobility in the forced swim test. *Eur. J. Pharmacol.* 650, 249–255. doi: 10.1016/j.ejphar.2010.10.008

Israelsson, C., Wang, Y., Kylberg, A., Pick, C. G., Hoffer, B. J., and Ebendal, T. (2009). Closed head injury in a mouse model results in molecular changes indicating inflammatory responses. *J. Neuro.* 26, 1307–1314. doi: 10.1089/neu.2008-0676

Iwai, T., Ito, S., Tanimitsu, K., Udagawa, S., and Oka, J. I. (2006). Glucagon-like peptide-1 inhibits LPS-induced IL-1 beta production in cultured rat astrocytes. *Neurosci. Res.* 55, 352–360. doi: 10.1016/j.neures.2006.04.008

Kappe, C., Tracy, L. M., Patrone, C., Iverfeldt, K., and Sjöholm, Å. (2012). GLP-1 secretion by microglial cells and decreased CNS expression in obesity. *J. Neuroinflamm.* 9:766. doi: 10.1186/1742-2094-9-276

Kim, D. S., Choi, H. I, Wang, Y., Luo, Y., Hoffer, B. J., and Greig, N. H. (2017). A new treatment strategy for Parkinson's disease through the gut-brain Axis: the glucagon-like peptide-1 receptor pathway. *Cell Transpl.* 26, 1560–1571. doi: 10.1177/0963689717721234

Kim, S., Moon, M., and Park, S. (2009). Exendin-4 protects dopaminergic neurons by inhibition of microglial activation and matrix metalloproteinase-3 expression in an animal model of Parkinson's disease. *J. Endocrinol.* 202:431. doi: 10.1677/JOE-09-0132

Levin, H. S., and Diaz-Arrastia, R. R. (2015). Diagnosis, prognosis, and clinical management of mild traumatic brain injury. *Lancet Neurol.* 14, 506–517. doi: 10.1016/S1474-4422(15)00002-2

Li, Y., Bader, M., Tamargo, I., Rubovitch, V., Tweedie, D., Pick, C. G., et al. (2015). Liraglutide is neurotrophic and neuroprotective in neuronal cultures and mitigates mild traumatic brain injury in mice. *J. Neurochem.* 135, 1203–1217. doi: 10.1111/jnc.13169

Li, Y., Chigurupati, S., Holloway, H. W., Mughal, M., Tweedie, D., Bruestle, D. A., et al. (2012). Exendin-4 ameliorates motor neuron degeneration in cellular and animal models of amyotrophic lateral sclerosis. *PLoS One* 7:e32008. doi: 10.1371/journal.pone.0032008

Li, Y., Hansotia, T., Yusta, B., Ris, F., Halban, P. A., and Drucker, D. J. (2003). Glucagon-like peptide-1 receptor signaling modulates β cell apoptosis. *J. Biol. Chem.* 278, 471–478. doi: 10.1074/jbc.m209423200

Li, Y., Liu, W., Li, L., and Holscher, C. (2016). Neuroprotective effects of a GIP analogue in the MPTP Parkinson's disease mouse model. *Neuropharmacology* 101, 255–263. doi: 10.1016/j.neuropharm.2015.10.002

Li, Y., Perry, T., Kindy, M. S., Harvey, B. K., Tweedie, D., Holloway, H. W., et al. (2009). GLP-1 receptor stimulation preserves primary cortical and dopaminergic neurons in cellular and rodent models of stroke and Parkinsonism. *Proc. Natl. Acad. Sci. U.S.A.* 106, 1285–1290. doi: 10.1073/pnas.0806720106

Li, Y., Tweedie, D., Mattson, M. P., Holloway, H. W., and Greig, N. H. (2010b). Enhancing the GLP-1 receptor signaling pathway leads to proliferation and neuroprotection in human neuroblastoma cells. *J. Neurochem.* 113, 1621–1631. doi: 10.1111/j.1471-4159.2010.06731.x

Li, Y., Duffy, K. B., Ottinger, M. A., Ray, B., Bailey, J. A., Holloway, H. W., et al. (2010a). GLP-1 receptor stimulation reduces amyloid-beta peptide accumulation and cytotoxicity in cellular and animal models of Alzheimer's disease. *J. Alzheimers. Dis.* 19, 1205–1219. doi: 10.3233/JAD-2010-1314

Liddelow, S. A., Guttenplan, K. A., Clarke, L. E., Bennett, F. C., Bohlen, C. J., Schirmer, L., et al. (2017). Neurotoxic reactive astrocytes are induced by activated microglia. *Nature* 541, 481–487. doi: 10.1038/nature21029

Lovshin, J. A., and Drucker, D. J. (2009). Incretin-based therapies for type 2 diabetes mellitus. *Nat. Rev. Endocrinol.* 5, 262–269. doi: 10.1038/nrendo.2009.48

Maas, A. I., Stocchetti, N., and Bullock, R. (2008). Moderate and severe traumatic brain injury in adults. *Lancet Neurol.* 7, 728–741. doi: 10.1016/S1474-4422(08)70164-9

Martin, B., Golden, E., Carlson, O. D., Pistell, P., Zhou, J., Kim, W., et al. (2009). Exendin-4 improves glycemic control, ameliorates brain and pancreatic pathologies, and extends survival in a mouse model of Huntington's disease. *Diabetes Metab. Res. Rev* 58, 318–328. doi: 10.2337/db08-0799

McClean, P. L., Parthsarathy, V., Faivre, E., and Holscher, C. (2011). The diabetes drug liraglutide prevents degenerative processes in a mouse model of Alzheimer's disease. *J. Neurosci.* 31, 6587–6594. doi: 10.1523/JNEUROSCI.0529-11.2011

McGrath, R., Glastras, S., and Hocking, S. (2015). Central functions of glucagon-like peptide-1: roles in energy regulation and neuroprotection. *J. Steroids Horm Sci.* 6: 152. doi: 10.4239/wjd.v6.i6.807

McInnes, K., Friesen, C. L., MacKenzie, D. E., Westwood, D. A., and Boe, S. G. (2017). Mild Traumatic Brain Injury (mTBI) and chronic cognitive impairment: a scoping review. *PLoS One* 12:e0174847. doi: 10.1371/journal.pone.0174847

Milman, A., Rosenberg, A., Weizman, R., and Pick, C. G. (2005). Mild traumatic brain injury induces persistent cognitive deficits and behavioral disturbances in mice. *J. Neurotrauma* 22, 1003–1010. doi: 10.1089/neu.2005.22.1003

Moppett, I. K. (2007). Traumatic brain injury: assessment, resuscitation and early management. *Br. J. Anaesth.* 99, 18–31. doi: 10.1093/bja/aem128

U.S. Department of Health and Human Services, Centers for Disease Control and Prevention, and National Center for Health Statistics, (2016). *Data From the National Health and Nutrition Examination Survey; Anthropometric Reference Data for Children and Adults: United States, 2011–2014. DHHS Publication No. 2016–1604 (Hyattsville, MD, USA)*. Available at: https://www.cdc.gov/nchs/data/series/sr_03/sr03_039.pdf (accessed August 14, 2019)

Nyberg, J., Anderson, M. F., Meister, B., Alborn, A. M., Strom, A. K., Brederlau, A., et al. (2005). Glucose-dependent insulinotropic polypeptide is expressed in adult hippocampus and induces progenitor cell proliferation. *J. Neurosci.* 25, 1816–1825. doi: 10.1523/jneurosci.4920-04.2005

Paratore, S., Ciotti, M. T., Basille, M., Vaudry, D., Gentile, A., Parenti, R., et al. (2011). Gastric inhibitory polypeptide and its receptor are expressed in the central nervous system and support neuronal survival. *Cent. Nerv. Syst. Agents Med. Chem.* 11, 210–222. doi: 10.2174/187152411798047771

Patterson, Z. R., and Holahan, M. R. (2012). Understanding the neuroinflammatory response following concussion to develop treatment strategies. *Front. Cell. Neurosci.* 6:58. doi: 10.3389/fncel.2012.00058

Perry, T., and Greig, N. H. (2003). The glucagon-like peptides: a double-edged therapeutic sword? *Trends Pharmacol. Sci.* 24, 377–383. doi: 10.1016/s0165-6147(03)00160-3

Perry, T., Haughey, N. J., Mattson, M. P., Egan, J. M., and Greig, N. H. (2002). Protection and reversal of excitotoxic neuronal damage by glucagon-like peptide-1 and exendin-4. *J. Pharmacol. Exp. Ther.* 302, 881–888. doi: 10.1124/jpet.102.037481

Perry, T., Holloway, H. W., Weerasuriya, A., Mouton, P. R., Duffy, K., Mattison, J. A., et al. (2007). Evidence of GLP-1-mediated neuroprotection in an animal model of pyridoxine-induced peripheral sensory neuropathy. *Exp. Neurol.* 203, 293–301. doi: 10.1016/j.expneurol.2006.09.028

Portron, A., Jadidi, S., Sarkar, N., DiMarchi, R., and Schmitt, C. (2017). Pharmacodynamics, pharmacokinetics, safety and tolerability of the novel dual glucose-dependent insulinotropic polypeptide/glucagon-like peptide-1 agonist RG7697 after single subcutaneous administration in healthy subjects. *Diabetes. Obes. Metab.* 19, 1446–1453. doi: 10.1111/dom.13025

Rachmany, L., Tweedie, D., Li, Y., Rubovitch, V., Holloway, H. W., Miller, J., et al. (2013). Exendin-4 induced glucagon-like peptide-1 receptor activation reverses behavioral impairments of mild traumatic brain injury in mice. *Age* 35, 1621–1636. doi: 10.1007/s11357-012-9464-0

Rubovitch, V., Edut, S., Sarfstein, R., Werner, H., and Pick, C. G. (2010). The intricate involvement of the Insulin-like growth factor receptor signaling in mild traumatic brain injury in mice. *Neurobiol. Dis.* 38, 299–303. doi: 10.1016/j.nbd.2010.01.021

Schmitt, C., Portron, A., Jadidi, S., Sarkar, N., and DiMarchi, R. (2017). Pharmacodynamics, pharmacokinetics and safety of multiple ascending doses of the novel dual glucose-dependent insulinotropic polypeptide/glucagon-like peptide-1 agonist RG7697 in people with type 2 diabetes mellitus. *Diabetes. Obes. Metab.* 19, 1436–1445. doi: 10.1111/dom.13024

Schmued, L. C., and Hopkins, K. J. (2000). Fluoro-Jade B: a high affinity fluorescent marker for the localization of neuronal degeneration. *Brain Res.* 874, 123–130. doi: 10.1016/s0006-8993(00)02513-0

Seino, Y., Fukushima, M., and Yabe, D. (2010). GIP and GLP-1, the two incretin hormones: similarities and differences. *J. Diabetes Invest.* 1, 8–23. doi: 10.1111/j.2040-1124.2010.00022.x

Shen, M., Wang, S., Wen, X., Han, X. R., Wang, Y. J., Zhou, X. M., et al. (2017). Dexmedetomidine exerts neuroprotective effect via the activation of the PI3K/Akt/mTOR signaling pathway in rats with traumatic brain injury. *Biomed. Pharmacother.* 95, 885–893. doi: 10.1016/j.biopha.2017.08.125

Shi, L., Zhang, Z., Li, L., and Holscher, C. (2017). A novel dual GLP-1/GIP receptor agonist alleviates cognitive decline by re-sensitizing insulin signaling in the Alzheimer icv. STZ rat model. *Behav. Brain Res.* 327, 65–74. doi: 10.1016/j.bbr.2017.03.032

Spielman, L. J., Gibson, D. L., and Klegeris, A. (2017). Incretin hormones regulate microglia oxidative stress, survival and expression of trophic factors. *Eur. J. Cell Biol.* 96, 240–253. doi: 10.1016/j.ejcb.2017.03.004

Tabuchi, A., Sakaya, H., Kisukeda, T., Fushiki, H., and Tsuda, M. (2002). Involvement of an upstream stimulatory factor as well as cAMP-responsive element-binding protein in the activation of brain-derived neurotrophic factor gene promoter I. *J. Biol. Chem.* 277, 35920–35931. doi: 10.1074/jbc.m204784200

Tagliaferri, F., Compagnone, C., Korsic, M., Servadei, F., and Kraus, J. (2006). A systematic review of brain injury epidemiology in Europe. *Acta Neurochir.* 148, 255–268. doi: 10.1007/s00701-005-0651-y

Tamargo, I. A., Bader, M., Li, Y., Yu, S.-J., Wang, Y., Talbot, K., et al. (2017). Novel GLP-1R/GIPR co-agonist "twincretin" is neuroprotective in cell and rodent models of mild traumatic brain injury. *Exp. Neurol.* 288, 176–186. doi: 10.1016/j.expneurol.2016.11.005

Tashlykov, V., Katz, Y., Gazit, V., Zohar, O., Schreiber, S., and Pick, C. G. (2007). Apoptotic changes in the cortex and hippocampus following minimal brain trauma in mice. *Brain Res.* 1130, 197–205. doi: 10.1016/j.brainres.2006.10.032

Trümper, A., Trümper, K., Trusheim, H., Arnold, R., Göke, B., and Hörsch, D. (2001). Glucose-dependent insulinotropic polypeptide is a growth factor for β (INS-1) cells by pleiotropic signaling. *Mol. Endocrinol.* 15, 1559–1570. doi: 10.1210/mend.15.9.0688

Tweedie, D., Rachmany, L., Rubovitch, V., Li, Y., Holloway, H. W., Lehrmann, E., et al. (2016b). Blast traumatic brain injury-induced cognitive deficits are attenuated by preinjury or postinjury treatment with the glucagon-like peptide-1 receptor agonist, exendin-4. *Alzheimers Dement* 12, 34–48. doi: 10.1016/j.jalz.2015.07.489

Tweedie, D., Rachmany, L., Kim, D. S., Rubovitch, V., Lehrmann, E., Zhang, Y., et al. (2016a). Mild traumatic brain injury-induced hippocampal gene expressions: the identification of target cellular processes for drug development. *J. Neurosci. Methods* 272, 4–18. doi: 10.1016/j.jneumeth.2016.02.003

Tweedie, D., Rachmany, L., Rubovitch, V., Zhang, Y. Q., Becker, K. G., Perez, E., et al. (2013). Changes in mouse cognition and hippocampal gene expression observed in a mild physical- and blast-traumatic brain injury. *Neurobiol. Dis.* 54, 1–11. doi: 10.1016/j.nbd.2013.02.006

Verma, M. K., Goel, R., Krishnadas, N., and Nemmani, K. V. S. (2018). Targeting glucose-dependent insulinotropic polypeptide receptor for neurodegenerative disorders. *Expert. Opin. Ther.* 22, 615–628. doi: 10.1080/14728222.2018.1487952

Verma, M. K., Goel, R., Nandakumar, K., and Nemmani, K. V. S. (2017). Effect of D-Ala(2)GIP, a stable GIP receptor agonist on MPTP-induced neuronal impairments in mice. *Eur. J. Pharmacol.* 804, 38–45. doi: 10.1016/j.ejphar.2017.03.059

Wang, W., Shen, M., Sun, K., Wang, Y., Wang, X., Jin, X., et al. (2018). Aminoguanidine reverses cognitive deficits and activation of cAMP/CREB/BDNF pathway in mouse hippocampus after traumatic brain injury (TBI). *Brain Inj.* 32, 1858–1865. doi: 10.1080/02699052.2018.1537513

Wang, Z. F., Pan, Z. Y., Xu, C. S., and Li, Z. Q. (2017). Activation of G-protein coupled estrogen receptor 1 improves early-onset cognitive impairment via PI3K/Akt pathway in rats with traumatic brain injury. *Biochem. Biophys. Res. Commun.* 482, 948–953. doi: 10.1016/j.bbrc.2016.11.138

Washington, P. M., Forcelli, P. A., Wilkins, T., Zapple, D. N., Parsadanian, M., and Burns, M. P. (2012). The effect of injury severity on behavior: a phenotypic study of cognitive and emotional deficits after mild, moderate, and severe controlled cortical impact injury in mice. *J. Neurotraum.* 29, 2283–2296. doi: 10.1089/neu.2012.2456

Werner, C., and Engelhard, K. (2007). Pathophysiology of traumatic brain injury. *Br. J. Anaesth.* 99, 4–9.

Wu, H. Y., Tang, X. Q., Liu, H., Mao, X. F., and Wang, Y. X. (2018). Both classic Gs- cAMP/PKA/CREB and alternative Gs-cAMP/PKA/p38β/CREB signal pathways mediate exenatide-stimulated expression of M2 microglial markers. *J. Neuroimmunol.* 316, 17–22. doi: 10.1016/j.jneuroim.2017.12.005

Yu, Y. W., Hsieh, T. H., Chen, K. Y., Wu, J. C., Hoffer, B. J., Greig, N. H., et al. (2016). Glucose-dependent insulinotropic polypeptide ameliorates mild traumatic brain injury-induced cognitive and sensorimotor deficits and neuroinflammation in rats. *J. Neurotrauma* 33, 2044–2054. doi: 10.1089/neu.2015.4229

Yuan, Z., Li, D., Feng, P., Xue, G., Ji, C., Li, G., et al. (2017). A novel GLP-1/GIP dual agonist is more effective than liraglutide in reducing inflammation and enhancing GDNF release in the MPTP mouse model of Parkinson's disease. *Eur. J. Pharmacol.* 812, 82–90. doi: 10.1016/j.ejphar.2017.06.029

Yun, S. P., Kam, T. I., Panicker, N., Kim, S., Oh, Y., Park, J. S., et al. (2018). Block of A1 astrocyte conversion by microglia is neuroprotective in models of Parkinson's disease. *Nat. Med.* 24:931. doi: 10.1038/s41591-018-0051-5

Zohar, O., Rubovitch, V., Milman, A., Schreiber, S., and Pick, C. G. (2011). Behavioral consequences of minimal traumatic brain injury in mice. *Acta Neurobiol. Exp.* 71, 36–45.

Zohar, O., Schreiber, S., Getslev, V., Schwartz, J. P., Mullins, P. G., and Pick, C. G. (2003). Closed-head minimal traumatic brain injury produces long-term cognitive deficits in mice. *Neuroscience* 118, 949–955. doi: 10.1016/s0306-4522(03)00048-4

**Conflict of Interest:** RD is a co-inventor on patent applications (US2011/0166062 A1; US 12/999,285; "GIP-based mixed agonists for treatment of metabolic disorders and obesity") owned by Indiana University that pertain to the twincretin peptide in this paper.

The remaining authors declare that the research was conducted in the absence of any commercial or financial relationships that could be construed as a potential conflict of interest.

frontiers in Cell and Developmental Biology

MINI REVIEW
published: 07 February 2020
doi: 10.3389/fcell.2020.00053

# Improving Cerebrovascular Function to Increase Neuronal Recovery in Neurodegeneration Associated to Cardiovascular Disease

*Lotte Vanherle[1,2†], Hana Matuskova[1,2,3,4†], Nicholas Don-Doncow[1,2], Franziska E. Uhl[1,2] and Anja Meissner[1,2,4*]*

[1] Department of Experimental Medical Science, Lund University, Lund, Sweden, [2] Wallenberg Centre for Molecular Medicine, Lund University, Lund, Sweden, [3] Department of Neurology, University Hospital Bonn, Bonn, Germany, [4] German Center for Neurodegenerative Diseases (DZNE), Bonn, Germany

OPEN ACCESS

**Edited by:**
Luis B. Tovar-y-Romo, National Autonomous University of Mexico, Mexico

**Reviewed by:**
Marietta Zille, Universität zu Lübeck, Germany
Ximena Castillo, National Autonomous University of Mexico, Mexico

***Correspondence:**
Anja Meissner
anja.meissner@med.lu.se

[†] These authors have contributed equally to this work

**Specialty section:**
This article was submitted to Molecular Medicine, a section of the journal Frontiers in Cell and Developmental Biology

**Received:** 11 December 2019
**Accepted:** 21 January 2020
**Published:** 07 February 2020

**Citation:**
Vanherle L, Matuskova H, Don-Doncow N, Uhl FE and Meissner A (2020) Improving Cerebrovascular Function to Increase Neuronal Recovery in Neurodegeneration Associated to Cardiovascular Disease. Front. Cell Dev. Biol. 8:53. doi: 10.3389/fcell.2020.00053

Mounting evidence indicates that the presence of cardiovascular disease (CVD) and risk factors elevates the incidence of cognitive impairment (CI) and dementia. CVD and associated decline in cardiovascular function can impair cerebral blood flow (CBF) regulation, leading to the disruption of oxygen and nutrient supply in the brain where limited intracellular energy storage capacity critically depends on CBF to sustain proper neuronal functioning. During hypertension and acute as well as chronic CVD, cerebral hypoperfusion and impaired cerebrovascular function are often associated with neurodegeneration and can lead to CI and dementia. Currently, all forms of neurodegeneration associated to CVD lack effective treatments, which highlights the need to better understand specific mechanisms linking cerebrovascular dysfunction and CBF deficits to neurodegeneration. In this review, we discuss vascular targets that have already shown attenuation of neurodegeneration or CI associated to hypertension, heart failure (HF) and stroke by improving cerebrovascular function or CBF deficits.

**Keywords: cerebral blood flow, cerebrovascular function, hypertension, heart failure, stroke**

## INTRODUCTION

The cerebral circulation plays a critical role in matching nutrient and oxygen supply to neuronal activity and thus, is intimately linked to proper brain function (Iadecola, 2013, 2017; Wolters et al., 2017; Leeuwis et al., 2018). However, it appears to have been long under-recognized in the field of neurodegenerative research despite mounting evidence that associates also classical neurodegenerative diseases, such as Alzheimer's disease and Parkinson's disease, to impairments in cerebrovascular structure and function (Freitag et al., 2006; Kovacs et al., 2014; Bos et al., 2017). We have come a long way, and focus has shifted to include the vascular origins of neurodegeneration (Iadecola, 2013; Castillo et al., 2019).

In recent years, it came apparent that during cardiovascular disease (CVD), the most prevalent disease burden worldwide (GBD 2017 Causes of Death Collaborators, 2018), structural and functional impairments of the cerebral circulation majorly contribute to the development of neurodegeneration and cognitive impairment (CI) (Kuller et al., 2005; Jefferson et al., 2010;

Gorelick et al., 2011; Haring et al., 2013; Takeda et al., 2019). Cerebrovascular alterations, ranging from endothelial dysfunction, vascular remodeling and inflammation to capillary rarefaction, blood-brain-barrier (BBB) damage and neurovascular uncoupling promote neurodegeneration in CVD (Iadecola, 2013, 2017) and have also been associated to the pathogenesis of Alzheimer's disease (Carnevale et al., 2016). Precise mechanisms underlying neurodegenerative processes and CI in CVD are reviewed in detail elsewhere (Iadecola, 2013; O'Brien and Thomas, 2015; Castillo et al., 2019), but it is generally considered that such cerebromicrovascular alterations contribute to a decline in cerebral blood flow (CBF) that reduces metabolic support for neural signaling, thereby exacerbating neuronal dysfunction (Iadecola, 2013). Strong epidemiological and experimental evidence suggest an exacerbation of cognitive dysfunction during *hypertension* and *heart failure* (HF) (Jefferson et al., 2010; Gorelick et al., 2011). Thus, controlling cardiovascular risk factors has become increasingly important not only in the prevention of deleterious acute consequences (i.e., *stroke*), but also for reducing the risk of developing CVD-associated neurodegeneration that may lead to the development of CI and dementia (Sprint Mind Investigators for the Sprint Research Group, Williamson et al., 2019). Although the association between CVD and increased dementia risk is well established (Kuller et al., 2005; Jefferson et al., 2010; Gorelick et al., 2011; Haring et al., 2013), it is still unclear if treatments would reverse already established CI. Because of its intimate link to neuronal function, targeting the cerebral vasculature to improve CBF has yielded some promising results in respect to neuro-regenerative processes (Meissner et al., 2012; Lidington et al., 2019). This article summarizes vascular targets that have shown to attenuate neuronal degeneration or cognitive function associated to hypertension, HF and stroke by improving cerebrovascular function or CBF deficits. For this purpose, we mainly included studies in this review that discussed mechanisms related to cerebrovascular function or CBF regulation, which showed improvements of vascular function and/or a mitigation of neurodegeneration (e.g., impairment of neuronal structure, memory function, neurological function) after targeting these mechanisms. We apologize to all researchers whose work is only indirectly mentioned through review article citations.

# TARGETING CEREBROVASCULAR MECHANISMS TO IMPROVE CBF AND ATTENUATE NEURODEGENERATION DURING HYPERTENSION AND CARDIOVASCULAR DISEASE

## Hypertension

Chronic hypertension is the most prevalent cardiovascular disorder and the leading cause of cardiovascular and cerebrovascular morbidity and mortality worldwide (Drozdz and Kawecka-Jaszcz, 2014; Ibekwe, 2015). It is one of the most important modifiable risk factors for stroke and HF (Ibekwe, 2015), and has also been associated to the pathogenesis of Alzheimer's disease (Carnevale et al., 2016). Hypertension alters the morphology as well as the function of cerebral vessels (Joutel et al., 2010; Meissner, 2016; Meissner et al., 2017), however, our knowledge about its effects on neurovascular coupling and hypertension-induced molecular changes in the different cell types of the neurovascular unit is still very fragmented.

Angiotensin II (AngII), the primary effector hormone of the renin angiotensin system (RAS), is considered the main contributor to impairments of neurovascular coupling independent of blood pressure (Kazama et al., 2004). It is suggested that vascular and glial cells, but not neurons, drive the changes in neurovascular coupling in response to AngII (Kazama et al., 2004; Capone et al., 2011). In the group of hypertensive drugs, angiotensin II receptor type 1 (AT1R) antagonists have been shown to prevent a decline in CBF in elderly hypertensive patients (Bloch et al., 2015) by potentially counteracting cerebrovascular dysfunction and local reactive oxygen species (ROS) production. Interestingly, treatment with Ang-(1-7), which are opposing many AngII effects on AT1R, lowered AngII levels in spontaneously hypertensive rats (SHR) and most interestingly, associated to decreased neuronal apoptosis. Favorable Ang-(1-7) effects on CBF are thought to result from effects on bradykinin levels (Lu et al., 2008), nitric oxide (NO) release, and endothelial NO synthase (NOS) expression (Zhang et al., 2008), and through Mas receptors (Jiang et al., 2013) that are thought to be involved in astrocyte-mediated calcium signaling during hypertension (Guo et al., 2010).

Recent evidence has emerged that statins, cholesterol-lowering drugs, may be beneficial in hypertension, specifically for the reversal of cognitive decline (Don-Doncow et al., 2018). Hypertension-induced BBB impairment was reversed after atorvastatin treatment, suggesting a novel role for statins in hypertension-associated brain dysfunction (Kalayci et al., 2005). Moreover, simvastatin normalized cerebromicrovascular perfusion and increased cerebral capillary density in SHR (Freitas et al., 2017). Precise mechanisms underlying these favorable effects on the cerebral microvasculature are yet to be determined. Besides affecting cerebromicrovascular perfusion and BBB stability, statin-mediated anti-inflammatory effects decreased in both rolling leukocyte presence and leukocyte adhesion to cerebral endothelial cells (Freitas et al., 2017), which may hinder leukocyte infiltration into the brain and thus, reduce neuroinflammation (Don-Doncow et al., 2018). Adverse immune activation and infiltration is considered a key mechanism in neurodegeneration associated to hypertension or hypertensive stimuli (Faraco et al., 2016, 2018; Don-Doncow et al., 2019). High dietary salt concentrations have been shown to suppress endothelial function and CBF, resulting in CI by mechanisms involving an expansion of the Th17 cells in the small intestine that leads to a systemic increase in IL-17 (Faraco et al., 2018). By inhibiting the phosphorylation of endothelial NOS and thus, NO production in cerebral endothelial cells, IL-17 is thought to contribute to the neurovascular dysfunction and thus, the development of CI (Faraco et al., 2018). Neuroinflammation is generally accepted as a key player in the pathophysiology of hypertension, involving higher oxidative stress levels, immune activation and recruitment, and BBB impairment

(Rodriguez-Iturbe et al., 2017). To date, only little is known about the precise mechanisms linking hypertension-associated inflammation to cerebrovascular dysfunction or CBF and hence, its link to neurodegeneration and CI is mostly elusive. A recent study showed the role of perivascular macrophages (PVMs) as mediators of hypertension-associated neuronal dysfunction and memory impairment in response to AngII (Faraco et al., 2016). The activation of the AT1R on PVMs, which was shown to induce NADPH oxidase 2 (NOX2)-mediated ROS production, is not only thought to trigger BBB impairment but also CBF reduction. Depletion of PVMs as well as PVM-specific AT1R deletion protected against the development of neurovascular uncoupling, CBF deficits and memory impairment induced by hypertension (Faraco et al., 2016). Overexpression of CuZn-superoxide dismutase in the subfornical organ prevented hypertension-induced alteration in neurovascular coupling and endothelium-dependent responses in somatosensory cortex, confirming an AngII-mediated neurovascular unit dysfunction during hypertension that involves ROS (Capone et al., 2012). Despite proven mechanistic involvement, ROS inhibition or immunomodulation have not yet been evaluated therapeutically in hypertension-associated neurodegeneration. Like ROS, many other targets have been identified as mechanisms linking neurodegeneration and hypertension, but their effective therapeutic potential to promote neuro-regeneration in the hypertensive brain is yet to be tested.

## Heart Failure

Heart failure-associated morbidity has grown as the frequently accompanying cognitive decline majorly affects disease outcome, accelerating disease progression by reducing the ability to execute self-care activities and treatment compliance (Hajduk et al., 2013). Epidemiological studies not only showed that the majority of HF patients develop some form of cognitive decline or memory loss, but that they develop them earlier in life compared to the healthy population (Cacciatore et al., 1998; Pressler, 2008; Pressler et al., 2010; Hajduk et al., 2013; Leto and Feola, 2014; Meissner et al., 2015). To date, no therapeutic options exist. Restoring hemodynamic properties and correcting vascular risk factors seem to be the primary approach in the management of CI in HF patients. Experimental mouse models emulate several key features of HF-associated brain complications, including reduced CBF and compromised neurological function (Meissner et al., 2015), and are therefore valuable model systems to study molecular mechanisms underlying neurodegeneration and CI associated to HF.

In healthy patients, cerebral auto-regulatory mechanisms can compensate for fluctuations in cardiac output and blood pressure by lowering cerebrovascular resistance (Paulson et al., 1990; Willie et al., 2014). During HF, however, increased vascular tone successes vasodilation that normally counterbalances increased vasoconstriction (Gruhn et al., 2001; Choi et al., 2006; Yang et al., 2012). Hence, cerebral autoregulation might not be able to fully compensate hemodynamic changes, leading to decreased CBF that may directly translate to structural and functional alterations in the brain (Yang et al., 2012). Previous work identified a novel microvascular mechanism by which HF critically reduces CBF and thus, impairs memory function (i.e., tested in a novel object recognition task) in a mouse model of congestive HF. Here, augmented sphingosine-1-phosphate (S1P) signaling associates to enhanced myogenic tone that translates into compromised autoregulation and restricted CBF (Meissner et al., 2012; Yang et al., 2012). Pharmacological inhibition as well as genetic deletion of S1P receptor 2 (S1PR2) abolished the HF-induced augmentation of myogenic tone in isolated posterior cerebral arteries (Yang et al., 2012). Such augmented cerebrovascular S1PR2 signaling results from disturbances in S1P homeostasis during HF where an acquired cystic fibrosis transmembrane regulator (CFTR) dysfunction critically impairs the cerebrovascular S1P degradation, and hence increases S1P bioavailability for S1PR2 signaling on vascular smooth muscle cells (Meissner et al., 2012). Augmented tumor necrosis factor alpha (TNF-α) signaling in cerebral arteries was identified as molecular link that not only stimulates S1P production but also limits S1P degradation by down-regulating CFTR (Meissner et al., 2012; Yang et al., 2012; **Figure 1**). Scavenging TNF-α with Etanercept successfully abolished the pathological augmentation of cerebrovascular vasoconstriction in HF and thus, improved cerebral perfusion (Meissner et al., 2015). As a clinical intervention, however, Etanercept carries significant unwanted risks associated to its importance in neuronal function and blood pressure control (Baune et al., 2008; Kroetsch et al., 2017). Similarly, directly targeting S1P and its receptors bears considerable disadvantages due to its pleiotropy and cell-type specific functionality. Thus, correcting S1P homeostasis by normalizing S1P homeostasis (i.e., through stabilizing CFTR function) yielded beneficial effects (Lidington et al., 2019). Pharmacological treatment of HF mice improved neuronal integrity (i.e., dendritic lengths and spine density) and memory function through normalizing pathological alterations in cerebral artery CFTR expression, vascular reactivity, and CBF (Lidington et al., 2019). Targeting S1P-CFTR signaling, therefore, may emerge as valuable tool to manage cerebrovascular dysfunction, impaired cerebral perfusion, and neuronal injury contributing to HF-associated neurodegeneration and memory deficits. CFTR therapeutics could have unanticipated, non-beneficial effects in other tissues by for instance, increasing CFTR expression above normal levels. Thus, repurposing of clinically approved CFTR correctors necessitates more rigorous pre-clinical testing.

Another target of pre-clinical investigation in attempt to link HF and neurodegeneration is inflammation associated to CBF deficits. In a mouse model of slowly developing HF, vascular CI was observed during the early stages of HF and interestingly, preceded the development of left ventricular dysfunction (Adamski et al., 2018). Precise non-cardiac-dependent contributors to such early onset vascular CI still need to be confirmed. However, platelet hyperactivity, contributing to BBB impairment and in turn, cerebral endothelial inflammation and impairment of NO−dependent vasoregulation was put forward to promote the development of CI and lead to a chronic manifestation of CBF deficits during advanced HF (Adamski et al., 2018). Key players involved in this signaling cascade remain unknown and hence, platelet-targeting therapy as strategy

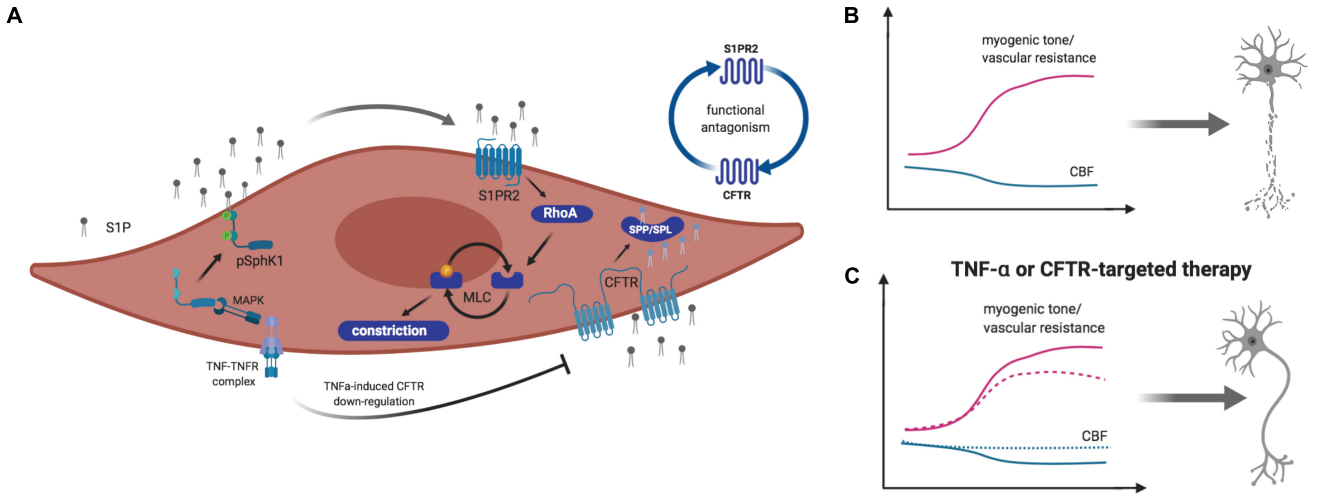


**FIGURE 1 |** Schematic illustration of sphingosine-1-phosphate (S1P) signaling-mediated myogenic tone regulation in vascular smooth muscle cells. **(A)** Tumor necrosis factor alpha (TNF-α) stimulates sphingosine kinase 1 (Sphk1)-mediated S1P production in a mitogen activated protein kinase (MAPK)-dependent manner. S1P is released to the extracellular space, where it activates S1P receptor (S1PR) 2–dependent signaling pathways, leading to vasoconstriction. TNF-α stimulates the downregulation of the cystic fibrosis transmembrane conductance regulator (CFTR), which transports S1P across the plasma membrane for degradation by S1P phosphohydrolases (SPP) or S1P lyases (SPL). **(B)** During heart failure (HF) and hemorrhagic stroke, augmented S1P production by SphK1 and limited S1P degradation enhance S1PR2-mediated vasoconstriction that leads to reduced cerebral blood flow (CBF) and neurodegeneration. **(C)** Targeting S1PR2 signaling by inhibiting S1PR2 or improving S1P degradation by enhancing CFTR expression and activity normalizes myogenic tone and cerebral perfusion. This normalization associates to reduced neuronal injury. Image created by BioRender.

to reverse neurodegeneration and CI associated to early HF is yet to be validated. To date, only few studies have investigated molecular targets to re-establish normal CBF during HF, which highlights the need for more pre-clinical research efforts to identify targetable mechanisms with capacity to improve brain function during HF.

## Stroke

Stroke is associated with the highest incidence of severe disability, of which neurological deficits are reported in 50% of all patients 6 months after a stroke event (Bordet et al., 2017; Merriman et al., 2018). Ischemic stroke leads to complete blood flow disruption, resulting in irreversible changes and cell death in the ischemic core and in parts of the surrounding area, the so-called penumbra. Reperfusion in the penumbra in the acute phase after ischemia onset limits the extent of tissue damage and helps improving functional outcome. It is, therefore, the main target of acute neuroprotective treatments (Lin et al., 2013), of which tissue plasminogen activator (tPA) is currently the only approved medication. The therapeutic window of tPA, however, is limited to 3–4.5 h post-stroke onset as tPA administration beyond 4.5 h increases the risk of developing edema and hemorrhagic transformation that in turn, is associated with delayed ischemia (Pena et al., 2017). Targeting vascular function and re-establishing proper CBF has been focus of many preclinical research efforts and yielded some promising results that warrant testing in humans (Iwasawa et al., 2018; Lidington et al., 2019).

The stimulation of angiogenesis via the vascular endothelial growth factor (VEGF) represents one of the most researched targets to improve CBF after stroke despite the controversy regarding its effects. Studies using VEGF treatment post-stroke revealed a clear importance of administration route and timing. VEGF injected systematically in the acute post-stroke phase induces BBB leakage and hemorrhagic transformation (Abumiya et al., 2005) accompanied by augmented ischemic lesions. Intravenous injection of human recombinant VEGF 48 h post-stroke on the other hand promoted angiogenesis and reduced neurological deficit in rats (Zhang et al., 2000). Mice overexpressing VEGF post-stroke had smaller ischemic volume and more pronounced new vessel formation, interestingly, without CBF improvements in the ischemic area or aggravating effects on the BBB (Wang et al., 2005). In addition to angiogenesis, the beneficial effect of exogenous VEGF may also be mediated by its anti-apoptotic and pro-survival effects in neurons (Sanchez et al., 2010). Accordingly, brain derived neurotrophic factor (BDNF) was identified as major regulator of angiogenic processes (Usui et al., 2014) that mediates its angiogenic effects via a crosstalk with VEGF (Li et al., 2006). In stroke patients significant lower BDNF levels were detected, which were positively correlated with poor functional outcome (Schabitz et al., 2007). Similar to VEGF, exogenous BDNF administration post-stroke resulted in smaller ischemic size and significantly improved functional outcome in rat models by inducing hippocampal neurogenesis and reducing neuroinflammation in the acute phase of stroke (Schabitz et al., 2007; Ravina et al., 2018). Its effects on CBF related to improved stroke outcome, however, are still elusive. Nerve growth factor (NGF) seems to be similarly linked to VEGF-mediated pro-angiogenic effects in the ischemic brain. In rodent

models, intranasal administration of NGF increased VEGF serum levels, increased microvessel density in the penumbra region, improved neurological outcome, and reduced ischemic injury 7 days post-stroke (Li et al., 2018). The beneficial effects of intranasal application of NGF are currently tested in a clinical trial in patients after acute ischemic stroke (ClinicalTrials.gov Identifier: NCT03686163). Although effects on CBF are warranted for most of these studies, angiogenesis-boosting therapy to re-establish proper perfusion evolved as promising therapeutic target in acute stroke therapy. Besides testing the classical growth factor-mediated therapy approaches in rodent models, AT1R blockers, which are widely used anti-hypertensive medications, were re-discovered to show pro-angiogenic effects after stroke and were reported to increase CBF in the ipsilateral hemisphere (Ito et al., 2002; Engelhorn et al., 2004; Alhusban et al., 2013). Similarly, AngII type 2 receptor (AT2R) agonists were shown to result in enhanced relaxation of basilar arteries and improved CBF after permanent middle cerebral artery occlusion (Faure et al., 2008). Nonetheless, the effectiveness of Angiotensin receptor (ATR) treatment is under debate as LIFE, ACCESS and MOSES trials demonstrated a decrease in the frequency of stroke after AT1R blockade (Dahlof et al., 2002; Schrader et al., 2003, 2005), while such treatment failed to show beneficial effects in other trials (Sandset et al., 2011).

Similar to cerebrovascular ATR effects, modulation of S1P receptors has shown beneficial effects on cerebrovascular function and CBF in experimental stroke. The selective S1PR1 agonist SEW2871 revealed positive effects on CBF, potentially resulting from increased diameter of leptomeningeal collateral vessels and enhanced vasodilatation in leptomeningeal anastomoses associated with increased phosphorylation of endothelial NOS in the ipsilateral hemisphere during chronic cerebral hypoperfusion (Iwasawa et al., 2018). Besides CBF improvements, researchers also reported an attenuation of infarct size and an improvement of neurological function assessed by neuroscoring.

In a model of subarachnoid hemorrhage (SAH), a form of stroke that originates from a hemorrhage but often exacerbates through secondary ischemia (van Gijn et al., 2007), increased cerebrovascular myogenic tone and hence, increased cerebrovascular resistance and reduced CBF was associated to augmented S1PR2 signaling in vascular smooth muscle cells (Yagi et al., 2015). Therapeutic administration of S1PR2 antagonist JTE013 improved cerebrovascular function, reduced neuronal injury and significantly enhanced neurological function (i.e., neuroscore reduction). TNF-α inhibition resulted in a similarly improved functional outcome (Yagi et al., 2015). TNF-α-induced impairment of cerebrovascular function that associates to CBF deficits and secondary ischemia during SAH (Vecchione et al., 2009; Yagi et al., 2015) are thought to stem from altered S1P signaling as TNF-α alters S1P degradation, which leaves more S1P available for pro-constrictive S1PR2 signaling in mural cells (**Figure 1**). Improving S1P degradation normalized the perfusion deficits, reduced neuronal injury, and improved neurological function in this SAH model (Lidington et al., 2019).

Overall, targeting the cerebral vasculature and improving vascular function and thus, normalizing CBF post-stroke evolved as promising path to improve post-stroke recovery. More studies are needed that evaluate CBF effects of different treatment strategies in addition to the commonly used assessment criteria for stroke outcome, such as infarct volume and neuroscore.

## OUTLOOK

We have come a long way to appreciate the association between CVD and cognitive function. Hence, efforts to preserve and restore cerebrovascular function and integrity drastically increased. The identification of important drivers of vasoregulation and thus, CBF is more and more valued to possess the capacity as therapeutic intervention early in disease processes to either prevent neurodegeneration or boost neuro-regeneration not only in CVD but also in classical neurodegenerative diseases. However, our mechanistic knowledge relating CVD-associated cerebrovascular dysfunction to neurodegeneration and potentially CI is still very fragmented, with only few targets with larger applicability emerging thus far. Particularly, the modulation of AT1R or S1P signaling has shown promising effects on cerebrovascular function and CBF and in turn, neuronal function in different pre-clinical disease models (Meissner et al., 2012; Yang et al., 2012; Yagi et al., 2015). Other emerging targets with a wider applicability still warrant a validation in CVD models. Transcranial infrared brain stimulation (TIBS) is suggested to stabilize patients with CI and memory deficits through stimulation of mitochondrial ATP production in the brain (de la Torre et al., 2019). This approach may not only counteract reduced energy availability but also increase CBF through augmenting endothelial NO production and thereby, limit neuronal degeneration (Uozumi et al., 2010). Further research is needed to identify unifying mechanisms that are applicable to several diseases. In light of that, engagement of different pre-clinical and clinical communities in concerted efforts is required to successfully answering still outstanding question.

## AUTHOR CONTRIBUTIONS

LV, HM, and AM wrote the first draft of the manuscript. ND-D and FU wrote sections of the manuscript. All authors contributed to the manuscript revision, read, and approved the submitted version.

## FUNDING

We gratefully acknowledge the following funding sources: The Swedish Research Council (VR 2017-01243), the German Research Foundation (DFG ME 4667/2-1), the Hedlunds Stiftelse (M-2019-1101), the Åke Wibergs Stiftelse (M19-0380), the Sparbanken Stiftelse (2019/670), and the Knut and Alice Wallenberg Foundation.

## REFERENCES


Abumiya, T., Yokota, C., Kuge, Y., and Minematsu, K. (2005). Aggravation of hemorrhagic transformation by early intraarterial infusion of low-dose vascular endothelial growth factor after transient focal cerebral ischemia in rats. *Brain Res.* 1049, 95–103. doi: 10.1016/j.brainres.2005.05.011

Adamski, M. G., Sternak, M., Mohaissen, T., Kaczor, D., Wieronska, J. M., Malinowska, M., et al. (2018). Vascular cognitive impairment linked to brain endothelium inflammation in early stages of heart failure in mice. *J. Am. Heart Assoc.* 7:e007694. doi: 10.1161/JAHA.117.007694

Alhusban, A., Kozak, A., Ergul, A., and Fagan, S. C. (2013). AT1 receptor antagonism is proangiogenic in the brain: BDNF a novel mediator. *J. Pharmacol. Exp. Ther.* 344, 348–359. doi: 10.1124/jpet.112.197483

Baune, B. T., Wiede, F., Braun, A., Golledge, J., Arolt, V., and Koerner, H. (2008). Cognitive dysfunction in mice deficient for TNF- and its receptors. *Am. J. Med. Genet. B Neuropsychiatr. Genet.* 147B, 1056–1064. doi: 10.1002/ajmg.b.30712

Bloch, S., Obari, D., and Girouard, H. (2015). Angiotensin and neurovascular coupling: beyond hypertension. *Microcirculation* 22, 159–167. doi: 10.1111/micc.12193

Bordet, R., Ihl, R., Korczyn, A. D., Lanza, G., Jansa, J., Hoerr, R., et al. (2017). Towards the concept of disease-modifier in post-stroke or vascular cognitive impairment: a consensus report. *BMC Med.* 15:107. doi: 10.1186/s12916-017-0869-6

Bos, I., Verhey, F. R., Ramakers, I., Jacobs, H. I. L., Soininen, H., Freund-Levi, Y., et al. (2017). Cerebrovascular and amyloid pathology in predementia stages: the relationship with neurodegeneration and cognitive decline. *Alzheimers Res. Ther.* 9:101. doi: 10.1186/s13195-017-0328-9

Cacciatore, F., Abete, P., Ferrara, N., Calabrese, C., Napoli, C., Maggi, S., et al. (1998). Congestive heart failure and cognitive impairment in an older population. Osservatorio geriatrico campano study group. *J. Am. Geriatr. Soc.* 46, 1343–1348. doi: 10.1111/j.1532-5415.1998.tb05999.x

Capone, C., Faraco, G., Park, L., Cao, X., Davisson, R. L., and Iadecola, C. (2011). The cerebrovascular dysfunction induced by slow pressor doses of angiotensin II precedes the development of hypertension. *Am. J. Physiol. Heart Circ. Physiol.* 300, H397–H407. doi: 10.1152/ajpheart.00679.2010

Capone, C., Faraco, G., Peterson, J. R., Coleman, C., Anrather, J., Milner, T. A., et al. (2012). Central cardiovascular circuits contribute to the neurovascular dysfunction in angiotensin II hypertension. *J. Neurosci.* 32, 4878–4886. doi: 10.1523/JNEUROSCI.6262-11.2012

Carnevale, D., Perrotta, M., Lembo, G., and Trimarco, B. (2016). Pathophysiological Links Among Hypertension and Alzheimer's Disease. *High Blood Press Cardiovasc. Prev.* 23, 3–7. doi: 10.1007/s40292-015-0108-1

Castillo, X., Castro-Obregon, S., Gutierrez-Becker, B., Gutierrez-Ospina, G., Karalis, N., Khalil, A. A., et al. (2019). Re-thinking the etiological framework of neurodegeneration. *Front. Neurosci.* 13:728. doi: 10.3389/fnins.2019.00728

Choi, B. R., Kim, J. S., Yang, Y. J., Park, K. M., Lee, C. W., Kim, Y. H., et al. (2006). Factors associated with decreased cerebral blood flow in congestive heart failure secondary to idiopathic dilated cardiomyopathy. *Am. J. Cardiol.* 97, 1365–1369. doi: 10.1016/j.amjcard.2005.11.059

Dahlof, B., Devereux, R. B., Kjeldsen, S. E., Julius, S., Beevers, G., de Faire, U., et al. (2002). Cardiovascular morbidity and mortality in the Losartan Intervention For Endpoint reduction in hypertension study (LIFE): a randomised trial against atenolol. *Lancet* 359, 995–1003. doi: 10.1016/s0140-6736(02)08089-3

de la Torre, J. C., Olmo, A. D., and Valles, S. (2019). Can mild cognitive impairment be stabilized by showering brain mitochondria with laser photons?. *Neuropharmacology* [Epub ahead of print].

Don-Doncow, N., Vanherle, L., Zhang, Y., and Meissner, A. (2019). T-cell accumulation in the hypertensive brain: a role for sphingosine-1-phosphate-mediated chemotaxis. *Int. J. Mol. Sci.* 20:E537. doi: 10.3390/ijms20030537

Don-Doncow, N., Zhang, Y., Rattik, S., Bjorkbackal, H., and Meissner, A. (2018). Anti-inflammatory properties of simvastatin mediate improvement of memory function in aged ApoE-/- mice. *Atherosclerosis* 32:98. doi: 10.1016/j.atherosclerosissup.2018.04.298

Drozdz, D., and Kawecka-Jaszcz, K. (2014). Cardiovascular changes during chronic hypertensive states. *Pediatr. Nephrol.* 29, 1507–1516. doi: 10.1007/s00467-013-2614-5

Engelhorn, T., Goerike, S., Doerfler, A., Okorn, C., Forsting, M., Heusch, G., et al. (2004). The angiotensin II type 1-receptor blocker candesartan increases cerebral blood flow, reduces infarct size, and improves neurologic outcome after transient cerebral ischemia in rats. *J. Cereb. Blood Flow Metab.* 24, 467–474. doi: 10.1097/00004647-200404000-00012

Faraco, G., Brea, D., Garcia-Bonilla, L., Wang, G., Racchumi, G., Chang, H., et al. (2018). Dietary salt promotes neurovascular and cognitive dysfunction through a gut-initiated TH17 response. *Nat. Neurosci.* 21, 240–249. doi: 10.1038/s41593-017-0059-z

Faraco, G., Sugiyama, Y., Lane, D., Garcia-Bonilla, L., Chang, H., Santisteban, M. M., et al. (2016). Perivascular macrophages mediate the neurovascular and cognitive dysfunction associated with hypertension. *J. Clin. Invest.* 126, 4674–4689. doi: 10.1172/JCI86950

Faure, S., Bureau, A., Oudart, N., Javellaud, J., Fournier, A., and Achard, J. M. (2008). Protective effect of candesartan in experimental ischemic stroke in the rat mediated by AT2 and AT4 receptors. *J. Hypertens.* 26, 2008–2015. doi: 10.1097/HJH.0b013e32830dd5ee

Freitag, M. H., Peila, R., Masaki, K., Petrovitch, H., Ross, G. W., White, L. R., et al. (2006). Midlife pulse pressure and incidence of dementia: the honolulu-asia aging study. *Stroke* 37, 33–37. doi: 10.1161/01.str.0000196941.58869.2d

Freitas, F., Estato, V., Reis, P., Castro-Faria-Neto, H. C., Carvalho, V., Torres, R., et al. (2017). Acute simvastatin treatment restores cerebral functional capillary density and attenuates angiotensin II-induced microcirculatory changes in a model of primary hypertension. *Microcirculation* 24:e12416. doi: 10.1111/micc.12416

GBD 2017 Causes of Death Collaborators (2018). Global, regional, and national age-sex-specific mortality for 282 causes of death in 195 countries and territories, 1980-2017: a systematic analysis for the global burden of disease study 2017. *Lancet* 392, 1736–1788. doi: 10.1016/S0140-6736(18)32203-7

Gorelick, P. B., Scuteri, A., Black, S. E., Decarli, C., Greenberg, S. M., Iadecola, C., et al. (2011). Vascular contributions to cognitive impairment and dementia: a statement for healthcare professionals from the american heart association/american stroke association. *Stroke* 42, 2672–2713. doi: 10.1161/str.0b013e3182299496

Gruhn, N., Larsen, F. S., Boesgaard, S., Knudsen, G. M., Mortensen, S. A., Thomsen, G., et al. (2001). Cerebral blood flow in patients with chronic heart failure before and after heart transplantation. *Stroke* 32, 2530–2533. doi: 10.1161/hs1101.098360

Guo, F., Liu, B., Tang, F., Lane, S., Souslova, E. A., Chudakov, D. M., et al. (2010). Astroglia are a possible cellular substrate of angiotensin(1-7) effects in the rostral ventrolateral medulla. *Cardiovasc. Res.* 87, 578–584. doi: 10.1093/cvr/cvq059

Hajduk, A. M., Kiefe, C. I., Person, S. D., Gore, J. G., and Saczynski, J. S. (2013). Cognitive change in heart failure: a systematic review. *Circ. Cardiovasc. Q. Outcomes* 6, 451–460. doi: 10.1161/CIRCOUTCOMES.113.000121

Haring, B., Leng, X., Robinson, J., Johnson, K. C., Jackson, R. D., Beyth, R., et al. (2013). Cardiovascular disease and cognitive decline in postmenopausal women: results from the Women's health initiative memory study. *J. Am. Heart Assoc.* 2:e000369. doi: 10.1161/JAHA.113.000369

Iadecola, C. (2013). The pathobiology of vascular dementia. *Neuron* 80, 844–866. doi: 10.1016/j.neuron.2013.10.008

Iadecola, C. (2017). The neurovascular unit coming of age: a journey through neurovascular coupling in health and disease. *Neuron* 96, 17–42. doi: 10.1016/j.neuron.2017.07.030

Ibekwe, R. (2015). Modifiable risk factors of hypertension and socio-demographic profile in oghara, delta state; prevalence and correlates. *Ann. Med. Health Sci. Res.* 5, 71–77. doi: 10.4103/2141-9248.149793

Ito, T., Yamakawa, H., Bregonzio, C., Terron, J. A., Falcon-Neri, A., and Saavedra, J. M. (2002). Protection against ischemia and improvement of cerebral blood flow in genetically hypertensive rats by chronic pretreatment with an angiotensin II AT1 antagonist. *Stroke* 33, 2297–2303. doi: 10.1161/01.str.0000027274.03779.f3

Iwasawa, E., Ishibashi, S., Suzuki, M., Li, F., Ichijo, M., Miki, K., et al. (2018). Sphingosine-1-phosphate receptor 1 activation enhances leptomeningeal collateral development and improves outcome after stroke in mice. *J. Stroke Cerebrovasc. Dis.* 27, 1237–1251. doi: 10.1016/j.jstrokecerebrovasdis.2017.11.040

Jefferson, A. L., Himali, J. J., Beiser, A. S., Au, R., Massaro, J. M., Seshadri, S., et al. (2010). Cardiac index is associated with brain aging: the framingham

heart study. *Circulation* 122, 690–697. doi: 10.1161/CIRCULATIONAHA.109.905091

Jiang, T., Gao, L., Shi, J., Lu, J., Wang, Y., and Zhang, Y. (2013). Angiotensin-(1-7) modulates renin–angiotensin system associated with reducing oxidative stress and attenuating neuronal apoptosis in the brain of hypertensive rats. *Pharmacol. Res.* 67, 84–93. doi: 10.1016/j.phrs.2012.10.014

Joutel, A., Monet-Lepretre, M., Gosele, C., Baron-Menguy, C., Hammes, A., Schmidt, S., et al. (2010). Cerebrovascular dysfunction and microcirculation rarefaction precede white matter lesions in a mouse genetic model of cerebral ischemic small vessel disease. *J. Clin. Invest.* 120, 433–445. doi: 10.1172/JCI39733

Kalayci, R., Kaya, M., Elmas, I., Arican, N., Ahishali, B., Uzun, H., et al. (2005). Effects of atorvastatin on blood–brain barrier permeability during l-NAME hypertension followed by angiotensin-II in rats. *Brain Res.* 1042, 184–193. doi: 10.1016/j.brainres.2005.02.044

Kazama, K., Anrather, J., Zhou, P., Girouard, H., Frys, K., Milner, T. A., et al. (2004). Angiotensin II impairs neurovascular coupling in neocortex through NADPH oxidase-derived radicals. *Circ. Res.* 95, 1019–1026. doi: 10.1161/01.res.0000148637.85595.c5

Kovacs, K. R., Bajko, Z., Szekeres, C. C., Csapo, K., Olah, L., Magyar, M. T., et al. (2014). Elevated LDL-C combined with hypertension worsens subclinical vascular impairment and cognitive function. *J. Am. Soc. Hypertens.* 8, 550–560. doi: 10.1016/j.jash.2014.04.007

Kroetsch, J. T., Levy, A. S., Zhang, H., Aschar-Sobbi, R., Lidington, D., Offermanns, S., et al. (2017). Constitutive smooth muscle tumour necrosis factor regulates microvascular myogenic responsiveness and systemic blood pressure. *Nat. Commun.* 8:14805. doi: 10.1038/ncomms14805

Kuller, L. H., Lopez, O. L., Jagust, W. J., Becker, J. T., DeKosky, S. T., Lyketsos, C., et al. (2005). Determinants of vascular dementia in the cardiovascular health cognition study. *Neurology* 64, 1548–1552. doi: 10.1212/01.wnl.0000160115.55756.de

Leeuwis, A. E., Smith, L. A., Melbourne, A., Hughes, A. D., Richards, M., Prins, N. D., et al. (2018). Cerebral blood flow and cognitive functioning in a community-based, multi-ethnic cohort: the SABRE study. *Front. Aging Neurosci.* 10:279. doi: 10.3389/fnagi.2018.00279

Leto, L., and Feola, M. (2014). Cognitive impairment in heart failure patients. *J. Geriatr. Cardiol.* 11, 316–328.

Li, Q., Ford, M. C., Lavik, E. B., and Madri, J. A. (2006). Modeling the neurovascular niche: VEGF- and BDNF-mediated cross-talk between neural stem cells and endothelial cells: an in vitro study. *J. Neurosci. Res.* 84, 1656–1668. doi: 10.1002/jnr.21087

Li, X., Li, F., Ling, L., Li, C., and Zhong, Y. (2018). Intranasal administration of nerve growth factor promotes angiogenesis via activation of PI3K/Akt signaling following cerebral infarction in rats. *Am. J. Transl. Res.* 10, 3481–3492.

Lidington, D., Fares, J. C., Uhl, F. E., Dinh, D. D., Kroetsch, J. T., Sauvé, M., et al. (2019). CFTR therapeutics normalize cerebral perfusion deficits in mouse models of heart failure and subarachnoid hemorrhage. *JACC* 4, 940–958. doi: 10.1016/j.jacbts.2019.07.004

Lin, L., Bivard, A., and Parsons, M. W. (2013). Perfusion patterns of ischemic stroke on computed tomography perfusion. *J. Stroke* 15, 164–173. doi: 10.5853/jos.2013.15.3.164

Lu, J., Zhang, Y., and Shi, J. (2008). Effects of intracerebroventricular infusion of angiotensin-(1-7) on bradykinin formation and the kinin receptor expression after focal cerebral ischemia-reperfusion in rats. *Brain Res.* 1219, 127–135. doi: 10.1016/j.brainres.2008.04.057

Meissner, A. (2016). Hypertension and the brain: a risk factor for more than heart disease. *Cerebrovasc. Dis.* 42, 255–262. doi: 10.1159/000446082

Meissner, A., Minnerup, J., Soria, G., and Planas, A. M. (2017). Structural and functional brain alterations in a murine model of angiotensin II-induced hypertension. *J. Neurochem.* 140, 509–521. doi: 10.1111/jnc.13905

Meissner, A., Visanji, N. P., Momen, M. A., Feng, R., Francis, B. M., Bolz, S.-S., et al. (2015). Tumor necrosis factor-α underlies loss of cortical dendritic spine density in a mouse model of congestive heart failure. *J. Am. Heart Assoc.* 4:e001920.

Meissner, A., Yang, J., Kroetsch, J. T., Sauve, M., Dax, H., Momen, A., et al. (2012). Tumor necrosis factor-alpha-mediated downregulation of the cystic fibrosis transmembrane conductance regulator drives pathological sphingosine-1-phosphate signaling in a mouse model of heart failure. *Circulation* 125, 2739–2750. doi: 10.1161/CIRCULATIONAHA.111.047316

Merriman, N. A., Sexton, E., Donnelly, N. A., McCabe, G., Walsh, M. E., Rohde, D., et al. (2018). Managing cognitive impairment following stroke: protocol for a systematic review of non-randomised controlled studies of psychological interventions. *BMJ Open* 8:e019001. doi: 10.1136/bmjopen-2017-019001

O'Brien, J. T., and Thomas, A. (2015). Vascular dementia. *Lancet* 386, 1698–1706. doi: 10.1016/S0140-6736(15)00463-8

Paulson, O. B., Strandgaard, S., and Edvinsson, L. (1990). Cerebral autoregulation. *Cerebrovasc. Brain Metab. Rev.* 2, 161–192.

Pena, I. D., Borlongan, C., Shen, G., and Davis, W. (2017). Strategies to extend thrombolytic time window for ischemic stroke treatment: an unmet clinical need. *J. Stroke* 19, 50–60. doi: 10.5853/jos.2016.01515

Pressler, S. J. (2008). Cognitive functioning and chronic heart failure: a review of the literature (2002-July 2007). *J. Cardiovasc. Nurs.* 23, 239–249. doi: 10.1097/01.JCN.0000305096.09710.ec

Pressler, S. J., Subramanian, U., Kareken, D., Perkins, S. M., Gradus-Pizlo, I., Sauvé, M. J., et al. (2010). Cognitive deficits in chronic heart failure. *Nurs. Res.* 59, 127–139. doi: 10.1097/NNR.0b013e3181d1a747

Ravina, K., Briggs, D. I., Kislal, S., Warraich, Z., Nguyen, T., Lam, R. K., et al. (2018). Intracerebral delivery of brain-derived neurotrophic factor using Hystem((R))-C Hydrogel implants improves functional recovery and reduces neuroinflammation in a rat model of ischemic stroke. *Int. J. Mol. Sci.* 19:E3782. doi: 10.3390/ijms19123782

Rodriguez-Iturbe, B., Pons, H., and Johnson, R. J. (2017). Role of the immune system in hypertension. *Physiol. Rev.* 97, 1127–1164. doi: 10.1152/physrev.00031.2016

Sanchez, A., Wadhwani, S., and Grammas, P. (2010). Multiple neurotrophic effects of VEGF on cultured neurons. *Neuropeptides* 44, 323–331. doi: 10.1016/j.npep.2010.04.002

Sandset, E. C., Bath, P. M., Boysen, G., Jatuzis, D., Korv, J., Luders, S., et al. (2011). The angiotensin-receptor blocker candesartan for treatment of acute stroke (SCAST): a randomised, placebo-controlled, double-blind trial. *Lancet* 377, 741–750. doi: 10.1016/S0140-6736(11)60104-9

Schabitz, W. R., Steigleder, T., Cooper-Kuhn, C. M., Schwab, S., Sommer, C., Schneider, A., et al. (2007). Intravenous brain-derived neurotrophic factor enhances poststroke sensorimotor recovery and stimulates neurogenesis. *Stroke* 38, 2165–2172. doi: 10.1161/strokeaha.106.477331

Schrader, J., Luders, S., Kulschewski, A., Berger, J., Zidek, W., Treib, J., et al. (2003). The access study: evaluation of acute candesartan cilexetil therapy in stroke survivors. *Stroke* 34, 1699–1703. doi: 10.1161/01.str.0000075777.18006.89

Schrader, J., Luders, S., Kulschewski, A., Hammersen, F., Plate, K., Berger, J., et al. (2005). Morbidity and mortality after stroke, eprosartan compared with nitrendipine for secondary prevention: principal results of a prospective randomized controlled study (MOSES). *Stroke* 36, 1218–1226.

Sprint Mind Investigators for the Sprint Research Group, Williamson, J. D., Pajewski, N. M., Auchus, A. P., Bryan, R. N., Chelune, G., et al. (2019). Effect of intensive vs standard blood pressure control on probable dementia: a randomized clinical trial. *JAMA* 321, 553–561.

Takeda, S., Rakugi, H., and Morishita, R. (2019). Roles of vascular risk factors in the pathogenesis of dementia. *Hypertens. Res*. [Epub ahead of print].

Uozumi, Y., Nawashiro, H., Sato, S., Kawauchi, S., Shima, K., and Kikuchi, M. (2010). Targeted increase in cerebral blood flow by transcranial near-infrared laser irradiation. *Lasers Surg. Med.* 42, 566–576. doi: 10.1002/lsm.20938

Usui, T., Naruo, A., Okada, M., Hayabe, Y., and Yamawaki, H. (2014). Brain-derived neurotrophic factor promotes angiogenic tube formation through generation of oxidative stress in human vascular endothelial cells. *Acta Physiol.* 211, 385–394. doi: 10.1111/apha.12249

van Gijn, J., Kerr, R. S., and Rinkel, G. J. (2007). Subarachnoid haemorrhage. *Lancet* 369, 306–318.

Vecchione, C., Frati, A., Di Pardo, A., Cifelli, G., Carnevale, D., Gentile, M. T., et al. (2009). Tumor necrosis factor-alpha mediates hemolysis-induced vasoconstriction and the cerebral vasospasm evoked by subarachnoid hemorrhage. *Hypertension* 54, 150–156. doi: 10.1161/HYPERTENSIONAHA.108.128124

Wang, Y., Kilic, E., Kilic, U., Weber, B., Bassetti, C. L., Marti, H. H., et al. (2005). VEGF overexpression induces post-ischaemic neuroprotection, but facilitates haemodynamic steal phenomena. *Brain* 128, 52–63. doi: 10.1093/brain/awh325

Willie, C. K., Tzeng, Y. C., Fisher, J. A., and Ainslie, P. N. (2014). Integrative regulation of human brain blood flow. *J. Physiol.* 592, 841–859. doi: 10.1113/jphysiol.2013.268953

Wolters, F. J., Zonneveld, H. I., Hofman, A., van der Lugt, A., Koudstaal, P. J., Vernooij, M. W., et al. (2017). Cerebral perfusion and the risk of dementia: a population-based study. *Circulation* 136, 719–728. doi: 10.1161/CIRCULATIONAHA.117.027448

Yagi, K., Lidington, D., Wan, H., Fares, J. C., Meissner, A., Sumiyoshi, M., et al. (2015). Therapeutically targeting tumor necrosis factor-alpha/sphingosine-1-phosphate signaling corrects myogenic reactivity in subarachnoid hemorrhage. *Stroke* 46, 2260–2270. doi: 10.1161/STROKEAHA.114.006365

Yang, J., Noyan-Ashraf, M. H., Meissner, A., Voigtlaender-Bolz, J., Kroetsch, J. T., Foltz, W., et al. (2012). Proximal cerebral arteries develop myogenic responsiveness in heart failure via tumor necrosis factor-alpha-dependent activation of sphingosine-1-phosphate signaling. *Circulation* 126, 196–206. doi: 10.1161/CIRCULATIONAHA.111.039644

Zhang, Y., Lu, J., Shi, J., Lin, X., Dong, J., Zhang, S., et al. (2008). Central administration of angiotensin-(1-7) stimulates nitric oxide release and upregulates the endothelial nitric oxide synthase expression following focal cerebral ischemia/reperfusion in rats. *Neuropeptides* 42, 593–600. doi: 10.1016/j.npep.2008.09.005

Zhang, Z. G., Zhang, L., Jiang, Q., Zhang, R., Davies, K., Powers, C., et al. (2000). VEGF enhances angiogenesis and promotes blood-brain barrier leakage in the ischemic brain. *J. Clin. Invest.* 106, 829–838. doi: 10.1172/jci9369

**Conflict of Interest:** The authors declare that the research was conducted in the absence of any commercial or financial relationships that could be construed as a potential conflict of interest.

frontiers in Cell and Developmental Biology

MINI REVIEW
published: 13 March 2020
doi: 10.3389/fcell.2020.00116

# Deconstructing Neurogenesis, Transplantation and Genome-Editing as Neural Repair Strategies in Brain Disease

*Muhammad O. Chohan*[1,2]*

[1] Department of Psychiatry, Division of Integrative Neuroscience, New York State Psychiatric Institute, New York, NY, United States, [2] Department of Psychiatry, Division of Child and Adolescent Psychiatry, Columbia University, New York, NY, United States

Neural repair in injury and disease presents a pressing unmet need in regenerative medicine. Due to the intrinsically reduced ability of the brain to replace lost and damaged neurons, reversing long-term cognitive and functional impairments poses a unique problem. Over the years, advancements in cellular and molecular understanding of neurogenesis mechanisms coupled with sophistication of biotechnology tools have transformed neural repair into a cross-disciplinary field that integrates discoveries from developmental neurobiology, transplantation and tissue engineering to design disease- and patient-specific remedies aimed at boosting either native rehabilitation or delivering exogenous hypoimmunogenic interventions. Advances in deciphering the blueprint of neural ontogenesis and annotation of the human genome has led to the development of targeted therapeutic opportunities that have the potential of treating the most vulnerable patient populations and whose findings from benchside suggest looming clinical translation. This review discusses how findings from studies of adult neurogenesis have informed development of interventions that target endogenous neural regenerative machineries and how advances in biotechnology, including the use of new gene-editing tools, have made possible the development of promising, complex neural transplant-based strategies. Adopting a multi-pronged strategy that is tailored to underlying neural pathology and that encompasses facilitation of endogenous regeneration, correction of patient's genomic mutations and delivery of transformed neural precursors and mature disease-relevant neuronal populations to replace injured or lost neural tissue remains no longer a fantasy.

**Keywords: neural stem cells, transplantation, adult neurogenesis, neurological disorders, genome-editing**

OPEN ACCESS

***Edited by:***
*Luis B. Tovar-y-Romo, National Autonomous University of Mexico, Mexico*

***Reviewed by:***
*Caghan Kizil, German Center for Neurodegenerative Diseases (DZNE), Germany*
*Sara Xapelli, University of Lisbon, Portugal*
*Jorge Valero, Achucarro Basque Center for Neuroscience, Spain*

***Correspondence:**
*Muhammad O. Chohan*
*muhammad.chohan@nyspi.columbia.edu*

***Specialty section:***
*This article was submitted to Molecular Medicine, a section of the journal Frontiers in Cell and Developmental Biology*

***Received:*** *02 December 2019*
***Accepted:*** *11 February 2020*
***Published:*** *13 March 2020*

***Citation:***
*Chohan MO (2020) Deconstructing Neurogenesis, Transplantation and Genome-Editing as Neural Repair Strategies in Brain Disease. Front. Cell Dev. Biol. 8:116. doi: 10.3389/fcell.2020.00116*

## INTRODUCTION

Contrary to long held belief, adult neurogenesis (AN) is now a well-recognized phenomenon in mammals. While constitutively active AN is restricted to two forebrain regions, the subgranular zone (SGZ) of the dentate gyrus (DG) of the hippocampus and the subventricular zone (SVZ) lining the ventricles, variable degrees of reactive neurogenesis is present in several other brain regions that is activated in response to injury or disease onset (Jin et al., 2006). Importantly, impairments

in AN have been linked to a number of neurological and psychiatric diseases (Hoglinger et al., 2004; Reif et al., 2006), indicating the value of developing therapies that boost AN potential of cell replacement in tackling brain dysfunction.

In contrast to mammals, lower vertebrates such as teleost fish and amphibians (such as axolotl and salamander) have expanded neurogenic capacities. Unsurprisingly, most of our understanding of human AN processes continues to be informed by findings in lower vertebrate models that also display comparable expression patterns and functions of neurogenic molecular controls. Intriguingly, some amphibian species display life-long de-differentiation and *trans*-differentiation processes during repair (as seen during retinal and lens regeneration in newts), phenomenon absent in mammals. Using recently developed gene-editing toolkits, studies in these species can provide mechanistic insights into why such phenomenon are scaled down in mammals and be informative for developing novel disease relevant cell-replacement strategies.

The remarkable ability of the adult mammalian brain to functionally integrate new neurons into existing circuitries (Falkner et al., 2016) combined with the progress in our understanding of these phenomenon in non-mammalian and mammalian models has now made possible the development of therapies that can awaken latent neurogenic programs, direct resident neuronal fates into cell types of need and replace injured or diseased neurons in brain regions within and outside that of DG and SVZ. This review discusses AN in mammalian and non-mammalian brains, the reparative potential of cell-based transplant therapy in neurodegenerative diseases and the therapeutic application of novel gene-editing approaches in the framework of designing disease- and patient-specific curative strategies (**Figure 1**).

# ADULT NEUROGENESIS IN THE MAMMALIAN BRAIN

## Evidence of Adult Neurogenesis in Mammals: A Brief History

Initial anatomical evidence of the existence of AN in mammals did not arrive until the 1960s when, using thymidine-$H^3$ autoradiographic techniques, Joseph Altman reported evidence of the formation of newborn neurons in the adult brain (Altman, 1962, 1963; Altman and Das, 1965, 1967). Follow-up electron microscopic studies extended support to the claim of radio-labeled cells as being neuronal (Kaplan and Hinds, 1977), still, a lack of use of definitive neuronal markers to co-label radio-labeled cells and a failure to replicate this in non-human primates (Rakic, 1985; Eckenhoff and Rakic, 1988) prevented the field from reaching consensus.

Almost a decade after Altman's initial findings, Fernando Nottebohm, following up on his discovery of sexually dimorphic and seasonally regulated song-control system in the songbird (Nottebohm and Arnold, 1976; Nottebohm, 1981), crucially demonstrated adult-born cells' neuronal identity and functional integration into adult circuits (Goldman and Nottebohm, 1983; Paton and Nottebohm, 1984; Alvarez-Buylla et al., 1990a). Soon after, the glial nature of NSCs in songbirds was described (Alvarez-Buylla et al., 1990b), which was followed by similar observations in the mammalian SVZ (Doetsch et al., 1999) and hippocampus (Seri et al., 2001, 2004). Later, the isolation of mitogen-responsive multipotent cells and successful induction of reactive neurogenesis suggested continuance of prenatal permissive regenerative programs into the adult mammalian brain (Reynolds and Weiss, 1992; Lois and Alvarez-Buylla, 1993; Luskin, 1993; Palmer et al., 1995). Finally, AN in the SVZ and hippocampus was shown to exist in humans (Eriksson et al., 1998; Spalding et al., 2013; Ernst et al., 2014).

### Adult Neurogenesis in the Sub-Ventricular Zone

Initial characterization of the adult human SVZ by Alvarez-Buylla et al., reported a ribbon of astrocytes lining the lateral ventricles with few surrounding proliferating cells (Sanai et al., 2004). In particular, the human SVZ was reported to lack the cellular organizational structure and rostral migratory stream (RMS) characteristics of its rodent counterpart (**Figure 1**, legend). A follow-up study by the same group reported strong expression of immature cell markers and RMS in the infant human SVZ, both of which sharply declined after birth (Sanai et al., 2011). In addition, a novel migratory stream to the cortex was described in the infant brain (Sanai et al., 2011). In contrast, another group found robust SVZ proliferation and a RMS containing glial cells, proliferating cells and neuroblasts organized around a lateral ventricular extension reaching the olfactory bulb (OB) in the adult (Curtis et al., 2007; Kam et al., 2009). These disparate adult human data underscore the importance of applying more reliable, species-specific progenitor/immature cell markers and optimizing methodological approaches for identifying NSCs (see also below). From a therapeutic perspective, the existence of SVZ neurogenesis in humans could have important implications for neurodegenerative disorders as neuroblasts were recently shown to migrate to and differentiate into interneurons in the striatum (Ernst et al., 2014) [but also see Dennis et al. (2016)] and carbon-14 birth-dating studies have suggested that adult-born striatal neurons might be preferentially depleted in Huntington's disease (HD) (Ernst et al., 2014). Moreover, in animals models of PD, stimulation of SVZ precursors has been shown to rescue dopamine (DA) mediated behaviors (Spalding et al., 2005; Androutsellis-Theotokis et al., 2009).

### Adult Neurogenesis in the Hippocampal Dentate Gyrus

Whether the adult human hippocampus contains self-renewing NSCs is a topic of much interest. Eriksson et al. (1998) initially reported newly generated BrdU-labeled cells in the human DG that co-expressed neuronal markers. This finding was corroborated by studies demonstrating the presence of neural progenitors in surgically excised brain specimens (Roy et al., 2000; Palmer et al., 2001) and carbon-14 birth-dating studies that revealed substantial DG neuronal turnover (Spalding et al., 2013). Recently, Boldrini et al. (2018) also found preserved DG neurogenesis in individuals 14–79 years

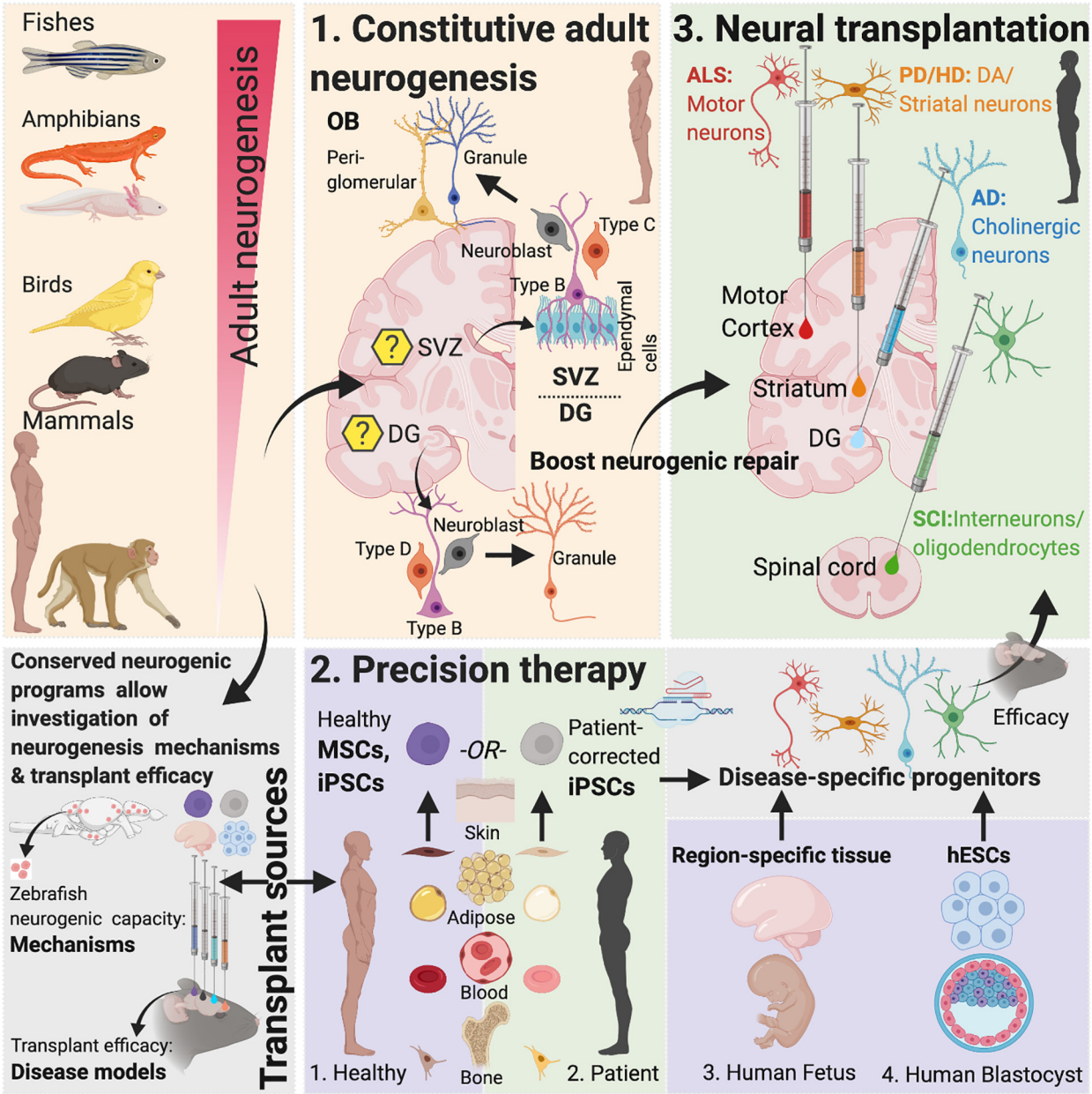


**FIGURE 1 |** Adult neurogenesis in mammals and non-mammals. Lessons from non-vertebrate neurogenesis and implications for designing cell-based transplant therapies. Mammalian SVZ Neurogenesis: Characterization of neurogenesis in the rodent SVZ has revealed the existence of quiescent and active populations of proliferating cells. While heterogenous populations of NSCs have been described, "type-B" cells maintaining close proximity with the ependymal cell layer include nestin-expressing populations that asymmetrically divide to form Ascli and Dlx2 expressing "type-C" cells, also called transit-amplifying cells, which then symmetrically divide to form Dcx-positive type-A neuroblasts. These neuroblasts constitute the rostral migratory stream (RMS) that eventually contributes to OB peri-glomerular and granule cells. Recent studies have suggested that "type-B" cells are derived from embryonic NSCs that also generate striatal, septal or cortical neurons and become quiescent between E13.5-15.5 until their activation in adulthood (Fuentealba et al., 2015). Within the OB, granule cells form >95% of the adult-born population (Winner et al., 2002; Naritsuka et al., 2009; Merkle et al., 2014). Optogenetic activation paired with odor stimulation of adult-born neurons has been shown to facilitate difficult olfactory discrimination learning, an effect that is absent following photoactivation of early postnatal born neurons (Alonso et al., 2012). In addition, two photon-targeted recordings from peri-glomerular neurons have revealed that adult-born cells functionally integrate in the OB circuitry and whose activity is regulated by experience-dependent plasticity (Livneh et al., 2014). Mammalian DG Neurogenesis: Whether the adult mammalian hippocampus contains self-renewing NSCs or whether the neighboring lateral ventricular niche containing true NSCs maintains neurogenesis in the hippocampus has been contested (Seaberg and van der Kooy, 2002; Bull and Bartlett, 2005) but several recent studies have documented the presence of self-renewing, multipotent cells expressing embryonic NSC markers in the DG with fate mapping analysis confirming their stem cell behavior *in vivo* (Seri et al., 2001; Lagace et al., 2007; Imayoshi et al., 2008; Lugert et al., 2010; Bonaguidi et al., 2011; Encinas et al., 2011; Urban et al., 2016; Pilz et al., 2018). In the adult hippocampus (DG), SGZ radial glia-like cells give rise to proliferative non-radial-like populations that differentiate into neuroblasts. Upon differentiation, these neuroblasts develop into granule cells (Pilz et al., 2018). The embryonic origin of adult precursors in the DG in rodents was recently traced to a common Hopx-positive precursor population that is responsible for

*(Continued)*

**FIGURE 1 |** Continued
generating both developmental and AN, with the precursors not undergoing a lineage specification change during any stage of development (Berg et al., 2019). Non-mammalian Vertebrates: In contrast to mammals, non-mammalian vertebrates including certain fish and salamander species display a remarkable amount of neurogenic capacity in the adult. More than a dozen constitutive neurogenic zones have been described in the adult teleost (Grandel et al., 2006; Maruska et al., 2012), and while constitutive neurogenesis is limited to the forebrain in the newt (Berg et al., 2010) and the forebrain and ventricular zone in the axolotl (Maden et al., 2013), neuronal loss in these species following injury leads to complete regeneration (Bernardos et al., 2007; Parish et al., 2007; Berg et al., 2010; Skaggs et al., 2014). This latter capacity is reminiscent of, albeit less efficacious, reparative recruitment of quiescent progenitors found in rodents (Barnabe-Heider et al., 2010; Sirko et al., 2013; Magnusson et al., 2014). Implications for Designing Brain Repair Strategies: The limited ability of AN in mammals to enable neural repair could be due to a presence of reduced number of NSCs, available progenitors that maybe fate-restricted or strong inhibitory cues from glia. As mentioned, studies focused on naturally occurring neurogenic process that are present in lower vertebrates can yield important insights into why those mechanisms are restricted in mammals (Bhattarai et al., 2016, 2020). Evidence for the presence of evolutionary conserved genes related to regeneration as revealed by recent genome sequencing of species with enhanced regenerative capacities and the development of techniques that make those species amenable to gene-editing (Howe et al., 2013; Irion et al., 2014; Elewa et al., 2017; Nowoshilow et al., 2018) has paved the way for in-depth investigation of neurogenic molecular controls and their comparison across mammals and non-mammalian species to design novel therapies. Created with Biorender.com.

of age, with older individuals having a smaller quiescent progenitor pool. The existence of lifelong hippocampal AN was further confirmed in two very recent studies that examined neurogenesis throughout normal and pathological aging in AD patients (Moreno-Jimenez et al., 2019) and in individuals with mild cognitive impairment (Tobin et al., 2019), with findings suggesting impaired neurogenesis in both conditions. This is not surprising since an enhanced DG neurogenic capacity has been linked to reduced susceptibility to cognitive impairments in patients with AD pathology (Briley et al., 2016) and enhancing hippocampal neurogenesis improved cognition in an AD mouse model (Choi et al., 2018). In stark contrast, other groups have observed a sharp decline in proliferating cells in childhood, observing only sparse number of proliferating cells in the adult hippocampus that were of microglia lineage (Dennis et al., 2016). In addition, Sorrells et al. (2018), using DCX and PSA-NCAM to label immature neurons, found a sharp reduction in hippocampal neurogenesis in childhood observing no new neurons in the adult. Intriguingly, the authors found that both these markers, which are widely used to identify neurogenesis in other species, can label mature neurons and glial cells in humans. Marker expression can depend on tissue preservation techniques and DCX is known to be sensitive to postmortem breakdown (Boekhoorn et al., 2006) posing significant challenges to cross-study comparisons. Future studies could benefit by allocating efforts to documenting the clinical profile and mode of death of patients as both these factors can drastically influence neurogenesis rates. In addition, applying quality control procedures, including minimizing postmortem delay, optimizing brain fixation methods to preserve neuronal morphology and marker expression, standardization of protocols for identification of neurogenic neurons and examination of gene expression patterns, along with development of more specific markers of neurogenic neurons in humans may be beneficial.

### Adult Neurogenesis in the Non-mammalian Brain: Similarities to Adult Mammalian Neurogenesis

Several similarities exist between mammalian and non-mammalian species regarding AN. These include the sites of neurogenesis [the ventricular lining within the telencephalon appears to be the site of origin of new neurons in many mammalian and non-mammalian species (Goldman and Nottebohm, 1983; Doetsch et al., 1999; Ganz et al., 2010; Rothenaigner et al., 2011)], identity of neurogenic progenitors as well as the molecular machineries that regulate proliferation of NSCs. Like in mammals (Doetsch et al., 1999), some progenitor populations in birds, fishes and amphibians also have glial characteristics (Alvarez-Buylla et al., 1990b; Rothenaigner et al., 2011; Kirkham et al., 2014). Moreover, molecular controls governing quiescence of NSCs show remarkable conservation between vertebrate species: e.g., Notch signaling has been shown to regulate radial glial quiescence in zebrafish (Alunni et al., 2013), newt (Kirkham et al., 2014) and adult mouse (Imayoshi et al., 2010) and transcription factors Id1 and Fezf2 that are associated with increased quiescence in adult mouse NSCs (Nam and Benezra, 2009) have also been identified in zebrafish (Berberoglu et al., 2014; Rodriguez Viales et al., 2015). Intriguingly, Ascl1 upregulation has been linked to the activation of the retinal latent progenitors, Muller glia, in zebrafish during retinal regeneration following lesions (Ramachandran et al., 2011) and forced overexpression of Ascl1 in Muller glia in young mice coaxes these progenitors toward a neurogenic fate (Ueki et al., 2015) rather than the gliogenic fate that is normally seen in older mice (Dyer and Cepko, 2000). Comparative studies of species can thus yield important insights into the biology of AN and be informative for therapeutic strategies that harness AN potential of tissue repair (Kizil and Bhattarai, 2018; **Figure 1**).

## NEURAL TRANSPLANTATION AS CELL-BASED THERAPY

On the other hand, transplantation of NSCs or progenitors to replace diseased neurons is an alternate strategy that comes with the opportunity of directing therapy to brain regions where it is most needed (**Figure 1** and **Table 1**). Also, the self-renewing attribute and migratory nature of NSCs/progenitors make them attractive therapeutic candidates in the setting of diffuse damage to the brain.

### Fetal and Embryonic Tissue-Based Transplants in Pre-clinical Models and Clinical Trials

Initial proof-of-concept transplantation studies carried out during 70 and 80s demonstrated long-term viability of grafted

**TABLE 1 |** Summary of select studies involving cell-transplant based repair strategies in *in vivo* pre-clinical neurodegenerative disease models.

| Repair strategy | References | Type of cell grafted/manipulated | Disease/ model | Functional impact |
|---|---|---|---|---|
| Fetal-tissue based | (Bjorklund and Stenevi, 1979) | Fetal ventral midbrain tissue | PD/rat 6-OHDA | Restoration of DA innervation and motor improvement |
| | (Isacson et al., 1984) | Fetal striatal tissue | HD/rat Ibotenic-acid | Reduction in locomotor and metabolic hyperactivity |
| | (Low et al., 1982; Gage et al., 1984) | Fetal substantia nigra and septal nuclei | Aging, hippocampal lesions | Improved motor coordination and spatial learning |
| | (Gaillard et al., 2007; Falkner et al., 2016) | Fetal tissue | Motor, visual cortex | Long range, synaptic, functional integration with host circuitries |
| MSCs-based | (Hellmann et al., 2006) | mBM-MSCs | PD/rat 6-OHDA | Cells migrate to lesioned hemisphere and differentiate into neurons |
| | (Bahat-Stroomza et al., 2009) | hBM-MSCs | PD/rat 6-OHDA | Reduction in motor impairments, regeneration of DA terminals |
| | (Lee et al., 2009) | hAD-MSCs | HD/rat QA-lesion, mouse R6/2 | Improved motor performance, reduced huntingtin aggregates |
| | (Lin et al., 2011) | hBM-MSCs | HD/mouse QA-lesion, R6/2 | Improved motor performance in QA-lesion model |
| | (Shin et al., 2014) | hMSCs | AD/mouse Aβ treated | Increased autophagy and Aβ clearance |
| | (Garcia et al., 2014) | VEGF overexpressing BM-MSCs | AD/mouse APPswe/PS1 double transgenic | Increased vascularization, cognition, decreased Aβ plagues |
| | (Kim et al., 2010) | ALS-hBM-MSCs | ALS/mouse $SOD1^{G93A}$ | Increased lifespan, increased MN survival |
| | (Kim et al., 2014) | hAD-MSCs | ALS/mouse $SOD1^{G93A}$ | Release of growth factors, increased life span |
| hESCs-based | (Kriks et al., 2011) | hESC-DA neurons | PD/mouse, rat 6-OHDA, monkey MPTP | Long term survival and motor restoration |
| | (Grealish et al., 2014) | hESC-DA neurons | PD/rat 6-OHDA | Motor restoration comparable to human fetal grafts |
| | (Steinbeck et al., 2015) | Inhibitory opsin-expressing hESC-DA neurons | PD/mouse 6-OHDA | Light-induced silencing of grafts re-introduced motor defects |
| | (Chen et al., 2016) | CRISPR-engineered DREADD expressing hESC-DA neurons | PD/mouse 6-OHDA | Control of motor behaviors by CNO |
| | (Aubry et al., 2008) | hESC-striatal progenitors | HD/rat QA-lesion | DARPP32 + differentiation |
| | (Ma et al., 2012) | hESC-striatal progenitors | HD/mouse QA-lesion | Correction of locomotive deficits and circuit integration |
| | (Faedo et al., 2017) | hESC-striatal progenitors | HD/rat QA-lesion | Long-range circuit integration |
| | (Espuny-Camacho et al., 2017) | hESC-cortical progenitors | AD/chimeric APP/PS1 mouse | Susceptibility of human neurons to Tau |
| | (Yue et al., 2015) | hESC-basal forebrain cholinergic neurons | AD/mouse 5XFAD, APP/PS1 | Improvement in learning and memory |
| | (Rossi et al., 2010) | hESC-MNP | SCI/rat | Improvement in motor function |
| | (Wyatt et al., 2011) | hESC-MNP | ALS, SMA, SCI | Increased growth factor secretion |
| iPSCs-based | (Hargus et al., 2010) | DA neurons differentiated from patient fibroblasts | PD/rat 6-OHDA | Correction of AMPH-induced rotation behavior |
| | (Samata et al., 2016) | DA progenitors differentiated from human PSCs | PD/rat 6-OHDA, monkey MPTP | Restoration of motor deficits |
| | (Kikuchi et al., 2017a) | DA neurons differentiated from healthy and PD fibroblasts | PD/monkey MPTP | Long-term survival of DA cells. Increase in spontaneous movement. |
| | (Kikuchi et al., 2017b) | Healthy or idiopathic PD-iPSCs differentiated from fibroblasts and peripheral blood cells | PD/mouse α-Synuclein, rat 6-OHDA | Lack of α-Synuclein accumulation. Motor improvement |

*(Continued)*

**TABLE 1** | Continued

| Repair strategy | References | Type of cell grafted/manipulated | Disease/ model | Functional impact |
|---|---|---|---|---|
| | (Jeon et al., 2012) | CAG-repeat HD-iPSCs | HD/rat QA-lesion | Initial behavioral recovery. Development of HD pathology. |
| | (An et al., 2012) | CAG-repeat-corrected HD-iPSCs | HD/mouse R6/2 | Rescue of pathogenic HD signaling |
| | (Mu et al., 2014) | Mouse iPSCs | HD/rat QA-lesion | Improved learning and memory |
| | (Cha et al., 2017) | Mouse iPSCs | AD/mouse 5XFAD | Reduced Aβ plaque, improved cognition |
| | (Fujiwara et al., 2013) | hiPSCs- cholinergic neurons | AD/mouse PDAPP | Improved spatial memory |
| | (Popescu et al., 2013) | hiPSCs-MNP | ALS/rat $SOD1^{G93A}$ | Motor neuron generation |
| | (Nizzardo et al., 2014) | hiPSCs-NSC | ALS/mouse $SOD1^{G93A}$ | Improved neuromuscular function, reduced motor neuron loss |
| *In vivo* direct reprogramming | (Torper et al., 2013) | Exogenous human astrocytes. Endogenous mouse striatal astrocytes | PD/mouse 6-OHDA | Conversion into DA neurons |
| | (Rivetti di Val Cervo et al., 2017) | Endogenous mouse striatal astrocytes | PD/mouse 6-OHDA | Conversion into DA neurons. Correction of gait |
| | (Pereira et al., 2017) | Endogenous midbrain and striatal NG2 glia | PD/mouse 6-OHDA | Conversion into PV neurons |
| | (Niu et al., 2013) | Endogenous striatal astrocytes | Aging/mouse | Conversion into neuroblasts and mature neurons |
| | (Guo et al., 2014) | Endogenous cortical astrocytes and NG2 glia | AD, Stab-injury/mouse | Conversion into glutamatergic and GABA neurons |
| | (Su et al., 2014) | Endogenous and exogenous astrocytes | SCI/T8 hemi-section mouse | Neurogenesis and conversion into GABA neurons |
| | (El Waly et al., 2018) | Endogenous mouse neuroblasts | Demyelination/ cuprizone-induced | Conversion into myelin producing oligodendrocytes |
| | (Torper et al., 2015) | Endogenous mouse NG2 glia | Mouse | Conversion into glutamatergic and GABA neurons |

*MSC, Mesenchymal Stem Cell; hESC, human Embryonic Stem Cell; hiPSC, human induced Pluripotent Stem Cell; PD, Parkinson's Disease; 6-OHDA, 6-hydroxydopamine; MPTP, 1-methyl-4-phenyl-1,2,3,6-tetrahydropyridine; HD, Huntington Disease; QA, Quinolinic Acid; R6/2, Huntingtin transgene insertion 62; hBM, human bone marrow; hAD, human Adipose; Aβ, beta-amyloid; AD, Alzheimer's Disease; APPswe/PS1, amyloid beta precursor protein/presenilin 1; 5XFAD, mice express human APP and PSN1 transgenes with a total of five AD-linked mutations; PDAPP, APP expressed under PDGF promoter; ALS, amyotrophic lateral sclerosis; SOD1, superoxide dismutase 1; SCI, spinal cord injury; SMA, spinal muscular atrophy.*

neural tissue and evidence for functional replacement for missing neurons. In animal models of PD and HD, transplanted fetal rat substantia nigra tissue established connections with host striatum and reversed motor and metabolic deficits (Perlow et al., 1979; Isacson et al., 1984). Additional support came from the long-term survival of human fetal neural tissue in monkeys (Redmond et al., 1988), that led to the commencement of transplantation of fetal tissue into the striatum of PD patients (Lindvall et al., 1990; Spencer et al., 1992). Intriguingly, the initial open-label clinical trials demonstrated restoration of DA synthesis resulting in significant and long-lasting clinical improvements of motor function (Hauser et al., 1999; Piccini et al., 1999). Though variable clinical efficacy was observed, the ability of allografts to survive, integrate and function in diseased host environment, in some cases up to 20 years (Bega and Krainc, 2014), was in itself an exciting finding. Subsequent double-blinded, placebo controlled clinical trials, however, failed to reveal definitive results and long-term follow up studies revealed the development of α-synuclein aggregates in grafted fetal neurons (Kordower et al., 2008) and graft-induced dyskinesias (Freed et al., 2001; Hagell et al., 2002; Olanow et al., 2003), effects later attributed to heterogenous spread of transplanted cells and/or graft contamination by serotonergic cells (Politis et al., 2010). In addition, early withdrawal of immunosuppression, severe phenotype of transplanted patients and grafts' non-innervation of the ventral striatum were identified as some of the limiting factors. Based on these findings, a new multi-center trial with fetal-based transplantation to PD patients is currently underway that hopes to address these concerns (Moore et al., 2014; Kirkeby et al., 2017). Therapeutic potential of neural transplantation was similarly first explored for HD in rodent and non-human primate models (Wictorin et al., 1989; Peschanski et al., 1995; Kendall et al., 1998), the positive results of which led to fetal striatal implantation in patients in the mid- to late-90s (Bachoud-Levi et al., 2000, 2006; Hauser et al., 2002). However, disease-like neuronal degeneration of grafted tissue upon postmortem analysis raised uncertainty about this approach (Cicchetti et al., 2009; **Table 1**).

### Limitations of Using Fetal and Embryonic Origin Cell-Based Transplantation Strategies

It is worth mentioning here that both PD and HD, at least in their earlier stages, involve relatively specific cellular and regional pathologies: nigrostriatal DA neurons in PD and striatal medium spiny neurons in HD, making them suitable to tissue grafts dissected from fetal regions that contain the target cell population. However, it should also be kept in mind that pathologies in these conditions are not region-specific. For instance, in PD, non-DA and non-motor symptoms can cause significant disability, especially in patients with advanced pathology (Chaudhuri et al., 2006) and while striatal pathology dominates initial stages of HD, cell loss in the motor and cingulate cortices correlates with the degree of motor and mood dysfunction characteristic of the disease in later stages (Thu et al., 2010). Therefore, to alleviate the full repertoire of advanced disease symptomatology, adjuvant therapy for secondary disease processes maybe required. Indeed, widespread brain degenerative changes have been proposed to offset therapeutic efficacy of an otherwise viable graft (Li et al., 2016). Such a strategy may also not be applicable to disorders of diffuse pathology such as stroke, AD, SCI, and ALS, that involve pathological alterations in multiple neuronal and glial cellular phenotypes and brain regions. Lastly, the most obvious limitation to fetal transplants is the limited availability of graft sources which have traditionally been derived from human embryos causing significant logistical and ethical concerns.

## PRECISION THERAPEUTICS

### Human Embryonic and Induced Pluripotent Stem Cell Technologies

Given the variable clinical efficacy, risk of contamination by non-specific cell types and ethical concerns associated with fetal grafts, alternative transplant sources have been sought to boost endogenous reparative mechanisms. Recently, pluripotent stem cells (PSCs) (Gurdon, 1962; Evans and Kaufman, 1981; Martin, 1981) including hESCs (Thomson et al., 1998; Reubinoff et al., 2000) derived from pre-implantation embryos, and hiPSCs (Takahashi and Yamanaka, 2006; Yu et al., 2007; Park et al., 2008) that are reprogrammed from somatic cells using a defined cocktail of transcription factors, have attracted tremendous interest in the field of regenerative medicine. Use of autologous hiPSCs can also overcome immune mismatch-mediated graft rejection and circumvent ethical and logistical issues associated with the use of hESCs. While hiPSC technology is by design usable to treat donor patients limiting its cost-effectiveness and scalability (Nakatsuji et al., 2008), hypo-immunogenicity in hiPSCs was recently achieved via inactivation of the major histocompatibility complex (MHC) and overexpression of the transmembrane protein CD47 (Deuse et al., 2019), potentially conferring a remarkable universal donor capability to hiPSCs (**Figure 1** and **Table 1**).

### Genome-Editing

The development of biotechnology allowing generation of hiPSCs from non-viral techniques and gene-editing tools that enable site-specific corrections of disease-causing gene mutations have made genome-edited hiPSC-based cell therapy an ideal choice in the field of precision therapeutics. Using genome-editing tools, such as zinc finger nucleases (ZFNs) (Bibikova et al., 2003), TAL effector nucleases (Boch et al., 2009) and the more specific clustered regulatory interspaced short palindromic repeats (CRISPR)/CRISPR-associated (Cas) system (Mali et al., 2013), that enable precise corrections of deleterious mutations, genome corrected-iPSCs are now being generated. Already, advances have led to generation of engineered cells that are able to deliver therapeutic factors and that carry minimal risks of tumorigenicity in preclinical models of PD (Kriks et al., 2011; Grealish et al., 2014; Hallett et al., 2015; Steinbeck et al., 2015; Kikuchi et al., 2017a; Shi et al., 2017). Using ZFNs, generation of isogenic disease and control hiPSCs from PD patients' cortical neurons carrying the α-synuclein mutations A53T (Chung et al., 2013) and LRRK2 (Reinhardt et al., 2013) and their insertion into hESCs (Soldner et al., 2011) have been described. Lately, CRISPR/Cas system has been used to correct α-synuclein mutations in PD hiPSCs (Heman-Ackah et al., 2016; Soldner et al., 2016), remove HTT-repeat expansion mutation in HD hiPSCs (Xu et al., 2017) and correct mutations in presenilin (PSEN) in AD basal forebrain cholinergic neurons (Ortiz-Virumbrales et al., 2017). While majority of these studies have employed *ex vivo* manipulation of hiPSCs, successful *in vivo* gene editing of post mitotic cells, as has been shown in five-familial AD and amyloid precursor protein (APP) knock-in mice (Park et al., 2019), has opened up the tantalizing prospect of eliminating the need for cell transplants for brain repair. In theory, *in vivo* gene editing is a similar concept to the one used for *in vivo* direct reprogramming in which non-neuronal cells are converted into disease-specific neurons directly *in situ* with preclinical studies showing successful integration of reprogrammed cells into host circuits within the cerebral cortex (Guo et al., 2014), striatum (Torper et al., 2015), midbrain (Torper et al., 2013) and the spinal cord (Su et al., 2014) in heterogenous disease contexts (**Figure 1** and **Table 1**).

## DISCUSSION

### Applying a Multi-Pronged Strategy for Repair of Neural Tissue

Alterations in AN appear to be a common feature in many neurological and psychiatric disorders (Sahay and Hen, 2007; Winner et al., 2011; Niv et al., 2012; Pun et al., 2012). Studies in experimental models can yield important insights into AN biology including its potential for cell replacement in disease and injury contexts (van Tijn et al., 2011; Newman et al., 2014). Yet to achieve successful tissue restoration, a combinatorial therapeutic strategy might be required that includes boosting of endogenous neurogenic processes, *in vivo* genome-correction of endogenously generated NSCs/progenitors/mature neurons,

transplantation of *ex vivo* gene-corrected neurons and the delivery of neurotherapeutic factors. Transplantation of fate-restricted progenitors that retain the capability to migrate and differentiate into mature neurons and functionally integrate into existing circuits has the benefit of decreasing the number of transplants and chances of developing non-specificity issues. Still, multiple cellular phenotypes might be required to construct a therapeutically efficacious graft, whose composition must be geared toward correcting primary genetic deficits and secondary phenotypes. Transplant composition for chronic neurodegenerative diseases, especially in advanced stages, might require a greater dependence on exogenous cells due to the extensive damage to host tissue, while also attempting to correct mutations in remaining diseased neuronal populations. Acute injuries, on the other hand, would require a greater role for neurotrophic factors and modification of extracellular matrix to facilitate regeneration of existing tissue, while at the same time replacing lost or damaged neural populations by promoting endogenous neurogenesis and transplanting fate-restricted precursors and/or reprogrammed mature neurons. Given the above, perhaps the most effective approach while designing cell-based therapy might be to adopt a multi-pronged strategy that cumulatively addresses the shortcomings of the above-mentioned tissue restoration strategies and that is tailored to the brain disease in hand.

## AUTHOR CONTRIBUTIONS

MC developed the concepts and wrote the manuscript.

## FUNDING

This work was supported by the New York State Office of Mental Health.

## REFERENCES


Alonso, M., Lepousez, G., Sebastien, W., Bardy, C., Gabellec, M. M., Torquet, N., et al. (2012). Activation of adult-born neurons facilitates learning and memory. *Nat. Neurosci.* 15, 897–904. doi: 10.1038/nn.3108

Altman, J. (1962). Are new neurons formed in the brains of adult mammals? *Science* 135, 1127–1128. doi: 10.1126/science.135.3509.1127

Altman, J. (1963). Autoradiographic investigation of cell proliferation in the brains of rats and cats. *Anat. Rec.* 145, 573–591. doi: 10.1002/ar.1091450409

Altman, J., and Das, G. D. (1965). Post-natal origin of microneurones in the rat brain. *Nature* 207, 953–956. doi: 10.1038/207953a0

Altman, J., and Das, G. D. (1967). Postnatal neurogenesis in the guinea-pig. *Nature* 214, 1098–1101. doi: 10.1038/2141098a0

Alunni, A., Krecsmarik, M., Bosco, A., Galant, S., Pan, L., Moens, C. B., et al. (2013). Notch3 signaling gates cell cycle entry and limits neural stem cell amplification in the adult pallium. *Development* 140, 3335–3347. doi: 10.1242/dev.095018

Alvarez-Buylla, A., Kirn, J. R., and Nottebohm, F. (1990a). Birth of projection neurons in adult avian brain may be related to perceptual or motor learning. *Science* 249, 1444–1446. doi: 10.1126/science.1698312

Alvarez-Buylla, A., Theelen, M., and Nottebohm, F. (1990b). Proliferation "hot spots" in adult avian ventricular zone reveal radial cell division. *Neuron* 5, 101–109. doi: 10.1016/0896-6273(90)90038-h

An, M. C., Zhang, N., Scott, G., Montoro, D., Wittkop, T., Mooney, S., et al. (2012). Genetic correction of Huntington's disease phenotypes in induced pluripotent stem cells. *Cell Stem Cell* 11, 253–263. doi: 10.1016/j.stem.2012.04.026

Androutsellis-Theotokis, A., Rueger, M. A., Park, D. M., Mkhikian, H., Korb, E., Poser, S. W., et al. (2009). Targeting neural precursors in the adult brain rescues injured dopamine neurons. *Proc. Natl. Acad. Sci. U.S.A.* 106, 13570–13575. doi: 10.1073/pnas.0905125106

Aubry, L., Bugi, A., Lefort, N., Rousseau, F., Peschanski, M., and Perrier, A. L. (2008). Striatal progenitors derived from human ES cells mature into DARPP32 neurons *in vitro* and in quinolinic acid-lesioned rats. *Proc. Natl. Acad. Sci. U.S.A.* 105, 16707–16712. doi: 10.1073/pnas.0808488105

Bachoud-Levi, A. C., Gaura, V., Brugieres, P., Lefaucheur, J. P., Boisse, M. F., Maison, P., et al. (2006). Effect of fetal neural transplants in patients with Huntington's disease 6 years after surgery: a long-term follow-up study. *Lancet Neurol.* 5, 303–309. doi: 10.1016/s1474-4422(06)70381-7

Bachoud-Levi, A. C., Remy, P., Nguyen, J. P., Brugieres, P., Lefaucheur, J. P., Bourdet, C., et al. (2000). Motor and cognitive improvements in patients with Huntington's disease after neural transplantation. *Lancet* 356, 1975–1979. doi: 10.1016/s0140-6736(00)03310-9

Bahat-Stroomza, M., Barhum, Y., Levy, Y. S., Karpov, O., Bulvik, S., Melamed, E., et al. (2009). Induction of adult human bone marrow mesenchymal stromal cells into functional astrocyte-like cells: potential for restorative treatment in Parkinson's disease. *J. Mol. Neurosci.* 39, 199–210. doi: 10.1007/s12031-008-9166-3

Barnabe-Heider, F., Goritz, C., Sabelstrom, H., Takebayashi, H., Pfrieger, F. W., Meletis, K., et al. (2010). Origin of new glial cells in intact and injured adult spinal cord. *Cell Stem Cell* 7, 470–482. doi: 10.1016/j.stem.2010.07.014

Bega, D., and Krainc, D. (2014). Long-term clinical outcomes after fetal cell transplantation in parkinson disease: implications for the future of cell therapy. *JAMA* 311, 617–618.

Berberoglu, M. A., Dong, Z., Li, G., Zheng, J., Trejo, M., Ldel, C., et al. (2014). Heterogeneously expressed fezf2 patterns gradient Notch activity in balancing the quiescence, proliferation, and differentiation of adult neural stem cells. *J. Neurosci.* 34, 13911–13923. doi: 10.1523/JNEUROSCI.1976-14.2014

Berg, D. A., Kirkham, M., Beljajeva, A., Knapp, D., Habermann, B., Ryge, J., et al. (2010). Efficient regeneration by activation of neurogenesis in homeostatically quiescent regions of the adult vertebrate brain. *Development* 137, 4127–4134. doi: 10.1242/dev.055541

Berg, D. A., Su, Y., Jimenez-Cyrus, D., Patel, A., Huang, N., Morizet, D., et al. (2019). A common embryonic origin of stem cells drives developmental and adult neurogenesis. *Cell* 177, 654.e15–668.e15. doi: 10.1016/j.cell.2019.02.010

Bernardos, R. L., Barthel, L. K., Meyers, J. R., and Raymond, P. A. (2007). Late-stage neuronal progenitors in the retina are radial Muller glia that function as retinal stem cells. *J. Neurosci.* 27, 7028–7040. doi: 10.1523/jneurosci.1624-07.2007

Bhattarai, P., Cosacak, M. I., Mashkaryan, V., Demir, S., Popova, S. D., Govindarajan, N., et al. (2020). Neuron-glia interaction through Serotonin-BDNF-NGFR axis enables regenerative neurogenesis in Alzheimer's model of adult zebrafish brain. *PLoS Biol.* 18:e3000585. doi: 10.1371/journal.pbio.3000585

Bhattarai, P., Hickman, L., and Phillips, J. L. (2016). Pain among hospitalized older people with heart failure and their preparation to manage this symptom on discharge: a descriptive-observational study. *Contemp. Nurs.* 52, 204–215. doi: 10.1080/10376178.2016.1175311

Bibikova, M., Beumer, K., Trautman, J. K., and Carroll, D. (2003). Enhancing gene targeting with designed zinc finger nucleases. *Science* 300:764. doi: 10.1126/science.1079512

Bjorklund, A., and Stenevi, U. (1979). Reconstruction of the nigrostriatal dopamine pathway by intracerebral nigral transplants. *Brain Res.* 177, 555–560. doi: 10.1016/0006-8993(79)90472-4

Boch, J., Scholze, H., Schornack, S., Landgraf, A., Hahn, S., Kay, S., et al. (2009). Breaking the code of DNA binding specificity of TAL-type III effectors. *Science* 326, 1509–1512. doi: 10.1126/science.1178811

Boekhoorn, K., Joels, M., and Lucassen, P. J. (2006). Increased proliferation reflects glial and vascular-associated changes, but not neurogenesis in the presenile Alzheimer hippocampus. *Neurobiol. Dis.* 24, 1–14. doi: 10.1016/j.nbd.2006.04.017

Boldrini, M., Fulmore, C. A., Tartt, A. N., Simeon, L. R., Pavlova, I., Poposka, V., et al. (2018). Human hippocampal neurogenesis persists throughout aging. *Cell Stem Cell* 22, 589.e5–599.e5.

Bonaguidi, M. A., Wheeler, M. A., Shapiro, J. S., Stadel, R. P., Sun, G. J., Ming, G. L., et al. (2011). *In vivo* clonal analysis reveals self-renewing and multipotent adult neural stem cell characteristics. *Cell* 145, 1142–1155. doi: 10.1016/j.cell.2011.05.024

Briley, D., Ghirardi, V., Woltjer, R., Renck, A., Zolochevska, O., Taglialatela, G., et al. (2016). Preserved neurogenesis in non-demented individuals with AD neuropathology. *Sci. Rep.* 6:27812. doi: 10.1038/srep27812

Bull, N. D., and Bartlett, P. F. (2005). The adult mouse hippocampal progenitor is neurogenic but not a stem cell. *J. Neurosci.* 25, 10815–10821. doi: 10.1523/jneurosci.3249-05.2005

Cha, M. Y., Kwon, Y. W., Ahn, H. S., Jeong, H., Lee, Y. Y., Moon, M., et al. (2017). Protein-induced pluripotent stem cells ameliorate cognitive dysfunction and reduce abeta deposition in a mouse model of Alzheimer's disease. *Stem Cells Transl. Med.* 6, 293–305. doi: 10.5966/sctm.2016-0081

Chaudhuri, K. R., Healy, D. G., Schapira, A. H., and National Institute for Clinical Excellence, (2006). Non-motor symptoms of Parkinson's disease: diagnosis and management. *Lancet Neurol.* 5, 235–245.

Chen, Y., Xiong, M., Dong, Y., Haberman, A., Cao, J., Liu, H., et al. (2016). Chemical control of grafted human PSC-derived neurons in a mouse model of Parkinson's disease. *Cell Stem Cell.* 18, 817–826. doi: 10.1016/j.stem.2016.03.014

Choi, S. H., Bylykbashi, E., Chatila, Z. K., Lee, S. W., Pulli, B., Clemenson, G. D., et al. (2018). Combined adult neurogenesis and BDNF mimic exercise effects on cognition in an Alzheimer's mouse model. *Science* 361:eaan8821. doi: 10.1126/science.aan8821

Chung, C. Y., Khurana, V., Auluck, P. K., Tardiff, D. F., Mazzulli, J. R., Soldner, F., et al. (2013). Identification and rescue of alpha-synuclein toxicity in Parkinson patient-derived neurons. *Science* 342, 983–987. doi: 10.1126/science.1245296

Cicchetti, F., Saporta, S., Hauser, R. A., Parent, M., Saint-Pierre, M., Sanberg, P. R., et al. (2009). Neural transplants in patients with Huntington's disease undergo disease-like neuronal degeneration. *Proc. Natl. Acad. Sci. U.S.A.* 106, 12483–12488. doi: 10.1073/pnas.0904239106

Curtis, M. A., Kam, M., Nannmark, U., Anderson, M. F., Axell, M. Z., Wikkelso, C., et al. (2007). Human neuroblasts migrate to the olfactory bulb via a lateral ventricular extension. *Science* 315, 1243–1249. doi: 10.1126/science.1136281

Dennis, C. V., Suh, L. S., Rodriguez, M. L., Kril, J. J., and Sutherland, G. T. (2016). Human adult neurogenesis across the ages: an immunohistochemical study. *Neuropathol. Appl. Neurobiol.* 42, 621–638. doi: 10.1111/nan.12337

Deuse, T., Hu, X., Gravina, A., Wang, D., Tediashvili, G., De, C., et al. (2019). Hypoimmunogenic derivatives of induced pluripotent stem cells evade immune rejection in fully immunocompetent allogeneic recipients. *Nat. Biotechnol.* 37, 252–258. doi: 10.1038/s41587-019-0016-3

Doetsch, F., Caille, I., Lim, D. A., Garcia-Verdugo, J. M., and Alvarez-Buylla, A. (1999). Subventricular zone astrocytes are neural stem cells in the adult mammalian brain. *Cell* 97, 703–716. doi: 10.1016/s0092-8674(00)80783-7

Dyer, M. A., and Cepko, C. L. (2000). Control of Muller glial cell proliferation and activation following retinal injury. *Nat. Neurosci.* 3, 873–880. doi: 10.1038/78774

Eckenhoff, M. F., and Rakic, P. (1988). Nature and fate of proliferative cells in the hippocampal dentate gyrus during the life span of the rhesus monkey. *J. Neurosci.* 8, 2729–2747. doi: 10.1523/jneurosci.08-08-02729.1988

El Waly, B., Cayre, M., and Durbec, P. (2018). Promoting myelin repair through *in* vivo neuroblast reprogramming. *Stem Cell Rep.* 10, 1492–1504. doi: 10.1016/j.stemcr.2018.02.015

Elewa, A., Wang, H., Talavera-Lopez, C., Joven, A., Brito, G., Kumar, A., et al. (2017). Reading and editing the Pleurodeles waltl genome reveals novel features of tetrapod regeneration. *Nat. Commun.* 8:2286. doi: 10.1038/s41467-017-01964-9

Encinas, J. M., Michurina, T. V., Peunova, N., Park, J. H., Tordo, J., Peterson, D. A., et al. (2011). Division-coupled astrocytic differentiation and age-related depletion of neural stem cells in the adult hippocampus. *Cell Stem Cell* 8, 566–579. doi: 10.1016/j.stem.2011.03.010

Eriksson, P. S., Perfilieva, E., Bjork-Eriksson, T., Alborn, A. M., Nordborg, C., Peterson, D. A., et al. (1998). Neurogenesis in the adult human hippocampus. *Nat. Med.* 4, 1313–1317.

Ernst, A., Alkass, K., Bernard, S., Salehpour, M., Perl, S., Tisdale, J., et al. (2014). Neurogenesis in the striatum of the adult human brain. *Cell* 156, 1072–1083. doi: 10.1016/j.cell.2014.01.044

Espuny-Camacho, I., Arranz, A. M., Fiers, M., Snellinx, A., Ando, K., Munck, S., et al. (2017). Hallmarks of Alzheimer's disease in stem-cell-derived human neurons transplanted into mouse brain. *Neuron* 93, 1066.e8–1081.e8. doi: 10.1016/j.neuron.2017.02.001

Evans, M. J., and Kaufman, M. H. (1981). Establishment in culture of pluripotential cells from mouse embryos. *Nature* 292, 154–156. doi: 10.1038/292154a0

Faedo, A., Laporta, A., Segnali, A., Galimberti, M., Besusso, D., Cesana, E., et al. (2017). Differentiation of human telencephalic progenitor cells into MSNs by inducible expression of Gsx2 and Ebf1. *Proc. Natl. Acad. Sci. U.S.A.* 114, E1234–E1242. doi: 10.1073/pnas.1611473114

Falkner, S., Grade, S., Dimou, L., Conzelmann, K. K., Bonhoeffer, T., Gotz, M., et al. (2016). Transplanted embryonic neurons integrate into adult neocortical circuits. *Nature* 539, 248–253. doi: 10.1038/nature20113

Freed, C. R., Greene, P. E., Breeze, R. E., Tsai, W. Y., DuMouchel, W., Kao, R., et al. (2001). Transplantation of embryonic dopamine neurons for severe Parkinson's disease. *N. Engl. J. Med.* 344, 710–719. doi: 10.1056/nejm200103083441002

Fuentealba, L. C., Rompani, S. B., Parraguez, J. I., Obernier, K., Romero, R., Cepko, C. L., et al. (2015). Embryonic origin of postnatal neural stem cells. *Cell* 161, 1644–1655. doi: 10.1016/j.cell.2015.05.041

Fujiwara, N., Shimizu, J., Takai, K., Arimitsu, N., Saito, A., Kono, T., et al. (2013). Restoration of spatial memory dysfunction of human APP transgenic mice by transplantation of neuronal precursors derived from human iPS cells. *Neurosci. Lett.* 557(Pt B), 129–134. doi: 10.1016/j.neulet.2013.10.043

Gage, F. H., Bjorklund, A., Stenevi, U., Dunnett, S. B., and Kelly, P. A. (1984). Intrahippocampal septal grafts ameliorate learning impairments in aged rats. *Science* 225, 533–536. doi: 10.1126/science.6539949

Gaillard, A., Prestoz, L., Dumartin, B., Cantereau, A., Morel, F., Roger, M., et al. (2007). Reestablishment of damaged adult motor pathways by grafted embryonic cortical neurons. *Nat. Neurosci.* 10, 1294–1299. doi: 10.1038/nn1970

Ganz, J., Kaslin, J., Hochmann, S., Freudenreich, D., and Brand, M. (2010). Heterogeneity and Fgf dependence of adult neural progenitors in the zebrafish telencephalon. *Glia* 58, 1345–1363. doi: 10.1002/glia.21012

Garcia, K. O., Ornellas, F. L., Martin, P. K., Patti, C. L., Mello, L. E., Frussa-Filho, R., et al. (2014). Therapeutic effects of the transplantation of VEGF overexpressing bone marrow mesenchymal stem cells in the hippocampus of murine model of Alzheimer's disease. *Front. Aging Neurosci.* 6:30. doi: 10.3389/fnagi.2014.00030

Goldman, S. A., and Nottebohm, F. (1983). Neuronal production, migration, and differentiation in a vocal control nucleus of the adult female canary brain. *Proc. Natl. Acad. Sci. U.S.A.* 80, 2390–2394. doi: 10.1073/pnas.80.8.2390

Grandel, H., Kaslin, J., Ganz, J., Wenzel, I., and Brand, M. (2006). Neural stem cells and neurogenesis in the adult zebrafish brain: origin, proliferation dynamics, migration and cell fate. *Dev. Biol.* 295, 263–277. doi: 10.1016/j.ydbio.2006.03.040

Grealish, S., Diguet, E., Kirkeby, A., Mattsson, B., Heuer, A., Bramoulle, Y., et al. (2014). Human ESC-derived dopamine neurons show similar preclinical efficacy and potency to fetal neurons when grafted in a rat model of Parkinson's disease. *Cell Stem Cell* 15, 653–665. doi: 10.1016/j.stem.2014.09.017

Guo, Z., Zhang, L., Wu, Z., Chen, Y., Wang, F., and Chen, G. (2014). *In vivo* direct reprogramming of reactive glial cells into functional neurons after brain injury and in an Alzheimer's disease model. *Cell Stem Cell* 14, 188–202. doi: 10.1016/j.stem.2013.12.001

Gurdon, J. B. (1962). The developmental capacity of nuclei taken from intestinal epithelium cells of feeding tadpoles. *J. Embryol. Exp. Morphol.* 10, 622–640.

Hagell, P., Piccini, P., Bjorklund, A., Brundin, P., Rehncrona, S., Widner, H., et al. (2002). Dyskinesias following neural transplantation in Parkinson's disease. *Nat. Neurosci.* 5, 627–628.

Hallett, P. J., Deleidi, M., Astradsson, A., Smith, G. A., Cooper, O., Osborn, T. M., et al. (2015). Successful function of autologous iPSC-derived dopamine neurons following transplantation in a non-human primate model of Parkinson's disease. *Cell Stem Cell* 16, 269–274. doi: 10.1016/j.stem.2015.01.018

Hargus, G., Cooper, O., Deleidi, M., Levy, A., Lee, K., Marlow, E., et al. (2010). Differentiated Parkinson patient-derived induced pluripotent stem cells grow in the adult rodent brain and reduce motor asymmetry in Parkinsonian rats. *Proc. Natl. Acad. Sci. U.S.A.* 107, 15921–15926. doi: 10.1073/pnas.1010209107

Hauser, R. A., Freeman, T. B., Snow, B. J., Nauert, M., Gauger, L., Kordower, J. H., et al. (1999). Long-term evaluation of bilateral fetal nigral transplantation in Parkinson disease. *Arch. Neurol.* 56, 179–187.

Hauser, R. A., Sandberg, P. R., Freeman, T. B., and Stoessl, A. J. (2002). Bilateral human fetal striatal transplantation in Huntington's disease. *Neurology* 58, 687–695. doi: 10.1212/wnl.58.5.687

Hellmann, M. A., Panet, H., Barhum, Y., Melamed, E., and Offen, D. (2006). Increased survival and migration of engrafted mesenchymal bone marrow stem cells in 6-hydroxydopamine-lesioned rodents. *Neurosci. Lett.* 395, 124–128. doi: 10.1016/j.neulet.2005.10.097

Heman-Ackah, S. M., Bassett, A. R., and Wood, M. J. (2016). Precision modulation of neurodegenerative disease-related gene expression in human iPSC-derived neurons. *Sci. Rep.* 6:28420. doi: 10.1038/srep28420

Hoglinger, G. U., Rizk, P., Muriel, M. P., Duyckaerts, C., Oertel, W. H., Caille, I., et al. (2004). Dopamine depletion impairs precursor cell proliferation in Parkinson disease. *Nat. Neurosci.* 7, 726–735. doi: 10.1038/nn1265

Howe, K., Clark, M. D., Torroja, C. F., Torrance, J., Berthelot, C., Muffato, M., et al. (2013). The zebrafish reference genome sequence and its relationship to the human genome. *Nature* 496, 498–503.

Imayoshi, I., Sakamoto, M., Ohtsuka, T., Takao, K., Miyakawa, T., Yamaguchi, M., et al. (2008). Roles of continuous neurogenesis in the structural and functional integrity of the adult forebrain. *Nat. Neurosci.* 11, 1153–1161. doi: 10.1038/nn.2185

Imayoshi, I., Sakamoto, M., Yamaguchi, M., Mori, K., and Kageyama, R. (2010). Essential roles of Notch signaling in maintenance of neural stem cells in developing and adult brains. *J. Neurosci.* 30, 3489–3498. doi: 10.1523/JNEUROSCI.4987-09.2010

Irion, U., Krauss, J., and Nusslein-Volhard, C. (2014). Precise and efficient genome editing in zebrafish using the CRISPR/Cas9 system. *Development* 141, 4827–4830. doi: 10.1242/dev.115584

Isacson, O., Brundin, P., Kelly, P. A., Gage, F. H., and Bjorklund, A. (1984). Functional neuronal replacement by grafted striatal neurones in the ibotenic acid-lesioned rat striatum. *Nature* 311, 458–460. doi: 10.1038/311458a0

Jeon, I., Lee, N., Li, J. Y., Park, I. H., Park, K. S., Moon, J., et al. (2012). Neuronal properties, *in vivo* effects, and pathology of a Huntington's disease patient-derived induced pluripotent stem cells. *Stem Cells* 30, 2054–2062. doi: 10.1002/stem.1135

Jin, K., Wang, X., Xie, L., Mao, X. O., Zhu, W., Wang, Y., et al. (2006). Evidence for stroke-induced neurogenesis in the human brain. *Proc. Natl. Acad. Sci. U.S.A.* 103, 13198–13202. doi: 10.1073/pnas.0603512103

Kam, M., Curtis, M. A., McGlashan, S. R., Connor, B., Nannmark, U., and Faull, R. L. (2009). The cellular composition and morphological organization of the rostral migratory stream in the adult human brain. *J. Chem. Neuroanat.* 37, 196–205. doi: 10.1016/j.jchemneu.2008.12.009

Kaplan, M. S., and Hinds, J. W. (1977). Neurogenesis in the adult rat: electron microscopic analysis of light radioautographs. *Science* 197, 1092–1094. doi: 10.1126/science.887941

Kendall, A. L., Rayment, F. D., Torres, E. M., Baker, H. F., Ridley, R. M., and Dunnett, S. B. (1998). Functional integration of striatal allografts in a primate model of Huntington's disease. *Nat. Med.* 4, 727–729. doi: 10.1038/nm0698-727

Kikuchi, T., Morizane, A., Doi, D., Magotani, H., Onoe, H., Hayashi, T., et al. (2017a). Human iPS cell-derived dopaminergic neurons function in a primate Parkinson's disease model. *Nature* 548, 592–596. doi: 10.1038/nature23664

Kikuchi, T., Morizane, A., Doi, D., Okita, K., Nakagawa, M., Yamakado, H., et al. (2017b). Idiopathic Parkinson's disease patient-derived induced pluripotent stem cells function as midbrain dopaminergic neurons in rodent brains. *J. Neurosci. Res.* 95, 1829–1837. doi: 10.1002/jnr.24014

Kim, H., Kim, H. Y., Choi, M. R., Hwang, S., Nam, K. H., Kim, H. C., et al. (2010). Dose-dependent efficacy of ALS-human mesenchymal stem cells transplantation into cisterna magna in SOD1-G93A ALS mice. *Neurosci. Lett.* 468, 190–194. doi: 10.1016/j.neulet.2009.10.074

Kim, K. S., Lee, H. J., An, J., Kim, Y. B., Ra, J. C., Lim, I., et al. (2014). Transplantation of human adipose tissue-derived stem cells delays clinical onset and prolongs life span in ALS mouse model. *Cell Transplant.* 23, 1585–1597. doi: 10.3727/096368913X673450

Kirkeby, A., Parmar, M., and Barker, R. A. (2017). Strategies for bringing stem cell-derived dopamine neurons to the clinic: a European approach (STEM-PD). *Prog. Brain Res.* 230, 165–190. doi: 10.1016/bs.pbr.2016.11.011

Kirkham, M., Hameed, L. S., Berg, D. A., Wang, H., and Simon, A. (2014). Progenitor cell dynamics in the Newt Telencephalon during homeostasis and neuronal regeneration. *Stem Cell Rep.* 2, 507–519. doi: 10.1016/j.stemcr.2014.01.018

Kizil, C., and Bhattarai, P. (2018). Is Alzheimer's also a stem cell disease? - The zebrafish perspective. *Front. Cell Dev. Biol.* 6:159. doi: 10.3389/fcell.2018.00159

Kordower, J. H., Chu, Y., Hauser, R. A., Freeman, T. B., and Olanow, C. W. (2008). Lewy body-like pathology in long-term embryonic nigral transplants in Parkinson's disease. *Nat. Med.* 14, 504–506. doi: 10.1038/nm1747

Kriks, S., Shim, J. W., Piao, J., Ganat, Y. M., Wakeman, D. R., Xie, Z., et al. (2011). Dopamine neurons derived from human ES cells efficiently engraft in animal models of Parkinson's disease. *Nature* 480, 547–551. doi: 10.1038/nature10648

Lagace, D. C., Whitman, M. C., Noonan, M. A., Ables, J. L., DeCarolis, N. A., Arguello, A. A., et al. (2007). Dynamic contribution of nestin-expressing stem cells to adult neurogenesis. *J. Neurosci.* 27, 12623–12629. doi: 10.1523/jneurosci.3812-07.2007

Lee, S. T., Chu, K., Jung, K. H., Im, W. S., Park, J. E., Lim, H. C., et al. (2009). Slowed progression in models of Huntington disease by adipose stem cell transplantation. *Ann. Neurol.* 66, 671–681. doi: 10.1002/ana.21788

Li, W., Englund, E., Widner, H., Mattsson, B., van Westen, D., Latt, J., et al. (2016). Extensive graft-derived dopaminergic innervation is maintained 24 years after transplantation in the degenerating parkinsonian brain. *Proc. Natl. Acad. Sci. U.S.A.* 113, 6544–6549. doi: 10.1073/pnas.1605245113

Lin, Y. T., Chern, Y., Shen, C. K., Wen, H. L., Chang, Y. C., Li, H., et al. (2011). Human mesenchymal stem cells prolong survival and ameliorate motor deficit through trophic support in Huntington's disease mouse models. *PLoS One* 6:e22924. doi: 10.1371/journal.pone.0022924

Lindvall, O., Brundin, P., Widner, H., Rehncrona, S., Gustavii, B., Frackowiak, R., et al. (1990). Grafts of fetal dopamine neurons survive and improve motor function in Parkinson's disease. *Science* 247, 574–577. doi: 10.1126/science.2105529

Livneh, Y., Adam, Y., and Mizrahi, A. (2014). Odor processing by adult-born neurons. *Neuron* 81, 1097–1110. doi: 10.1016/j.neuron.2014.01.007

Lois, C., and Alvarez-Buylla, A. (1993). Proliferating subventricular zone cells in the adult mammalian forebrain can differentiate into neurons and glia. *Proc. Natl. Acad. Sci. U.S.A.* 90, 2074–2077. doi: 10.1073/pnas.90.5.2074

Low, W. C., Lewis, P. R., Bunch, S. T., Dunnett, S. B., Thomas, S. R., Iversen, S. D., et al. (1982). Function recovery following neural transplantation of embryonic septal nuclei in adult rats with septohippocampal lesions. *Nature* 300, 260–262. doi: 10.1038/300260a0

Lugert, S., Basak, O., Knuckles, P., Haussler, U., Fabel, K., Gotz, M., et al. (2010). Quiescent and active hippocampal neural stem cells with distinct morphologies respond selectively to physiological and pathological stimuli and aging. *Cell Stem Cell* 6, 445–456. doi: 10.1016/j.stem.2010.03.017

Luskin, M. B. (1993). Restricted proliferation and migration of postnatally generated neurons derived from the forebrain subventricular zone. *Neuron* 11, 173–189. doi: 10.1016/0896-6273(93)90281-u

Ma, L., Hu, B., Liu, Y., Vermilyea, S. C., Liu, H., Gao, L., et al. (2012). Human embryonic stem cell-derived GABA neurons correct locomotion deficits in quinolinic acid-lesioned mice. *Cell Stem Cell* 10, 455–464. doi: 10.1016/j.stem.2012.01.021

Maden, M., Manwell, L. A., and Ormerod, B. K. (2013). Proliferation zones in the axolotl brain and regeneration of the telencephalon. *Neural Dev.* 8:1. doi: 10.1186/1749-8104-8-1

Magnusson, J. P., Goritz, C., Tatarishvili, J., Dias, D. O., Smith, E. M., Lindvall, O., et al. (2014). A latent neurogenic program in astrocytes regulated by Notch signaling in the mouse. *Science* 346, 237–241. doi: 10.1126/science.346.6206.237

Mali, P., Yang, L., Esvelt, K. M., Aach, J., Guell, M., DiCarlo, J. E., et al. (2013). RNA-guided human genome engineering via Cas9. *Science* 339, 823–826. doi: 10.1126/science.1232033

Martin, G. R. (1981). Isolation of a pluripotent cell line from early mouse embryos cultured in medium conditioned by teratocarcinoma stem cells. *Proc. Natl. Acad. Sci. U.S.A.* 78, 7634–7638. doi: 10.1073/pnas.78.12.7634

Maruska, K. P., Carpenter, R. E., and Fernald, R. D. (2012). Characterization of cell proliferation throughout the brain of the African cichlid fish Astatotilapia burtoni and its regulation by social status. *J. Comp. Neurol.* 520, 3471–3491. doi: 10.1002/cne.23100

Merkle, F. T., Fuentealba, L. C., Sanders, T. A., Magno, L., Kessaris, N., and Alvarez-Buylla, A. (2014). Adult neural stem cells in distinct microdomains

generate previously unknown interneuron types. *Nat. Neurosci.* 17, 207–214. doi: 10.1038/nn.3610

Moore, S. F., Guzman, N. V., Mason, S. L., Williams-Gray, C. H., and Barker, R. A. (2014). Which patients with Parkinson's disease participate in clinical trials? One centre's experiences with a new cell based therapy trial (TRANSEURO). *J. Parkinsons Dis.* 4, 671–676. doi: 10.3233/JPD-140432

Moreno-Jimenez, E. P., Flor-Garcia, M., Terreros-Roncal, J., Rabano, A., Cafini, F., Pallas-Bazarra, N., et al. (2019). Adult hippocampal neurogenesis is abundant in neurologically healthy subjects and drops sharply in patients with Alzheimer's disease. *Nat. Med.* 25, 554–560. doi: 10.1038/s41591-019-0375-9

Mu, S., Wang, J., Zhou, G., Peng, W., He, Z., Zhao, Z., et al. (2014). Transplantation of induced pluripotent stem cells improves functional recovery in Huntington's disease rat model. *PLoS One* 9:e101185. doi: 10.1371/journal.pone.0101185

Nakatsuji, N., Nakajima, F., and Tokunaga, K. (2008). HLA-haplotype banking and iPS cells. *Nat. Biotechnol.* 26, 739–740. doi: 10.1038/nbt0708-739

Nam, H. S., and Benezra, R. (2009). High levels of Id1 expression define B1 type adult neural stem cells. *Cell Stem Cell* 5, 515–526. doi: 10.1016/j.stem.2009.08.017

Naritsuka, H., Sakai, K., Hashikawa, T., Mori, K., and Yamaguchi, M. (2009). Perisomatic-targeting granule cells in the mouse olfactory bulb. *J. Comp. Neurol.* 515, 409–426. doi: 10.1002/cne.22063

Newman, M., Ebrahimie, E., and Lardelli, M. (2014). Using the zebrafish model for Alzheimer's disease research. *Front. Genet.* 5:189. doi: 10.3389/fgene.2014.00189

Niu, W., Zang, T., Zou, Y., Fang, S., Smith, D. K., Bachoo, R., et al. (2013). *In vivo* reprogramming of astrocytes to neuroblasts in the adult brain. *Nat. Cell Biol.* 15, 1164–1175. doi: 10.1038/ncb2843

Niv, F., Keiner, S., Krishna, Witte, O. W., Lie, D. C., and Redecker, C. (2012). Aberrant neurogenesis after stroke: a retroviral cell labeling study. *Stroke* 43, 2468–2475. doi: 10.1161/STROKEAHA.112.660977

Nizzardo, M., Simone, C., Rizzo, F., Ruggieri, M., Salani, S., Riboldi, G., et al. (2014). Minimally invasive transplantation of iPSC-derived ALDHhiSSCloVLA4+ neural stem cells effectively improves the phenotype of an amyotrophic lateral sclerosis model. *Hum. Mol. Genet.* 23, 342–354. doi: 10.1093/hmg/ddt425

Nottebohm, F. (1981). A brain for all seasons: cyclical anatomical changes in song control nuclei of the canary brain. *Science* 214, 1368–1370. doi: 10.1126/science.7313697

Nottebohm, F., and Arnold, A. P. (1976). Sexual dimorphism in vocal control areas of the songbird brain. *Science* 194, 211–213. doi: 10.1126/science.959852

Nowoshilow, S., Schloissnig, S., Fei, J. F., Dahl, A., Pang, A. W. C., Pippel, M., et al. (2018). The axolotl genome and the evolution of key tissue formation regulators. *Nature* 554, 50–55. doi: 10.1038/nature25458

Olanow, C. W., Goetz, C. G., Kordower, J. H., Stoessl, A. J., Sossi, V., Brin, M. F., et al. (2003). A double-blind controlled trial of bilateral fetal nigral transplantation in Parkinson's disease. *Ann. Neurol.* 54, 403–414. doi: 10.1002/ana.10720

Ortiz-Virumbrales, M., Moreno, C. L., Kruglikov, I., Marazuela, P., Sproul, A., Jacob, S., et al. (2017). CRISPR/Cas9-Correctable mutation-related molecular and physiological phenotypes in iPSC-derived Alzheimer's PSEN2 (N141I) neurons. *Acta Neuropathol. Commun.* 5:77. doi: 10.1186/s40478-017-0475-z

Palmer, T. D., Ray, J., and Gage, F. H. (1995). FGF-2-responsive neuronal progenitors reside in proliferative and quiescent regions of the adult rodent brain. *Mol. Cell. Neurosci.* 6, 474–486. doi: 10.1006/mcne.1995.1035

Palmer, T. D., Schwartz, P. H., Taupin, P., Kaspar, B., Stein, S. A., and Gage, F. H. (2001). Cell culture. Progenitor cells from human brain after death. *Nature* 411, 42–43. doi: 10.1038/35075141

Parish, C. L., Beljajeva, A., Arenas, E., and Simon, A. (2007). Midbrain dopaminergic neurogenesis and behavioural recovery in a salamander lesion-induced regeneration model. *Development* 134, 2881–2887. doi: 10.1242/dev.002329

Park, H., Oh, J., Shim, G., Cho, B., Chang, Y., Kim, S., et al. (2019). *In vivo* neuronal gene editing via CRISPR-Cas9 amphiphilic nanocomplexes alleviates deficits in mouse models of Alzheimer's disease. *Nat. Neurosci.* 22, 524–528. doi: 10.1038/s41593-019-0352-0

Park, I. H., Zhao, R., West, J. A., Yabuuchi, A., Huo, H., Ince, T. A., et al. (2008). Reprogramming of human somatic cells to pluripotency with defined factors. *Nature* 451, 141–146. doi: 10.1038/nature06534

Paton, J. A., and Nottebohm, F. N. (1984). Neurons generated in the adult brain are recruited into functional circuits. *Science* 225, 1046–1048. doi: 10.1126/science.6474166

Pereira, M., Birtele, M., Shrigley, S., Benitez, J. A., Hedlund, E., Parmar, M., et al. (2017). Direct Reprogramming of Resident NG2 Glia into Neurons with Properties of Fast-Spiking Parvalbumin-Containing Interneurons. *Stem Cell Rep.* 9, 742–751. doi: 10.1016/j.stemcr.2017.07.023

Perlow, M. J., Freed, W. J., Hoffer, B. J., Seiger, A., Olson, L., and Wyatt, R. J. (1979). Brain grafts reduce motor abnormalities produced by destruction of nigrostriatal dopamine system. *Science* 204, 643–647. doi: 10.1126/science.571147

Peschanski, M., Cesaro, P., and Hantraye, P. (1995). Rationale for intrastriatal grafting of striatal neuroblasts in patients with Huntington's disease. *Neuroscience* 68, 273–285. doi: 10.1016/0306-4522(95)00162-c

Piccini, P., Brooks, D. J., Bjorklund, A., Gunn, R. N., Grasby, P. M., Rimoldi, O., et al. (1999). Dopamine release from nigral transplants visualized *in vivo* in a Parkinson's patient. *Nat. Neurosci.* 2, 1137–1140. doi: 10.1038/16060

Pilz, G. A., Bottes, S., Betizeau, M., Jorg, D. J., Carta, S., Simons, B. D., et al. (2018). Live imaging of neurogenesis in the adult mouse hippocampus. *Science* 359, 658–662. doi: 10.1126/science.aao5056

Politis, M., Wu, K., Loane, C., Quinn, N. P., Brooks, D. J., Rehncrona, S., et al. (2010). Serotonergic neurons mediate dyskinesia side effects in Parkinson's patients with neural transplants. *Sci. Transl. Med.* 2:38ra46. doi: 10.1126/scitranslmed.3000976

Popescu, I. R., Nicaise, C., Liu, S., Bisch, G., Knippenberg, S., Daubie, V., et al. (2013). Neural progenitors derived from human induced pluripotent stem cells survive and differentiate upon transplantation into a rat model of amyotrophic lateral sclerosis. *Stem Cells Transl. Med.* 2, 167–174. doi: 10.5966/sctm.2012-0042

Pun, R. Y., Rolle, I. J., Lasarge, C. L., Hosford, B. E., Rosen, J. M., Uhl, J. D., et al. (2012). Excessive activation of mTOR in postnatally generated granule cells is sufficient to cause epilepsy. *Neuron* 75, 1022–1034. doi: 10.1016/j.neuron.2012.08.002

Rakic, P. (1985). Limits of neurogenesis in primates. *Science* 227, 1054–1056. doi: 10.1126/science.3975601

Ramachandran, R., Zhao, X. F., and Goldman, D. (2011). Ascl1a/Dkk/beta-catenin signaling pathway is necessary and glycogen synthase kinase-3beta inhibition is sufficient for zebrafish retina regeneration. *Proc. Natl. Acad. Sci. U.S.A.* 108, 15858–15863. doi: 10.1073/pnas.1107220108

Redmond, D. E. Jr., Naftolin, F., Collier, T. J., Leranth, C., Robbins, R. J., Sladek, C. D., et al. (1988). Cryopreservation, culture, and transplantation of human fetal mesencephalic tissue into monkeys. *Science* 242, 768–771. doi: 10.1126/science.2903552

Reif, A., Fritzen, S., Finger, M., Strobel, A., Lauer, M., Schmitt, A., et al. (2006). Neural stem cell proliferation is decreased in schizophrenia, but not in depression. *Mol. Psychiatry* 11, 514–522. doi: 10.1038/sj.mp.4001791

Reinhardt, P., Schmid, B., Burbulla, L. F., Schondorf, D. C., Wagner, L., Glatza, M., et al. (2013). Genetic correction of a LRRK2 mutation in human iPSCs links parkinsonian neurodegeneration to ERK-dependent changes in gene expression. *Cell Stem Cell* 12, 354–367. doi: 10.1016/j.stem.2013.01.008

Reubinoff, B. E., Pera, M. F., Fong, C. Y., Trounson, A., and Bongso, A. (2000). Embryonic stem cell lines from human blastocysts: somatic differentiation *in vitro*. *Nat. Biotechnol.* 18, 399–404. doi: 10.1038/74447

Reynolds, B. A., and Weiss, S. (1992). Generation of neurons and astrocytes from isolated cells of the adult mammalian central nervous system. *Science* 255, 1707–1710. doi: 10.1126/science.1553558

Rivetti di Val Cervo, P., Romanov, R. A., Spigolon, G., Masini, D., et al. (2017). Induction of functional dopamine neurons from human astrocytes *in vitro* and mouse astrocytes in a Parkinson's disease model. *Nat. Biotechnol.* 35, 444–452. doi: 10.1038/nbt.3835

Rodriguez Viales, R., Diotel, N., Ferg, M., Armant, O., Eich, J., Alunni, A., et al. (2015). The helix-loop-helix protein id1 controls stem cell proliferation during regenerative neurogenesis in the adult zebrafish telencephalon. *Stem Cells* 33, 892–903. doi: 10.1002/stem.1883

Rossi, S. L., Nistor, G., Wyatt, T., Yin, H. Z., Poole, A. J., Weiss, J. H., et al. (2010). Histological and functional benefit following transplantation of motor neuron progenitors to the injured rat spinal cord. *PLoS One* 5:e11852. doi: 10.1371/journal.pone.0011852

Rothenaigner, I., Krecsmarik, M., Hayes, J. A., Bahn, B., Lepier, A., Fortin, G., et al. (2011). Clonal analysis by distinct viral vectors identifies bona fide neural stem cells in the adult zebrafish telencephalon and characterizes their division properties and fate. *Development* 138, 1459–1469. doi: 10.1242/dev.058156

Roy, N. S., Wang, S., Jiang, L., Kang, J., Benraiss, A., Harrison-Restelli, C., et al. (2000). *In vitro* neurogenesis by progenitor cells isolated from the adult human hippocampus. *Nat. Med.* 6, 271–277. doi: 10.1038/73119

Sahay, A., and Hen, R. (2007). Adult hippocampal neurogenesis in depression. *Nat. Neurosci.* 10, 1110–1115. doi: 10.1038/nn1969

Samata, B., Doi, D., Nishimura, K., Kikuchi, T., Watanabe, A., Sakamoto, Y., et al. (2016). Purification of functional human ES and iPSC-derived midbrain dopaminergic progenitors using LRTM1. *Nat. Commun.* 7:13097. doi: 10.1038/ncomms13097

Sanai, N., Nguyen, T., Ihrie, R. A., Mirzadeh, Z., Tsai, H. H., Wong, M., et al. (2011). Corridors of migrating neurons in the human brain and their decline during infancy. *Nature* 478, 382–386. doi: 10.1038/nature10487

Sanai, N., Tramontin, A. D., Quinones-Hinojosa, A., Barbaro, N. M., Gupta, N., Kunwar, S., et al. (2004). Unique astrocyte ribbon in adult human brain contains neural stem cells but lacks chain migration. *Nature* 427, 740–744. doi: 10.1038/nature02301

Seaberg, R. M., and van der Kooy, D. (2002). Adult rodent neurogenic regions: the ventricular subependyma contains neural stem cells, but the dentate gyrus contains restricted progenitors. *J. Neurosci.* 22, 1784–1793. doi: 10.1523/jneurosci.22-05-01784.2002

Seri, B., Garcia-Verdugo, J. M., Collado-Morente, L., McEwen, B. S., and Alvarez-Buylla, A. (2004). Cell types, lineage, and architecture of the germinal zone in the adult dentate gyrus. *J. Comp. Neurol.* 478, 359–378. doi: 10.1002/cne.20288

Seri, B., Garcia-Verdugo, J. M., McEwen, B. S., and Alvarez-Buylla, A. (2001). Astrocytes give rise to new neurons in the adult mammalian hippocampus. *J. Neurosci.* 21, 7153–7160. doi: 10.1523/jneurosci.21-18-07153.2001

Shi, Y., Inoue, H., Wu, J. C., and Yamanaka, S. (2017). Induced pluripotent stem cell technology: a decade of progress. *Nat. Rev. Drug Discov.* 16, 115–130. doi: 10.1038/nrd.2016.245

Shin, J. Y., Park, H. J., Kim, H. N., Oh, S. H., Bae, J. S., Ha, H. J., et al. (2014). Mesenchymal stem cells enhance autophagy and increase beta-amyloid clearance in Alzheimer disease models. *Autophagy* 10, 32–44. doi: 10.4161/auto.26508

Sirko, S., Behrendt, G., Johansson, P. A., Tripathi, P., Costa, M., Bek, S., et al. (2013). Reactive glia in the injured brain acquire stem cell properties in response to sonic hedgehog. [corrected]. *Cell Stem Cell* 12, 426–439. doi: 10.1016/j.stem.2013.01.019

Skaggs, K., Goldman, D., and Parent, J. M. (2014). Excitotoxic brain injury in adult zebrafish stimulates neurogenesis and long-distance neuronal integration. *Glia* 62, 2061–2079. doi: 10.1002/glia.22726

Soldner, F., Laganiere, J., Cheng, A. W., Hockemeyer, D., Gao, Q., Alagappan, R., et al. (2011). Generation of isogenic pluripotent stem cells differing exclusively at two early onset Parkinson point mutations. *Cell* 146, 318–331. doi: 10.1016/j.cell.2011.06.019

Soldner, F., Stelzer, Y., Shivalila, C. S., Abraham, B. J., Latourelle, J. C., Barrasa, M. I., et al. (2016). Parkinson-associated risk variant in distal enhancer of alpha-synuclein modulates target gene expression. *Nature* 533, 95–99. doi: 10.1038/nature17939

Sorrells, S. F., Paredes, M. F., Cebrian-Silla, A., Sandoval, K., Qi, D., Kelley, K. W., et al. (2018). Human hippocampal neurogenesis drops sharply in children to undetectable levels in adults. *Nature* 555, 377–381. doi: 10.1038/nature25975

Spalding, K. L., Bergmann, O., Alkass, K., Bernard, S., Salehpour, M., Huttner, H. B., et al. (2013). Dynamics of hippocampal neurogenesis in adult humans. *Cell* 153, 1219–1227. doi: 10.1016/j.cell.2013.05.002

Spalding, K. L., Bhardwaj, R. D., Buchholz, B. A., Druid, H., and Frisen, J. (2005). Retrospective birth dating of cells in humans. *Cell* 122, 133–143. doi: 10.1016/j.cell.2005.04.028

Spencer, D. D., Robbins, R. J., Naftolin, F., Marek, K. L., Vollmer, T., Leranth, C., et al. (1992). Unilateral transplantation of human fetal mesencephalic tissue into the caudate nucleus of patients with Parkinson's disease. *N. Engl. J. Med.* 327, 1541–1548. doi: 10.1056/nejm199211263272201

Steinbeck, J. A., Choi, S. J., Mrejeru, A., Ganat, Y., Deisseroth, K., Sulzer, D., et al. (2015). Optogenetics enables functional analysis of human embryonic stem cell-derived grafts in a Parkinson's disease model. *Nat. Biotechnol.* 33, 204–209. doi: 10.1038/nbt.3124

Su, Z., Niu, W., Liu, M. L., Zou, Y., and Zhang, C. L. (2014). *In vivo* conversion of astrocytes to neurons in the injured adult spinal cord. *Nat. Commun.* 5:3338. doi: 10.1038/ncomms4338

Takahashi, K., and Yamanaka, S. (2006). Induction of pluripotent stem cells from mouse embryonic and adult fibroblast cultures by defined factors. *Cell* 126, 663–676. doi: 10.1016/j.cell.2006.07.024

Thomson, J. A., Itskovitz-Eldor, J., Shapiro, S. S., Waknitz, M. A., Swiergiel, J. J., Marshall, V. S., et al. (1998). Embryonic stem cell lines derived from human blastocysts. *Science* 282, 1145–1147. doi: 10.1126/science.282.5391.1145

Thu, D. C., Oorschot, D. E., Tippett, L. J., Nana, A. L., Hogg, V. M., Synek, B. J., et al. (2010). Cell loss in the motor and cingulate cortex correlates with symptomatology in Huntington's disease. *Brain* 133(Pt 4), 1094–1110. doi: 10.1093/brain/awq047

Tobin, M. K., Musaraca, K., Disouky, A., Shetti, A., Bheri, A., Honer, W. G., et al. (2019). Human hippocampal neurogenesis persists in aged adults and Alzheimer's disease patients. *Cell Stem Cell* 24, 974.e3–982.e3.

Torper, O., Ottosson, D. R., Pereira, M., Lau, S., Cardoso, T., Grealish, S., et al. (2015). *In vivo* reprogramming of striatal NG2 glia into functional neurons that integrate into local host circuitry. *Cell Rep.* 12, 474–481. doi: 10.1016/j.celrep.2015.06.040

Torper, O., Pfisterer, U., Wolf, D. A., Pereira, M., Lau, S., Jakobsson, J., et al. (2013). Generation of induced neurons via direct conversion *in vivo*. *Proc. Natl. Acad. Sci. U.S.A.* 110, 7038–7043. doi: 10.1073/pnas.1303829110

Ueki, Y., Wilken, M. S., Cox, K. E., Chipman, L., Jorstad, N., Sternhagen, K., et al. (2015). Transgenic expression of the proneural transcription factor Ascl1 in Muller glia stimulates retinal regeneration in young mice. *Proc. Natl. Acad. Sci. U.S.A.* 112, 13717–13722. doi: 10.1073/pnas.1510595112

Urban, N., van den Berg, D. L., Forget, A., Andersen, J., Demmers, J. A., Hunt, C., et al. (2016). Return to quiescence of mouse neural stem cells by degradation of a proactivation protein. *Science* 353, 292–295. doi: 10.1126/science.aaf4802

van Tijn, P., Kamphuis, W., Marlatt, M. W., Hol, E. M., and Lucassen, P. J. (2011). Presenilin mouse and zebrafish models for dementia: focus on neurogenesis. *Prog. Neurobiol.* 93, 149–164. doi: 10.1016/j.pneurobio.2010.10.008

Wictorin, K., Ouimet, C. C., and Bjorklund, A. (1989). Intrinsic organization and connectivity of intrastriatal striatal transplants in rats as revealed by DARPP-32 immunohistochemistry: specificity of connections with the lesioned host brain. *Eur. J. Neurosci.* 1, 690–701. doi: 10.1111/j.1460-9568.1989.tb00375.x

Winner, B., Cooper-Kuhn, C. M., Aigner, R., Winkler, J., and Kuhn, H. G. (2002). Long-term survival and cell death of newly generated neurons in the adult rat olfactory bulb. *Eur. J. Neurosci.* 16, 1681–1689. doi: 10.1046/j.1460-9568.2002.02238.x

Winner, B., Kohl, Z., and Gage, F. H. (2011). Neurodegenerative disease and adult neurogenesis. *Eur. J. Neurosci.* 33, 1139–1151. doi: 10.1111/j.1460-9568.2011.07613.x

Wyatt, T. J., Rossi, S. L., Siegenthaler, M. M., Frame, J., Robles, R., Nistor, G., et al. (2011). Human motor neuron progenitor transplantation leads to endogenous neuronal sparing in 3 models of motor neuron loss. *Stem Cells Int.* 2011, 207230. doi: 10.4061/2011/207230

Xu, X., Tay, Y., Sim, B., Yoon, S. I., Huang, Y., Ooi, J., et al. (2017). Reversal of phenotypic abnormalities by CRISPR/Cas9-mediated gene correction in huntington disease patient-derived induced pluripotent stem cells. *Stem Cell Rep.* 8, 619–633. doi: 10.1016/j.stemcr.2017.01.022

Yu, J., Vodyanik, M. A., Smuga-Otto, K., Antosiewicz-Bourget, J., Frane, J. L., Tian, S., et al. (2007). Induced pluripotent stem cell lines derived from human somatic cells. *Science* 318, 1917–1920.

Yue, W., Li, Y., Zhang, T., Jiang, M., Qian, Y., Zhang, M., et al. (2015). ESC-derived basal forebrain cholinergic neurons ameliorate the cognitive symptoms associated with Alzheimer's disease in mouse models. *Stem Cell Rep.* 5, 776–790. doi: 10.1016/j.stemcr.2015.09.010

**Conflict of Interest:** The author declares that the research was conducted in the absence of any commercial or financial relationships that could be construed as a potential conflict of interest.

frontiers in Cell and Developmental Biology

BRIEF RESEARCH REPORT
published: 20 March 2020
doi: 10.3389/fcell.2020.00173

# Inhibition of Gamma-Secretase Promotes Axon Regeneration After a Complete Spinal Cord Injury

*Daniel Sobrido-Cameán[1†], Diego Robledo[2†], Daniel Romaus-Sanjurjo[1‡], Vanessa Pérez-Cedrón[3], Laura Sánchez[3], María Celina Rodicio[1*†] and Antón Barreiro-Iglesias[1*†]*

[1] Department of Functional Biology, CIBUS, Faculty of Biology, Universidade de Santiago de Compostela, Santiago de Compostela, Spain, [2] The Roslin Institute and Royal (Dick) School of Veterinary Studies, The University of Edinburgh, Edinburgh, United Kingdom, [3] Department of Genetics, Universidade de Santiago de Compostela, Santiago de Compostela, Spain

In a recent study, we showed that GABA and baclofen (a GABAB receptor agonist) inhibit caspase activation and promote axon regeneration in descending neurons of the sea lamprey brainstem after a complete spinal cord injury (Romaus-Sanjurjo et al., 2018a). Now, we repeated these treatments and performed 2 independent Illumina RNA-Sequencing studies in the brainstems of control and GABA or baclofen treated animals. GABA treated larval sea lampreys with their controls were analyzed 29 days after a complete spinal cord injury and baclofen treated larvae with their controls 9 days after the injury. One of the most significantly downregulated genes after both treatments was a HES gene (*HESB*). HES proteins are transcription factors that are key mediators of the Notch signaling pathway and gamma-secretase activity is crucial for the activation of this pathway. So, based on the RNA-Seq results we subsequently treated spinal cord injured larval sea lampreys with a novel gamma-secretase inhibitor (PF-3804014). This treatment also reduced the expression of *HESB* in the brainstem and significantly enhanced the regeneration of individually identifiable descending neurons after a complete spinal cord injury. Our results show that gamma-secretase could be a novel target to promote axon regeneration after nervous system injuries.

**Keywords: notch, gamma-secretase, axon regeneration, GABA, baclofen, RNA-Seq, lamprey, spinal cord injury**

OPEN ACCESS

***Edited by:***
*Luis B. Tovar-y-Romo, National Autonomous University of Mexico, Mexico*

***Reviewed by:***
*Jeffrey C. Petruska, University of Louisville, United States*
*David Parker, University of Cambridge, United Kingdom*
*Hermelinda Salgado-Ceballos, Mexican Social Security Institute (IMSS), Mexico*

****Correspondence:***
*María Celina Rodicio*
*mcelina.rodicio@usc.es*
*Antón Barreiro-Iglesias*
*anton.barreiro@usc.es*

*[†] These authors have contributed equally to this work*

***[‡] Present address:***
*Daniel Romaus-Sanjurjo, Department of Neurosciences, School of Medicine, University of California, San Diego, La Jolla, CA, United States*

***Specialty section:***
*This article was submitted to Molecular Medicine, a section of the journal Frontiers in Cell and Developmental Biology*

***Received:*** *16 December 2019*
***Accepted:*** *02 March 2020*
***Published:*** *20 March 2020*

***Citation:***
*Sobrido-Cameán D, Robledo D, Romaus-Sanjurjo D, Pérez-Cedrón V, Sánchez L, Rodicio MC and Barreiro-Iglesias A (2020) Inhibition of Gamma-Secretase Promotes Axon Regeneration After a Complete Spinal Cord Injury. Front. Cell Dev. Biol. 8:173. doi: 10.3389/fcell.2020.00173*

## INTRODUCTION

In mammals, including humans, spinal cord injury (SCI) is a devastating event that can lead to permanent disability. The death of neurons that are not replaced after the injury and lack of axon regeneration of axotomized neurons are two of the main causes of permanent neurological deficits after SCI. In striking contrast to mammals, lampreys, as other basal vertebrates, are able to recover locomotion spontaneously after a complete SCI (Rodicio and Barreiro-Iglesias, 2012; Romaus-Sanjurjo et al., 2018b). During recovery from a complete SCI, lampreys are able to regenerate approximately 50% of their brainstem descending neurons and this partial axonal regeneration is needed for recovery (Davis and McClellan, 1994; Jacobs et al., 1997; Cornide-Petronio et al., 2011; Parker, 2017). This offers an interesting vertebrate model to find new signaling pathways responsible for neuronal survival and axon regeneration in descending neurons after SCI.

In a recent study, we showed that endogenous GABA promotes axon regeneration in descending neurons of lampreys after a complete SCI, and that GABOB (a GABA analog) and baclofen (a GABAB receptor agonist) treatments further promoted axon regeneration (Romaus-Sanjurjo et al., 2018a, 2019). GABA and baclofen treatments also inhibited caspase activation in giant individually identifiable descending neurons following the complete SCI (Romaus-Sanjurjo et al., 2018a). Here, we repeated the GABA and baclofen treatments and carried out 2 independent Illumina RNA sequencing (RNA-Seq) studies in the brainstems of control non-treated animals and treated animals. The aim of these RNA-Seq studies was to obtain gene expression data that could reveal secondary pathways modulated by GABAergic signaling in injured neurons and identify new signaling pathways that could be involved in the control of neuronal survival and axon regeneration in lampreys.

As shown below, results from these RNA-Seq experiments revealed changes in the expression of a *HES* gene. HES proteins are key mediators of the Notch signaling pathway (Engler et al., 2018). In the developing central nervous system, Notch signaling is mainly known for its role in neurogenesis and neuronal differentiation (see Imayoshi and Kageyama, 2011; Engler et al., 2018; Sagner et al., 2018), a feature that is conserved in developing lampreys (Lara-Ramirez et al., 2019). But, interestingly, a recent study showed that Notch signaling also inhibits axon regeneration in worms (El Bejjani and Hammarlund, 2012; Po et al., 2012). Whether this is also the case in vertebrates was not known. Here, we provide evidence showing that the pharmacological inhibition of gamma-secretase promotes axon regeneration after a complete SCI in lampreys.

# MATERIALS AND METHODS

## Animals, SCI and Drug Treatments

All experiments involving animals were approved by the Bioethics Committee at the University of Santiago de Compostela and the *Conselleria do Medio Rural e do Mar* of the *Xunta de Galicia* (license reference JLPV/IId; Spain), and were performed in accordance with European Union and Spanish guidelines on animal care and experimentation. Animals were deeply anesthetized with 0.1% MS-222 (Sigma, St Louis, MO) in lamprey Ringer solution before all experimental procedures.

Mature and developmentally stable larval sea lampreys, *Petromyzon marinus* L. ($n$ = 149; between 100 and 120 mm in body length, 5–7 years of age), were used in this study. Larval lampreys were collected from the river Ulla (Galicia, north-western Spain), with permission from the *Xunta de Galicia*, and maintained in aerated freshwater aquaria at 15°C with a bed of river sediment until their use in experimental procedures. Larval lampreys were randomly distributed between the different experimental groups.

SCI surgical procedures and drug treatments with GABA and baclofen were performed as previously described (Romaus-Sanjurjo et al., 2018a; **Figure 1**). Briefly, the rostral spinal cord was exposed from the dorsal midline at the level of the 5th gill. A complete spinal cord transection was performed with Castroviejo scissors and the spinal cord cut ends were visualized under the stereomicroscope. After SCI, animals were returned to individual freshwater tanks. Each injured animal was examined 24 h after surgery to confirm that there was no movement caudal to the lesion site. The animals were allowed to recover in individual freshwater tanks at 19.5°C. GABA and baclofen were applied in the water where the animals were left after the SCI surgical procedures (GABA at a concentration of 500 μM and baclofen at a concentration of 125 μM). GABA treated animals and their controls were processed for RNA extraction 29 days post-lesion (dpl) [when spontaneous axon regrowth begins to predominate Zhang et al. (2005); **Figure 1**]. Baclofen treated animals and their controls were processed for RNA extraction 9 days post-lesion [at a time in which caspase activation begins to be detected in injured neurons (Barreiro-Iglesias and Shifman, 2012, 2015) and axon retraction predominates Zhang et al., 2005; **Figure 1**].

PF-3804014 [a novel gamma-secretase inhibitor (Lanz et al., 2010) that has been used in recent studies to inhibit Notch signaling (e.g., Samon et al., 2012; Wu et al., 2017); Tocris Bioscience, United Kingdom] treatment after a complete SCI (see previous paragraph) was done as previously described for taurine treatments (Sobrido-Cameán et al., 2019). In these experiments, PF-3804014 was dissolved in lamprey Ringer solution (137 mM NaCl, 2.9 mM KCl, 2.1 mM CaCl2, 2 mM HEPES; pH 7.4) at a concentration of 5 mM, soaked in a small piece of Gelfoam (Pfizer; New York, NY) and placed on top of the site of injury at the time of spinal cord transection. Control animals went through the same surgical procedures but were only treated with Gelfoam soaked in lamprey Ringer. Axon regeneration was assessed 11 weeks post-lesion (wpl) in control ($n$ = 16) and PF-3804014 ($n$ = 21) treated animals using Neurobiotin (Vector, Burlingame, CA) as a retrograde tracer as previously described (Sobrido-Cameán et al., 2019). Briefly, at 11 wpl a second complete spinal cord transection was performed 5 mm below the site of the original transection and Neurobiotin (Vector) was applied in the rostral end of the transected spinal cord with the aid of a minute pin (#000). The animals were allowed to recover for 1 week to allow transport of the tracer from the application point to the neuronal soma of descending neurons. Since the original SCI was a complete spinal cord transection, only neurons whose axons regenerated at least 5 mm below the site of injury were labeled by the tracer. The presence of Neurobiotin in whole-mounted brains/spinal cords was detected using Avidin-D-FITC conjugated (Vector; 1:500).

## Imaging and Quantifications

A spectral confocal microscope (model TCS-SP2; Leica, Wetzlar, Germany) was used to acquire images of the whole-mounted brains/spinal cords. The identity of regenerated (Neurobiotin labeled) and non-regenerated identifiable descending neurons was determined for each brain. Giant descending neurons are always identifiable by their know location and big size (Jacobs et al., 1997) regardless of the presence of the tracer. Then, we calculated the percentage of regenerated identifiable neurons per animal and the total number of regenerated and non-regenerated neurons for all animals in the control and treated groups.

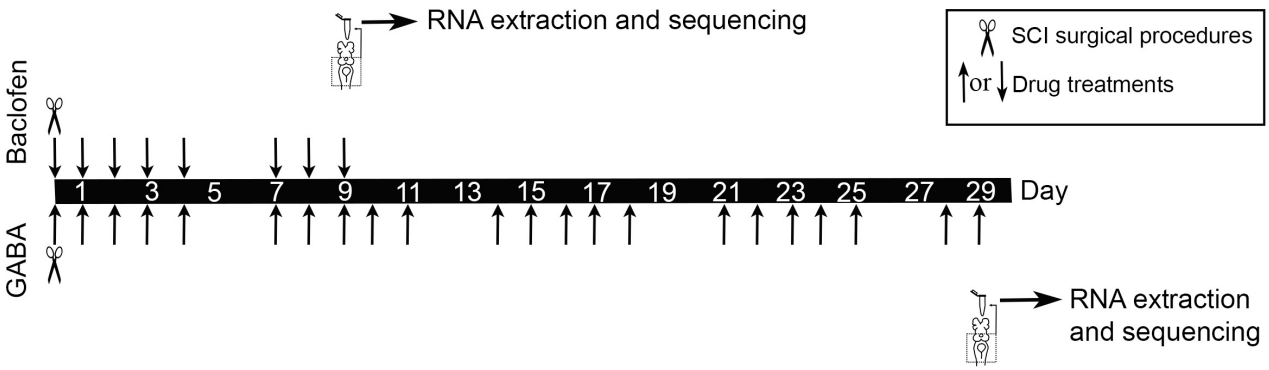


**FIGURE 1 |** Experimental design for the RNA-Seq experiments.

For axon quantification, we scanned the rostral spinal cord (starting at the obex) using a 20x objective. Then, we traced a horizontal line through the middle of the spinal cord confocal stack (**Figure 2A**) using the Fiji software and manually quantified the number of axons crossing this line. To avoid missing overlapping axons we counted through the stack of optical sections using the counting plugin in Fiji. Only the axons that regenerate through the site of injury (ascending or descending) are labeled with the tracer. Note that with this preparation, we can only quantify the coarsest axons; therefore, it is likely that more axons actually regenerated both in control and treated animals. The experimenter was blinded during all quantifications.

## Total RNA Isolation

After the GABA or baclofen treatment periods (29 days in the GABA experiment and 9 days in the baclofen experiment) the brainstems of control and treated larvae were dissected out and immediately put in RNAlater (Ambion Inc., TX, United States) (**Figure 1**). RNA extraction was performed using the RNeasy mini kit (Qiagen, Germany) with DNase treatment following the manufacturer's instructions. Isolated RNAs were eluted in nuclease free water. RNA quality and quantity were evaluated in a Bioanalyzer (Bonsai Technologies, Spain) and in a NanoDrop® ND-1000 spectrophotometer (NanoDrop® Technologies Inc., DE, United States). RNAs were stored at −80°C until use for RNA-Seq.

## RNA Sequencing

In the GABA experiment, 3 GABA treated and 3 control samples (each sample containing the RNA from 4 brainstems of 4 different animals; $n = 24$ in total) were sent to the Wellcome Trust Centre for Human Genetics (Oxford, United Kingdom) for library preparation and sequencing. RNA quality was checked again in a Bioanalyzer (Bonsai Technologies). All samples had RNA integrity number (RIN) of >8 (RIN measures how degraded the RNA is on a 0–10 scale, 10 being the least degraded). mRNA sequencing libraries were prepared from poly dT selected mRNA using the Illumina TrueSeq Stranded mRNA Library Preparation kit according to the manufacturer's protocol. The average insert size of the libraries was approximately 300 bp. A different barcode was used for each sample to enable demultiplexing of the sequencing data. Sequencing was conducted on an Illumina HiSeq 4000 as 150 bp paired-end reads, yielding 23.2 to 27.8 million reads per sample.

In the baclofen experiment, 5 baclofen treated and 5 control samples (each sample containing the RNA of 8 brainstems of 8 different animals; $n = 80$ animals in total) were sent to Edinburgh Genomics (Edinburg, United Kingdom) for library preparation and sequencing. RNA quality was checked again in a Bioanalyzer (Bonsai Technologies). All samples had RNA integrity number (RIN) of >7.5. mRNA sequencing libraries were prepared from poly dT selected mRNA using the Illumina TrueSeq Stranded mRNA Library Preparation kit according to the manufacturer's protocol. The average insert size of the libraries was approximately 300 bp. A different barcode was used for each sample to enable demultiplexing of the sequencing data. Sequencing was conducted on an Illumina NovaSeq S1 flowcell as 100 bp paired-end reads, yielding 26.8 to 37.6 million reads per sample.

## Quality Validation and Read Mapping

Between 23.2 and 37.6 million paired-end reads per sample were obtained (individual figures are shown in **Supplementary Table S1**). Sequencing quality was evaluated using FastQC. The quality of the baclofen experiment was significantly better than that of the GABA experiment (**Supplementary Figure S1**), non-etheless the sequencing output of both experiments showed average base qualities above 30 (reliability of the base call, the error probability of a quality of 30 is 0.001), except for the very last bases of the right reads of the GABA experiment (bases 141–150). Raw paired-end FASTQ files were quality filtered using Fastp (Chen et al., 2018) to remove leading or trailing bases with Phred quality scores <15 ('-q 15'), reads with length <30 base pairs ('-l 30'), polyG tails ('–trim_poly_g') and trim adaptor sequences (detected by per-read overlap, default). Significantly more reads were trimmed from the GABA experiment, congruent with the sequence quality assessment. The resulting trimmed FASTQ files were aligned against the latest lamprey genome assembly (Pmar_germline 1.0) (Smith et al., 2018) using STAR (Dobin et al., 2013) in 2-pass mapping mode (–twopassMode Basic) with the following

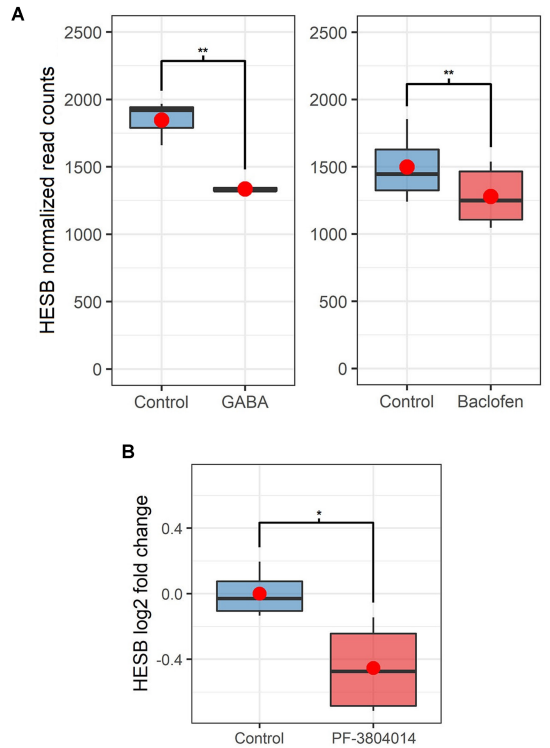


**FIGURE 2 |** Changes in *HESB* expression in the brainstem of injured animals after drug treatments. **(A)** Changes in the expression of *HESB* in the brainstem of injured animals after GABA or baclofen treatments (RNA-Seq). *HESB* gene expression is represented as read counts normalized by DESeq's median of ratios, and ** represents that the differences between the two groups are significant with false discovery rate corrected *p*-values between 0.01 and 0.001. Note that results are not comparable between the 2 RNA-Seq experiments. **(B)** Change in the expression of *HESB* in the brainstem of 1 wpl animals after the PF-3804014 treatment (qPCR). *HESB* expression is represented as log2 fold change in comparison to the mean of the controls, and * represents that the differences between the two groups are significant with *p*-value between 0.05 and 0.01. For both A and B, boxplots show the median, 25th and 75th percentiles, red dots represent the mean and whiskers extend to the most extreme data point which is no more than 1.5 times the length of the box away from the box.

parameters: 10 maximum multiple alignments allowed per read (–outFilterMultimapNmax 10), 10 maximum mismatches per read pair (–outFilterMismatchNmax 10), minimum and maximum intron lengths of 20 and 1 M bp, respectively (–alignIntronMin 20; –alignIntronMax 1000000), maximum distance of 1 Mb between mate reads (–alignMatesGapMax 1000000) and detection of chimeric sequences with a minimum mapped length of 20 bp (–chimSegmentMin 20; –chimScoreMin 1). The percentage of unique mapped reads ranged between 60.2 to 73.7%, with multimapping reads representing 9.3 to 26.1% and unaligned reads 13.1 to 18.1% (**Supplementary Table S1**).

## Transcriptome Reconstruction and Gene Expression

StringTie (Pertea et al., 2015) with default parameters (fr-firststrand, '–rf') was used to construct the lamprey transcriptome from our samples using the genome alignment files. The resulting genome-guided transcriptome has 110,157 transcripts distributed in 57,134 genes. Transcript length ranged from 80 to 73,302 bp, with an average of 2314 bp, N50 of 5,304 bp and N90 of 987 bp. FeatureCounts (Liao et al., 2014) was used to quantify gene expression at the gene level with the following parameters: fragments (paired-end reads) were counted instead of individual reads ('-p'), only fragments with both ends mapped were considered ('-B'), chimeric fragments were not considered ('-C'), and strand specified as reversely stranded ('-s 2'). Statistical analyses related to differential expression were performed using R v.3.5.2[1]. The output matrix was input into the R/Bioconductor package DESeq2 (Love et al., 2014).

The Benjamini-Hochberg false discovery rate (FDR) was applied, and transcripts with corrected *P*-values $< 0.05$ were considered differentially expressed genes. Heatmaps were drawn using the R package 'gplots' v.3.01.1[2]. Pathway analyses were performed using Reactome (Fabregat et al., 2018), converting all non-human gene identifiers to their human equivalents.

## RNA-Seq Data Records

Raw FASTQ files for all samples were uploaded to the NCBI Sequence Read Archive (SRA), and are publicly available under BioProject accession numbers PRJNA561093 (GABA) and PRJNA561123 (Baclofen). The constructed transcriptome is available in the NCBI Transcriptome Shotgun Assembly (TSA) database under accession GHVE00000000. Read counts for each transcript were deposited in NCBI Gene Expression Omnibus (GEO) and are available under accession number GSE137860.

## qPCR Experiments After PF-3804014 Treatment

4 brainstems ($n = 4$ animals) from control 1 wpl vehicle treated animals and 4 brainstems ($n = 4$ animals) from 1 wpl PF-3804014 treated animals were processed for qPCR analyses of *HESB* (GenBank accession number: MN833804) expression. Specific primers for targeted genes were designed using Primer3: *HESB*-forward AAAGCAAAGACGGGACAGGA, *HESB*-reverse GATGTCCGCCTTCTCCAGTT, *GAPDH*-forward CAGATTCGTCCAGCTCCGTT, *GAPDH*-reverse CCATTGTGGAGCGGATGTCA. qPCR was performed on a Stratagene Mx3005P thermocycler (Agilent Technologies) using Brilliant III Ultra-Fast SYBR Green QPCR Master Mix in a final volume of 12.5 μL following the manufacturer's protocol with 1 μL of cDNA per reaction. Primer concentration was 300 nM and each sample was run in duplicate. The cycling parameters were: 50°C for 2 min, 95°C for 10 min, followed by 40 cycles of amplification at 95°C for 15 s and 60°C for 1 min. After amplification, a dissociation step was performed raising the temperature from 65 to 95°C to create a melting curve and ensure the presence of a single amplification product. qPCR data were obtained by the MxPro software (Agilent Technologies)

[1]http://www.R-project.org/

[2]https://cran.r-project.org/web/packages/gplots/index.html

and quantification cycle values (Cq) calculated for each replicate and then averaged to obtain the final Cq value. *HESB* Cq values were normalized using the reference gene (*GAPDH*), and fold changes were calculated for each sample using the average of the controls as reference.

## Statistical Analyses

Statistical analysis was carried out using Prism 6 (GraphPad software, La Jolla, CA). Data were presented as mean ± SEM. Normality of the data was determined by D'Agostino–Pearson omnibus test and all data passed the normality test. A Student's *t*-test was used to determine significant differences in the qPCR experiment and between control and PF-3804014 treated animals (percentage of regenerated neurons per animal and number of regenerated axons per animal). A Fisher's exact test was used to determine significant differences between control and PF-3804014 treated animals (total number of regenerated neurons).

# RESULTS

## RNA-Seq Differential Expression Analyses

In previous work, we showed that both GABA and baclofen promote axon regeneration after a complete SCI in lampreys (Romaus-Sanjurjo et al., 2018a). Here, we aimed to identify new genes involved in axon regeneration in lampreys that might be regulated by GABAergic signaling. For this we carried out 2 independent RNA-Seq studies in the brainstems of injured animals after GABA or baclofen treatments. 23 differentially expressed genes were detected between GABA-treated and control samples, and 82 differentially expressed genes between baclofen-treated and control samples (**Supplementary File 1**). At 29 dpl, treatment with GABA induced mostly the downregulation of genes compared to control animals (**Supplementary File 1**; 7 up-regulated and 16 down-regulated genes). The opposite trend was seen at 9 dpl with baclofen, which induced the upregulation of a higher number of genes (**Supplementary File 1**; 63 upregulated and 18 downregulated genes). This included changes in the expression of genes known to promote axon regeneration, like the transcription factor KLF7 (increased expression after baclofen treatment; see discussion).

A HES transcription factor [annotated as *HESB* in another lamprey species *Lampetra planeri* (Lara-Ramirez et al., 2019)] was the most significantly downregulated gene in response to GABA (logFC = −0.47; **Figure 2A**, and **Supplementary File 1**); and it was also one of the most significantly down-regulated genes in response to baclofen (logFC = -0.44; **Figure 2**; **Supplementary File 1**). The sea lamprey *HESB* transcript sequence was deposited in GenBank under accession number MN833804. HES proteins are key transcription factors in the Notch signaling pathway (Ohtsuka et al., 1999). Concordantly, Reactome pathway analysis revealed a significant enrichment of many pathways relating to Notch signaling (FDR $p$-value $< 0.05$) amongst differentially expressed genes after both treatments (see **Supplementary File 2**). This suggests that Notch signaling might play a crucial role in axon regeneration in lampreys.

## Pharmacological Inhibition of Gamma-Secretase Promotes Axon Regeneration After a Complete SCI

Gamma-secretase activity is crucial for the release of the Notch intracellular domain (NICD) to activate the transcription of target genes like the HES family of transcription factors (see Fischer and Gessler, 2007). So, based on the RNA-Seq results we decided to treat larval sea lampreys after a complete spinal cord transection with the novel gamma-secretase inhibitor PF-3804014. First, qPCR experiments showed that the PF-3804014 treatment also caused a significant decrease in *HESB* expression in the brainstem of spinal cord injured animals (1 wpl) as compared to vehicle treated controls (logFC = −0.45; Student's *t*-test, $p = 0.0307$; **Figure 2B**). At 11 wpl, the PF-3804014 treatment significantly promoted axon regeneration of individually identifiable descending neurons (**Figure 3A**; the M1-3, I1-6, B1-B6, Mth, and Mth' descending neurons) of the sea lamprey (**Figures 3B–D**); both when looking at the percentage of regenerated identifiable descending neurons per animal (Student's *t*-test, $p = 0.0132$; **Figures 3B,C**) or at the total number of regenerated identifiable neurons (Fisher's exact test, $p = 0.0032$; **Figures 3B,D**). Moreover, the acute PF-3804014 treatment significantly increased the number of regenerated axons (ascending or descending) in the spinal cord following a complete SCI (Student's *t*-test, $p = 0.0134$; **Figures 3E,F**). These results show that inhibiting gamma-secretase activity acutely after a complete spinal cord transection enhances true axon regeneration in sea lamprey neurons.

# DISCUSSION

Our 2 RNA-Seq studies in the brainstem of spinal cord injured larval sea lampreys revealed a significant downregulation of a HES transcription factor (*HESB*) and a significant enrichment of the Notch signaling pathway after GABA and baclofen treatments. The fact that this was detected in 2 independent RNA-Seq studies carried out in different sequencing platforms, using 2 different GABAergic drugs and at 2 different time points after injury provided strong confidence on the possible importance of this signaling pathway during regeneration. Gamma-secretase activity is crucial for the release of NICD to activate the transcription of target genes like the HES family of transcription factors (see Fischer and Gessler, 2007). Treatments with the gamma-secretase inhibitor PF-3804014 also caused a significant decrease in the expression of *HESB* in the brainstem and a significant increase in axon regeneration after a complete SCI. Specifically, this treatment led to a significant increase in the regeneration of individually identifiable descending neurons of the lamprey brainstem. This is in agreement with our previous results showing improved axon regeneration after baclofen or GABOB treatments after SCI in lampreys (Romaus-Sanjurjo et al., 2018a). So, the Notch signaling pathway appears to be of crucial importance in the regulation of axon regrowth after SCI in lampreys. Our results also suggest that GABA signaling promotes

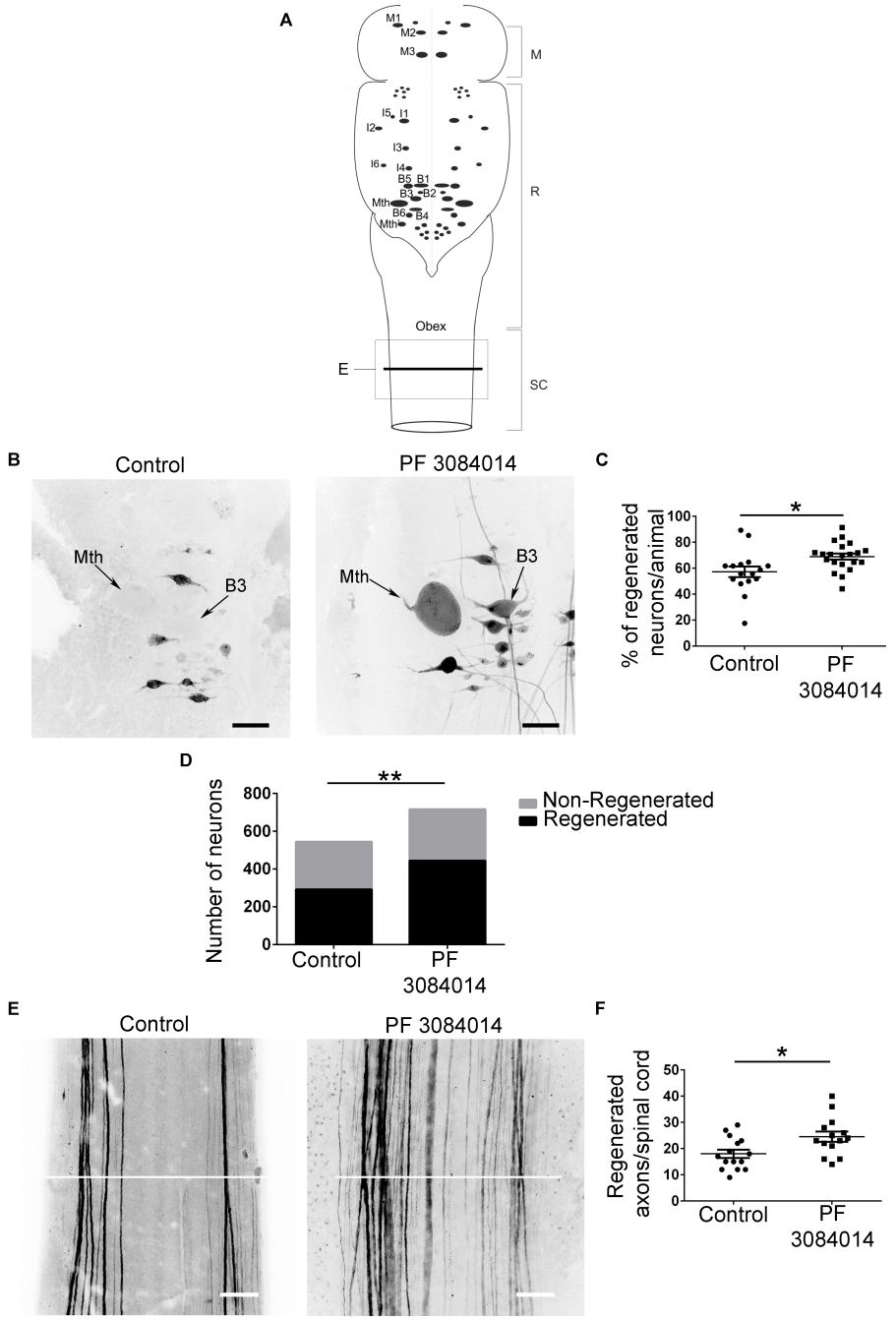


**FIGURE 3 |** PF-3804014 promotes axon regeneration after a complete SCI. **(A)** Schematic drawing of a dorsal view of the sea lamprey brainstem showing the location of giant individually identifiable descending neurons (modified from Sobrido-Cameán and Barreiro-Iglesias, 2018). The box marked "E" indicates the spinal cord region shown in Panel E. The line used to count the number of regenerated axons in the spinal cord is also indicated. M, mesencephalon; R, rhombencephalon; SC, spinal cord. **(B)** Photomicrographs of dorsal views of whole-mounted brains showing regenerated identifiable descending neurons, as identified by retrograde tracer labeling, in control and PF-3804014 treated animals. Note the increased number of labeled (regenerated) identifiable neurons in PF-3804014 treated animals. **(C)** Graph showing significant changes (asterisk) in the percentage of regenerated identifiable descending neurons per animal (controls: $n$ = 16 animals; PF-3804014 treated: $n$ = 21 animals) after the PF-3804014 treatment (control: 57,22 ± 4.132%; PF-3804014: 68.95 ± 2.354%). **(D)** Graph showing significant changes (asterisks) in the total number of regenerated neurons after the PF-3804014 treatment (control: 292 neurons regenerated, 252 non-regenerated; PF-3804014: 444 neurons regenerated, 272 non-regenerated). **(E)** Photomicrographs of whole-mounted spinal cords showing regenerated axons, as identified by tracer labeling, in control and PF-3804014 treated animals. Note the increased number of regenerated axons in PF-3804014 treated animals. The line used to count the number of regenerated axons in the spinal cord is also indicated in white. **(F)** Graph showing significant changes (asterisk) in the number of regenerated axons per spinal cord after the PF-3804014 treatment (control: 18 ± 1.588 axons, $n$ = 15 animals; PF-3804014: 24.57 ± 1.955 axons, $n$ = 14 animals). Rostral is up and scale bars correspond to 100 μm.

axon regeneration, at least partially, by inhibiting the Notch signaling pathway.

A previous study in *Caenorhabditis elegans* revealed that Notch signaling inhibits axon regeneration in identifiable neurons of this nematode (El Bejjani and Hammarlund, 2012). Importantly, our findings extend these results to vertebrates and the SCI situation. As in lampreys, treatments with a gamma-secretase inhibitor (DAPT in their case) improved axon regeneration in worms (El Bejjani and Hammarlund, 2012). Interestingly, gamma-secretase activity had to be inhibited right after injury in worms to improve regeneration (El Bejjani and Hammarlund, 2012), which coincides with our results using also early pharmacological inhibition in lampreys. In *C. elegans*, genetic manipulations showed that Notch signaling acts autonomously in the injured neuron to prevent growth cone formation (El Bejjani and Hammarlund, 2012). Our current data in lampreys analyzing whole brainstems (which include descending neurons but also other types of neurons and glial cells) in the RNA-Seq/qPCR experiments and pharmacological inhibition (present results) does not allow us to differentiate between direct or indirect effects of this signaling pathway in the regeneration of descending neurons. In future work it would be important to study if Notch signaling acts directly on lamprey descending neurons during regeneration or if the positive effects of gamma-secretase inhibition come through an indirect mechanism.

Notch1 expression increases in the rodent spinal cord after SCI (Yamamoto et al., 2001; Chen et al., 2005), and treating human induced pluripotent stem cell-derived neural stem/progenitor cells with a gamma-secretase inhibitor promoted axon growth from these cells after transplantation to the injured spinal cord of mice (Okubo et al., 2018). So, putting together previous data in rodents and our results in lampreys we propose that gamma-secretase could be an interesting target to promote axon regeneration after SCI in mammalian models. Moreover, gamma-secretase could also serve as a target to promote other regenerative aspects, for example gamma-secretase inhibition promotes stem cell proliferation and generation of new motor neurons after SCI in zebrafish (Dias et al., 2012). Future work should test the effects of gamma-secretase inhibition in preclinical rodent models of SCI to evaluate both positive and negative outcomes of this treatment.

Finally, it is important to mention that our 2 RNA-Seq studies revealed significant changes in the expression of other genes (see **Supplementary File 1**), which provides a resource for future studies on the role of these genes during regeneration. A comparison between the GABA and baclofen RNA-Seq experiments reveals differences in the changes of gene expression (see **Supplementary File 1**). This might be related to the different time points of analysis (29 or 9 dpl) and due to a potential influence of GABAA receptors during GABA treatment. Changes in gene expression after SCI in lampreys have been also observed even at later time points when looking at the expression of specific genes like with the *HDAC1* gene (Chen et al., 2016); therefore, new RNA-Seq studies at different time points might reveal more genes involved in the positive effects of GABA signaling. Regarding a possible contribution of GABAA receptors, we have recently shown that a muscimol (a GABAA agonist) treatment inhibits caspase activation in identifiable descending neurons of lampreys after a complete SCI (Sobrido-Cameán et al., 2018), which supports the possibility of an influence of GABAA receptors during the GABA treatment.

As an example of other genes, the baclofen treatment caused a significant increase in the expression of 2 members of the Krüppel-like family of transcription factors (KLFs): *KLF7* and *KLF10*. Changes in the expression of different KLFs (including *KLF7* and *KLF10*) were previously detected over the course of recovery in an RNA-Seq study after SCI in lampreys (Herman et al., 2018). Previous work in mammalian models has revealed a differential implication of different KLFs in the control of axon regeneration after different types of nervous system injuries Moore et al., 2009 (for reviews see Moore and Goldberg, 2011; Moore et al., 2011). KLF7 promotes axon regeneration in mammals (Blackmore et al., 2012; Wang et al., 2016), which coincides well with our results revealing increased expression of KLF7 after baclofen treatment in lampreys with a complete SCI. As far as we are aware, the implication of KLF10 in axon regeneration has not yet been elucidated. Our results open the way to study the role of these or other genes in both neuronal survival and axon regeneration after SCI.

## DATA AVAILABILITY STATEMENT

Raw FASTQ files for all samples were uploaded to the NCBI Sequence Read Archive (SRA), and are publicly available under BioProject accession numbers PRJNA561093 (GABA) and PRJNA561123 (Baclofen). The constructed transcriptome is available in the NCBI Transcriptome Shotgun Assembly (TSA) database under accession GHVE00000000. Read counts for each transcript were deposited in NCBI Gene Expression Omnibus (GEO) and are available under accession number GSE137860.

## ETHICS STATEMENT

The animal study was reviewed and approved by the Bioethics Committee of the University of Santiago de Compostela Santiago de Compostela, A Coruña, Spain.

## AUTHOR CONTRIBUTIONS

DS-C and DR-S performed the SCI surgeries, drug treatments and brainstem dissections. VP-C performed the RNA extractions. DR performed the bioinformatic analyses. LS, MR, and AB-I supervised the study. MR and AB-I conceived the study. DR and AB-I wrote the manuscript. All authors have approved the final manuscript.

## FUNDING

Grant sponsors: FEDER/Ministerio de Ciencia, Innovación y Universidades – Agencia Estatal de Investigación (Grant

number: BFU-2017-87079-P) and the Xunta de Galicia (Grant number: ED431C 2018/28). DR was supported by the BBSRC Institute Strategic Programme Grants to the Roslin Institute (BB/P013732/1, BB/P013740/1, and BB/P013759/1).

## ACKNOWLEDGMENTS

We thank the staff of the Ximonde Biological Station for providing lampreys used in this study and Dr. Mercedes Rivas Cascallar for confocal microscope facilities and help. We acknowledge the support of the *Centro de Supercomputación de Galicia* (CESGA, Spain) in the completion of this work.

## SUPPLEMENTARY MATERIAL

The Supplementary Material for this article can be found online at: https://www.frontiersin.org/articles/10.3389/fcell.2020.00173/full#supplementary-material

## REFERENCES

Barreiro-Iglesias, A., and Shifman, M. I. (2012). Use of fluorochrome-labeled inhibitors of caspases to detect neuronal apoptosis in the whole-mounted lamprey brain after spinal cord injury. *Enzyme Res.* 2012:835731. doi: 10.1155/2012/835731

Barreiro-Iglesias, A., and Shifman, M. I. (2015). Detection of activated caspase-8 in injured spinal axons by using fluorochrome-labeled inhibitors of caspases (FLICA). *Methods Mol. Biol.* 1254, 329–339. doi: 10.1007/978-1-4939-2152-2_23

Blackmore, M. G., Wang, Z., Lerch, J. K., Motti, D., Zhang, Y. P., Shields, C. B., et al. (2012). Krüppel-like Factor 7 engineered for transcriptional activation promotes axon regeneration in the adult corticospinal tract. *Proc. Natl. Acad. Sci. U.S.A.* 109, 7517–7522. doi: 10.1073/pnas.1120684109

Chen, J., Laramore, C., and Shifman, M. I. (2016). Differential expression of HDACs and KATs in high and low regeneration capacity neurons during spinal cord regeneration. *Exp. Neurol.* 280, 50–59. doi: 10.1016/j.expneurol.2016.04.001

Chen, J., Leong, S. Y., and Schachner, M. (2005). Differential expression of cell fate determinants in neurons and glial cells of adult mouse spinal cord after compression injury. *Eur. J. Neurosci.* 22, 1895–1906. doi: 10.1111/j.1460-9568.2005.04348.x

Chen, S., Zhou, Y., Chen, Y., and Gu, J. (2018). fastp: an ultra-fast all-in-one FASTQ preprocessor. *Bioinformatics* 34, i884–i890. doi: 10.1093/bioinformatics/bty560

Cornide-Petronio, M. E., Ruiz, M. S., Barreiro-Iglesias, A., and Rodicio, M. C. (2011). Spontaneous regeneration of the serotonergic descending innervation in the sea lamprey after spinal cord injury. *J. Neurotrauma* 28, 2535–2540. doi: 10.1089/neu.2011.1766

Davis, G. R. Jr., and McClellan, A. D. (1994). Long distance axonal regeneration of identified lamprey reticulospinal neurons. *Exp. Neurol.* 127, 94–105. doi: 10.1006/exnr.1994.1083

Dias, T. B., Yang, Y. J., Ogai, K., Becker, T., and Becker, C. G. (2012). Notch signaling controls generation of motor neurons in the lesioned spinal cord of adult zebrafish. *J. Neurosci.* 32, 3245–3252. doi: 10.1523/JNEUROSCI.6398-11.2012

Dobin, A., Davis, C. A., Schlesinger, F., Drenkow, J., Zaleski, C., Jha, S., et al. (2013). STAR: ultrafast universal RNA-seq aligner. *Bioinformatics* 29, 15–21. doi: 10.1093/bioinformatics/bts635

El Bejjani, R., and Hammarlund, M. (2012). Notch signaling inhibits axon regeneration. *Neuron* 73, 268–278. doi: 10.1016/j.neuron.2011.11.017

Engler, A., Zhang, R., and Taylor, V. (2018). Notch and neurogenesis. *Adv. Exp. Med. Biol.* 1066, 223–234. doi: 10.1007/978-3-319-89512-3_11

Fabregat, A., Korninger, F., Viteri, G., Sidiropoulos, K., Marín-García, P., Ping, P., et al. (2018). Reactome graph database: efficient access to complex pathway data. *PLoS Comput. Biol.* 14:e1005968. doi: 10.1371/journal.pcbi.1005968

Fischer, A., and Gessler, M. (2007). Delta-notch–and then? protein interactions and proposed modes of repression by Hes and Hey bHLH factors. *Nucleic Acids Res.* 35, 4583–4596. doi: 10.1093/nar/gkm477

Herman, P. E., Papatheodorou, A., Bryant, S. A., Waterbury, C. K. M., Herdy, J. R., Arcese, A. A., et al. (2018). Highly conserved molecular pathways, including Wnt signaling, promote functional recovery from spinal cord injury in lampreys. *Sci. Rep.* 8:742. doi: 10.1038/s41598-017-18757-1

Imayoshi, I., and Kageyama, R. (2011). The role of notch signaling in adult neurogenesis. *Mol. Neurobiol.* 44, 7–12. doi: 10.1007/s12035-011-8186-0

Jacobs, A. J., Swain, G. P., Snedeker, J. A., Pijak, D. S., Gladstone, L. J., and Selzer, M. E. (1997). Recovery of neurofilament expression selectively in regenerating reticulospinal neurons. *J. Neurosci.* 17, 5206–5220. doi: 10.1523/jneurosci.17-13-05206.1997

Lanz, T. A., Wood, K. M., Richter, K. E., Nolan, C. E., Becker, S. L., Pozdnyakov, N., et al. (2010). Pharmacodynamics and pharmacokinetics of the gamma-secretase inhibitor PF-3084014. *J. Pharmacol. Exp. Ther.* 334, 269–277. doi: 10.1124/jpet.110.167379

Lara-Ramirez, R., Pérez-González, C., Anselmi, C., Patthey, C., and Shimeld, S. M. A. (2019). Notch-regulated proliferative stem cell zone in the developing spinal cord is an ancestral vertebrate trait. *Development* 146:dev166595. doi: 10.1242/dev.166595

Liao, Y., Smyth, G. K., and Shi, W. (2014). featureCounts: an efficient general purpose program for assigning sequence reads to genomic features. *Bioinformatics* 30, 923–930. doi: 10.1093/bioinformatics/btt656

Love, M. I., Huber, W., and Anders, S. (2014). Moderated estimation of fold change and dispersion for RNA-seq data with DESeq2. *Genome Biol.* 15:550. doi: 10.1186/s13059-014-0550-8

Moore, D. L., Apara, A., and Goldberg, J. L. (2011). Krüppel-like transcription factors in the nervous system: novel players in neurite outgrowth and axon regeneration. *Mol. Cell Neurosci.* 47, 233–243. doi: 10.1016/j.mcn.2011.05.005

Moore, D. L., Blackmore, M. G., Hu, Y., Kaestner, K. H., Bixby, J. L., Lemmon, V. P., et al. (2009). KLF family members regulate intrinsic axon regeneration ability. *Science* 326, 298–301. doi: 10.1126/science.1175737

Moore, D. L., and Goldberg, J. L. (2011). Multiple transcription factor families regulate axon growth and regeneration. *Dev. Neurobiol.* 71, 1186–1211. doi: 10.1002/dneu.20934

Ohtsuka, T., Ishibashi, M., Gradwohl, G., Nakanishi, S., Guillemot, F., and Kageyama, R. (1999). Hes1 and Hes5 as notch effectors in mammalian neuronal differentiation. *EMBO J.* 18, 2196–2207. doi: 10.1093/emboj/18.8.2196

Okubo, T., Nagoshi, N., Kohyama, J., Tsuji, O., Shinozaki, M., Shibata, S., et al. (2018). Treatment with a gamma-secretase inhibitor promotes functional recovery in human IPSC- derived transplants for chronic spinal cord injury. *Stem Cell Rep.* 11, 1416–1432. doi: 10.1016/j.stemcr.2018.10.022

Parker, D. (2017). The lesioned spinal cord is a "new" spinal cord: evidence from functional changes after spinal injury in lamprey. *Front. Neural Circuits* 11:84. doi: 10.3389/fncir.2017.00084

Pertea, M., Pertea, G. M., Antonescu, C. M., Chang, T. C., Mendell, J. T., and Salzberg, S. L. (2015). StringTie enables improved reconstruction of a transcriptome from RNA-seq reads. *Nat. Biotechnol.* 33, 290–295. doi: 10.1038/nbt.3122

Po, M. D., Calarco, J. A., and Zhen, M. (2012). Releasing the inner inhibition for axon regeneration. *Neuron* 73, 207–209. doi: 10.1016/j.neuron.2012.01.002

Rodicio, M. C., and Barreiro-Iglesias, A. (2012). Lampreys as an animal model in regeneration studies after spinal cord injury. *Rev. Neurol.* 55, 157–166.

Romaus-Sanjurjo, D., Ledo-García, R., Fernández-López, B., Hanslik, K., Morgan, J. R., Barreiro-Iglesias, A., et al. (2018a). GABA promotes survival and axonal regeneration in identifiable descending neurons after spinal cord injury in larval lampreys. *Cell Death Dis.* 9:663.

Romaus-Sanjurjo, D., Rodicio, M. C., and Barreiro-Iglesias, A. (2019). Gamma-aminobutyric acid (GABA) promotes recovery from spinal cord injury in

lampreys: role of GABA receptors and perspective on the translation to mammals. *Neural Regen. Res.* 14, 1695–1696.

Romaus-Sanjurjo, D., Valle-Maroto, S. M., Barreiro-Iglesias, A., Fernández-López, B., and Rodicio, M. C. (2018b). Anatomical recovery of the GABAergic system after a complete spinal cord injury in lampreys. *Neuropharmacology* 131, 389–402. doi: 10.1016/j.neuropharm.2018.01.006

Sagner, A., Gaber, Z. B., Delile, J., Kong, J. H., Rousso, D. L., Pearson, C. A., et al. (2018). Olig2 and Hes regulatory dynamics during motor neuron differentiation revealed by single cell transcriptomics. *PLoS Biol.* 16:e2003127. doi: 10.1371/journal.pbio.2003127

Samon, J. B., Castillo-Martin, M., Hadler, M., Ambesi-Impiobato, A., Paietta, E., Racevskis, J., et al. (2012). Preclinical analysis of the γ-secretase inhibitor PF-03084014 in combination with glucocorticoids in T-cell acute lymphoblastic leukemia. *Mol. Cancer Ther.* 11, 1565–1575. doi: 10.1158/1535-7163.mct-11-0938

Smith, J. J., Timoshevskaya, N., Ye, C., Holt, C., Keinath, M. C., Parker, H. J., et al. (2018). The sea lamprey germline genome provides insights into programmed genome rearrangement and vertebrate evolution. *Nat. Genet.* 50, 270–277. doi: 10.1038/s41588-017-0036-1

Sobrido-Cameán, D., and Barreiro-Iglesias, A. (2018). Role of caspase-8 and Fas in cell death after spinal cord injury. *Front. Mol. Neurosci.* 11:101. doi: 10.3389/fnmol.2018.00101

Sobrido-Cameán, D., Fernández-López, B., Pereiro, N., Lafuente, A., Rodicio, M. C., and Barreiro-Iglesias, A. (2019). Taurine promotes axonal regeneration after a complete spinal cord injury in lampreys. *J. Neurotrauma* (in press). doi: 10.1089/neu.2019.6604

Sobrido-Cameán, D., Rodicio, M. C., and Barreiro-Iglesias, A. (2018). Data on the effect of a muscimol treatment in caspase activation in descending neurons of lampreys after a complete spinal cord injury. *Data Brief* 21, 2037–2041.

Wang, Y., Li, W. Y., Sun, P., Jin, Z. S., Liu, G. B., Deng, L. X., et al. (2016). Sciatic nerve regeneration in KLF7-transfected acellular nerve allografts. *Neurol. Res.* 38, 242–254. doi: 10.1080/01616412.2015.1105584

Wu, C. X., Xu, A., Zhang, C. C., Olson, P., Chen, L., Lee, T. K., et al. (2017). Notch inhibitor PF-03084014 inhibits hepatocellular carcinoma growth and metastasis via suppression of cancer stemness due to reduced activation of Notch1-Stat3. *Mol. Cancer Ther.* 16, 1531–1543.

Yamamoto, S., Nagao, M., Sugimori, M., Kosako, H., Nakatomi, H., Yamamoto, N., et al. (2001). Transcription factor expression and Notch-dependent regulation of neural progenitors in the adult rat spinal cord. *J. Neurosci.* 21, 9814–9823. doi: 10.1523/JNEUROSCI.21-24-09814.2001

Zhang, G., Jin, L. Q., Sul, J. Y., Haydon, P. G., and Selzer, M. E. (2005). Live imaging of regenerating lamprey spinal axons. *Neurorehabil. Neural Repair* 19, 46–57.

**Conflict of Interest:** The authors declare that the research was conducted in the absence of any commercial or financial relationships that could be construed as a potential conflict of interest.

frontiers in Cellular Neuroscience

ORIGINAL RESEARCH
published: 20 March 2020
doi: 10.3389/fncel.2020.00038

# Time-Course Changes and Role of Autophagy in Primary Spinal Motor Neurons Subjected to Oxygen-Glucose Deprivation: Insights Into Autophagy Changes in a Cellular Model of Spinal Cord Ischemia

*Shudong Chen*[1†], *Ruimin Tian*[1,2†], *Dan Luo*[1], *Zhifeng Xiao*[1], *Hui Li*[3] *and Dingkun Lin*[1,2*]

[1]*The Second Affiliated Hospital of Guangzhou University of Chinese Medicine, Guangzhou, China,* [2]*Guangdong Provincial Academy of Chinese Medical Sciences, Guangzhou, China,* [3]*School of Basic Medical Sciences, Guangzhou University of Chinese Medicine, Guangzhou, China*

Spinal cord ischemia is a severe clinical complication induced by thoracoabdominal aortic surgery, severe trauma, or compression to the spinal column. As one of the most important functional cells in the spinal cord, spinal motor neurons (SMNs) suffer most during the process since they are vulnerable to ischemic injury due to high demands of energy. Previous researches have tried various animal models or organotypic tissue experiments to mimic the process and get to know the pathogenesis and mechanism. However, little work has been performed on the cellular model of spinal cord ischemia, which has been hampered by the inability to obtain a sufficient number of pure primary SMNs for *in vitro* study. By optimizing the isolation and culture of SMNs, our laboratory has developed an improved culture system of primary SMNs, which allows cellular models and thus mechanism studies. In the present study, by establishing an *in vitro* model of spinal cord ischemia, we intended to observe the dynamic time-course changes of SMNs and investigate the role of autophagy in SMNs during the process. It was found that oxygen-glucose deprivation (OGD) resulted in destruction of neural networks and decreased cell viability of primary SMNs, and the severity increased with the prolonging of the OGD time. The OGD treatment enhanced autophagy, which reached a peak at 5 h. Further investigation demonstrated that inhibition of autophagy exacerbated the injury, evidencing that autophagy plays a protective role during the process.

**Keywords: spinal motor neurons (SMNs), spinal cord ischemia, cellular model, oxygen-glucose deprivation (OGD), autophagy**

OPEN ACCESS

***Edited by:***
*Luis B. Tovar-y-Romo, National Autonomous University of Mexico, Mexico*

***Reviewed by:***
*James N. Sleigh, University College London, United Kingdom*
*Lourdes Massieu, National Autonomous University of Mexico, Mexico*

***Correspondence:**
*Dingkun Lin*
*lindingkun_tcm@163.com*

*[†]These authors have contributed equally to this work*

***Received:*** *01 August 2019*
***Accepted:*** *07 February 2020*
***Published:*** *20 March 2020*

***Citation:***
*Chen S, Tian R, Luo D, Xiao Z, Li H and Lin D (2020) Time-Course Changes and Role of Autophagy in Primary Spinal Motor Neurons Subjected to Oxygen-Glucose Deprivation: Insights Into Autophagy Changes in a Cellular Model of Spinal Cord Ischemia. Front. Cell. Neurosci. 14:38. doi: 10.3389/fncel.2020.00038*

## INTRODUCTION

Spinal cord ischemia is a devastating complication following thoracoabdominal aortic surgery (Drinkwater et al., 2010; Shimizu and Yozu, 2011; Etz et al., 2014), and it frequently occurs as well when the spinal cord suffers from direct trauma during spinal cord injury (Rivlin and Tator, 1978; Aslan et al., 2009), or compression from vertebral stenosis and various other spinal lesions (Gooding et al., 1975; Griffiths et al., 1979; Yang et al., 2015), which may lead to various degrees of disability or even paraparesis/paraplegia (Coselli et al., 1997; Etz et al., 2008; Suarez et al., 2013). During the spinal cord ischemia, the blood flow of the spinal cord is reduced, and the tissue auto-regulation is disrupted (Kise et al., 2015; Weidauer et al., 2015), which takes an essential part in the pathophysiological mechanisms. During the past decades, numerous studies, by adopting various animal models (in rats, mice, rabbits, cats, pigs, and primates; Griffiths et al., 1979; Kato et al., 1997; Kolenda et al., 2003; Wang et al., 2010; Hwang et al., 2012, 2017; Nazli et al., 2015; Yang et al., 2015) and tissue (organotypic spinal cord slices) experiments (Turner and Johnson, 2011; Esposito et al., 2012) of spinal cord ischemia, have been studied for the pathogenesis and developed some methods to reduce the injury; however, up until now, the treatment options remain strongly controversial and limited, and the concrete mechanisms and roles of certain types of cells involved in this process are still far from clear. Besides *in vivo* or organotypic models, cellular models of a certain disease to mimic a certain cell type phenotype hold the key to understand the pathogenesis of a disease; nevertheless, progress in performing researches about spinal cord ischemia have been impeded by the inability to gain sufficient number with well uniformity of certain types of cells *in vitro*.

In eukaryotic cells, the maintenance of normal metabolic balance relies on two major protein catabolism pathways: the ubiquitin–proteasome pathway (UPS) and autophagy lysosomal pathway. A number of neurological disorders have been discovered to be associated with autophagy. Autophagy (means "self-eating" in Greek, "auto" oneself, "phagy" to eat), a term which was first coined by Christian de Duve in 1963 (De Duve, 1963; Klionsky, 2008), is a highly regulated process in which protein aggregates and damaged organelles are degraded *via* the lysosomal pathway. It is an evolutionary conserved catabolic system where unnecessary or dysfunctional cellular components, including cytosolic proteins and organelles, are detained in a double-membrane vesicle, and the resulting vacuoles (autophagosomes) are degraded after they are transmitted to the lysosomal compartment (Klionsky and Emr, 2000; Mizushima and Komatsu, 2011; Feng et al., 2014). It serves like a cellular housekeeper, to keep the amino acid/energy recycling and try to mitigate various metabolic stresses (Levine and Kroemer, 2008; Wirawan et al., 2012). Although some of abovementioned functions overlap with those of the UPS, autophagy mainly contributes to the turnover of long-lived proteins and the maintenance of amino acid pools in the setting of cellular stresses (Ciechanover et al., 2000; Nedelsky et al., 2008; Lu et al., 2013). This process is considered to be adaptive and essential for survival, differentiation, development, and homeostasis under both physiological and pathological conditions. In various neurological diseases, autophagy may be either upregulated or downregulated or even impaired (Komatsu et al., 2006; Lee et al., 2010; Lynch-Day et al., 2012; Gu et al., 2013; Martin et al., 2015). Previous *in vivo* studies have indicated that autophagy is implicated in the spinal cord ischemic injury (Kanno et al., 2009a; Fan et al., 2014; Fujita et al., 2015; Fang et al., 2016), whereas the concrete mechanisms during the process are controversial, and the impact of autophagy in primary spinal neurons has not been fully understood. Accumulating evidence suggested that autophagy may act as a "double-edged sword" with regard to central nervous system injury. The role of autophagy varies with the type or degree of injuries. Mounting studies showed that autophagy activation may be involved in neuroprotection in cerebral or spinal cord injury (Sheng et al., 2010; Mariño et al., 2011; Wang P. et al., 2012; Sun et al., 2016), but some investigators reported that the ischemic injury may induce "autophagic cell death," and inhibition of autophagy can prevent neuron death after ischemic injury (Yu et al., 2004; Rami et al., 2008; Uchiyama et al., 2008; Kanno et al., 2009b). Some *in vivo* studies have also documented that, in the model of cerebral ischemia, autophagy is activated in various cell types—neurons, astrocytes, and vascular endothelial cells, while in the model of spinal cord injury (Kanno et al., 2009a; Fang et al., 2016), autophagesomes mainly accumulate in neurons, microglia, or oligodendrocytes, rather than in astrocytes. Nevertheless, the concrete change in a certain cell type during the process of spinal cord injury has never been reported, and the underlying mechanisms deserve further investigation.

Spinal motor neurons (SMNs), the nerve cells that connect the ventral horn of the spinal cord to directly or indirectly control muscles or glands, act as one of the most important neurons in the spinal cord. Existing studies have demonstrated that SMNs are vulnerable to ischemic injury due to their high demands of energy (Kanno et al., 2009a; Fujita et al., 2015; Fang et al., 2016). The ischemia induces changes in SMNs, which can, in turn, affect the process. Nevertheless, little is known about the dynamic time-course changes and the function of autophagy in SMNs during the process. By optimizing the isolation and culture of SMNs, our laboratory has developed an improved culture system of SMNs, which allows establishing cellular models and performing mechanism studies. Based on this culture system, we also tried some *in vitro* models of SMNs to mimic the metabolic perturbation occurring *in vivo* during the spinal cord ischemic injury, which may include the state of hypoxia, aglycemia, acidosis, oxidative stress, etc. Oxygen-glucose deprivation (OGD), which has been widely utilized to study the cerebral ischemia injury or ischemia/reperfusion injury, is a commonly used model to mimic an ischemic milieu *in vitro* (Fontella et al., 2005; Cimarosti et al., 2012; Wang R. et al., 2012; Tasca et al., 2015). Performing OGD-induced SMNs injury model can well mimic the extracellular condition in spinal ischemia and results in neuronal insult; however, unlike cerebral ischemia injury and ischemia/reperfusion injury, which have been studied by numerous researches, investigations about the spinal neurons are far from enough.

To date, no studies have addressed the time-course changes and the role of autophagy in primary SMNs subjected to OGD conditions. In the current study, by establishing a cellular model of spinal cord ischemia *in vitro*, we intended to investigate the potential involvement of autophagy and its time course in primary SMNs. Furthermore, by treating with the autophagy inhibitor, the role of autophagy during the process was clearly observed.

# MATERIALS AND METHODS

## Reagents and Chemicals

Neurobasal™ medium, B-27™ supplement, HBSS, PBS, and trypsin were purchased from Gibco. Brain-derived neurotrophic factor (BDNF), glial cell-derived neurotrophic factor (GDNF), glutamate, L-glutamine, Dnase, poly-D-lysine (PDL), paraformaldehyde (PFA), and 4′,6-diamidino-2-phenylindole (DAPI) were all obtained from Sigma-Aldrich. RIPA Lysis and Extraction Buffer, as well as Pierce™ BCA Protein Assay Kit were purchased from Thermo Scientific. The protease inhibitor cocktail was from Bimake. Primary antibodies against NGF receptor ($p75^{NTR}$; ab6172), CHAT (ab6168), and β-actin (ab8226) were provided by Abcam. Antibody against SMI 32 (NE1023), Cy3-conjugated sheep anti-rabbit IgG secondary antibody (AC111C), and polyvinylidene difluoride (PVDF) membranes were purchased from EMD Millippore. Primary antibody against light chain 3 (LC3; M152-3) was purchased from MBL International. Primary antibodies against Beclin1 (#3738), SQSTM1/p62 (#5114), as well as horseradish peroxidase (HRP)-linked secondary antibodies (#7074, #7076) were obtained from Cell Signaling Technology. Alexa fluor 488-conjugated donkey anti-mouse IgG secondary antibody (A-21202) was bought from Invitrogen. Clarity™ Western ECL Substrate was obtained from Bio-rad. CCK8 kit were purchased from Dojindo. Bafilomycin A1 (Baf-A1) and 3-Methyladenine (3-MA) were purchased from Selleck Chemicals.

## Isolation and Culture of Primary Spinal Motor Neurons (SMNs)

Pregnant Sprague–Dawley rats were used in the experiments in accordance with internationally accepted standard guidelines for animal use and care, and our study protocol was reviewed and approved by the ethical committee of Guangzhou University of Chinese Medicine. SMNs were prepared from 14- to 16-day embryonic rats as we have reported previously (Chen et al., 2018). Briefly, the spinal cords from embryonic rats were dissected, with vessels and menings gently removed. Then, tissues were washed and cut into small slices and transferred a new dish for trypsinization (0.25% trypsin and 0.4% Dnase) for 20 min at 37°C, followed by adding complete media to inactivate the trypsin, Later, the tissues were gently triturated using Gilson blue pipette tips and a 100-mesh filter to obtain the single-cell suspension. Cells were harvested by centrifugation, re-suspended by Neurobasal™ medium supplemented with 2% B27, and plated on panning dishes, which had been coated with affinity-purified goat anti-mouse IgG in Tris-HCl buffer at 4°C overnight, washed, and then incubated with $p75^{NTR}$ antibody (1–10 μg/ml in PBS). After immunopanning, panning dishes were gently washed to remove those loosely attached cells. Adherent cells (phase bright and quite big under the inverted phase-contrast microscope) were collected by trypsinization and centrifugation, then re-suspended by plating media, whose components were Neurobasal medium supplemented with 2% B27 and 25 μM Glutamate. An aliquot (2 μl) was used for counting before cells were seeded at a proper density ($2 \times 10^4$/ml–$5 \times 10^4$/ml) on Petri dishes or a 96-well plate, which had been pre-treated with PDL (20 μg/ml, for 30 min at room temperature). 24 hours after plating, media was fully replaced by growth media, whose components were Neurobasal medium supplemented with 2% B27, 2 mM of L-Glutamine, 10 ng/ml of BDNF, and 10 ng/ml of GDNF. Neurons were maintained at 37°C in a humidified 5% $CO_2$ incubator, and half volume of the medium was changed with fresh media every 3 days. Experiments were performed after day *in vitro* (DIV) 7–14.

## Oxygen-Glucose Deprivation (OGD) Exposure of SMNs

OGD has been utilized as a simulation model of hypoxic insult *in vitro*. OGD experiments were performed between DIV 7 and DIV 14, at which time SMNs represented at least 95% of the population as assessed by SMN marker and DAPI staining. To initiate OGD, the cultured primary SMNs were rinsed with HBSS and then incubated with Earle's balanced salt solution (EBSS), whose components were (in mg/L): 6,800 NaCl, 400 KCl, 200 $CaCl_2$, 200 $MgSO_4$–$7H_2O$, 140 $NaH_2PO_4$–$H_2O$, 2,200 $NaHCO_3$, pH 7.4, and placed in a tri-gas incubator (Thermo Fisher Scientific), which was set at 5% $O_2$ and 5% $CO_2$ at 37°C for certain hours to mimic ischemic insult. The experimental schedule is shown in **Figure 1**. Control cells were cultured in normal culture medium (Neurobasal medium supplemented with 2% B27 and 2 mM L-Glutamine) and placed in the regular incubator (95% air and 5% $CO_2$ at 37°C).

## Quantification of Cell Viability With CCK8 Assay

Cell viability of cultured SMNs was tested with a nonradioactive cell counting kit (CCK8) following the manufacturer's instructions. In brief, the primary SMNs were seeded on 96-well plates at a density of $2.5 \times 10^3$ per well. After cells were subjected to OGD for 0.5, 1, 2, 3, 5, and 7 h, 10 μl of CCK8 was added to each well, and the mixture was incubated for 4 h at 37°C. Then, absorbance was determined at 450 nm by a microplate reader. Results were expressed as the percentage of CCK8 reduction, and the absorbance of control cells was set at 100%.

## Immunofluorescence Assay

Isolated SMNs were plated on confocal dishes for immunofluorescence assay. Cells were washed with ice-cold PBS, fixed with 4% paraformaldehyde solution for 15 min at room temperature, permeabilized by 0.2% Triton X-100 (in PBS, pH 7.4) and further blocked in 5% goat serum for 1 h at room temperature. Cells were then incubated with appropriate primary

antibodies at 4°C overnight. For double immunofluorescence, different primary antibodies from different species were simultaneously incubated. For the identification of SMNs, mouse anti-SMI 32 (1:500) and/or rabbit anti-CHAT (1:500) were used. While for the identification of autophagic marker, mouse anti-LC3 (1:500) was used. After being washed, cells were incubated with Alexa fluor 488-conjugated donkey anti-mouse IgG (1:1,000) or/and Cy3 conjugated sheep anti-rabbit secondary antibody (1:1,000) for 1 h in dark. For nuclear counterstaining, DAPI was used. Labeled cells were identified using Olympus FX-70 fluorescence microscope or Zeiss LSM 510 META laser scanning confocal microscope, and digital images were recorded by Adobe Photoshop software and Zeiss LSM Image Examiner software.

## Protein Isolation, Quantification, and Western Blot Analysis

Isolated SMNs were plated on Petri dishes for Western blot analysis. After OGD treatment, cells were harvested and lysed in ice-cold RIPA lysis buffer with protease inhibitor cocktail. Protein concentrations were detected using BCA protein assay kit, and proteins in each group were adjusted to the same concentrations. Equivalent amounts of protein were loaded and electrophoretically on 12% or 15% sodium dodecyl sulfate polyacrylamide gel electrophoresis (SDS-PAGE), and blotted onto PVDF membranes. Then, the nonspecific binding was blocked by incubating membranes in 5% skimmed milk (in TBS containing 0.05% Tween 20) for 1 h. The membranes were incubated with primary antibodies diluted in TBST as follows: mouse anti-LC3 (1:1,000), rabbit anti-Beclin1 (1:1,000), rabbit anti-SQSTM1/p62 (1:1,000), and mouse anti-β-actin (1:3,000) overnight at 4°C. The next day, membranes were washed three times with TBST for 5 min each wash, followed by incubating with anti-mouse IgG HRP-linked antibody (1:2,000) or anti-rabbit IgG HRP-linked antibody (1:2,000) for 1 h at room temperature. Immunoreactivity was detected with Clarity™ Western ECL Substrate, and reacting bands were captured by Bio-rad ChemiDoc™ XRS+ system, and analyzed for final determination of protein expression with Image Lab and normalized by β-actin as internal controls.

## Electron Microscopy

The neurons were harvested and fixed in 2.5% glutaraldehyde in 0.1 M phosphate buffer (pH 7.4) for 8 h, followed by treatment with 1% osmium tetroxide for an additional 1 h, and dehydrated by gradient ethanol and acetone. Samples were immersed in resin, hardened, and sectioned (50–70 nm). Later, the ultrathin sections were stained with lead citrate and uranyl acetate and observed by electron microscopy (Zeiss EM910).

## Statistical Analysis

All experiments were performed at least three times independently. Statistical analysis of all data was performed using SPSS 22.0 and GraphPad Prism 7. Results were presented as mean ± standard deviation (SD). Statistical comparisons between two groups were determined using unpaired Student's *t*-test. Differences among groups were evaluated with one-way analysis of variance (ANOVA) followed by Tukey's or Dunnett's *post hoc* test when appropriate, or two-way ANOVA followed by

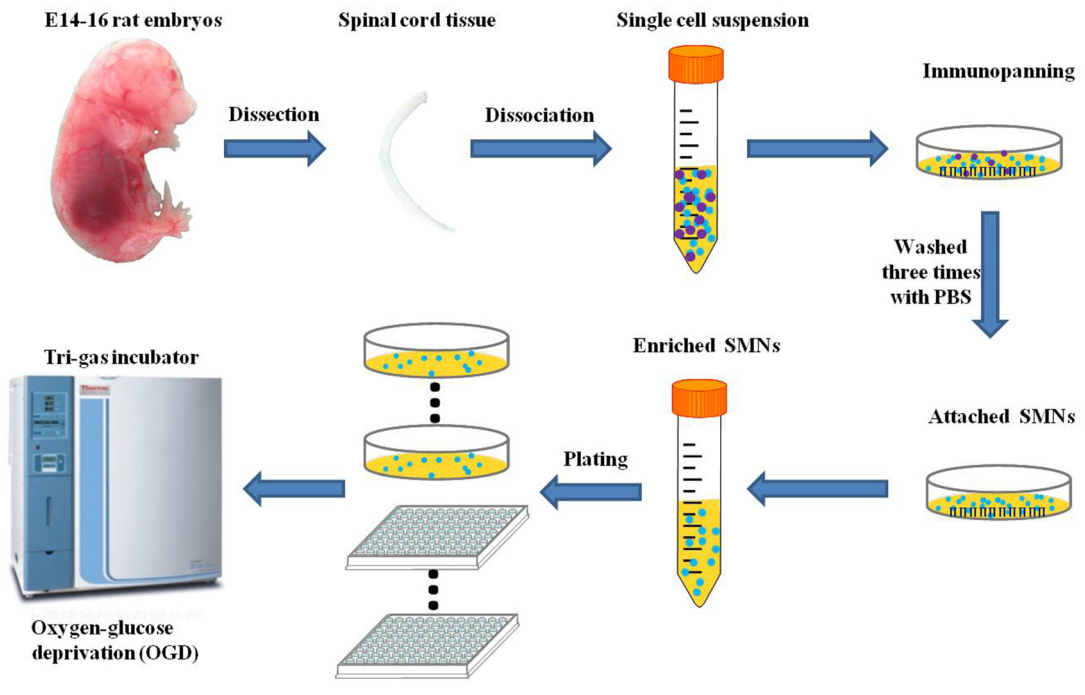


**FIGURE 1** | Schematic diagram of the isolation and purification of primary spinal motor neurons (SMNs) and oxygen-glucose deprivation (OGD) modeling process.

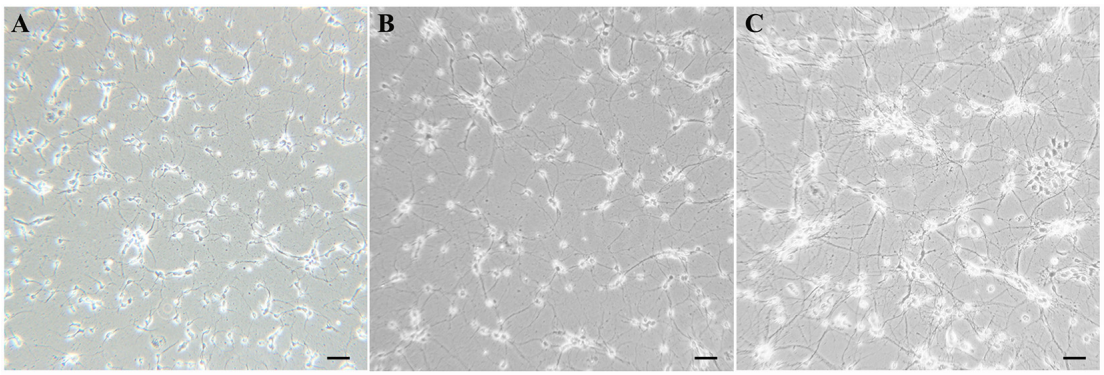


**FIGURE 2 |** Visual characterization of cultured primary SMNs. **(A)** Morphology of cultured cells after plating for 2 days. **(B)** SMNs developed large cell bodies with long neurites. **(C)** Mature SMNs formed vastly interconnected neurite networks.

Sidak's multiple comparisons test. A difference was considered statistically significant when $p < 0.05$.

# RESULTS

## Characterization, Identification, and Purity of Primary SMNs

Within 24 h after plating, most cells were adherent to the bottom, and some even grew tiny neurites, but all cells were solitary. After the first media replacement (24 h) to remove the floating cells and change some media components, larger cells appeared, cell outgrowths grew longer and formed multiple branches. After 7 days in culture, cells grew mature with plump soma and high refraction, and formed interconnected neural networks diffusely (**Figure 2**).

In order to identify motor neurons in the culture system, SMI-32 and CHAT antibodies were both used. As shown in **Figure 3**, the SMI-32 and CHAT stainings showed cell bodies, dendrites, and large axons. On the 10th day, as signs for maturation and high differentiation, the cultured SMNs developed large cell bodies with long neurites, which formed interconnected neurite networks and showed prominent arborization. The purity of SMNs was calculated by motor neuron marker (CHAT and SMI-32) immunofluorescence and DAPI staining. The results showed that the proportion of SMNs reached over 95%, which can meet the requirements of subsequent experiments.

## Morphological Changes of Primary SMNs Under OGD at Different Time Points

OGD-induced SMN injury acts as a model to mimic spinal cord ischemia injury *in vitro* and results in neuronal insult. In this experiment, primary SMNs were cultured under OGD condition for 1, 2, 3, 5, 7, and 24 h, with motor neurons cultured in normal media and normoxia serving as control. As shown in **Figures 4A–F**, it seems that cells showed no obvious morphological changes within 1 h; however, most SMNs exhibited atrophic cyton and disrupted neurofilament after 3 h, and the injury continued to aggravate as time prolonged, with apparent impaired neural networks after 7 h and even massive cell loss for 24 h.

## Cell Viability Is Reduced Under OGD in a Time-Dependent Manner

We assessed the survival rate of SMNs after OGD insult. It was reduced under OGD in a time-dependent manner. According to **Figure 4G**, the cell viability declined sharply when cells were initially subjected to OGD (1 h), with significant changes every half an hour (control vs. 0.5 h, 0.5 vs. 1 h), but later declined relative slowly within 3 h (without significant change 1 vs. 2 h, and 2 vs. 3 h). Until 5 h upon OGD stress, viability declined markedly compared with 3 h. As time prolonged, cell viability declined more slowly, reaching a nearly 50% viability decrease in 7 h, but with no significant difference with 5 h.

## OGD Treatment Enhances Autophagy in Primary SMNs, and Autophagy Reaches a Peak at 5 h

To determine whether autophagy was involved in SMNs under OGD conditions, we first examined the classical autophagy makers by Western blot assays. The microtubule-associated protein LC3, a mammalian homol of the yeast ATG8 gene (Aut7/Apg8), serves as the markers for autophagy. As shown in **Figure 5**, the bands showed the time course of autophagy induction under OGD, and the ratio of LC3-II/LC3-I was seen as a dramatic increase in SMNs after OGD for 3 h and reached a peak at 5 h. Immunofluorescence assay revealed strong and punctate LC3 staining in the OGD group (**Figure 6**), whose trends were consistent with that of Western blot analysis. Intriguingly, we can also observe that strong, punctate LC3 appeared much more in soma than in axons.

P62, also called sequestosome 1 (SQSTM1), is the selective cargo receptor for autophagy to degenerate misfolded proteins and serves as the marker for autophagic degradation. We detected the expression of SQSTM1/p62 and found that its level was diminished significantly after OGD for 3 h, which corresponded to the results of LC3. Additionally, Beclin1, the mammalian homolog of the yeast Agt6, forms a protein complex with class III phosphatidyl inositol-3 kinase within the

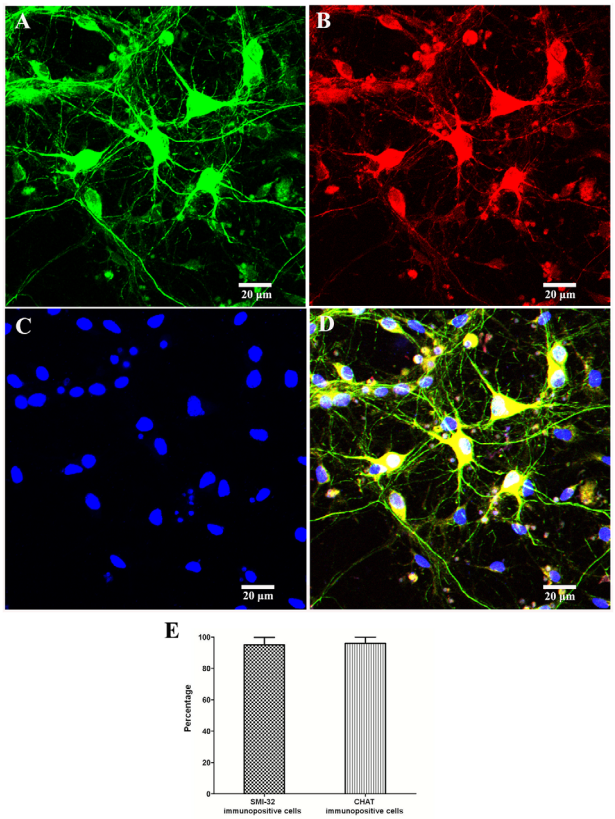


**FIGURE 3 |** Identification and purity of SMNs by immunofluorescence with motor neuron-specific markers against SMI-32 and CHAT. The immunofluorescence assay of motor neuron marker SMI-32 (green, **A**) and CHAT (red, **B**) showed cell bodies, dendrites, and large axons, with 4′,6-diamidino-2-phenylindole (DAPI) staining (blue, **C**) showing the nuclei. **(D)** Merged image. **(E)** The percentage of SMI-32 or CHAT-immuopositive cells were calculated. Data were presented as mean ± SD ($n$ = 5 independent experiments). At least 10 random fields from one sample were averaged in each independent experiment. Scale bars represent 20 μm.

autophagosome. Results showed that Beclin 1 expression was upregulated markedly and continually after OGD within 7 h.

## OGD Treatment Induces Autophagic Flux in Primary SMNs

Given that autophagy was involved in primary SMNs upon OGD stress, we next decided to confirm that the enhancement of autophagy markers during the process was due to induction of autophagy or blockage of autophagosome maturation. For this purpose, lysosome inhibitor Bafilomycin A1 (Baf-A1) needs to be added in the culture medium to assess the responses of SMNs, which is a classical approach to observing the real state of autophagic flux. Baf A1 is a late-phase autophagy inhibitor, which acts by inhibiting vacuolar H + ATPase (V-ATPase) and thus prevents the maturation of autophagic vacuole fusion between autophagosomes and lysosomes (Gómez-Sánchez et al., 2015; Klionsky et al., 2016). Results in **Figure 7** demonstrated that, in the presence of Baf-A1, LC3 II increased and accumulated, LC3-II/LC3-I displayed a much higher level

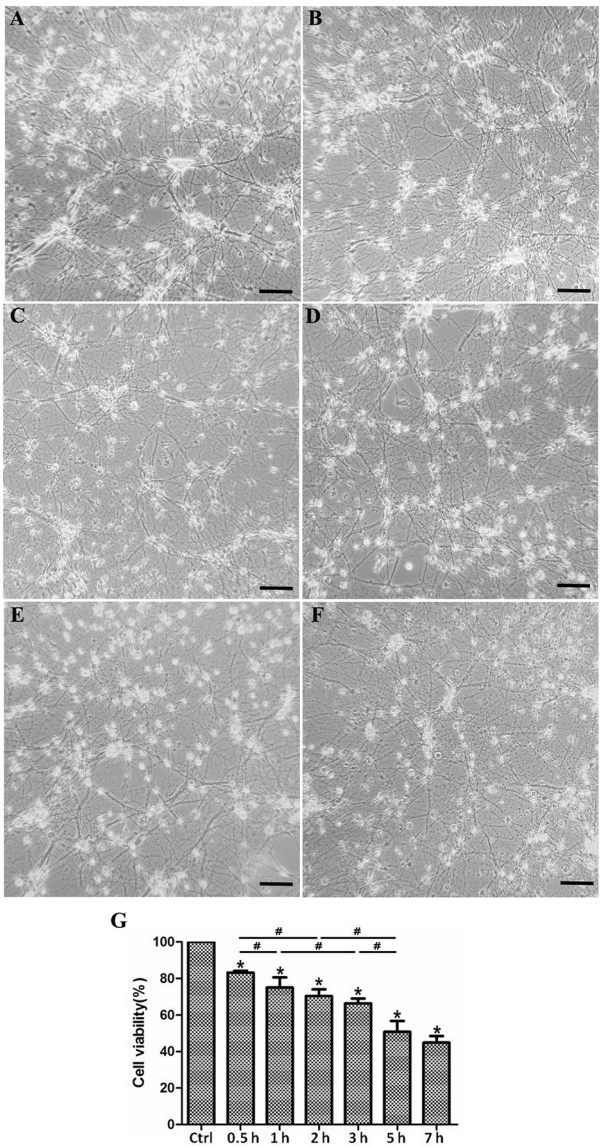


**FIGURE 4 |** Morphological changes and cell viability of cultured SMNs under OGD for different time. Primary SMNs were cultured normally **(A)** or subjected to OGD for various periods of time (**B**: 1 h, **C**: 3 h, **D**: 5 h, **E**: 7 h, or **F**: 24 h, respectively), and the representative phase photomicrographs showed the morphologic changes (×250). **(A–F)** OGD resulted in destruction of neural networks, and the severity increased with the prolonging of OGD time. **(G)** Cell viability was reduced under OGD in a time-dependent manner. The cell viability was assessed using the CCK8 kit, and results were expressed as the percentage of CCK8 reduction. The absorbance of control cells was set at 100%. Data were presented as mean ± SD ($n$ = 5 independent experiments). Statistical comparisons were carried out with one-way analysis of variance (ANOVA). $^{*}p < 0.05$ compared with control group. $^{\#}p < 0.05$ between groups.

when SMNs were treated with OGD plus Baf-A1 than OGD alone. This indicated that the increase in LC3-II levels by OGD was because of an increase in production rather than the decreased recycling of autophagy.

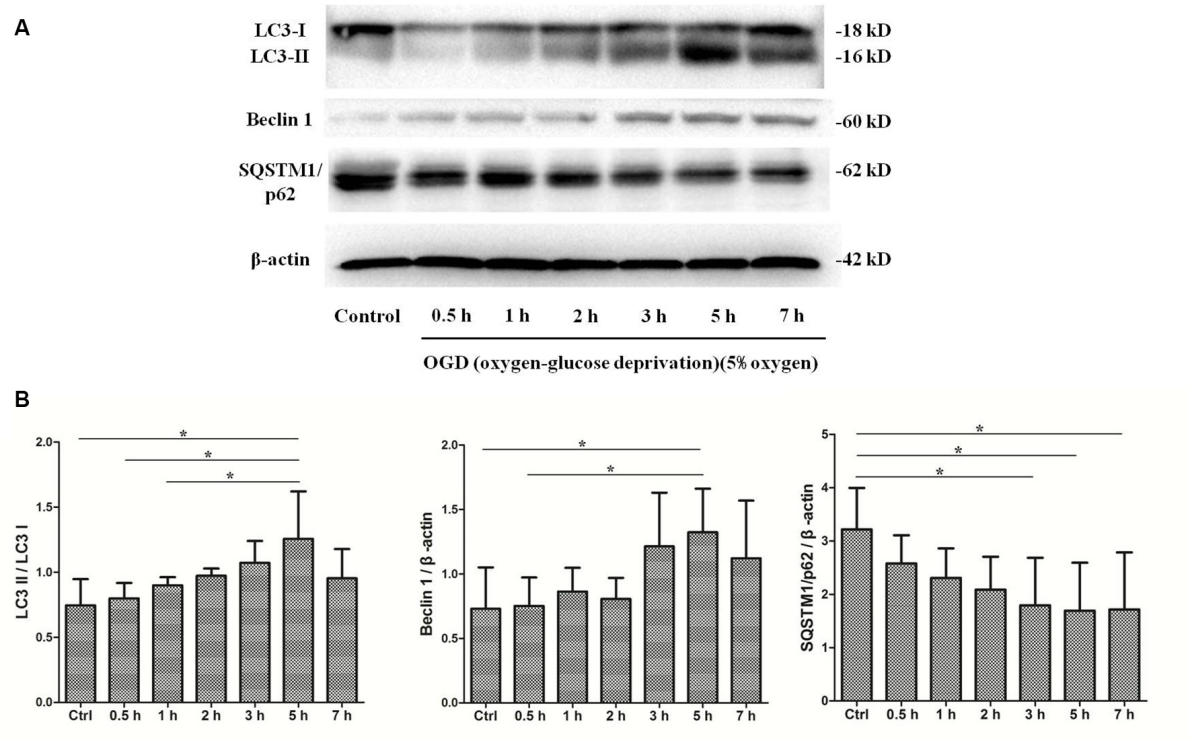


**FIGURE 5 |** OGD treatment induces autophagy activation. SMNs were exposed to OGD for and indicated time, and the expression of light chain 3 (LC3) I, LC3 II, Beclin1, and SQSTM1/p62 were detected by Western blot **(A)**. **(B)** The quantitative results are shown after normalizing with β-actin as an internal control. Data were presented as mean ± SD ($n$ = 3 independent experiments). Statistical comparisons were carried out with one-way ANOVA. *$p < 0.05$.

## Results of Transmission Electron Microscopy

The transmission electron microscopy (TEM) acts as one of the most important methods for monitoring autophagy (Swanlund et al., 2010). Autophagy was first detected by TEM in the 1950s, and it was originally observed as a focal degradation of cytoplasmic areas performed by lysosomes, which still remains the hallmarks of this process. Up until now, TEM is still the only tool that reveals the morphology of autophagic structures at a resolution in the nm range and shows the cellular substructure during the process, which allows the exact identification (Martinet et al., 2014). Therefore, we used TEM to examine the ultrastructural changes of SMNs subjected to OGD insult. In order to identify the typical differences, we chose the control cells and SMNs after 5 h of OGD. As shown in **Figure 8**, control cells contained normal-looking organelles, nucleus, and chromatin. The mitochondria had a dense matrix, neatly aligned cristae, and no signs of autophagy were observed. While after OGD insults, SMNs were found to contain many vesicles with typical morphological features of autophagosomes (AP). A number of double or multi-membrane structures, which engulfed cytoplasm fractions and organelles, can be observed in the cytoplasm. When autophagosomes fused with lysosomes, the inner membranes disappeared, and autophagosomes turned to be single-membrane autophagic vacuoles. The mitochondria displayed swelling with partially broken or dilated cristae. The TEM strongly once again suggested that overactivation of autophagy was triggered in primary SMNs subjected to OGD.

## Inhibition of Autophagy Exacerbates the Injury of Primary SMNs Exposed to OGD

In order to clarify the effects of autophagy in OGD-induced neuron injury, primary cultured SMNs were treated with autophagy inhibitor 3-MA, whose dosage has been selected to avoid cytotoxity (**Figure 9A**), and its corresponding inhibition effect was confirmed by Western blot (**Figure 9B**), followed by OGD for an indicated time, and then the cell viability was measured.

3-MA, a well-established inhibitor of autophagy, relatively selectively inhibits the class III phosphatidylinositol kinase (Wu et al., 2010), whose activity is required for autophagosome formation. It has been generally accepted and widely used as an inhibitor of autophagy. Our data showed that the cell viability was even decreased by 3-MA treatment (**Figure 9C**), indicating that inhibition of autophagy exacerbates the injury of primary SMNs exposed to OGD.

# DISCUSSION

In the current study, we identified the dynamic time-course changes and role of autophagy in primary SMNs subjected to OGD. To the best of our knowledge, this report is among the

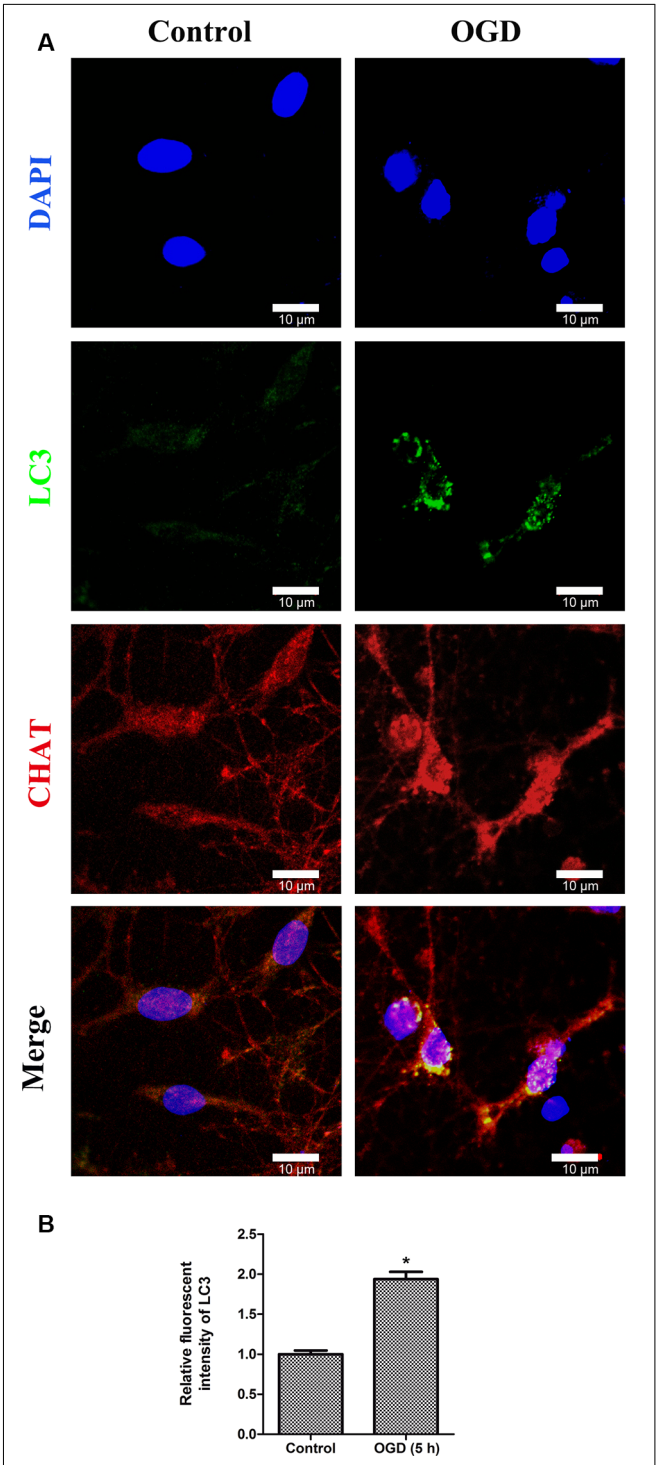


**FIGURE 6 |** Double immunofluorescence stainings show the LC3-positive puncta in primary SMNs under OGD. **(A)** Representative fluorescent confocal images of cells counterstained with DAPI (blue, nuclei), autophagy-specific marker—LC3 (green) as well as motor neuron marker—CHAT (red) are shown ($n$ = 3 independent experiments). Strong, punctate LC3 staining can be observed in primary SMNs under OGD. Scale bar presents 10 μm. **(B)** The relative fluorescent intensity of LC3 was analyzed using ImageJ. Data were presented as mean ± SD ($n$ = 3 independent experiments). Statistical comparisons were carried out with unpaired Student's $t$-test. $^{*}p < 0.05$.

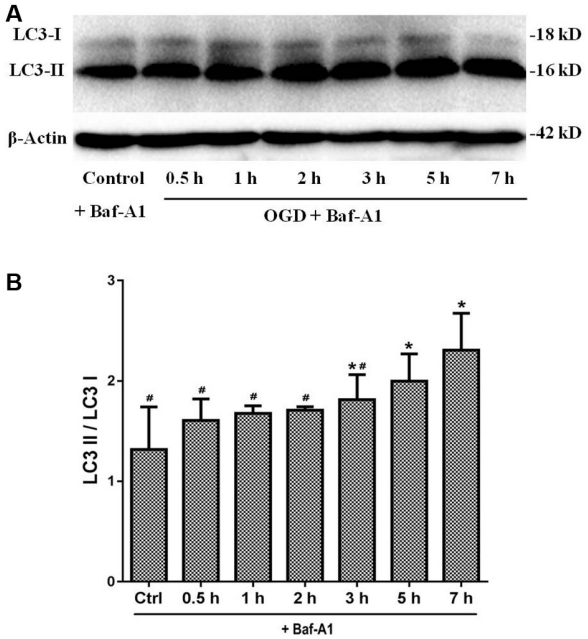


**FIGURE 7 |** LC3 expression under OGD with Baf-A1 to observe the real state of autophagic flux. **(A)** The expression of LC3 I and LC3 II were detected by Western blot. In the presence of Baf-A1, LC3 II dramatically increased and accumulated. **(B)** The quantitative results are shown in the bar chart. Data were presented as mean ± SD ($n$ = 3 independent experiments). Statistical comparisons were carried out with one-way ANOVA. $^{*}p < 0.05$ compared with the control group. $^{\#}p < 0.05$ compared with the 7-h group.

first to clarify the autophagic expression changes in a primary cell model of spinal cord ischemia.

Primary cultures facilitate the limitation of similar *in situ* counterpart morphology and physiology. However, due to the low yields of motor neuron cultures from spinal cord before, hybrid cell lines of motor neurons (NSC 34 and VSC 4.1) have long been utilized and tacitly regarded as the most stable motor neuron cell line to mimic the pathophysiology of motor neuron disorders (Mosier et al., 1995; Eggett et al., 2000; Samantaray et al., 2006; Maier et al., 2013; Perera et al., 2018). Whereas, with the deepening and development of research, it has been found that there are obvious differences between the hybrid cell lines and primary cells, including the susceptibility of glutamate-induced death and calcium influx (Madji Hounoum et al., 2016). Hence, more and more scholars suggest that primary cells are more suitable as experimental models.

The isolation and culture of primary SMNs had been reported and described well (Schaffner et al., 1987; Martinou et al., 1989; Camu and Henderson, 1992, 1994; Graber and Harris, 2013); however, scarcely rapid and easy protocols have been achieved, let alone cellular models of SMNs. Previous literature mainly focuses on the possibility of successful isolation and culture of SMNs, by density gradient centrifugation, fluorescence-activated cell sorting or immunopanning, or a combination of these methods. Their results are inspiring, but the processes are often complicated, time-consuming, and hard to obtain sufficient quantities of SMNs once, which make it impossible

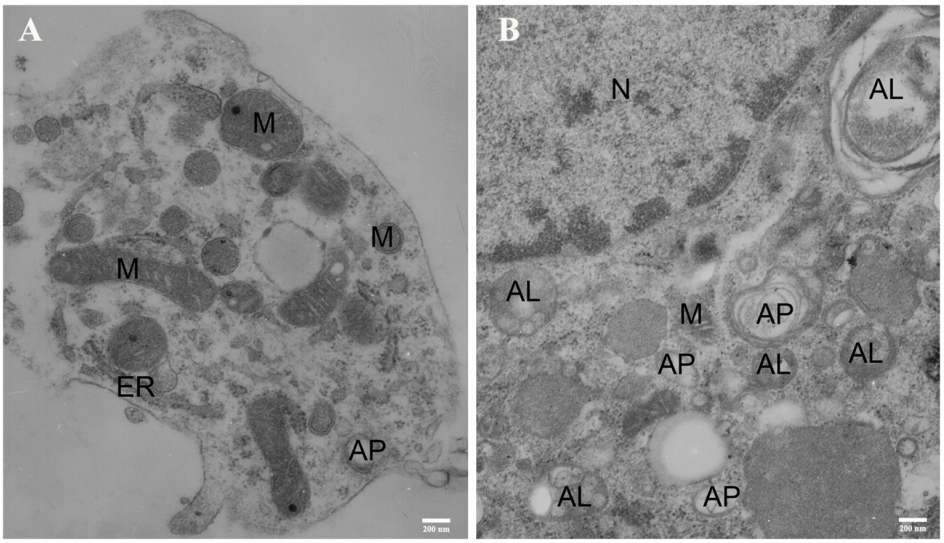


**FIGURE 8 |** Representative electron micrographs (EM) of primary SMNs in the control **(A)** and OGD group **(B)**. The ultrastructural changes in primary SMNs after OGD injury are shown, and distinct autophagic structures are marked: autophagosome (AP), autolysosome (AL), mitochondria (M), endoplasmic reticulum (ER), cell nucleus (N). **(A)** The neuronal soma was plump and showed a normal morphology, with intact nuclear and plasma membranes. In addition, the mitochondria had a dense matrix and neatly aligned cristae, and no signs of autophagy were observed. **(B)** After OGD insults, crescent-shaped or goblet-like phagophores with double- or multiple-layer membrane structures and formation of autophagosomes can be observed, and autophagic vacuoles fused with lysosomes to form autolysosomes with single-layer membrane structures can also be seen. Images shown are representative examples from three independent experiments. Scale bars presents 200 nm.

to perform protein or RNA profiling systematically. Rapid and easy protocols facilitate mechanism studies or drug screens by performing downstream analyses (protein or RNA profiling), which require enough quantities of motor neurons *in vitro*. Therefore, we developed rapid, efficient, and reproducible procedures for the dissection of spinal cords and harvest of SMNs with high survival and purity (Chen et al., 2018), and develop cellular models of SMNs, which allow performing mechanism studies or drug screens.

Autophagy is an indispensable catabolic process in cell survival, differentiation, development, and homeostasis (Levine and Kroemer, 2008; Mizushima and Komatsu, 2011). The dual role of autophagy varies, either to protect cells through adaptive regulation or induce "autophagic cell death." Accumulating studies have confirmed that autophagy activation is involved in the central nervous system injury and some neurodegenerative diseases (Tan et al., 2014; Martinez-Vicente, 2015; Guo et al., 2018), yet researches on autophagy in spinal cord injury are far from enough. Meanwhile, it is still debatable whether autophagy exerts a protective or destructive role in spinal cord injury. For instance, there are studies documenting that autophagy plays a protective role in spinal ischemia *via* sustaining autophagy (Fan et al., 2014). However, transient spinal cord ischemia can induce autophagy in motor neurons, which may result in neuronal death (Baba et al., 2009; Fujita et al., 2015). Meanwhile, even some research provided evidence that autophagy exerts opposing impact on early and later stages after spinal I/R injury: early activated autophagy alleviates spinal cord I/R injury by inhibiting apoptosis and inflammation, while later, excessively enhanced autophagy aggravates the injury (Fang et al., 2016). Nonetheless, the abovementioned researches are mainly *in vivo* studies, which did not show the concrete change of a certain cell type during the process of spinal cord ischemia injury, which we have tried to investigate in our studies.

Lack or deprivation of energy, such as oxygen or glucose, may lead to low physiological function, abnormal metabolism, and even cell death. In our experiment, the cell viability was reduced under OGD (**Figure 4**). According to the cell viability curve (**Figure 4G**), we clearly found that the cell viability declined sharply when cells were initially subjected to OGD, but later declined relatively slowly. Correspondingly, we detected the autophagic expression changes during the process (**Figure 5**). Concomitant with the rate of viability changes, it was interesting to find that autophagy was upregulated and kept increasing in the first few hours, reaching a peak at 5 h, suggesting that cells started to maintain the balance of internal environment after receiving adverse stimulus. However, since the OGD insult existed persistently, the cell viability continued to decline. Morphologically (**Figures 4A–F**), the SMNs showed slight injury in the first few hours and apparent impaired neural networks after 7 h, indicating that the normal physiological functions were unable to be maintained after stimulated by persistent adverse factors.

The microtubule-associated protein LC3, a mammalian homolog of the yeast ATG8 gene (Aut7/Apg8), takes an important part in the formation of autophagic vacuoles (Klionsky et al., 2016). The cytoplasmic form LC3 (LC3-I) is distributed throughout the cytoplasm diffusely and uniformly, but during autophagy activation, it will be conjugated to phosphatidylethanolamine to form

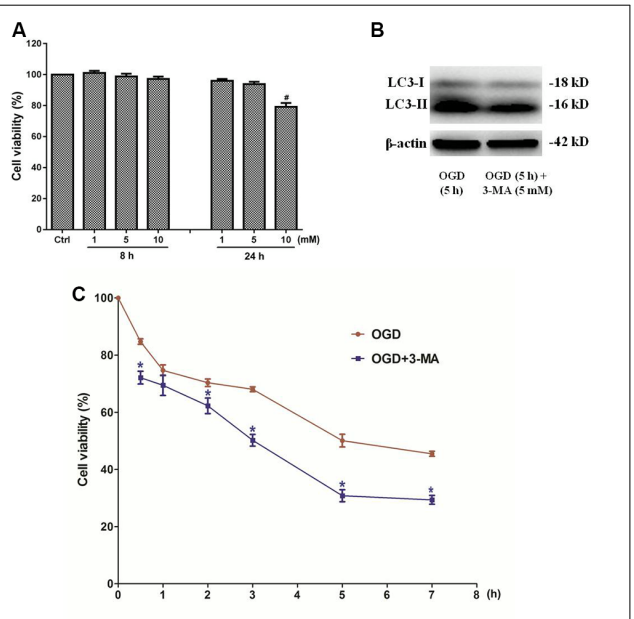


**FIGURE 9 |** Inhibition of autophagy by 3-methyladenine (3-MA) exacerbates the injury of primary SMNs exposed to OGD. **(A)** Primary SMNs in normal conditions were treated with different dosages of 3-MA to select its safe dosage. **(B)** The autophagy inhibition effect of 5 mM 3-MA was confirmed by Western blot. To test it simple and clear, SMNs were subjected to OGD for 5 h in the presence or absence of 3-MA, and their expressions of LC3 I and LC3 II were detected. Results indicated that this dosage can significantly block autophagy in SMNs under OGD conditions. **(C)** The dosage 5 mM was applied in all the time points, and the cell viability of primary SMNs with or without 3-MA was assessed at different time points using the CCK8 kit. Results were expressed as the percentage of CCK8 reduction, and the absorbance of the control cells was set at 100%. Data were presented as mean ± SD ($n$ = 5 independent experiments). Statistical comparisons were carried out with one-way ANOVA **(A)** or two-way ANOVA **(C)**. $^{\#}p < 0.05$ compared with the control group. $^{*}p < 0.05$ compared with cell viability in the same time point under OGD conditions.

LC3–phosphatidylethanolamine conjugate (LC3-II) and recruited to autophagosomal membranes (Mizushima and Yoshimori, 2007). When associated with autophagosomes, LC3 exhibits a typically apparent mobility in electrophoresis, changing from 18 kD to 16 kD and indicated as "LC3 puncta processing," which is commonly referred to as LC3-II. Autophagosomes fuse with lysosomes to form autolysosomes, and intra-autophagosomal components are degraded by lysosomal hydrolases. At the same time, LC3-II in autolysosomal lumen is degraded. Therefore, lysosomal turnover of the autophagosomal marker LC3-II can reflect the autophagic activity to some extent, and detecting LC3 by immunoblotting and immunofluorescence have become reliable methods for monitoring autophagy and autophagy-related processes. The level of autophagy can be assessed by the ratio of LC3-II/I by immunoblotting and positive puncta of LC3 by immunofluorescence. In our study, the Western blot analysis revealed a significantly increase in LC3 level (**Figure 5**), which was further corroborated by immunofluorescence assays (**Figure 6**) and TEM (**Figure 8**). Meanwhile, the marker of autophagic degradation (SQSTM1/p62) diminished significantly after OGD for 3 h, and Beclin 1 expression was upregulated markedly and continually after OGD within 7 h (**Figure 5**).

Besides the fact that immunofluorescence assays confirmed the induction of autophagy during OGD, intriguingly, from the immunofluorescence images, strong LC3 puncta were assembly visualized in soma rather than in axons (**Figure 6**). Previous studies have demonstrated that retrograde transportation along axons back toward the neuronal cell bodies are critical during the autophagic process of neurons (Maday et al., 2012; Maday and Holzbaur, 2014; Zheng et al., 2019). It has already been proven that the process of retrograde transport along axons back toward the neuronal soma occurs in hippocampal, DRG, and cortical neurons (Lee et al., 2011; Maday et al., 2012; Maday and Holzbaur, 2014; Zheng et al., 2019). Our findings may provide some support for this theory in SMNs.

Detecting LC3 by immunoblotting and immunofluorescence are the basic ways to monitor autophagy and autophagy-related processes; however, these results can hardly represent the real state of autophagic flux since autophagy is a dynamic process with multiple steps. In this regard, lysosome inhibitor Baf-A1 was added to the culture medium to assess the responses of SMNs, which is a classical approach in observing the real state of autophagic flux. Actually, up until now, besides the lysosomal or vacuolar degradation inhibitor present or not in Western blot analysis, an alternative way to detect the autophagic flux is to measure the GFP–LC3 fusion protein with the aid of the GFP–LC3 expressing plasmid. In our experiment, we have tried both of the methods, but limited to the low transfection efficiency of GFP–LC3 expressing plasmid in primary SMNs, we only showed the results of autophagic flux detection by adding Baf-A1. In the presence of Baf-A1, LC3 II increased and accumulated (**Figure 7**), which indicated the increase in LC3-II levels by OGD owing to an increase in production rather than the decreased recycling of autophagy.

Later, in order to evaluate the role of autophagy, the autophagy inhibitor 3-MA was added in the culture system. It showed that blockade of autophagy activation by 3-MA aggravated cell injury, presenting worse cell viability.

## CONCLUSION

Taken together, by successfully establishing a primary cellular model of spinal cord ischemia *in vitro*, the dynamic time-course changes of autophagy and autophagy flux in SMNs was clearly investigated. Autophagy was upregulated in primary SMNs subjected to OGD, and autophagy reached a peak at 5 h. Besides, inhibition of autophagy exacerbated the injury of primary SMNs exposed to OGD, suggesting that autophagy plays a protective role during the process. Further studies need to explore the possible pathway and mechanisms underlying the effects of autophagy overactivation.

## DATA AVAILABILITY STATEMENT

The datasets generated for this study are available on request to the corresponding author.

## ETHICS STATEMENT

The animal study was reviewed and approved by the Ethical Committee of Guangzhou University of Chinese Medicine.

## AUTHOR CONTRIBUTIONS

SC and DLi conceived and designed the experiments. SC, RT, DLu, and ZX performed the experiments, analyzed the data, and wrote the manuscript. HL and DLi revised the manuscript. All authors have read and approved the manuscript for publication.

## FUNDING

This research was funded by the National Natural Science Foundation of China (Nos. 81704095 and 81673992), Administration of Traditional Chinese Medicine of Guangdong Province (No. 20173022), and Science and Technology Project of Guangdong Province (No. 2016A020226008).

## REFERENCES

Aslan, A., Cemek, M., Buyukokuroglu, M. E., Altunbas, K., Bas, O., Yurumez, Y., et al. (2009). Dantrolene can reduce secondary damage after spinal cord injury. *Eur. Spine J.* 18, 1442–1451. doi: 10.1007/s00586-009-1033-6

Baba, H., Sakurai, M., Abe, K., and Tominaga, R. (2009). Autophagy-mediated stress response in motor neuron after transient ischemia in rabbits. *J. Vasc. Surg.* 50, 381–387. doi: 10.1016/j.jvs.2009.03.042

Camu, W., and Henderson, C. E. (1992). Purification of embryonic rat motoneurons by panning on a monoclonal antibody to the low-affinity NGF receptor. *J. Neurosci. Methods* 44, 59–70. doi: 10.1016/0165-0270(92)90114-s

Camu, W., and Henderson, C. E. (1994). Rapid purification of embryonic rat motoneurons: an *in vitro* model for studying MND/ALS pathogenesis. *J. Neurol. Sci.* 124, 73–74. doi: 10.1016/0022-510x(94)90185-6

Chen, S., Tian, R., Li, H., Chen, M., Zhang, H., and Lin, D. (2018). Optimized methods for rapidly dissecting spinal cords and harvesting spinal motor neurons with high survival and purity from rats at different embryonic stages. *J. Spinal Cord Med.* 41, 281–291. doi: 10.1080/10790268.2017.1329075

Ciechanover, A., Orian, A., and Schwartz, A. L. (2000). Ubiquitin-mediated proteolysis: biological regulation *via* destruction. *Bioessays* 22, 442–451. doi: 10.1002/(sici)1521-1878(200005)22:5<442::aid-bies6>3.0.co;2-q

Cimarosti, H., Ashikaga, E., Jaafari, N., Dearden, L., Rubin, P., Wilkinson, K. A., et al. (2012). Enhanced SUMOylation and SENP-1 protein levels following oxygen and glucose deprivation in neurones. *J. Cereb. Blood Flow Metab.* 32, 17–22. doi: 10.1038/jcbfm.2011.146

Coselli, J. S., LeMaire, S. A., de Figueiredo, L. P., and Kirby, R. P. (1997). Paraplegia after thoracoabdominal aortic aneurysm repair: is dissection a risk factor? *Ann. Thorac. Surg.* 63, 28–35; discussion 35–26. doi: 10.1016/s0003-4975(96)01029-6

De Duve, C. (1963). The lysosome. *Sci. Am.* 208, 64–72. doi: 10.1038/scientificamerican0563-64

Drinkwater, S. L., Goebells, A., Haydar, A., Bourke, P., Brown, L., Hamady, M., et al. (2010). The incidence of spinal cord ischaemia following thoracic and thoracoabdominal aortic endovascular intervention. *Eur. J. Vasc. Endovasc. Surg.* 40, 729–735. doi: 10.1016/j.ejvs.2010.08.013

Eggett, C. J., Crosier, S., Manning, P., Cookson, M. R., Menzies, F. M., McNeil, C. J., et al. (2000). Development and characterisation of a glutamate-sensitive motor neurone cell line. *J. Neurochem.* 74, 1895–1902. doi: 10.1046/j.1471-4159.2000.0741895.x

Esposito, E., Paterniti, I., Meli, R., Bramanti, P., and Cuzzocrea, S. (2012). GW0742, a high-affinity PPAR-delta agonist, mediates protection in an organotypic model of spinal cord damage. *Spine* 37, E73–E78. doi: 10.1097/brs.0b013e3182276d88

Etz, D. C., Luehr, M., Aspern, K. V., Misfeld, M., Gudehus, S., Ender, J., et al. (2014). Spinal cord ischemia in open and endovascular thoracoabdominal aortic aneurysm repair: new concepts. *J. Cardiovasc. Surg.* 55, 159–168.

Etz, C. D., Luehr, M., Kari, F. A., Bodian, C. A., Smego, D., Plestis, K. A., et al. (2008). Paraplegia after extensive thoracic and thoracoabdominal aortic aneurysm repair: does critical spinal cord ischemia occur postoperatively? *J. Thorac. Cardiovasc. Surg.* 135, 324–330. doi: 10.1016/j.jtcvs.2007.11.002

Fan, J., Zhang, Z., Chao, X., Gu, J., Cai, W., Zhou, W., et al. (2014). Ischemic preconditioning enhances autophagy but suppresses autophagic cell death in rat spinal neurons following ischemia-reperfusion. *Brain Res.* 1562, 76–86. doi: 10.1016/j.brainres.2014.03.019

Fang, B., Li, X. Q., Bao, N. R., Tan, W. F., Chen, F. S., Pi, X. L., et al. (2016). Role of autophagy in the bimodal stage after spinal cord ischemia reperfusion injury in rats. *Neuroscience* 328, 107–116. doi: 10.1016/j.neuroscience.2016.04.019

Feng, Y., He, D., Yao, Z., and Klionsky, D. J. (2014). The machinery of macroautophagy. *Cell Res.* 24, 24–41. doi: 10.1038/cr.2013.168

Fontella, F. U., Cimarosti, H., Crema, L. M., Thomazi, A. P., Leite, M. C., Salbego, C., et al. (2005). Acute and repeated restraint stress influences cellular damage in rat hippocampal slices exposed to oxygen and glucose deprivation. *Brain Res. Bull.* 65, 443–450. doi: 10.1016/j.brainresbull.2005.02.026

Fujita, S., Sakurai, M., Baba, H., Abe, K., and Tominaga, R. (2015). Autophagy-mediated stress response in motor neurons after hypothermic spinal cord ischemia in rabbits. *J. Vasc. Surg.* 62, 1312–1319. doi: 10.1016/j.jvs.2014.03.297

Gómez-Sánchez, R., Pizarro-Estrella, E., Yakhine-Diop, S. M., Rodríguez-Arribas, M., Bravo-San Pedro, J. M., Fuentes, J. M., et al. (2015). Routine Western blot to check autophagic flux: cautions and recommendations. *Anal. Biochem.* 477, 13–20. doi: 10.1016/j.ab.2015.02.020

Gooding, M. R., Wilson, C. B., and Hoff, J. T. (1975). Experimental cervical myelopathy. Effects of ischemia and compression of the canine cervical spinal cord. *J. Neurosurg.* 43, 9–17. doi: 10.3171/jns.1975.43.1.0009

Graber, D. J., and Harris, B. T. (2013). Purification and culture of spinal motor neurons from rat embryos. *Cold Spring Harb. Protoc.* 2013, 319–326. doi: 10.1101/pdb.prot074161

Griffiths, I. R., Trench, J. G., and Crawford, R. A. (1979). Spinal cord blood flow and conduction during experimental cord compression in normotensive and hypotensive dogs. *J. Neurosurg.* 50, 353–360. doi: 10.3171/jns.1979.50.3.0353

Gu, Z., Sun, Y., Liu, K., Wang, F., Zhang, T., Li, Q., et al. (2013). The role of autophagic and lysosomal pathways in ischemic brain injury. *Neural Regen. Res.* 8, 2117–2125. doi: 10.3969/j.issn.1673-5374.2013.23.001

Guo, F., Liu, X., Cai, H., and Le, W. (2018). Autophagy in neurodegenerative diseases: pathogenesis and therapy. *Brain Pathol.* 28, 3–13. doi: 10.1111/bpa.12545

Hwang, J., Huh, J., Kim, J., Jeon, Y., Cho, S., and Han, S. (2012). Pretreatment with erythropoietin attenuates the neurological injury after spinal cord ischemia. *Spinal Cord* 50, 208–212. doi: 10.1038/sc.2011.136

Hwang, J. Y., Sohn, H. M., Kim, J. H., Park, S., Park, J. W., Lim, M. S., et al. (2017). Reproducible motor deficit following aortic occlusion in a rat model of spinal cord ischemia. *J. Vis. Exp.* 125:e55814. doi: 10.3791/55814

Kanno, H., Ozawa, H., Sekiguchi, A., and Itoi, E. (2009a). The role of autophagy in spinal cord injury. *Autophagy* 5, 390–392. doi: 10.4161/auto.5.3.7724

Kanno, H., Ozawa, H., Sekiguchi, A., and Itoi, E. (2009b). Spinal cord injury induces upregulation of Beclin 1 and promotes autophagic cell death. *Neurobiol. Dis.* 33, 143–148. doi: 10.1016/j.nbd.2008.09.009

Kato, H., Kanellopoulos, G. K., Matsuo, S., Wu, Y. J., Jacquin, M. F., Hsu, C. Y., et al. (1997). Neuronal apoptosis and necrosis following spinal cord ischemia in the rat. *Exp. Neurol.* 148, 464–474. doi: 10.1006/exnr.1997.6707

Kise, Y., Kuniyoshi, Y., Inafuku, H., Nagano, T., Hirayasu, T., and Yamashiro, S. (2015). Directly measuring spinal cord blood flow and spinal cord perfusion pressure *via* the collateral network: correlations with changes in systemic blood pressure. *J. Thorac. Cardiovasc. Surg.* 149, 360–366. doi: 10.1016/j.jtcvs.2014.09.121

Klionsky, D. J. (2008). Autophagy revisited: a conversation with Christian de Duve. *Autophagy* 4, 740–743. doi: 10.4161/auto.6398

Klionsky, D. J., Abdelmohsen, K., Abe, A., Abedin, M. J., Abeliovich, H., Acevedo Arozena, A., et al. (2016). Guidelines for the use and interpretation

of assays for monitoring autophagy (3rd edition). *Autophagy* 12, 1–222. doi: 10.1080/15548627.2015.1100356

Klionsky, D. J., and Emr, S. D. (2000). Autophagy as a regulated pathway of cellular degradation. *Science* 290, 1717–1721. doi: 10.1126/science.290.5497.1717

Kolenda, H., Steffens, H., Hagenah, J., and Schomburg, E. D. (2003). Different susceptibility of facilitatory and inhibitory spinal pathways to ischemia in the cat. *Neurosci. Res.* 47, 357–366. doi: 10.1016/j.neures.2003.07.001

Komatsu, M., Waguri, S., Chiba, T., Murata, S., Iwata, J., Tanida, I., et al. (2006). Loss of autophagy in the central nervous system causes neurodegeneration in mice. *Nature* 441, 880–884. doi: 10.1038/nature04723

Lee, S., Sato, Y., and Nixon, R. A. (2011). Lysosomal proteolysis inhibition selectively disrupts axonal transport of degradative organelles and causes an Alzheimer's-like axonal dystrophy. *J. Neurosci.* 31, 7817–7830. doi: 10.1523/JNEUROSCI.6412-10.2011

Lee, J. H., Yu, W. H., Kumar, A., Lee, S., Mohan, P. S., Peterhoff, C. M., et al. (2010). Lysosomal proteolysis and autophagy require presenilin 1 and are disrupted by Alzheimer-related PS1 mutations. *Cell* 141, 1146–1158. doi: 10.1016/j.cell.2010.05.008

Levine, B., and Kroemer, G. (2008). Autophagy in the pathogenesis of disease. *Cell* 132, 27–42. doi: 10.1016/j.cell.2007.12.018

Lu, H., Li, G., Liu, L., Feng, L., Wang, X., and Jin, H. (2013). Regulation and function of mitophagy in development and cancer. *Autophagy* 9, 1720–1736. doi: 10.4161/auto.26550

Lynch-Day, M. A., Mao, K., Wang, K., Zhao, M., and Klionsky, D. J. (2012). The role of autophagy in Parkinson's disease. *Cold Spring Harb. Perspect. Med.* 2:a009357. doi: 10.1101/cshperspect.a009357

Maday, S., and Holzbaur, E. L. (2014). Autophagosome biogenesis in primary neurons follows an ordered and spatially regulated pathway. *Dev. Cell* 30, 71–85. doi: 10.1016/j.devcel.2014.06.001

Maday, S., Wallace, K. E., and Holzbaur, E. L. (2012). Autophagosomes initiate distally and mature during transport toward the cell soma in primary neurons. *J. Cell Biol.* 196, 407–417. doi: 10.1083/jcb.201106120

Madji Hounoum, B., Vourc'h, P., Felix, R., Corcia, P., Patin, F., Gueguinou, M., et al. (2016). NSC-34 motor neuron-like cells are unsuitable as experimental model for glutamate-mediated excitotoxicity. *Front. Cell. Neurosci.* 10:118. doi: 10.3389/fncel.2016.00118

Maier, O., Böhm, J., Dahm, M., Brück, S., Beyer, C., and Johann, S. (2013). Differentiated NSC-34 motoneuron-like cells as experimental model for cholinergic neurodegeneration. *Neurochem. Int.* 62, 1029–1038. doi: 10.1016/j.neuint.2013.03.008

Mariño, G., Madeo, F., and Kroemer, G. (2011). Autophagy for tissue homeostasis and neuroprotection. *Curr. Opin. Cell Biol.* 23, 198–206. doi: 10.1016/j.ceb.2010.10.001

Martin, D. D., Ladha, S., Ehrnhoefer, D. E., and Hayden, M. R. (2015). Autophagy in Huntington disease and huntingtin in autophagy. *Trends Neurosci.* 38, 26–35. doi: 10.1016/j.tins.2014.09.003

Martinet, W., Timmermans, J. P., and De Meyer, G. R. (2014). Methods to assess autophagy *In situ*—transmission electron microscopy versus immunohistochemistry. *Methods Enzymol.* 543, 89–114. doi: 10.1016/b978-0-12-801329-8.00005-2

Martinez-Vicente, M. (2015). Autophagy in neurodegenerative diseases: from pathogenic dysfunction to therapeutic modulation. *Semin. Cell Dev. Biol.* 40, 115–126. doi: 10.1016/j.semcdb.2015.03.005

Martinou, J. C., Le Van Thai, A., Cassar, G., Roubinet, F., and Weber, M. J. (1989). Characterization of two factors enhancing choline acetyltransferase activity in cultures of purified rat motoneurons. *J. Neurosci.* 9, 3645–3656. doi: 10.1523/JNEUROSCI.09-10-03645.1989

Mizushima, N., and Komatsu, M. (2011). Autophagy: renovation of cells and tissues. *Cell* 147, 728–741. doi: 10.1016/j.cell.2011.10.026

Mizushima, N., and Yoshimori, T. (2007). How to interpret LC3 immunoblotting. *Autophagy* 3, 542–545. doi: 10.4161/auto.4600

Mosier, D. R., Baldelli, P., Delbono, O., Smith, R. G., Alexianu, M. E., Appel, S. H., et al. (1995). Amyotrophic lateral sclerosis immunoglobulins increase $Ca^{2+}$ currents in a motoneuron cell line. *Ann. Neurol.* 37, 102–109. doi: 10.1002/ana.410370119

Nazli, Y., Colak, N., Alpay, M. F., Uysal, S., Uzunlar, A. K., and Cakir, O. (2015). Neuroprotective effect of atorvastatin in spinal cord ischemia-reperfusion injury. *Clinics* 70, 52–60. doi: 10.6061/clinics/2015(01)10

Nedelsky, N. B., Todd, P. K., and Taylor, J. P. (2008). Autophagy and the ubiquitin-proteasome system: collaborators in neuroprotection. *Biochim. Biophys. Acta* 1782, 691–699. doi: 10.1016/j.bbadis.2008.10.002

Perera, N. D., Sheean, R. K., Lau, C. L., Shin, Y. S., Beart, P. M., Horne, M. K., et al. (2018). Rilmenidine promotes MTOR-independent autophagy in the mutant SOD1 mouse model of amyotrophic lateral sclerosis without slowing disease progression. *Autophagy* 14, 534–551. doi: 10.1080/15548627.2017.1385674

Rami, A., Langhagen, A., and Steiger, S. (2008). Focal cerebral ischemia induces upregulation of Beclin 1 and autophagy-like cell death. *Neurobiol. Dis.* 29, 132–141. doi: 10.1016/j.nbd.2007.08.005

Rivlin, A. S., and Tator, C. H. (1978). Regional spinal cord blood flow in rats after severe cord trauma. *J. Neurosurg.* 49, 844–853. doi: 10.3171/jns.1978.49.6.0844

Samantaray, S., Ray, S. K., Ali, S. F., and Banik, N. L. (2006). Calpain activation in apoptosis of motoneurons in cell culture models of experimental parkinsonism. *Ann. N Y Acad. Sci.* 1074, 349–356. doi: 10.1196/annals.1369.034

Schaffner, A. E., St John, P. A., and Barker, J. L. (1987). Fluorescence-activated cell sorting of embryonic mouse and rat motoneurons and their long-term survival *in vitro*. *J. Neurosci.* 7, 3088–3104. doi: 10.1523/JNEUROSCI.07-10-03088.1987

Sheng, R., Zhang, L. S., Han, R., Liu, X. Q., Gao, B., and Qin, Z. H. (2010). Autophagy activation is associated with neuroprotection in a rat model of focal cerebral ischemic preconditioning. *Autophagy* 6, 482–494. doi: 10.4161/auto.6.4.11737

Shimizu, H., and Yozu, R. (2011). Current strategies for spinal cord protection during thoracic and thoracoabdominal aortic aneurysm repair. *Gen. Thorac. Cardiovasc. Surg.* 59, 155–163. doi: 10.1007/s11748-010-0705-9

Suarez, N. C., Levi, R., and Bullington, J. (2013). Regaining health and wellbeing after traumatic spinal cord injury. *J. Rehabil. Med.* 45, 1023–1027. doi: 10.2340/16501977-1226

Sun, Y., Liu, D., Su, P., Lin, F., and Tang, Q. (2016). Changes in autophagy in rats after spinal cord injury and the effect of hyperbaric oxygen on autophagy. *Neurosci. Lett.* 618, 139–145. doi: 10.1016/j.neulet.2016.02.054

Swanlund, J. M., Kregel, K. C., and Oberley, T. D. (2010). Investigating autophagy: quantitative morphometric analysis using electron microscopy. *Autophagy* 6, 270–277. doi: 10.4161/auto.6.2.10439

Tan, C. C., Yu, J. T., Tan, M. S., Jiang, T., Zhu, X. C., and Tan, L. (2014). Autophagy in aging and neurodegenerative diseases: implications for pathogenesis and therapy. *Neurobiol. Aging* 35, 941–957. doi: 10.1016/j.neurobiolaging.2013.11.019

Tasca, C. I., Dal-Cim, T., and Cimarosti, H. (2015). *In vitro* oxygen-glucose deprivation to study ischemic cell death. *Methods Mol. Biol.* 1254, 197–210. doi: 10.1007/978-1-4939-2152-2_15

Turner, S. M., and Johnson, S. M. (2011). Delta-opioid receptor activation prolongs respiratory motor output during oxygen-glucose deprivation in neonatal rat spinal cord *in vitro*. *Neuroscience* 187, 70–83. doi: 10.1016/j.neuroscience.2011.04.059

Uchiyama, Y., Koike, M., and Shibata, M. (2008). Autophagic neuron death in neonatal brain ischemia/hypoxia. *Autophagy* 4, 404–408. doi: 10.4161/auto.5598

Wang, P., Guan, Y. F., Du, H., Zhai, Q. W., Su, D. F., and Miao, C. Y. (2012). Induction of autophagy contributes to the neuroprotection of nicotinamide phosphoribosyltransferase in cerebral ischemia. *Autophagy* 8, 77–87. doi: 10.4161/auto.8.1.18274

Wang, Z., Yang, W., Britz, G. W., Lombard, F. W., Warner, D. S., and Sheng, H. (2010). Development of a simplified spinal cord ischemia model in mice. *J. Neurosci. Methods* 189, 246–251. doi: 10.1016/j.jneumeth.2010.04.003

Wang, R., Zhang, X., Zhang, J., Fan, Y., Shen, Y., Hu, W., et al. (2012). Oxygen-glucose deprivation induced glial scar-like change in astrocytes. *PLoS One* 7:e37574. doi: 10.1371/journal.pone.0037574

Weidauer, S., Nichtweiß, M., Hattingen, E., and Berkefeld, J. (2015). Spinal cord ischemia: aetiology, clinical syndromes and imaging features. *Neuroradiology* 57, 241–257. doi: 10.1007/s00234-014-1464-6

Wirawan, E., Vanden Berghe, T., Lippens, S., Agostinis, P., and Vandenabeele, P. (2012). Autophagy: for better or for worse. *Cell Res.* 22, 43–61. doi: 10.1038/cr.2011.152

Wu, Y. T., Tan, H. L., Shui, G., Bauvy, C., Huang, Q., Wenk, M. R., et al. (2010). Dual role of 3-methyladenine in modulation of autophagy *via* different temporal patterns of inhibition on class I and III phosphoinositide 3-kinase. *J. Biol. Chem.* 285, 10850–10861. doi: 10.1074/jbc.M109.080796

Yang, T., Wu, L., Wang, H., Fang, J., Yao, N., and Xu, Y. (2015). Inflammation level after decompression surgery for a rat model of chronic severe spinal cord compression and effects on ischemia-reperfusion injury. *Neurol. Med. Chir.* 55, 578–586. doi: 10.2176/nmc.oa.2015-0022

Yu, L., Alva, A., Su, H., Dutt, P., Freundt, E., Welsh, S., et al. (2004). Regulation of an ATG7-beclin 1 program of autophagic cell death by caspase-8. *Science* 304, 1500–1502. doi: 10.1126/science.1096645

Zheng, Y., Zhang, X., Wu, X., Jiang, L., Ahsan, A., Ma, S., et al. (2019). Somatic autophagy of axonal mitochondria in ischemic neurons. *J. Cell Biol.* 218, 1891–1907. doi: 10.1083/jcb.201804101

**Conflict of Interest**: The authors declare that the research was conducted in the absence of any commercial or financial relationships that could be construed as a potential conflict of interest.

frontiers in Cell and Developmental Biology

REVIEW
published: 25 March 2020
doi: 10.3389/fcell.2020.00190

# The Influence of Neuron-Extrinsic Factors and Aging on Injury Progression and Axonal Repair in the Central Nervous System

*Theresa C. Sutherland*† *and Cédric G. Geoffroy**†

*Department of Neuroscience and Experimental Therapeutics, Texas A&M Health Science Center, Bryan, TX, United States*

In the aging western population, the average age of incidence for spinal cord injury (SCI) has increased, as has the length of survival of SCI patients. This places great importance on understanding SCI in middle-aged and aging patients. Axon regeneration after injury is an area of study that has received substantial attention and made important experimental progress, however, our understanding of how aging affects this process, and any therapeutic effort to modulate repair, is incomplete. The growth and regeneration of axons is mediated by both neuron intrinsic and extrinsic factors. In this review we explore some of the key extrinsic influences on axon regeneration in the literature, focusing on inflammation and astrogliosis, other cellular responses, components of the extracellular matrix, and myelin proteins. We will describe how each element supports the contention that axonal growth after injury in the central nervous system shows an age-dependent decline, and how this may affect outcomes after a SCI.

**Keywords: aging, neuron-extrinsic factors, inflammation, microglia, astrocytes, extra-cellular matrix, signaling, spinal cord injury**

OPEN ACCESS

***Edited by:***
*Alicia Guemez-Gamboa, Northwestern University, United States*

***Reviewed by:***
*Michael G. Fehlings, Toronto Western Hospital, Canada*
*Jason R. Plemel, University of Alberta, Canada*

****Correspondence:***
*Cédric G. Geoffroy*
*geoffroy@tamu.edu*

*†These authors have contributed equally to this work*

***Specialty section:***
*This article was submitted to Molecular Medicine, a section of the journal Frontiers in Cell and Developmental Biology*

***Received:*** *15 January 2020*
***Accepted:*** *06 March 2020*
***Published:*** *25 March 2020*

***Citation:***
*Sutherland TC and Geoffroy CG (2020) The Influence of Neuron-Extrinsic Factors and Aging on Injury Progression and Axonal Repair in the Central Nervous System. Front. Cell Dev. Biol. 8:190. doi: 10.3389/fcell.2020.00190*

## INTRODUCTION

Spinal Cord Injury (SCI) is the second most common cause of paralysis, following stroke, and places a significant and life-long burden on patients. Globally, the SCI incidence rate is approximately 13 cases per 100,000 population, with an average of 0.93 million new cases occurring each year (James et al., 2019). In the United States the incidence is approximately 54 cases per million people, with around 17,730 new cases each year (Singh et al., 2014; NSCISC, 2019). In the

**Abbreviations:** AD, Alzheimer's disease; ALS, amyotrophic lateral sclerosis; BBB, blood-brain barrier; BDNF, brain-derived neurotrophic factor; BMP, bone morphogenetic protein; BSCB, blood-spinal cord barrier; ChABC, chondroitinase ABC; CNS, central nervous system; CNTF, ciliary neurotrophic factor; CSPG, chondroitin sulfate proteoglycans; CST, cortico-spinal tract; DSPG, dermatan sulfate proteoglycans; EGF, epidermal growth factor; ERK, extracellular signal-regulated kinases; FGF, fibroblast growth factors; GABA, gamma aminobutyric acid; GDNF, glial cell-derived neurotrophic factor; GFAP, glial fibrillary acidic protein; HD, Huntington's disease; HSPG, heparan sulfate proteoglycans; IGF, insulin-like growth factor; IL, interleukin; JAK, Janus kinase; JNK, C-Jun N-Terminal Kinase; KLFs, Krüppel-like factors; KSPG, keratan sulfate proteoglycans; LPS, lipopolysaccharide; MAG, myelin-associated glycoprotein; MAPK, mitogen activated protein kinase; MEK, mitogen-activated protein kinase kinase; mTOR, mammalian target of rapamycin; NFκB, nuclear factor Kappa-light-chain-enhancer of activated B cells; NGF, nerve growth factor; NOX, NADPH-oxidase; NTs, neurotrophins; OMgp, oligodendrocyte myelin glycoprotein; OPCs, oligodendrocyte progenitor cells; PNS, peripheral nervous system; PTEN, phosphatase and tensin homolog; RNS, reactive nitrogen species; ROS, reactive oxygen species; SCI, spinal cord injury; SOCS3, suppressor of cytokine signaling 3; STAT3, signal transducer and activator of transcription 3; TBI, traumatic brain injury; TGF, transforming growth factor; TNF, tumor necrosis factor; VEGF, vascular endothelial growth factor.

past decades, SCI has shown an important shift in the demographic population affected. There is a peak in SCI in a younger cohort (<30 years) followed by a second peak in an aging cohort (65 years and over) (Devivo, 2012; Singh et al., 2014). The incidence of SCI in middle-aged and aging populations is increasing (Devivo and Chen, 2011; Devivo, 2012; Singh et al., 2014). In the United States the average age of incidence of SCI is ∼43 (NSCISC, 2019) and the average age of people living with SCI who reported paralysis due to a SCI is ∼48 (Christopher and Dana Reeve Foundation, 2009). The likelihood of complications and co-morbidities increases with age; this is accompanied by a decline in prognosis and rehabilitation outcome (Devivo et al., 1990).

Age has been recognized as an important factor influencing the severity and outcome of spinal cord injury. Indeed, studies have demonstrated that old animals recover less than their younger counterparts after SCI (Gwak et al., 2004; Siegenthaler et al., 2008; von Leden et al., 2017), however, the exact mechanisms involved are unknown. The majority of studies in SCI, especially in the field of axon growth and regeneration, use young animals to model the injury, due to the relative ease compared to older animal models. Experimentally the average age of rat used to model SCI is 96 days old (±28) and less than 0.35% of the animals are 12 months, which corresponds to ∼40 years old in humans, or older (Nielson et al., 2014; Fouad et al., 2019). This creates a dichotomy between the experimental models and the aging human SCI population that may have significant impacts on the translation of research into clinically relevant therapeutic strategies. Therefore, a better understanding of the impacts of age and aging on SCI recovery and repair at the cellular and molecular level is imperative, especially to the continued development and tailoring of therapeutic interventions.

Axon regeneration is an important part of recovering function after injury to the nervous system. Long-distance axon regeneration and substantial functional recovery has been observed in the adult mammalian peripheral nervous system (PNS) (Huebner and Strittmatter, 2009). PNS neurons have demonstrated an ability to modulate gene expression in response to injury, in order to promote axon growth (He and Jin, 2016). In contrast, the central nervous system (CNS) shows little to no tangible regenerative potential after injury and limited plasticity. One major limiting factor for the success of regeneration in mature CNS axons is their poor intrinsic regenerative capacity (Lu et al., 2014). This is combined with complex interactions of both neuron-intrinsic and extrinsic factors in the injury that result in a failure to successfully regenerate healthy axons. Corticospinal neurons, in particular, have a very low capacity for axon regrowth, even after manipulations to create a permissive extrinsic environment, neutralization of inhibitory molecules or tissue grafts (Lu et al., 2014). In some cases, it has been observed that while CNS axons severed by trauma show immediate local sprouting, this progresses to become swollen, disorganized and dystrophic (He and Jin, 2016). The lack of intrinsic regenerative ability of CNS neurons results in the poor regeneration, and limited functional recovery observed after SCI. This lack of intrinsic capacity is also compounded by interaction with a wide range of inhibitory neuron-extrinsic factors.

Despite the rapid progress in understanding the cellular and molecular regulation of axon growth after injury, a major gap exists in our knowledge of how aging impacts CNS axon growth. An age-dependent decline in axon growth has been reported in a variety of model organisms, including *C. elegans* (Byrne et al., 2014; Hammarlund and Jin, 2014), zebrafish (Graciarena et al., 2014), and mammals PNS (Pestronk et al., 1980; Verdú et al., 1995, 2000). The minimal natural ability of CNS axons to regenerate under normal conditions makes the observation of further reduction with age extremely difficult. Only recently has this age-dependent decline in axon regeneration potential been shown after SCI (Geoffroy et al., 2016).

The relationship between age/aging and axon growth is complicated and multifactorial. Both neuron-intrinsic and extrinsic factors play significant roles in the capability for axon regeneration after damage, and the age-dependent weakening of this capability. In the following review, we examine the current evidence for an age-dependent decline in axon growth after CNS injury, with specific focus on the role of neuron-extrinsic factors. The neuron-intrinsic factors have been addressed in a previous review, and will only briefly be discussed (Geoffroy et al., 2017). We will discuss how inflammation, astrogliosis, other cells around the injury site, the components of the extracellular matrix and the myelin proteins are altered with age and SCI, and their respective potential involvement in the age-dependent axon regeneration decline. Understanding the underlying mechanisms of age-dependent decline in recovery potential is critical for the development of therapies to stimulate repair in patients regardless of age.

## Evidence for Age Dependent Axon Growth Decline

There is growing evidence for an age-dependent decline in axon growth, and regeneration potential, across a variety of model organisms. In aging zebrafish, axon regeneration has been shown to occur at a reduced speed and with increased latency (Graciarena et al., 2014). A similar decline in axon regeneration efficiency has been observed in *C. elegans* (Zou et al., 2013; Hammarlund and Jin, 2014) with both models putatively linked to altered neuron-intrinsic mechanisms.

In mammalian models, regrowth of aged peripheral axons is delayed, slower and less effective than that in younger animals (Verdú et al., 1995; Kerezoudi and Thomas, 1999; Kang and Lichtman, 2013). Pharmaceutical denervation also failed to elicit any growth response in aged (28 month old) rats (Pestronk et al., 1980). While the exact mechanisms and etiology of the decline of PNS regeneration with are unclear (Willcox and Scott, 2004), both neuron-intrinsic or extrinsic mechanisms seem to be at play. The processes of myelin clearance is also delayed in aging and is associated with decreases in fibers in the affected nerves (Vaughan, 1992; Kang and Lichtman, 2013). Adult DRG neurons *in vitro* present approximately 30% slower growth than their neonate counterparts (Lamoureux et al., 2010). The axonal atrophy observed in aged nerve fibers may be attributable to the

reduced expression and transport of cytoskeletal proteins (Verdú et al., 2000), reduction in the rate of axonal transport (Stromska and Ochs, 1982; Kerezoudi and Thomas, 1999) as well as the decreased expression of nerve growth factor receptors (Parhad et al., 1995). Peripheral neuropathies resulting from these axonal changes with age are common in elderly populations (Cho et al., 2006). The age-related changes and decline are ambiguous, and do not progress linearly with age, exhibiting variation between studies (Verdú et al., 2000).

The relationship between age and axon regeneration in the CNS has received much less attention due to its already limited natural ability of CNS axons to regenerate. There is growing evidence for the same age-dependent decline that is seen in the PNS. Developmental studies have shown that changes in both the neuron-extrinsic environment of the spinal cord and intrinsic changes can reduce regeneration with age (Blackmore and Letourneau, 2006). In mammalian models of SCI, aging reduces locomotor recovery (Gwak et al., 2004) and is linked to changes in inflammation (von Leden et al., 2017) and myelination (Siegenthaler et al., 2008). Additionally, aging has varied effects on axon growth depending on the axon tract examined, with reduced rostral sprouting in the majority of major tracts at the lesion site (Jaerve et al., 2011). The neuronal deletion of phosphatase and tensin homolog (PTEN), a negative regulator of mammalian target of rapamycin (mTOR), has emerged as an effective target to promote the regeneration of the cortical spinal tract (CST) axons after an injury in young animals (Sun et al., 2011; Geoffroy et al., 2015). Recently, an age-dependent decline in mammalian CNS axon regeneration has been documented using PTEN-deletion strategies (Du et al., 2015; Geoffroy et al., 2016).

The regeneration, repair and regrowth of damaged axons is a complex process that relies on both internal mechanisms and responses to external signals. A balance of intrinsic and extrinsic cues determines the innate ability of injured CNS neurons to promote axon growth, and to elongate over distance. Both neuron-intrinsic and extrinsic mechanisms are altered in the normal aging process, resulting in a decline in the growth and regenerative potential of axons. There are a myriad of neuronal-intrinsic factors that interact and can impact axon growth after damage, including different pathways (PTEN/mTOR pathway, Park et al., 2008; Sun et al., 2011; Geoffroy et al., 2015), Suppressor of Cytokine Signaling 3 (SOCS3)/Signal Transducer and Activator of Transcription 3 (STAT3), Wnt/Ryk, insulin-like growth factor (IGF)-1, tumor suppressor p53, and Krüppel-like factors (KLFs), mitochondrial function, neuronal viscosity and axonal transport. These have been addressed in depth in our previous review focusing on the changes of neuron-intrinsic mechanisms with age (Geoffroy et al., 2017). The current review will only concentrate on the neuron-extrinsic factors influencing axon regeneration.

## The Impact of Extra-Neuronal Components on Axon Growth Potential

It is widely accepted that the pathophysiology of SCI consists of two distinct components (Kwon et al., 2004; Donnelly and Popovich, 2008). The primary injury results in the disruption of axons, the surrounding glial cells and blood vessels. The secondary injury is delayed and manifests in a broad spectrum of pathologies that exacerbate the injury and can continue for years after the primary trauma (Profyris et al., 2004; Rowland et al., 2008).

A range of cell signals and processes, which are intrinsically linked, influence the lesion microenvironment and the ongoing injury response (**Figure 1**). These include- microvascular disruption, hemorrhage, and disruption of cellular membranes resulting in the release of cytotoxic molecules, and excess ions and glutamate which causes damage to the surrounding cells by excitotoxicity (Brown et al., 2005), oxidative stress (Potts et al., 2006), lipid peroxidation of membranes (Shetye et al., 2014), disruption of intercellular ion balance (Potts et al., 2006), and induction of cell death signals. A hallmark of the secondary injury phase is a strong and persistent pro-inflammatory cascade, characterized by neutrophil and macrophage infiltration, microglial activation and astrogliosis (Profyris et al., 2004; Potts et al., 2006; Rowland et al., 2008). The injury environment is also influenced by contributions from fibroblasts, endothelial cells, pericytes and oligodendrocyte progenitor cells (OPCs) (**Figure 2**). This is characterized by degenerating myelin, increases in neuro-inhibitory molecules and oxidative stressors, alterations in the extracellular matrix (ECM), and fibrotic scar formation in the affected area.

# NEUROINFLAMMATION AND PHAGOCYTES IN THE CENTRAL NERVOUS SYSTEM

## Inflammation and the Immune Response in the Central Nervous System

In the inflammatory cascade occurring post-injury in the CNS, neutrophils are recruited, and endogenous microglia and astrocytes are activated. Blood monocytes migrate to the injury site and differentiate into macrophages nearly indistinguishable from activated microglia. There is a prolonged and dysregulated inflammatory response propagated by pro-inflammatory macrophages (Gensel and Zhang, 2015). Many elements of the inflammatory response have both neuroprotective and neurotoxic potential (Kwon et al., 2004). Infiltrating neutrophils produce oxidative and proteolytic enzymes that prepare the area for repair; however, the overwhelming numbers drawn to the lesion can be detrimental to the surrounding tissues. Macrophages and microglia are capable of producing factors that may help promote axonal growth, as well as molecules that are neurotoxic (Fleming et al., 2006). For in depth reviews see Hohlfeld et al. (2007).

### Inter- and Intra-Cellular Immune Signaling in the Injured Nervous System

After neurotrauma cytokines are secreted from a variety cells, and a range of receptors are expressed on the surface of multiple cell types (Pineau and Lacroix, 2007). Microglia monitor the extracellular environment, and express a large range of cytokine

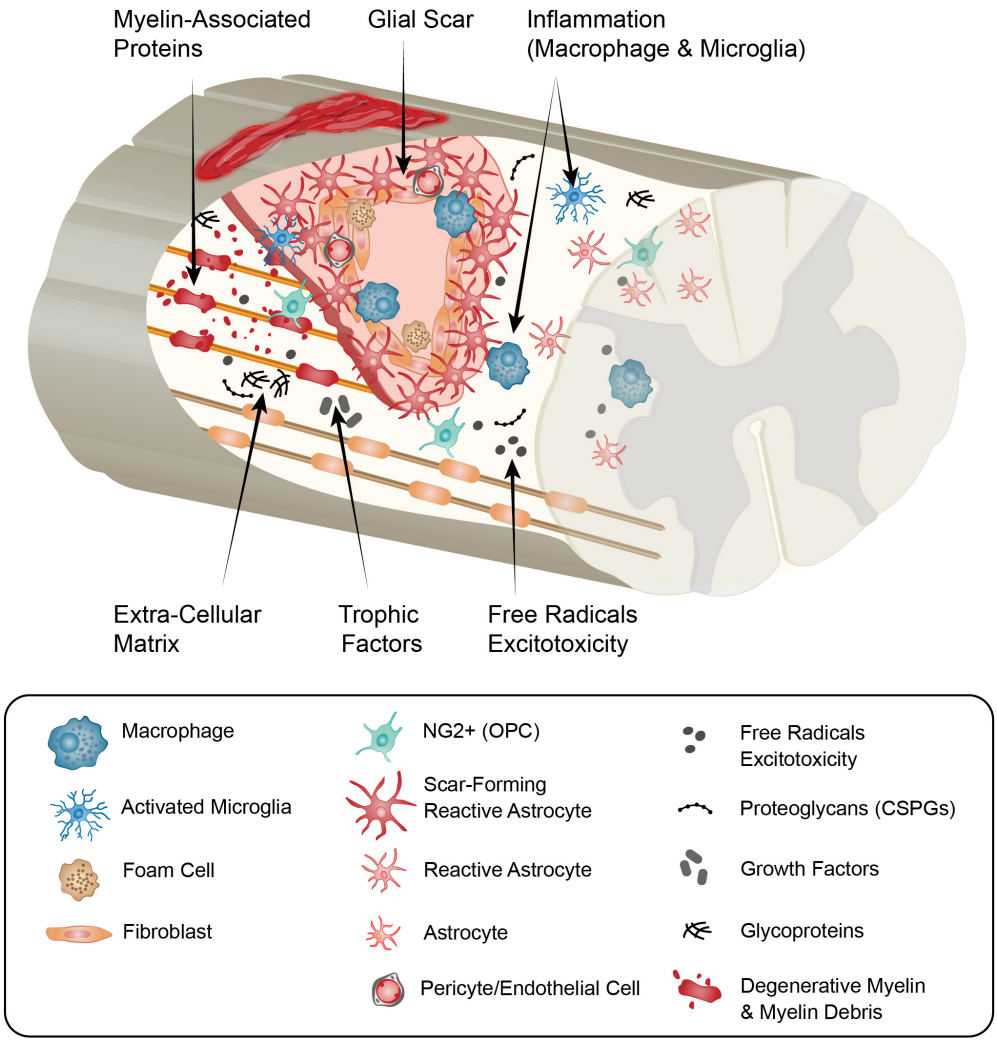


**FIGURE 1 |** Summary schematic of the cellular and extracellular cellular factors that can influence axon growth in the chronic spinal cord injury scar and that may be altered with age. In response to traumatic spinal injury, many cellular and molecular mechanisms are activated, including an inflammatory response (neutrophils, monocytes, microglia, macrophages), astrocytic response (forming the astroglial scar), and fibroblast response (from different origins, forming the fibrotic scar). With age, the initial injury response is altered and a reduction of locomotor functional recovery is observed. There is more BSCB permeability (resulting in more blood cells and molecules entering the injury), more pro-inflammatory response (more "M1-phenotype"), reduction in wound healing (linked to the alteration in the astrocytic response), induction of cell death (including neurons and oligodendrocytes). In the more chronic phase of the injury, age keeps changing the cellular response compared to young animals (inflammatory cells, astrocytes, fibroblasts, OPCs, endothelial, pericytes) which alters the environment: there is more debris present (including axon and myelin debris), alteration in the growth factors produced, changes in ECM composition (changes in glycoproteins and proteoglycans production), and less revascularization. All of these can participate in the age-dependent decline in axon regeneration. BSCB, blood spinal cord barrier; ECM, extracellular matrix; OPCs, oligodendrocytes precursor cells.

and chemokine receptors (Dheen et al., 2007). Astrocytes have an active involvement in the inflammatory response, expressing receptors to a variety of signals (Sofroniew, 2015). OPCs have also been shown to be capable of modulating and influencing the immune response in EAE, a multiple sclerosis model (Falcão et al., 2018). Oligodendrocytes also express some cytokine receptors, differing from the expression profiles of OPCs, astrocytes and microglia (Sawada et al., 1993). Neural stem/progenitor cells (NSPCs) have recently been discovered to be modulators of the inflammatory response, expressing a range of receptors for cytokines and growth factors (Ziv et al., 2006). Even mature neurons can express low levels of some cytokine receptors (Sawada et al., 1993).

Mitogen activated protein kinases (MAPKs) are known to mediate many fundamental cellular processes and responses to extrinsic stressors. p38 and c-Jun N-terminal kinase (JNK) signaling cascades have been implicated in the regulation of inflammatory mediator transcription and translation, making them attractive targets in multiple disease models (Kaminska, 2005). Interestingly, both the p38 and JNK MAPK pathways are required to promote axon regeneration, and in the absence of either pathway axon regeneration will fail (Nix et al., 2011). In

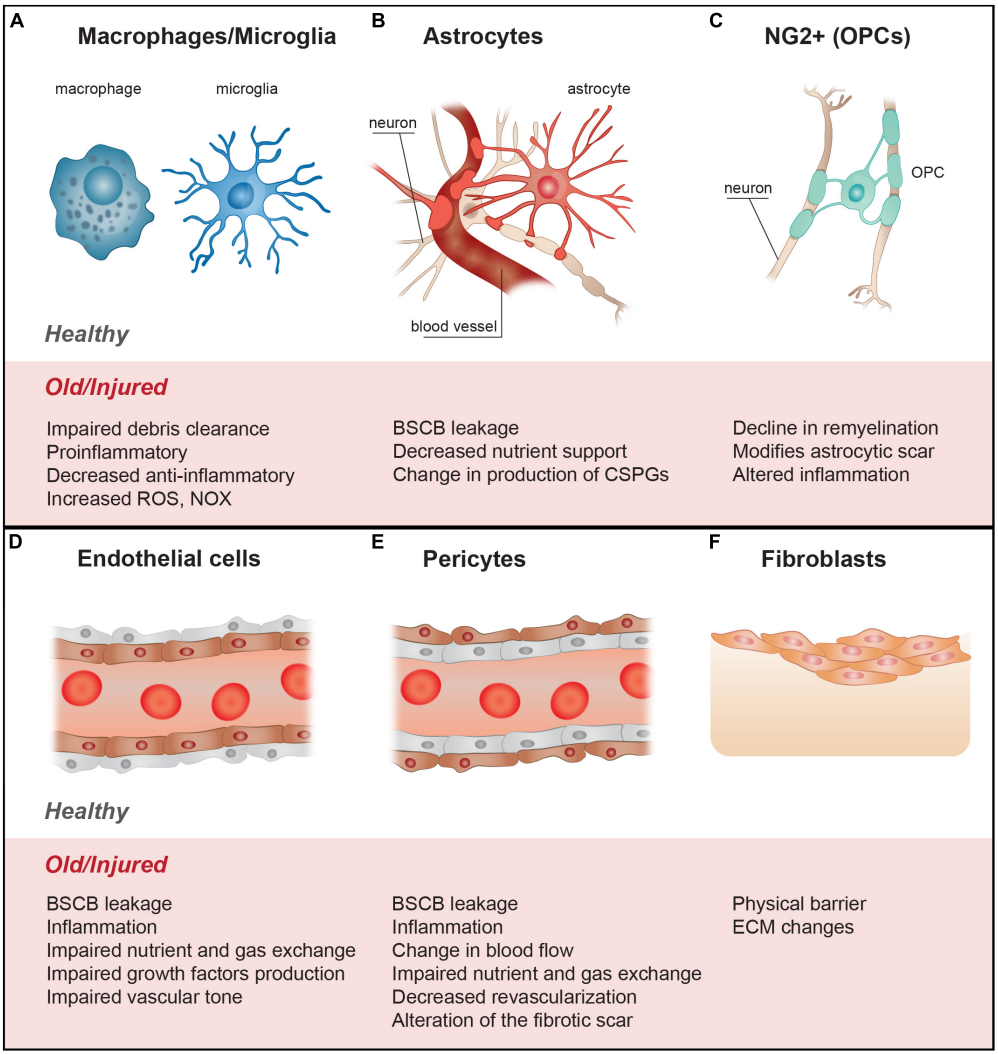


**FIGURE 2 |** The cellular contributors to spinal cord injury altered in aging further reduce injury repair and axon growth. **(A)** Inflammatory response by microphages and microglia results in more a pro-inflammatory and less anti-inflammatory profile, associated with a reduction in debris clearance efficiency, and increase in ROS and NOX. **(B)** Astrocytes form the astroglial scar and their alteration with age and injury may include changes in ECM molecule expression profiles (growth factors, glycoproteins, proteoglycan production - CSPGs). Astrocytes become pro-inflammatory, resulting in increases in ROS and NOX. Changes in astrocyte functions also include increases in BSBC leakiness and reduction in nutrient availability. **(C)** Fibroblasts, from different origins, form the fibrotic scar; with age and injury, the profile of the ECM molecules they produce changes, making the injury more anti-regenerative, altering the injury stiffness, and making a physical barrier to growth. **(D)** Changes in the state of the endothelial cells with age can lead to increases in BSBC leakiness, infiltration of inflammatory molecules, reduction in growth factor production, and reduction in control of the vascular tone, leading to local hypoxia and reduction in nutrients entry. **(E)** Similar to endothelial cells, alteration in the functions of pericytes with age and injury may lead to vascular dysfunction, reduction in trophic support, increase in local hypoxia and decrease in angiogenesis. The roles of pericytes in the fibrotic scar and production of ECM molecules may also be altered. **(F)** With age, the proliferation and differentiation potential of OPCs is reduced, which can diminish the potential for remyelination, alter neuroinflammation and reduce neuron survival after SCI. These changes can also alter the astrocytic scar, making it more inhibitory. BSCB, blood spinal cord barrier; CSPGs, chondroitin sulfate proteoglycans; ECM, extracellular matrix; OPCs, oligodendrocytes precursor cells; NOX, NADPH-oxidase; ROS, reactive oxygen species.

cerebral ischemia sustained activation of p38 has been observed in microglia and the use of a MAPK inhibitor has been found to reduce the size of the resulting infarct (Sugino et al., 2000). Similar results, and decreases in neurological deficits, have been seen in models of stroke (Barone et al., 2001). An inhibition of MAPK signaling, and resulting reduction in inflammation, has also been shown to be neuroprotective after SCI in rats (Qu et al., 2012). The mTOR pathway is also well known for its contribution to multiple cellular functions, including cell growth and metabolism, which has made it an attractive target. In the CNS, mTOR is involved in neuronal cell growth and survival, axonal and dendritic development, and synaptic plasticity (Lin et al., 2017). Pharmaceutical inhibition of mTOR has increased autophagy, reduced neuronal loss and cell death, and improved locomotor function after SCI in mice (Kanno et al., 2012). These pathways highlight the complexity of the secondary injury

phase of SCI, the inter-linked nature of the responses and the prominent role of the inflammatory response after traumatic injury to the CNS.

### The Inflammatory Response Changes With Age: 'Inflamm-Aging'

The gradual increase in inflammatory signaling documented with age has been termed 'inflamm-aging' (De Martinis et al., 2005). 'Inflamm-aging' is largely microglia-driven; however, the accumulated effects are seen on a wide variety of cells and can fundamentally alter these cells' normal physiological behavior. There are empirical links between inflammation and typical features of aging brains, such as decreased re-myelination, gray matter loss and cortical thinning, shrinkage in hippocampal volume, and deficits in learning and memory (Koellhoffer et al., 2017). It has also been suggested that age-related increases in ROS lead to chronic inflammation. Microglia are responsible for the bulk of oxidation products and inflammatory mediators in the aged brain, and contribute to a gradual increase in ROS generation with age. They are also key mediators of ROS-induced neural injury and ROS contribution to neurodegeneration (see Stewart et al., 2019 for review). NADPH-oxidase (NOX) has been linked to the classical activation of microglia and demonstrated to contribute the bulk of superoxide in neurodegenerative disorders (Bordt and Polster, 2014). NOX levels have been seen to increase in the CNS with age. Increased production of ROS from macrophage NOX with age exacerbates secondary injury after SCI (Zhang B. et al., 2019). Dystrophic microglia in aging have been observed to contain degenerated mitochondria (Wierzba-Bobrowicz et al., 2004). When stimulated with lipopolysaccharide (LPS) microglia that are deficient in NOX exhibited decreased tumor necrosis factor (TNF) expression, decreased levels of intracellular ROS and extracellular superoxide, and subsequent decreases in neurotoxicity (Qin et al., 2004). The increase in ROS production in the aging CNS can be directly toxic to adjacent neurons and can influence them via secondary signaling pathways, such as the NFκB or MAPK pathways.

## Macrophages, Microglia and Phagocytes in the Central Nervous System

Microglia play an important role in the development, monitoring and maintenance of the CNS. These cells, alongside peripheral monocytes/macrophages, also have a significant role in the post-injury environment (Fleming et al., 2006; Benowitz and Popovich, 2011). The dichotomy of macrophages and microglia stems from the heterogeneity of these cells. Their different activation phenotypes play different roles in the potential deterioration or repair of the surrounding tissue (Kigerl et al., 2009; Murray and Wynn, 2011), especially in relation to neuronal survival and axon growth. Activated microglia and macrophages have been suggested to both promote (Rabchevsky and Streit, 1997) and inhibit (Popovich et al., 2002) neurite outgrowth under different conditions (Gensel et al., 2009).

The functional states of macrophages are broadly categorized along a spectrum between classically activated pro-inflammatory (M1-like) and alternatively activated anti-inflammatory macrophages (M2-like) (Kigerl et al., 2009; Gensel and Zhang, 2015). Classically activated macrophages are efficient producers of potentially neurotoxic effector molecules and pro-inflammatory cytokines, while the alternatively activated phenotype is involved in dampening the inflammatory response and promoting tissue remodeling (Mantovani et al., 2013). While in the adult brain microglial density remains fairly stable over a lifetime, there is constant steady turn-over of microglia (cells surviving an average of 4.2 years) (Tan et al., 2020), allowing for the population to be refreshed and renewed multiple times in a lifetime (Askew et al., 2017).

### The Microglial and Macrophage Response to Injury in the Young Nervous System

The microenvironment of the lesion after SCI affects the function and polarization of macrophages (Brennan and Popovich, 2018). Constituents of the injury microenvironment, including myelin debris, can switch phagocytes toward a classically activated phenotype, propagating the pro-inflammatory response (Brennan and Popovich, 2018). The temporal distribution and the magnitude of pro-inflammatory and anti-inflammatory responses after SCI may have a significant role in determining the efficacy of injury resolution (Gordon and Martinez, 2010). Classically pro-inflammatory macrophages are prominent in the initial inflammatory response to SCI, persist at increased levels (Donnelly and Popovich, 2008), which can be detrimental to injury resolution. The transient nature of the anti-inflammatory macrophage response, and its lower magnitude (Gordon and Martinez, 2010; Sutherland et al., 2017) contribute to the persistence of pro-inflammatory responses, and the development of a neurotoxic inflammatory state (Ren and Young, 2013). This translates into poor neural tissue regeneration and wound resolution, resulting in poorer functional recovery.

Macrophages and activated microglia in contact with axons at the site of a CNS injury promote 'dieback' of axons from the lesion, signaled through both cell surface molecules and released soluble factors (Horn et al., 2008; Busch et al., 2011). Macrophages activated by intra-spinal zymosan displayed concurrent pro-regenerative and neurotoxic functions in a non-traumatic model (Gensel et al., 2009). This model showed a significant increase in axon growth up to the foci of activated macrophages. However, the axon growth was transient and the neurotoxic effects resulting from prolonged exposure to inflammatory factors produced by the activated macrophages persisted, resulting in impaired axon growth and increased cell death. LPS elicited a strong pro-inflammatory response without any accompanying axon growth enhancement, further demonstrating the heterogeneity of macrophage responses (Gensel et al., 2009).

Despite the evidence suggesting a negative effect of microglia on neuronal regeneration after CNS trauma (reviewed in Silver et al., 2015), these cells are essential to the CNS. The complete depletion or blocking of microglia after injury has been shown to exacerbate injury pathology and impair recovery (Lalancette-Hébert et al., 2007). Non-specific immune therapies are largely ineffective and can often worsen the injury outcome (Brennan and Popovich, 2018). After traumatic injury microglia and macrophages are capable of producing neurotrophic factors

such as brain-derived neurotrophic factor (BDNF) (Dougherty et al., 2000) and the macrophage derived protein oncomodulin (Yin et al., 2006) that can promote axonal growth. In the post-injury environment pro-inflammatory modulators prevail. Pro-inflammatory cytokines play a necessary role when kept in balance, and a complete blockade of their activity may be detrimental to recovery (Ikeda et al., 1996; Streit et al., 1998). Both pro- and anti-inflammatory effectors are required; however, the response needs to be regulated and the magnitude and timing closely controlled. It is this balance and regulation that is currently missing in the inflammatory response to CNS injury.

## Altered Phagocyte Responses in the Aging Nervous System

In recent years, it has been recognized that a persistent mild pro-inflammatory state in elderly patients is correlated with significant degenerative diseases (Howcroft et al., 2013). The relationship between systematic inflammation and neuroinflammation in aged subjects is still unclear. Evidence indicates that peripheral activation of the innate immune system in aged animals leads to exacerbated neuroinflammation in the CNS (Godbout et al., 2005; Howcroft et al., 2013). It has been demonstrated in mice that activation of the peripheral innate immune system by LPS can induce CNS microglia to produce pro-inflammatory cytokines, resulting in reduction in locomotor and social behaviors (Godbout et al., 2005). The complement pathway, and molecules associated with microglial activation, are up-regulated in the naive aged spinal cord, suggesting that a para-inflammatory state develops with aging (Galbavy et al., 2017).

With aging cellular senescence, dysregulated inflammatory signaling and defects in phagocytosis can result in maladaptive immune responses, chronic inflammation, and worsened outcomes after injury (Streit et al., 2008; Koellhoffer et al., 2017; Ritzel et al., 2019). PNS axons recover more efficiently when debris is cleared; however, aged Schwann cells exhibit diminished plasticity, and impairments in clearance of myelin debris as well as in recruitment of other phagocytes (Painter et al., 2014). In the aging brain the number and density of microglia increase in the parenchyma of various compartments, however, the reason for this increase is still unclear (Mouton et al., 2002). The distribution of microglia is altered in the aging cortex, moving away from a uniform, organized 'mosaic' to a less even distribution (Tremblay et al., 2012). Additionally, the normal ramified appearance of microglia shifts toward a de-ramified appearance with shorter and less branched processes (Damani et al., 2011). This is likely to have detrimental functional consequences as the microglial processes are dynamic structures important to the surveillance and support functions of microglia (Wong, 2013). Aged microglia are considered 'primed' and have exaggerated responsiveness to acute inflammatory stimulus (O'Neil et al., 2018) as well as systemic inflammation (d'Avila et al., 2018). Age-associated changes to microglia have been implicated in the progression of neurodegenerative disorders, such as Parkinson's (Lecours et al., 2018) and Alzheimer's (AD) (Hickman et al., 2008) diseases, and their prevalence in aging populations documented (Wong, 2013).

A beneficial inflammatory response to injury is reliant on correct regulation, magnitude, and balance between pro-and anti-inflammatory impetuses. Inhibitory receptors on microglia are required to prevent the initiation of undesirable inflammation and to resolve inflammation. In aged nervous tissue these receptors show an impaired ability to maintain microglial quiescence, which may be partially due to a reduction in the expression of the receptors' cognate ligands (Koellhoffer et al., 2017). Two examples shown to be impaired in the aged CNS are the immune-inhibitory signaling axes CD200/CD200R1 (Wang X. J. et al., 2011) and CX3CL1/CX3CR1 (Wynne et al., 2010). Both of these are associated with downregulating microglial activation and maintaining homeostasis in the CNS. The CD200/CD200R signaling axis is involved in microglia retaining a quiescent state. In the aging brain, there is a decreased of CD200 expression at both the mRNA and protein levels, accompanied by an enhancement of microglial response (Wang X. J. et al., 2011). CX3CL1/CX3CR1 signaling, which is involved in modulation of microglia activity, is impaired in the aging brain and CX3CL1 protein levels are reduced. Specifically in isolated microglia, there is a decrease in CX3CR1, with a concurrent increase in pro-inflammatory cytokine IL-1β. There is also down-regulated surface expression of CX3CR1 on a subset of aged microglia, compared to their younger adult counterparts. This may be a key contributor to the exaggerated microglial response to LPS challenge observed and correspond to delayed recovery from sickness behavior, and prolonged IL-1β induction in the aged brain (Wynne et al., 2010). The limited lifetime turnover of microglia leaves them vulnerable to age-related deficits. Forced microglial repopulation in the aged (16–18 months) mouse brain reversed age-related deficits; however, the age-associated inflammatory signature in the whole brain was not rescued by microglial repopulation alone (O'Neil et al., 2018). Similar to O'Neil et al. (2018) another study found that microglial repopulation did not broadly alter the inflammatory gene expression profile of the brain, or the response to immune challenges. There were, however, reversals of age-related alterations in neuronal gene expression profiles and neuronal complexity, accompanied by rescue of deficits in long-term potentiation in aged neurons (Elmore et al., 2018). This study observed improvements in spatial memory and in physiological characteristics of microglia in 24 months old mice within a month of microglial repopulation. These studies suggest that microglia can be targeted to ameliorate some age-related deficits but they cannot be separated from the complex post-injury environment.

There have been studies demonstrating that aged microglia contribute to enhanced pathology and worse outcomes in traumatic brain injury (TBI) (Ritzel et al., 2019), Stroke (Moraga et al., 2015), and AD (Hickman et al., 2008). In SCI, macrophages and microglia play an important role in the secondary injury phase. The age-related differences in the pro-inflammatory properties of the endogenous microglia is thought to be a potentially important contributor to the more detrimental inflammatory response seen in adult animals (Kumamaru et al., 2012). Both aging and CNS trauma prime microglia and the inflammatory response, and as such, each

can exacerbate the other. Aged individuals have been shown to have worse post-TBI outcomes, which may be associated with not just inflammation but also endocrine disfunction. Endocrine disruption is common in TBI, potentially stemming from hypotension, hypoxia, anemia, and inflammation in the secondary injury (Ziebell et al., 2017). Together these studies suggest that age exacerbates microglial activation, and inflammatory gene expression, detrimentally in CNS injury.

With age, phagocytosis and debris clearance by macrophages and monocytes declines (Linehan et al., 2014). Deficits in phagocytosis have also been observed in the normal and challenged CNS in aged animals (Neumann et al., 2008; Natrajan et al., 2015; Ritzel et al., 2015). The fragmentation of the myelin sheaths increases with age and leads to the formation of insoluble lysosomal inclusions in microglia, contributing to age-related microglial senescence and immune dysfunction (Safaiyan et al., 2016). The increased myelin debris in the aged CNS also affects the phenotype of phagocytes in CNS injury. Infiltrating macrophages often present an anti-inflammatory phenotype upon entering the CNS and migrate toward the injury epicenter where they switch to a more pro-inflammatory phenotype. Anti-inflammatory primed blood-derived macrophages respond to myelin debris in culture, shifting to resemble more classically activated macrophages (Wang et al., 2015). In a model of demyelination, aged macrophages and microglia showed excessive accumulation of myelin debris which led to cholesterol crystal formation, phagolysosomal membrane rupture and stimulated inflammasomes (Cantuti-Castelvetri et al., 2018). The alterations in microglia with injury and aging are shown in **Figure 3**. The interactions between the inhibitory factors in the lesion, and the macrophages, microglia and astroglia, creates a largely neurotoxic and inhibitory environment post-injury, exacerbated in aging.

### 'Inflamm-Aging,' Axon Growth and Recovery From Spinal Cord Injury

Inflammation is viewed as an important driver of age-related CNS dysfunction. There is very little known about how the changes in the inflammatory response that occur with age influences the response to SCI. The literature in this area is sparse. Both microglial and astroglial responses are increased and more sustained in older animals, however, aged microglia may be less efficient at debris clearance (Li, 2013). Up to 30 days post-injury there is a greater increase in phagocytes after contusion SCI in middle aged rats, compared to their younger counterparts. Older animals exhibited a significant increase in CD68-positive cells and demonstrated a more pronounced sub-acute CD68 upregulation around the injury site (von Leden et al., 2017). In a thoracic SCI study greater locomotor deficits have been observed in aged (18 months) animals compared to their younger (3 months) counterparts (Hooshmand et al., 2014). The lesion size and amount of cell death was increased, with much lower tissue sparing in the aged animals. The acute localized inflammatory response was also significantly higher. Microglial markers and activation have been observed to increase with age, however, the function of these activated microglia is still largely unknown as is whether this increase is causative or reactive to neurodegeneration (Howcroft et al., 2013). The affect the aging inflammatory response has on recovery from SCI is an area that needs greater attention with the aging SCI population.

Age-related differences in inflammation have been explored to some extent in infants and younger adult animals, particularly in rodents (Sutherland et al., 2017) but have yet to be explored in middle-aged and aging animals. It is believed that the alternative activation of either microglia or macrophages to a M2a phenotype by interleukin (IL)-4/IL-13 may support neuronal growth and repair processes (Kigerl et al., 2009; Murray and Wynn, 2011). Aged (18–19 months old) mice have demonstrated impaired induction of the IL-4α receptor (IL-4Rα) in microglia, accompanied by attenuated downstream Arginase gene expression (anti-inflammatory associated), as well as decreased recruitment of IL-4 receptor expressing macrophages. Aged mice, both wild-type and IL-4Rα knockout, also displayed decreased functional recovery after contusion SCI (Fenn et al., 2014). Macrophages in 14 months old mice exhibited significantly reduced IL-10 expression and CD86/IL-10 (M2b) macrophages in the spinal cord after spinal contusion. This decrease in M2-like phenotype coincided with increased tissue damage and greater functional impairment (Zhang et al., 2015). In a contusion SCI study in mice significantly higher generation of ROS occurred in 14 months old mice compared to their 4 months old counterparts. This was accompanied by NOX2 increases and increased indications of lipid peroxidation. This suggests that macrophages and NOX contribute to SCI oxidative stress that is exacerbated in aging (Zhang B. et al., 2016). In middle-aged rats, both naïve and after a moderate contusion SCI, there were significant increases in markers of oxidative stress, microglial marker Iba1, and inflammatory and NOX2 component gene expression compared to their younger counterparts. These middle-aged rats also exhibited greater lesion volume and showed significantly reduced hind-limb motor scores after the contusion SCI (von Leden et al., 2017). These studies suggest the aged inflammatory state is more detrimental to the surrounding tissue and inhibitory to ongoing regeneration and repair. Both aging and spinal cord injury prime microglia, produce a pro-inflammatory environment and a detrimental oxidative environment, it follows that in combination these two factors will compound one another to worsen recovery after SCI.

## ASTROGLIOSIS AND THE ASTROGLIAL SCAR IN THE CENTRAL NERVOUS SYSTEM

### Normal Role and Functions of Young Astrocytes

Astrocytes have a broad range of roles in the development and maintenance of the CNS. In the mature CNS, they are involved in the cellular, molecular and metabolic homeostasis essential for normal neuronal function. Astrocytes monitor and maintain the extracellular ionic environment and pH, as well as clear extracellular glutamate and gamma aminobutyric acid (GABA).

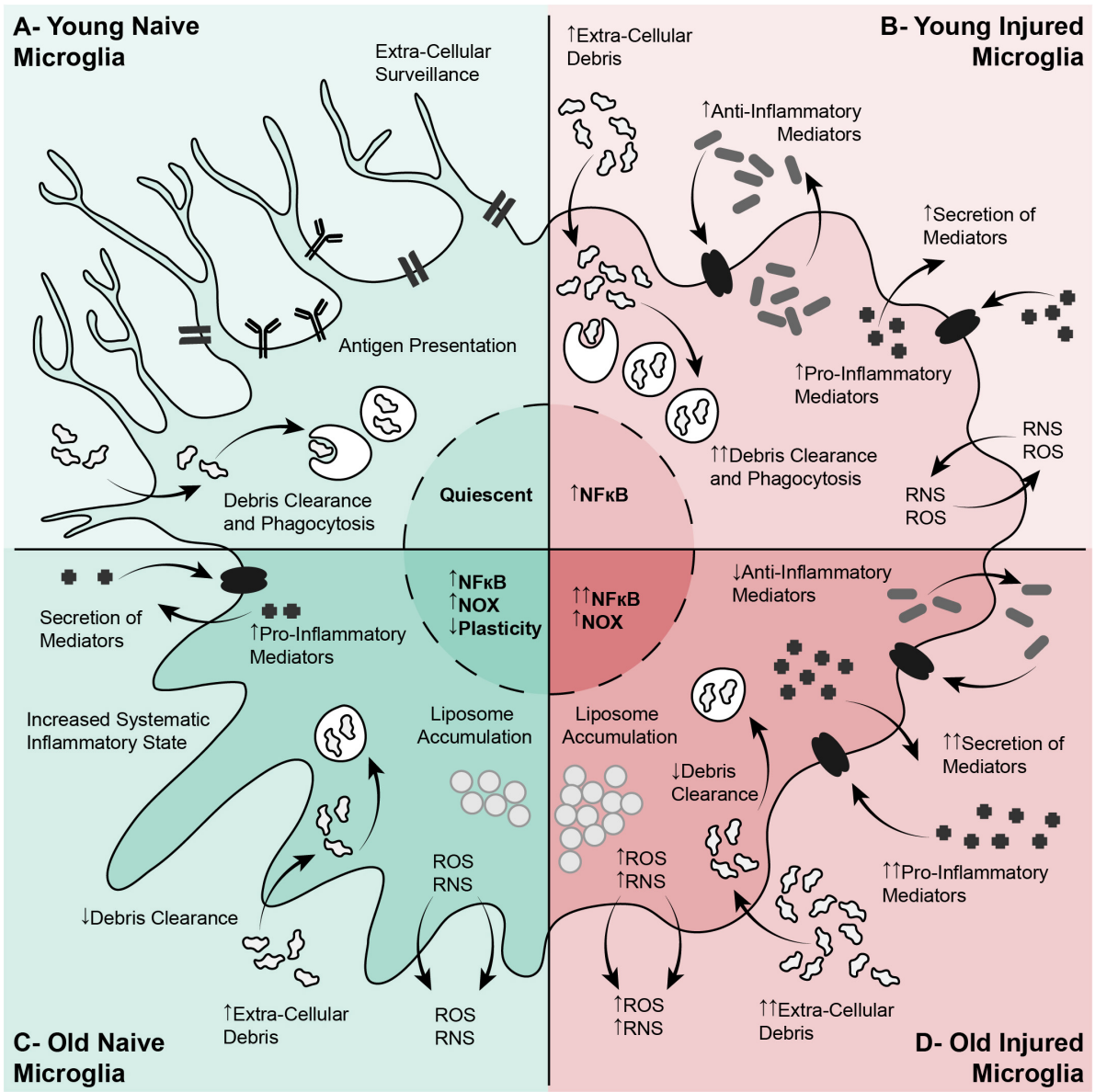


**FIGURE 3 |** Alterations in microglia in aging, and their responses to spinal cord injury, exacerbate the injury and reduce axon growth. **(A)** Young Naïve Microglia. In the young naïve CNS, resting microglia have a ramified appearance with branched processes, and have an organized distribution. These cells are involved in extracellular surveillance, debris clearance, environmental maintenance, and antigen presentation. **(B)** Young Activated Microglia. In the young CNS, microglia are activated after a SCI, becoming more ameboid and phagocytic. This is characterized by increased debris clearance, upregulation of inflammatory mediators (mostly pro- and some anti-inflammatory), activation of inflammatory signaling pathways, and the production of ROS and RNS. **(C)** Aged Naïve Microglia. In the aging CNS, microglia undergo physiological and functional changes linked with a systematic para-inflammatory state. Aged microglia have a de-ramified appearance and a more disorganized distribution. These cells are less plastic and become 'primed,' characterized by increased expression of pro-inflammatory mediators, increased NOX, ROS and RNS, impaired debris clearance, and liposome accumulation. **(D)** Aged Activated Microglia. After a SCI in the aged CNS, aged microglia respond similarly to the younger microglia. However, these aged cells are already 'primed,' pro-inflammatory, and have impaired debris clearance. This results in exacerbation of the detrimental elements of microglial activation, such as excessive production of pro-inflammatory mediators into the lesion environment, excessive NOS, ROS and RNS leading to increased oxidative stress, and inefficient debris clearance. CNS, Central Nervous System; NOX:, NADPH-oxidase; ROS, Reactive Oxygen Species; RNS, Reactive Nitrogen Species; SCI, Spinal Cord Injury.

It has emerged that astrocytes also play a role in detoxifying free radicals to prevent excitotoxicity. These cells also have a role in synthesizing precursors for glutamate and GABA production. Furthermore, astrocytes have been shown to sequester and redistribute potassium ($K^+$) for neuronal activity. These glia cells produce metabolic substrates for neuron function, including lactate and the production and release of ATP. Astrocytes store glycogen and can produce energy substrates to subsist on

anaerobic ATP production. For in depth review see Ransom et al. (2003). Astroglia are also involved in the maintenance of the blood-brain barrier (BBB) and can release factors that modulate endothelial permeability (Abbott, 2002) allowing for the exchange of essential nutrients into the CNS. The processes of astrocytes are associated with capillaries and involved in maintaining cerebral blood flow to support neuronal activity (Mulligan and MacVicar, 2004). Additionally, astrocytes can regulate brain microvascular permeability via $Ca^{2+}$ signaling (Erdő et al., 2017).

Astrocytes are also involved in the sculpting, maintenance and modulation of excitatory and inhibitory synapses and regulation of synaptogenesis (Ransom et al., 2003). They produce factors to induce synapse formation and maturation, and are involved in 'synaptic pruning' in the developing nervous system. In the functional synapse perisynaptic astrocytic processes house transporters and enzymes responsible for ion and transmitter homeostasis in the synaptic cleft, as well as for metabolic support (Pekny et al., 2016).

## Alterations in Astrocytes in Normal Aging

Astrocytes are vital to homeostasis, defense and regeneration of the CNS. In the aging brain, there are alterations in astrocyte morphology, and loss of functionality and reactivity. These changes are heterogeneous, disease-related, and region-specific (Clarke et al., 2018; Cunningham et al., 2019; Matias et al., 2019). In aging the brain, astrocytes play a role in the hypometabolic state that impinges on mitochondrial metabolism and neuronal survival (Jiang and Cadenas, 2014). With age, astrocytes exhibit an early stage of reactive astrogliosis, even in the absence of disease or trauma (Cotrina and Nedergaard, 2002; Boisvert et al., 2018). This is observed in cellular hypertrophy and variations in the expression of structural elements, such as glial fibrillary acidic protein (GFAP) and vimentin, and growth factors, such as ciliary neurotrophic factor (CNTF). An increase in oxidoreductive enzymes is also observed (Cotrina and Nedergaard, 2002). These are hallmarks of reactive astrogliosis that are seen in pathological conditions in the younger CNS. Similar astrocytic changes have been found in the aging spinal cord (Duan et al., 2009). There is evidence that astrocytes undergo cellular senescence with aging. The increase in neuroinflammatory function and loss of normal homeostatic function associated with astrocytic senescence may be an important component of neurodegenerative disorders prevalent in aging (Cohen and Torres, 2019). It has also been observed that the number of astrocytes in some brain regions, especially the cortex, increase significantly with aging (Cotrina and Nedergaard, 2002). Astrocytes in aging are extensively reviewed in Palmer and Ousman (2018).

The physiological changes in astrocytes with aging affect ability to perform their core functions, and can contribute to BBB disfunction (Erdő et al., 2017), alterations in antioxidant systems and increases in oxidative stress (Pertusa et al., 2007; Duan et al., 2009), an increased and altered inflammatory state (Clarke et al., 2018), and reduced neuronal support (Das and Svendsen, 2015). Age-dependent astrocytic alterations may affect synaptic efficacy in normal tissue and also hinder neuronal survival in pathological conditions. Aged astrocytes have been shown to upregulate genes that partially resemble reactive astrocytes, and also those associated with synapse elimination, that varies region to region within the brain. These alterations in aged astrocytes result in an environment susceptible to neuronal damage, a potential factor in age-related diseases and decline (Boisvert et al., 2018). Astrocytic differences in aging animals may impact the efficiency of post-SCI astrogliosis, specifically, the ability of reactive astrocytes to quickly sequester the inflammatory response and reduce its spread, which may result in worse outcomes for patients. One possibility is that a greater imbalance between the protective effects and the neuro-inhibitory effects of reactive astrogliosis develops with aging. Astrocytes undergo an increase in basal mRNA levels of activated astrocyte markers GFAP and S100B in the aged brain (Popa-Wagner et al., 2011). In the normal brain, the region-specific transcriptional identities of astrocytes change with age and astrocytes in the aged brain show the neuroinflammatory phenotype of A1-like reactive astrocytes (Clarke et al., 2018). The differences in astrocyte properties and reactive astrogliosis that occur with age is not a new question, with comparative studies as far back as the 1980s, however, it is still an area with many unanswered questions. In a cortical/hippocampal needle-puncture model, both 3 and 16–19 months old rats showed robust early astrocyte proliferation. This response was heterogenous and regional, with the older rats demonstrating greater proliferation in the cortex not in the hippocampus (Topp et al., 1989). After chemically induced excitotoxity in the striatum aged (22–24 months) rats exhibited an earlier onset and a more pronounced astrogliosis than young (3 months) rats. This is correlated with a delayed progression of neurodegeneration in the aged striatum, and reduced tissue injury and edema size (Castillo-Ruiz et al., 2007).

Reactive astrogliosis and astrogliopathy play an important role in diseases of the nervous system, especially neurodegenerative diseases, that increase in prevalence with age. In aging-prevalent diseases, such as AD, tauopathies, Lewy body diseases, Huntington's disease (HD), amyotrophic lateral sclerosis (ALS) and Creutzfeldt-Jakob disease, astrogliopathy is often characterized by increased GFAP and abnormal protein aggregates (Ferrer, 2017). After cerebral ischemia, astrocytes form an astroglial scar around the infarct. In a stroke model, aged rats (18–24 months) demonstrated more severe functional impairment, accompanied by an accelerated glial response, compared to their young (2 months) counterparts. This suggests alteration in the temporal progression of the glial response with age may result in altered scar formation and an environment that is more inhibitory to axon growth (Badan et al., 2003). After stroke, levels of the immune modulator transforming growth factor (TGF)-β are increased in astrocytes, activated microglia and macrophages, suggesting that this increase may be associated with regulation of the astroglial scar formation and the immune response. TGF-β is involved in the maintenance of homeostasis, especially vascular homeostasis (Walshe et al., 2009), therefore, an increase in astrocytic TGF-β may suggest a deviation from homeostasis and vascular dysfunction. While TGF-β signaling is increased in the aged brain, it is yet to be correlated with infarct size or functional outcomes (Doyle et al., 2010). In a rodent model of ALS, an age-dependent acceleration in

acquiring a senescent phenotype has been observed in astrocytes, accompanied by a reduction in their support of motor neurons (Das and Svendsen, 2015).

## Trauma and Reactive Astrocytes in the Young Nervous System

One of the hallmarks of trauma to the CNS is reactive astrogliosis, and the formation of a glial and fibrotic scar (Orr and Gensel, 2018). Reactive astrogliosis is the molecular and morphological changes that astrocytes undergo (Sofroniew, 2009). Astrocytes become reactive and undergo functional and physiological changes in trauma, disease and aging (Matias et al., 2019). These alterations include proliferation, hypertrophy of the soma and processes, branching, and upregulation of GFAP expression, and occur in a heterogeneous, context dependent manner regulated by different signaling events (Sofroniew and Vinters, 2010; Anderson et al., 2014). In severe cases reactive astrogliosis results in the formation of the astroglial scar. This is an important process after injury as these cells wall off the damaged areas and seal the lesion to protect the surrounding intact tissue from further damage (Faulkner et al., 2004). Indeed, removal of reactive astrocytes after neurotrauma results in failure of BBB repair, widespread tissue disruption, pronounced cellular degeneration, and severe motor deficits (Faulkner et al., 2004), indicating the role of reactive astrocytes in restoration of the BBB. However, there is still some contention as to whether reactive astrogliosis, and the formation of the astroglial scar, are beneficial or detrimental to functional recovery after SCI (Fawcett and Asher, 1999; Silver and Miller, 2004; Sofroniew, 2009). The role of astrocytes and microglia in regenerative failure in the CNS has been extensively reviewed previously (Silver et al., 2015).

There have been many studies demonstrating that reactive astrocytes have a substantial effect on axon regeneration after SCI. *In vitro* studies have shown that activated astrocytes produce both pro- and anti-inflammatory effector molecules, which can both help and hinder functional recovery (Sofroniew, 2009; Kawano et al., 2012; Pekny and Pekna, 2014). The astroglial scar is not only a physical barrier, obstructive to axon growth, it also produces a variety of potent growth inhibitory ECM molecules, and the lectican family of chondroitin sulphate proteoglycans (CSPGs) (McKeon et al., 1991, 1999; Li et al., 2013). For decades, the glial scar has been acknowledged as a source of molecules which can inhibit neurite outgrowth (Bovolenta et al., 1992). A 2011 study also suggested that reactive astrocytes also contribute to the failure of re-myelination by high expression of bone morphogenic protein (BMP) (Wang Y. et al., 2011). A study in adult mice demonstrated that neither complete prevention of the astroglial scar formation, attenuation of reactive astrocytes, or the deletion of chronic astroglial scars resulted in increased spontaneous growth of severed axons through a thoracic SCI. Even with the introduction of axon-specific growth factors, preventing the formation of the astroglial scar still significantly reduced the stimulated axon (Anderson et al., 2016).

Recently reactive astrocytes have been shown to be a highly heterogeneous population (Zamanian et al., 2012; Pekny and Pekna, 2014). Neuroinflammation and ischemia induce two different types of reactive astrocytes, referred to as 'A1' and 'A2' astrocytes respectively. A1 astrocytes demonstrate a more detrimental neuroinflammatory profile whereas A2 astrocytes upregulate many neurotrophic factors and appear more beneficial to injury resolution (Zamanian et al., 2012). A1 reactive astrocytes exhibit impaired ability to carry out normal astrocytic functions, and also release neurotoxic elements that may contribute to damage (Clarke et al., 2018). This heterogeneity of the reactive astrocyte population may go some way to explaining the dichotomy of results around reactive astrogliosis after CNS injury. In the field of SCI there is a large body of literature demonstrating both neuro-protective and neuro-inhibitory elements of post-traumatic reactive astrogliosis (Fawcett and Asher, 1999; Silver and Miller, 2004; Sofroniew, 2009). The duality of the astroglial scar and reactive astrogliosis is still a complicating factor in potential treatments for SCI, which is further impacted by changes in the aging CNS. This is an interesting path to explore in the context of the astrocytic response to SCI and also how this is altered with age.

In the astrocytes, several molecular pathways have been shown to be involved as regulator of reactive astrogliosis in trauma and disease. Studies have pointed to the Janus Kinase (JAK)/STAT3 signaling as an important pathway (Okada et al., 2006; Herrmann et al., 2008). In models of AD and HD the over-expression of SOCS3 in astrocytes inhibited the activation of the JAK/STAT3 pathway and attenuated astrocyte reactivity (Haim et al., 2015). Astrocytic *STAT3* deletion reduces GFAP upregulation and scar formation after SCI, as well as increased spread of inflammation, tissue disruption and locomotor deficits (Herrmann et al., 2008). Conversely, astrocytic *SOCS3* deletion, an endogenous inhibitor of STAT3, results in rapid astrocyte migration, deceased lesion area and better motor outcomes (Okada et al., 2006). Activation of the PI3K/Akt/mTOR signaling pathway is involved in astrogliosis. In culture, mTOR induces astrocyte proliferation, and its blockade suppresses proliferation, attenuates astrocytic migration, and reduces production of astrocytic-induced inflammatory factors (Li et al., 2015). Overexpression of *PTEN* in astrocytes attenuates astroglial scar formation, alters CSPG expression and improves axon regeneration into the lesion site (Chen et al., 2016). However, the role of mTOR signaling in both the astrocytic and inflammatory responses, is yet to be fully elucidated. There are mixed reports as how the MAPK pathways are involved in astrogliosis. After traumatic SCI, proliferation of reactive astrocytes in the lesion is accompanied by an increase in the expression and phosphorylation of mitogen-activated protein kinase kinase-extracellular signal-regulated kinases (MEK-ERK). A specific increase in the level of ERK phosphorylation was detected specifically in astrocytes after SCI (Ito et al., 2009). Inhibition of p38 MAPK or ERK has been demonstrated to be protective ischemia or brain injury models (Kang and Hébert, 2011). In another study, inhibition of p38 MAPK appeared to worsen ischemic damage (Lennmyr et al., 2003). Recently, leucine zipper-bearing kinase (LZK) has been shown to mediate astrogliosis, as its deletion in astrocytes reduces astrogliosis after SCI, subsequently increasing the lesion size, while its over-expression enhances astrogliosis and decreases the lesion

size (Chen et al., 2018). Together, these suggest that the role of the MAPK signaling in astrocytes response still needs to be elucidated. Others pathways such as NFκB may also be involved in astrogliosis (Kang and Hébert, 2011). NFκB, mTOR, JNK/STAT3 and MAPK pathways are all linked to not just astrocytes and reactive astrogliosis, but are also involved in the inflammatory and neuronal response, demonstrating the complex interlinking of extrinsic factors as well as neuron-intrinsic factors after CNS trauma.

## The Aged Astrocyte Response to SCI

Astrocytes in aging exhibit a range of physiological changes and functional alterations that can impact their response to trauma. Variations in structural elements, growth factors, and oxidoreductive systems (Cotrina and Nedergaard, 2002) in naïve aged astrocytes can compound the existing neurotoxic elements of the injury micro-environment by increasing the detrimental oxidative state and decreasing support for neuron regeneration. The loss of antioxidant tolerance capacity and increased vulnerability to oxidative stress with age (Pertusa et al., 2007; Duan et al., 2009) may be a significant contributor to the increase in post-injury ROS, and oxidative stress after CNS trauma. Significantly, the increased inflammatory state, and skew toward pro-inflammatory phenotypes (Clarke et al., 2018) in aging astrocytes can have a significant impact on the response to trauma. *In vitro* aged astrocytes show amplified responses to inflammatory cytokines, IL-1β, and TNF-α (Jiang and Cadenas, 2014). The primed, early activation state of these cells (Cotrina and Nedergaard, 2002) may have a cumulative effect with the injury induced reactive astrogliosis, exacerbating the negative effects of the persistent pro-inflammatory response. This warrants investigation, especially in the field of SCI.

There have been few studies comparing younger and aged astrocytes responses to SCI. In primary spinal cord astrocytes aged *in vitro* (60 DIV), increased expression of ferritin and GFAP were observed along with decreases in glutamate transporter 1 and transferrin receptor 1, and in mitochondrial membrane potential (Duan et al., 2009). Coincidently, in the naïve middle-aged (13 months) mouse spinal cord, decrease in antioxidant enzymes heme oxygenase 1 and NAD(P)H/quinone oxidoreductase 1, and in nuclear factor E2-related factor 2 (Nrf2) which directs expression of these enzymes, were observed (Duan et al., 2009). *In vitro,* aged astrocytes display an age-dependent increase in mitochondrial oxidative metabolism. The activation of NFκB signaling in these cells results in increased expression of NOX2 and elevated nitric oxide production. This was also associated with an age-dependent increase in hydrogen peroxide generation (Jiang and Cadenas, 2014). Alterations in the antioxidant capabilities and mitochondrial function may have significant flow-on effects in injury scenarios where there is oxidative damage and a detrimental increase in ROS and RNS. In response to SCI in older animals, astrocytes may also present changes in the production profile in CSPGs, and in their role in maintaining blood-spinal cord barrier (BSCB) integrity, which could have far-reaching consequences through the entry of inflammatory and potentially neurotoxic elements into the CNS and which also impact the availability of nutrients and support for potentially regenerative tissue after trauma.

In the area of SCI, the differences in astrocyte reactivity that occur in aging may have significant and far-reaching consequences. Aging astrocytes have been observed to lose their capacity to support neurite outgrowth and their efficacy stimulating axon growth (Smith et al., 1990). In the aging spinal cord, astrocytes exhibit higher basal GFAP mRNA levels, however, their ability to respond to a non-invasive CNS injury was observed to be reduced compared to their younger counterparts (Kane et al., 1997). This is potentially significant in the context of SCI as astrogliosis is an important element of the post-injury response and the interaction between astrocytes and axons is highly influential for axon growth potential. Recently, neuronal *PTEN* deletion was shown to promote mTOR signaling and axon growth in both the rubrospinal and corticospinal tracts, regardless of the age of the mice, but the axonal regeneration was still greatly diminished in the older animals compared to their younger counterparts (Geoffroy et al., 2016). An increase in astrogliosis, as well as inflammatory marker CD68, was observed in older animals at sub-chronic time-points, suggesting that differences in neuron-extrinsic environmental influences could mediate the age-dependent decrease in axon regeneration. It would be interested to assess whether modification of the astroglial scar with neuronal *PTEN* deletion could enhance axon regeneration in middle-age animals.

Reactive astrogliosis and the formation of an astroglial scar are significant parts of the post-injury response in the CNS and can influence outcomes after injury. The glial response contributes significantly to the nature of the post-injury environment and may be an important extrinsic factor in regulating axon regeneration, however, this is an area that still needs to be examined in detail. Astrocytes exhibit changes in reactivity and response in the aging CNS that can have significant consequences for the progression of injury, and the development of CNS disorders. The significant alterations in astrocytic response with injury and aging are shown in **Figure 4**. This is potentially an important factor and one that we have little knowledge about. In the aging CNS these responses are robust but also irregular, which may contribute to the age-related decline in axon regeneration and also to worsening post-injury outcomes after SCI. This potential relationship between aging, the glial response and injury resolution is an area of great interest that requires a considerably more study.

# CELLULAR INFLUENCES BEYOND INFLAMMATION AND ASTROGLIOSIS

While a great deal of attention and therapeutic efforts are directed at axon regeneration, with increasing focus falling on the inflammatory response and reactive astrogliosis, the secondary injury environment is potentiated by not just astrocytes and microglia but also fibroblasts, pericytes, endothelial cells, and other cells present around the injury epicenter (summarized in **Figure 2**). However, the specific role of each cell type in the age-dependent regeneration decline remains to be determined.

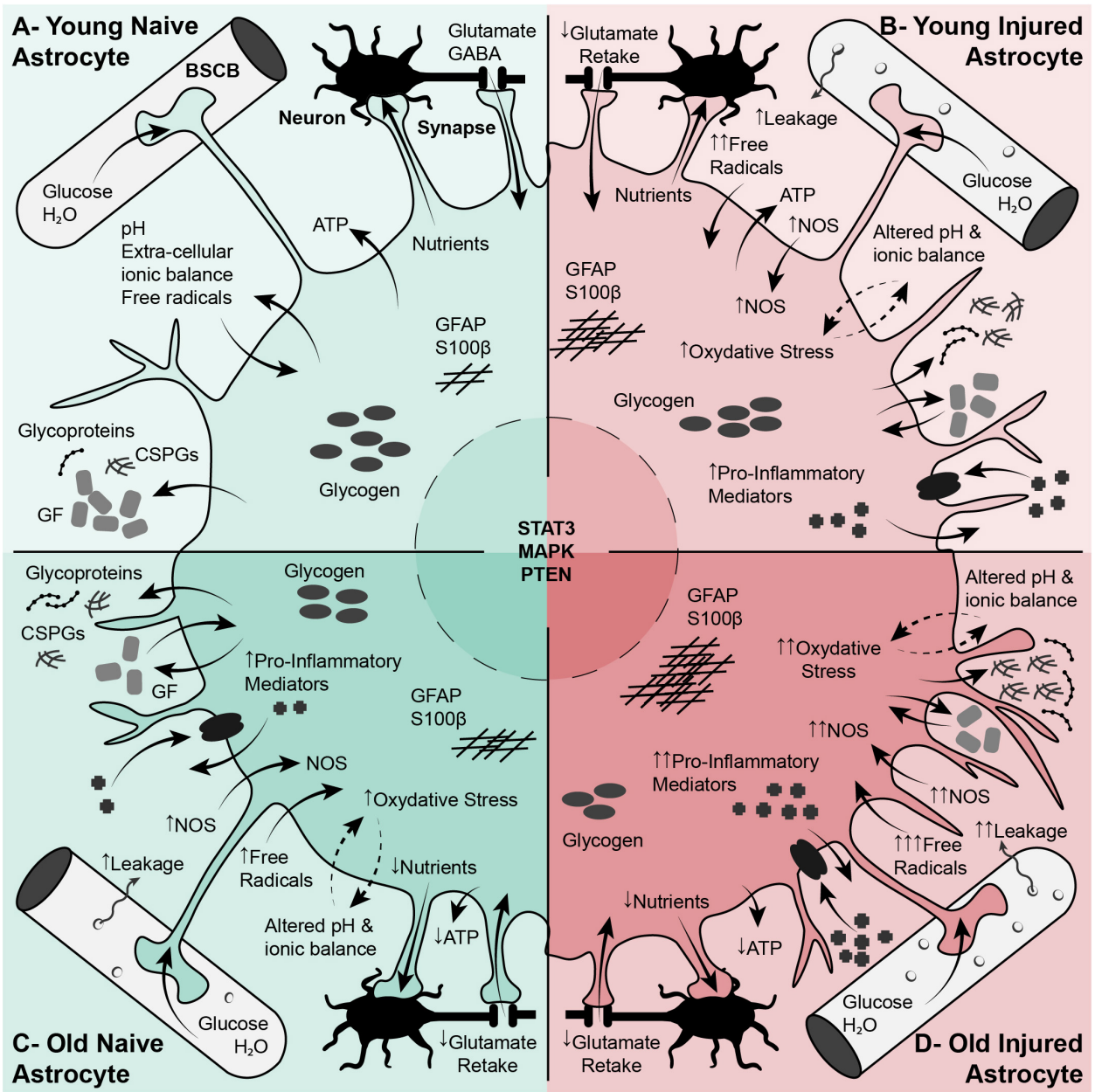


**FIGURE 4 |** Differences in astrocyte phenotypes, functions and responses with aging play a significant role in central nervous system health as well as spinal cord injury response. **(A)** Regular Function of Young Astrocytes. Astrocytes play a vital role in cellular, molecular, and metabolic homeostasis in the naïve CNS. These cells are involved in synaptogenesis and support mature synapses. They also support neurons and neuronal function through the uptake of glutamate, K+, and GABA, the production and release of transmitters, cytokines and ATP, and by stocking glycogen. Astrocyte processes interact with vascular endothelial cells and are an important element of the BBB. **(B)** Young Reactive Astrocytes. After SCI, astrocytes become reactive, increasing in size and branching. These reactive astrocytes are characterized by a suite of molecular changes including increased GFAP expression, increased proteoglycan (CSPGs) production, increased NOS and ROS, and production of inflammatory cytokines. Reactive astrocytes are involved in BBB repair, and sequestering the inflammatory lesion and fibrotic scar. **(C)** Normal Aging Astrocytes. In the aging CNS, astrocytes become larger and more branched than their younger un-injured counterparts. These cells exhibit an early stage of reactive astrogliosis characterized by increased GFAP, vimentin and S100β expression, increased expression of growth factors (such as CNTF and TGF-β) and increased oxidoreductive enzymes and oxidative stress. These cells show impaired ability to perform normal functions such as BBB/vascular maintenance and neuronal support. **(D)** Aged Reactive Astrocytes. After SCI, the alterations in astrocytes with aging are exacerbated. Aged astrocytes are already in an early reactive state, this is compounded by injury and activation cues in the lesion environment. The result is greater increase in GFAP, increase in oxidative stress and inflammation, increased excitotoxicity, impaired BBB repair, and, significantly, impaired sequestering of the inflammatory lesion. All of this will have profound effects on neuronal survival and axon re-growth. BBB, Blood-Brain Barrier; CNS, Central Nervous System; CNTF, Ciliary Neurotrophic Factor; CSPGs, Chondroitin Sulfate Proteoglycans; GFAP, Glial Fibrillary Acidic Protein; NOS, Nitric Oxide Synthase; ROS, Reactive Oxygen Species; SCI, Spinal Cord Injury.

## Fibroblasts

After SCI, fibroblasts from different origins proliferate and form the fibrotic scar, which is isolated from the spare tissue by the reactive astrocytes. For detailed review see Dias and Göritz (2018). Fibroblasts are a major source of fibronectin, collagen and other ECM components known to inhibit regeneration. Reducing the fibrotic scar can enhance axon regeneration and increase functional recovery (Ruschel et al., 2015; Dias et al., 2018) in young animals. However, while most studies aim to reduce the fibrotic scar, ablation of fibroblasts may compromise tissue integrity after injury, elements of the fibrotic scar may play supporting roles, and removing them acutely after injury may have negative effects (Göritz et al., 2011; Bradbury and Burnside, 2019). In non-nervous tissue, aging is known to alter fibroblasts (Varani, 2010). Different pathways are altered in skin and cardiac fibroblasts with aging, including a decrease in ERK and Akt expression, an increase in JNK and TGF-β/Smad signaling, which can alter their proliferation and production of ECM proteins. Therefore, it is likely that age affects the fibrotic response after SCI. There is a need to understand how age specifically modify this response.

## Endothelial Cells

The vascular and nervous system are closely juxtaposed, and endothelial cells respond to similar patterning cues as growth cones (Adams and Eichmann, 2010). There is increasing interest in taking advantage of this interaction to control axon regeneration by controlling vascular patterning after SCI (Partyka et al., 2019; Tran et al., 2020). Endothelial cells secrete vascular endothelial growth factor (VEGF), which promotes cell survival and axonal outgrowth (Sondell et al., 1999). These cells can also secrete other neurotrophic factors promoting axon growth (Grasman and Kaplan, 2017). With age, the production of different factors by endothelial cells, such as VEGF, declines with age (Shetty et al., 2005), which can result in a decrease in cell survival and in axon growth with age. The production of endothelin-1 and nitric oxide by endothelial cells are also altered, resulting in the modification of vascular tone (vasoconstriction/vasodilation). Lack of control of the vascular tone can be result in inability to meet the metabolic demand of the tissue, increase of local hypoxia, and reduction in waste removal (Bosetti et al., 2016; Jacob et al., 2016). Alteration of this balance at the injury site is likely to have negative effect on axon regeneration. Finally, changes in vascular permeability and BBB leakiness with aging can result in infiltration of molecules into the CNS, alteration in the microenvironment, and increase in neurotoxicity. This demonstrates the need to better understand how SCI and age can impact endothelial cell function and their relation to axon growth potential.

## Pericytes

Pericytes are closely associated with endothelial cells, and have projections encircling CNS vessels. These cells not only play a role in regulating and maintaining vascular barrier integrity (Sá-Pereira et al., 2012), they have a wide range of physiological functions (Muramatsu and Yamashita, 2014). CNS trauma often leads to vascular disruption and dysfunction, closely linked to neuronal dysfunction. One significant element of this is the reduction in trophic support for the CNS cells. After SCI, excess of monoamine receptors (5-HT1) on pericytes leads to local constriction of capillaries and chronic hypoxia. Inhibiting this receptor increases locomotor recovery (Picoli et al., 2019).

Pericytes have emerged as potential targets to increase functional recovery after SCI. For a detailed review, see Picoli et al. (2019). Pericytes in the spinal cord are heterogenous. After SCI, a subtype of pericyte gives rise to a population of stromal cells integral to the glial and fibrotic scars, and play a role in post-injury fibrosis. These cells were shown to be essential to the successful sealing of the lesion (Göritz et al., 2011). Inhibiting the proliferation of pericytes reduces the fibrotic scar tissue after SCI, and improves the regeneration of axon tracts, prompting improved sensorimotor functional recovery (Dias et al., 2018). After SCI, pericytes contribute a significant amount of collagen to the scar formation (Birbrair et al., 2014) and NG2+ pericytes are also involved with angiogenesis (Hesp et al., 2018).

To our knowledge, how the age factor impacts the response of pericytes in SCI models has not been characterized. Pericyte loss and neurovascular dysfunction have been linked to age-dependent neurodegeneration. Alteration of the BBB is observed in different neurogenerative conditions (ALS, HD) as well as neurotrauma (TBI and stroke). For review see Lendahl et al. (2019) and Li et al. (2019). Therefore, it is conceivable that SCI in older animals' results in enhanced BBB breakdown, increase in serum proteins leakage to the spinal lesion, increase in neurotoxicity as well as worse functional outcome. Additionally, a poorly functioning vascular system will likely result in less nutrients reaching potentially growing axons. Modulating pericytes integrity and activity could be of therapeutic interest in the context of middle-age and age SCI.

## NG2+ Cell Population

Different cell types can express NG2 in the CNS. Here, we refer to NG2+ cells as OPCs. OPCs are present throughout the CNS. They react to injury by proliferating and migrating toward the lesion, and differentiating into oligodendrocytes and astrocytes (Nishiyama et al., 2009; Hackett et al., 2018). For review see Hackett and Lee (2016). Removing NG2+ cells (both OPCs and pericytes) results in astrocytic and fibrotic scar disruption, with reduction in scar density and less distinct borders (Hesp et al., 2018). This was surprisingly accompanied by axon growth into the lesion as well as persistent functional impairment. While previous studies show that NG2 proteoglycan inhibits axon growth, NG2+ cells themselves may facilitate growth (Hackett and Lee, 2016). NG2+ cells proliferation and differentiation is reduced (Sim et al., 2002; Psachoulia et al., 2009) and OPCs heterogenicity altered with age (Spitzer et al., 2019). NG2+ cells have been shown to maintain neuron survival, via reduction of IL-1β pro-inflammatory pathway in the hippocampus (Nakano et al., 2017). Additionally, intracellular pathways involved in OPCs differentiation and myelination include ERK/MAPK, PI3K/Akt/mTOR and Wnt/β-catenin (Gaesser and Fyffe-Maricich, 2016), all of which can be altered with aging. An attractive hypothesis would be that the reduction in NG2+

activity with age and injury participates to neuroinflammation and inducing neuron death, and the reduction in NG2 cells proliferation and differentiation results in an environment less favorable to axon growth.

# THE INFLUENCE OF EXTRACELLULAR COMPONENTS ON AXON REGENERATION POTENTIAL

## The Extra-Cellular Matrix

The importance of the ECM and extracellular elements of the environment in an age-dependent decline in regeneration potential is highlighted in a study by Kawano et al. comparing postnatal 7, 14, and 21 with adult mice (P60-80) (Kawano et al., 2005). Transected axons regenerated across the lesion only in P7; in P14 and older, the axons stop at the lesion site. The fibrotic scar, containing type IV collagen, was not present in the P7 mice. Inhibition of collagen synthesis in older mice prevented the formation of this scar resulting in a greater number of axons extending across the lesion. These elements are intrinsically connected to the cellular elements and the formation of CNS scar tissue, as well as influencing the nature of the injury microenvironment. Overall, there has been very little done to elucidate the changes in extracellular components in aging and how it plays a role in the reduction of axon regeneration potential; the changes with age and traumatic spinal injury is still yet to be elucidated.

### Glycoproteins

#### *Fibronectin*

After CNS trauma, the glial scar surrounds the lesion site, accompanied by infiltration of plasma fibronectin, fibronectin secretion from various fibroblast-like cells and formation of a fibrotic scar (Farooque et al., 1992; Zhu et al., 2015). While fibrosis restores BBB integrity and restricts lesion spread, it also disrupts the CNS structural matrix and produces both a physical and biochemical barrier to axon growth (Kawano et al., 2012). Astrocyte-associated fibronectin participates in axon growth (Tom et al., 2004) but fibronectin aggregates reduce remyelination (Stoffels et al., 2013). Fibronectin is an early trigger of glial scar formation through the TGF-β/Smad signaling pathway, and increases inhibitory proteoglycan expression (Schachtrup et al., 2010). Fibronectin can also activate microglia and infiltrating macrophages (Milner and Campbell, 2003). Reduction of the fibrotic scar, via reduction of fibronectin, could be an interesting strategy to increase axon growth. While changes in fibronectin expression with age after neurotrauma are unknown, one could predict an increase in expression level, as fibronectin increases with age in other tissue (Kumazaki et al., 1993; Dorner et al., 1996; Labat-Robert, 2004). This could lead to an increase in astroglial and inflammatory response, as well as a more inhibitory fibrotic scar.

#### *Collagen*

Collagens expression levels are increased after CNS injury (Frisen et al., 1995; Zhu et al., 2015). Although not inhibitory in itself, collagen IV serves as a mesh for other inhibitory molecules to bind (Liesi and Kauppila, 2002). Inhibition of deposition of Collagen IV facilitates axon regeneration (Stichel et al., 1999). An increase in collagens within the SCI lesion induces astrocytic scar formation via the integrin pathway (Hara et al., 2017). Blockage of collagen interaction with astrocytes reduces astrocytic scar formation and promotes functional recovery. However, collagen concentration is known to increase with age (Uspenskaia et al., 2004). It will be interesting to test whether alteration of the collagen composition with age after SCI is linked to the increase in the reactive astrocytes and formation of the astrocytic scar observed.

#### *Laminin*

Laminins are widely express in the CNS, and play important roles, mostly via the integrin pathway (Nirwane and Yao, 2019). Astrocyte-produced laminins maintain BBB (by regulating pericyte differentiation), and the increase in laminin observed after TBI may be an attempt in restoring the BBB integrity (Tate et al., 2007; Yao et al., 2014). Laminins participate in angiogenesis and revascularization after injury (Simon-Assmann et al., 2011; Wappler et al., 2011). They also support axon growth both *in vitro* and *in vivo* (Frisen et al., 1995; Plantman et al., 2008). The expression of most of the prominent laminin chains are reduced in the adult brain, compared to development (Sanes, 1989). There are also deposits of laminin and laminin-like material seen in the aged brain, especially associated with AD (Jucker et al., 1996). Altered laminin isoforms in aging can impair endothelial cell function (Bell et al., 2010; Wagner et al., 2018). Alteration of laminin expression level and form in response to injury in older animals is likely to play an important role in maintaining BBB integrity and in participating in the reduction of axon growth.

### Proteoglycans

Proteoglycans include dermatan sulfate proteoglycans (DSPGs), heparan sulfate proteoglycans (HSPGs), keratan sulfate proteoglycans (KSPGs) and CSPGs (George and Geller, 2018). CSPGs are the most studied in their role in pathfinding in development and restricting plasticity in adult CNS (Bartus et al., 2012). CSPGs are associated with glial scaring and reactive gliosis after SCI and inhibit axon growth. Thus, disruption of the CSPGs after SCI was thought to be a promising strategy to modify the glial scar, promote plasticity, axon growth and functional recovery. One strategy is the use of chondroitinase ABC (ChABC). There is flourishing literature on this topic (Muir et al., 2019). Proteoglycans composition changes during aging and accumulates in the brain (Reed et al., 2018; Richard et al., 2018). Increased proteoglycan sulfation with aging may reduce plasticity and memory (Foscarin et al., 2017). It will be of interest to assess the proteoglycans changes with age and SCI and to determine the effects of ChABC in middle-age and age animals.

### Biomechanical Properties of the Injured Spinal Cord

The ECM composition alters the tissue stiffness. Stiffness has recently been advanced as an important factor for regeneration (Moeendarbary et al., 2017; Thompson et al., 2019). Changes in collagen, laminin, and increases in intermediate filaments GFAP and vimentin, modify the stiffness of the tissue. Axons growth

decreases on a softer tissue, such as the glial scar in the SCI (Koser et al., 2016). Increase in tissue stiffness with age has been shown to reduce OPCs proliferation and differentiation (Segel et al., 2019). Therefore, changes of the ECM composition with age and injury are likely to alter the biomechanical properties and impede any attempt at promoting axon regeneration in aged animals.

## Growth Factors

Numerous growth factors are known to promote axon regeneration, including IGFs, nerve growth factor (NGF), BDNF, glial cell-derived neurotrophic factor (GDNF), neurotrophins (NTs), fibroblast growth factors (FGFs), epidermal growth factors (EGF), and CNTF (Duraikannu et al., 2019).

### *Insulin-like growth factor*

In the developing brain, IGF-1 promotes oligodendrocytes proliferation and differentiation and axonal growth (Ye et al., 2002; Dyer et al., 2016). IGF-1 has been shown to increase axon regeneration (Ozdinler and Macklis, 2006; Zhang Y. et al., 2019) although not in adult, most likely because of the lack of IGF-1 receptor (Hollis et al., 2009; Dupraz et al., 2013). Recently, IGF-1, only in combination with osteopontin, was shown to increase CST sprouting (Liu et al., 2017). IGF-1 expression levels decline with age. This reduction, associated with longevity, is proposed to be a neuroprotective after injury, as higher level of IGF-1 is associated with cognitive dysfunction (Shetty et al., 2005; Mao et al., 2018). Indeed, IGF-1/insulin inhibits axon regeneration in *C. elegans* in aging neurons (Byrne et al., 2014). Whether IGF-1 reduces regeneration in aged mammals needs to be determined. On the other hand, IGF-1 may have anti-inflammatory effect in the CNS (Sukhanov et al., 2007; Labandeira-Garcia et al., 2017) and may reduce the astrocytic response (Genis et al., 2014; Hernandez-Garzón et al., 2016). Therefore, a reduction of IGF-1 with age may participate to the age-related CNS inflammation and increase astrogliosis. Regardless, the involvement of the IGF1/IGF-1 receptor in the modulation of inflammation, astrogliosis and axon regeneration in the context of aging and neurotrauma is complicated.

### *Nerve growth factor*

After SCI, NGF is increased (Brown et al., 2004). Infusion or overexpression of NGF increases axon growth after SCI (Oudega and Hagg, 1996; Romero et al., 2000) and reduces neuronal apoptosis, via activation of the PI3K/Akt and MAPK pathways (Zhang et al., 2014). However, NGF is decreased and its precursor, proNGF, is increased with aging (Al-Shawi et al., 2007; Budni et al., 2015). While proNGF promotes neurite growth in young rodents, it induces cell death but no growth in old animals (Al-Shawi et al., 2008). After SCI, proNGF mediates oligodendrocytes death (Beattie et al., 2002). Therefore, increase of proNGF with age after SCI is likely neurotoxic, and may not promote axon growth. However, it remains possible that infusion or overexpression NGF in older animal still promote axon growth after SCI.

### *Brain-derived neurotrophic factor*

Brain-derived neurotrophic factor has repeatedly been shown to be neuroprotective and to enhance regeneration/sprouting after SCI through the MAPK, PI3K, and PLC γ signaling (Weishaupt et al., 2012; Garraway and Huie, 2016). However, it is not known if similar effects would be observed in older animals in the context of SCI. BDNF/TrkB is altered with age. TrkB receptor expression level declines with age in the pituitary (Rage et al., 2007) and aging is associated with BDNF and/or TrkB expression decrease at the neuromuscular junction (Greising et al., 2015; Greising et al., 2017). Reduction of BDNF with age is linked to cognitive, memory deficit and hippocampal shrinkage (Erickson et al., 2010; von Bohlen Und Halbach, 2010; Petzold et al., 2015). In sum, there is evidence that BDNF or its receptor, TrkB, are reduced in the context of injury in middle-age and aged animals. Thus, we speculate that BDNF-based treatments in older animal may still enhance axon growth after SCI but only to a limited degree, and that it may be necessary to combine them with other approaches, such as overexpression of TrkB in the neurons.

### *NT3*

NT3 plays a role in neuron survival and axon regeneration (Keefe et al., 2017). NT3 overexpression also improves recovery after SCI by reducing dendritic atrophy and dendritic regrowth in young animals (Wang et al., 2018; Han et al., 2019). NT-3 binds preferentially to TrkC receptor (Keefe et al., 2017). However, a reduction of TrkC is observed with age in sensory neurons, which could reduce NT3 activity in older animals (Vaughan et al., 2017). Importantly, in a stroke model, delayed viral delivery of NT3 promotes recovery in both adult (6 months) and aged (18 months) rats, via increase in CST sprouting (Duricki et al., 2016). Therefore, the effects of this therapy on adult and elderly animals with SCI may also enhance CST sprouting, despite the potential reduction of TrkC in neurons.

### *Glial cell-derived neurotrophic factor*

Member of the TGF-ß superfamily, GDNF has been shown to promote survival of neurons (Paratcha and Ledda, 2008). After SCI, administration of GDNF promotes functional recovery via different mechanisms, such as enhancing axon regeneration and sprouting, altering astrogliosis via reduction of GFAP and CSPGs production, reducing BSCB permeability and reduction of nitric oxide production. For review see Rosich et al. (2017). While a decrease in GDNF expression level with age and SCI would be expected, it has not been characterized. Similarly, the effect of GDNF delivery on functional recovery after SCI in age animals remains to be tested.

### *Fibroblast growth factors*

Several members of the FGFs family, especially FGF1 and FGF2, have been shown to be involved in neuron survival and neurite extension (Teng et al., 1999). FGF1 also reduces inflammation (Lee et al., 2008) and astrogliosis (Lee et al., 2011; Kang et al., 2014). Different FGF treatment, alone or in combination, promote recovery after SCI (Rabchevsky et al., 2000; Zhou et al., 2018). Pathways activated by FGFs include ERK/MAPK, PLCγ and AKT. FGF2 and FGF receptors expression levels decline with age (Shetty et al., 2005; Hurley et al., 2016). However, changes of these factors and their receptors in the aged spinal cord have not been described. A decline of FGF receptors with age would

indicate less potential for clinical translation potential and calls for further investigation.

***Epidermal growth factors***

Epidermal Growth Factors inhibits axon regeneration (Koprivica et al., 2005) and promotes reactive astrocytes (Liu et al., 2006; Codeluppi et al., 2009) through mTOR and AKT signaling. Inhibiting EGF receptor was found to promote functional recovery after SCI via modification of the glial scar, reducing inflammation and increasing OPC proliferation (Erschbamer et al., 2007; Li et al., 2011; Zhang S. et al., 2016). However, an opposite effect was later described, with an increase in lesion size and reduction in functional recovery (Berry et al., 2011; Sharp et al., 2012). EGF administration reduces BSCB disruption (Zheng et al., 2016). Decrease in EGF-Receptor with age has been documented in the skin fibroblasts (Shiraha et al., 2000), the aged hippocampus (Enwere et al., 2004) and other systems (Rongo, 2011; Siddiqui et al., 2012). How age and SCI affect expression levels of EGF and EGFR is not known. One could speculate that EGFR expression is reduced within the spinal cord of age animals, and that its inhibition, regardless of its positive or negative impact on recovery in young animals, will likely have minimal impact on functional recovery in aged animals.

While manipulation of the growth factors to promote axon growth after injury seem complex, the general consensus is that a combinatorial approach is needed. This has been elegantly demonstrated in the recent work from the Sofroniew lab (Anderson et al., 2018). In this study, 3 mechanisms were targeted: increase of the neuron-intrinsic capacity (with osteopontin, IGF-1 and CDNF), increase in growth support at the injury site (with FGF2 and EGF), and chemoattractant caudal to the injury (GDNF). Only the combination of these three factors lead to strong axon regeneration. These data warrant further testing in the context of aging.

## Myelin Proteins and Constituents

Studies have found multiple potent neurite growth inhibitory factors that are enriched in CNS myelin, such as Nogo-A, myelin-associated glycoprotein (MAG), oligodendrocyte/myelin glycoprotein (OMgp). After injury, myelin sheaths are damaged, and these factors are released into the extra-cellular environment. These molecules alter the regenerative potential after CNS and targeting them or their receptors can enhance axon growth after SCI, although, some conflicting results have been reported. Indeed, some groups reported a beneficial effect of genetic Nogo deletion on axon regeneration and sprouting and others only on sprouting (Cafferty et al., 2010; Lee et al., 2010). For review (Geoffroy and Zheng, 2014).

Few studies examined how age alters the expression of these proteins. Nogo-A levels are significantly decreased in aged animals (Trifunovski et al., 2006; Kumari and Thakur, 2014). A decrease in recovery is surprisingly observed in 12-month-old Nogo A/B deficient mice after TBI, compared to young adults, possibly related to hypomyelination (Marklund et al., 2009). Aged brains with stroke present a unique profile in growth-inhibitory molecule changes (Li and Carmichael, 2006). In aged brains OMgp is increased earlier than in young animals; MAG is increased in old injured brains but decreased in young; and Nogo-A is decreased in the aged while increased in young mice Nogo receptor 1 (NgR1) antagonist has been shown to increase OPC maturation and remyelination, and motor recovery after stroke in aged mice (Sozmen et al., 2016). While Nogo-A is not altered in 12-month-old mice, at least at 6 weeks post injury (Geoffroy et al., 2016), the exact age-related profile change of these molecules at different time point after SCI has not been characterized. Indeed, as discussed in Section "The Inflammatory Response Changes with Age: 'Inflamm-Aging,'" there are been reports of reduction in debris clearance by aged macrophages and monocytes (Neumann et al., 2008; Natrajan et al., 2015). Therefore, one would speculate that the inhibitory myelin proteins stay longer at the injury site of older animals, and reduce axon growth potential. Additionally, the expression of the MHC1 receptor, PirB, is increased with age in the hippocampus, localized primarily in neurons. Induction of the MHC1 pathway in neurons is potentially linked to increased neuro-immune signaling and altered synaptic homeostasis, contributing to age-related hippocampal dysfunction (VanGuilder Starkey et al., 2012). If a similar pattern occurs in spinal neurons, it may lead to greater inhibition in aged neurons than their younger counterparts with the same amount of myelin proteins. PirB is increased in the spinal cord after injury (Zhou et al., 2010), while how age alters spinal expression of PirB is still to be elucidated. Similarly, NgR1, and its ligands, are increased in the hippocampus with age (VanGuilder Starkey et al., 2013). These data suggest that, even absent alterations in myelin protein levels, changes in neuronal expression of receptors may increase the inhibitory effects of these proteins on axon regeneration.

# CONCLUSION

The regeneration of damaged axons has been extensively studied in the PNS, and it has long been accepted that there is an age-dependent decline in regeneration after injury. Axon injury in the CNS is a more complex matter, however, it has recently been recognized that the CNS also present an age-dependent decline in axon regeneration. Our current understanding of this decline is still limited and requires greater exploration. The aging population, increasing average age of SCI incidence and longer life-expectancies of people living with SCI, creates a strong need to increase our understanding of the age-dependent obstacles for axonal repair. Axon regeneration is dependent on a myriad of neuron intrinsic and extrinsic factors. The nature and balance of these factors can result in the promotion or inhibition of growth. After CNS injury, there is no significant axonal regeneration which has been associated with a variety of neuron-intrinsic elements as well as interactions with the injury environment. There is currently a lack of published literature reviews, and preclinical studies at the intersection of aging and SCI research. In this review we have concentrated on the impact of the interaction with the inflammatory response, the resident glial cells and the extracellular environment, and how these are altered both in an injury and in an aging paradigm. We propose that the interaction

between injury and aging will compound the inherent difficulties and further inhibit the limited regenerative capability of the CNS. Finally, while this review focuses on the extrinsic factors that can influence the success of axon regeneration, the importance of the neuron-intrinsic factors and how these also interact with each other cannot be ignored.

## AUTHOR CONTRIBUTIONS

TS and CG conceived and wrote the manuscript.

## FUNDING

CG is a TIRR Foundation Fellow, and is supported by Mission Connect (018-002-1), Craig H. Neilsen Foundation (599148).

## ACKNOWLEDGMENTS

We thank Arthur Sefiani for help editing the manuscript. We also thank Graphit Science & Art, LLC for preparing the illustrations used in the figures.

## REFERENCES

Abbott, N. J. (2002). Astrocyte–endothelial interactions and blood–brain barrier permeability. *J. Anat.* 200, 629–638. doi: 10.1046/j.1469-7580.2002.00064.x

Adams, R. H., and Eichmann, A. (2010). Axon guidance molecules in vascular patterning. *Cold Spring Harb. Perspect. Biol.* 2:a001875. doi: 10.1101/cshperspect.a001875

Al-Shawi, R., Hafner, A., Chun, S., Raza, S., Crutcher, K., Thrasivoulou, C., et al. (2007). ProNGF, sortilin, and age-related neurodegeneration. *Ann. N. Y. Acad. Sci.* 1119, 208–215. doi: 10.1196/annals.1404.024

Al-Shawi, R., Hafner, A., Olson, J., Chun, S., Raza, S., Thrasivoulou, C., et al. (2008). Neurotoxic and neurotrophic roles of proNGF and the receptor sortilin in the adult and ageing nervous system. *Eur. J. Neurosci.* 27, 2103–2114. doi: 10.1111/j.1460-9568.2008.06152.x

Anderson, M. A., Ao, Y., and Sofroniew, M. V. (2014). Heterogeneity of reactive astrocytes. *Neurosci. Lett.* 565, 23–29. doi: 10.1016/j.neulet.2013.12.030

Anderson, M. A., Burda, J. E., Ren, Y., Ao, Y., O'shea, T. M., Kawaguchi, R., et al. (2016). Astrocyte scar formation aids central nervous system axon regeneration. *Nature* 532, 195–200. doi: 10.1038/nature17623

Anderson, M. A., O'shea, T. M., Burda, J. E., Ao, Y., Barlatey, S. L., Bernstein, A. M., et al. (2018). Required growth facilitators propel axon regeneration across complete spinal cord injury. *Nature* 561, 396–400. doi: 10.1038/s41586-018-0467-6

Askew, K., Li, K., Olmos-Alonso, A., Garcia-Moreno, F., Liang, Y., Richardson, P., et al. (2017). Coupled proliferation and apoptosis maintain the rapid turnover of microglia in the adult brain. *Cell Rep.* 18, 391–405. doi: 10.1016/j.celrep.2016.12.041

Badan, I., Buchhold, B., Hamm, A., Gratz, M., Walker, L., Platt, D., et al. (2003). Accelerated glial reactivity to stroke in aged rats correlates with reduced functional recovery. *J. Cereb. Blood Flow Metab.* 23, 845–854. doi: 10.1097/01.wcb.0000071883.63724.a7

Barone, F., Irving, E., Ray, A., Lee, J., Kassis, S., Kumar, S., et al. (2001). SB 239063, a second-generation p38 mitogen-activated protein kinase inhibitor, reduces brain injury and neurological deficits in cerebral focal ischemia. *J. Pharmacol. Exp. Ther.* 296, 312–321.

Bartus, K., James, N. D., Bosch, K. D., and Bradbury, E. J. (2012). Chondroitin sulphate proteoglycans: key modulators of spinal cord and brain plasticity. *Exp. Neurol.* 235, 5–17. doi: 10.1016/j.expneurol.2011.08.008

Beattie, M. S., Harrington, A. W., Lee, R., Kim, J. Y., Boyce, S. L., Longo, F. M., et al. (2002). ProNGF induces p75-mediated death of oligodendrocytes following spinal cord injury. *Neuron* 36, 375–386. doi: 10.1016/s0896-6273(02)01005-x

Bell, R. D., Winkler, E. A., Sagare, A. P., Singh, I., Larue, B., Deane, R., et al. (2010). Pericytes control key neurovascular functions and neuronal phenotype in the adult brain and during brain aging. *Neuron* 68, 409–427. doi: 10.1016/j.neuron.2010.09.043

Benowitz, L. I., and Popovich, P. G. (2011). Inflammation and axon regeneration. *Curr. Opin. Neurol.* 24, 577–583. doi: 10.1097/WCO.0b013e32834c208d

Berry, M., Ahmed, Z., Douglas, M. R., and Logan, A. (2011). Epidermal growth factor receptor antagonists and CNS axon regeneration: mechanisms and controversies. *Brain Res. Bull.* 84, 289–299. doi: 10.1016/j.brainresbull.2010.08.004

Birbrair, A., Zhang, T., Files, D. C., Mannava, S., Smith, T., Wang, Z.-M., et al. (2014). Type-1 pericytes accumulate after tissue injury and produce collagen in an organ-dependent manner. *Stem Cell Res. Ther.* 5:122. doi: 10.1186/scrt512

Blackmore, M., and Letourneau, P. C. (2006). Changes within maturing neurons limit axonal regeneration in the developing spinal cord. *J. Neurobiol.* 66, 348–360. doi: 10.1002/neu.20224

Boisvert, M. M., Erikson, G. A., Shokhirev, M. N., and Allen, N. J. (2018). The aging astrocyte transcriptome from multiple regions of the mouse brain. *Cell Rep.* 22, 269–285. doi: 10.1016/j.celrep.2017.12.039

Bordt, E. A., and Polster, B. M. (2014). NADPH oxidase-and mitochondria-derived reactive oxygen species in proinflammatory microglial activation: a bipartisan affair? *Free Radic. Biol. Med.* 76, 34–46. doi: 10.1016/j.freeradbiomed.2014.07.033

Bosetti, F., Galis, Z. S., Bynoe, M. S., Charette, M., Cipolla, M. J., Zoppo, G. J. D., et al. (2016). Small blood vessels: big health problems: scientific recommendations of the national institutes of health workshop. *J. Am. Heart Assoc.* 5:e004389.

Bovolenta, P., Wandosell, F., and Nieto-Sampedro, M. (1992). CNS glial scar tissue: a source of molecules which inhibit central neurite outgrowth. *Prog. Brain Res.* 94, 367–379. doi: 10.1016/s0079-6123(08)61765-3

Bradbury, E. J., and Burnside, E. R. (2019). Moving beyond the glial scar for spinal cord repair. *Nat. Commun.* 10:3879. doi: 10.1038/s41467-019-11707-7

Brennan, F. H., and Popovich, P. G. (2018). Emerging targets for reprograming the immune response to promote repair and recovery of function after spinal cord injury. *Curr. Opin. Neurol.* 31, 334–344. doi: 10.1097/WCO.0000000000000550

Brown, A., Ricci, M. J., and Weaver, L. C. (2004). NGF message and protein distribution in the injured rat spinal cord. *Exp. Neurol.* 188, 115–127. doi: 10.1016/j.expneurol.2004.03.017

Brown, K. M., Wolfe, B. B., and Wrathall, J. R. (2005). Rapid functional recovery after spinal cord injury in young rats. *J. Neurotrauma* 22, 559–574. doi: 10.1089/neu.2005.22.559

Budni, J., Bellettini-Santos, T., Mina, F., Garcez, M. L., and Zugno, A. I. (2015). The involvement of BDNF, NGF and GDNF in aging and Alzheimer's disease. *Aging Dis.* 6, 331–341. doi: 10.14336/AD.2015.0825

Busch, S. A., Hamilton, J. A., Horn, K. P., Cuascut, F. X., Cutrone, R., Lehman, N., et al. (2011). Multipotent adult progenitor cells prevent macrophage-mediated axonal dieback and promote regrowth after spinal cord injury. *J. Neurosci.* 31, 944–953. doi: 10.1523/JNEUROSCI.3566-10.2011

Byrne, A. B., Walradt, T., Gardner, K. E., Hubbert, A., Reinke, V., and Hammarlund, M. (2014). Insulin/IGF1 signaling inhibits age-dependent axon regeneration. *Neuron* 81, 561–573. doi: 10.1016/j.neuron.2013.11.019

Cafferty, W. B., Duffy, P., Huebner, E., and Strittmatter, S. M. (2010). MAG and OMgp synergize with Nogo-A to restrict axonal growth and neurological recovery after spinal cord trauma. *J. Neurosci.* 30, 6825–6837. doi: 10.1523/JNEUROSCI.6239-09.2010

Cantuti-Castelvetri, L., Fitzner, D., Bosch-Queralt, M., Weil, M.-T., Su, M., Sen, P., et al. (2018). Defective cholesterol clearance limits remyelination in the aged central nervous system. *Science* 359, 684–688. doi: 10.1126/science.aan4183

Castillo-Ruiz, M., Campuzano, O., Acarin, L., Castellano, B., and Gonzalez, B. J. E. G. (2007). Delayed neurodegeneration and early astrogliosis after excitotoxicity to the aged brain. *Exp. Gerontol.* 42, 343–354. doi: 10.1016/j.exger.2006.10.008

Chen, M., Geoffroy, C. G., Meves, J. M., Narang, A., Li, Y., Nguyen, M. T., et al. (2018). Leucine zipper-bearing kinase is a critical regulator of astrocyte reactivity in the adult mammalian CNS. *Cell Rep.* 22, 3587–3597. doi: 10.1016/j.celrep.2018.02.102

Chen, M., Geoffroy, C. G., Wong, H. N., Tress, O., Nguyen, M. T., Holzman, L. B., et al. (2016). Leucine zipper-bearing kinase promotes axon growth in mammalian central nervous system neurons. *Sci. Rep.* 6:31482. doi: 10.1038/srep31482

Cho, D. Y., Mold, J. W., and Roberts, M. (2006). Further investigation of the negative association between hypertension and peripheral neuropathy in the elderly: an Oklahoma physicians resource/research network (OKPRN) study. *J. Am. Board Fam. Med.* 19, 240–250. doi: 10.3122/jabfm.19.3.240

Christopher and Dana Reeve Foundation (2009). *One Degree of Separation: Paralysis and Spinal Cord Injury in the United States*. Millburn, NJ: Christopher and Dana Reeve Foundation. Available online at: http://s3.amazonaws.com/reeve-assets-production/8112REPTFINAL.PDF

Clarke, L. E., Liddelow, S. A., Chakraborty, C., Münch, A. E., Heiman, M., and Barres, B. A. (2018). Normal aging induces A1-like astrocyte reactivity. *Proc. Natl. Acad. Sci. U.S.A.* 115, E1896–E1905. doi: 10.1073/pnas.1800165115

Codeluppi, S., Svensson, C. I., Hefferan, M. P., Valencia, F., Silldorff, M. D., Oshiro, M., et al. (2009). The Rheb-mTOR pathway is upregulated in reactive astrocytes of the injured spinal cord. *J. Neurosci.* 29, 1093–1104. doi: 10.1523/JNEUROSCI.4103-08.2009

Cohen, J., and Torres, C. (2019). Astrocyte senescence: evidence and significance. *Aging Cell* 18:e12937. doi: 10.1111/acel.12937

Cotrina, M. L., and Nedergaard, M. (2002). Astrocytes in the aging brain. *J. Neurosci. Res.* 67, 1–10.

Cunningham, C., Dunne, A., and Lopez-Rodriguez, A. B. (2019). Astrocytes: heterogeneous and dynamic phenotypes in neurodegeneration and innate immunity. *Neuroscientist* 25, 455–474. doi: 10.1177/1073858418809941

Damani, M. R., Zhao, L., Fontainhas, A. M., Amaral, J., Fariss, R. N., and Wong, W. T. (2011). Age-related alterations in the dynamic behavior of microglia. *Aging Cell* 10, 263–276. doi: 10.1111/j.1474-9726.2010.00660.x

Das, M. M., and Svendsen, C. N. (2015). Astrocytes show reduced support of motor neurons with aging that is accelerated in a rodent model of ALS. *Neurobiol. Aging* 36, 1130–1139. doi: 10.1016/j.neurobiolaging.2014.09.020

d'Avila, J. C., Siqueira, L. D., Mazeraud, A., Azevedo, E. P., Foguel, D., Castro-Faria-Neto, H. C., et al. (2018). Age-related cognitive impairment is associated with long-term neuroinflammation and oxidative stress in a mouse model of episodic systemic inflammation. *J. Neuroinflammation* 15:28. doi: 10.1186/s12974-018-1059-y

De Martinis, M., Franceschi, C., Monti, D., and Ginaldi, L. (2005). Inflamm-ageing and lifelong antigenic load as major determinants of ageing rate and longevity. *FEBS Lett.* 579, 2035–2039. doi: 10.1016/j.febslet.2005.02.055

Devivo, M. J. (2012). Epidemiology of traumatic spinal cord injury: trends and future implications. *J. Spinal. Cord.* 50, 365–372. doi: 10.1038/sc.2011.178

Devivo, M. J., and Chen, Y. (2011). Trends in new injuries, prevalent cases, and aging with spinal cord injury. *Arch. Phys. Med. Rehabil.* 92, 332–338. doi: 10.1016/j.apmr.2010.08.031

Devivo, M. J., Kartus, P. L., Rutt, R. D., Stover, S. L., and Fine, P. R. (1990). The influence of age at time of spinal cord injury on rehabilitation outcome. *Arch. Neurol.* 47, 687–691.

Dheen, S. T., Kaur, C., and Ling, E. A. (2007). Microglial activation and its implications in the brain diseases. *Curr. Med. Chem.* 14, 1189–1197. doi: 10.2174/092986707780597961

Dias, D. O., and Göritz, C. (2018). Fibrotic scarring following lesions to the central nervous system. *Matrix Biol.* 68, 561–570. doi: 10.1016/j.matbio.2018.02.009

Dias, D. O., Kim, H., Holl, D., Solnestam, B. W., Lundeberg, J., Carlén, M., et al. (2018). Reducing pericyte-derived scarring promotes recovery after spinal cord injury. *Cell* 173, 153–165.e22. doi: 10.1016/j.cell.2018.02.004

Donnelly, D. J., and Popovich, P. G. (2008). Inflammation and its role in neuroprotection, axonal regeneration and functional recovery after spinal cord injury. *Exp. Neurol.* 209, 378–388. doi: 10.1016/j.expneurol.2007.06.009

Dorner, H., Fischer, B., Platt, D., Kessler, C., and Popa-Wagner, A. (1996). V+ fibronectin mRNA is increased in the brains of aged rats: effect of food restriction. *Brain Res.* 726, 198–206. doi: 10.1016/0006-8993(96)00334-4

Dougherty, K. D., Dreyfus, C. F., and Black, I. B. (2000). Brain-derived neurotrophic factor in astrocytes, oligodendrocytes, and microglia/macrophages after spinal cord injury. *Neurobiol. Dis.* 7, 574–585. doi: 10.1006/nbdi.2000.0318

Doyle, K. P., Cekanaviciute, E., Mamer, L. E., and Buckwalter, M. S. J. J. O. N. (2010). TGFβ signaling in the brain increases with aging and signals to astrocytes and innate immune cells in the weeks after stroke. *J. Neuroinflammation* 7:62. doi: 10.1186/1742-2094-7-62

Du, K., Zheng, S., Zhang, Q., Li, S., Gao, X., Wang, J., et al. (2015). Pten deletion promotes regrowth of corticospinal tract axons 1 year after spinal cord injury. *J. Neurosci.* 35, 9754–9763. doi: 10.1523/JNEUROSCI.3637-14.2015

Duan, W., Zhang, R., Guo, Y., Jiang, Y., Huang, Y., Jiang, H., et al. (2009). Nrf2 activity is lost in the spinal cord and its astrocytes of aged mice. *In Vitro Cell. Dev. Biol. Anim.* 45, 388–397. doi: 10.1007/s11626-009-9194-5

Dupraz, S., Grassi, D., Karnas, D., Nieto Guil, A. F., Hicks, D., and Quiroga, S. (2013). The insulin-like growth factor 1 receptor is essential for axonal regeneration in adult central nervous system neurons. *PLoS One* 8:e54462. doi: 10.1371/journal.pone.0054462

Duraikannu, A., Krishnan, A., Chandrasekhar, A., and Zochodne, D. W. (2019). Beyond trophic factors: exploiting the intrinsic regenerative properties of adult neurons. *Front. Cell. Neurosci.* 13:128. doi: 10.3389/fncel.2019.00128

Duricki, D. A., Hutson, T. H., Kathe, C., Soleman, S., Gonzalez-Carter, D., Petruska, J. C., et al. (2016). Delayed intramuscular human neurotrophin-3 improves recovery in adult and elderly rats after stroke. *Brain* 139, 259–275. doi: 10.1093/brain/awv341

Dyer, A. H., Vahdatpour, C., Sanfeliu, A., and Tropea, D. (2016). The role of insulin-like growth factor 1 (IGF-1) in brain development, maturation and neuroplasticity. *Neuroscience* 325, 89–99. doi: 10.1016/j.neuroscience.2016.03.056

Elmore, M. R., Hohsfield, L. A., Kramár, E. A., Soreq, L., Lee, R. J., Pham, S. T., et al. (2018). Replacement of microglia in the aged brain reverses cognitive, synaptic, and neuronal deficits in mice. *Aging Cell* 17:e12832. doi: 10.1111/acel.12832

Enwere, E., Shingo, T., Gregg, C., Fujikawa, H., Ohta, S., and Weiss, S. (2004). Aging results in reduced epidermal growth factor receptor signaling, diminished olfactory neurogenesis, and deficits in fine olfactory discrimination. *J. Neurosci.* 24, 8354–8365. doi: 10.1523/jneurosci.2751-04.2004

Erdő, F., Denes, L., and De Lange, E. (2017). Age-associated physiological and pathological changes at the blood–brain barrier: a review. *J. Cereb. Blood Flow Metab.* 37, 4–24. doi: 10.1177/0271678x16679420

Erickson, K. I., Prakash, R. S., Voss, M. W., Chaddock, L., Heo, S., Mclaren, M., et al. (2010). Brain-derived neurotrophic factor is associated with age-related decline in hippocampal volume. *J. Neurosci.* 30, 5368–5375. doi: 10.1523/JNEUROSCI.6251-09.2010

Erschbamer, M., Pernold, K., and Olson, L. (2007). Inhibiting epidermal growth factor receptor improves structural, locomotor, sensory, and bladder recovery from experimental spinal cord injury. *J. Neurosci.* 27, 6428–6435. doi: 10.1523/jneurosci.1037-07.2007

Falcão, A. M., Van Bruggen, D., Marques, S., Meijer, M., Jäkel, S., Agirre, E., et al. (2018). Disease-specific oligodendrocyte lineage cells arise in multiple sclerosis. *Nat. Med.* 24, 1837–1844. doi: 10.1038/s41591-018-0236-y

Farooque, M., Zhang, Y., Holtz, A., and Olsson, Y. (1992). Exudation of fibronectin and albumin after spinal cord injury in rats. *Acta Neuropathol.* 84, 613–620.

Faulkner, J. R., Herrmann, J. E., Woo, M. J., Tansey, K. E., Doan, N. B., and Sofroniew, M. V. (2004). Reactive astrocytes protect tissue and preserve function after spinal cord injury. *J. Neurosci.* 24, 2143–2155. doi: 10.1523/jneurosci.3547-03.2004

Fawcett, J. W., and Asher, R. A. (1999). The glial scar and central nervous system repair. *Brain Res. Bull.* 49, 377–391. doi: 10.1016/s0361-9230(99)00072-6

Fenn, A. M., Hall, J. C., Gensel, J. C., Popovich, P. G., and Godbout, J. P. (2014). IL-4 signaling drives a unique arginase+/IL-1β+ microglia phenotype and recruits macrophages to the inflammatory CNS: consequences of age-related deficits in IL-4Rα after traumatic spinal cord injury. *J. Neurosci.* 34, 8904–8917. doi: 10.1523/jneurosci.1146-14.2014

Ferrer, I. (2017). Diversity of astroglial responses across human neurodegenerative disorders and brain aging. *J. Brain Pathol.* 27, 645–674. doi: 10.1111/bpa.12538

Fleming, J. C., Norenberg, M. D., Ramsay, D. A., Dekaban, G. A., Marcillo, A. E., Saenz, A. D., et al. (2006). The cellular inflammatory response in human spinal cords after injury. *Brain* 129, 3249–3269. doi: 10.1093/brain/awl296

Foscarin, S., Raha-Chowdhury, R., Fawcett, J. W., and Kwok, J. C. F. (2017). Brain ageing changes proteoglycan sulfation, rendering perineuronal nets more inhibitory. *Aging* 9, 1607–1622. doi: 10.18632/aging.101256

Fouad, K., Bixby, J. L., Callahan, A., Grethe, J. S., Jakeman, L. B., Lemmon, V. P., et al. (2019). FAIR SCI ahead: the evolution of the open data commons for pre-clinical spinal cord injury research. *J. Neurotrauma* doi: 10.1089/neu.2019.6674 [Epub ahead of print].

Frisen, J., Haegerstrand, A., Risling, M., Fried, K., Johansson, C. B., Hammarberg, H., et al. (1995). Spinal axons in central nervous system scar tissue are closely related to laminin-immunoreactive astrocytes. *Neuroscience* 65, 293–304. doi: 10.1016/0306-4522(94)00467-j

Gaesser, J. M., and Fyffe-Maricich, S. L. (2016). Intracellular signaling pathway regulation of myelination and remyelination in the CNS. *Exp. Neurol.* 283, 501–511. doi: 10.1016/j.expneurol.2016.03.008

Galbavy, W., Lu, Y., Kaczocha, M., Puopolo, M., Liu, L., and Rebecchi, M. J. (2017). Transcriptomic evidence of a para-inflammatory state in the middle aged lumbar spinal cord. *Immun. Ageing* 14:9. doi: 10.1186/s12979-017-0091-6

Garraway, S. M., and Huie, J. R. (2016). Spinal plasticity and behavior: BDNF-induced neuromodulation in uninjured and injured spinal cord. *Neural Plast.* 2016:9857201.

Genis, L., Dávila, D., Fernandez, S., Pozo-Rodrigálvarez, A., Martínez-Murillo, R., and Torres-Aleman, I. (2014). Astrocytes require insulin-like growth factor I to protect neurons against oxidative injury [version 2; peer review: 3 approved]. *F1000Res.* 3:28. doi: 10.12688/f1000research.3-28.v2

Gensel, J. C., Nakamura, S., Guan, Z., Van Rooijen, N., Ankeny, D. P., and Popovich, P. G. (2009). Macrophages promote axon regeneration with concurrent neurotoxicity. *J. Neurosci.* 29, 3956–3968. doi: 10.1523/JNEUROSCI.3992-08.2009

Gensel, J. C., and Zhang, B. (2015). Macrophage activation and its role in repair and pathology after spinal cord injury. *Brain Res.* 1619, 1–11. doi: 10.1016/j.brainres.2014.12.045

Geoffroy, C. G., Hilton, B. J., Tetzlaff, W., and Zheng, B. (2016). Evidence for an age-dependent decline in axon regeneration in the adult mammalian central nervous system. *Cell Rep.* 15, 238–246. doi: 10.1016/j.celrep.2016.03.028

Geoffroy, C. G., Lorenzana, A. O., Kwan, J. P., Lin, K., Ghassemi, O., Ma, A., et al. (2015). Effects of PTEN and Nogo codeletion on corticospinal axon sprouting and regeneration in mice. *J. Neurosci.* 35, 6413–6428. doi: 10.1523/JNEUROSCI.4013-14.2015

Geoffroy, C. G., Meves, J. M., and Zheng, B. (2017). The age factor in axonal repair after spinal cord injury: a focus on neuron-intrinsic mechanisms. *Neurosci. Lett.* 652, 41–49. doi: 10.1016/j.neulet.2016.11.003

Geoffroy, C. G., and Zheng, B. (2014). Myelin-associated inhibitors in axonal growth after CNS injury. *Curr. Opin. Neurobiol.* 27, 31–38. doi: 10.1016/j.conb.2014.02.012

George, N., and Geller, H. M. (2018). Extracellular matrix and traumatic brain injury. *J. Neurosci. Res.* 96, 573–588. doi: 10.1002/jnr.24151

Godbout, J., Chen, J., Abraham, J., Richwine, A., Berg, B., Kelley, K., et al. (2005). Exaggerated neuroinflammation and sickness behavior in aged mice following activation of the peripheral innate immune system. *FASEB J.* 19, 1329–1331. doi: 10.1096/fj.05-3776fje

Gordon, S., and Martinez, F. O. (2010). Alternative activation of macrophages: mechanism and functions. *Immunity* 32, 593–604. doi: 10.1016/j.immuni.2010.05.007

Göritz, C., Dias, D. O., Tomilin, N., Barbacid, M., Shupliakov, O., and Frisén, J. (2011). A pericyte origin of spinal cord scar tissue. *Science* 333, 238–242. doi: 10.1126/science.1203165

Graciarena, M., Dambly-Chaudière, C., and Ghysen, A. (2014). Dynamics of axonal regeneration in adult and aging zebrafish reveal the promoting effect of a first lesion. *Proc. Natl. Acad. Sci. U.S.A.* 111, 1610–1615. doi: 10.1073/pnas.1319405111

Grasman, J. M., and Kaplan, D. L. (2017). Human endothelial cells secrete neurotropic factors to direct axonal growth of peripheral nerves. *Sci. Rep.* 7, 4092–4092. doi: 10.1038/s41598-017-04460-8

Greising, S. M., Ermilov, L. G., Sieck, G. C., and Mantilla, C. B. (2015). Ageing and neurotrophic signalling effects on diaphragm neuromuscular function. *J. Physiol.* 593, 431–440. doi: 10.1113/jphysiol.2014.282244

Greising, S. M., Vasdev, A. K., Zhan, W.-Z., Sieck, G. C., and Mantilla, C. B. (2017). Chronic TrkB agonist treatment in old age does not mitigate diaphragm neuromuscular dysfunction. *Physiol. Rep.* 5:e13103. doi: 10.14814/phy2.13103

Gwak, Y. S., Hains, B. C., Johnson, K. M., and Hulsebosch, C. E. (2004). Effect of age at time of spinal cord injury on behavioral outcomes in rat. *J. Neurotrauma* 21, 983–993. doi: 10.1089/0897715041650999

Hackett, A. R., and Lee, J. K. (2016). Understanding the NG2 glial scar after spinal cord injury. *Front. Neurol.* 7:199. doi: 10.3389/fneur.2016.00199

Hackett, A. R., Yahn, S. L., Lyapichev, K., Dajnoki, A., Lee, D.-H., Rodriguez, M., et al. (2018). Injury type-dependent differentiation of NG2 glia into heterogeneous astrocytes. *Exp. Neurol.* 308, 72–79. doi: 10.1016/j.expneurol.2018.07.001

Haim, L. B., Ceyzériat, K., Carrillo-De Sauvage, M. A., Aubry, F., Auregan, G., Guillermier, M., et al. (2015). The JAK/STAT3 pathway is a common inducer of astrocyte reactivity in Alzheimer's and Huntington's diseases. *J. Neurosci.* 35, 2817–2829. doi: 10.1523/JNEUROSCI.3516-14.2015

Hammarlund, M., and Jin, Y. (2014). Axon regeneration in *C. elegans*. *Curr. Opin. Neurobiol.* 27, 199–207. doi: 10.1016/j.conb.2014.04.001

Han, Q., Ordaz, J. D., Liu, N.-K., Richardson, Z., Wu, W., Xia, Y., et al. (2019). Descending motor circuitry required for NT-3 mediated locomotor recovery after spinal cord injury in mice. *Nat. Commun.* 10:5815. doi: 10.1038/s41467-019-13854-3

Hara, M., Kobayakawa, K., Ohkawa, Y., Kumamaru, H., Yokota, K., Saito, T., et al. (2017). Interaction of reactive astrocytes with type I collagen induces astrocytic scar formation through the integrin-N-cadherin pathway after spinal cord injury. *Nat. Med.* 23, 818–828. doi: 10.1038/nm.4354

He, Z., and Jin, Y. (2016). Intrinsic control of axon regeneration. *Neuron* 90, 437–451. doi: 10.1016/j.neuron.2016.04.022

Hernandez-Garzón, E., Fernandez, A. M., Perez-Alvarez, A., Genis, L., Bascuñana, P., Fernandez De La Rosa, R., et al. (2016). The insulin-like growth factor I receptor regulates glucose transport by astrocytes. *Glia* 64, 1962–1971. doi: 10.1002/glia.23035

Herrmann, J. E., Imura, T., Song, B., Qi, J., Ao, Y., Nguyen, T. K., et al. (2008). STAT3 is a critical regulator of astrogliosis and scar formation after spinal cord injury. *J. Neurosci.* 28, 7231–7243. doi: 10.1523/jneurosci.1709-08.2008

Hesp, Z. C., Yoseph, R. Y., Suzuki, R., Jukkola, P., Wilson, C., Nishiyama, A., et al. (2018). Proliferating NG2-cell-dependent angiogenesis and scar formation alter axon growth and functional recovery after spinal cord injury in mice. *J. Neurosci.* 38, 1366–1382. doi: 10.1523/JNEUROSCI.3953-16.2017

Hickman, S. E., Allison, E. K., and El Khoury, J. (2008). Microglial dysfunction and defective β-amyloid clearance pathways in aging Alzheimer's disease mice. *J. Neurosci.* 28, 8354–8360. doi: 10.1523/JNEUROSCI.0616-08.2008

Hohlfeld, R., Kerschensteiner, M., and Meinl, E. (2007). Dual role of inflammation in CNS disease. *Neurology* 68, S58–S63.

Hollis, E. R., Lu, P., Blesch, A., and Tuszynski, M. H. (2009). IGF-I gene delivery promotes corticospinal neuronal survival but not regeneration after adult CNS injury. *Exp. Neurol.* 215, 53–59. doi: 10.1016/j.expneurol.2008.09.014

Hooshmand, M. J., Galvan, M. D., Partida, E., and Anderson, A. J. (2014). Characterization of recovery, repair, and inflammatory processes following contusion spinal cord injury in old female rats: is age a limitation? *Immun. Ageing* 11:15. doi: 10.1186/1742-4933-11-15

Horn, K. P., Busch, S. A., Hawthorne, A. L., Van Rooijen, N., and Silver, J. (2008). Another barrier to regeneration in the CNS: activated macrophages induce extensive retraction of dystrophic axons through direct physical interactions. *J. Neurosci.* 28, 9330–9341. doi: 10.1523/JNEUROSCI.2488-08.2008

Howcroft, T. K., Campisi, J., Louis, G. B., Smith, M. T., Wise, B., Wyss-Coray, T., et al. (2013). The role of inflammation in age-related disease. *Aging* 5, 84–93.

Huebner, E. A., and Strittmatter, S. M. (2009). "Axon regeneration in the peripheral and central nervous systems," in *Cell Biology of the Axon. Results and Problems in Cell Differentiation*, Vol. 48, ed. E. Koenig (Berlin: Springer).

Hurley, M. M., Gronowicz, G., Zhu, L., Kuhn, L. T., Rodner, C., and Xiao, L. (2016). Age-related changes in FGF-2, fibroblast growth factor receptors and β-catenin expression in human mesenchyme-derived progenitor cells. *J. Cell. Biochem.* 117, 721–729. doi: 10.1002/jcb.25357

Ikeda, K., Iwasaki, Y., Shiojima, T., and Kinoshita, M. (1996). Neuroprotective effect of various cytokines on developing spinal motoneurons following axotomy. *J. Neurol. Sci.* 135, 109–113. doi: 10.1016/0022-510x(95)00263-2

Ito, M., Natsume, A., Takeuchi, H., Shimato, S., Ohno, M., Wakabayashi, T., et al. (2009). Type I interferon inhibits astrocytic gliosis and promotes functional recovery after spinal cord injury by deactivation of the MEK/ERK pathway. *J. Neurotrauma* 26, 41–53. doi: 10.1089/neu.2008.0646

Jacob, M., Chappell, D., and Becker, B. F. (2016). Regulation of blood flow and volume exchange across the microcirculation. *Crit. Care* 20:319.

Jaerve, A., Schiwy, N., Schmitz, C., and Mueller, H. W. (2011). Differential effect of aging on axon sprouting and regenerative growth in spinal cord injury. *Exp. Neurol.* 231, 284–294. doi: 10.1016/j.expneurol.2011.07.002

James, S. L., Theadom, A., Ellenbogen, R. G., Bannick, M. S., Montjoy-Venning, W., Lucchesi, L. R., et al. (2019). Global, regional, and national burden of traumatic brain injury and spinal cord injury, 1990–2016: a systematic analysis for the global burden of disease study 2016. *Lancet Neurol.* 18, 56–87.

Jiang, T., and Cadenas, E. (2014). Astrocytic metabolic and inflammatory changes as a function of age. *Aging Cell* 13, 1059–1067. doi: 10.1111/acel.12268

Jucker, M., Tian, M., and Ingram, D. K. (1996). Laminins in the adult and aged brain. *Mol. Chem. Neuropathol.* 28, 209–218. doi: 10.1007/bf02815224

Kaminska, B. (2005). MAPK signalling pathways as molecular targets for anti-inflammatory therapy—from molecular mechanisms to therapeutic benefits. *Biochim. Biophys. Acta* 1754, 253–262. doi: 10.1016/j.bbapap.2005.08.017

Kane, C. J., Sims, T. J., and Gilmore, S. A. (1997). Astrocytes in the aged rat spinal cord fail to increase GFAP mRNA following sciatic nerve axotomy. *Brain Res.* 759, 163–165. doi: 10.1016/s0006-8993(97)00359-4

Kang, H., and Lichtman, J. W. (2013). Motor axon regeneration and muscle reinnervation in young adult and aged animals. *J. Neurosci.* 33, 19480–19491. doi: 10.1523/JNEUROSCI.4067-13.2013

Kang, W., Balordi, F., Su, N., Chen, L., Fishell, G., and Hebert, J. M. (2014). Astrocyte activation is suppressed in both normal and injured brain by FGF signaling. *Proc. Natl. Acad. Sci. U.S.A.* 111, E2987–E2995. doi: 10.1073/pnas.1320401111

Kang, W., and Hébert, J. M. (2011). Signaling pathways in reactive astrocytes, a genetic perspective. *Mol. Neurobiol.* 43, 147–154. doi: 10.1007/s12035-011-8163-7

Kanno, H., Ozawa, H., Sekiguchi, A., Yamaya, S., Tateda, S., Yahata, K., et al. (2012). The role of mTOR signaling pathway in spinal cord injury. *Cell Cycle* 11, 3175–3179. doi: 10.4161/cc.21262

Kawano, H., Kimura-Kuroda, J., Komuta, Y., Yoshioka, N., Li, H. P., Kawamura, K., et al. (2012). Role of the lesion scar in the response to damage and repair of the central nervous system. *Cell Tissue Res.* 349, 169–180. doi: 10.1007/s00441-012-1336-5

Kawano, H., Li, H. P., Sango, K., Kawamura, K., and Raisman, G. (2005). Inhibition of collagen synthesis overrides the age-related failure of regeneration of nigrostriatal dopaminergic axons. *J. Neurosci. Res.* 80, 191–202. doi: 10.1002/jnr.20441

Keefe, K. M., Sheikh, I. S., and Smith, G. M. (2017). Targeting neurotrophins to specific populations of neurons: NGF, BDNF, and NT-3 and their relevance for treatment of spinal cord injury. *Int. J. Mol. Sci.* 18:548. doi: 10.3390/ijms18030548

Kerezoudi, E., and Thomas, P. (1999). Influence of age on regeneration in the peripheral nervous system. *Gerontology* 45, 301–306. doi: 10.1159/000022109

Kigerl, K. A., Gensel, J. C., Ankeny, D. P., Alexander, J. K., Donnelly, D. J., and Popovich, P. G. (2009). Identification of two distinct macrophage subsets with divergent effects causing either neurotoxicity or regeneration in the injured mouse spinal cord. *J. Neurosci.* 29, 13435–13444. doi: 10.1523/jneurosci.3257-09.2009

Koellhoffer, E., Mccullough, L., and Ritzel, R. (2017). Old maids: aging and its impact on microglia function. *Int. J. Mol. Sci.* 18:769. doi: 10.3390/ijms18040769

Koprivica, V., Cho, K. S., Park, J. B., Yiu, G., Atwal, J., Gore, B., et al. (2005). EGFR activation mediates inhibition of axon regeneration by myelin and chondroitin sulfate proteoglycans. *Science* 310, 106–110. doi: 10.1126/science.1115462

Koser, D. E., Thompson, A. J., Foster, S. K., Dwivedy, A., Pillai, E. K., Sheridan, G. K., et al. (2016). Mechanosensing is critical for axon growth in the developing brain. *Nat. Neurosci.* 19, 1592–1598. doi: 10.1038/nn.4394

Kumamaru, H., Saiwai, H., Ohkawa, Y., Yamada, H., Iwamoto, Y., and Okada, S. (2012). Age-related differences in cellular and molecular profiles of inflammatory responses after spinal cord injury. *J. Cell. Physiol.* 227, 1335–1346. doi: 10.1002/jcp.22845

Kumari, A., and Thakur, M. K. (2014). Age-dependent decline of nogo-a protein in the mouse cerebrum. *Cell. Mol. Neurobiol.* 34, 1131–1141. doi: 10.1007/s10571-014-0088-z

Kumazaki, T., Kobayashi, M., and Mitsui, Y. (1993). Enhanced expression of fibronectin during in vivo cellular aging of human vascular endothelial cells and skin fibroblasts. *Exp. Cell Res.* 205, 396–402. doi: 10.1006/excr.1993.1103

Kwon, B. K., Tetzlaff, W., Grauer, J. N., Beiner, J., and Vaccaro, A. R. J. T. S. J. (2004). Pathophysiology and pharmacologic treatment of acute spinal cord injury. *Spine J.* 4, 451–464. doi: 10.1016/j.spinee.2003.07.007

Labandeira-Garcia, J. L., Costa-Besada, M. A., Labandeira, C. M., Villar-Cheda, B., and Rodríguez-Perez, A. I. (2017). Insulin-like growth factor-1 and neuroinflammation. *Front. Aging Neurosci.* 9:365. doi: 10.3389/fnagi.2017.00365

Labat-Robert, J. (2004). Cell-matrix interactions in aging: role of receptors and matricryptins. *Ageing Res. Rev.* 3, 233–247. doi: 10.1016/j.arr.2003.10.002

Lalancette-Hébert, M., Gowing, G., Simard, A., Weng, Y. C., and Kriz, J. (2007). Selective ablation of proliferating microglial cells exacerbates ischemic injury in the brain. *J. Neurosci.* 27, 2596–2605. doi: 10.1523/jneurosci.5360-06.2007

Lamoureux, P. L., O'toole, M. R., Heidemann, S. R., and Miller, K. E. (2010). Slowing of axonal regeneration is correlated with increased axonal viscosity during aging. *BMC Neurosci.* 11:140. doi: 10.1186/1471-2202-11-140

Lecours, C., Bordeleau, M., Cantin, L., Parent, M., Dipaolo, T., and Tremblay, M.-E. (2018). Microglial implication in Parkinson's disease: loss of beneficial physiological roles or gain of inflammatory functions? *Front. Cell. Neurosci.* 12:282. doi: 10.3389/fncel.2018.00282

Lee, J. K., Geoffroy, C. G., Chan, A. F., Tolentino, K. E., Crawford, M. J., Leal, M. A., et al. (2010). Assessing spinal axon regeneration and sprouting in Nogo-, MAG-, and OMgp-deficient mice. *Neuron* 66, 663–670. doi: 10.1016/j.neuron.2010.05.002

Lee, M. J., Chen, C. J., Cheng, C. H., Huang, W. C., Kuo, H. S., Wu, J. C., et al. (2008). Combined treatment using peripheral nerve graft and FGF-1: changes to the glial environment and differential macrophage reaction in a complete transected spinal cord. *Neurosci. Lett.* 433, 163–169. doi: 10.1016/j.neulet.2007.11.067

Lee, M. J., Chen, C. J., Huang, W. C., Huang, M. C., Chang, W. C., Kuo, H. S., et al. (2011). Regulation of chondroitin sulphate proteoglycan and reactive gliosis after spinal cord transection: effects of peripheral nerve graft and fibroblast growth factor 1. *Neuropathol. Appl. Neurobiol.* 37, 585–599. doi: 10.1111/j.1365-2990.2011.01182.x

Lendahl, U., Nilsson, P., and Betsholtz, C. (2019). Emerging links between cerebrovascular and neurodegenerative diseases—a special role for pericytes. *EMBO Rep.* 20:e48070. doi: 10.15252/embr.201948070

Lennmyr, F., Ericsson, A., Gerwins, P., Ahlström, H., and Terént, A. (2003). Increased brain injury and vascular leakage after pretreatment with p38-inhibitor SB203580 in transient ischemia. *Acta Neurol. Scand.* 108, 339–345. doi: 10.1034/j.1600-0404.2003.00129.x

Li, C.-Y., Li, X., Liu, S.-F., Qu, W.-S., Wang, W., and Tian, D.-S. (2015). Inhibition of mTOR pathway restrains astrocyte proliferation, migration and production of inflammatory mediators after oxygen–glucose deprivation and reoxygenation. *Neurochem. Int.* 83, 9–18. doi: 10.1016/j.neuint.2015.03.001

Li, H.-P., Komuta, Y., Kimura-Kuroda, J., Van Kuppevelt, T. H., and Kawano, H. (2013). Roles of chondroitin sulfate and dermatan sulfate in the formation of a lesion scar and axonal regeneration after traumatic injury of the mouse brain. *J. Neurotrauma* 30, 413–425. doi: 10.1089/neu.2012.2513

Li, S., and Carmichael, S. T. (2006). Growth-associated gene and protein expression in the region of axonal sprouting in the aged brain after stroke. *Neurobiol. Dis.* 23, 362–373. doi: 10.1016/j.nbd.2006.03.011

Li, W. (2013). Phagocyte dysfunction, tissue aging and degeneration. *Ageing Res. Rev.* 12, 1005–1012. doi: 10.1016/j.arr.2013.05.006

Li, Y., Xie, L., Huang, T., Zhang, Y., Zhou, J., Qi, B., et al. (2019). Aging neurovascular unit and potential role of DNA damage and repair in combating vascular and neurodegenerative disorders. *Front. Neurosci.* 13:778. doi: 10.3389/fnins.2019.00778

Li, Z.-W., Tang, R.-H., Zhang, J.-P., Tang, Z.-P., Qu, W.-S., Zhu, W.-H., et al. (2011). Inhibiting epidermal growth factor receptor attenuates reactive

astrogliosis and improves functional outcome after spinal cord injury in rats. *Neurochem. Int.* 58, 812–819. doi: 10.1016/j.neuint.2011.03.007

Liesi, P., and Kauppila, T. (2002). Induction of type IV collagen and other basement-membrane-associated proteins after spinal cord injury of the adult rat may participate in formation of the glial scar. *Exp. Neurol.* 173, 31–45. doi: 10.1006/exnr.2001.7800

Lin, J., Huo, X., and Liu, X. (2017). "mTOR signaling pathway": a potential target of curcumin in the treatment of spinal cord injury. *Biomed Res. Int.* 2017:1634801. doi: 10.1155/2017/1634801

Linehan, E., Dombrowski, Y., Snoddy, R., Fallon, P. G., Kissenpfennig, A., and Fitzgerald, D. C. (2014). Aging impairs peritoneal but not bone marrow-derived macrophage phagocytosis. *Aging Cell* 13, 699–708. doi: 10.1111/acel.12223

Liu, B., Chen, H., Johns, T. G., and Neufeld, A. H. (2006). Epidermal growth factor receptor activation: an upstream signal for transition of quiescent astrocytes into reactive astrocytes after neural injury. *J. Neurosci.* 26, 7532–7540. doi: 10.1523/jneurosci.1004-06.2006

Liu, Y., Wang, X., Li, W., Zhang, Q., Li, Y., Zhang, Z., et al. (2017). A sensitized IGF1 treatment restores corticospinal axon-dependent functions. *Neuron* 95, 817–833.e4. doi: 10.1016/j.neuron.2017.07.037

Lu, Y., Belin, S., and He, Z. (2014). Signaling regulations of neuronal regenerative ability. *Curr. Opin. Neurobiol.* 27, 135–142. doi: 10.1016/j.conb.2014.03.007

Mantovani, A., Biswas, S. K., Galdiero, M. R., Sica, A., and Locati, M. (2013). Macrophage plasticity and polarization in tissue repair and remodelling. *J. Pathol.* 229, 176–185. doi: 10.1002/path.4133

Mao, K., Quipildor, G. F., Tabrizian, T., Novaj, A., Guan, F., Walters, R. O., et al. (2018). Late-life targeting of the IGF-1 receptor improves healthspan and lifespan in female mice. *Nat. Commun.* 9:2394. doi: 10.1038/s41467-018-04805-5

Marklund, N., Morales, D., Clausen, F., Hånell, A., Kiwanuka, O., Pitkänen, A., et al. (2009). Functional outcome is impaired following traumatic brain injury in aging Nogo-A/B-deficient mice. *Neuroscience* 163, 540–551. doi: 10.1016/j.neuroscience.2009.06.042

Matias, I., Morgado, J., and Gomes, F. C. A. (2019). Astrocyte heterogeneity: impact to brain aging and disease. *Front. Aging Neurosci.* 11:59. doi: 10.3389/fnagi.2019.00059

McKeon, R. J., Jurynec, M. J., and Buck, C. R. (1999). The chondroitin sulfate proteoglycans neurocan and phosphacan are expressed by reactive astrocytes in the chronic CNS glial scar. *J. Neurosci.* 19, 10778–10788. doi: 10.1523/jneurosci.19-24-10778.1999

McKeon, R. J., Schreiber, R. C., Rudge, J. S., and Silver, J. (1991). Reduction of neurite outgrowth in a model of glial scarring following CNS injury is correlated with the expression of inhibitory molecules on reactive astrocytes. *J. Neurosci.* 11, 3398–3411. doi: 10.1523/jneurosci.11-11-03398.1991

Milner, R., and Campbell, I. L. (2003). The extracellular matrix and cytokines regulate microglial integrin expression and activation. *J. Immunol.* 170, 3850–3858. doi: 10.4049/jimmunol.170.7.3850

Moeendarbary, E., Weber, I. P., Sheridan, G. K., Koser, D. E., Soleman, S., Haenzi, B., et al. (2017). The soft mechanical signature of glial scars in the central nervous system. *Nat. Commun.* 8:14787. doi: 10.1038/ncomms14787

Moraga, A., Pradillo, J. M., García-Culebras, A., Palma-Tortosa, S., Ballesteros, I., Hernández-Jiménez, M., et al. (2015). Aging increases microglial proliferation, delays cell migration, and decreases cortical neurogenesis after focal cerebral ischemia. *J. Neuroinflammation* 12:87. doi: 10.1186/s12974-015-0314-8

Mouton, P. R., Long, J. M., Lei, D.-L., Howard, V., Jucker, M., Calhoun, M. E., et al. (2002). Age and gender effects on microglia and astrocyte numbers in brains of mice. *Brain Res.* 956, 30–35. doi: 10.1016/s0006-8993(02)03475-3

Muir, E., De Winter, F., Verhaagen, J., and Fawcett, J. (2019). Recent advances in the therapeutic uses of chondroitinase ABC. *Exp. Neurol.* 321:113032. doi: 10.1016/j.expneurol.2019.113032

Mulligan, S. J., and MacVicar, B. A. (2004). Calcium transients in astrocyte endfeet cause cerebrovascular constrictions. *Nature* 431, 195–199. doi: 10.1038/nature02827

Muramatsu, R., and Yamashita, T. (2014). Pericyte function in the physiological central nervous system. *Neurosci. Res.* 81, 38–41. doi: 10.1016/j.neures.2014.01.007

Murray, P. J., and Wynn, T. A. (2011). Protective and pathogenic functions of macrophage subsets. *Nat. Rev. Immunol.* 11, 723–737. doi: 10.1038/nri3073

Nakano, M., Tamura, Y., Yamato, M., Kume, S., Eguchi, A., Takata, K., et al. (2017). NG2 glial cells regulate neuroimmunological responses to maintain neuronal function and survival. *Sci. Rep.* 7:42041. doi: 10.1038/srep42041

Natrajan, M. S., De La Fuente, A. G., Crawford, A. H., Linehan, E., Nuñez, V., Johnson, K. R., et al. (2015). Retinoid X receptor activation reverses age-related deficiencies in myelin debris phagocytosis and remyelination. *Brain* 138, 3581–3597. doi: 10.1093/brain/awv289

Neumann, H., Kotter, M. R., and Franklin, R. J. M. (2008). Debris clearance by microglia: an essential link between degeneration and regeneration. *Brain* 132, 288–295. doi: 10.1093/brain/awn109

Nielson, J. L., Guandique, C. F., Liu, A. W., Burke, D. A., Lash, A. T., Moseanko, R., et al. (2014). Development of a database for translational spinal cord injury research. *J. Neurotrauma* 31, 1789–1799. doi: 10.1089/neu.2014.3399

Nirwane, A., and Yao, Y. (2019). Laminins and their receptors in the CNS. *Biol. Rev.* 94, 283–306. doi: 10.1111/brv.12454

Nishiyama, A., Komitova, M., Suzuki, R., and Zhu, X. (2009). Polydendrocytes (NG2 cells): multifunctional cells with lineage plasticity. *Nat. Rev. Neurosci.* 10, 9–22. doi: 10.1038/nrn2495

Nix, P., Hisamoto, N., Matsumoto, K., and Bastiani, M. (2011). Axon regeneration requires coordinate activation of p38 and JNK MAPK pathways. *Proc. Natl. Acad. Sci. U.S.A.* 108, 10738–10743. doi: 10.1073/pnas.1104830108

NSCISC (2019). *Spinal Cord Injury (SCI) Facts and Figures at a Glance*. Birmingham: National Spinal Cord Injury Statistics Center. Available online at: https://www.nscisc.uab.edu/Public/Facts%20and%20Figures%20-%202017.pdf

Okada, S., Nakamura, M., Katoh, H., Miyao, T., Shimazaki, T., Ishii, K., et al. (2006). Conditional ablation of Stat3 or Socs3 discloses a dual role for reactive astrocytes after spinal cord injury. *Nat. Med.* 12, 829–834. doi: 10.1038/nm1425

O'Neil, S. M., Witcher, K. G., Mckim, D. B., and Godbout, J. P. (2018). Forced turnover of aged microglia induces an intermediate phenotype but does not rebalance CNS environmental cues driving priming to immune challenge. *Acta Neuropathol. Commun.* 6:129. doi: 10.1186/s40478-018-0636-8

Orr, M. B., and Gensel, J. C. (2018). Spinal cord injury scarring and inflammation: therapies targeting glial and inflammatory responses. *Neurotherapeutics* 15, 541–553. doi: 10.1007/s13311-018-0631-6

Oudega, M., and Hagg, T. (1996). Nerve growth factor promotes regeneration of sensory axons into adult rat spinal cord. *Exp. Neurol.* 140, 218–229. doi: 10.1006/exnr.1996.0131

Ozdinler, P. H., and Macklis, J. D. (2006). IGF-I specifically enhances axon outgrowth of corticospinal motor neurons. *Nat. Neurosci.* 9, 1371–1381. doi: 10.1038/nn1789

Painter, M. W., Lutz, A. B., Cheng, Y.-C., Latremoliere, A., Duong, K., Miller, C. M., et al. (2014). Diminished Schwann cell repair responses underlie age-associated impaired axonal regeneration. *Neuron* 83, 331–343. doi: 10.1016/j.neuron.2014.06.016

Palmer, A. L., and Ousman, S. S. (2018). Astrocytes and aging. *Front. Aging Neurosci.* 10:337. doi: 10.3389/fnagi.2018.00337

Paratcha, G., and Ledda, F. (2008). GDNF and GFRalpha: a versatile molecular complex for developing neurons. *Trends Neurosci.* 31, 384–391. doi: 10.1016/j.tins.2008.05.003

Parhad, I., Scott, J., Cellars, L., Bains, J., Krekoski, C., and Clark, A. (1995). Axonal atrophy in aging is associated with a decline in neurofilament gene expression. *J. Neurosci. Res.* 41, 355–366. doi: 10.1002/jnr.490410308

Park, K. K., Liu, K., Hu, Y., Smith, P. D., Wang, C., Cai, B., et al. (2008). Promoting axon regeneration in the adult CNS by modulation of the PTEN/mTOR pathway. *Science* 322, 963–966. doi: 10.1126/science.1161566

Partyka, P. P., Jin, Y., Bouyer, J., Dasilva, A., Godsey, G. A., Nagele, R. G., et al. (2019). Harnessing neurovascular interaction to guide axon growth. *Sci. Rep.* 9:2190. doi: 10.1038/s41598-019-38558-y

Pekny, M., and Pekna, M. (2014). Astrocyte reactivity and reactive astrogliosis: costs and benefits. *Physiol. Rev.* 94, 1077–1098. doi: 10.1152/physrev.00041.2013

Pekny, M., Pekna, M., Messing, A., Steinhäuser, C., Lee, J.-M., Parpura, V., et al. (2016). Astrocytes: a central element in neurological diseases. *Acta Neuropathol.* 131, 323–345. doi: 10.1007/s00401-015-1513-1

Pertusa, M., García-Matas, S., Rodríguez-Farré, E., Sanfeliu, C., and Cristòfol, R. (2007). Astrocytes aged in vitro show a decreased neuroprotective capacity. *J. Neurochem.* 101, 794–805. doi: 10.1111/j.1471-4159.2006.04369.x

Pestronk, A., Drachman, D. B., and Griffin, J. W. (1980). Effects of aging on nerve sprouting and regeneration. *Exp. Neurol.* 70, 65–82. doi: 10.1016/0014-4886(80)90006-0

Petzold, A., Psotta, L., Brigadski, T., Endres, T., and Lessmann, V. (2015). Chronic BDNF deficiency leads to an age-dependent impairment in spatial learning. *Neurobiol. Learn. Mem.* 120, 52–60. doi: 10.1016/j.nlm.2015.02.009

Picoli, C. C., Coimbra-Campos, L. M., Guerra, D. A., Silva, W. N., Prazeres, P. H., Costa, A. C., et al. (2019). Pericytes Act as key players in spinal cord injury. *Am. J. Pathol.* 189, 1327–1337. doi: 10.1016/j.ajpath.2019.03.008

Pineau, I., and Lacroix, S. (2007). Proinflammatory cytokine synthesis in the injured mouse spinal cord: multiphasic expression pattern and identification of the cell types involved. *J. Comp. Neurol.* 500, 267–285. doi: 10.1002/cne.21149

Plantman, S., Patarroyo, M., Fried, K., Domogatskaya, A., Tryggvason, K., Hammarberg, H., et al. (2008). Integrin-laminin interactions controlling neurite outgrowth from adult DRG neurons in vitro. *Mol. Cell. Neurosci.* 39, 50–62. doi: 10.1016/j.mcn.2008.05.015

Popa-Wagner, A., Buga, A.-M., and Kokaia, Z. (2011). Perturbed cellular response to brain injury during aging. *Ageing Res. Rev.* 10, 71–79. doi: 10.1016/j.arr.2009.10.008

Popovich, P., Guan, Z., Mcgaughy, V., Fisher, L., Hickey, W., Basso, D. M., et al. (2002). The neuropathological and behavioral consequences of intraspinal microglial/macrophage activation. *J. Neuropathol. Exp. Neurol.* 61, 623–633. doi: 10.1093/jnen/61.7.623

Potts, M. B., Koh, S.-E., Whetstone, W. D., Walker, B. A., Yoneyama, T., Claus, C. P., et al. (2006). Traumatic injury to the immature brain: inflammation, oxidative injury, and iron-mediated damage as potential therapeutic targets. *Neurorx* 3, 143–153. doi: 10.1007/bf03207045

Profyris, C., Cheema, S. S., Zang, D., Azari, M. F., Boyle, K., and Petratos, S. (2004). Degenerative and regenerative mechanisms governing spinal cord injury. *Neurobiol. Dis.* 15, 415–436. doi: 10.1016/j.nbd.2003.11.015

Psachoulia, K., Jamen, F., Young, K. M., and Richardson, W. D. (2009). Cell cycle dynamics of NG2 cells in the postnatal and ageing brain. *Neuron Glia Biol.* 5, 57–67. doi: 10.1017/S1740925X09990354

Qin, L., Liu, Y., Wang, T., Wei, S.-J., Block, M. L., Wilson, B., et al. (2004). NADPH oxidase mediates lipopolysaccharide-induced neurotoxicity and proinflammatory gene expression in activated microglia. *J. Biol. Chem.* 279, 1415–1421. doi: 10.1074/jbc.m307657200

Qu, W.-S., Tian, D.-S., Guo, Z.-B., Fang, J., Zhang, Q., Yu, Z.-Y., et al. (2012). Inhibition of EGFR/MAPK signaling reduces microglial inflammatory response and the associated secondary damage in rats after spinal cord injury. *J. Neuroinflammation* 9:178. doi: 10.1186/1742-2094-9-178

Rabchevsky, A., and Streit, W. (1997). Grafting of cultured microglial cells into the lesioned spinal cord of adult rats enhances neurite outgrowth. *J. Neurosci. Res.* 47, 34–48.

Rabchevsky, A. G., Fugaccia, I., Turner, A. F., Blades, D. A., Mattson, M. P., and Scheff, S. W. (2000). Basic fibroblast growth factor (bFGF) enhances functional recovery following severe spinal cord injury to the rat. *Exp. Neurol.* 164, 280–291. doi: 10.1006/exnr.2000.7399

Rage, F., Silhol, M., Biname, F., Arancibia, S., and Tapia-Arancibia, L. (2007). Effect of aging on the expression of BDNF and TrkB isoforms in rat pituitary. *Neurobiol. Aging* 28, 1088–1098. doi: 10.1016/j.neurobiolaging.2006.05.013

Ransom, B., Behar, T., and Nedergaard, M. (2003). New roles for astrocytes (stars at last). *Trends Neurosci.* 26, 520–522. doi: 10.1016/j.tins.2003.08.006

Reed, M. J., Damodarasamy, M., Pathan, J. L., Erickson, M. A., Banks, W. A., and Vernon, R. B. (2018). The effects of normal aging on regional accumulation of hyaluronan and chondroitin sulfate proteoglycans in the mouse brain. *J. Histochem. Cytochem.* 66, 697–707. doi: 10.1369/0022155418774779

Ren, Y., and Young, W. (2013). Managing inflammation after spinal cord injury through manipulation of macrophage function. *Neural Plast.* 2013:945034. doi: 10.1155/2013/945034

Richard, A. D., Tian, X. L., El-Saadi, M. W., and Lu, X. H. (2018). Erasure of striatal chondroitin sulfate proteoglycan-associated extracellular matrix rescues aging-dependent decline of motor learning. *Neurobiol. Aging* 71, 61–71. doi: 10.1016/j.neurobiolaging.2018.07.008

Ritzel, R. M., Doran, S. J., Glaser, E. P., Meadows, V. E., Faden, A. I., Stoica, B. A., et al. (2019). Old age increases microglial senescence, exacerbates secondary neuroinflammation, and worsens neurological outcomes after acute traumatic brain injury in mice. *Neurobiol. Aging* 77, 194–206. doi: 10.1016/j.neurobiolaging.2019.02.010

Ritzel, R. M., Patel, A. R., Pan, S., Crapser, J., Hammond, M., Jellison, E., et al. (2015). Age-and location-related changes in microglial function. *Neurobiol. Aging* 36, 2153–2163. doi: 10.1016/j.neurobiolaging.2015.02.016

Romero, M. I., Rangappa, N., Li, L., Lightfoot, E., Garry, M. G., and Smith, G. M. (2000). Extensive sprouting of sensory afferents and hyperalgesia induced by conditional expression of nerve growth factor in the adult spinal cord. *J. Neurosci.* 20, 4435–4445. doi: 10.1523/jneurosci.20-12-04435.2000

Rongo, C. (2011). Epidermal growth factor and aging: a signaling molecule reveals a new eye opening function. *Aging* 3, 896–905. doi: 10.18632/aging.100384

Rosich, K., Hanna, B. F., Ibrahim, R. K., Hellenbrand, D. J., and Hanna, A. (2017). The effects of glial cell line-derived neurotrophic factor after spinal cord injury. *J. Neurotrauma* 34, 3311–3325. doi: 10.1089/neu.2017.5175

Rowland, J. W., Hawryluk, G. W., Kwon, B., and Fehlings, M. G. (2008). Current status of acute spinal cord injury pathophysiology and emerging therapies: promise on the horizon. *Neurosurg. Focus* 25:E2. doi: 10.3171/FOC.2008.25.11.E2

Ruschel, J., Hellal, F., Flynn, K. C., Dupraz, S., Elliott, D. A., Tedeschi, A., et al. (2015). Systemic administration of epothilone B promotes axon regeneration after spinal cord injury. *Science* 348, 347–352. doi: 10.1126/science.aaa2958

Safaiyan, S., Kannaiyan, N., Snaidero, N., Brioschi, S., Biber, K., Yona, S., et al. (2016). Age-related myelin degradation burdens the clearance function of microglia during aging. *Nat. Neurosci.* 19, 995–998. doi: 10.1038/nn.4325

Sanes, J. R. (1989). Extracellular matrix molecules that influence neural development. *Annu. Rev. Neurosci.* 12, 491–516. doi: 10.1146/annurev.ne.12.030189.002423

Sá-Pereira, I., Brites, D., and Brito, M. A. (2012). Neurovascular unit: a focus on pericytes. *Mol. Neurobiol.* 45, 327–347. doi: 10.1007/s12035-012-8244-2

Sawada, M., Itoh, Y., Suzumura, A., and Marunouchi, T. (1993). Expression of cytokine receptors in cultured neuronal and glial cells. *Neurosci. Lett.* 160, 131–134. doi: 10.1016/0304-3940(93)90396-3

Schachtrup, C., Ryu, J. K., Helmrick, M. J., Vagena, E., Galanakis, D. K., Degen, J. L., et al. (2010). Fibrinogen triggers astrocyte scar formation by promoting the availability of active TGF-β after vascular damage. *J. Neurosci.* 30, 5843–5854. doi: 10.1523/JNEUROSCI.0137-10.2010

Segel, M., Neumann, B., Hill, M. F. E., Weber, I. P., Viscomi, C., Zhao, C., et al. (2019). Niche stiffness underlies the ageing of central nervous system progenitor cells. *Nature* 573, 130–134. doi: 10.1038/s41586-019-1484-9

Sharp, K., Yee, K. M., and Steward, O. (2012). A re-assessment of the effects of treatment with an epidermal growth factor receptor (EGFR) inhibitor on recovery of bladder and locomotor function following thoracic spinal cord injury in rats. *Exp. Neurol.* 233, 649–659. doi: 10.1016/j.expneurol.2011.04.013

Shetty, A. K., Hattiangady, B., and Shetty, G. A. (2005). Stem/progenitor cell proliferation factors FGF-2, IGF-1, and VEGF exhibit early decline during the course of aging in the hippocampus: role of astrocytes. *Glia* 51, 173–186. doi: 10.1002/glia.20187

Shetye, S. S., Troyer, K. L., Streijger, F., Lee, J. H., Kwon, B. K., Cripton, P. A., et al. (2014). Nonlinear viscoelastic characterization of the porcine spinal cord. *Acta Biomater.* 10, 792–797. doi: 10.1016/j.actbio.2013.10.038

Shiraha, H., Gupta, K., Drabik, K., and Wells, A. (2000). Aging fibroblasts present reduced epidermal growth factor (EGF) responsiveness due to preferential loss of EGF receptors. *J. Biol. Chem.* 275, 19343–19351. doi: 10.1074/jbc.m000008200

Siddiqui, S., Fang, M., Ni, B., Lu, D., Martin, B., and Maudsley, S. (2012). Central role of the EGF receptor in neurometabolic aging. *Int. J. Endocrinol.* 2012:739428. doi: 10.1155/2012/739428

Siegenthaler, M. M., Ammon, D. L., and Keirstead, H. S. (2008). Myelin pathogenesis and functional deficits following SCI are age-associated. *Exp. Neurol.* 213, 363–371. doi: 10.1016/j.expneurol.2008.06.015

Silver, J., and Miller, J. H. (2004). Regeneration beyond the glial scar. *Nat. Rev. Neurosci.* 5, 146–156. doi: 10.1038/nrn1326

Silver, J., Schwab, M. E., and Popovich, P. G. (2015). Central nervous system regenerative failure: role of oligodendrocytes, astrocytes, and microglia. *Cold Spring Harb. Perspect. Biol.* 7:a020602. doi: 10.1101/cshperspect.a020602

Sim, F. J., Zhao, C., Penderis, J., and Franklin, R. J. (2002). The age-related decrease in CNS remyelination efficiency is attributable to an impairment of both oligodendrocyte progenitor recruitment and differentiation. *J. Neurosci.* 22, 2451–2459. doi: 10.1523/jneurosci.22-07-02451.2002

Simon-Assmann, P., Orend, G., Mammadova-Bach, E., Spenle, C., and Lefebvre, O. (2011). Role of laminins in physiological and pathological angiogenesis. *Int. J. Dev. Biol.* 55, 455–465. doi: 10.1387/ijdb.103223ps

Singh, A., Tetreault, L., Kalsi-Ryan, S., Nouri, A., and Fehlings, M. G. (2014). Global prevalence and incidence of traumatic spinal cord injury. *Clin. Epidemiol.* 6, 309–331. doi: 10.2147/CLEP.S68889

Smith, G. M., Rutishauser, U., Silver, J., and Miller, R. H. (1990). Maturation of astrocytes in vitro alters the extent and molecular basis of neurite outgrowth. *Dev. Biol.* 138, 377–390. doi: 10.1016/0012-1606(90)90204-v

Sofroniew, M. V. (2009). Molecular dissection of reactive astrogliosis and glial scar formation. *Trends Neurosci.* 32, 638–647. doi: 10.1016/j.tins.2009.08.002

Sofroniew, M. V. (2015). Astrocyte barriers to neurotoxic inflammation. *Nat. Rev. Neurosci.* 16, 249–263. doi: 10.1038/nrn3898

Sofroniew, M. V., and Vinters, H. V. (2010). Astrocytes: biology and pathology. *Acta Neuropathol.* 119, 7–35. doi: 10.1007/s00401-009-0619-8

Sondell, M., Lundborg, G., and Kanje, M. (1999). Vascular endothelial growth factor has neurotrophic activity and stimulates axonal outgrowth, enhancing cell survival and Schwann cell proliferation in the peripheral nervous system. *J. Neurosci.* 19, 5731–5740. doi: 10.1523/jneurosci.19-14-05731.1999

Sozmen, E. G., Rosenzweig, S., Llorente, I. L., Ditullio, D. J., Machnicki, M., Vinters, H. V., et al. (2016). Nogo receptor blockade overcomes remyelination failure after white matter stroke and stimulates functional recovery in aged mice. *Proc. Natl. Acad. Sci. U.S.A.* 113, E8453–E8462. doi: 10.1073/pnas.1615322113

Spitzer, S. O., Sitnikov, S., Kamen, Y., Evans, K. A., Kronenberg-Versteeg, D., Dietmann, S., et al. (2019). Oligodendrocyte progenitor cells become regionally diverse and heterogeneous with age. *Neuron* 101, 459–471.e5. doi: 10.1016/j.neuron.2018.12.020

Stewart, A. N., Gensel, J. C., and Zhang, B. (2019). Therapeutic implications of advanced age at time of spinal cord injury. *Neural Regene. Res.* 14, 1895–1896.

Stichel, C. C., Hermanns, S., Luhmann, H. J., Lausberg, F., Niermann, H., D'urso, D., et al. (1999). Inhibition of collagen IV deposition promotes regeneration of injured CNS axons. *Eur. J. Neurosci.* 11, 632–646. doi: 10.1046/j.1460-9568.1999.00466.x

Stoffels, J. M., De Jonge, J. C., Stancic, M., Nomden, A., Van Strien, M. E., Ma, D., et al. (2013). Fibronectin aggregation in multiple sclerosis lesions impairs remyelination. *Brain* 136, 116–131. doi: 10.1093/brain/aws313

Streit, W. J., Miller, K. R., Lopes, K. O., and Njie, E. (2008). Microglial degeneration in the aging brain–bad news for neurons. *Front. Biosci.* 13, 3423–3438.

Streit, W. J., Semple-Rowland, S. L., Hurley, S. D., Miller, R. C., Popovich, P. G., and Stokes, B. T. (1998). Cytokine mRNA profiles in contused spinal cord and axotomized facial nucleus suggest a beneficial role for inflammation and gliosis. *Exp. Neurol.* 152, 74–87. doi: 10.1006/exnr.1998.6835

Stromska, D., and Ochs, S. (1982). Axoplasmic transport in aged rats. *Exp. Neurol.* 77, 215–224. doi: 10.1016/0014-4886(82)90155-8

Sugino, T., Nozaki, K., Takagi, Y., Hattori, I., Hashimoto, N., Moriguchi, T., et al. (2000). Activation of mitogen-activated protein kinases after transient forebrain ischemia in gerbil hippocampus. *J. Neurosci.* 20, 4506–4514. doi: 10.1523/jneurosci.20-12-04506.2000

Sukhanov, S., Higashi, Y., Shai, S.-Y., Vaughn, C., Mohler, J., Li, Y., et al. (2007). IGF-1 reduces inflammatory responses, suppresses oxidative stress, and decreases atherosclerosis progression in ApoE-deficient mice. *Arterioscler. Thromb. Vasc. Biol.* 27, 2684–2690. doi: 10.1161/atvbaha.107.156257

Sun, F., Park, K. K., Belin, S., Wang, D., Lu, T., Chen, G., et al. (2011). Sustained axon regeneration induced by co-deletion of PTEN and SOCS3. *Nature* 480, 372–375. doi: 10.1038/nature10594

Sutherland, T. C., Mathews, K. J., Mao, Y., Nguyen, T., and Gorrie, C. A. (2017). Differences in the cellular response to acute spinal cord injury between developing and mature rats highlights the potential significance of the inflammatory response. *Front. Cell. Neurosci.* 10:310. doi: 10.3389/fncel.2016.00310

Tan, Y.-L., Yuan, Y., and Tian, L. (2020). Microglial regional heterogeneity and its role in the brain. *Mol. Psychiatry* 25, 351–367. doi: 10.1038/s41380-019-0609-8

Tate, C. C., Tate, M. C., and Laplaca, M. C. (2007). Fibronectin and laminin increase in the mouse brain after controlled cortical impact injury. *J. Neurotrauma* 24, 226–230. doi: 10.1089/neu.2006.0043

Teng, Y. D., Mocchetti, I., Taveira-Dasilva, A. M., Gillis, R. A., and Wrathall, J. R. (1999). Basic fibroblast growth factor increases long-term survival of spinal motor neurons and improves respiratory function after experimental spinal cord injury. *J. Neurosci.* 19, 7037–7047. doi: 10.1523/jneurosci.19-16-07037.1999

Thompson, A. J., Pillai, E. K., Dimov, I. B., Foster, S. K., Holt, C. E., and Franze, K. (2019). Rapid changes in tissue mechanics regulate cell behaviour in the developing embryonic brain. *eLife* 8:e39356. doi: 10.7554/eLife.39356

Tom, V. J., Doller, C. M., Malouf, A. T., and Silver, J. (2004). Astrocyte-associated fibronectin is critical for axonal regeneration in adult white matter. *J. Neurosci.* 24, 9282–9290. doi: 10.1523/jneurosci.2120-04.2004

Topp, K. S., Faddis, B. T., and Vijayan, V. K. (1989). Trauma-induced proliferation of astrocytes in the brains of young and aged rats. *Glia* 2, 201–211. doi: 10.1002/glia.440020309

Tran, K. A., Partyk, P. P., Jin, Y., Bouyer, J., Fischer, I., and Galie, P. A. (2020). Vascularization of self-assembled peptide scaffolds for spinal cord injury repair. *Acta Biomater.* 104, 76–84. doi: 10.1016/j.actbio.2019.12.033

Tremblay, M. È., Zettel, M. L., Ison, J. R., Allen, P. D., and Majewska, A. K. (2012). Effects of aging and sensory loss on glial cells in mouse visual and auditory cortices. *Glia* 60, 541–558. doi: 10.1002/glia.22287

Trifunovski, A., Josephson, A., Bickford, P. C., Olson, L., and Brené, S. (2006). Selective decline of Nogo mRNA in the aging brain. *Neuroreport* 17, 913–916. doi: 10.1097/01.wnr.0000221831.95598.a3

Uspenskaia, O., Liebetrau, M., Herms, J., Danek, A., and Hamann, G. F. (2004). Aging is associated with increased collagen type IV accumulation in the basal lamina of human cerebral microvessels. *BMC Neurosci.* 5:37. doi: 10.1186/1471-2202-5-37

VanGuilder Starkey, H. D., Sonntag, W. E., and Freeman, W. M. (2013). Increased hippocampal NgR1 signaling machinery in aged rats with deficits of spatial cognition. *Eur. J. Neurosci.* 37, 1643–1658. doi: 10.1111/ejn.12165

VanGuilder Starkey, H. D., Van Kirk, C. A., Bixler, G. V., Imperio, C. G., Kale, V. P., Serfass, J. M., et al. (2012). Neuroglial expression of the MHCI pathway and PirB receptor is upregulated in the hippocampus with advanced aging. *J. Mol. Neurosci.* 48, 111–126. doi: 10.1007/s12031-012-9783-8

Varani, J. (2010). Fibroblast aging: intrinsic and extrinsic factors. *Drug Discov. Today Ther. Strateg.* 7, 65–70. doi: 10.1016/j.ddstr.2011.06.001

Vaughan, D. W. (1992). Effects of advancing age on peripheral nerve regeneration. *J. Comp. Neurol.* 323, 219–237. doi: 10.1002/cne.903230207

Vaughan, S. K., Stanley, O. L., and Valdez, G. (2017). Impact of aging on proprioceptive sensory neurons and intrafusal muscle fibers in mice. *J. Gerontol. A Biol. Sci. Med. Sci.* 72, 771–779. doi: 10.1093/gerona/glw175

Verdú, E., Butí, M., and Navarro, X. (1995). The effect of aging on efferent nerve fibers regeneration in mice. *Brain Res.* 696, 76–82. doi: 10.1016/0006-8993(95)00762-f

Verdú, E., Ceballos, D., Vilches, J. J., and Navarro, X. (2000). Influence of aging on peripheral nerve function and regeneration. *J. Peripher. Nerv. Syst.* 5, 191–208. doi: 10.1111/j.1529-8027.2000.00026.x

von Bohlen Und Halbach, O. (2010). Involvement of BDNF in age-dependent alterations in the hippocampus. *Front. Aging Neurosci.* 2:36. doi: 10.3389/fnagi.2010.00036

von Leden, R. E., Khayrullina, G., Moritz, K. E., and Byrnes, K. R. (2017). Age exacerbates microglial activation, oxidative stress, inflammatory and NOX2 gene expression, and delays functional recovery in a middle-aged rodent model of spinal cord injury. *J. Neuroinflammation* 14:161. doi: 10.1186/s12974-017-0933-3

Wagner, J. U., Chavakis, E., Rogg, E.-M., Muhly-Reinholz, M., Glaser, S. F., Günther, S., et al. (2018). Switch in laminin β2 to laminin β1 isoforms during aging controls endothelial cell functions—brief report. *Arterioscler. Thromb. Vasc. Biol.* 38, 1170–1177. doi: 10.1161/atvbaha.117.310685

Walshe, T. E., Saint-Geniez, M., Maharaj, A. S., Sekiyama, E., Maldonado, A. E., and D'amore, P. A. (2009). TGF-β is required for vascular barrier function, endothelial survival and homeostasis of the adult microvasculature. *PLoS One* 4:e5149. doi: 10.1371/journal.pone.0005149

Wang, X., Cao, K., Sun, X., Chen, Y., Duan, Z., Sun, L., et al. (2015). Macrophages in spinal cord injury: phenotypic and functional change from exposure to myelin debris. *Glia* 63, 635–651. doi: 10.1002/glia.22774

Wang, X.-J., Zhang, S., Yan, Z.-Q., Zhao, Y.-X., Zhou, H.-Y., Wang, Y., et al. (2011). Impaired CD200–CD200R-mediated microglia silencing enhances midbrain dopaminergic neurodegeneration: roles of aging, superoxide, NADPH oxidase, and p38 MAPK. *Free Radic. Biol. Med.* 50, 1094–1106. doi: 10.1016/j.freeradbiomed.2011.01.032

Wang, Y., Cheng, X., He, Q., Zheng, Y., Kim, D. H., Whittemore, S. R., et al. (2011). Astrocytes from the contused spinal cord inhibit oligodendrocyte differentiation of adult oligodendrocyte precursor cells by increasing the expression of bone morphogenetic proteins. *J. Neurosci.* 31, 6053–6058. doi: 10.1523/JNEUROSCI.5524-09.2011

Wang, Y., Wu, W., Wu, X., Sun, Y., Zhang, Y. P., Deng, L. X., et al. (2018). Remodeling of lumbar motor circuitry remote to a thoracic spinal cord injury promotes locomotor recovery. *eLife* 7:e39016. doi: 10.7554/eLife.39016

Wappler, E. A., Adorjan, I., Gal, A., Galgoczy, P., Bindics, K., and Nagy, Z. (2011). Dynamics of dystroglycan complex proteins and laminin changes due to angiogenesis in rat cerebral hypoperfusion. *Microvasc. Res.* 81, 153–159. doi: 10.1016/j.mvr.2010.12.005

Weishaupt, N., Blesch, A., and Fouad, K. (2012). BDNF: the career of a multifaceted neurotrophin in spinal cord injury. *Exp. Neurol.* 238, 254–264. doi: 10.1016/j.expneurol.2012.09.001

Wierzba-Bobrowicz, T., Lewandowska, E., Kosno-Kruszewska, E., Lechowicz, W., Pasennik, E., and Schmidt-Sidor, B. (2004). Degeneration of microglial cells in frontal and temporal lobes of chronic schizophrenics. *Folia Neuropathol.* 42, 157–166.

Willcox, B. J., and Scott, J. N. (2004). Growth-associated proteins and regeneration-induced gene expression in the aging neuron. *Mech. Ageing Dev.* 125, 513–516. doi: 10.1016/j.mad.2004.04.004

Wong, W. T. (2013). Microglial aging in the healthy CNS: phenotypes, drivers, and rejuvenation. *Front. Cell. Neurosci.* 7:22. doi: 10.3389/fncel.2013.00022

Wynne, A. M., Henry, C. J., Huang, Y., Cleland, A., and Godbout, J. P. (2010). Protracted downregulation of CX3CR1 on microglia of aged mice after lipopolysaccharide challenge. *Brain Behav. Immun.* 24, 1190–1201. doi: 10.1016/j.bbi.2010.05.011

Yao, Y., Chen, Z. L., Norris, E. H., and Strickland, S. (2014). Astrocytic laminin regulates pericyte differentiation and maintains blood brain barrier integrity. *Nat. Commun.* 5:3413. doi: 10.1038/ncomms4413

Ye, P., Li, L., Richards, R. G., Diaugustine, R. P., and D'ercole, A. J. (2002). Myelination is altered in insulin-like growth factor-I null mutant mice. *J. Neurosci.* 22, 6041–6051. doi: 10.1523/jneurosci.22-14-06041.2002

Yin, Y., Henzl, M. T., Lorber, B., Nakazawa, T., Thomas, T. T., Jiang, F., et al. (2006). Oncomodulin is a macrophage-derived signal for axon regeneration in retinal ganglion cells. *Nat. Neurosci.* 9, 843–852. doi: 10.1038/nn1701

Zamanian, J. L., Xu, L., Foo, L. C., Nouri, N., Zhou, L., Giffard, R. G., et al. (2012). Genomic analysis of reactive astrogliosis. *J. Neurosci.* 32, 6391–6410. doi: 10.1523/jneurosci.6221-11.2012

Zhang, B., Bailey, W. M., Braun, K. J., and Gensel, J. C. (2015). Age decreases macrophage IL-10 expression: implications for functional recovery and tissue repair in spinal cord injury. *Exp. Neurol.* 273, 83–91. doi: 10.1016/j.expneurol.2015.08.001

Zhang, B., Bailey, W. M., Mcvicar, A. L., and Gensel, J. C. (2016). Age increases reactive oxygen species production in macrophages and potentiates oxidative damage after spinal cord injury. *Neurobiol. Aging* 47, 157–167. doi: 10.1016/j.neurobiolaging.2016.07.029

Zhang, B., Bailey, W. M., Mcvicar, A. L., Stewart, A. N., Veldhorst, A. K., and Gensel, J. C. (2019). Reducing age-dependent monocyte-derived macrophage activation contributes to the therapeutic efficacy of NADPH oxidase inhibition in spinal cord injury. *Brain Behav. Immun.* 76, 139–150. doi: 10.1016/j.bbi.2018.11.013

Zhang, S., Ju, P., Tjandra, E., Yeap, Y., Owlanj, H., and Feng, Z. (2016). Inhibition of epidermal growth factor receptor improves myelination and attenuates tissue damage of spinal cord injury. *Cell. Mol. Neurobiol.* 36, 1169–1178. doi: 10.1007/s10571-015-0313-4

Zhang, H., Wu, F., Kong, X., Yang, J., Chen, H., Deng, L., et al. (2014). Nerve growth factor improves functional recovery by inhibiting endoplasmic reticulum stress-induced neuronal apoptosis in rats with spinal cord injury. *J. Transl. Med.* 12:130. doi: 10.1186/1479-5876-12-130

Zhang, Y., Williams, P. R., Jacobi, A., Wang, C., Goel, A., Hirano, A. A., et al. (2019). Elevating growth factor responsiveness and axon regeneration by modulating presynaptic inputs. *Neuron* 103, 39–51.e5. doi: 10.1016/j.neuron.2019.04.033

Zheng, B., Ye, L., Zhou, Y., Zhu, S., Wang, Q., Shi, H., et al. (2016). Epidermal growth factor attenuates blood-spinal cord barrier disruption via PI3K/Akt/Rac1 pathway after acute spinal cord injury. *J. Cell. Mol. Med.* 20, 1062–1075. doi: 10.1111/jcmm.12761

Zhou, Y., Qian, R., Rao, J., Weng, M., and Yi, X. (2010). Expression of PirB in normal and injured spinal cord of rats. *J. Huazhong Univ. Sci. Technolog. Med. Sci.* 30, 482–485. doi: 10.1007/s11596-010-0453-1

Zhou, Y., Wang, Z., Li, J., Li, X., and Xiao, J. (2018). Fibroblast growth factors in the management of spinal cord injury. *J. Cell. Mol. Med.* 22, 25–37. doi: 10.1111/jcmm.13353

Zhu, Y., Soderblom, C., Trojanowsky, M., Lee, D.-H., and Lee, J. K. (2015). Fibronectin matrix assembly after spinal cord injury. *J. Neurotrauma* 32, 1158–1167. doi: 10.1089/neu.2014.3703

Ziebell, J. M., Rowe, R. K., Muccigrosso, M. M., Reddaway, J. T., Adelson, P. D., Godbout, J. P., et al. (2017). Aging with a traumatic brain injury: could behavioral morbidities and endocrine symptoms be influenced by microglial priming? *Brain Behav. Immun.* 59, 1–7. doi: 10.1016/j.bbi.2016.03.008

Ziv, Y., Avidan, H., Pluchino, S., Martino, G., and Schwartz, M. (2006). Synergy between immune cells and adult neural stem/progenitor cells promotes functional recovery from spinal cord injury. *Proc. Natl. Acad. Sci. U.S.A.* 103, 13174–13179. doi: 10.1073/pnas.0603747103

Zou, Y., Chiu, H., Zinovyeva, A., Ambros, V., Chuang, C.-F., and Chang, C. (2013). Developmental decline in neuronal regeneration by the progressive change of two intrinsic timers. *Science* 340, 372–376. doi: 10.1126/science.1231321

**Conflict of Interest:** The authors declare that the research was conducted in the absence of any commercial or financial relationships that could be construed as a potential conflict of interest.

frontiers in Cell and Developmental Biology

BRIEF RESEARCH REPORT
published: 25 May 2020
doi: 10.3389/fcell.2020.00371

# Caveolin-1 Regulates Perivascular Aquaporin-4 Expression After Cerebral Ischemia

*Irina Filchenko[1,2,3†], Camille Blochet[1,3†], Lara Buscemi[1,3], Melanie Price[1,3], Jerome Badaut[4,5*†] and Lorenz Hirt[1,3*†]*

*[1] Service of Neurology, Department of Clinical Neurosciences, CHUV, Lausanne, Switzerland, [2] North-Western State Medical University named after I.I. Mechnikov, Saint-Petersburg, Russia, [3] Department of Fundamental Neurosciences, University of Lausanne, Lausanne, Switzerland, [4] Brain Molecular Imaging Lab, CNRS UMR 5287, INCIA, University of Bordeaux, Bordeaux, France, [5] Basic Science Department, Loma Linda University School of Medicine, Loma Linda, CA, United States*

Edema is a hallmark of many brain disorders including stroke. During vasogenic edema, blood-brain barrier (BBB) permeability increases, contributing to the entry of plasma proteins followed by water. Caveolae and caveolin-1 (Cav-1) are involved in these BBB permeability changes. The expression of the aquaporin-4 (AQP4) water channel relates to brain swelling, however, its regulation is poorly understood. Here we tested whether Cav-1 regulates AQP4 expression in the perivascular region after brain ischemia in mice. We showed that Cav-1 knockout mice had enhanced hemispheric swelling and decreased perivascular AQP4 expression in perilesional and contralateral cortical regions compared to wild-type. Glial fibrillary acidic protein-positive astrocytes displayed less branching and ramification in Cav-1 knockout mice compared to wild-type animals. There was a positive correlation between the area of perivascular AQP4-immunolabelling and branch length of Glial fibrillary acidic protein-positive astrocytes in wild-type mice, not seen in Cav-1 knockout mice. In summary, we show for the first time that loss of Cav-1 results in decreased AQP4 expression and impaired perivascular AQP4 covering after cerebral ischemia associated with altered reactive astrocyte morphology and enhanced brain swelling. Therapeutic approaches targeting Cav-1 may provide new opportunities for improving stroke outcome.

## SIGNIFICANCE STATEMENT

Severe brain edema worsens outcome in stroke patients. Available treatments for stroke-related edema are not efficient and molecular and cellular mechanisms are poorly understood. Cellular water channels, aquaporins (AQPs), are mainly expressed in astrocytes in the brain and play a key role in water movements and cerebral edema, while endothelial caveolins have been suggested to play a role in vasogenic edema. Here we used an integrative approach to study possible interaction between AQP4 and caveolin-1 (Cav-1) after stroke. Absence of Cav-1 was associated with perivascular changes in AQP4 expression and enhanced brain swelling at 3 days after cerebral ischemia. The present work indicates a direct or indirect effect of Cav-1 on perivascular AQP4, which may lead to novel edema therapy.

**Keywords: stroke, aquaporin (AQP)-4, caveolin-1 (CAV1), recovery, astrocytes, endfeet**

OPEN ACCESS

***Edited by:***
*João M. N. Duarte, Lund University, Sweden*

***Reviewed by:***
*Paul G. Mermelstein, University of Minnesota Twin Cities, United States*
*Cecilia Jacques G. de Almeida, Oswaldo Cruz Foundation (Fiocruz), Brazil*

****Correspondence:***
*Jerome Badaut*
*jerome.badaut@u-bordeaux.fr*
*Lorenz Hirt*
*lorenz.hirt@chuv.ch*

*† These authors have contributed equally to this work*

***Specialty section:***
*This article was submitted to Molecular Medicine, a section of the journal Frontiers in Cell and Developmental Biology*

***Received:*** *30 March 2020*
***Accepted:*** *27 April 2020*
***Published:*** *25 May 2020*

***Citation:***
*Filchenko I, Blochet C, Buscemi L, Price M, Badaut J and Hirt L (2020) Caveolin-1 Regulates Perivascular Aquaporin-4 Expression After Cerebral Ischemia. Front. Cell Dev. Biol. 8:371. doi: 10.3389/fcell.2020.00371*

## INTRODUCTION

Cerebral edema is a hallmark of many brain diseases including stroke. It is characterized by a net increase in water in the brain tissue, triggering tissue swelling. Brain edema has a simple definition, hiding a very complex phenomenon with heterogeneous processes depending on the brain disease (Michinaga and Koyama, 2015; Jha et al., 2019). Underlying molecular and cellular mechanisms of edema formation and resolution are not well understood. Recently, brain edema was divided into three categories, cytotoxic, ionic and vasogenic, based on changes in BBB properties (Simard et al., 2007; Michinaga and Koyama, 2015; Clement et al., 2020). Brain endothelium, critical for the BBB function, restricts the passage of molecules from blood to the brain tissue via the presence of tight junctions between endothelial cells and specific transporters (Villabona-Rueda et al., 2019) and a low level of transcytosis (Ayloo and Gu, 2019). The increase in BBB permeability after stroke (Sadeghian et al., 2018) has been linked to an early increase in transcytosis (Knowland et al., 2014), which is caveolae and Cav-1 dependent (Knowland et al., 2014; Sadeghian et al., 2018). Cav-1 belongs to the caveolin family and contributes to the formation of caveolae (plasma membrane invaginations), transcytosis and signal transduction (Parton and del Pozo, 2013). In brain Cav-1 is found in endothelial cells (Knowland et al., 2014; Badaut et al., 2015; Blochet et al., 2020), astrocytes (Badaut et al., 2015; Blochet et al., 2020) and neurons (Xu et al., 2015) of the neurovascular unit (NVU). We recently demonstrated in Cav-1 knockout (KO) mice (JAX stock #007083) that presence of Cav-1 is associated with better survival and recovery after stroke, suggesting a protective role for endogenous Cav-1. We also showed that Cav-1 plays a role in neovascularization and astrogliosis after ischemic injury (Blochet et al., 2020). Choi and colleagues showed that Cav-1 overexpression attenuated brain edema after cerebral ischemia in the rat (Choi et al., 2016).

Several AQPs are present in the brain, the most abundant being the water channel AQP4. AQP4 is important for water movement and edema in the NVU (Badaut et al., 2014) and is expressed in astrocytes (Bi et al., 2017; Hirt et al., 2018a). An early increase in AQP4 expression occurs 1 h after stroke onset on perivascular end-feet and a late increase on astrocyte processes 48 h after stroke onset (de Castro Ribeiro et al., 2006; Hirt et al., 2009). AQP4 may have a dual role in edema, contributing to edema formation (Manley et al., 2000) and facilitating water clearance (Hirt et al., 2009). Moreover, the presence of AQP4 on perivascular astrocyte end-feet is important for perivascular cerebro-spinal fluid flow and protein clearance (Iliff et al., 2012). In perivascular end-feet expression depends on syntrophin, dystrophin–dystroglycan and agrin complex (Noell et al., 2011; Vella et al., 2015). Changes in pericyte properties and platelet-derived growth factor subunit B signaling have been linked to decreased AQP4 polarization (Lindblom et al., 2003; Gundersen et al., 2014; Munk et al., 2019). However, little is known about the molecular mechanisms involved in regulation of presence of AQP4 in perivascular end-feet after brain ischemia.

Outside the brain, endothelial Cav-1 has been shown to contribute to the presence of AQPs in the cell membrane (Jablonski and Hughes, 2006; Aoki et al., 2012; Li et al., 2012; Kim et al., 2013; Jung et al., 2015). Interestingly, Bi et al. (2017) proposed Cav-1 phosphorylation affects AQP4 subcellular distribution. Here, we investigated if Cav-1 is involved in AQP4 expression and cellular distribution after brain ischemia relating to astrogliosis and brain swelling.

## MATERIALS AND METHODS

Animal experiments and care complied with the guidelines of the Swiss Veterinary Office and were approved by the Animal Care and Use Committee (license VD2017.5). Animal reporting was according to ARRIVE guidelines.

### Animal Groups and Experimental Design

Male C57Bl/6J wild-type (WT) mice (6 weeks) were from Charles River ($n$ = 16). Cav-1 KO mice in a C57Bl/6J background from Jackson Laboratory (JAX stock #007083) were bred on site ($n$ = 18). Animals were housed for at least 1 week in a temperature-controlled animal facility on a 12-h light-dark cycle with *ad libitum* access to food and water. Cages contained standard bedding and enrichment material.

(1) Immunofluorescence experiments with $n$ = 9 WT and n = 9 Cav-1 KO animals, two to three different samples at three different time points (sham and middle cerebral artery occlusion (MCAO) at 6 and 72 h post injury). Animals were perfused (see below) at 6 and 72 h. Our veterinary authority requested the following humane termination endpoints: loss of righting reflex from 24 h post-injury, status epilepticus, body weight loss of more than 25%.
(2) Brain swelling was assessed in mice from a previous experiment (Blochet et al., 2020) with $n$ = 7 WT and $n$ = 9 Cav-1 KO mice. Briefly, brains were frozen in liquid nitrogen vapor and twelve 20 μm-thick coronal cryostat (Leica CM3050) sections per brain collected on Superfrost-Plus slides (Fisher Scientific). Sections were stained with cresyl violet, imaged with a stereomicroscope (Nikon SMZ 25) at 5× magnification with blinded analysis using ImageJ/FIJI software.

### Experimental Model of Cerebral Ischemia

Focal cerebral ischemia was induced by left MCAO with a monofilament (Doccol Corporation) for 35 min under isoflurane anesthesia as described (Blochet et al., 2020). Ischemia was considered successful if cerebral blood flow during MCAO was below 20% of baseline and over 50% of baseline at reperfusion according to laser Doppler flowmetry (Perimed). Rectal temperature was kept at 37.0 ± 0.5°C during surgery. We performed sham surgery under anesthesia by placing the Doppler probe onto the skull and dissecting the carotid arteries without filament insertion. After surgery, animals were maintained overnight at 28°C. We assessed the coat, eyes and nose, neurological deficit, epileptic seizures, body weight loss and dehydration of all animals daily.

## Immunofluorescence Staining

For tissue collection for immunofluorescence staining mice were transcardially perfused with PBS followed by 4% paraformaldehyde (PFA) at 4°C, 10 mL/min, at 6 and 72 h post injury. Following overnight post-fixation in PFA, brains were incubated in phosphate buffered saline (PBS) with 30% sucrose for 48 h, then frozen in isopentane on dry ice. Coronal cryostat sections (25 μm-thick) were collected, stored in PBS with 30% sucrose at −20°C.

Immunofluorescence staining was performed on above sections with antigen retrieval using cold 33% acetic acid, 66% ethanol and blocking with 1% bovine serum albumin, 5% horse serum, 0.1% Triton X100 solution for 1 h at room temperature. Primary antibodies were: Mouse anti-microtubule associated protein 2 (MAP-2, 1:500, Millipore Merck, cat # MAB3418), Rabbit anti-AQP4 (1:500, Merck cat # AB3594-200UL), Rat anti-cluster of differentiation 31 (CD31) (1:100, BD Biosciences, cat # 550274), Mouse anti-Glial Acidic Fibrillary Protein (GFAP) (1:2000, Merck, cat # MAB3402), Mouse anti-glutamine synthetase (GS, 1:1000, Merck, cat # MAB302). Primary antibodies were incubated in 1% bovine serum albumin (BSA), 0.3% Triton X100 in PBS overnight at 4°C. Alexa Fluor-labeled (Invitrogen) secondary antibodies were incubated in the same solution with 4',6-diamidino-2-phenylindole (DAPI) for 1 h at room temperature. Sections were mounted on SuperFrost-Plus slides (Fischer Scientific) with FluorSave medium (Calbiochem) and coverslipped.

## Image Acquisition and Analysis

We captured images of coronal brain sections using a slide-scanner (Zeiss AxioScan Z1) at 10× magnification. We acquired higher magnification images (63×) of ipsilateral and contralateral striatum and cortex to the lesion with a confocal microscope (Zeiss LSM 710 Quasar).

For AQP4 expression patterns, vessel density analysis and astrocyte morphological analysis Images were acquired in ipsilateral and contralateral striatum and cortex to the lesion with the same confocal microscope at 40× magnification (**Figures 2**, **3**). We analyzed AQP4 expression and then vessel density using the Fiji vessel density plugin (open source image processing package). This software analyzes vessel-like signals and calculates vascular density = vessel area/total area × 100% and vascular length density = skeletonized vessel area/total area × 100%. Quantification was done on averaged z-projections using Fiji on stacks of seven to nine images with 2 μm-spacing with three images for each region of interest per animal (ipsilateral and contralateral striatum and cortex in animals following stroke and striatum and cortex in sham animals, **Supplementary Figure S1**), three animals per group (Cav-1 KO and WT). Astrocyte morphology was analyzed in the same regions using Fiji's bandpass and unsharp mask filtering, binarization, skeletonization and analysis on the averaged z-projections as described previously (Blochet et al., 2020). Quantification was done on averaged z-projections using Fiji on stacks of seven to nine images with 2 μm-spacing on three images for each brain region per animal (ipsilateral and contralateral cortex in animals following stroke and cortex in sham animals), three animals per group (Cav-1 KO and WT). AQP4 expression pattern, vessel density and astrocyte morphology analyses were performed blinded.

## Statistical Analysis

Data were expressed as median, interquartile range, minimal and maximal values and analyzed with IBM SPSS Statistics 25 and Graphpad Prism 8. Data normalization was conducted in a two-step approach as described previously. We carried out one-way ANOVA with Tukey's correction for multiple comparisons of six groups (Cav-1 KO/WT ipsilateral/contralateral and Cav-1 KO/WT sham cortex/striatum) for immunofluorescence analysis of AQP4 and CD31 expression patterns in the cortex and comparison of six groups (Cav-1 KO/WT ipsilateral/contralateral cortex and Cav-1 KO/WT sham cortex) for immunofluorescence analysis of astrocyte morphology. The association between AQP4 expression patterns and astrocyte morphology was assessed with Pearson correlation coefficient. Statistical significance was set at $^{*}p < 0.05$, $^{**}p < 0.01$, $^{***}p < 0.005$ and $^{****}p < 0.001$.

# RESULTS

## AQP4 Expression in WT and in Cav-1 KO Mice and Brain Swelling

Using an anti-body to the neuronal marker microtubule associated protein 2 (MAP-2), we delineated the lesion area by lack of MAP-2 labeling on coronal brain sections (white dashed lines, **Figure 1A**). GFAP staining was performed at 6 and 72 h post injury (**Figure 1B**). Decreased GFAP staining was observed in the ipsilateral striatum of both genotypes after stroke with a larger decrease in Cav-1 KO mice than WT mice at 72 h after stroke onset (**Figure 1B**). The area of enhanced GFAP labeling corresponding to the glial scar in the perilesion was smaller in Cav-1 KOs than WTs (yellow arrows, **Figure 1B**).

AQP4 staining was observed in the periventricular areas and in the glia limitans with no significant difference between the two genotypes (**Figure 1C**). AQP4-labeling was absent in the striatum of Cav-1 KO mice at six but not in WTs, indicating a difference in AQP4 expression after stroke. Similarly, AQP4 labeling in the perilesion and contralateral cortex was decreased in Cav-1 KO mice compared to WT at 6 and 72h after stroke onset (red arrows, **Figure 1C**).

Brain swelling (**Figure 1D**) was higher in Cav-1 KO than in WT mice (outlined by white dotted lines corresponding to the ipsilateral hemisphere relative to the contralateral hemisphere in **Figure 1C**). Quantification of GFAP and AQP4 staining was done on higher magnification images to assess cell morphology (GFAP) and cellular location (AQP4) respectively.

## Perivascular AQP4 Expression

AQP4 was present on GFAP-positive astrocyte end-feet encircling the CD31-immunolabelled endothelial cells (**Figure 1E**) in all brain regions investigated. In contrast, AQP4 staining pattern in the lesion (ipsilateral striatum) was punctate without perivascular

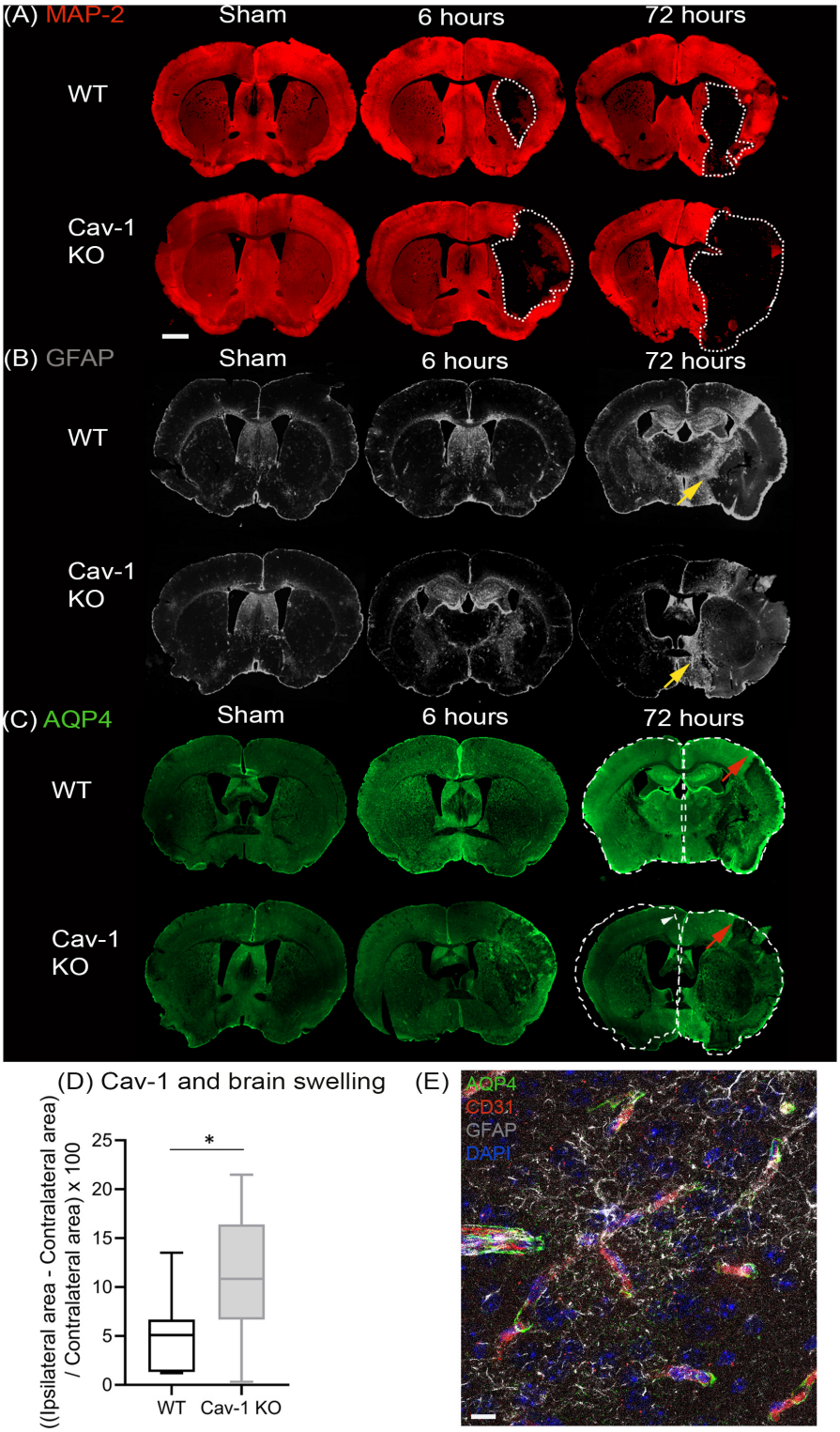


**FIGURE 1 |** Immunostaining of coronal slices of WT and Cav-1 KO mice after sham surgery and at 6 and 72 h after MCAO: **(A)** MAP-2 expression (red) showing the lesion outlined by a white dotted line. **(B)** GFAP expression (gray) showing the extent of the astrocyte scar highlighted by yellow arrows. **(C)** AQP4 expression (green); the contralateral hemisphere area is delineated by a white dotted line relative to the ipsilateral hemisphere to appreciate the swelling and the white arrowhead points to the shift of the midline due to swelling. Red arrows highlight AQP4 staining in the cortical perilesion. Scale bar = 1 mm. **(D)** Brain swelling at 7 days after MCAO in WT and Cav-1 KO mice. **(E)** Immuno-staining at ×63 magnification illustrating the relationship between AQP4 (green), vessels labeled by CD31 (red) and reactive astrocytes (gray), scale bar = 10 μm.

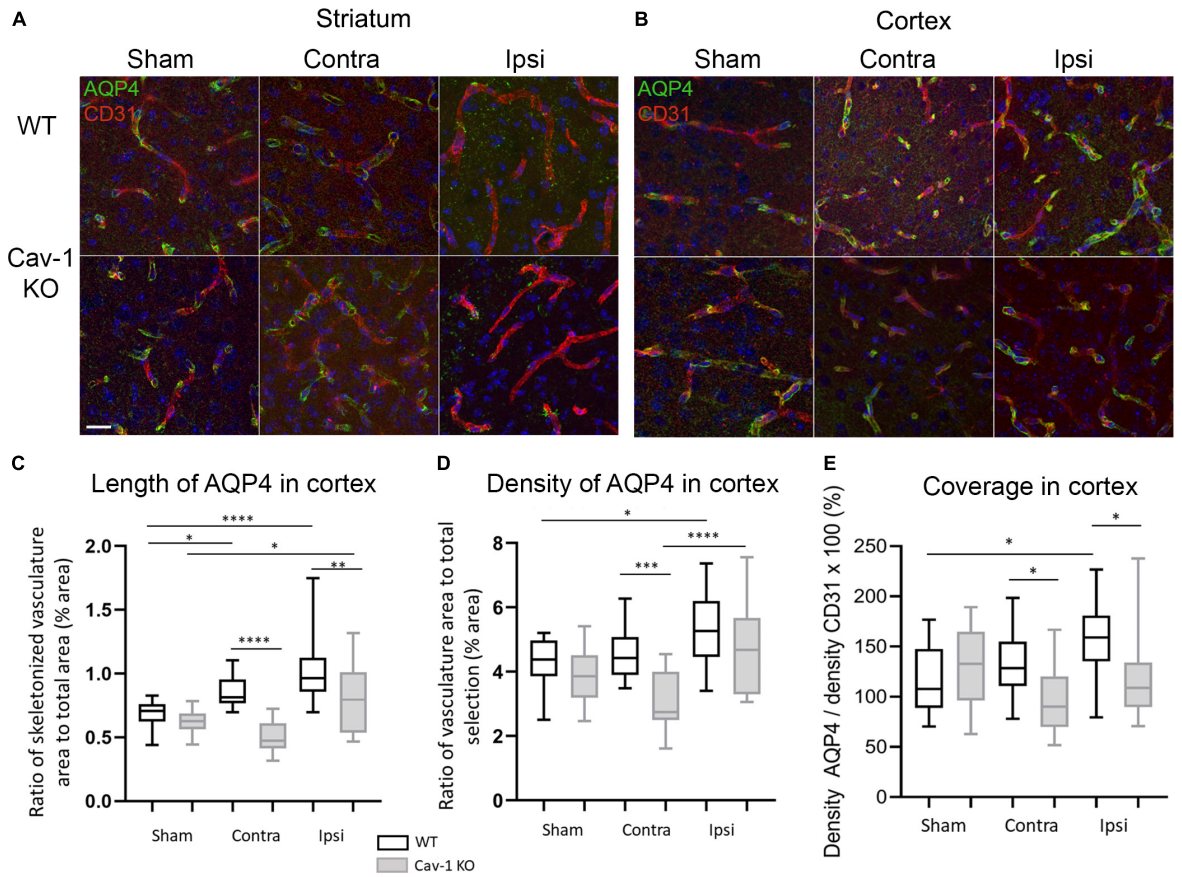


**FIGURE 2 | (A)** High magnification images of AQP4 on vessels stained by CD31 at 72 h post-MCAO (×63 magnification) in the striatum. **(B)** High magnification images of AQP4 on vessels stained with CD31 at 72 h post-MCAO (×63 magnification) in the cortex. **(C)** Analysis of the length of AQP4-immunolabeled vessel-like structures with Fiji vascular density plug-in in WT and Cav-1 KO after MCAO and in sham animals; $n = 3$ areas per animal with three animals per group. Black and gray plots refer to WT and Cav-1 KO animals, respectively. Significant differences between WT and Cav-1 KO animals are noted as $^{*}p < 0.05$, $^{**}p < 0.01$, $^{***}p < 0.005$ and $^{****}p < 0.001$. WT-Sham compared to WT-Ipsi: 95% CI [−0.4949 to −0.1666], $p < 0.0001$, WT-Sham compared to WT-Contra: 95% CI [−0.3330 to −0.004702], $p = 0.04$, KO-Sham compared to KO-Ipsi: 95% CI [−0.3355 to −0.007202], $p = 0.0354$, WT-Contra compared to KO-Contra: 95% CI [0.1888 to 0.5171], $p < 0.0001$, and WT-Ipsi compared to KO-Ipsi: 95% CI [0.05398 to 0.3822], $p = 0.0027$. **(D)** Analysis of the density of AQP4-immunolabeled vessel-like structures assessed by the same Fiji plug-in. WT-Sham compared to WT-Ipsi: 95% CI [−1.985 to −0.09168], $p = 0.0229$, WT-Contra compared to KO-Contra: 95% CI [0.5432 to 2.436], $p = 0.0002$, KO-Contra compared to KO-Ipsi: 95% CI [−2.594 to −0.7009], $p < 0.0001$. **(E)** Analysis of the coverage of AQP4 on vessels measured as the ratio between the density of AQP-4 vessel-like pattern and CD31-labeled vessels. WT-Sham compared to WT-Ipsi: 95% CI [−73.27 to −1.223], $p = 0.0384$, WT-Contra compared to KO-Contra: 95% CI [3.157 to 75.20], $p = 0.0247$, WT-Ipsi compared to KO-Ipsi: 95% CI [3.509 to 75.55], $p = 0.0228$. Contra: contralateral hemisphere to the lesion, Ipsi: ipsilateral hemisphere to the lesion. Scale bar = 20 μm. Comparisons were carried out by one-way ANOVA with Tukey's multiple comparisons post-test.

staining in WT and KOs (**Figure 2A**). Note, in the lesion the decrease in AQP4-staining is more pronounced in the Cav-1 KO mice.

AQP4 staining was observed around the blood vessels in the perilesion and contralateral cortex in both genotypes. A significant increase in the length of perivascular-AQP4 staining was observed in the ipsilateral and contralateral cortex of WT stroke animals compared to WT sham (Tukey's multiple comparisons test, 95% CI [−0.4949 to −0.1666], $p < 0.0001$ and 95% CI −0.3330 to −0.004702], $p = 0.04$ respectively) (**Figure 2B**). The same was observed in sham Cav-1 KO mice compared to ipsilateral cortex (KO-Sham compared to KO-Ipsi: 95% CI [−0.3355 to −0.007202], $p = 0.0354$) but not for the contralateral cortex. Interestingly, the length of AQP4 staining was significantly decreased in the ipsi- and contralateral cortex of the Cav-1 KO mice compared to WTs after stroke (WT-Contra compared to KO-Contra: 95% CI [0.1888 to 0.5171], $p < 0.0001$, and WT-Ipsi compared to KO-Ipsi: 95% CI [0.05398 to 0.3822], $p = 0.0027$) (**Figure 2C**). Blood vessels were stained with CD31 (**Figure 2A**) and measurements (not shown) showed a significant increase in vascular density in the lesion compared to sham, consistent with what has been previously reported (Blochet et al., 2020). The coverage of CD31-positive blood vessels by perivascular AQP4 was significantly increased in the perilesion/ipsilateral cortex WT stroke animals compared to sham (WT-Sham compared to WT-Ipsi: 95% CI [−73.27 to −1.223], $p = 0.0384$) (**Figure 2E**). However, perivascular AQP4 coverage was significantly lower in Cav-1 KO mice compared to WT in the ipsi- and contralateral cortex (WT-Contra

compared to KO-Contra: 95% CI [3.157 to 75.20], $p = 0.0247$, WT-Ipsi compared to KO-Ipsi: 95% CI [3.509 to 75.55], $p = 0.0228$.) (**Figure 2E**).

## Morphological Alterations of GFAP-Positive Astrocytes

In both genotypes there was GFAP staining in the ipsi- and contralateral cortex (**Figure 3A**) and the labeling was significantly decreased in the lesion (**Figure 1A**). Images of GFAP-positive astrocytes were skeletonized for morphological analysis (**Figure 3B**). There were significantly fewer GFAP positive astrocytes in the ipsilateral cortex of Cav-1 KO mice compared to WT (WT-Ipsi compared to KO-Ipsi: 95% CI [10.92 to 19.31], $p < 0.0001$) (**Figure 3C**). Morphological analysis showed a significant increase in the branch length of astrocytes in the ipsi- and contralateral cortex of WT stroke mice compared to sham (WT-Sham compared to WT-Ipsi: 95% CI [−2.455 to −1.005], $p < 0.0001$, WT-Sham compared to WT-Contra: 95% CI [−1.648 to −0.1988], $p = 0.0054$, WT-Ipsi compared to WT-Contra: 95% CI: [−1.531 to −0.08208], $p = 0.0210$). It also showed shorter process length in Cav-1 KO stroke mice in the ipsilateral cortex compared to WT (WT-Ipsi compared to KO-Ipsi: 95% CI [0.5799 to 2.029], $p < 0.0001$) (**Figure 3C**). Similar results were obtained for GS-positive astrocytes (**Supplementary Figure S2**). As observed for AQP4-labeling, there was no change in the length of GFAP-positive branches in Cav-1 KO stroke mice compared to sham (**Figure 3D**). These results suggested a potential relationship between AQP4 expression and astrocyte morphology. Analysis of AQP4 staining and reactive astrocyte morphology exhibited positive correlation between the length of AQP4-immunolabelled vessel-like structures and number of GFAP-positive branches in WT mice (Pearson correlation coefficient = 0.532, $p = 0.005$; **Figure 3E**). Conversely, in Cav-1 KO mice a negative correlation between length of AQP4-immunolabelled vessel-like structures and branch length (Pearson correlation coefficient = −0.443, $p = 0.021$) was observed (**Figure 3E**). No association between AQP4 expression patterns and selected morphological features of GS-immunolabeled astrocytes was observed.

# DISCUSSION

Cav-1 deficient mice are vulnerable to stroke as they develop larger lesions and recover less well than WT mice (Blochet et al., 2020). We show now that mice lacking Cav-1 have significantly less astrocytic AQP4 in the lesion core, perilesion and contralateral cortex after stroke. In addition, there was less perivascular coverage by AQP4 in these areas. Concomitant with the changes in AQP4 expression and coverage, reactive astrocyte morphological changes were severely diminished and brain swelling was increased in the Cav-1 KO mice after stroke. The work indicates a link between Cav-1, reactive astrocyte morphology and perivascular astrocytic AQP4 expression, brain edema and consequent recovery after stroke.

## Diminished Perivascular AQP4 Expression: Consequence on Brain Edema After Stroke

There is abundant literature on the role of AQP4 in brain edema (for review Badaut et al., 2014). The contribution of AQP4 varies greatly depending on time post-injury, brain region, amongst others leading to apparently contradictory results on edema, lesion size and outcome in AQP4 KO mice after stroke (Manley et al., 2000; Yao et al., 2008; Zeng et al., 2012; Hirt et al., 2017). AQP4 expression was rapidly up-regulated in the lesion and perilesion at 6 h in WT mice in agreement with our earlier description of an increase 1 h after stroke onset in the infarct core and ischemic penumbra (de Castro Ribeiro et al., 2006; Hirt et al., 2009). However, there was less increase in AQP4-staining in Cav-1 KOs indicating that the absence of Cav-1 affects AQP4 expression. The lower AQP4 expression is associated with a larger edema formation, which is in agreement with our earlier observation that up-regulating AQP4 on astrocytic end-feet, attenuated the early phase of hemispheric enlargement 1 h after MCAO (Hirt et al., 2009). WT mice exhibited higher perivascular expression of AQP4 (**Figure 2**). Interestingly, disrupted perivascular AQP4 polarization caused by reactive astrogliosis was shown to impair glymphatic clearance in the models of Alzheimer disease and senescence (Kress et al., 2014). Altogether, increased perivascular AQP4 after stroke could be a protective mechanism by promoting edema resolution and facilitating water and debris clearance from the perivascular space.

## Role of Cav-1 in Perivascular AQP4 Changes: Potential Mechanisms

Lower perivascular AQP4 expression was observed after stroke in absence of Cav-1, suggesting a role for Cav-1 in AQP4 expression in astrocyte perivascular end-feet (**Figure 2**). In support of our observations, Cav-1 has recently been implicated in movement of AQP4 to the cell surface after oxidative stress (Bi et al., 2017). Insertion of AQP4-heterotetramers depend on the syntrophin, dystrophin-dystroglycan complex in association with the extracellular matrix protein agrin (Noell et al., 2011; Vella et al., 2015; Tham et al., 2016). Interestingly, Cav-1 binds β-dystroglycan in smooth muscle cells, linking the extracellular matrix and actin cytoskeleton (Sharma et al., 2010). Neuronal nitric-oxide synthase has been shown to down-regulate the level of expression α-syntrophin (Brenman et al., 1996; Hashida-Okumura et al., 1999; Sato et al., 2004; Zhang, 2017). As a hypothesis, Cav-1 might act on α-syntrophin levels via inhibition of eNOS, which in turn might influence the level of AQP4 on the perivascular end-feet membranes.

Another possibility for the decrease in perivascular AQP4 is a change in laminin expression in astrocytes and endothelial cells. The lack of astrocytic laminin expression in conditional knockout mice has been shown to prevent pericyte differentiation and inhibit AQP4 expression, causing BBB breakdown (Yao et al., 2014). Cav1-KO mice showed less laminin-labeled endothelial cells in the ipsilateral hemisphere following ischemic stroke than

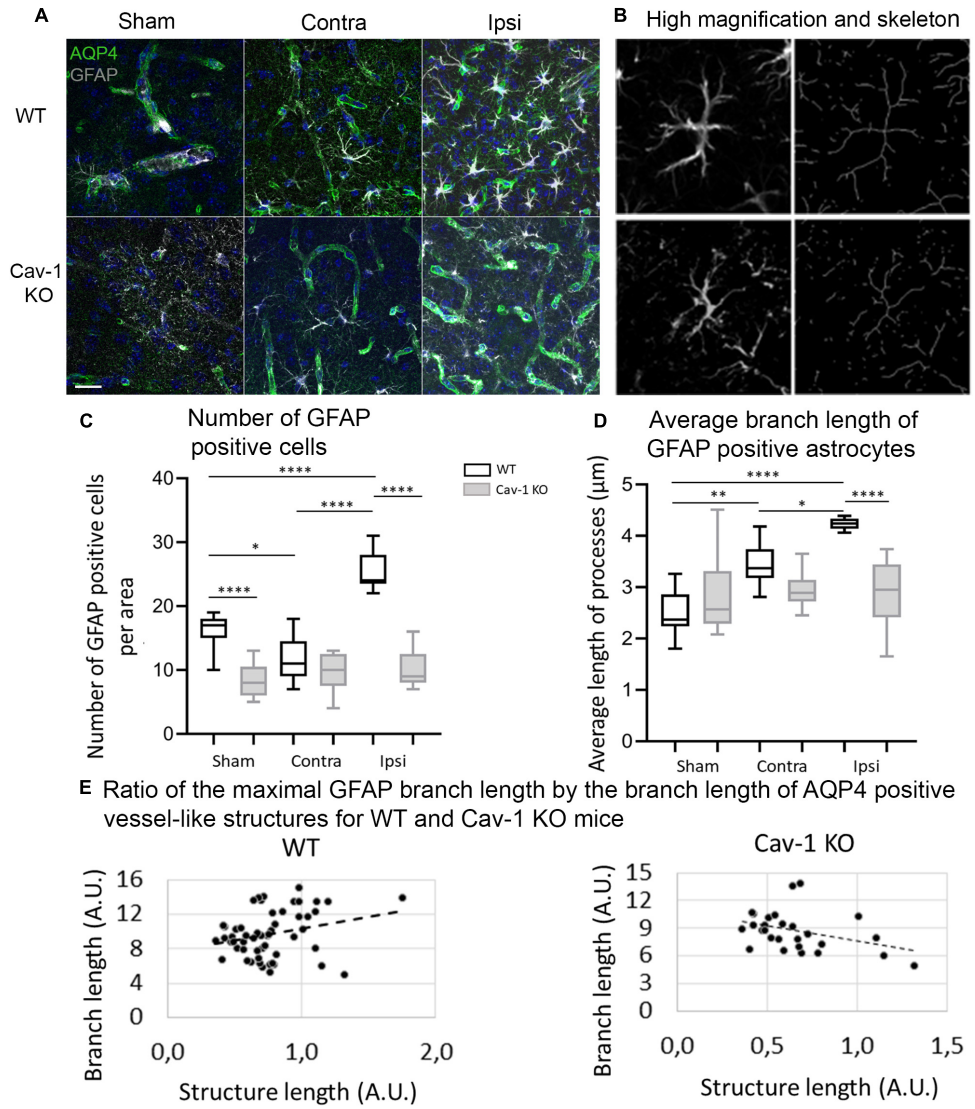


**FIGURE 3 | (A)** Immunofluorescence staining with AQP4 (green) and GFAP (gray) in WT and Cav-1 KO mice at 72 h post-MCAO (63× magnification). AQP4 co-localized with GFAP-positive astrocyte end-feet. Scale bar = 20 μm. **(B)** Single-channel confocal microscopy ROIs obtained from 40× magnification images, illustrating the overview of a GFAP-positive astrocyte morphology and its skeletonization. **(C)** Number of GFAP-positive reactive astrocytes. WT-Sham compared to WT-Ipsi: 95% CI: [−13.42 to −5.027], $p < 0.0001$, WT-Sham compared to WT-Contra: 95% CI [0.4716 to 8.862], $p = 0.0212$, WT-Sham compared to KO-Sham: 95% CI: [3.805 to 12.20], $p < 0.0001$, WT-Ipsi compared to WT-Contra: 95% CI [−18.08 to −9.694], $p < 0.0001$, and WT-Ipsi compared to KO-Ipsi: 95% CI [10.92 to 19.31], $p < 0.0001$. **(D)** Average branch length of GFAP-positive astrocytes. WT-Sham compared to WT-Ipsi: 95% CI [−2.455 to −1.005], $p < 0.0001$, WT-Sham compared to WT-Contra: 95% CI [−1.648 to −0.1988], $p = 0.0054$, WT-Ipsi compared to WT-Contra: 95% CI: [−1.531 to −0.08208], $p = 0.0210$, and WT-Ipsi compared to KO-Ipsi: 95% CI [0.5799 to 2.029], $p < 0.0001$. Comparisons were carried out by one-way ANOVA with Tukey's multiple comparisons post-test. **(E)** The positive correlation between the length of AQP4-immunolabeled vessel-like structures and the maximal branch length of GFAP-immunolabeled astrocytes in WT mice (Pearson correlation coefficient = 0.451, $p = 0.024$) and Cav-1 KO mice (Pearson correlation coefficient = −0.443, $p = 0.021$).

WT mice (Jasmin et al., 2007). Therefore, lower perivascular AQP4 after stroke in cav-1 KO mice could be a consequence of decreased laminin.

## Altered Reactive Astrocyte Morphology in Cav-1 KO Mice: Relation With AQP4

In contrast to our previous analysis in the striatal perilesion (Blochet et al., 2020), we observed a lower number of GFAP-labeled astrocytes in the ipsilateral cortex of MCAO Cav-1 KO animals compared to WT animals. Cav-1 KO mice also had a lower degree of GFAP branching after stroke in the perilesional and contralateral cortex than WTs (**Figure 3**) in agreement with our earlier work (Blochet et al., 2020). Interestingly, the number of GFAP-positive processes correlated positively with perivascular AQP4 expression in WT animals after stroke but negatively in Cav-1 KO mice. This suggests that the attenuated morphological alterations of astrocytes after stroke in Cav-1 KO mice are linked

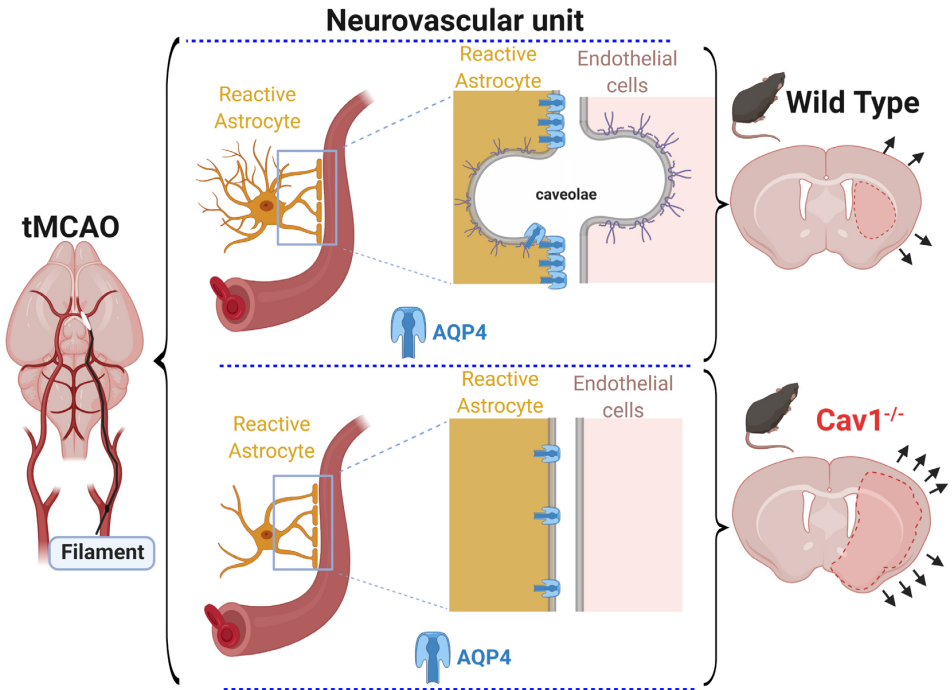


**FIGURE 4 |** After transient filament MCAO (left), Cav 1 KO mice had larger lesions, enhanced cerebral edema and higher hemispheric swelling (bottom right) compared to WT mice (top right). At the level of the NVU (center images), the absence of caveolae* and Cav-1 correlated with altered astroglial reaction and expression of AQP4 on astrocytic end-feet in Cav-1 KO mice (bottom center) compared to WT mice (top center).

to decreased AQP4 expression. Previously, reduced AQP4 expression and loss of perivascular AQP4 localization were related to disorganized intermediate filaments in reactive astrocytes (de Castro Ribeiro et al., 2006; Allnoch et al., 2019). Cav-1 may influence AQP4 expression levels by inhibiting nitric oxide synthase, as nitric oxide was described to increase AQP4 expression and to influence astrocyte volume (Yu et al., 2012; Oku et al., 2015). AQPs seem to contribute to reactive astrocyte morphology and we showed the importance of AQP9 in astrocyte morphological changes *in vitro* and *in vivo* (Hirt et al., 2018b).

In summary, Cav-1 appears to influence AQP4 expression and distribution along vessels contributing to changes in reactive astrogliosis and brain edema observed in Cav-1 KO mice after experimental stroke (**Figure 4**). We are currently investigating a therapeutic approach targeting Cav-1 and have shown that the administration of cavtratin, a peptide containing the scaffolding domain of Cav-1 after MCAO improves outcome and enhances angiogenesis (Blochet et al., 2019; Blochet et al., in preparation), perhaps via some of the effects seen in this work. Indeed, understanding Cav-1 changes after stroke may lead to new treatment options for improving outcome after stroke.

## DATA AVAILABILITY STATEMENT

All datasets presented in this study are included in the article/**Supplementary Material**.

## ETHICS STATEMENT

The animal study was reviewed and approved by Commission cantonal d'expérimentation animale, canton de Vaud. Autorisation N°2017.5.

## AUTHOR CONTRIBUTIONS

IF: immunos, image analysis, data analysis, manuscript preparation. CB: surgery, immunos, image analysis, data analysis, manuscript preparation. MP and LB: scientific discussion and manuscript preparation. LH and JB: study concept and manuscript preparation.

## FUNDING

This work was supported by the Swiss Science Foundation grant 31003A_163465/1, by the Biaggi and Juchum Foundations, by the Novartis Foundation for Biomedical Research grant #18C170 and by a Boehringer Ingelheim Fonds Travel Grant grant to Irina Filchenko. EraNet Neuron TRAINS (JB) and MISST (JB).

## SUPPLEMENTARY MATERIAL

The Supplementary Material for this article can be found online at: https://www.frontiersin.org/articles/10.3389/fcell.2020.00371/full#supplementary-material

**FIGURE S1 | (A)** Coronal brain sections at 72 h after sham and MCAO injury showing the different regions of interest (ROIs) for on high magnification images and respective quantifications. **(B)** Analysis of cortical astrocytic morphology on GS- and GFAP-immunolabeled images and by skeletonization; $n = 3$ areas per animal with 3 animals per group. The data are shown as median and interquartile range; only significant differences are displayed.

**FIGURE S2 | (A)** Immunofluorescence staining with AQP4 (green) and Glutamine Synthetase (GS) (gray) in WT and Cav-1 KO mice at 72 h post-MCAO (×63 magnification). AQP4 co-localized with GS-positive astrocyte end-feet. Scale bar = 20 μm. **(B)** Single-channel confocal microscopy ROIs obtained from 40× magnification images, illustrating the overview of GS-positive astrocyte morphology and skeletonization. **(C)** Number of GS-positive astrocytes. WT-Ipsi compared to WT-Contra: 95% CI [−18.54 to −1.904], $p = 0.0081$, and WT-Ipsi compared to KO-Ipsi: 95% CI [6.348 to 22.99], $p < 0.0001$. **(D)** Ramification of GS-positive astrocytes assessed by the number of quadruple points of GS-positive astrocytes. WT-Sham compared to WT-Ipsi: 95% CI [−0.9914 to −0.03480], $p = 0.0289$, and WT-Ipsi compared to KO-Ipsi: 95% CI [0.09476 to 1.051], $p = 0.0105$. Comparisons were carried out by one-way ANOVA with Tukey's multiple comparisons post-test.

## REFERENCES


Allnoch, L., Baumgartner, W., and Hansmann, F. (2019). Impact of astrocyte depletion upon inflammation and demyelination in a murine animal model of multiple sclerosis. *Int. J. Mol. Sci.* 20:3922. doi: 10.3390/ijms20163922

Aoki, T., Suzuki, T., Hagiwara, H., Kuwahara, M., Sasaki, S., Takata, K., et al. (2012). Close association of aquaporin-2 internalization with caveolin-1. *Acta Histochem. Cytochem.* 45, 139–146. doi: 10.1267/ahc.12003

Ayloo, S., and Gu, C. (2019). Transcytosis at the blood-brain barrier. *Curr. Opin. Neurobiol.* 57, 32–38. doi: 10.1016/j.conb.2018.12.014

Badaut, J., Ajao, D. O., Sorensen, D. W., Fukuda, A. M., and Pellerin, L. (2015). Caveolin expression changes in the neurovascular unit after juvenile traumatic brain injury: signs of blood-brain barrier healing? *Neuroscience* 285, 215–226. doi: 10.1016/j.neuroscience.2014.10.035

Badaut, J., Fukuda, A. M., Jullienne, A., and Petry, K. G. (2014). Aquaporin and brain diseases. *Biochim. Biophys. Acta* 1840, 1554–1565. doi: 10.1016/j.bbagen.2013.10.032

Bi, C., Tham, D. K. L., Perronnet, C., Joshi, B., Nabi, I. R., and Moukhles, H. (2017). The oxidative stress-induced increase in the membrane expression of the water-permeable channel aquaporin-4 in astrocytes is regulated by caveolin-1 phosphorylation. .*Front Cell Neurosci.* 11:412. doi: 10.3389/fncel.2017.00412

Blochet, C., Buscemi, L., Clement, T., Badaut, J., and Hirt, L. (2019). "Caveolin-1 role in neovascularization and astrogliosis after stroke and effects of cavtratin as a neuroprotectant," in *Proceedings of the 29th International Symposium on Cerebral Blood Flow, Metabolism and Function / 14th International Conference on Quantification of Brain*, (Yokohama: Sage).

Blochet, C., Buscemi, L., Clement, T., Gehri, S., Badaut, J., and Hirt, L. (2020). Involvement of caveolin-1 in neurovascular unit remodeling after stroke: effects on neovascularization and astrogliosis. *J. Cereb. Blood Flow Metab.* 40, 163–176. doi: 10.1177/0271678X18806893

Brenman, J. E., Chao, D. S., Gee, S. H., McGee, A. W., Craven, S. E., Santillano, D. R., et al. (1996). Interaction of nitric oxide synthase with the postsynaptic density protein PSD-95 and alpha1-syntrophin mediated by PDZ domains. *Cell* 84, 757–767. doi: 10.1016/s0092-8674(00)81053-3

Choi, K. H., Kim, H. S., Park, M. S., Lee, E. B., Lee, J. K., Kim, J. T., et al. (2016). Overexpression of caveolin-1 attenuates brain edema by inhibiting tight junction degradation. *Oncotarget* 7, 67857–67867. doi: 10.18632/oncotarget.12346

Clement, T., Rodriguez-Grande, B., and Badaut, J. (2020). Aquaporins in brain edema. *J. Neurosci. Res.* 98, 9–18. doi: 10.1002/jnr.24354

de Castro Ribeiro, M., Hirt, L., Bogousslavsky, J., Regli, L., and Badaut, J. (2006). Time course of aquaporin expression after transient focal cerebral ischemia in mice. *J. Neurosci. Res.* 83, 1231–1240. doi: 10.1002/jnr.20819

Gundersen, G. A., Vindedal, G. F., Skare, O., and Nagelhus, E. A. (2014). Evidence that pericytes regulate aquaporin-4 polarization in mouse cortical astrocytes. *Brain Struct. Funct.* 219, 2181–2186. doi: 10.1007/s00429-013-0629-0

Hashida-Okumura, A., Okumura, N., Iwamatsu, A., Buijs, R. M., Romijn, H. J., and Nagai, K. (1999). Interaction of neuronal nitric-oxide synthase with alpha1-syntrophin in rat brain. *J. Biol. Chem.* 274, 11736–11741. doi: 10.1074/jbc.274.17.11736

Hirt, L., Fukuda, A. M., Ambadipudi, K., Rashid, F., Binder, D., Verkman, A., et al. (2017). Improved long-term outcome after transient cerebral ischemia in aquaporin-4 knockout mice. *J. Cereb. Blood Flow Metab.* 37, 277–290. doi: 10.1177/0271678X15623290

Hirt, L., Price, M., Benakis, C., and Badaut, J. (2018a). Aquaporins in neurological disorders. *Cln. Transl. Neurosci.* 2, 1–7. doi: 10.1177/2514183X17752902

Hirt, L., Price, M., Mastour, N., Brunet, J. F., Barriere, G., Friscourt, F., et al. (2018b). Increase of aquaporin 9 expression in astrocytes participates in astrogliosis. *J. Neurosci. Res.* 96, 194–206. doi: 10.1002/jnr.24061

Hirt, L., Ternon, B., Price, M., Mastour, N., Brunet, J. F., and Badaut, J. (2009). Protective role of early aquaporin 4 induction against postischemic edema formation. *J. Cereb. Blood Flow Metab.* 29, 423–433. doi: 10.1038/jcbfm.2008.133

Iliff, J. J., Wang, M., Liao, Y., Plogg, B. A., Peng, W., Gundersen, G. A., et al. (2012). A paravascular pathway facilitates CSF flow through the brain parenchyma and the clearance of interstitial solutes, including amyloid beta. *Sci. Transl. Med.* 4:147ra111. doi: 10.1126/scitranslmed.3003748

Jablonski, E. M., and Hughes, F. M. (2006). The potential role of caveolin-1 in inhibition of aquaporins during the AVD. *Biol. Cell.* 98, 33–42. doi: 10.1042/BC20040131

Jasmin, J. F., Malhotra, S., Singh Dhallu, M., Mercier, I., Rosenbaum, D. M., and Lisanti, M. P. (2007). Caveolin-1 deficiency increases cerebral ischemic injury. *Circ. Res.* 100, 721–729. doi: 10.1161/01.RES.0000260180.42709.29

Jha, R. M., Kochanek, P. M., and Simard, J. M. (2019). Pathophysiology and treatment of cerebral edema in traumatic brain injury. *Neuropharmacology* 145(Pt B), 230–246. doi: 10.1016/j.neuropharm.2018.08.004

Jung, S., Kim, S. O., Cho, K. A., Song, S. H., Kang, T. W., Park, K., et al. (2015). Loss of caveolin 1 is associated with the expression of aquaporin 1 and bladder dysfunction in mice. *Int. Neurourol. J.* 19, 34–38. doi: 10.5213/inj.2015.19.1.34

Kim, S. O., Song, S. H., Park, K., and Kwon, D. (2013). Overexpression of aquaporin-1 and caveolin-1 in the rat urinary bladder urothelium following bladder outlet obstruction. *Int. Neurourol. J.* 17, 174–179. doi: 10.5213/inj.2013.17.4.174

Knowland, D., Arac, A., Sekiguchi, K. J., Hsu, M., Lutz, S. E., Perrino, J., et al. (2014). Stepwise recruitment of transcellular and paracellular pathways underlies blood-brain barrier breakdown in stroke. *Neuron* 82, 603–617. doi: 10.1016/j.neuron.2014.03.003

Kress, B. T., Iliff, J. J., Xia, M., Wang, M., Wei, H. S., Zeppenfeld, D., et al. (2014). Impairment of paravascular clearance pathways in the aging brain. *Ann. Neurol.* 76, 845–861. doi: 10.1002/ana.24271

Li, X., McClellan, M. E., Tanito, M., Garteiser, P., Towner, R., Bissig, D., et al. (2012). Loss of caveolin-1 impairs retinal function due to disturbance of subretinal microenvironment. *J. Biol. Chem.* 287, 16424–16434. doi: 10.1074/jbc.M112.353763

Lindblom, P., Gerhardt, H., Liebner, S., Abramsson, A., Enge, M., Hellstrom, M., et al. (2003). Endothelial PDGF-B retention is required for proper investment of pericytes in the microvessel wall. *Genes Dev.* 17, 1835–1840. doi: 10.1101/gad.266803

Manley, G. T., Fujimura, M., Ma, T., Noshita, N., Filiz, F., Bollen, A. W., et al. (2000). Aquaporin-4 deletion in mice reduces brain edema after acute water intoxication and ischemic stroke. *Nat. Med.* 6, 159–163. doi: 10.1038/72256

Michinaga, S., and Koyama, Y. (2015). Pathogenesis of brain edema and investigation into anti-edema drugs. *Int. J. Mol. Sci.* 16, 9949–9975. doi: 10.3390/ijms16059949

Munk, A. S., Wang, W., Bechet, N. B., Eltanahy, A. M., Cheng, A. X., Sigurdsson, B., et al. (2019). PDGF-B is required for development of the glymphatic system. *Cell. Rep.* 26, 2955.e3–2969.e3. doi: 10.1016/j.celrep.2019.02.050

Noell, S., Wolburg-Buchholz, K., Mack, A. F., Beedle, A. M., Satz, J. S., Campbell, K. P., et al. (2011). Evidence for a role of dystroglycan regulating the membrane architecture of astroglial endfeet. *Eur. J. Neurosci.* 33, 2179–2186. doi: 10.1111/j.1460-9568.2011.07688.x

Oku, H., Morishita, S., Horie, T., Kida, T., Mimura, M., Fukumoto, M., et al. (2015). Nitric oxide increases the expression of aquaporin-4 protein in rat optic nerve astrocytes through the cyclic guanosine monophosphate/protein kinase G pathway. *Ophthalmic Res.* 54, 212–221. doi: 10.1159/000440846

Parton, R. G., and del Pozo, M. A. (2013). Caveolae as plasma membrane sensors, protectors and organizers. *Nat. Rev. Mol. Cell. Biol.* 14, 98–112. doi: 10.1038/nrm3512

Sadeghian, H., Lacoste, B., Qin, T., Toussay, X., Rosa, R., Oka, F., et al. (2018). Spreading depolarizations trigger caveolin-1-dependent endothelial transcytosis. *Ann. Neurol.* 84, 409–423. doi: 10.1002/ana.25298

Sato, Y., Sagami, I., and Shimizu, T. (2004). Identification of caveolin-1-interacting sites in neuronal nitric-oxide synthase. Molecular mechanism for inhibition of NO formation. *J. Biol. Chem.* 279, 8827–8836. doi: 10.1074/jbc.M310327200

Sharma, P., Ghavami, S., Stelmack, G. L., McNeill, K. D., Mutawe, M. M., Klonisch, T., et al. (2010). beta-Dystroglycan binds caveolin-1 in smooth muscle: a functional role in caveolae distribution and Ca2+ release. *J. Cell Sci.* 123(Pt 18), 3061–3070. doi: 10.1242/jcs.066712

Simard, J. M., Kent, T. A., Chen, M., Tarasov, K. V., and Gerzanich, V. (2007). Brain oedema in focal ischaemia: molecular pathophysiology and theoretical implications. *Lancet Neurol.* 6, 258–268. doi: 10.1016/S1474-4422(07)70055-8

Tham, D. K., Joshi, B., and Moukhles, H. (2016). Aquaporin-4 cell-surface expression and turnover are regulated by dystroglycan, dynamin, and the extracellular matrix in astrocytes. *PLoS One* 11:e0165439. doi: 10.1371/journal.pone.0165439

Vella, J., Zammit, C., Di Giovanni, G., Muscat, R., and Valentino, M. (2015). The central role of aquaporins in the pathophysiology of ischemic stroke. *Front. Cell Neurosci.* 9:108. doi: 10.3389/fncel.2015.00108

Villabona-Rueda, A., Erice, C., Pardo, C. A., and Stins, M. F. (2019). The evolving concept of the blood brain barrier (BBB): from a single static barrier to a heterogeneous and dynamic relay center. *Front. Cell. Neurosci.* 13:405. doi: 10.3389/fncel.2019.00405

Xu, L., Guo, R., Xie, Y., Ma, M., Ye, R., and Liu, X. (2015). Caveolae: molecular insights and therapeutic targets for stroke. *Expert Opin. Ther. Targets* 19, 633–650. doi: 10.1517/14728222.2015.1009446

Yao, X., Hrabetova, S., Nicholson, C., and Manley, G. T. (2008). Aquaporin-4-deficient mice have increased extracellular space without tortuosity change. *J. Neurosci.* 28, 5460–5464. doi: 10.1523/JNEUROSCI.0257-08.2008

Yao, Y., Chen, Z. L., Norris, E. H., and Strickland, S. (2014). Astrocytic laminin regulates pericyte differentiation and maintains blood brain barrier integrity. *Nat. Commun.* 5:3413. doi: 10.1038/ncomms4413

Yu, L., Yi, J., Ye, G., Zheng, Y., Song, Z., Yang, Y., et al. (2012). Effects of curcumin on levels of nitric oxide synthase and AQP-4 in a rat model of hypoxia-ischemic brain damage. *Brain Res.* 1475, 88–95. doi: 10.1016/j.brainres.2012.07.055

Zeng, X. N., Xie, L. L., Liang, R., Sun, X. L., Fan, Y., and Hu, G. (2012). AQP4 knockout aggravates ischemia/reperfusion injury in mice. *CNS Neurosci. Ther.* 18, 388–394. doi: 10.1111/j.1755-5949.2012.00308.x

Zhang, Y. H. (2017). Nitric oxide signalling and neuronal nitric oxide synthase in the heart under stress. *F1000Research* 6:742. doi: 10.12688/f1000research.10128.1

**Conflict of Interest:** The authors declare that the research was conducted in the absence of any commercial or financial relationships that could be construed as a potential conflict of interest.

frontiers in Cell and Developmental Biology

ORIGINAL RESEARCH
published: 02 July 2020
doi: 10.3389/fcell.2020.00544

# Caspase-3 Activation Correlates With the Initial Mitochondrial Membrane Depolarization in Neonatal Cerebellar Granule Neurons

*Edaena Benítez-Rangel[1,2†], Mauricio Olguín-Albuerne[2], María Cristina López-Méndez[1†], Guadalupe Domínguez-Macouzet[2], Agustín Guerrero-Hernández[1]* and Julio Morán[2]**

[1] Departamento de Bioquímica, CINVESTAV-IPN, Mexico City, Mexico, [2] División de Neurociencias, Instituto de Fisiología Celular, Universidad Nacional Autónoma de México, Mexico City, Mexico

OPEN ACCESS

**Edited by:**
João M. N. Duarte,
Lund University, Sweden

**Reviewed by:**
Alexandra Latini,
Federal University of Santa Catarina, Brazil
Cláudia Pereira,
University of Coimbra, Portugal

***Correspondence:**
Agustín Guerrero-Hernández
aguerrero@cinvestav.mx
Julio Morán
jmoran@ifc.unam.mx

**†Present address:**
Edaena Benítez-Rangel,
Unidad de Morfología y Función,
Facultad de Estudios Superiores Iztacala, Universidad Nacional Autónoma de México, Tlalnepantla, Mexico
María Cristina López-Méndez,
Tecnológico Nacional de México/Instituto Tecnológico Superior de Misantla, Misantla, Mexico

**Specialty section:**
This article was submitted to Molecular Medicine, a section of the journal Frontiers in Cell and Developmental Biology

**Received:** 11 March 2020
**Accepted:** 09 June 2020
**Published:** 02 July 2020

**Citation:**
Benítez-Rangel E, Olguín-Albuerne M, López-Méndez MC, Domínguez-Macouzet G, Guerrero-Hernández A and Morán J (2020) Caspase-3 Activation Correlates With the Initial Mitochondrial Membrane Depolarization in Neonatal Cerebellar Granule Neurons. Front. Cell Dev. Biol. 8:544. doi: 10.3389/fcell.2020.00544

In this study we evaluated the effect of the reduction in the endoplasmic reticulum calcium concentration ($[Ca^{2+}]_{ER}$), changes in the cytoplasmic calcium concentration ($[Ca^{2+}]_i$), alteration of the mitochondrial membrane potential, and the ER stress in the activation of caspase-3 in neonatal cerebellar granule cells (CGN). The cells were loaded with Fura-2 to detect changes in the $[Ca^{2+}]_i$ and with Mag-fluo-4 to measure variations in the $[Ca^{2+}]_{ER}$ or with TMRE to follow modifications in the mitochondrial membrane potential in response to five different inducers of CGN cell death. These inducers were staurosporine, thapsigargin, tunicamycin, nifedipine and plasma membrane repolarization by switching culture medium from 25 mM KCl (K25) to 5 mM KCl (K5). Additionally, different markers of ER stress were determined and all these parameters were correlated with the activation of caspase-3. The different inducers of cell death in CGN resulted in three different levels of activation of caspase-3. The highest caspase-3 activity occurred in response to K5. At the same time, staurosporine, nifedipine, and tunicamycin elicited an intermediate activation of caspase-3. Importantly, thapsigargin did not activate caspase-3 at any time. Both K5 and nifedipine rapidly decreased the $[Ca^{2+}]_i$, but only K5 immediately reduced the $[Ca^{2+}]_{ER}$ and the mitochondrial membrane potential. Staurosporine and tunicamycin increased the $[Ca^{2+}]_i$ and they decreased both the $[Ca^{2+}]_{ER}$ and mitochondrial membrane potential, but at a much lower rate than K5. Thapsigargin strongly increased the $[Ca^{2+}]_i$, but it took 10 min to observe any decrease in the mitochondrial membrane potential. Three cell death inducers - K5, staurosporine, and thapsigargin- elicited ER stress, but they took 30 min to have any effect. Thapsigargin, as expected, displayed the highest efficacy activating PERK. Moreover, a specific PERK inhibitor did not have any impact on cell death triggered by these cell death inducers. Our data suggest that voltage-gated $Ca^{2+}$ channels, that are not dihydropyridine-sensitive, load the ER with $Ca^{2+}$ and this $Ca^{2+}$ flux plays a critical role in keeping the mitochondrial membrane potential polarized. A rapid decrease in the $[Ca^{2+}]_{ER}$ resulted in rapid mitochondrial membrane depolarization and strong activation of caspase-3 without the intervention of the ER stress in CGN.

**Keywords: neuronal death, cerebellar granule neurons, calcium, endoplasmic reticulum, mitochondria, endoplasmic reticulum stress**

## INTRODUCTION

The endoplasmic reticulum (ER) is one of the most important intracellular $Ca^{2+}$ stores. It is well documented that a sustained reduction in the luminal [$Ca^{2+}$] of the ER can result in a condition known as ER stress that eventually can lead to cell death (Boyce and Yuan, 2006; Szegedi et al., 2006; Sun et al., 2013). This condition may result in the activation of the ER stress receptor pathways. Particularly, IRE1 can lead to apoptotic cell death by the activation of JNK (Szegedi et al., 2006). We have previously shown that JNK is involved in the apoptotic cell death of cultured neonatal cerebellar granule neurons (CGN) induced by potassium deprivation (K5), but not by staurosporine (Ramiro-Cortés and Morán, 2009). The possible mechanisms relating ER stress activation with the apoptotic death remain to be elucidated. One possibility is that the cytoplasmic $Ca^{2+}$ reduction induced by potassium deprivation could lead to a decrease of the luminal ER [$Ca^{2+}$], which in turn could cause an ER stress in this model.

Alternatively, alterations in the transfer of $Ca^{2+}$ from the ER to the mitochondria could be the reason behind CGN apoptotic death-induced by the decreased $[Ca^{2+}]_i$. It has been calculated that about half of the $Ca^{2+}$ released from the ER is taken up by the mitochondria (Pacher et al., 2000; Lam and Galione, 2013) and that $Ca^{2+}$ movement from the ER to the mitochondria via $IP_3R$ regulates energy production by increasing respiration and accelerating the Krebs cycle (Cardenas et al., 2010, 2015). It is then feasible that a reduction of $Ca^{2+}$ movement from the ER to the mitochondria might result in cell death (Rizzuto et al., 2012).

Programmed cell death is critical for the physiology of the nervous system. Alterations in this program result in different neurological ailments; for instance, an excess of neuronal cell death leads to neurodegenerative diseases such as Parkinson's, Alzheimer's, among others. During development, a large proportion of CGN die (Wood et al., 1993) with features of apoptotic death (Lossi et al., 1998). CGN have been used as a model to study apoptosis during neuronal development. In that regard, it is known that calcium ions ($Ca^{2+}$) are involved in the apoptotic death of CGN. These cells need a sustained $Ca^{2+}$ influx for survival, which can be achieved by culturing cells in high $K^+$ (25 mM, K25), which in turn activates voltage-gated $Ca^{2+}$ channels (VGCC) resulting in a continuous $Ca^{2+}$ influx and increased intracellular calcium concentration ($[Ca^{2+}]_i$) (Gallo et al., 1987; Moran and Patel, 1989; Alavez et al., 1996).

In support of the role played by sustained calcium influx in avoiding apoptosis in CGN, it has been shown that apoptotic cell death of CGN chronically cultured in K25 can be induced by blocking their VGCC (Kingsbury and Balazs, 1987; Balazs et al., 1988; Pearson et al., 1992; Copani et al., 1995). Thus, CGN prepared from postnatal rats maintained in the K25 medium can survive and mature in culture conditions. Moreover, CGN that had been chronically cultured in K25 would die by apoptosis when they are transferred to a non-depolarizing medium containing 5 mM KCl (K5) (Moran and Patel, 1989; D'Mello et al., 1993, 1997; Alavez et al., 1996; Ishitani et al., 1997; Nardi et al., 1997; Villalba et al., 1997; Morán et al., 1999).

The repolarization of plasma membrane potential by transferring cells to 5 mM $K^+$ leads to the deactivation of VGCC. This, in turn, results in the inhibition of $Ca^{2+}$ influx and subsequent cell death. A result that can be prevented by increasing the $[Ca^{2+}]_i$ with the addition of a $Ca^{2+}$ ionophore (Morán et al., 1999). We have also found that caspase-3 transcription and activation induced by K5 is mediated by the fall in the $[Ca^{2+}]_i$ in CGN (Morán et al., 1999). In contrast to K5, the apoptotic death of CGN evoked by other conditions such as the incubation with staurosporine, a generalized kinase inhibitor, turned out to be $Ca^{2+}$-independent. Despite the experimental evidence showing that a reduction in $Ca^{2+}$ influx leads to apoptotic death for CGN, there is not enough information to propose a mechanism of action for $Ca^{2+}$, particularly during the early phase of the apoptotic death in this model.

To test these possibilities, we have evaluated the effect of different inducers of apoptosis on $Ca^{2+}$ release from the ER in cultured neonatal CGN and we have looked into the correlation between this calcium release and caspase-3 activation, mitochondrial depolarization, and ER stress. Based on the present results, we propose that the survival of CGN requires a sustained $Ca^{2+}$ transfer from the ER to the mitochondria to keep this organelle polarized and the inhibition of this $Ca^{2+}$ transfer leads to a rapid mitochondrial partial depolarization that in turn leads to apoptotic death in this neuronal survival model.

## MATERIALS AND METHODS

### Cerebellar Granule Neurons Cultures

All animals used in this study were treated following the accepted standards of animal care and with the procedures approved by the local Committee of Research and Ethics of the Instituto de Fisiología Celular, Universidad Nacional Autónoma de México. The protocol used followed the Guidelines for the Care and Use of Mammals in Neuroscience as well as guidelines released by the Mexican Institutes of Health Research and the National Institutes of Health Guide for the care and use of laboratory animals (NIH Publication No. 8023, revised 1978). All efforts were made to minimize animal suffering and to reduce the number of animals used.

CGN cultures were prepared as previously described (Morán et al., 1999). Briefly, cell suspensions dissociated from 8 day-old rat cerebellum were plated at a density of $1.5 \times 10^6$ or $2 \times 10^6$ cells /ml in 12 or 6 well culture plates with or without coverslips coated with poly-L-lysine (5 μg/ml). They were maintained for 6–8 days *in vitro*. Culture medium contained basal Eagle's medium supplemented with 10% (v/v) heat-inactivated fetal calf serum, 2 mM glutamine, 25 mM KCl, 50 U/ml penicillin, and 50 mg/ml streptomycin. This medium is denoted in the text as K25 and is the control condition. The culture dishes were incubated at 37 °C in a humidified 5% $CO_2$/95% air atmosphere. Cytosine arabinoside (10 mM) was added 24 h after seeding to avoid the presence of non-neuronal cells. To trigger cell death, CGN were treated with staurosporine (0.5 μM), thapsigargin (2 μM), tunicamycin (20 μg/ml), and

nifedipine (10 μM) or they were transferred to a medium identical to K25 except that KCl was 5 mM (it is denoted as K5).

## Simultaneous Recording of Changes in the Cytosolic and the ER $Ca^{2+}$ Concentrations

CGN (6–7 days) seeded on coverslips ($1.5 \times 10^6$ or $2 \times 10^6$ cells/ml) were incubated with MagFluo4-AM (0.25 μM) in the dark and at room temperature for 1 h. Subsequently, Fura2-AM (1.5 μM) was added for 1 h, without removing the first dye. Cells were washed with K25 for 10–30 min and the coverslips were mounted in a device into the cuvette. The dyes were excited at 340, 360, and 380 nm wavelength for Fura-2 and 495 nm wavelength for MagFluo-4 (Dagnino-Acosta and Guerrero-Hernández, 2009) and fluorescence emission was collected at 530 nm wavelength by using a QM-8 spectrofluorometer (PTI). Changes in both the $[Ca^{2+}]_i$ (fura-2) and $[Ca^{2+}]_{ER}$ (Magfluo-4) in response to the addition of staurosporine, thapsigargin, nifedipine, or tunicamycin were carried out in CGN maintained in K25. $Ca^{2+}$ release from the ER for CGN in K25 was stimulated with either histamine or glutamate. Changes in the $[Ca^{2+}]_i$ and the $[Ca^{2+}]_{ER}$ were induced by exchanging K25 with K5 or vice versa.

To convert Fura-2 fluorescence ratios into $[Ca^{2+}]_i$, digitonin was added to obtain Rmax followed by EGTA (5 mM) to get Rmin. The background fluorescence was determined at the end by adding $Mn^{2+}$, and this value was subtracted before doing the ratio 340/380. To correct for coverslip movements and the autofluorescence of staurosporine, the 360 nm fluorescence signal was subtracted from the 340 and 380 nm signals, as previously indicated (Benitez-Rangel et al., 2015). Briefly,

Ec (1): $(\lambda_{exc}\ 340 - \lambda_{exc}\ 360) + C = \lambda_{exc}\ 340$ corrected
Ec (2): $(\lambda_{exc}\ 380 - \lambda_{exc}\ 360) + C = \lambda_{exc}\ 380$ corrected

where C corresponds to 360 nm basal fluorescence.

These corrected values became intracellular $Ca^{2+}$ using the following equation (3) (Grynkiewicz et al., 1985):

Ec (3): $Ca^{2+} = K_d\ \beta\ [(R - R_{min})/(R_{max} - R)]$

MagFluo-4 fluorescence was normalized using the initial signal as Fo. Since we do not know the resting level of the $[Ca^{2+}]_{ER}$ in CGN, then changes in the $[Ca^{2+}]_{ER}$ are indicated as ΔF/Fo.

## Detection of Mitochondrial Membrane Potential

Initially, we attempted to study changes in the mitochondrial $[Ca^{2+}]$ and for this reason, CGN were incubated with 1 μM rhod-2/AM for 1 h in the dark and at room temperature. However, this dye, in agreement with previous reports (Fonteriz et al., 2010), modified mitochondrial morphology when compared to the one observed with TMRE (**Supplementary Figure S1**). For this reason, we discarded the use of rhod-2 and decided to follow changes in the mitochondrial membrane potential with TMRE as a better indicator of the metabolic state of this organelle.

To this end, CGN grown for 6–7 days on coverslips, were incubated with TMRE (50 nM) in the dark and at room temperature for 30 min. The cells were washed with K25 for 5–10 min and the coverslip was placed in a cuvette using a homemade holder. The dye was excited at 549 nm and emission was recorded at 575 nm using a QM-8 spectrofluorometer (PTI). Initial fluorescence (Fo) was recorded, and then changes in mitochondrial membrane potential were induced by switching solutions (K25 to K5) and by adding different inducers of apoptosis in K25. At the end of the experiment, FCCP (20 μM) was added as a depolarization control. Negative values of ΔF/Fo reflect depolarization of mitochondrial membrane potential, as shown by the application of FCCP. Simultaneous changes in the $[Ca^{2+}]_i$ and the $[Ca^{2+}]_{ER}$ were obtained in the same CGN. Changes in the mitochondrial membrane potential with TMRE were acquired from the same cultured CGN, but using a different coverslip.

## Determination of Caspase-3 Activity

CGN cultured for 6–8 days were incubated with ER stressors (thapsigargin, tunicamycin) or cell death inducers (K25 to K5, staurosporine) for 6 h. Cells were placed on ice, lysed with caspase-3 assay buffer (50 mM HEPES, 5 mM DTT, and Triton X-100 1%), and the cell suspension was stirred for 30 min. Cells were scraped with a rubber cell scraper, and the cell lysate was recovered and kept frozen until the caspase-3 activity assay was carried out. Caspase-3 activity was determined using a fluorescent assay determined by a QM-8 spectrofluorometer (PTI) according to the manufacturer specifications, but with slight modifications as previously described (Morán et al., 1999; Benitez-Rangel et al., 2011). Briefly, determinations were carried out in assay buffer (20 mM HEPES, 5 mM DTT, 2 mM EDTA, and 0.1% Triton X-100, pH 7.4). For each determinations, assay buffer contained Ac-DEVD-AMC (caspase-3 substrate) with or without 2 μM Ac-DEVD-CHO (caspase-3 inhibitor) and 50 μl of cell lysate. The reactions were recorded for 20–30 min after the addition of the caspase substrate (1 μM) and cell lysate (30–60 mg/ml). Caspase-3 activity was the difference in fluorescence between the caspase-3 inhibitor being present or not. Basal caspase-3 activity was obtained from CGN that were kept in K25 without any treatment. Signal obtained from control cells (K25) was taken as one fold response.

## Western Blot

Cells were washed twice in ice-cold PBS and homogenized in lysis buffer (25mM Trizma, 50mM NaCl, 2% Igepal, 0.2% SDS, and complete protease and phosphatases inhibitors, pH7.4). The protein concentration of cellular homogenates was determined by using the Bradford method. A total of 40μg of soluble protein per lane were subjected to 15% SDS-PAGE and transferred to polyvinylidene difluoride membranes. Membranes were blocked with fat-free milk (5% in Tris-buffered saline (TBS)/Tween 20 (TTBS) buffer [100mM Trizma, 150mM NaCl, and 0.1% Tween, pH7.5]) and incubated overnight at 4 ℃ with the following specific primary antibodies: 1:1000 rabbit anti-eIF2α, 1:1000 mouse anti-GRP78, and 1:2000 mouse anti-β-Tubulin. β-Tubulin was used as a loading control.

Bands were visualized using chemiluminescence according to the manufacturer's recommendations and exposed to Kodak BioMax-LightFilm. The optical density (O.D.) of each band was divided by the corresponding O.D. for β-tubulin and this ratio was compared to the one obtained from CGN extracts maintained in K25 (this value represents onefold response).

## Imaging CGN in the Confocal Microscope

CGN grown for 6–7 days on coverslips were incubated with the combination of TMRE (50 nM, 1 h) and MagFluo-4 (250 nM, 2 h) or with Rhod-2 (1 μM, 1 h) in the dark and at room temperature. Cells were washed with K25 for 5–10 min. The coverslip was mounted to a recording chamber placed on the stage of the microscope. The fluorescence images were collected using a confocal microscope Carl Zeiss LSM 700 with a 63x oil immersion objective. The excitation wavelengths were 488 nm for Mag-fluo-4 and 555 nm for Rhod-2 and TMRE.

## Statistical Analysis

Statistical analysis was done by using SigmaPlot 12.1 software. Data are expressed as means ± SEM. Pairwise comparison within multiples groups was made by analysis of variance (ANOVA) followed by the Holm Sidak *post hoc* test or by the non-parametric analysis Kruskal–Wallis followed by the Dunnett *post hoc* test; *p*-values less than 0.05 were considered statistically significant.

# RESULTS

Neonatal CGN were cultured on coverslips and loaded with both Mag-fluo-4/AM to determine luminal ER calcium concentration and with TMRE to measure the mitochondrial membrane potential and imaged with a confocal microscope (**Figure 1**). Cell bodies are seen in the bright field image (**Figure 1A**), but not in fluorescence images because they are out of focus. Neurites were heavily stained with both TMRE (**Figure 1B**) and Mag-fluo-4 (**Figure 1C**), the latter indicating regions of high luminal $[Ca^{2+}]$ that did not colocalize with the mitochondrial membrane potential indicator (**Figure 1D**). These data confirm that Mag-fluo-4 is not reporting mitochondrial deposits under our dye loading conditions and most likely is reporting changes in the luminal ER $[Ca^{2+}]$, so the Mag-fluo-4 signal is referred as the $[Ca^{2+}]_{ER}$. The simultaneous recording of CGN $[Ca^{2+}]_i$ and

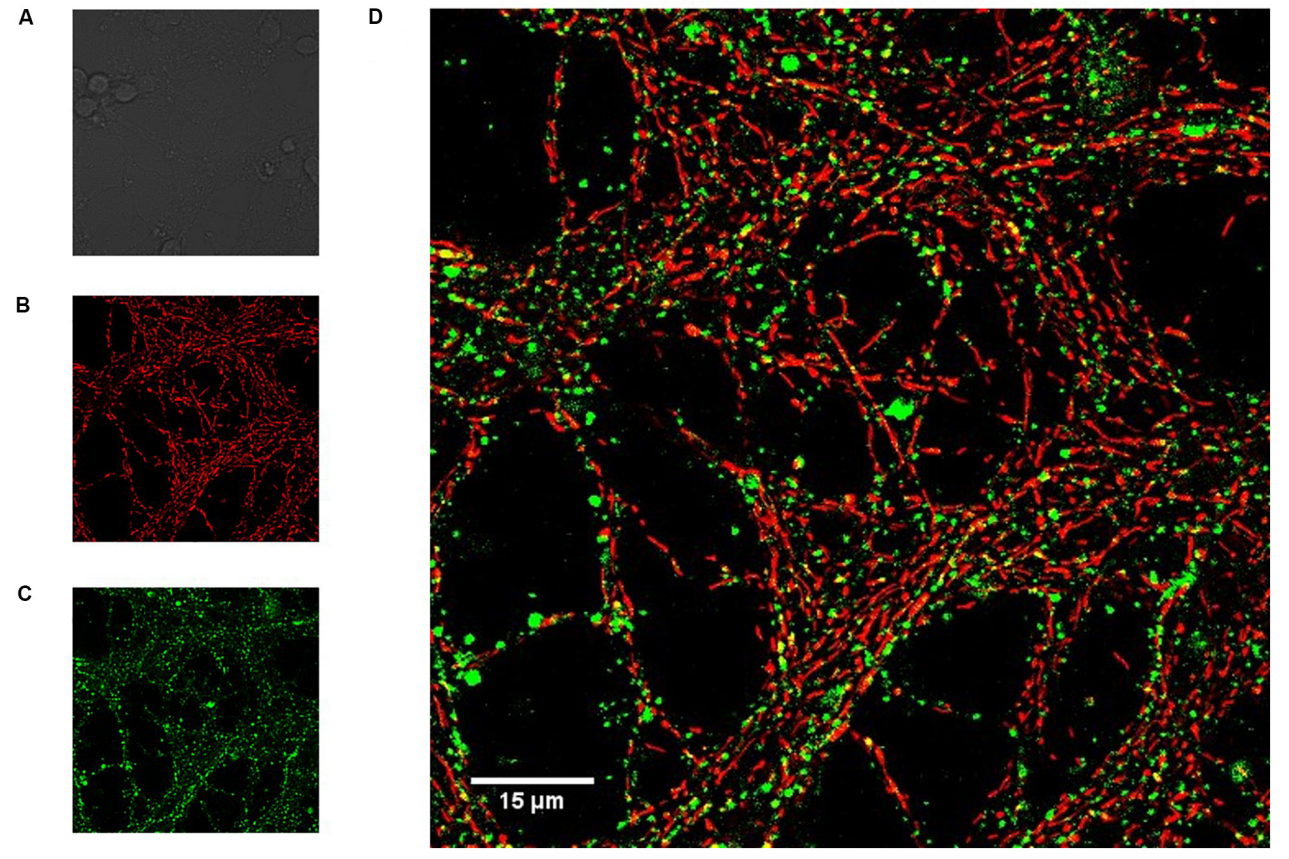


**FIGURE 1 |** Magfluo-4 signal did not colocalize with mitochondria stained with TMRE in CGN. Cerebellar granule neurons (CGN) loaded with calcium indicator Magfluo-4 and mitochondrial membrane potential indicator TMRE were visualized with a Zeiss LSM 710 confocal microscope (600x). MagFluo-4 and TMRE dyes were located in different areas within the same CGN group. **(A)** Bright field, showing the soma of different CGN; **(B)** TMRE signal (red, mitochondria); **(C)** MagFluo-4 signal (green, high calcium areas); **(D)** the merged images showed a minimal colocalization of the labels as noted by the absence of yellow pixels.

$[Ca^{2+}]_{ER}$ was obtained by loading cells with fura-2/AM and Mag-fluo-4/AM, respectively, and using a spectrofluorometer.

CGN that were in K5 displayed a normal resting $[Ca^{2+}]_i$ below 100 nM (**Supplementary Figure S2**), which is in line with the idea that these cells are repolarized (high membrane potential). Plasma membrane depolarization by adding K25 (**Supplementary Figure S2A**) produced an immediate increase in the $[Ca^{2+}]_i$ (blue trace). This elevation was followed by a slow rise in the $[Ca^{2+}]_{ER}$ (green trace) without any significant change in the mitochondrial membrane potential (red trace) for the initial 10 min after membrane depolarization. The application of thapsigargin, to inhibit the sarco/endoplasmic reticulum $Ca^{2+}$-ATPase (SERCA) pump, resulted in a slow reduction in the $[Ca^{2+}]_{ER}$. In this case, the plasma membrane depolarization with K25 derived in a much larger increase in the $[Ca^{2+}]_i$ than the one observed in those CGN with active SERCA pump and as expected, no increase in the $[Ca^{2+}]_{ER}$ was attained (**Supplementary Figure S2B**). These data suggest that membrane depolarization of CGN activates voltage-gated calcium channels at the plasma membrane and a significant fraction of the $Ca^{2+}$ entering the cell is sequestered in the ER by the action of SERCA pump. CGN in K25 were challenged with either histamine (400 μM) or glutamate (200 μM) to verify the ER $Ca^{2+}$ store. Both agonists produced a similar initial increase in the $[Ca^{2+}]_i$. Nevertheless, the ER $Ca^{2+}$ reduction was smaller and slower with histamine (**Supplementary Figure S2C**) than with glutamate (**Supplementary Figure S2D**). The addition of thapsigargin resulted in a significant decrease in the $[Ca^{2+}]_{ER}$ after the application of glutamate.

CGN in K25 showed a significantly larger resting $[Ca^{2+}]_i$, above 200 nM, that was immediately decreased to below 100 nM by switching from K25 to K5 (**Figure 2**, blue trace). We verified that a mechanical stimulus by the change of solution could not be the explanation for the reduction in the $[Ca^{2+}]_i$ because switching solutions from K25 for another K25 did not have any apparent effect on the $[Ca^{2+}]_i$, the luminal $[Ca^{2+}]_{ER}$, or the mitochondrial membrane potential (**Supplementary Figure S3**). Interestingly, with practically the same time course, both the $[Ca^{2+}]_{ER}$ (**Figure 2**, green trace) and the mitochondrial membrane potential (**Figure 2**, red trace) were significantly decreased by replacing K25 with K5. Importantly, this effect of plasma membrane repolarization on mitochondria membrane potential was much faster but smaller than the decrease seen with FCCP. The latter produces a complete mitochondrial membrane depolarization (**Supplementary Figure S4**).

It is known that cell depolarization and the subsequent activation of voltage-gated calcium channels are responsible for $Ca^{2+}$ entering the cytoplasm. We employed nifedipine (10 μM) to inhibit this $Ca^{2+}$ entry. This dihydropyridine reduced the $[Ca^{2+}]_i$ similarly, as seen with K5 (compare **Figure 3** with **Figure 2**). Nevertheless, the effect of nifedipine on the $[Ca^{2+}]_{ER}$ was smaller and slower when compared to K5 (**Figure 3**). Additionally, the mitochondrial membrane depolarization (**Figure 3**, red trace) followed the same time

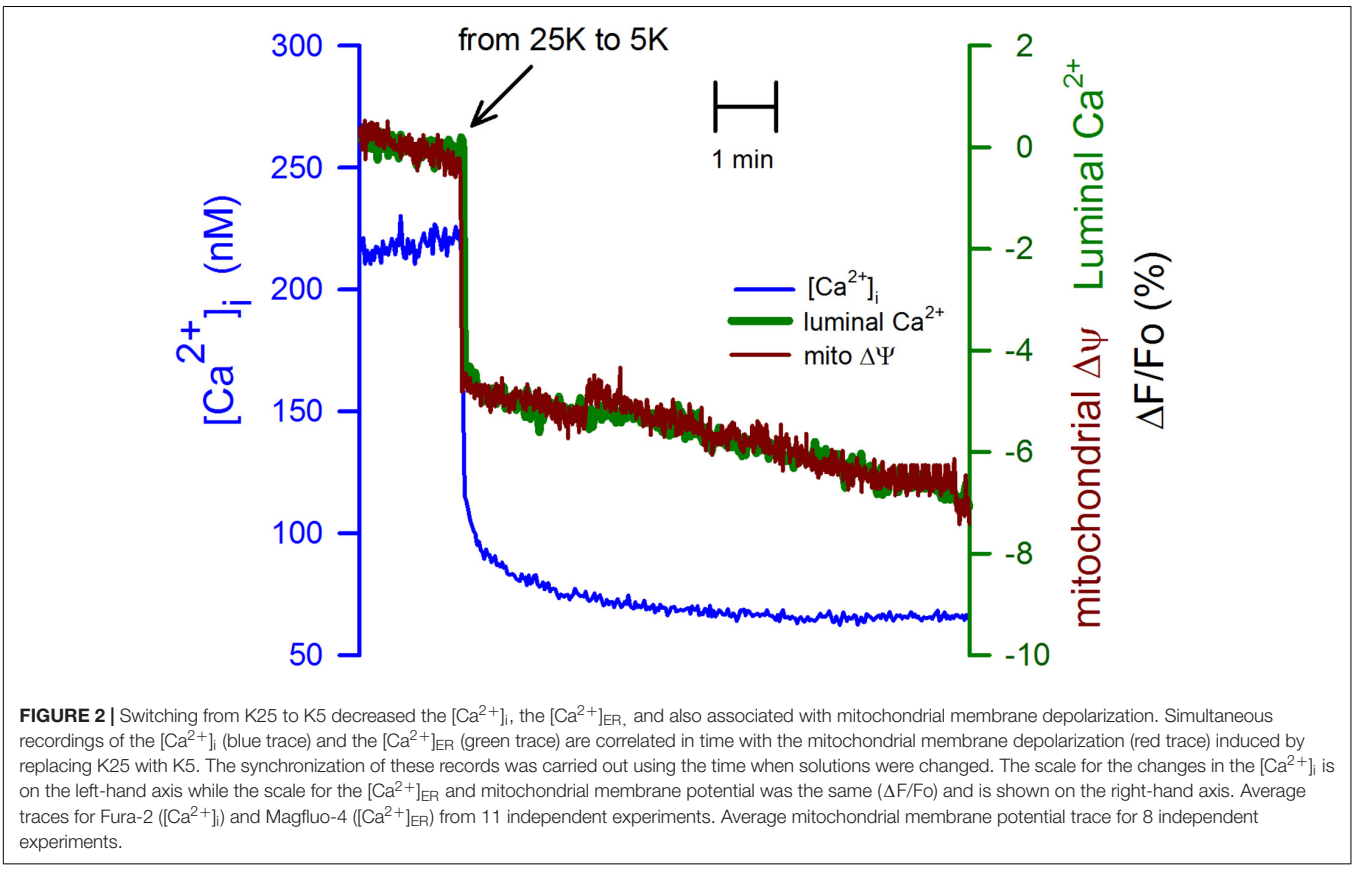


**FIGURE 2 |** Switching from K25 to K5 decreased the $[Ca^{2+}]_i$, the $[Ca^{2+}]_{ER}$, and also associated with mitochondrial membrane depolarization. Simultaneous recordings of the $[Ca^{2+}]_i$ (blue trace) and the $[Ca^{2+}]_{ER}$ (green trace) are correlated in time with the mitochondrial membrane depolarization (red trace) induced by replacing K25 with K5. The synchronization of these records was carried out using the time when solutions were changed. The scale for the changes in the $[Ca^{2+}]_i$ is on the left-hand axis while the scale for the $[Ca^{2+}]_{ER}$ and mitochondrial membrane potential was the same (ΔF/Fo) and is shown on the right-hand axis. Average traces for Fura-2 ($[Ca^{2+}]_i$) and Magfluo-4 ($[Ca^{2+}]_{ER}$) from 11 independent experiments. Average mitochondrial membrane potential trace for 8 independent experiments.

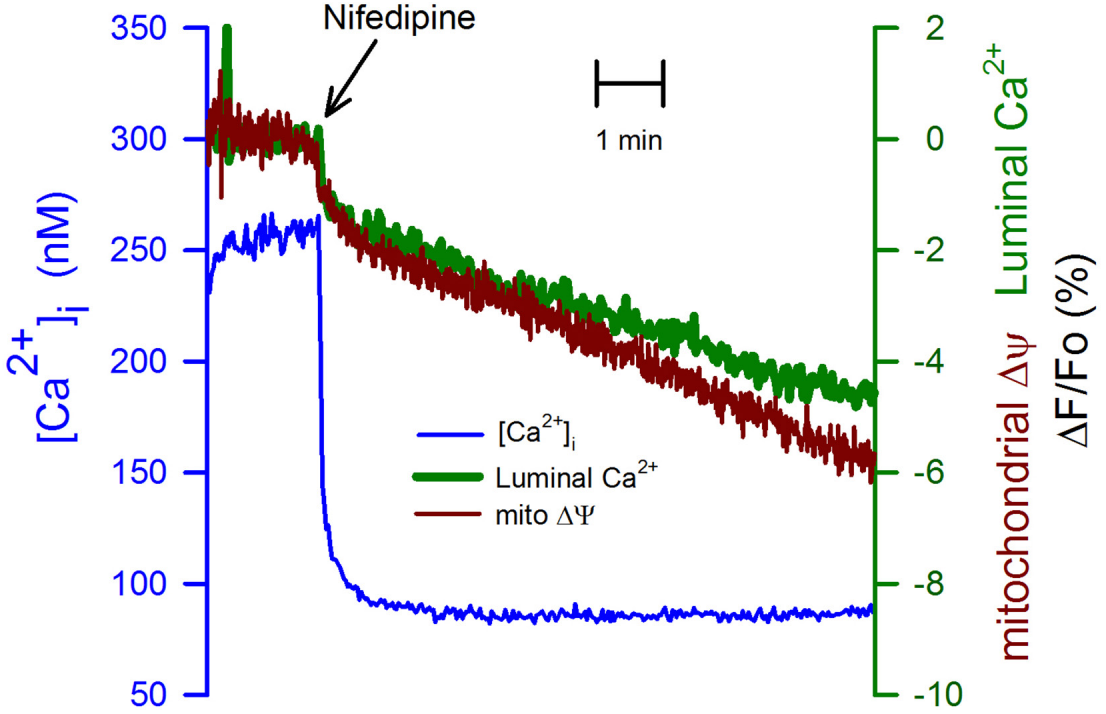


**FIGURE 3 |** Inhibition of VGCCs with nifedipine while inhibiting $Ca^{2+}$ entry to the cytoplasm did not have the same effect on the $[Ca^{2+}]_{ER}$ or the mitochondrial membrane potential. CGN in K25 were exposed to nifedipine (10 μM) at the indicated time (black arrow) to mimic the deactivation of VGCCs as produced by going from K25 to K5. The reduction in the $[Ca^{2+}]_i$ (blue trace) was of the same amplitude as the one seen with K5 (**Figure 2**). However, the $[Ca^{2+}]_{ER}$ (green trace) was resistant to the reduction in the $[Ca^{2+}]_i$ suggesting the presence of $Ca^{2+}$ entry via a dihydropyridine-resistant VGCCs which is also replenishing the ER $Ca^{2+}$ store. The mitochondrial membrane depolarization (red trace) showed the same time course of the decrease in the $[Ca^{2+}]_{ER}$. Average traces ($n$ = 8) for the $[Ca^{2+}]_i$ and the $[Ca^{2+}]_{ER}$. Average TMRE trace for six independent experiments.

course as the one observed for the $[Ca^{2+}]_{ER}$. These data suggest that there are other voltage-gated calcium channels, different from the dihydropyridine receptors, and that they efficiently load the ER with $Ca^{2+}$. Moreover, it appears that mitochondria membrane potential strongly depends on the $Ca^{2+}$ loading of the ER. Our data suggest that plasma membrane VGCCs, different from dihydropyridine-sensitive L-type calcium channels, participate in $Ca^{2+}$ entry to the cytoplasm and that these channels, but not those sensitive to nifedipine, are in close connection with the SERCA pump of the ER. These data also suggest that the mitochondrial membrane potential is affected by rapid reductions in the luminal $[Ca^{2+}]_{ER}$.

We have used thapsigargin (2 μM) -a potent and specific inhibitor of SERCA pump (Lytton et al., 1991)- to test the connection between the ER and mitochondria in depolarized CGN. The inhibition of SERCA pumps produced an immediate but transient increase in the $[Ca^{2+}]_i$ (**Figure 4**, blue trace) with a delayed reduction in the luminal $[Ca^{2+}]_{ER}$ and even more delayed and a smaller reduction in the mitochondria membrane potential. These data suggest that mitochondrial membrane potential is sensitive to the luminal $[Ca^{2+}]_{ER}$, but an increase in the $[Ca^{2+}]_i$ could prevent mitochondrial depolarization.

To further study the connection between the ER and the mitochondria, we have used tunicamycin (20 μg/ml). This is an inhibitor of protein glycosylation, which also produces ER stress (Liu et al., 1997). Tunicamycin induced a slow but sustained elevation in the $[Ca^{2+}]_i$ that might result from the partial inhibition of the SERCA pump activity (**Figure 5**, blue trace). In this case, the mitochondrial membrane potential displayed a rapid reduction, followed by a slower rate of depolarization. Tunicamycin also produced an immediate and more gradual decrease in the $[Ca^{2+}]_{ER}$ (**Figure 5**, green trace). The observation that the time course between the mitochondrial membrane potential and the luminal $[Ca^{2+}]_{ER}$ is similar suggests that the luminal $[Ca^{2+}]_{ER}$ regulates mitochondria membrane potential. A situation also observed for K5 and nifedipine.

We have studied the effect of staurosporine (1 μm), a nonspecific inhibitor of kinases, which also has a well-established role as an inducer of apoptosis (Tamaoki et al., 1986; Deshmukh and Johnson, 2000). This kinase inhibitor produced a sustained increase in the $[Ca^{2+}]_i$ (**Figure 6**, blue trace), the origin of this response was not further investigated. This response was followed by a slower but continuous reduction in the mitochondrial membrane potential (**Figure 6**, red trace) in association with a delayed decline in the luminal $[Ca^{2+}]_{ER}$. The reduction in the mitochondrial membrane potential triggered by staurosporine preceded the decrease in the $[Ca^{2+}]_{ER}$. Therefore, the reduction in the $[Ca^{2+}]_{ER}$ appears cannot fully explain the staurosporine-induced mitochondrial depolarization. The nature

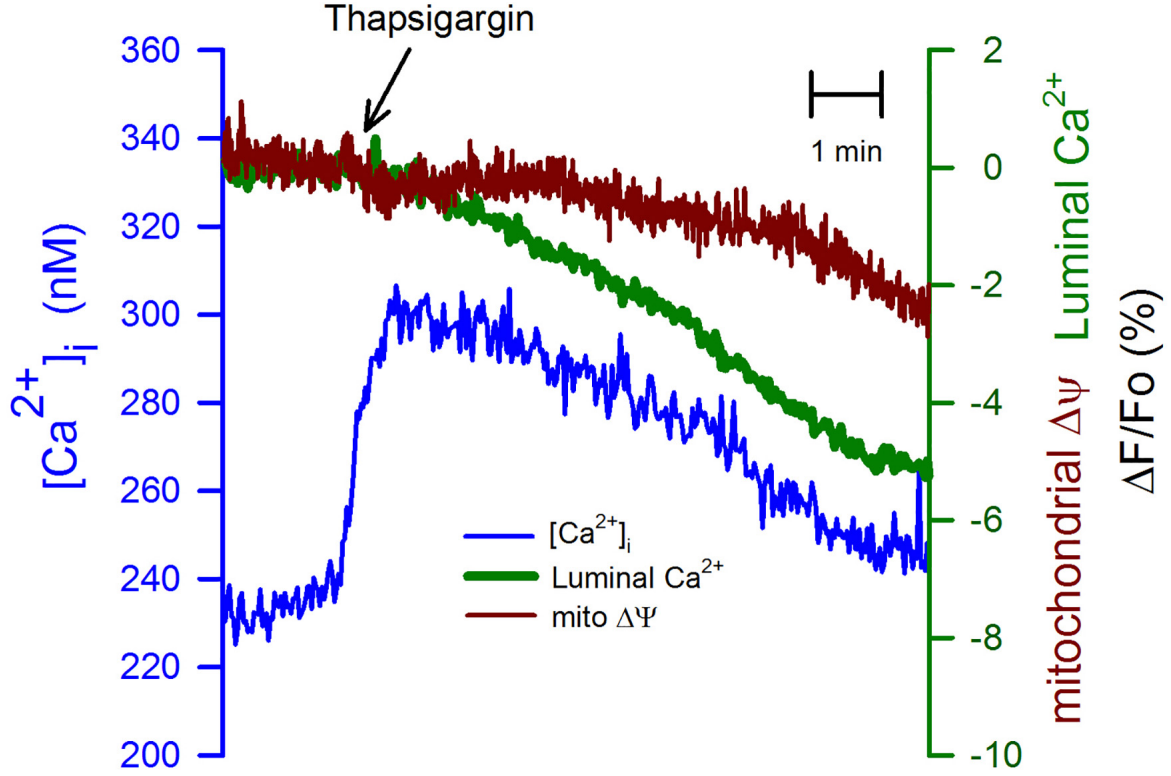


**FIGURE 4 |** Thapsigargin uncoupled the depletion of the $[Ca^{2+}]_{ER}$ from the mitochondrial membrane depolarization. Thapsigargin (2 μM) was applied at the indicated time (black arrow) to CGN in K25. This inhibitor of the SERCA pump produces a transient elevation of the $[Ca^{2+}]_i$ (blue trace), but a much slower reduction in the $[Ca^{2+}]_{ER}$ (green trace) and even slower reduction of the mitochondrial membrane potential (red trace). Average recordings ($n$ = 9) for the $[Ca^{2+}]_i$ and the $[Ca^{2+}]_{ER}$. Average trace for TMRE ($n$ = 4).

of the reduction in the $[Ca^{2+}]_{ER}$ induced by staurosporine was not further determined, however, it is clear that the time course for this reduction is quite different from the associated increase in the $[Ca^{2+}]_i$.

Both K5 and staurosporine induce apoptosis in these cells. We have studied the increase in caspase-3 activity caused by K5 in comparison with other inducers of cell death. CGN cultured in K25 were either switched to K5 for 6 h (**Figure 7A**, solid bar) or were incubated for 6 h with nifedipine (10 μM, **Figure 7A** red bar), staurosporine (1 μM, **Figure 7A** green bar), tunicamycin (20 μg/ml, **Figure 7A** yellow bar) or thapsigargin (2 μM, **Figure 7A** blue bar), and activity of caspase-3 was assessed as previously described (Morán et al., 1999; Benitez-Rangel et al., 2011). Incubation in K5 showed strong activation of caspase-3, while nifedipine produced a four-times smaller activation of this protease, similar to staurosporine and tunicamycin. Interestingly, thapsigargin did not significantly increase the activity of caspase-3. These data show that K5 is the most potent activator of caspase-3 in CGN, while the other conditions activate the protease to a lower extent, and thapsigargin is ineffective for the same incubation time.

Mitochondria is a critical element in the activation of caspase-3, thus, we decided to compare the effect of these chemicals on the mitochondrial membrane potential that had been previously recorded. The same pattern emerged as for activation of caspase-3 when compared with the initial (1 min) mitochondrial membrane depolarization induced by K5 (**Figure 7B**, solid bar), nifedipine (**Figure 7B**, red bar), staurosporine (**Figure 7B**, green bar), tunicamycin (**Figure 7B**, yellow bar), and thapsigargin (**Figure 7B**, blue bar). Remarkably, the mitochondria membrane depolarization is the same for all conditions at 10 min, except for thapsigargin (**Figure 7C**). Therefore it is only the initial mitochondrial membrane depolarization, and not the extent of this depolarization (**Figure 7C**), that better predicts the activation of caspase-3 by these five different inducers of apoptosis in CGN. These inducers of apoptosis displayed a different time course for the mitochondrial membrane depolarization (**Supplementary Figure S5**). K5 produced the fastest mitochondrial membrane depolarization, while staurosporine, tunicamycin, and nifedipine had a similar rate of reduction in the mitochondria membrane potential, and thapsigargin had the slowest time course. This time point of 1 min appears to correlate better for all five different conditions in the activation of caspase-3 because the mitochondrial membrane depolarization was the same at 10 min and yet the activation of caspase-3 was not the same 6 h later. Thapsigargin was unable to depolarize mitochondria at minute one, and accordingly, there was no activation of caspase-3 6 h

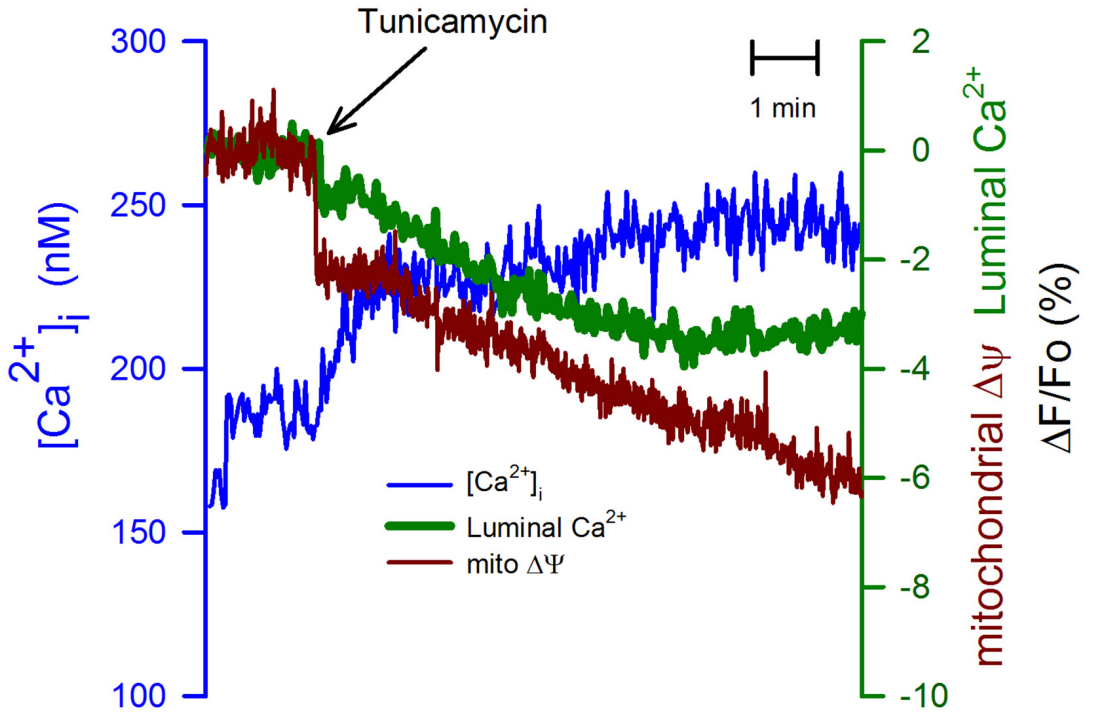


**FIGURE 5 |** Tunicamycin had a stronger effect on the mitochondrial membrane potential than on the $[Ca^{2+}]_{ER}$. The ER stressor tunicamycin (20 μg/ml) was applied at the time indicated (black arrow) to CGN in K25. Tunicamycin increased the ($[Ca^{2+}]_i$) and it also produced a slow reduction in the [Ca2+]ER, but the mitochondrial membrane potential displayed a biphasic response, an initial fast decrease followed by a much more gradual decline in the mitochondrial membrane potential (red trace). In this case, tunicamycin displayed a stronger effect on the mitochondrial membrane potential than on the two different calcium concentrations. Average traces ($n$ = 6) for all three various indicators.

later. These data suggest that it is the kinetics of mitochondrial membrane depolarization, and not the extent of depolarization, that predicts the extent of caspase-3 activation in CGN.

Interestingly, the 10 min level of mitochondria membrane depolarization (**Figure 7C**), the changes in the $[Ca^{2+}]_i$ (**Supplementary Figure S6**), and the extent of the reduction in the luminal $[Ca^{2+}]_{ER}$ (**Supplementary Figure S7**) did not show any correlation with the activation of caspase-3 in CGN. Collectively, these data suggest that membrane depolarization (K25) activates nifedipine-resistant VGCCs that are closely associated with the superficial ER, which in turn accumulates $Ca^{2+}$ via SERCA pump and releases this ion to the mitochondria. It appears that this constant $Ca^{2+}$ flux from the ER to the mitochondria is essential to keep mitochondria membrane potential and CGN survival. Accordingly, a drastic interruption of this $Ca^{2+}$ flux would lead to the activation of caspase-3, which eventually results in cell demise.

Since the decline in the $[Ca^{2+}]_{ER}$ produces ER stress that eventually could result in cell death (Tabas and Ron, 2011; Urra et al., 2013), we decided to study whether this reduction, more than mitochondrial membrane depolarization, could be the reason behind apoptosis in CGN. The cells were incubated in K5, or K25 with 0.5 μM staurosporine or 2 μM thapsigargin, and PERK activation was assessed by determining phosphorylation of eIF2α (**Figure 8**). All these three conditions significantly activated PERK at 30 min, which was the earliest time point evaluated. Thapsigargin was the most potent activator of PERK (**Figure 8C**), while staurosporine resulted in an intermediate effect, and K5 induced the smallest phosphorylation of eIF2$\alpha$. These data corroborate that these three different conditions, that decreased the luminal $[Ca^{2+}]_{ER}$ also activated PERK kinase reflecting the activation of ER stress.

Importantly, the observed activation of PERK did not correlate with the activation of caspase-3 because thapsigargin, the most effective activator of PERK, barely activated caspase-3 at 6 h. Moreover, we have used GSK2606414, a potent inhibitor of PERK (Axten et al., 2012), to study the role of this kinase in the induction of apoptosis in CGN. GSK2606414 at 20 μM did not modify the expression levels of eIF2a (**Supplementary Figure S8A**) and yet fully inhibited its phosphorylation by either K5 (**Supplementary Figure S8B**) or thapsigargin (**Supplementary Figure S8C**). However, this PERK inhibitor did not improve CGN viability after 12, 24, and 48 h incubation with these three different inducers of apoptosis (**Supplementary Figure S9**). Moreover, these data corroborated that thapsigargin, a potent inducer of ER stress, is a weak inducer of cell demise. These data suggest that ER stress was not the reason behind the activation of caspase-3 and cell death in CGN.

It has been shown that ER stress produces adaptive responses that should allow cells to cope with the stress and avoid cell demise program. One of these responses is an increase in the expression of GRP78 or BiP. Nevertheless, none of the conditions

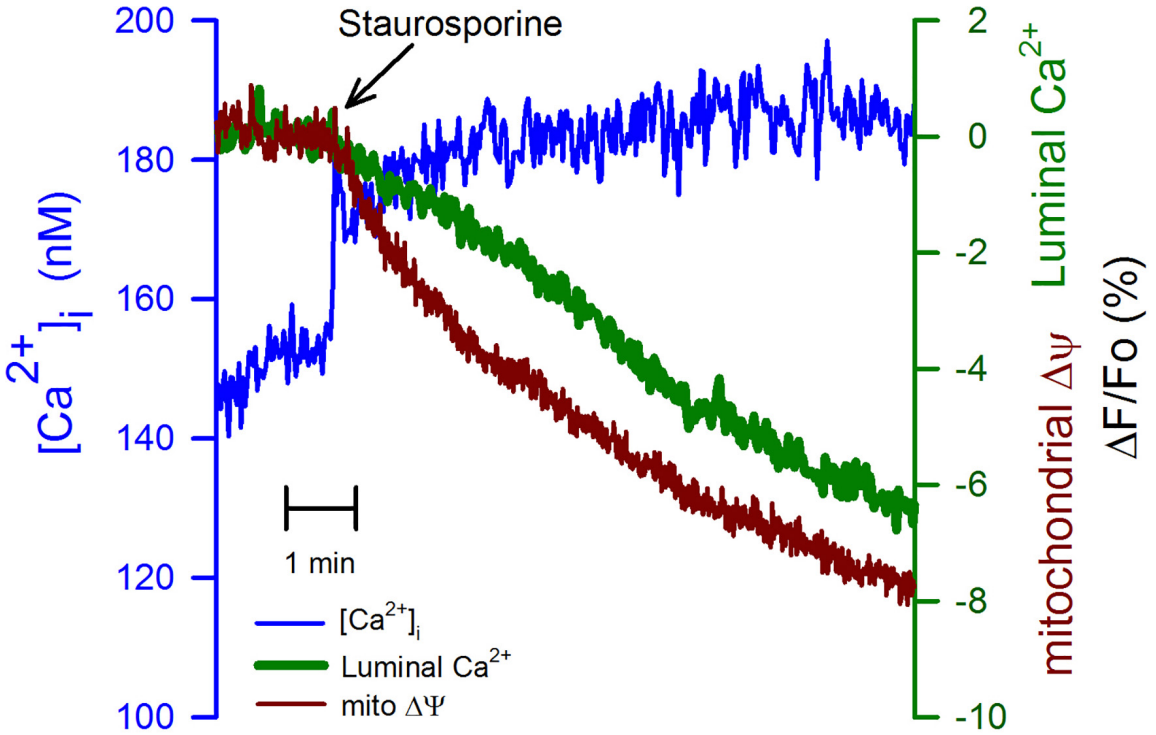


**FIGURE 6 |** Staurosporine reduces mitochondrial membrane potential faster than the $[Ca^{2+}]_{ER}$. The application of staurosporine (1 μM), a strong apoptosis inducer, to CGN in K25 at the time indicated (black arrow) produced a fast increase in the $[Ca^{2+}]_i$ (blue trace) trailed by an evident depolarization of the mitochondrial membrane potential (red trace) trailed by a slower reduction in the $[Ca^{2+}]_{ER}$ (green trace). Average traces ($n$ = 6) for all three different indicators.

that induce ER stress, based on the activation of PERK, led to an increased expression level of GRP78 (**Supplementary Figure S10** ). This situation was the same, whether at 30 min or 6 h of incubation with K5, staurosporine, or thapsigargin. Unexpectedly, staurosporine led to an apparent reduction in the expression of GRP78 at 6 h (**Supplementary Figure S10B**). These data suggest that an increase in Bip expression cannot explain the lack of correlation between the induction of ER stress and activation of caspase-3 in CGN. Overall, these data discard ER stress as the cause for cell death in CGN and point to a rapid mitochondrial membrane depolarization due to a reduction in the $Ca^{2+}$ release from the ER as the main reason for cell demise in this type of neurons.

## DISCUSSION

We have studied the role played by $Ca^{2+}$ in the induction of cell death in CGN by recording changes in the $[Ca^{2+}]_i$, the luminal $[Ca^{2+}]_{ER}$, and the mitochondrial membrane potential. We have found that the initial rate of mitochondrial membrane depolarization better predicts the extent of caspase-3 activation using five different cell death-inducing conditions in CGN. Nevertheless, all these five conditions, K5 (repolarization of plasma membrane potential), staurosporine, thapsigargin, nifedipine, and tunicamycin, have different mechanisms to induce cell death. Additionally, the ER stress does not seem to be associated with the activation of caspase-3 in CGN. Our data support the scenario where cell depolarization (25K), which is necessary for CGN survival, associates with sustained activation of VGCCs, increased $[Ca^{2+}]_i$, a higher level of the luminal $[Ca^{2+}]_{ER}$, and a larger mitochondrial membrane potential.

The use of nifedipine, to inhibit L-type VGCCs, has shown that this type of channel in CGN is fully responsible for the increase in the $[Ca^{2+}]_i$ in depolarizing conditions (K25). This is the case since both conditions, i.e., the addition of nifedipine in depolarizing medium (K25) or the repolarization of CGN by switching from K25 to K5, produced precisely the same reduction in the $[Ca^{2+}]_i$. These data argue that only L-type VGCCs are involved in the increase in the $[Ca^{2+}]_i$ induced by K25. Indeed, it has been shown that L-type VGCCs have a voltage activation curve more negative than the dihydropyridine-insensitive channels (Wheeler et al., 2012) in superior cervical ganglion neurons (SCGN).

Using Mag-fluo-4, we have corroborated that plasma membrane depolarization produced an increase in the luminal $[Ca^{2+}]_{ER}$ that required the activity of the SERCA pump while the plasma membrane repolarization resulted in a rapid reduction of the luminal $[Ca^{2+}]_{ER}$. However, the more interesting observation was a similar rate of decline for $[Ca^{2+}]_{ER}$ and $[Ca^{2+}]_i$, but only with K5 and not with nifedipine in K25. Nifedipine decreased the $[Ca^{2+}]_i$ very rapidly, but not

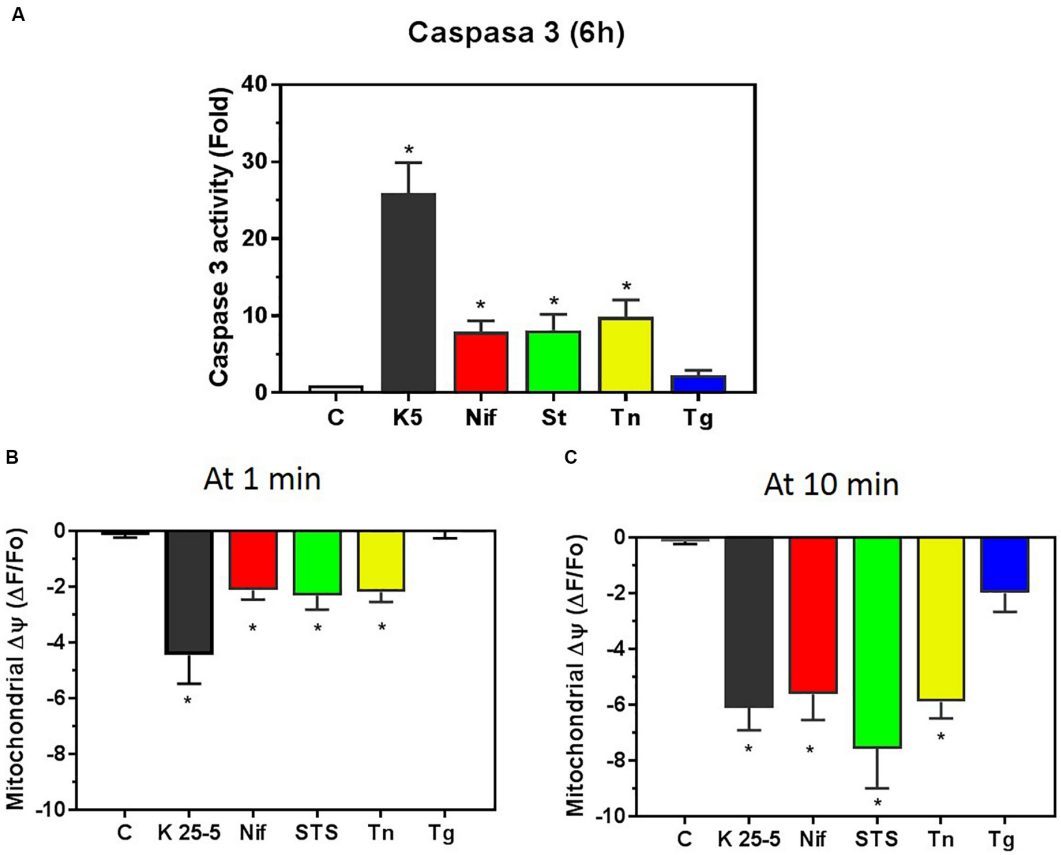


**FIGURE 7 |** Caspase-3 activation by different inducers of apoptosis correlated with the early mitochondrial membrane depolarization. **(A)** Caspase-3 activity was determined in CGN lysates obtained after 6 h incubation with the following chemicals nifedipine (10 μM, red bar), staurosporine (1μM, green bar), tunicamycin (20 μg/ml, yellow bar) and thapsigargin (2 μM, blue bar). Additionally, CGN were incubated for 6 h with K5 (black bar), and caspase-3 activity was measured in cell lysates as indicated in section "Materials and Methods." The caspase-3 activity for CGN in K25 was considered the basal level. Values indicate the average fold-increase normalized to the control ± SEM of 4 independent experiments. *$p < 0.05$ vs. control, C. **(B)** This panel shows the extent of mitochondrial membrane depolarization at 1 min after the addition of the different inducers of cell death. Bars show the same color code as in **(A)**. Values are means ± SEM of 4–6 independent experiments. *$p < 0.05$ vs. the level before the addition of the stimulus. **(C)** The mitochondrial membrane depolarization observed 10 min after the application of the indicated inducer of apoptosis. Note that thapsigargin-induced depolarization was not significant even at 10 min incubation time. Bars show the same color code as in **(A)**. Values indicate the means ± SEM of 4–11 independent experiments. *$p < 0.05$ vs. the level before the addition of the stimulus. Data shown in **(B,C)** come from the TMRE traces shown in **Figures 2–6**, and **Supplementary Figure S5** compares the different time courses of mitochondria depolarization.

the luminal $[Ca^{2+}]_{ER}$. These data argue for the presence of nifedipine-resistant VGCCs that are in the plasma membrane, but clustered just above the SERCA pump in the ER. This arrangement facilitates nifedipine-insensitive VGCCs to load the ER better than the L-type VGGCs (de Juan-Sanz et al., 2017). Indeed, the inhibition of the SERCA pump with thapsigargin produced a more significant increase in the $[Ca^{2+}]_i$ when CGN were depolarized by switching from K5 to K25, indicating that the ER is capturing a substantial amount of the $Ca^{2+}$ entering into CGN via active VGCCs. It has been shown in SCGN that inhibition of the SERCA pump with thapsigargin produces a much larger $[Ca^{2+}]_i$ response when nimodipine-insensitive VGCCs were activated instead of the nimodipine-sensitive channels (Wheeler et al., 2012). These data were interpreted to indicate that the ER was positioned just beneath the plasma membrane where the dihydropyridine-insensitive channels (CaV2) were located and that $Ca^{2+}$ entry mediated by these channels was loading ER Ca store by the action of SERCA pumps. Based on the data shown here, it appears then that the location of the SERCA pump underneath the dihydropyridine-insensitive VGCCs channels, observed for SCGN, is also present in CGN.

The functional interaction between VGCCs and ER and mitochondria seems to be highly complex. A recent study in cultured hippocampal neurons concluded that L-type VGCCs act in a bimodal way on the bioenergetics of the mitochondria depending on the magnitude of the stimulation of the VGCCs (Hotka et al., 2020). During low neuronal activity, VGCCs would promote an increase of $[Ca^{2+}]_{ER}$, which transfer $Ca^{2+}$ to mitochondria provoking an increase in

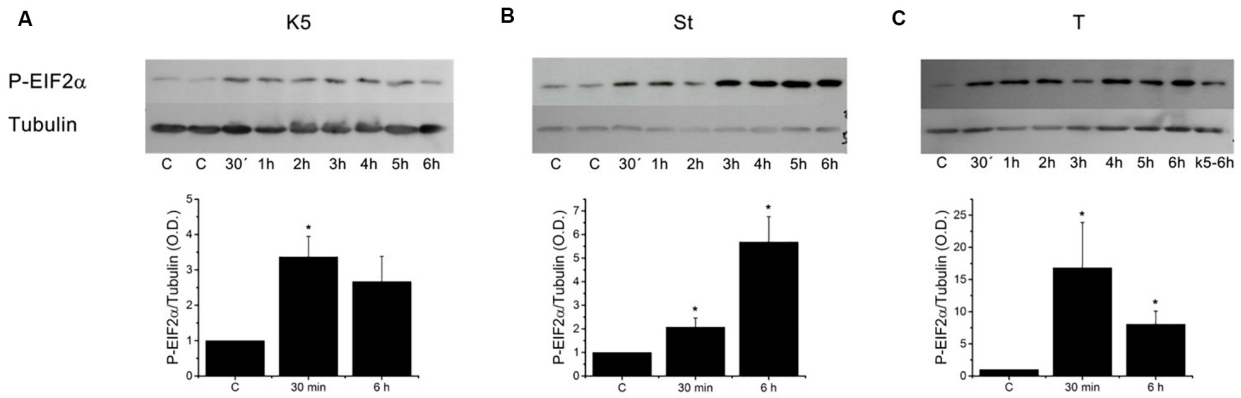


**FIGURE 8 |** Different inducers of apoptosis triggered eIF2α phosphorylation in CGN. Cerebellar granule neurons were incubated with **(A)** K5 or treated with **(B)** staurosporine (0.5 μM, St) and **(C)** thapsigargin (2 μM, T) for times from 30 min to 6 h and the activation of PERK was determined based on the phosphorylation of eIF2α (∼38 kDa) and tubulin (∼52 kDa) was used as a loading control. Densitometric analysis was carried out for the control condition (CGN in K25) and 30 min and 6 h for each treatment. Thapsigargin was the most effective activator of PERK at the earliest time tested. Data are mean ± SEM. **(A)** (*$p < 0.05$, ANOVA, $n = 4$). **(B)** (*$p < 0.05$, Kruskal–Wallis, $n = 4$). **(C)** (*$p < 0.05$, Kruskal–Wallis, $n = 3$).

mitochondrial respiration. In contrast, high activity conditions lead to a marked direct increase of $Ca^{2+}$ transport to mitochondria, without the participation of ER that affects mitochondrial respiration (Hotka et al., 2020). It has been shown that a high $Ca^{2+}$ influx is associated with CGN survival. However, it is not clear whether this survival was the consequence of a high level in the ER or of $Ca^{2+}$ uptake by mitochondria. The $Ca^{2+}$ reduction in the ER results in triggering ER-stress response, and this, in turn, can trigger apoptosis. We have found that thapsigargin was the most effective way of provoking ER-stress, but the least effective activator of caspase-3. Moreover, the inhibitor of PERK did not improve survival for K5 condition. Together these data suggest that the reduction in the luminal $[Ca^{2+}]_{ER}$ due to the VGCC deactivation is not the explanation for the associated CGN cell death.

We used Rhod-2 to determine whether the repolarization induces a change of the levels of $Ca^{2+}$ in the mitochondria. However, it has been described that this indicator deteriorates mitochondria, a situation that was observed in CGN. Another reliable way to assess the activity of mitochondria is to analyze the membrane potential; in this case, the repolarization of CGN resulted in an evident mitochondria depolarization, although of a much smaller magnitude than the one produced by a mitochondrial uncoupler. Interestingly, the rate of this membrane depolarization, and not the extent, showed a clear correlation with the amount of caspase-3 activated by the different inducers of cell death. For instance, K5 was the largest activator of caspase-3 and produced the fastest mitochondrial depolarization, while thapsigargin that activated the smallest amount of caspase-3 did not produce any early mitochondrial depolarization. Collectively, these data suggest that continuous $Ca^{2+}$ supply by the ER to mitochondria is the explanation behind the prosurvival activity of K25 in CGN. It has been shown that $Ca^{2+}$ transfer from the ER to mitochondria has a prosurvival effect in cancer cells and our results suggest that a similar situation occurs in CGN.

## DATA AVAILABILITY STATEMENT

The datasets generated for this study are available on request to any of the corresponding authors.

## ETHICS STATEMENT

The animal study was reviewed and approved by the Animal Care and Use Committee of the Instituto de Fisiología Celular, Universidad Nacional Autónoma de México (protocol number JMA120-17).

## AUTHOR CONTRIBUTIONS

EB-R carried out the experiments, contributed to analyze and interpret the data, participated in the design of the study, and to the draft of the manuscript. MO-A and GD-M carried out some of the experiments. ML-M contributed to obtaining and processing of images. AG-H and JM conceived the study, participated in its design, and contributed to draft the manuscript. All authors contributed to the article and approved the submitted version.

## FUNDING

This work was supported by the Consejo Nacional de Ciencia y Tecnología (CONACYT), grants numbers 285184 to JM and FC2016/2803 to AG-H and the Dirección General de Asuntos del Personal Académico (DGAPA-PAPIIT, UNAM), grant IN210716 to JM. EB-R was supported by a postdoctoral fellowship from DGAPA-UNAM.

## ACKNOWLEDGMENTS

We are grateful to Guadalupe Dominguez Macouzet (Instituto de Fisiologia Celular, UNAM) for excellent technical assistance.

## SUPPLEMENTARY MATERIAL

The Supplementary Material for this article can be found online at: https://www.frontiersin.org/articles/10.3389/fcell.2020.00544/full#supplementary-material

## REFERENCES

Alavez, S., Gutierrez-Kobeh, L., and Moran, J. (1996). Characterization of the activation of glutaminase induced by N-methyl-D-aspartate and potassium in cerebellar granule cells. *J. Neurosci. Res.* 45, 637–646. doi: 10.1002/(sici)1097-4547(19960901)45:5<637::aid-jnr13>3.0.co;2-w

Axten, J. M., Medina, J. R., Feng, Y., Shu, A., Romeril, S. P., Grant, S. W., et al. (2012). Discovery of 7-methyl-5-(1-{[3-(trifluoromethyl)phenyl]acetyl}-2,3-dihydro-1H-indol-5-yl)-7H-pyrrolo[2,3d]pyrimidin-4-amine (GSK2606414), a potent and selective first-in-class inhibitor of protein kinase R (PKR)-like endoplasmic reticulum kinase (PERK). *J. Med. Chem.* 55, 7193–7207. doi: 10.1021/jm300713s

Balazs, R., Jorgensen, O. S., and Hack, N. (1988). N-Methyl-D-aspartate promotes the survival of cerebellar granule cells in culture. *Neuroscience* 27, 437–451. doi: 10.1016/0306-4522(88)90279-5

Benitez-Rangel, E., Garcia, L., Namorado, M. C., Reyes, J. L., and Guerrero-Hernandez, A. (2011). Ion channel inhibitors block caspase activation by mechanisms other than restoring intracellular potassium concentration. *Cell Death Dis.* 2:e113. doi: 10.1038/cddis.2010.93

Benitez-Rangel, E., López-Méndez, M. C., Garcia, L., and Guerrero-Hernández, A. (2015). DIDS (4,4'-Diisothiocyanatostilbene-2,2'-disulfonate) directly inhibits caspase activity in HeLa cell lysates. *Cell Death Discov.* 1:15037.

Boyce, M., and Yuan, J. (2006). Cellular response to endoplasmic reticulum strees: a matter of life or death. *Cell Death Differ.* 13, 363–373. doi: 10.1038/sj.cdd.4401817

Cardenas, C., Miller, R. A., Smith, I., Bui, T., Molgo, J., Müller, M., et al. (2010). Essential regulation of cell bioenergetics by constitutive $InsP_3$ receptor Ca2+ transfer to mitochondria. *Cell* 142, 270–283. doi: 10.1016/j.cell.2010.06.007

Cardenas, C., Müller, M., McNeal, A., Lovy, A., Jana, F., Bustos, G., et al. (2015). Selective vulnerability of cancer cells by inhibition of $Ca^{2+}$ transfer from endoplasmic reticulum to mitochondria. *Cell Rep.* 14, 2313–2324. doi: 10.1016/j.celrep.2016.02.030

Copani, A., Bruno, V. M. G., Barresi, V., Battaglia, G., Condorelli, D. F., and Nicoletti, F. (1995). Activation of metabotropic glutamate receptors prevents neuronal apoptosis in culture. *J. Neurochem.* 64, 101–108. doi: 10.1046/j.1471-4159.1995.64010101.x

Dagnino-Acosta, A., and Guerrero-Hernández, A. (2009). Variable luminal sarcoplasmic reticulum Ca(2+) buffer capacity in smooth muscle cells. *Cell Calcium.* 46, 188–196. doi: 10.1016/j.ceca.2009.07.005

de Juan-Sanz, J., Holt, G. T., Schreiter, E. R., de Juan, E., Kim, D. S., and Ryan, T. A. (2017). Axonal endoplasmic reticulum $Ca^{2+}$ content controls release probability in CNS nerve terminals. *Neuron* 93, 867–881. doi: 10.1016/j.neuron.2017.01.010

Deshmukh, M., and Johnson, E. M. Jr. (2000). Staurosporine-induced neuronal death: multiple mechanisms and methodological implications. *Cell Death Differ.* 7, 250–261. doi: 10.1038/sj.cdd.4400641

D'Mello, S. R., Borodezt, K., and Soltoff, S. P. (1997). Insulin-like growth factor and potassium depolarization maintain neuronal survival by distinct pathways: possible involvement of PI 3-kinase in IGF-1 signaling. *J. Neurosci.* 17, 1548–1560. doi: 10.1523/JNEUROSCI.17-05-01548.1997

D'Mello, S. R., Galli, C., Ciotti, T., and Calissano, P. (1993). Induction of apoptosis in cerebellar granule neurons by low potassium: inhibition of death by insulin-like growth factor I and cAMP. *Proc. Natl. Acad. Sci. U.S.A.* 90, 10989–10993. doi: 10.1073/pnas.90.23.10989

Fonteriz, R. I., de la Fuente, S., Moreno, A., Lobatón, C. D., Montero, M., and Alvarez, J. (2010). Monitoring mitochondrial [$Ca^{2+}$] dynamics with rhod-2, ratiometric pericam and aequorin. *Cell Calcium* 48, 61–69. doi: 10.1016/j.ceca.2010.07.001

Gallo, V., Kingsbury, A., Balazs, R., and Jorgensen, O. S. (1987). The role of depolarization in the survival and differentiation of cerebellar granule cells in culture. *J. Neurosci.* 7, 2203–2213. doi: 10.1523/jneurosci.07-07-02203.1987

Grynkiewicz, G., Poenie, M., and Tsien, R. Y. (1985). A new generation of $Ca^{2+}$ indicators with greatly improved fluorescence properties. *J. Biol. Chem.* 260, 3440–3450.

Hotka, M., Cagalinec, M., Hilber, K., Hool, L., Boehm, S., and Kubista, H. (2020). L-type $Ca^{2+}$ channel-mediated $Ca^{2+}$ influx adjusts neuronal mitochondrial function to physiological and pathophysiological conditions. *Sci. Signal.* 13:618. doi: 10.1126/scisignal.aaw6923

Ishitani, R., Sunaga, K., Tanaka, M., Aishista, H., and Chuang, D.-M. (1997). Overexpression of glyceraldehyde-3-phosphate dehydrogenase is involved in low K+-induced apoptosis but not necrosis of cultured cerebellar granule cells. *Mol. Pharmacol.* 51, 542–550. doi: 10.1124/mol.51.4.542

Kingsbury, A., and Balazs, R. (1987). Effect of calcium agonists and antagonists on cerebellar granule cells. *Eur. J. Pharmacol.* 140, 275–283. doi: 10.1016/0014-2999(87)90284-6

Lam, A. K., and Galione, A. (2013). The endoplasmic reticulum and junctional membrane communication during calcium signaling. *Biochim. Biophys. Acta* 1833, 2542–2559. doi: 10.1016/j.bbamcr.2013.06.004

Liu, H., Bowes, R. C., van de Water, B., Sillence, C., Nagelkerke, J. F., and Stevens, J. L. (1997). Endoplasmic reticulum chaperones GRP78 and Calreticulin prevent oxidative stress, Ca2+ disturbances, and cell death in renal epithelial cells. *J. Biol. Chem.* 272, 21751–21759. doi: 10.1074/jbc.272.35.21751

Lossi, L., Zagzag, D., Greco, M. A., and Merighi, A. (1998). Apoptosis of undifferentiated progenitors and granule cell precursors in the postnatal human cerebellar cortex correlates with expression of BCL-2, ICE, and CPP32 proteins. *J. Comp. Neurol.* 399, 359–372. doi: 10.1002/(sici)1096-9861(19980928)399:3<359::aid-cne5>3.0.co;2-#

Lytton, J., Westlin, M., and Hanley, M. R. (1991). Thapsigargin inhibits the sarcoplasmic or endoplasmic reticulum Ca-ATPase family of calcium pumps. *J. Biol. Chem.* 266, 17067–17071.

Morán, J., Itoh, T., Reddy, U., Chen, M., and Pleasure, D. (1999). Caspase-3 expression by cerebellar granule neurons is regulated by calcium and cyclic AMP. *J. Neurochem.* 73, 568–577. doi: 10.1046/j.1471-4159.1999.0730568.x

Moran, J., and Patel, A. J. (1989). Effect of potassium depolarization on phosphate-activated glutaminase activity in primary cultures of cerebellar granule neurons and astroglial cells during development. *Dev. Brain. Res.* 46, 97–105. doi: 10.1016/0165-3806(89)90146-6

Nardi, N., Avidan, G., Daily, D., Zilkha-Falb, R., and Barzilai, A. (1997). Biochemical and temporal analysis of events associated with apoptosis induced by lowering the extracellular potassium concentration in mouse cerebellar granule neurons. *J. Neurochem.* 68, 750–759. doi: 10.1046/j.1471-4159.1997.68020750.x

Pacher, P., Csordas, P., Schneider, T., and Hajnoczky, G. (2000). Quantification of calcium signal transmission from sarco-endoplasmic reticulum to the mitochondria. *J. Physiol.* 529, 553–564. doi: 10.1111/j.1469-7793.2000.00553.x

Pearson, H., Graham, M. E., and Burgoyne, R. D. (1992). Relationship between intracellular free calcium concentration and NMDA-induced cerebellar granule cell survival in vitro. *Eur. J. Neurosci.* 4, 1369–1375. doi: 10.1111/j.1460-9568.1992.tb00162.x

Ramiro-Cortés, Y., and Morán, J. (2009). Role of oxidative stress and JNK pathway activation in apoptotic death induced by potassium deprivation and staurosporine in cerebellar granule neurons. *Neurochem. Int.* 55, 581–592. doi: 10.1016/j.neuint.2009.05.015

Rizzuto, R., De Stefani, D., Raffaello, A., and Mammucari, C. (2012). Mitochondria as sensors and regulators of calcium signalling. *Nat. Rev. Mol. Cell Biol.* 13, 566–578. doi: 10.1038/nrm3412

Sun, L., Zhao, Y., Zhou, K., Freeze, H. H., Zhang, Y. W., and Xu, H. (2013). Insufficient ER-stress response causes selective mouse cerebellar granule cell degeneration resembling that seen in congenital disorders of glycosylation. *Mol. Brain* 6:52. doi: 10.1186/1756-6606-6-52

Szegedi, E., Logue, S. E., Gorman, A. M., and Samali, A. (2006). Mediators of endoplasmic reticulum stress-induced apoptosis. *EMBO Rep.* 7, 880–885. doi: 10.1038/sj.embor.7400779

Tabas, I., and Ron, D. (2011). Integrating the mechanisms of apoptosis induced by endoplasmic reticulum stress. *Nat. Cell Biol.* 13, 184–190. doi: 10.1038/ncb0311-184

Tamaoki, T., Nomoto, H., Takahashi, I., Kato, Y., Morimoto, M., and Tomita, F. (1986). Staurosporine, a potent inhibitor of phospholipid/Ca++ dependent protein kinase. *Biochem. Biophys. Res. Commun.* 135, 397–402. doi: 10.1016/0006-291x(86)90008-2

Urra, H., Dufey, E., Lisbona, F., Rojas-Rivera, D., and Hetz, C. (2013). When ER stress reaches a dead end. *Biochim. Biophys. Acta* 1833, 3507–3517. doi: 10.1016/j.bbamcr.2013.07.024

Villalba, M., Bockaert, J., and Journot, L. (1997). Concomitant induction of apoptosis and necrosis in cerebellar granule cells following serum and potassium withdrawal. *Neuroreport* 8, 981–985. doi: 10.1097/00001756-199703030-00032

Wheeler, D. G., Groth, R. D., Ma, H., Barrett, C. F., Owen, S. F., Safa, P., et al. (2012). $Ca_V1$ and $Ca_V2$ channels engage distinct modes of $Ca^{2+}$ signling to control CREB-dependent gene expression. *Cell.* 149, 1112–1124. doi: 10.1016/j.cell.2012.03.041

Wood, K. A., Dipasquale, B., and Youle, R. J. (1993). In situ labeling of granule cells for apoptosis-associated DNA fragmentation reveals different mechanisms of cell loss in developing cerebellum. *Neuron* 11, 621–632. doi: 10.1016/0896-6273(93)90074-2

**Conflict of Interest:** The authors declare that the research was conducted in the absence of any commercial or financial relationships that could be construed as a potential conflict of interest.

frontiers in Cell and Developmental Biology

REVIEW
published: 18 August 2020
doi: 10.3389/fcell.2020.00736

# Functional Electrical Stimulation and the Modulation of the Axon Regeneration Program

*Juan Sebastián Jara[1], Sydney Agger[1] and Edmund R. Hollis II[1,2]**

[1] Burke Neurological Institute, White Plains, NY, United States, [2] Feil Family Brain and Mind Research Institute, Weill Cornell Medicine, New York, NY, United States

Neural injury in mammals often leads to persistent functional deficits as spontaneous repair in the peripheral nervous system (PNS) is often incomplete, while endogenous repair mechanisms in the central nervous system (CNS) are negligible. Peripheral axotomy elicits growth-associated gene programs in sensory and motor neurons that can support reinnervation of peripheral targets given sufficient levels of debris clearance and proximity to nerve targets. In contrast, while damaged CNS circuitry can undergo a limited amount of sprouting and reorganization, this innate plasticity does not re-establish the original connectivity. The utility of novel CNS circuitry will depend on effective connectivity and appropriate training to strengthen these circuits. One method of enhancing novel circuit connectivity is through the use of electrical stimulation, which supports axon growth in both central and peripheral neurons. This review will focus on the effects of CNS and PNS electrical stimulation in activating axon growth-associated gene programs and supporting the recovery of motor and sensory circuits. Electrical stimulation-mediated neuroplasticity represents a therapeutically viable approach to support neural repair and recovery. Development of appropriate clinical strategies employing electrical stimulation will depend upon determining the underlying mechanisms of activity-dependent axon regeneration and the heterogeneity of neuronal subtype responses to stimulation.

**Keywords: conditioning injury, regeneration associated genes, sprouting, plasticity, functional recovery, spinal cord injury**

OPEN ACCESS

***Edited by:***
*Luis B. Tovar-y-Romo, National Autonomous University of Mexico, Mexico*

***Reviewed by:***
*Fengquan Zhou, Johns Hopkins University, United States*
*Cedric G. Geoffroy, Texas A&M University, United States*

***Correspondence:**
*Edmund R. Hollis II*
*edh3001@med.cornell.edu*

***Specialty section:***
*This article was submitted to Molecular Medicine, a section of the journal Frontiers in Cell and Developmental Biology*

***Received:*** *18 April 2020*
***Accepted:*** *15 July 2020*
***Published:*** *18 August 2020*

***Citation:***
*Jara JS, Agger S and Hollis ER II (2020) Functional Electrical Stimulation and the Modulation of the Axon Regeneration Program. Front. Cell Dev. Biol. 8:736. doi: 10.3389/fcell.2020.00736*

## INTRODUCTION

Following injury to the adult mammalian central nervous system (CNS), neural circuits are permanently disrupted as severed axons fail to undergo spontaneous regeneration. The limited regenerative response of injured CNS neurons is due to both intrinsic and extrinsic factors. These growth-restrictive mechanisms play a large part in the poor clinical outcomes following brain or spinal cord trauma; however, despite limited regenerative capacity, mounting evidence has shown extensive spontaneous sprouting of CNS axon collaterals in the injured adult CNS.

The mammalian nervous system has an intrinsic capacity for structural and functional reorganization in response to a variety of stimuli during development, learning, or in response to pathological insults (Cramer et al., 2011; von Bernhardi et al., 2017). This innate plasticity is a key component of the system to adapt to a highly changing environment. Injury induced disruption of connectivity in the adult nervous system triggers plastic growth mechanisms and the sprouting of collaterals from spared, intact fibers (Maier and Schwab, 2006). Lesion-induced structural plasticity correlates with a limited degree of function recovery (Chen and Zheng, 2014); however, this innate plasticity falls far short of mediating recovery of damaged CNS circuits.

Recent findings suggest that manipulation of neuronal activity can drive plasticity related growth mechanisms and augment collateral sprouting, thereby enhancing the functional effect of axonal remodeling (Carmel and Martin, 2014). Electrical stimulation has long been known to enhance regeneration of peripheral axons (Hoffman and Binet, 1952; Pockett and Gavin, 1985). More recently, electrical stimulation has been used to enhance CNS plasticity in rodent models as well as to modulate and strengthen spared circuitry in individuals with spinal cord injury. Manipulation of activity-dependent neuroplasticity has great potential for improving neurological recovery from CNS injury. Herein we will discuss the systems-level effects of augmenting activity on injured neuronal circuits.

## Peripheral Nervous System Regeneration

In contrast to most CNS neurons, neurons of the peripheral nervous system (PNS) have a more robust regenerative response to injury (Ramón y Cajal, 1991; Mahar and Cavalli, 2018). This owes to the intrinsic regenerative program activated following PNS injury (McQuarrie and Grafstein, 1973). In the dorsal root ganglia (DRG), this program is characterized by a robust neuronal and non-neuronal response and regulation of a distinct transcriptional program (Tsujino et al., 2000; Costigan et al., 2002; Boeshore et al., 2004; Seijffers et al., 2007; Stam et al., 2007; Chandran et al., 2016). Within the damaged nerve, there is an activation and proliferation of Schwann cells and a robust inflammatory response, resulting in both trophic support and the clearance of myelin debris to allow for axon regeneration (Hall, 1986; Kang and Lichtman, 2013). Peripheral nerve injury has therefore proven to be an invaluable model for studying the underlying mechanisms that support axon regeneration and the structural plasticity of injured neurons.

Despite the innate regenerative potential of PNS neurons after injury, recovery of function remains limited. Several factors can hamper recovery, such as age, extent of injury and disruption of endoneurium, perineurium, or epineurium, and neuroma formation. One critical factor is the slow rate of regeneration in the adult PNS of 1–3 mm per day (Scheib and Hoke, 2013). Axons need to regrow over long distances before reaching appropriate targets, particularly in humans, and a significant delay in target-reinnervation leads to the irreversible atrophy of muscles and end-organs (Lee and Wolfe, 2000). In the absence of appropriate sensory end organs and motor endplate organization, the chances of successful restoration of function dwindle. In order to combat these effects and improve functional outcomes following PNS injury, an ideal treatment would be one that accelerates axon regeneration.

## Peripheral Conditioning and Molecular Pathways That Support Regeneration

The innate regenerative ability of adult mammalian PNS neurons has been used as a model to study the intrinsic mechanisms underlying the regenerative program. Primary sensory neurons are located in the DRG and extend axons into both CNS and PNS. Each axon exhibits a distinct response to injury in the adult. As described above, the peripheral axon retains the ability to regenerate following axotomy. In contrast, the CNS axon of the same cell will fail to regenerate after spinal cord injury. Intriguingly, the regenerative program activated by peripheral nerve injury conditions DRG neurons to mount an enhanced regenerative response to a second injury, whether in the peripheral or central axon (McQuarrie and Grafstein, 1973; Richardson and Issa, 1984). The process of peripheral conditioning results in the activation of a robust signaling cascade, inflammation, and transcriptional changes of thousands of genes in the DRG (Boeshore et al., 2004; Seijffers et al., 2007; Stam et al., 2007). Peripheral conditioning can be driven by axotomy (Richardson and Issa, 1984), inflammation (Steinmetz et al., 2005), demyelination (Hollis et al., 2015b), or electrical stimulation (Senger et al., 2018).

Another important change after conditioning lesion is the transient increase of second messenger cyclic nucleotide cAMP levels. Artificial elevation of cAMP can support a limited amount of sensory axon regeneration in the injured spinal cord (Qiu et al., 2002; Blesch et al., 2012). Downstream modulators of cAMP signaling have been directly linked to the regeneration program, including protein kinase A (Cai et al., 1999, 2001), cAMP response element-binding protein (CREB) (Gao et al., 2004), CREB binding protein (CBP) (Tedeschi et al., 2009) and arginase 1 (Cai et al., 2002).

Activation of the pro-regenerative transcriptional response in the somata of regenerating neurons requires a retrograde signal from the injury site. One candidate for this rapid signal is the early influx of calcium at the injury site (Ziv and Spira, 1995; Wolf et al., 2001; Mandolesi et al., 2004; Ghosh-Roy et al., 2010; Cho et al., 2013). Rapid calcium influx is a hallmark of injury conserved across species from invertebrates to mammals (Rishal and Fainzilber, 2014). Increased calcium levels in the axoplasm act locally on calcium-dependent enzymes related to protein synthesis, cytoskeletal modification, and growth cone formation (Chierzi et al., 2005; Bradke et al., 2012).

Additionally, early axotomy-induced calcium influx rapidly propagates retrogradely to the cell soma. Axotomy of cultured cortical neurons initiates a rapid membrane depolarization at the injury site triggering a fast-retrograde spiking activity and sustained cell body depolarization (Mandolesi et al., 2004). Injury-induced depolarization stimulates the calcium entry through activation of voltage-gated calcium channels (VGCC) or inversion of the sodium-calcium exchange pump following

a rise in cytosolic sodium concentration through voltage-gated sodium channels (Mandolesi et al., 2004). Intracellular calcium stores in sensory neurons are released following the initial increase in calcium concentration induced by peripheral injury (Rigaud et al., 2009). These stores are required for the propagation of the calcium wave as pre-emptive depletion of ryanodine receptor-sensitive intracellular calcium stores prevents back propagation and activation at the soma (Cho et al., 2013). It is likely that this calcium wave is a critical preliminary signal to prime neurons for regeneration as preventing it in cortical neurons by inhibiting TTX-sensitive sodium channels impairs neurite extension after *in vitro* injury (Mandolesi et al., 2004). Artificially elevating calcium influx in motor and sensory neurons by activation of the non-selective, light-sensitive cation channel channelrhodopsin can increase the rate of functional regeneration in mice (Ward et al., 2016, 2018). In *C. elegans* sensory neurons, this channelrhodopsin-mediated regeneration has been shown to depend on ryanodine receptor channel release of endoplasmic reticulum calcium stores (Sun et al., 2014). Interestingly, additional epigenetic-mediated changes by calcium increase after injury have been identified. Back propagation of calcium waves regulates epigenetic mechanisms including the release of histone deacetylase 5 (HDAC5) from the nucleus, and inactivation of HDAC3, leading to the initiation of a pro-regenerative transcriptional program (Cho et al., 2013; Hervera et al., 2019).

Electrical stimulation of peripheral nerves elicits this retrograde calcium signal. Genetically encoded calcium indicators can be used to image the calcium wave *in vivo* by fluorescent microscopy. Expression of the calcium indicator GCaMP6s in lumbar level 4 primary sensory neurons has been used to visualize calcium transients in response to sciatic nerve stimulation. Both large and small-diameter sensory somata show maximal calcium responses to low-frequency (20 Hz) stimulation (Chisholm et al., 2018). Short duration pulses (250 ms duration, 250 mA amplitude) preferentially activated large-diameter neurons, while longer duration (1 ms duration, 5 mA amplitude) activated most both A and C fiber cell bodies. Whether these distinct stimulation parameters elicit differential cellular responses is unknown.

The spatiotemporal regulation of calcium influx can regulate the regenerative program as calcium transients in the proximal segment after injury impair regeneration. In non-regenerating sensory neurons of drosophila, injury induces local calcium transients through the mechanosensitive cation channel dmPiezo, which inhibits axon regeneration by activating the calcium signaling regulator $Ca^{2+}$/calmodulin-dependent protein kinase II (CamKII) (Song et al., 2019). Nitric oxide synthase (NOS) and the cGMP-dependent kinase PKG act downstream of Piezo-mediated calcium signaling to inhibit axon regeneration in drosophila (Song et al., 2019). Piezo-mediated inhibition of regeneration is conserved in mouse models of sensory axotomy and conditional deletion of *Piezo1* enhances regeneration *in vivo* (Song et al., 2019). Furthermore, expression of the α2δ2 subunit of voltage gated calcium channels has been proposed to be a developmental switch underlying the decrease in axonal growth capacity that accompanies PNS maturation (Tedeschi et al., 2016). Genetic deletion of the encoding gene *Cacna2d2* promotes neurite elongation from cultured primary sensory neurons, while α2δ2 overexpression inhibits elongation through Cav2-mediated influx of pre-synaptic extracellular calcium (Tedeschi et al., 2016). Blockade of α2δ2 by clinically approved gabapentinoid drugs promotes neurite elongation *in vitro* and sensory axon regeneration and regenerative sprouting from injured corticospinal axons *in vivo* (Tedeschi et al., 2016; Sun et al., 2020).

## Neuronal Activity and Molecular Control Over Axon Growth

Neuronal activity can activate growth-associated molecular pathways. In an optic nerve model of CNS injury, driving activity in retinal ganglion cells (RGCs) by high-contrast visual stimulation or via chemogenetics approaches can enhance optic nerve regeneration (Lim et al., 2016). In contrast, suppressing neuronal activity with chemogenetics prevents the pro-regenerative effect of high-contrast visual stimulation (Lim et al., 2016). Furthermore, light-sensitive RGCs that express melanopsin are resistant to axotomy and exhibit high levels of phosphorylated ribosomal protein S6 (pS6) (Li et al., 2016). RGC pS6 levels decrease after axon elongation during development and this downregulation can be attenuated by deletion of the phosphatase and tensin homolog (PTEN) (Park et al., 2008). *PTEN* deletion from RGCs and other CNS neurons leads to elevated PI3K/mTOR (mammalian target of rapamycin) signaling, enhanced phosphorylation of S6, and an increased capacity for axonal growth after injury (Park et al., 2008; Liu et al., 2010). Alternatively, activating mTOR via over-expression of a constitutively active form of ras homolog enriched in brain 1 (cRheb1) appears to enhance RGC regeneration, though not nearly as robustly as *PTEN* deletion (Park et al., 2008; Lim et al., 2016).

Chronic electrical stimulation of the motor cortex over ten consecutive days leads to activation of the mTOR pathway, inactivation of PTEN, and increased phosphorylation of ribosomal protein S6 (Zareen et al., 2018). Additionally, this chronic stimulation drives increased levels of Janus kinase-signal transducer and activator of transcription (JAK/STAT) signaling (Zareen et al., 2018), a critical mediator of cytokine signaling. Enhancing JAK/STAT signaling through deletion of *suppressor of cytokine signaling 3* (*SOCS3*) increases optic nerve regeneration (Smith et al., 2009). JAK/STAT signaling acts independently of mTOR, while *SOCS3* and *PTEN* co-deletion deletion act synergistically to promote sustained optic nerve regeneration (Sun et al., 2011). In the motor cortex, the activation of these separate molecular pathways by chronic, daily electrical stimulation drives distinct aspects of structural remodeling in the intact corticospinal circuitry. New corticospinal collaterals sprout and form synaptic connections in the spinal cord during 10 days of stimulation. Pharmacological studies implicate mTOR signaling in collateral formation as corticospinal collateral sprouting is blocked by rapamycin;

whereas, inhibiting Stat3 activation with AG490 reduced both bouton-like structures on corticospinal axons as well as levels of cFos expression in ipsilateral cervical spinal cord neurons without affecting corticospinal collateral formation (Zareen et al., 2018). These studies demonstrate that not only can electrical stimulation activate growth-promoting molecular pathways, it can strengthen the formation of novel connections needed to elicit functional recovery.

Regeneration competent PNS neurons have been extensively studied to determine the molecular pathways critical for driving axon regeneration. Regeneration-associated genes (RAGs) have been largely defined as the coordinated and complementary genes activated by peripheral conditioning paradigms in PNS neurons. These include developmental growth-associated proteins (e.g., GAP-43, CAP23, and SPRR1A), transcription factors (e.g., ATF-3, c-Jun, Sox11, Smad1, Klf family members, and Stat3), and signaling pathways (MAPK, cytokine, JAK-STAT, TGF-b, neurotrophin) (Chandran et al., 2016; Mahar and Cavalli, 2018). In much the same manner that electrical stimulation of the cortex activates pro-regenerative molecular pathways, electrical stimulation of peripheral nerves has been shown to induce identified RAG expression in both sensory and motor neurons. Direct low-frequency electrical stimulation of the intact rodent sciatic nerves at 20 Hz for 1 h induces a significant upregulation in the expression of growth associated protein-43 (GAP-43), the neurotrophin BDNF and its high-affinity receptor trkB, as well as increased phosphorylation of the transcription factor cAMP response element binding protein (CREB) in DRGs neurons (English et al., 2007; Senger et al., 2018, 2019). This gene induction is comparable to injury-induced RAG induction (Senger et al., 2018, 2019). Similarly, brief electrical stimulation of the injured rat femoral nerve rapidly activates a RAGs response in motor neurons with upregulation of GAP43 and Tα1-Tubulin, as well as an increase in BDNF and trkB expression in stimulated motor neurons (Al-Majed et al., 2000a, 2004). The effects of electrical stimulation extend to perineuronal glial cells, with increased GFAP expression in satellite glia (Senger et al., 2018). In addition to the transcriptional regulation that occurs with electrical stimulation, 1 h of low-frequency stimulation of intact rat sciatic nerves increases intracellular cAMP levels in DRG neurons similar to nerve injury (Udina et al., 2008). Despite the fact that electrical stimulation and axotomy induce similar increases in cAMP, 1 h of low-frequency electrical stimulation is not sufficient to fully recapitulate the regenerative response of peripheral conditioning of sensory neurons to a central spinal cord injury (Udina et al., 2008; Goganau et al., 2018).

While electrical stimulation activates many of the same molecular pathways as peripheral conditioning via crush injury, it does not fully recapitulate the growth-promoting effects of conditioning. Following a subsequent peripheral injury, previous exposure to low-frequency electrical stimulation enhances the initiation of regeneration, but does not increase the rate of peripheral motor or sensory axon regeneration (Al-Majed et al., 2000b; Brushart et al., 2002). The limited effectiveness of electrical conditioning extends to the CNS as well, as regeneration of the central axon of dorsal column projecting sensory neurons after a spinal cord injury is less robust in rats conditioned 1 week prior with electrical stimulation than those subjected to nerve crush injury (Goganau et al., 2018). Electrical stimulation immediately following a dorsal column spinal cord injury allows for an increased initiation of regeneration; however, these axons fail to elongate through the injury site, in contrast to more robust regenerative effects of nerve crush injury (Udina et al., 2008). Despite the limitations of electrical stimulation compared to nerve crush, stimulation is a more attractive potential therapeutic approach to enhancing axon regeneration. The use of a conditioning nerve crush injury in patients is impractical as it would increase the risk of surgical complications and nerve crush elicits neuropathic pain (Hollis et al., 2015b).

Some of the limited effectiveness of current electrical conditioning may be alleviated by further optimization of stimulation parameters. Primary sensory neurons are sensitive to the frequency of electrically stimulated action potential patterns, activating discrete transcriptional programs based upon temporal changes in bursting patterns (Lee et al., 2017). It has long been known that specific patterns of induced neural activity in primary sensory neurons regulate immediate early gene expression independent of intracellular calcium levels (Sheng et al., 1993). The duration of neural activity induces unique gene expression profiles in a mechanistically distinct manner (Tyssowski et al., 2018). Defined action potential bursts underlie a temporal specificity in calcium influx through voltage gated calcium channels, leading to a tightly regulated activation of cAMP-responsive element binding protein (CREB) and mitogen-activated protein kinase (MAPK) signaling pathways (Fields et al., 1997; Wheeler et al., 2012). These same mechanisms may regulate the regenerative responses to discrete patterns of electrical stimulation. Indeed, modulation of stimulation frequency and current appears to alter the morphological and electrical properties of regenerated rat sciatic nerve (Lu et al., 2008, 2009). Despite the activation of the regenerative program found *in vivo* by low frequency (20 Hz) electrical stimulation, 20 Hz trains separated by 5 min intervals arrested neurite outgrowth of primary sensory neurons *in vitro* (Enes et al., 2010). Calcium influx through voltage-gated Cav1.2 calcium channels was proposed to mediate the stimulation evoked arrest of axon growth, with enhanced neurite outgrowth from cultured Cav1.2 deleted sensory neurons (Enes et al., 2010). Stimulation intensity of primary sensory neurons differentially regulates signaling through Cav1 and Cav2 channels (Wheeler et al., 2012), potentially driving distinct transcriptional responses and differences in the regenerative response.

Furthermore, maintenance of the energy supply in neurons is critical to meet metabolic demands and supporting physiological homeostasis. Axonal mitochondrial transport is crucial to this end. Following injury, the bioenergetic balance is highly disrupted, with mitochondrial depolarization and ATP depletion (Zhou et al., 2016). Increasing mitochondrial transport enhances peripheral and central axon regeneration (Cartoni et al., 2016; Zhou et al., 2016; Han et al., 2020). Electrical stimulation of peripheral nerves increases mitochondrial transport in a frequency dependent fashion (Sajic et al., 2013). Low frequency stimulation (1 Hz) mobilizes mitochondria transport in both

anterograde and retrograde directions, while higher frequency (50 Hz) stimulation further augmented anterograde transport only (Sajic et al., 2013). The increase in mitochondrial transport mediated by electrical stimulation may support the regenerative response following injury.

## Functional Effects of Electrical Stimulation on Circuit Recovery

Electrical stimulation has been used to hasten the recovery of both peripheral and central circuits after injury. While limited in comparison to the growth-promoting effects of conditioning crush injury, post-injury electrical stimulation has proven safe and effective in both animal models and humans. Low-frequency (4 Hz) stimulation of the soleus muscle in the rabbit was used to shorten the time for recovery of soleus function after axonotmesis of the soleus motor nerve (Nix and Hopf, 1983). This more rapid recovery of function elicited by post-injury electrical stimulation has also been observed in rodent models of nerve repair. A single hour of low-frequency electrical stimulation immediately following sciatic nerve transection and repair enhances axon regeneration and accelerates recovery of motor and sensory function, as measured by electrophysiological recordings and thermal sensitivity in the reinnervated hindpaw (**Figure 1**; Singh et al., 2012). Similar single 20 Hz electrical stimulation has been shown to enhance recovery after femoral nerve transection and epineurial suture repair, with quadriceps function returning 6-weeks earlier in stimulated mice than in controls (Ahlborn et al., 2007). Low-frequency stimulation post-surgery has been combined with daily locomotor training to accelerate the recovery of neurophysiological function after sciatic transection and epineurial suture repair (Asensio-Pinilla et al., 2009). More recently, the use of conditioning electrical stimulation was directly compared to nerve crush conditioning in a rat model of tibial nerve repair, in which the tibial nerve was conditioned 1 week prior to a nerve transection and epineurial suture repair (Senger et al., 2019). In these studies, conditioning by electrical stimulation was found to elicit greater physiological and functional recovery than conditioning by nerve crush. This apparent discrepancy with the effects observed *in vitro* and in models of subsequent spinal cord injury (Goganau et al., 2018) is likely due to slowing of the regenerating axons upon reaching the disrupted cytoarchitecture, proliferative Schwann cells, and inflammation at the nerve crush site. The efficacy of both pre- and post-injury electrical stimulation in enhancing regeneration of rodent peripheral nerves and accelerating functional outcomes, together with the feasibility of its use in bedside settings makes brief low frequency electrical stimulation a clinically relevant approach to mediate PNS repair. Indeed, clinical studies have found that electrical stimulation following surgical intervention to treat either full digital nerve transection or median nerve crush (carpal tunnel syndrome) is well-tolerated and enhances the recovery of both sensory and motor function (Gordon et al., 2010; Wong et al., 2015).

Within the CNS, chronic electrical stimulation drives collateral sprouting from intact descending corticospinal circuits (**Figure 2**). The corticospinal circuit is the primary motor pathway in primates and largely projects to the contralateral spinal cord. Ten days of stimulation (333 Hz, 45 ms bursts, every 2 s, for 6 h/day) of the medullary pyramid promotes sprouting of the corticospinal tract across the midline into the ipsilateral, denervated spinal cord (Brus-Ramer et al., 2007). This collateral sprouting is similar to what is observed following unilateral transection of the medullary pyramids (pyramidotomy), when the absence of corticospinal input to the spinal cord leads to cross-midline sprouting from the spared, intact corticospinal tract (Brus-Ramer et al., 2007; Lee et al., 2010). Performing chronic electrical stimulation after unilateral pyramidotomy results in an additive effect on corticospinal collateral sprouting (Brus-Ramer et al., 2007). Stimulation of the contralesional motor cortex mimics the direct stimulation of the pyramids, and this enhanced circuit plasticity drives recovery of skilled locomotor function after unilateral pyramidotomy in acute and chronic injury models (Carmel et al., 2010, 2014). Recovery is likely mediated by the formation of a novel, ipsilateral corticospinal circuit as inactivation of both ipsilateral and contralateral motor cortex impairs the behavioral recovery, while intact animals are only affected by contralateral cortical inactivation (Carmel et al., 2014). The growth-promoting effects of cortical stimulation are not restricted to intact circuits, as cortical electrical stimulation following cervical spinal cord injury drives corticospinal axon growth proximal to the injury site and enhances the recovery of forelimb function (Batty et al., 2020). In addition to the enhancement of axonal growth, the restoration of function through novel corticospinal circuits requires the synapse-promoting effects of cortical electrical stimulation. Pairing of cortical stimulation with peripheral afferents transiently strengthens the response to descending corticospinal input in acute experiments in rats (Mishra et al., 2017). Similar results have been demonstrated in healthy and spinal cord injured individuals (Bunday and Perez, 2012). In rats, repeated pairing of intermittent theta burst cortical stimulation with *trans*-spinal direct current stimulation after cervical spinal cord injury results in a strengthening of novel connections in the spinal cord. Furthermore, this paired stimulation paradigm can support the recovery of dextereous forelimb movements that depend on corticospinal function (Zareen et al., 2017; Yang et al., 2019). A brief summary of rodent electrical stimulation studies can be found in **Table 1**.

## Therapeutic Potential of Electrical Stimulation

In contrast to the robust regenerative response in rodents, injury of peripheral nerves in humans often results in incomplete or inadequate functional recovery (Scheib and Hoke, 2013). The efficacy of pre- and post-injury electrical stimulation in improving regeneration and functional outcomes has been demonstrated in multiple rodent models of peripheral nerve injury. This, combined with the feasibility of use in bedside settings, makes brief, low-frequency electrical stimulation a clinically viable approach in peripheral nerve repair as a means to mitigate the effects of slow regeneration

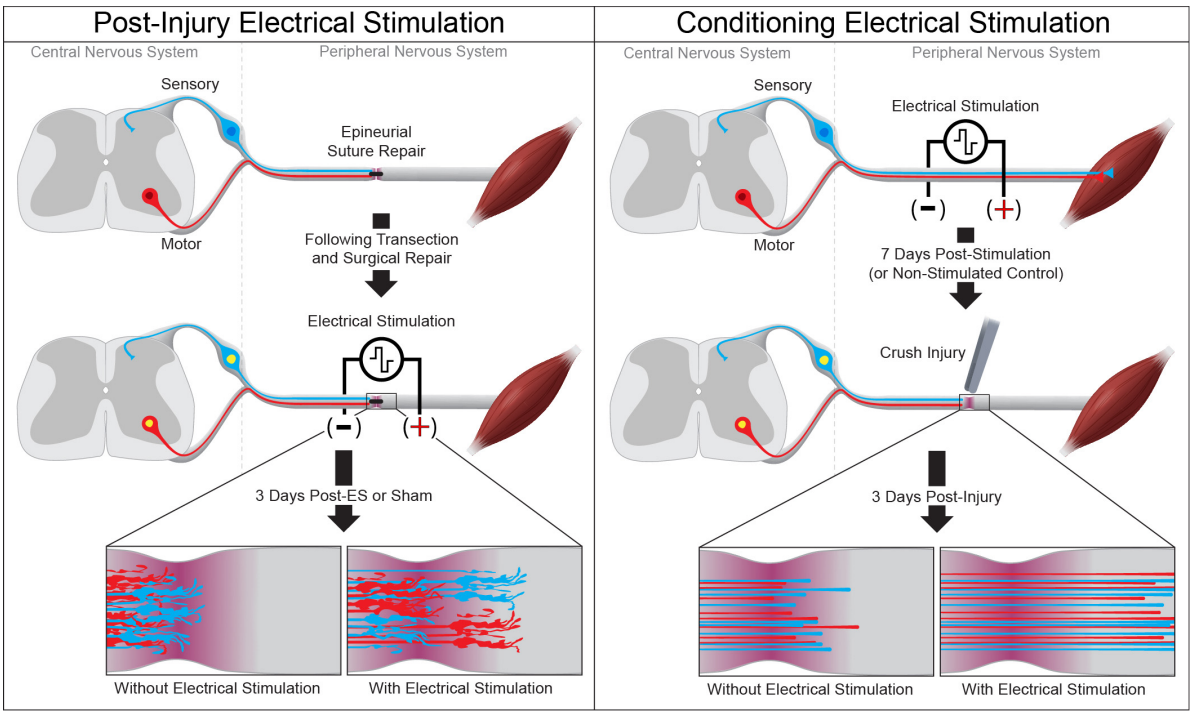


**FIGURE 1 |** Electrical stimulation enhances peripheral axon regeneration. A single session of low-frequency electrical stimulation (1 h, 20 Hz) can enhance motor and sensory axon regeneration following epineurial suture repair **(left)** or when used as a conditioning stimulus prior to subsequent axotomy **(right)**.

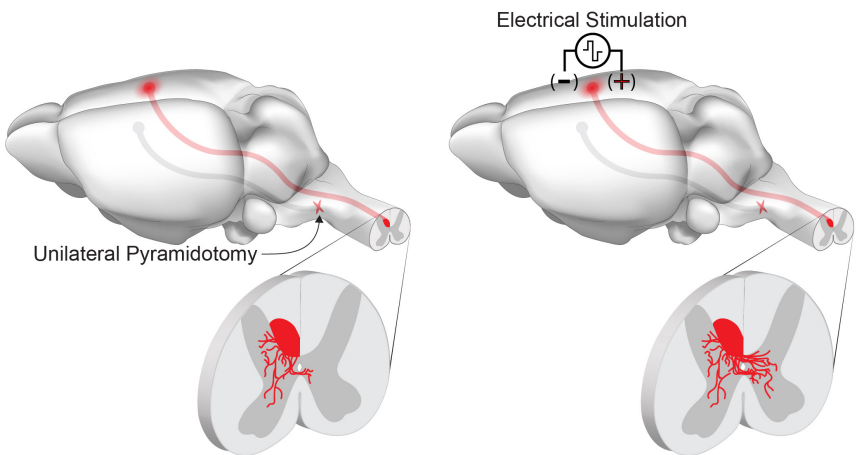


**FIGURE 2 |** Chronic electrical stimulation can drive corticospinal tract sprouting following injury. Unilateral pyramidotomy activates spontaneous collateral sprouting from the contralateral, intact corticospinal tract within the spinal cord. Chronic stimulation of the motor cortex activates neuron intrinsic growth pathways and enhances collateral sprouting and connectivity of spared corticospinal tract axons.

rate on the loss of end-organs and muscle atrophy (Lee and Wolfe, 2000). To date, 1 h of low-frequency (20 Hz) electrical stimulation has been successfully applied in clinical practice (Gordon et al., 2010; Wong et al., 2015). Individuals with motor axon loss from chronic median nerve compression at the wrist underwent decompression surgery. The group treated with single low-frequency electrical stimulation for 1 h after surgery showed enhanced reinnervation of thenar muscles characterized by improved motor and sensory nerve conduction in comparison to the surgery only group (Gordon et al., 2010). Electrical stimulation was also effective in improving physiological recovery and the return of normal sensory function when applied following epineurial repair of transected digital nerves (Wong et al., 2015). The effectiveness of these clinical findings on peripheral nerve repair are consistent with the evidence obtained from animal models. The recent

**TABLE 1 |** A brief summary of rodent electrical stimulation studies in the PNS and CNS.

| References | CNS/PNS | Stimulation substrate | Parameters | Effects |
|---|---|---|---|---|
| Al-Majed et al., 2000a | PNS | Electrode wired around injured rat femoral nerve | 20 Hz, 0.1 ms, 3 V, continous 1-h | Increased BDNF and trkB expression in motor neurons at 8 h and 2 days after ES. |
| Al-Majed et al., 2000b | PNS | Electrodes wired around injured rat femoral nerve | 20 Hz, 0.1 ms, 3 V, continous 1-h | ES enhanced initiation of motor neuron regeneration after femoral nerve repair. |
| Al-Majed et al., 2004 | PNS | Electrode wired around injured rat femoral nerve | 20 Hz, 0.1 ms, 3 V, continous 1-h | Upregulation of GAP43 and Tα1-Tubulin expression in motor neurons at 2days after ES. |
| English et al., 2007 | PNS | Cuff electrode around injured mouse common fibular nerve | 20 Hz, 0.1 ms, 0.5 to 5 V (2× motor threshold), continuous 1-h | Enhanced YFP+ axon regeneration through nerve allograft in a NT-4/5 dependent manner. Increased the levels of BDNF and trkB in injured and intact DRGs at 7 and 14 days after ES. |
| Geremia et al., 2007 | PNS | Stainless steel wire electrodes on opposite sides of injured femoral nerve | 20 Hz, 0.1 ms, 2× motor threshold 1-h | Increased sensory neuron regeneration after femoral nerve trunk repair, increased BDNF and GAP-43 expression in DRG neurons. |
| Udina et al., 2008 | PNS | Electrode wired around intact rat sciatic nerve | 20 Hz, 0.02 ms, ∼3 to 5 V (2× motor threshold), continous 1-h | ES enhanced central axon regeneration was less robust than nerve crush effects after SCI. Increased cAMP levels in DRGs 7 days after ES, comparable to nerve injury. |
| Chisholm et al., 2018 | PNS | Cuff electrodes surrounding intact mouse sciatic nerve | 1, 2, 5, and 20 Hz, ES-1: 250 μA, 250 μs. ES-2: 5 mA, 1 ms | Intensity- and frequency-dependent rapid calcium increase in DRG neurons |
| Goganau et al., 2018 | PNS | Cuff electrodes around intact rat sciatic nerve | 20 Hz, 0.2 ms, 2× motor threshold, continous 1-h (ES1), 7-h (ES2), or 1-h daily per 7 days (ES3). | ES enhanced central axon regeneration was less robust than nerve crush effects after SCI. 1 h of ES per day for 7 days and 7 hours of ES followed by 7 days of waiting resulted in similar *in vitro* neurite outgrowth. |
| Senger et al., 2018 | PNS | Electrode wired around intact rat common peroneal nerve | 20 Hz, 0.1 ms, continuos 1-h | Upregulation of GAP-43 and BDNF expression in DRG neurons and GFAP in satellite cells at 3 days after ES. Similar to injury-induced changes. |
| Senger et al., 2019 | PNS | Electrode wired around intact rat tibial nerve | 20 Hz, 0.1 ms, continuos 1-h | Increased pCREB levels in DRGs at 3 days after ES. 7 day prior electrical conditioning enhanced regeneration and reinnervation. |
| Brus-Ramer et al., 2007 | CNS | Tripolar electrodes on the surface of rats pyramidal tract | 333 Hz, 45 ms burst every 2 s, 6 h daily per 10 days. | Chronic ES enhanced intact corticospinal collateral sprouting. |
| Carmel et al., 2014 | CNS | Implanted electrodes into rat forelimb motor cortex | 333 Hz, 45 ms burst every 2 s, 6 h daily per 10 days | Chronic ES induced recovery of skilled locomotor function. |
| Zareen et al., 2017 | CNS | Combined bilateral rat epidural (M1) iTBS, and spinal cord (C4-T2) tsDCS stimulation 7 weeks after SCI | iTBS: stimulation intensity 75% of motor threshold. tsDCS: 1.5 mA for 2.5 s and returned to 0 over 2.5 s. Combined stimulation for 30 min daily per 10 day. | Combined ES enhanced injury-dependent corticospinal collateral sprouting below and above the level of injury, and enhanced skilled forelimb functional recovery. |
| Zareen et al., 2018 | CNS | Implanted electrodes into rat forelimb motor cortex | 333 Hz, 0.2 ms duration every 2 s, 1.1 to 2 mA, continous 6 h daily per 10 days | Chronic ES induced activation of mTOR and Jak/STAT pathways, inactivation of PTEN, and increased phosphorylation of ribosomal protein s6. Chronic ES induced mTOR-dependent collateral sprouting of intact corticospinal tract. |
| Jack et al., 2018 | CNS | Implanted electrodes into rat forelimb motor cortex | 333 Hz, 0.2 ms duration every 500 ms, 30 pulses per train | Single ES to injured CST increased collateral sprouting above injury site, with no further improvement in recovery of function. |
| Batty et al., 2020 | CNS | implanted electrodes into rats forelimb motor cortex | 333 Hz, 30 pulses of 0.2 ms width every 0.5 s, for 30 min | Single ES to intact CST enhanced corticospinal collateral sprouting above SCI and improved motor function recovery. |

findings that pre-conditioning of peripheral nerves with electrical stimulation has a robust effect on axon regeneration (Senger et al., 2019) suggests that there may be a benefit to performing pre-operative electrical stimulation in cases of surgical interventions involving intact nerves, such as nerve transfer. Further clinical studies are warranted to determine if the functional benefit of low-frequency electrical stimulation translates to long-distance nerve repair surgeries, such as brachial plexus repair. Additionally, the potential for peripheral nerve stimulation to enhance the sprouting of central sensory axons after spinal cord injury could be used to restore sensory function critical for movement (Takeoka et al., 2014). Strengthening ascending mechanosensory input to only a small proportion (<5%) of dorsal column nuclei is sufficient to support some level of functional recovery (Hollis et al., 2015a), so the translation of PNS electrical stimulation may prove to be a viable approach to restore sensory function after spinal cord injury.

Despite the limited regenerative capacity of CNS axons after spinal cord injury, some spontaneous compensatory sprouting from spared and injured axons can occur in both rodent and non-human primates (Ghosh et al., 2010; Rosenzweig et al., 2010). Mounting evidence indicates that this post-lesion plasticity can be increased by artificially driving neuronal activity. Epidural electrical stimulation has been employed in both animal models and in paraplegic individuals to engage motor circuits and support locomotor recovery. The extent to which this neuromodulation can have lasting impacts on motor circuit remodeling after injury is not yet known. Following complete thoracic spinal cord injury in rats, spinal motor networks are engaged during periods of epidural electrical stimulation, which allows for locomotion in the absence of descending input (Ichiyama et al., 2005). Chronically injured paraplegic individuals have similarly shown engagement of spinal motor circuits in the presence of epidural electric stimulation. Epidural stimulation in motor complete individuals allows for volitional movement of paralyzed leg muscles, including overground walking during stimulation (Harkema et al., 2011; Angeli et al., 2014, 2018). Furthermore, repeated pairing of activity-based training with epidural stimulation in a motor complete individual over several years has supported the recovery of trained volitional motor movements, independent of stimulation (Rejc et al., 2017). Patterning of epidural stimulation over the lumbar spinal cord to sequentially activate agonist-antagonist muscle groups supports the recovery of stimulation-mediated walking in chronic paraplegic individuals when paired with intensive rehabilitation (Wagner et al., 2018). Furthermore, some of the individuals enrolled in this study regained voluntary leg movements in the absence of stimulation. The underlying activity-dependent mechanism activated by epidural electrical stimulation paired with rehabilitation remains unknown. It is likely that the initial responses are activating motor circuits below the injury and residual supraspinal circuitry is able to engage these excited motor networks either directly or indirectly through spared propriospinal circuitry. The eventual recovery of limited volitional control in several individuals may result from engaging many of the same neuroplasticity mechanisms identified in electrical stimulation studies in animal models.

In contrast to implanted epidural stimulators, transcutaneous electrical spinal cord stimulation (TESS) is a non-invasive and painless neuromodulation strategy that augments motor and sensory function after SCI (Gerasimenko et al., 2015; Hofstoetter et al., 2015; Gad et al., 2018; Benavides et al., 2020). Cervical TESS, in combination with training, has been shown to induce a long-term improvement in volitional motor control and restoration of hand sensory function individuals with chronic incomplete SCI (Inanici et al., 2018). TESS utilizes currents from 5 to 50 Hz, with a carrier frequency (Russian current) between 5 and 10 kHz (Benavides et al., 2020). Changes in spinal sensory and motor circuit excitability have been proposed to underlie TESS-mediated functional effects, with neuroplasticity mechanisms facilitating a reorganization of spinal networks during intensive, rehabilitative training (Inanici et al., 2018; Benavides et al., 2020). The extent of anatomical circuit remodeling induced by TESS remains to be determined.

Among the different approaches that have been proposed to enhance post-lesion plasticity, extrinsic manipulation of neuronal activity by electrical stimulation is an attractive therapeutic approach. Electrical stimulation has been demonstrated to engage plasticity mechanisms in several central and peripheral neural circuits and has already shown feasibility in clinical settings. Development of appropriate strategies will likely depend upon the selective activation of desired neural subtypes in a temporally and spatially organized manner. Non-targeted electrical fields have been used to trigger population responses; however, it may be that distinct electrical stimulation parameters can selectively affect neuronal subtype responses and circuit-specific functional outcomes. Whether the molecular mechanisms activated by electrical stimulation are consistent across neuronal populations is unknown. The sprouting response of corticospinal axons to electrical stimulation contrasts with the elongation observed in stimulated PNS axons. These differences may arise from disparate stimulation parameters, discrete responses of these distinct populations to electrical stimulation, or from interactions of conserved stimulation-mediated molecular pathways with the intrinsic limitations of adult CNS neurons to axon elongation. Further studies will be required to identify whether CNS-tuned parameters of electrical stimulation can drive a regenerative response in transected corticospinal axons.

In the context of SCI, preclinical and clinical studies have clearly demonstrated that the stimulation of local spinal networks can drive lasting functional improvements (Ievins and Moritz, 2017; Courtine and Sofroniew, 2019; Hutson and Di Giovanni, 2019). Cortical and spinal cord paired electrical stimulation is an attractive approach to both enhance intrinsic sprouting and strengthen residual and newly formed collateral connections within the spinal cord (Dixon et al., 2016; Mishra et al., 2017). Additionally, it is likely that targeted rehabilitation or concurrent therapies, such as constraint-induced movement therapy, will be needed to strengthen and engage novel circuitry driven by electrical stimulation. The development of novel technologies will allow for the combining of biomedical devices for stimulation with rehabilitation and molecular or genetic control over neuroplasticity to support recovery after neurological injury and improve individuals' quality of life.

## AUTHOR CONTRIBUTIONS

JJ and EH wrote and edited the manuscript. SA created the illustrations. All authors contributed to the article and approved the submitted version.

## FUNDING

Financial support was provided by The Winifred Masterson Burke Foundation, the NIH Common Fund (1DP2NS106663), and the New York State Department of Health Spinal Cord Injury Research Board (C33267GG and C34463GG).

## ACKNOWLEDGMENTS

The authors would like to thank Amanda Bernstein for critical reading of the manuscript.

## REFERENCES

Ahlborn, P., Schachner, M., and Irintchev, A. (2007). One hour electrical stimulation accelerates functional recovery after femoral nerve repair. *Exper. Neurol.* 208, 137–144. doi: 10.1016/j.expneurol.2007.08.005

Al-Majed, A. A., Brushart, T. M., and Gordon, T. (2000a). Electrical stimulation accelerates and increases expression of BDNF and trkB mRNA in regenerating rat femoral motoneurons. *Eur. J. Neurosci.* 12, 4381–4390. doi: 10.1111/j.1460-9568.2000.01341.x

Al-Majed, A. A., Neumann, C. M., Brushart, T. M., and Gordon, T. (2000b). Brief electrical stimulation promotes the speed and accuracy of motor axonal regeneration. *J. Neurosci.* 20, 2602–2608. doi: 10.1523/jneurosci.20-07-02602.2000

Al-Majed, A. A., Tam, S. L., and Gordon, T. (2004). Electrical stimulation accelerates and enhances expression of regeneration-associated genes in regenerating rat femoral motoneurons. *Cell. Mol. Neurobiol.* 24, 379–402. doi: 10.1023/b:cemn.0000022770.66463.f7

Angeli, C. A., Boakye, M., Morton, R. A., Vogt, J., Benton, K., Chen, Y., et al. (2018). recovery of over-ground walking after chronic motor complete spinal cord injury. *New Engl. J. Med.* 379, 1244–1250. doi: 10.1056/nejmoa1803588

Angeli, C. A., Edgerton, V. R., Gerasimenko, Y. P., and Harkema, S. J. (2014). Altering spinal cord excitability enables voluntary movements after chronic complete paralysis in humans. *Brain* 137, 1394–1409. doi: 10.1093/brain/awu038

Asensio-Pinilla, E., Udina, E., Jaramillo, J., and Navarro, X. (2009). Electrical stimulation combined with exercise increase axonal regeneration after peripheral nerve injury. *Exper. Neurol.* 219, 258–265. doi: 10.1016/j.expneurol.2009.05.034

Batty, N. J., Torres-Espín, A., Vavrek, R., Raposo, P., and Fouad, K. (2020). Single-session cortical electrical stimulation enhances the efficacy of rehabilitative motor training after spinal cord injury in rats. *Exper. Neurol.* 324:113136. doi: 10.1016/j.expneurol.2019.113136

Benavides, F. D., Jo, H. J., Lundell, H., Edgerton, V. R., Gerasimenko, Y., and Perez, M. A. (2020). Cortical and subcortical effects of transcutaneous spinal cord stimulation in humans with tetraplegia. *J. Neurosci.* 40, 2633–2643. doi: 10.1523/jneurosci.2374-19.2020

Blesch, A., Lu, P., Tsukada, S., Alto, L. T., Roet, K., Coppola, G., et al. (2012). Conditioning lesions before or after spinal cord injury recruit broad genetic mechanisms that sustain axonal regeneration: Superiority to camp-mediated effects. *Exper. Neurol.* 235, 162–173. doi: 10.1016/j.expneurol.2011.12.037

Boeshore, K. L., Schreiber, R. C., Vaccariello, S. A., Sachs, H. H., Salazar, R., Lee, J., et al. (2004). Novel changes in gene expression following axotomy of a sympathetic ganglion: a microarray analysis. *J. Neurobiol.* 59, 216–235. doi: 10.1002/neu.10308

Bradke, F., Fawcett, J. W., and Spira, M. E. (2012). Assembly of a new growth cone after axotomy: the precursor to axon regeneration. *Nat. Rev. Neurosci.* 13, 183–193. doi: 10.1038/nrn3176

Brushart, T. M., Hoffman, P. N., Royall, R. M., Murinson, B. B., Witzel, C., and Gordon, T. (2002). Electrical stimulation promotes motoneuron regeneration without increasing its speed or conditioning the neuron. *J. Neurosci.* 22, 6631–6638. doi: 10.1523/jneurosci.22-15-06631.2002

Brus-Ramer, M., Carmel, J. B., Chakrabarty, S., and Martin, J. H. (2007). Electrical stimulation of spared corticospinal axons augments connections with ipsilateral spinal motor circuits after injury. *J. Neurosci.* 27, 13793–13801. doi: 10.1523/jneurosci.3489-07.2007

Bunday, K. L., and Perez, M. A. (2012). Motor recovery after spinal cord injury enhanced by strengthening corticospinal synaptic transmission. *Curr. Biol.* 22, 2355–2361. doi: 10.1016/j.cub.2012.10.046

Cai, D., Deng, K., Mellado, W., Lee, J., Ratan, R. R., and Filbin, M. T. (2002). Arginase I and polyamines act downstream from cyclic AMP in overcoming inhibition of axonal growth MAG and myelin in vitro. *Neuron* 35, 711–719. doi: 10.1016/s0896-6273(02)00826-7

Cai, D., Qiu, J., Cao, Z., Mcatee, M., Bregman, B. S., and Filbin, M. T. (2001). Neuronal cyclic AMP controls the developmental loss in ability of axons to regenerate. *J. Neurosci.* 21, 4731–4739. doi: 10.1523/jneurosci.21-13-04731.2001

Cai, D., Shen, Y., De Bellard, M., Tang, S., and Filbin, M. T. (1999). Prior exposure to neurotrophins blocks inhibition of axonal regeneration by MAG and Myelin via a cAMP-dependent mechanism. *Neuron* 22, 89–101. doi: 10.1016/s0896-6273(00)80681-9

Carmel, J. B., Berrol, L. J., Brus-Ramer, M., and Martin, J. H. (2010). Chronic electrical stimulation of the intact corticospinal system after unilateral injury restores skilled locomotor control and promotes spinal axon outgrowth. *J. Neurosci.* 30, 10918–10926. doi: 10.1523/jneurosci.1435-10.2010

Carmel, J. B., Kimura, H., and Martin, J. H. (2014). Electrical stimulation of motor cortex in the uninjured hemisphere after chronic unilateral injury promotes recovery of skilled locomotion through ipsilateral control. *J. Neurosci.* 34, 462–466. doi: 10.1523/jneurosci.3315-13.2014

Carmel, J. B., and Martin, J. H. (2014). Motor cortex electrical stimulation augments sprouting of the corticospinal tract and promotes recovery of motor function. *Front. Integr. Neurosci.* 8:51. doi: 10.3389/fnint.2014.00051

Cartoni, R., Norsworthy, M. W., Bei, F., Wang, C., Li, S., Zhang, Y., et al. (2016). The mammalian-specific protein armcx1 regulates mitochondrial transport during axon regeneration. *Neuron* 92, 1294–1307. doi: 10.1016/j.neuron.2016.10.060

Chandran, V., Coppola, G., Nawabi, H., Omura, T., Versano, R., Huebner, E. A., et al. (2016). A systems-level analysis of the peripheral nerve intrinsic axonal growth program. *Neuron* 89, 956–970. doi: 10.1016/j.neuron.2016.01.034

Chen, M., and Zheng, B. (2014). Axon plasticity in the mammalian central nervous system after injury. *Trends Neurosci.* 37, 583–593. doi: 10.1016/j.tins.2014.08.008

Chierzi, S., Ratto, G. M., Verma, P., and Fawcett, J. W. (2005). The ability of axons to regenerate their growth cones depends on axonal type and age, and is regulated by calcium, cAMP and ERK. *Eur. J. Neurosci.* 21, 2051–2062. doi: 10.1111/j.1460-9568.2005.04066.x

Chisholm, K. I., Khovanov, N., Lopes, D. M., La Russa, F., and Mcmahon, S. B. (2018). Large scale in vivo recording of sensory neuron activity with GCaMP6. *eNeuro* 5:ENEURO.0417-17.2018.

Cho, Y., Sloutsky, R., Naegle, K. M., and Cavalli, V. (2013). Injury-induced HDAC5 nuclear export is essential for axon regeneration. *Cell* 155, 894–908. doi: 10.1016/j.cell.2013.10.004

Costigan, M., Befort, K., Karchewski, L., Griffin, R. S., D'urso, D., Allchorne, A., et al. (2002). Replicate high-density rat genome oligonucleotide microarrays reveal hundreds of regulated genes in the dorsal root ganglion after peripheral nerve injury. *BMC Neurosci.* 3:16. doi: 10.1186/1471-2202-3-16

Courtine, G., and Sofroniew, M. V. (2019). Spinal cord repair: advances in biology and technology. *Nat. Med.* 25, 898–908. doi: 10.1038/s41591-019-0475-6

Cramer, S. C., Sur, M., Dobkin, B. H., O'brien, C., Sanger, T. D., Trojanowski, J. Q., et al. (2011). Harnessing neuroplasticity for clinical applications. *Brain* 134, 1591–1609.

Dixon, L., Ibrahim, M. M., Santora, D., and Knikou, M. (2016). Paired associative transspinal and transcortical stimulation produces plasticity in human cortical and spinal neuronal circuits. *J. Neurophysiol.* 116, 904–916. doi: 10.1152/jn.00259.2016

Enes, J., Langwieser, N., Ruschel, J., Carballosa-Gonzalez, M. M., Klug, A., Traut, M. H., et al. (2010). Electrical activity suppresses axon growth through Ca(v)1.2 channels in adult primary sensory neurons. *Curr. Biol.* 20, 1154–1164. doi: 10.1016/j.cub.2010.05.055

English, A. W., Schwartz, G., Meador, W., Sabatier, M. J., and Mulligan, A. (2007). Electrical stimulation promotes peripheral axon regeneration by enhanced neuronal neurotrophin signaling. *Dev. Neurobiol.* 67, 158–172. doi: 10.1002/dneu.20339

Fields, R. D., Eshete, F., Stevens, B., and Itoh, K. (1997). Action potential-dependent regulation of gene expression: temporal specificity in Ca*2*+, cAMP-responsive element binding proteins, and mitogen-activated protein kinase signaling. *J. Neurosci.* 17, 7252–7266. doi: 10.1523/jneurosci.17-19-07252.1997

Gad, P., Lee, S., Terrafranca, N., Zhong, H., Turner, A., Gerasimenko, Y., et al. (2018). Non-invasive activation of cervical spinal networks after severe paralysis. *J. Neurotraum.* 35, 2145–2158. doi: 10.1089/neu.2017.5461

Gao, Y., Deng, K., Hou, J., Bryson, J. B., Barco, A., Nikulina, E., et al. (2004). Activated CREB is sufficient to overcome inhibitors in myelin and promote spinal axon regeneration in vivo. *Neuron* 44, 609–621. doi: 10.1016/j.neuron.2004.10.030

Gerasimenko, Y., Gorodnichev, R., Moshonkina, T., Sayenko, D., Gad, P., and Reggie Edgerton, V. (2015). Transcutaneous electrical spinal-cord stimulation in humans. *Ann. Phys. Rehabil. Med.* 58, 225–231. doi: 10.1016/j.rehab.2015.05.003

Geremia, N. M., Gordon, T., Brushart, T. M., Al-Majed, A. A., and Verge, V. M. (2007). Electrical stimulation promotes sensory neuron regeneration and growth-associated gene expression. *Exp. Neurol.* 205, 347–359. doi: 10.1016/j.expneurol.2007.01.040

Ghosh, A., Haiss, F., Sydekum, E., Schneider, R., Gullo, M., Wyss, M. T., et al. (2010). Rewiring of hindlimb corticospinal neurons after spinal cord injury. *Nat. Neurosci.* 13, 97–104. doi: 10.1038/nn.2448

Ghosh-Roy, A., Wu, Z., Goncharov, A., Jin, Y., and Chisholm, A. D. (2010). Calcium and cyclic AMP promote axonal regeneration in *Caenorhabditis elegans* and require DLK-1 kinase. *J. Neurosci.* 30, 3175–3183. doi: 10.1523/jneurosci.5464-09.2010

Goganau, I., Sandner, B., Weidner, N., Fouad, K., and Blesch, A. (2018). Depolarization and electrical stimulation enhance in vitro and in vivo sensory axon growth after spinal cord injury. *Exp. Neurol.* 300, 247–258. doi: 10.1016/j.expneurol.2017.11.011

Gordon, T., Amirjani, N., Edwards, D. C., and Chan, K. M. (2010). Brief post-surgical electrical stimulation accelerates axon regeneration and muscle reinnervation without affecting the functional measures in carpal tunnel syndrome patients. *Exp. Neurol.* 223, 192–202. doi: 10.1016/j.expneurol.2009.09.020

Hall, S. M. (1986). The effect of inhibiting schwann cell mitosis on the re-innervation of acellular autografts in the peripheral nervous system of the mouse. *Neuropathol. Appl. Neurobiol.* 12, 401–414. doi: 10.1111/j.1365-2990.1986.tb00151.x

Han, Q., Xie, Y., Ordaz, J. D., Huh, A. J., Huang, N., Wu, W., et al. (2020). Restoring cellular energetics promotes axonal regeneration and functional recovery after spinal cord injury. *Cell Metab.* 31, 623–641.

Harkema, S., Gerasimenko, Y., Hodes, J., Burdick, J., Angeli, C., Chen, Y., et al. (2011). Effect of epidural stimulation of the lumbosacral spinal cord on voluntary movement, standing, and assisted stepping after motor complete paraplegia: a case study. *Lancet* 377, 1938–1947. doi: 10.1016/s0140-6736(11)60547-3

Hervera, A., Zhou, L., Palmisano, I., Mclachlan, E., Kong, G., Hutson, T. H., et al. (2019). PP4-dependent HDAC3 dephosphorylation discriminates between axonal regeneration and regenerative failure. *EMBO J.* 38:e101032.

Hoffman, H., and Binet, F. (1952). Acceleration and retardation of the process of axon-sprouting in partially denervated muscles. *Austr. J. Exper. Biol. Med. Sci.* 30, 541–566. doi: 10.1038/icb.1952.52

Hofstoetter, U. S., Krenn, M., Danner, S. M., Hofer, C., Kern, H., Mckay, W. B., et al. (2015). Augmentation of voluntary locomotor activity by transcutaneous spinal cord stimulation in motor-incomplete spinal cord-injured individuals. *Artif. Organ.* 39, E176–E186.

Hollis, E. R. II, Ishiko, N., Pessian, M., Tolentino, K., Lee-Kubli, C. A., Calcutt, N. A., et al. (2015a). Remodelling of spared proprioceptive circuit involving a small number of neurons supports functional recovery. *Nat. Commun.* 6:6079.

Hollis, E. R. II, Ishiko, N., Tolentino, K., Doherty, E., Rodriguez, M. J., Calcutt, N. A., et al. (2015b). A novel and robust conditioning lesion induced by ethidium bromide. *Exper. Neurol.* 265, 30–39. doi: 10.1016/j.expneurol.2014.12.004

Hutson, T. H., and Di Giovanni, S. (2019). The translational landscape in spinal cord injury: focus on neuroplasticity and regeneration. *Nat. Rev. Neurol.* 15, 732–745. doi: 10.1038/s41582-019-0280-3

Ichiyama, R. M., Gerasimenko, Y. P., Zhong, H., Roy, R. R., and Edgerton, V. R. (2005). Hindlimb stepping movements in complete spinal rats induced by epidural spinal cord stimulation. *Neurosci. Lett.* 383, 339–344. doi: 10.1016/j.neulet.2005.04.049

Ievins, A., and Moritz, C. T. (2017). Therapeutic stimulation for restoration of function after spinal cord injury. *Physiology* 32, 391–398. doi: 10.1152/physiol.00010.2017

Inanici, F., Samejima, S., Gad, P., Edgerton, V. R., Hofstetter, C. P., and Moritz, C. T. (2018). Transcutaneous electrical spinal stimulation promotes long-term recovery of upper extremity function in chronic tetraplegia. *IEEE Trans. Neural Syst. Rehabil. Eng.* 26, 1272–1278. doi: 10.1109/tnsre.2018.2834339

Jack, A. S., Hurd, C., Forero, J., Nataraj, A., Fenrich, K., Blesch, A., et al. (2018). Cortical electrical stimulation in female rats with a cervical spinal cord injury to promote axonal outgrowth. *J. Neurosci. Res.* 96, 852–862. doi: 10.1002/jnr.24209

Kang, H., and Lichtman, J. W. (2013). Motor axon regeneration and muscle reinnervation in young adult and aged animals. *J. Neurosci.* 33, 19480–19491. doi: 10.1523/jneurosci.4067-13.2013

Lee, J. K., Geoffroy, C. G., Chan, A. F., Tolentino, K. E., Crawford, M. J., Leal, M. A., et al. (2010). Assessing spinal axon regeneration and sprouting in Nogo-, MAG-, and OMgp-deficient mice. *Neuron* 66, 663–670. doi: 10.1016/j.neuron.2010.05.002

Lee, P. R., Cohen, J. E., Iacobas, D. A., Iacobas, S., and Fields, R. D. (2017). Gene networks activated by specific patterns of action potentials in dorsal root ganglia neurons. *Sci. Rep.* 7:43765.

Lee, S. K., and Wolfe, S. W. (2000). Peripheral nerve injury and repair. *J. Am. Acad. Orthop. Surg.* 8, 243–252.

Li, S., Yang, C., Zhang, L., Gao, X., Wang, X., Liu, W., et al. (2016). Promoting axon regeneration in the adult CNS by modulation of the melanopsin/GPCR signaling. *Proc. Natl. Acad. Sci. U.S.A.* 113, 1937–1942. doi: 10.1073/pnas.1523645113

Lim, J.-H. A., Stafford, B. K., Nguyen, P. L., Lien, B. V., Wang, C., Zukor, K., et al. (2016). Neural activity promotes long-distance, target-specific regeneration of adult retinal axons. *Nat. Neurosci.* 19, 1073–1084. doi: 10.1038/nn.4340

Liu, K., Lu, Y., Lee, J. K., Samara, R., Willenberg, R., Sears-Kraxberger, I., et al. (2010). PTEN deletion enhances the regenerative ability of adult corticospinal neurons. *Nat. Neurosci.* 13, 1075–1081. doi: 10.1038/nn.2603

Lu, M. C., Ho, C. Y., Hsu, S. F., Lee, H. C., Lin, J. H., Yao, C. H., et al. (2008). Effects of electrical stimulation at different frequencies on regeneration of transected peripheral nerve. *Neurorehabil. Neural Repair.* 22, 367–373. doi: 10.1177/1545968307313507

Lu, M. C., Tsai, C. C., Chen, S. C., Tsai, F. J., Yao, C. H., and Chen, Y. S. (2009). Use of electrical stimulation at different current levels to promote recovery after peripheral nerve injury in rats. *J. Traum.* 67, 1066–1072. doi: 10.1097/ta.0b013e318182351a

Mahar, M., and Cavalli, V. (2018). Intrinsic mechanisms of neuronal axon regeneration. *Nat. Rev. Neurosci.* 19, 323–337. doi: 10.1038/s41583-018-0001-8

Maier, I. C., and Schwab, M. E. (2006). Sprouting, regeneration and circuit formation in the injured spinal cord: factors and activity. *Philos. Trans. R. Soc. Lond. B Biol. Sci.* 361, 1611–1634. doi: 10.1098/rstb.2006.1890

Mandolesi, G., Madeddu, F., Bozzi, Y., Maffei, L., and Ratto, G. M. (2004). Acute physiological response of mammalian central neurons to axotomy: ionic regulation and electrical activity. *FASEB J.* 18, 1934–1936. doi: 10.1096/fj.04-1805fje

McQuarrie, I. G., and Grafstein, B. (1973). Axon outgrowth enhanced by a previous nerve injury. *Archiv. Neurol.* 29, 53–55. doi: 10.1001/archneur.1973.00490250071008

Mishra, A. M., Pal, A., Gupta, D., and Carmel, J. B. (2017). Paired motor cortex and cervical epidural electrical stimulation timed to converge in the spinal cord promotes lasting increases in motor responses. *J. Physiol.* 595, 6953–6968. doi: 10.1113/jp274663

Nix, W. A., and Hopf, H. C. (1983). Electrical stimulation of regenerating nerve and its effect on motor recovery. *Brain Res.* 272, 21–25. doi: 10.1016/0006-8993(83)90360-8

Park, K. K., Liu, K., Hu, Y., Smith, P. D., Wang, C., Cai, B., et al. (2008). Promoting axon regeneration in the adult CNS by modulation of the PTEN/mTOR pathway. *Science* 322, 963–966. doi: 10.1126/science.1161566

Pockett, S., and Gavin, R. M. (1985). Acceleration of peripheral nerve regeneration after crush injury in rat. *Neurosci. Lett.* 59, 221–224. doi: 10.1016/0304-3940(85)90203-4

Qiu, J., Cai, D., Dai, H., Mcatee, M., Hoffman, P. N., Bregman, B. S., et al. (2002). Spinal axon regeneration induced by elevation of cyclic AMP. *Neuron* 34, 895–903. doi: 10.1016/s0896-6273(02)00730-4

Ramón y Cajal, S. (1991). *Cajal's Degeneration and Regeneration of the Nervous System*. New York, NY: Oxford University Press.

Rejc, E., Angeli, C. A., Atkinson, D., and Harkema, S. J. (2017). Motor recovery after activity-based training with spinal cord epidural stimulation in a chronic motor complete paraplegic. *Sci. Rep.* 7:13476.

Richardson, P. M., and Issa, V. M. (1984). Peripheral injury enhances central regeneration of primary sensory neurones. *Nature* 309, 791–793. doi: 10.1038/309791a0

Rigaud, M., Gemes, G., Weyker, P. D., Cruikshank, J. M., Kawano, T., Wu, H.-E., et al. (2009). Axotomy depletes intracellular calcium stores in primary sensory neurons. *Anesthesiol. J. Am. Soc. Anesthesiol.* 111, 381–392. doi: 10.1097/aln.0b013e3181ae6212

Rishal, I., and Fainzilber, M. (2014). Axon-soma communication in neuronal injury. *Nat. Rev. Neurosci.* 15, 32–42. doi: 10.1038/nrn3609

Rosenzweig, E. S., Courtine, G., Jindrich, D. L., Brock, J. H., Ferguson, A. R., Strand, S. C., et al. (2010). Extensive spontaneous plasticity of corticospinal projections after primate spinal cord injury. *Nat. Neurosci.* 13, 1505–1510. doi: 10.1038/nn.2691

Sajic, M., Mastrolia, V., Lee, C. Y., Trigo, D., Sadeghian, M., Mosley, A. J., et al. (2013). Impulse conduction increases mitochondrial transport in adult mammalian peripheral nerves in vivo. *PLoS Biol.* 11:e1001754. doi: 10.1371/journal.pbio.1001754

Scheib, J., and Hoke, A. (2013). Advances in peripheral nerve regeneration. *Nat. Rev. Neurol.* 9, 668–676.

Seijffers, R., Mills, C. D., and Woolf, C. J. (2007). ATF3 increases the intrinsic growth state of DRG neurons to enhance peripheral nerve regeneration. *J. Neurosci.* 27, 7911–7920. doi: 10.1523/jneurosci.5313-06.2007

Senger, J. L., Chan, K. M., Macandili, H., Chan, A. W. M., Verge, V. M. K., Jones, K. E., et al. (2019). Conditioning electrical stimulation promotes functional nerve regeneration. *Exp. Neurol.* 315, 60–71. doi: 10.1016/j.expneurol.2019.02.001

Senger, J. L. B., Verge, V. M. K., Macandili, H. S. J., Olson, J. L., Chan, K. M., and Webber, C. A. (2018). Electrical stimulation as a conditioning strategy for promoting and accelerating peripheral nerve regeneration. *Exper. Neurol.* 302, 75–84. doi: 10.1016/j.expneurol.2017.12.013

Sheng, H. Z., Fields, R. D., and Nelson, P. G. (1993). Specific regulation of immediate early genes by patterned neuronal activity. *J. Neurosci. Res.* 35, 459–467. doi: 10.1002/jnr.490350502

Singh, B., Xu, Q.-G., Franz, C. K., Zhang, R., Dalton, C., Gordon, T., et al. (2012). Accelerated axon outgrowth, guidance, and target reinnervation across nerve transection gaps following a brief electrical stimulation paradigm. *Cell* 116:498. doi: 10.3171/2011.10.jns11612

Smith, P. D., Sun, F., Park, K. K., Cai, B., Wang, C., Kuwako, K., et al. (2009). SOCS3 deletion promotes optic nerve regeneration in vivo. *Neuron* 64, 617–623. doi: 10.1016/j.neuron.2009.11.021

Song, Y., Li, D., Farrelly, O., Miles, L., Li, F., Kim, S. E., et al. (2019). The mechanosensitive ion channel piezo inhibits axon regeneration. *Neuron* 102, 373–389.

Stam, F. J., Macgillavry, H. D., Armstrong, N. J., De Gunst, M. C., Zhang, Y., Van Kesteren, R. E., et al. (2007). Identification of candidate transcriptional modulators involved in successful regeneration after nerve injury. *Eur. J. Neurosci.* 25, 3629–3637. doi: 10.1111/j.1460-9568.2007.05597.x

Steinmetz, M. P., Horn, K. P., Tom, V. J., Miller, J. H., Busch, S. A., Nair, D., et al. (2005). Chronic enhancement of the intrinsic growth capacity of sensory neurons combined with the degradation of inhibitory proteoglycans allows functional regeneration of sensory axons through the dorsal root entry zone in the mammalian spinal cord. *J. Neurosci.* 25, 8066–8076. doi: 10.1523/jneurosci.2111-05.2005

Sun, F., Park, K. K., Belin, S., Wang, D., Lu, T., Chen, G., et al. (2011). Sustained axon regeneration induced by co-deletion of PTEN and SOCS3. *Nature* 480, 372–375. doi: 10.1038/nature10594

Sun, L., Shay, J., Mcloed, M., Roodhouse, K., Chung, S. H., Clark, C. M., et al. (2014). Neuronal regeneration in *C. elegans* requires subcellular calcium release by ryanodine receptor channels and can be enhanced by optogenetic stimulation. *J. Neurosci.* 34, 15947–15956. doi: 10.1523/jneurosci.4238-13.2014

Sun, W., Larson, M. J., Kiyoshi, C. M., Annett, A. J., Stalker, W. A., Peng, J., et al. (2020). Gabapentinoid treatment promotes corticospinal plasticity and regeneration following murine spinal cord injury. *J. Clin. Invest.* 130, 345–358. doi: 10.1172/jci130391

Takeoka, A., Vollenweider, I., Courtine, G., and Arber, S. (2014). Muscle spindle feedback directs locomotor recovery and circuit reorganization after spinal cord injury. *Cell* 159, 1626–1639. doi: 10.1016/j.cell.2014.11.019

Tedeschi, A., Dupraz, S., Laskowski, C. J., Xue, J., Ulas, T., Beyer, M., et al. (2016). The calcium channel subunit Alpha2delta2 suppresses axon regeneration in the adult CNS. *Neuron* 92, 419–434. doi: 10.1016/j.neuron.2016.09.026

Tedeschi, A., Nguyen, T., Puttagunta, R., Gaub, P., and Di Giovanni, S. (2009). A p53-CBP/p300 transcription module is required for GAP-43 expression, axon outgrowth, and regeneration. *Cell Death Differ.* 16, 543–554. doi: 10.1038/cdd.2008.175

Tsujino, H., Kondo, E., Fukuoka, T., Dai, Y., Tokunaga, A., Miki, K., et al. (2000). Activating transcription factor 3 (ATF3) induction by axotomy in sensory and motoneurons: a novel neuronal marker of nerve injury. *Mol. Cell. Neurosci.* 15, 170–182. doi: 10.1006/mcne.1999.0814

Tyssowski, K. M., Destefino, N. R., Cho, J. H., Dunn, C. J., Poston, R. G., Carty, C. E., et al. (2018). Different neuronal activity patterns induce different gene expression programs. *Neuron* 98, 530–546.

Udina, E., Furey, M., Busch, S., Silver, J., Gordon, T., and Fouad, K. (2008). Electrical stimulation of intact peripheral sensory axons in rats promotes outgrowth of their central projections. *Exper. Neurol.* 210, 238–247. doi: 10.1016/j.expneurol.2007.11.007

von Bernhardi, R., Bernhardi, L. E., and Eugenin, J. (2017). What is neural plasticity? *Adv. Exp. Med. Biol.* 1015, 1–15.

Wagner, F. B., Mignardot, J.-B., Le Goff-Mignardot, C. G., Demesmaeker, R., Komi, S., Capogrosso, M., et al. (2018). Targeted neurotechnology restores walking in humans with spinal cord injury. *Nature* 563, 65–71.

Ward, P. J., Clanton, S. L. II, and English, A. W. (2018). Optogenetically enhanced axon regeneration: motor versus sensory neuron-specific stimulation. *Eur. J. Neurosci.* 47, 294–304. doi: 10.1111/ejn.13836

Ward, P. J., Jones, L. N., Mulligan, A., Goolsby, W., Wilhelm, J. C., and English, A. W. (2016). Optically-induced neuronal activity is sufficient to promote functional motor axon regeneration in vivo. *PLoS One* 11:e0154243. doi: 10.1371/journal.pbio.154243

Wheeler, D. G., Groth, R. D., Ma, H., Barrett, C. F., Owen, S. F., Safa, P., et al. (2012). Ca(V)1 and Ca(V)2 channels engage distinct modes of Ca(2+) signaling to control CREB-dependent gene expression. *Cell* 149, 1112–1124. doi: 10.1016/j.cell.2012.03.041

Wolf, J. A., Stys, P. K., Lusardi, T., Meaney, D., and Smith, D. H. (2001). Traumatic axonal injury induces calcium influx modulated by tetrodotoxin-sensitive sodium channels. *J. Neurosci.* 21, 1923–1930. doi: 10.1523/jneurosci.21-06-01923.2001

Wong, J. N., Olson, J. L., Morhart, M. J., and Chan, K. M. (2015). Electrical stimulation enhances sensory recovery: a randomized controlled trial. *Ann. Neurol.* 77, 996–1006. doi: 10.1002/ana.24397

Yang, Q., Ramamurthy, A., Lall, S., Santos, J., Ratnadurai-Giridharan, S., Lopane, M., et al. (2019). Independent replication of motor cortex and cervical spinal cord electrical stimulation to promote forelimb motor function after spinal cord injury in rats. *Exper. Neurol.* 320:112962. doi: 10.1016/j.expneurol.2019.112962

Zareen, N., Dodson, S., Armada, K., Awad, R., Sultana, N., Hara, E., et al. (2018). Stimulation-dependent remodeling of the corticospinal tract requires reactivation of growth-promoting developmental signaling pathways. *Exper. Neurol.* 307, 133–144. doi: 10.1016/j.expneurol.2018.05.004

Zareen, N., Shinozaki, M., Ryan, D., Alexander, H., Amer, A., Truong, D. Q., et al. (2017). Motor cortex and spinal cord neuromodulation promote corticospinal tract axonal outgrowth and motor recovery after cervical contusion spinal cord injury. *Exper. Neurol.* 297, 179–189. doi: 10.1016/j.expneurol.2017.08.004

Zhou, B., Yu, P., Lin, M.-Y., Sun, T., Chen, Y., and Sheng, Z.-H. (2016). Facilitation of axon regeneration by enhancing mitochondrial transport and rescuing energy deficits. *J. Cell Biol.* 214, 103–119. doi: 10.1083/jcb.201605101

Ziv, N. E., and Spira, M. E. (1995). Axotomy induces a transient and localized elevation of the free intracellular calcium concentration to the millimolar range. *J. Neurophysiol.* 74, 2625–2637. doi: 10.1152/jn.1995.74.6.2625

**Conflict of Interest:** The authors declare that the research was conducted in the absence of any commercial or financial relationships that could be construed as a potential conflict of interest.

frontiers in Cell and Developmental Biology

REVIEW
published: 03 September 2020
doi: 10.3389/fcell.2020.567537

# GAP-43 and BASP1 in Axon Regeneration: Implications for the Treatment of Neurodegenerative Diseases

*Daayun Chung, Andrew Shum and Gabriela Caraveo**

*Department of Neurology, Feinberg School of Medicine, Northwestern University, Chicago, IL, United States*

Growth-associated protein-43 (GAP-43) and brain acid-soluble protein 1 (BASP1) regulate actin dynamics and presynaptic vesicle cycling at axon terminals, thereby facilitating axonal growth, regeneration, and plasticity. These functions highly depend on changes in GAP-43 and BASP1 expression levels and post-translational modifications such as phosphorylation. Interestingly, examinations of GAP-43 and BASP1 in neurodegenerative diseases reveal alterations in their expression and phosphorylation profiles. This review provides an overview of the structural properties, regulations, and functions of GAP-43 and BASP1, highlighting their involvement in neural injury response and regeneration. By discussing GAP-43 and BASP1 in the context of neurodegenerative diseases, we also explore the therapeutic potential of modulating their activities to compensate for neuron loss in neurodegenerative diseases.

**Keywords: GAP-43, BASP1, phosphorylation, neural injury response, axon regeneration, neurodegenerative diseases**

OPEN ACCESS

***Edited by:***
*João M. N. Duarte,*
*Lund University, Sweden*

***Reviewed by:***
*Annalisa Buffo,*
*University of Turin, Italy*
*Sol Sotillos,*
*Andalusian Center for Developmental Biology (CABD), Spain*
*Elisa Tamariz,*
*University of Veracruz, Mexico*

****Correspondence:***
*Gabriela Caraveo*
*gabriela.piso@northwestern.edu*

***Specialty section:***
*This article was submitted to Molecular Medicine, a section of the journal Frontiers in Cell and Developmental Biology*

***Received:*** *29 May 2020*
***Accepted:*** *14 August 2020*
***Published:*** *03 September 2020*

***Citation:***
*Chung D, Shum A and Caraveo G (2020) GAP-43 and BASP1 in Axon Regeneration: Implications for the Treatment of Neurodegenerative Diseases. Front. Cell Dev. Biol. 8:567537. doi: 10.3389/fcell.2020.567537*

## INTRODUCTION

Axons integrate external cues to grow toward and arborize their terminals onto their correct targets. Such axonal behavior is critical for establishing proper connections, regenerating injured nerves, and retaining anatomical plasticity in adult brains (Skene, 1989). A group of growth-associated proteins (>100) (Costigan et al., 2002; Xiao et al., 2002), whose expression is upregulated during neuronal development and regeneration, mediates these functions (Jacobson et al., 1986; Widmer and Caroni, 1990; Mason, 2002). Growth-associated protein-43 (GAP-43) and brain acid-soluble protein 1 (BASP1) are two members of this group with many shared structural properties and functions (Mosevitsky, 2005). GAP-43 is solely expressed in the nervous system (Karns et al., 1987), whereas BASP1 is highly expressed in the nervous system and some non-neural tissues including the kidney and testis (Mosevitsky et al., 1997; Mosevitsky and Silicheva, 2011). Within neurons, GAP-43, and BASP1 are enriched in axon terminals (Meiri et al., 1986; Widmer and Caroni, 1990), where they regulate the actin cytoskeleton (Wiederkehr et al., 1997; Laux et al., 2000). By modulating actin dynamics, GAP-43, and BASP1 achieve their physiological functions in neurodevelopment, synaptic function, and nerve regeneration.

# PHYSIOLOGICAL FUNCTIONS IN THE NERVOUS SYSTEM

## Neurodevelopment

Growth-associated protein-43 and BASP1 are highly expressed during periods of active axon growth and synaptogenesis (McGuire et al., 1988; De La Monte et al., 1989; Widmer and Caroni, 1990). Their critical involvement in neurodevelopment has been demonstrated by gene knockout studies. Homozygous knockout of GAP-43 (GAP-43$^{-/-}$) or BASP1 (BASP1$^{-/-}$) leads to high neonatal lethality, resulting in 5–10% survival to adulthood (Strittmatter et al., 1995; Frey et al., 2000; Metz and Schwab, 2004). Surviving GAP-43$^{-/-}$ animals exhibit defective pathfinding of retinal and commissural axons (Strittmatter et al., 1995; Shen et al., 2002), as well as an abnormal somatotopic map in the barrel cortex (Maier et al., 1999). In reflection of these anatomical defects, GAP-43$^{-/-}$ animals demonstrate motor, sensory, and behavioral impairments (Metz and Schwab, 2004). Surviving BASP1$^{-/-}$ animals also present evidence of impaired neurodevelopment including enlarged ventricles in the brain, axonal and synaptic abnormalities in the neocortex and hippocampus, and hyperactive behavior (Frey et al., 2000).

## Synaptic Function

As axons complete the innervation of their target areas, GAP-43 and BASP1 are downregulated in most brain regions. Interestingly, they remain highly expressed in areas of the adult brain implicated in learning and memory, including the neocortex and hippocampus (Benowitz et al., 1988; McGuire et al., 1988; Neve et al., 1988; Frey et al., 2000). In support of their importance in information storage, heterozygous GAP-43 knockout mice (GAP-43$^{+/-}$) exhibit a selective impairment in contextual memory (Rekart et al., 2005). This phenotype can be explained by various synaptic functions of GAP-43. GAP-43 was shown to regulate endocytosis via its interaction with rabaptin-5, which functions in endocytic membrane fusion (Neve et al., 1998), and as a substrate of caspase-3, which mediates AMPA receptor endocytosis (Han et al., 2013). Also, antibodies against GAP-43 decreased the release of glutamate and noradrenaline (Dekker et al., 1989a; Hens et al., 1998), indicating its importance in neurotransmitter release. This function is thought to be mediated, at least in part, by its interaction with the presynaptic vesicle fusion complex (Syntaxin, SNAP-25, and VAMP) (Haruta et al., 1997). Moreover, GAP-43 was shown to enhance long-term potentiation (Routtenberg and Lovinger, 1985; Lovinger et al., 1986; Hulo et al., 2002). The presence of BASP1 on synaptic vesicles (Yamamoto et al., 1997) and its identification as a caspase-3 substrate (Han et al., 2013) suggest its potential role in synaptic vesicle cycling, which may have implications for neurotransmission, synaptic plasticity, and information storage.

## Nerve Regeneration

Another circumstance under which GAP-43 and BASP1 are upregulated is nerve regeneration following injury (Skene and Willard, 1981; Caroni et al., 1997). An increase in GAP-43 and BASP1 mRNA levels strongly correlates with enhanced regenerative capacity. This is evidenced by their robust upregulation in the regenerating dorsal root ganglion (DRG) axons following sciatic nerve injury but not in the non-regenerating DRG axons following dorsal rhizotomy (Mason, 2002). The upregulation of GAP-43 and BASP1 also correlated with axonal sprouting after stroke in the barrel cortex (Carmichael et al., 2005). Additionally, an increase in GAP-43 was associated with optogenetic-induced functional recovery from stroke in the primary motor cortex (Cheng et al., 2014). In a different rodent model of stroke, antisense oligonucleotides to GAP-43 abolished the enhancement of functional recovery induced by the basic fibroblast growth factor (Kawamata et al., 1999). These observations from rodent stroke models hint at the importance of GAP-43 in neuronal recovery following injury. More importantly, GAP-43 was shown to be essential for the regenerative response through knockdown studies. In adult rodents, climbing fibers retain high levels of GAP-43 and demonstrate structural plasticity after injury (Grasselli and Strata, 2013). Knockdown of GAP-43 in climbing fibers inhibited the sprouting of their axonal branches following laser-axotomy (Allegra Mascaro et al., 2013) and lesion of the inferior olive, where these fibers originate (Grasselli et al., 2011). Overexpression studies involving GAP-43 and BASP1 show these proteins are sufficient for f-actin accumulation and subsequent neurite formation in primary sensory neurons (Aigner and Caroni, 1995) and in Purkinje neurons (Buffo et al., 1997). Moreover, co-overexpression of GAP-43 and BASP1 was sufficient to drive the regeneration of DRG axons following spinal cord lesion in adult mice when peripheral nerve graft was provided (Bomze et al., 2001).

# INVOLVEMENT IN NEURAL INJURY RESPONSE

In the central (CNS) and peripheral nervous systems (PNS), different external and internal factors lead to disparate outcomes of injury response. In the CNS, glial scar (Silver and Miller, 2004) and inhibitory glial factors such as myelin-associated glycoproteins and Nogo (Filbin, 2003) impede neuronal regeneration. Additionally, the inherent lack of axonal integrins and growth factor receptors limit the regrowth of neurons in the CNS (Koseki et al., 2017). As a result, positive outcomes of CNS injury remain limited to neuroprotection and marginal regenerative response. Neural injury stimulates neurons and glia to release cytokines and neurotrophic factors, which can activate growth-associated proteins such as GAP-43 and BASP1 to promote neuroprotection and regeneration.

## Cytokine Signaling

Upon injury, leakage from damaged or dying cells leads to an excess of glutamate in the extracellular space (Bullock et al., 1998). This stimulates astrocytes, microglia, and neurons to secrete cytokines such as interleukin-6 (IL-6) and -10 (IL-10) (Morganti-Kossman et al., 1997; Acarin et al., 2000). Accordingly, IL-6 and -10 were found to be elevated in

the cerebrospinal fluid and serum of patients with severe traumatic brain injury (TBI) (Kossmann et al., 1995; Csuka et al., 1999). After spinal cord injury, IL-6 treatment was shown to activate the JAK/STAT3 and PI3K/Akt pathways, upregulate GAP-43 and BASP1, and promote neurite outgrowth *in vitro* and synaptogenesis *in vivo* (Yang et al., 2012, 2015; **Figure 1**). The upregulation of GAP-43 and BASP1 was sensitive to the JAK2 inhibitor AG490 (Yang et al., 2015) but was not examined with a PI3K inhibitor. After oxygen-glucose deprivation, IL-10 treatment was shown to activate the JAK/STAT3 and PI3K/Akt pathways, upregulate GAP-43, and facilitate neuroprotection, neurite outgrowth, and synaptogenesis *in vitro* (Lin et al., 2015; Chen et al., 2016; **Figure 1**). The upregulation of GAP-43 was shown to be sensitive to the PI3K inhibitor LY294002 (Lin et al., 2015) but was not examined with a JAK2 inhibitor. The extent to which the neurite outgrowth observed *in vitro* translates into *in vivo* regeneration remains unclear.

## Neurotrophic Factor Signaling

Following injury, neurotrophic factors such as the nerve growth factor (NGF) (DeKosky et al., 1994; Chiaretti et al., 2009) and brain-derived neurotrophic factor (BDNF) (Miyake et al., 2002; Rostami et al., 2014) are upregulated in response to glutamate (Wetmore et al., 1994; Gwag et al., 1997) and cytokines (Kossmann et al., 1996). NGF and BDNF bind tropomyosin receptor kinase A and B, respectively, to initiate cell survival signaling via the PI3K/Akt pathway (Nguyen et al., 2010; **Figure 1**). In rodent models of stroke and TBI, the activation of NGF and BDNF signaling was shown to promote neuroprotection, synaptogenesis, and neurogenesis (Wu et al., 2008; Qi et al., 2014; Gudasheva et al., 2019). Such beneficial

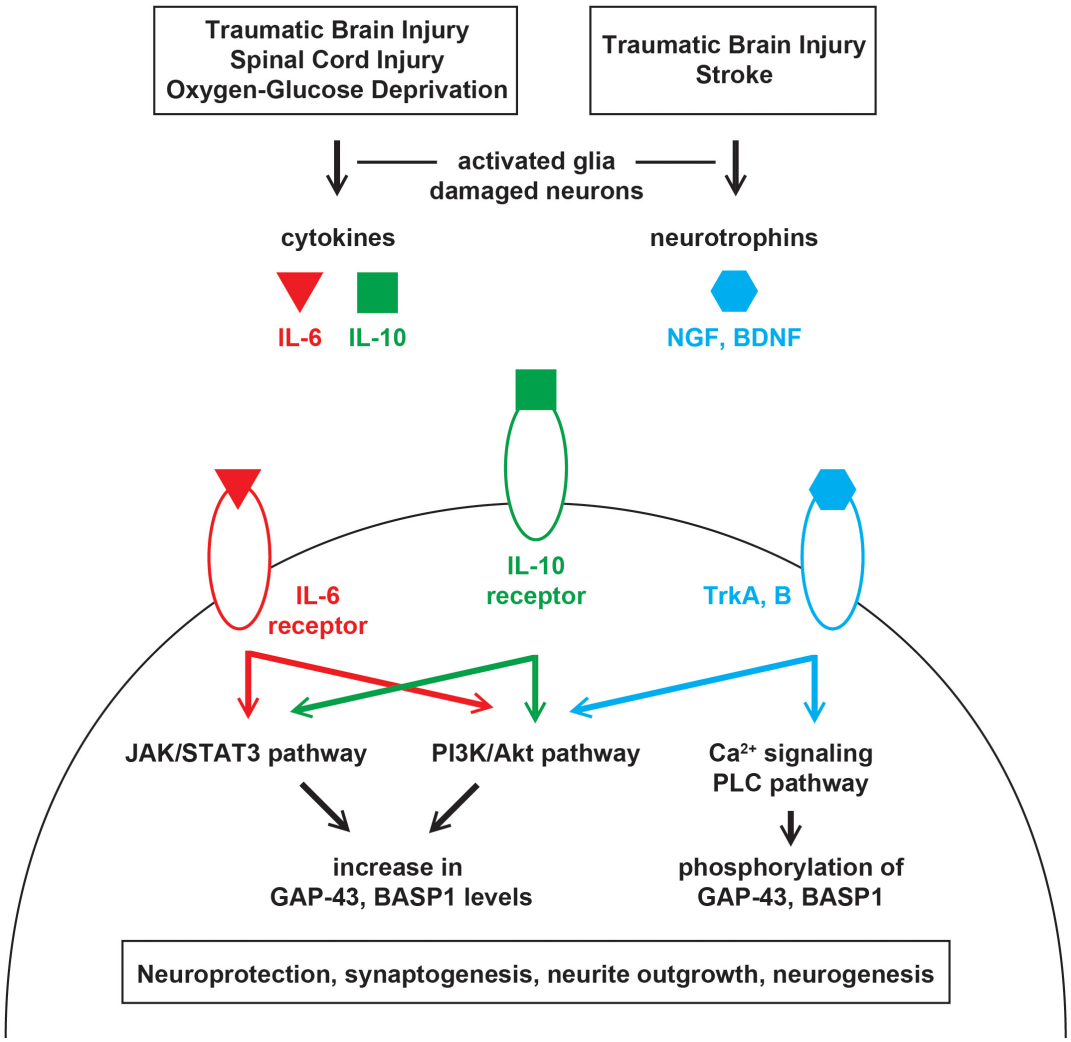


**FIGURE 1 |** Injury-induced signaling pathways that regulate GAP-43 and BASP1. Injuries in the central nervous system leads to the release of cytokines and neurotrophins from damaged neurons and activated glia. Cytokines and neurotrophins bind their receptors on surviving neurons to activate various signaling cascades that regulate the expression level and phosphorylation of GAP-43 and BASP1. Alterations in GAP-43 and BASP1 levels and phosphorylation are associated with neuroprotection, synaptogenesis, neurite outgrowth, and neurogenesis.

upregulation of NGF and BDNF was accompanied by an increase in GAP-43 levels when optogenetic stimulations were provided after stroke (Cheng et al., 2014). Given that BASP1 is similarly upregulated after stroke (Carmichael et al., 2005), its increase may also be mediated by NGF and BDNF. Moreover, GAP-43 was shown to be an essential effector of BDNF-driven neuroprotection (Gupta et al., 2009).

# STRUCTURAL PROPERTIES AND DOMAINS

## Intrinsic Disorder and Phase Separation

Growth-associated protein-43 and BASP1 are acidic proteins with isoelectric points of 4.4–4.6 (Mosevitsky et al., 1994). Their molecular weights are 23–25 kDa, but they appear at higher molecular weights on SDS-PAGE (Mosevitsky et al., 1994). These proteins are enriched in alanine (22% in GAP-43, 21% in BASP1) and proline (8% in GAP-43, 12% in BASP1), which gives rise to a high content of type II polyproline helix (32 ± 5% in GAP-43, 37 ± 2% in BASP1) characteristic of intrinsically disordered proteins (Forsova and Zakharov, 2016). Nuclear magnetic resonance spectroscopy also indicates that GAP-43 and BASP1 have unordered structures (Zhang et al., 1994; Geist et al., 2013). Intrinsically disordered proteins lack a stable three-dimensional structure and have the ability to engage in multivalent interactions (Haynes et al., 2006). Through multivalent interactions, intrinsically disordered proteins undergo liquid-liquid phase separation and form membraneless compartments that facilitate their functions (Li et al., 2012). Many proteins involved in actin assembly have intrinsically disordered regions, and phase separation mediated by these regions underlies their regulation of actin dynamics (Sun et al., 2017; Miao et al., 2018). Moreover, phosphorylation of intrinsically disordered proteins affects phase separation by modulating their charge and electrostatic interactions (Aumiller and Keating, 2016; Miao et al., 2018). Given that GAP-43 and BASP1 are phosphoproteins, they may transmit signals from kinases and phosphatases to the actin cytoskeleton via phase separation.

## PEST Sequence and High Turnover Rate

Growth-associated protein-43 and BASP1 have peptide sequences rich in proline, glutamate, serine, and threonine (PEST) (Barnes and Gomes, 1995; Mosevitsky et al., 1997). While PEST regions vary in their sequences and lengths, they all serve as signals for rapid proteolysis (Rechsteiner and Rogers, 1996). The presence of PEST sequences indicates that GAP-43 and BASP1 are short-lived proteins, however, this has yet to be experimentally verified.

## Effector Domain and CaM Binding

Growth-associated protein-43 and BASP1 have regions termed the effector domain (ED) that are enriched in basic and hydrophobic residues, bind calmodulin (CaM), and are phosphorylated by protein kinase C (PKC) (Cimler et al., 1985; Apel et al., 1990; Maekawa et al., 1993). The basic and hydrophobic residues in the ED also contribute to membrane association of these proteins (O'Neil and DeGrado, 1990; Mosevitsky et al., 1997; Mosevitsky, 2005). GAP-43 ED consists of residues 37–52 (KIQASFRGHITRKKLK) (Mosevitsky, 2005; **Figure 2**), which includes a canonical CaM-binding site termed the IQ motif (IQxxxRGxxxR) (Bähler and Rhoads, 2002). GAP-43 was shown to bind CaM with higher affinity in the absence of or at low $Ca^{2+}$ and to dissociate at high $Ca^{2+}$ (Andreasen et al., 1983; Alexander et al., 1987; Gamby et al., 1996). Hence, GAP-43 has been proposed to accumulate CaM at specific sites and release them upon local $Ca^{2+}$ elevation to sharpen the downstream response (Alexander et al., 1987; Mosevitsky, 2005). Unlike GAP-43, BASP1 ED is located at the N-terminal end (Myristoylation-GGKLSKKKKGY) (Mosevitsky, 2005; **Figure 2**). BASP1 lacks an IQ motif and instead binds CaM through alternating basic and hydrophobic residues (Takasaki et al., 1999). These alternating parts include the myristoyl moiety, which passes through a tunnel formed by hydrophobic pockets in the N- and C-terminal domains of CaM (Takasaki et al., 1999; Matsubara et al., 2004). BASP1 was shown to bind CaM with stronger affinity than GAP-43 (Maekawa et al., 1994) and in the presence of $Ca^{2+}$ (Maekawa et al., 1993), suggesting a different mode of action than GAP-43.

## Formation of Oligomers

Growth-associated protein-43 and BASP1 form oligomers in the presence of anionic phospholipids or sodium dodecyl sulfate (SDS) (Zakharov and Mosevitsky, 2010). Among anionic phospholipids, phosphatidylinositol 4,5-bisphosphate ($PI(4,5)P_2$) was the most potent driver of oligomerization (Zakharov and Mosevitsky, 2010). Interestingly, GAP-43 and BASP1 accumulate $PI(4,5)P_2$ on the inner surface of the plasma membrane, and this clustering is important for initiating signaling cascades that regulate the actin cytoskeleton (Laux et al., 2000). The role of $PI(4,5)P_2$ in driving oligomerization suggests that $PI(4,5)P_2$-induced oligomers may be important for this process. Oligomerization of GAP-43 and BASP1 results in α-helix formation within their EDs while preserving the overall structural disorder (Forsova and Zakharov, 2016). A significant level of disorder in oligomers has been proposed to enhance the flexibility of interactions and to enable the reversion to monomers (Tompa and Fuxreiter, 2008). In support of the flexibility in binding, GAP-43 and BASP1 were observed to form heterooligomers of different stoichiometries *in vitro* and in presynaptic membranes (Forsova and Zakharov, 2016). In agreement with the reversibility, GAP-43 and BASP1 oligomers were shown to dissociate into monomers upon removal of SDS or binding of CaM (Zakharov and Mosevitsky, 2010).

# TRANSCRIPTIONAL AND POST-TRANSCRIPTIONAL REGULATION

In developing and regenerating neurons, the levels of GAP-43 and BASP1 mRNAs and proteins are upregulated (Widmer and Caroni, 1990; Perrone-Bizzozero et al., 1991; Mason, 2002).

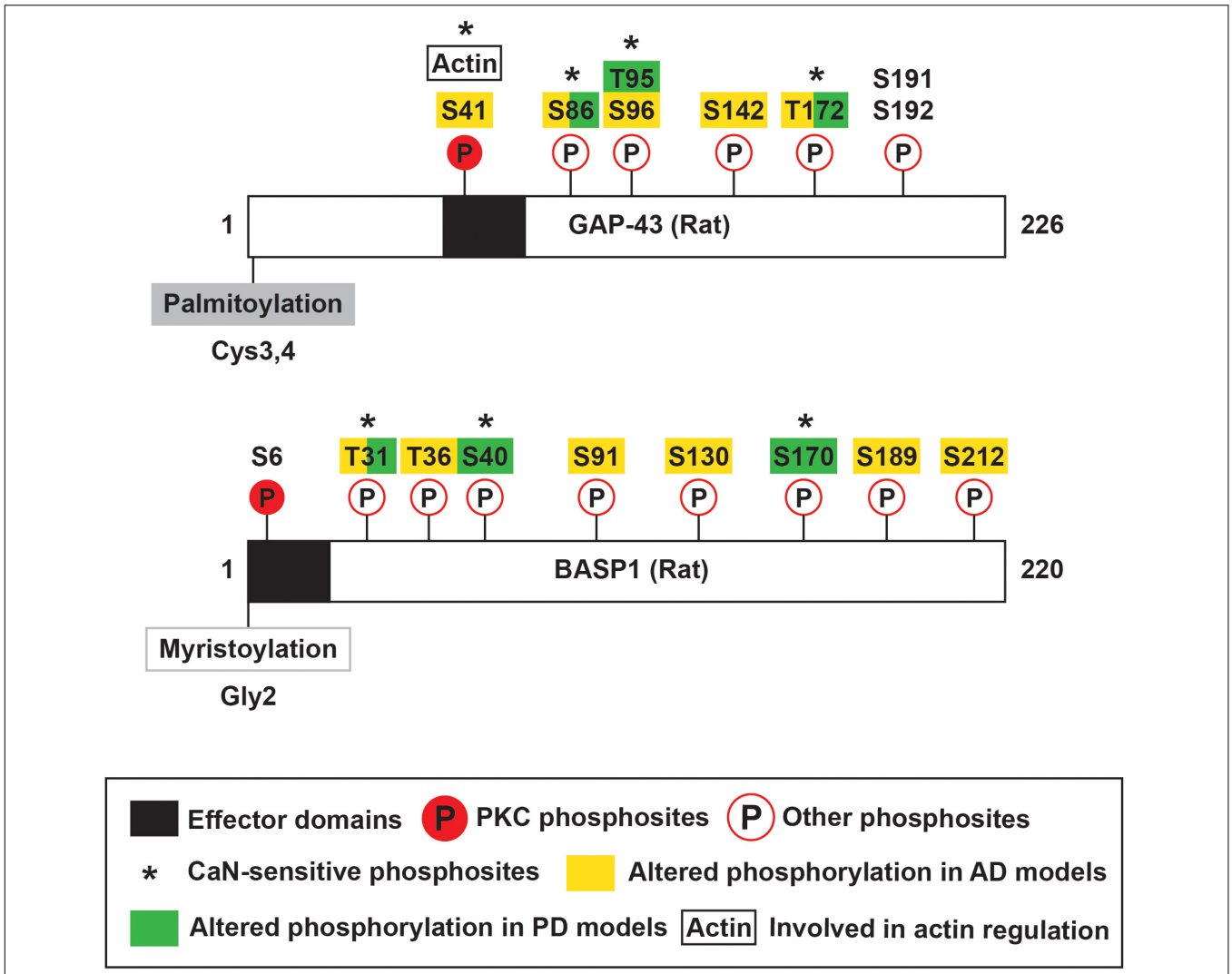


**FIGURE 2 |** Schematic of rat GAP-43 and BASP1 structure and post-translational modifications. GAP-43 and BASP1 are characterized by N-terminal fatty acylation, effector domains, and multiple phosphosites. GAP-43 is palmitoylated at Cysteine-3 and -4, and BASP1 is myristoylated at the N-terminal end. Their effector domains enable calmodulin binding and are subjected to phosphorylation by PKC. Phosphorylation of GAP-43 by PKC regulates various functions including actin cytoskeleton dynamics. GAP-43 and BASP1 are also regulated by other kinases and phosphatases, and such post-translational modifications are implicated in Alzheimer's and Parkinson's Diseases.

Studies present conflicting findings regarding the contributions of transcriptional activation to increased GAP-43 levels. The GAP-43 gene has two promoters, distal (P1) and proximal (P2), that are highly conserved between the rat and human genes (Eggen et al., 1994; de Groen et al., 1995). P1 contains classical promoter elements including TATA and CCAAT boxes (Nedivi et al., 1992), as well as a repressive element shown to inhibit GAP-43 expression in non-neuronal cells (Weber and Skene, 1997). P2 lacks classical promoter elements but contains a conserved enhancer box (E1) that can bind basic helix-loop-helix transcription factors (Chiaramello et al., 1996), which have critical roles in neural cell fate specification and differentiation (Dennis et al., 2019). In zebrafish, a 1 kb fragment spanning P1 and P2 of the rat GAP-43 gene was shown to developmentally regulate the expression of a downstream transgene in neurons (Udvadia et al., 2001). In contrast to this finding, developing rat cortical neurons and nerve growth factor-induced PC12 cells showed no change in GAP-43 pre-mRNA levels despite an increase in GAP-43 mRNA levels (Perrone-Bizzozero et al., 1991). This finding indicates that mRNA stability mainly contributes to the observed upregulation of GAP-43. The stabilization of GAP-43 mRNA is dependent on the highly conserved 3′ untranslated region (Kohn et al., 1996; Tsai et al., 1997), where the neural-specific RNA-binding protein HuD binds (Chung et al., 1997). The expression of HuD and GAP-43 are concomitantly increased during neuritogenesis (Anderson et al., 2001), in regenerating nerves (Anderson et al., 2003), and following spatial learning in rodent hippocampi (Quattrone et al., 2001; Pascale et al., 2004). Based on these observations, HuD was hypothesized to stabilize GAP-43 mRNA under physiological conditions. In

support of this hypothesis, transgenic mice overexpressing HuD exhibited an increase in GAP-43 mRNA but not pre-mRNA (Bolognani et al., 2006). Also, the half-life of GAP-43 mRNA from these transgenic mice was significantly longer than those from non-transgenic controls (Bolognani et al., 2006). The HuD-dependent stabilization of GAP-43 mRNA is positively regulated by PKC (Perrone-Bizzozero et al., 1993; Sanna et al., 2014) and is inhibited by the KH-type splicing regulatory protein, which competes with HuD to bind and promote the degradation of GAP-43 mRNA (Bird et al., 2013). Compared to GAP-43, little is known about the transcriptional and post-transcriptional control of BASP1. In the chicken BASP1 gene, a 135 bp region in the 5′ end of exon 1 was shown to bind the transcription factors Sp1 and Myc (Hartl et al., 2009). This regulatory region was sufficient to activate transcription and to mediate Myc-induced suppression of BASP1 (Hartl et al., 2009). Additionally, post-transcriptional regulation of BASP1 by its processed pseudogene has been proposed but not experimentally verified (Uzumcu et al., 2009).

# POST-TRANSLATIONAL MODIFICATIONS

## Fatty Acylation

Growth-associated protein-43 and BASP1 mainly localize to membranes (Skene et al., 1986; Maekawa et al., 1993), and their membrane associations are partially mediated by fatty acylation. GAP-43 is post-translationally palmitoylated at Cysteine-3 and -4 (Skene and Virág, 1989; **Figure 2**). Its palmitoylation can occur in the endoplasmic reticulum-Golgi intermediate compartment (ERGIC), Golgi apparatus, and plasma membrane (McLaughlin and Denny, 1999). Upon palmitoylation, GAP-43 can be sorted to the tips of growing neurites (Gauthier-Kemper et al., 2014). Palmitoylation of GAP-43 is dynamically regulated, as suggested by the low percentage (∼35%) of fatty acylated GAP-43 at steady state in PC12 and COS-1 cells (Liang et al., 2002). The dynamic regulation of palmitoylation affects GAP-43 functions. Changes in palmitoylation enable GAP-43 to cycle between pathways independent of and involving $G_o$, a heterotrimeric GTP-binding protein enriched in growth cones (Edmonds et al., 1990). N-terminal peptides of GAP-43 produced by the $Ca^{2+}$-dependent protease m-calpain interact with and activate $G_o$ signaling cascade that leads to growth cone collapse (Strittmatter et al., 1994; Zakharov and Mosevitsky, 2007; **Figure 3**). Palmitoylation reduces the ability of the N-terminal peptides to stimulate $G_o$, thereby blocking $G_o$ signaling-induced growth cone collapse (Sudo et al., 1992). Additionally, palmitoylation appears to be important for the switch from promoting axon growth to stabilizing synapses upon successful target innervation (Patterson and Skene, 1999). Experimental evidence shows that palmitoylation of GAP-43, when inhibited, reversibly stalls neurite outgrowth (Hess et al., 1993) and is significantly reduced at the early phase of synapse maturation (Patterson and Skene, 1999). Unlike GAP-43, BASP1 is co-translationally myristoylated at the N-terminal end (Mosevitsky et al., 1997; Takasaki et al., 1999; **Figure 2**). In the rat brain, BASP1 molecules and N-terminal fragments appear predominantly in the myristoylated form (Mosevitsky et al., 1997; Zakharov et al., 2003). Myristoylation of BASP1 was shown to promote membrane association and to enable CaM binding (Takasaki et al., 1999; Matsubara et al., 2004).

## Phosphorylation

Growth-associated protein-43 and BASP1 EDs undergo $Ca^{2+}$-dependent phosphorylation by PKC. PKC phosphosites in GAP-43 and BASP1 are Serine-41 and Serine-6, respectively (Apel et al., 1990; Maekawa et al., 1994; **Figure 2**). GAP-43 Serine-41 can also be dephosphorylated by the $Ca^{2+}$/CaM-dependent phosphatase calcineurin (CaN) (Liu and Storm, 1989). Phosphorylation by PKC abolishes CaM binding to both GAP-43 and BASP1 (Apel et al., 1990; Takasaki et al., 1999). More importantly, PKC-mediated phosphorylation has significant functional consequences. Phosphorylated GAP-43 not only promotes actin polymerization and stabilization (He et al., 1997; Korshunova et al., 2007) but also interacts with presynaptic vesicle fusion complex (Syntaxin, SNAP-25, and VAMP) (Haruta et al., 1997). Through these molecular pathways, phosphorylated GAP-43 facilitates axon guidance (Dent and Meiri, 1998), axon outgrowth (Aigner et al., 1995; Korshunova et al., 2007), neurotransmission (Dekker et al., 1989b; Heemskerk et al., 1990), and synaptic plasticity (Routtenberg and Lovinger, 1985; Lovinger et al., 1986; Hulo et al., 2002). The modulation of BASP1 functions by PKC remains to be studied. In addition to PKC phosphosites, many residues of GAP-43 and BASP1 were found to be phosphorylated. To name a few, GAP-43 was phosphorylated at Serine-96 and Threonine-172 by unknown kinase(s) (Spencer et al., 1992), Serine-191 and -192 by Casein Kinase II (Apel et al., 1991), and Serine-96 by c-Jun N-terminal kinase (JNK) (Kawasaki et al., 2018; **Figure 2**). Additional phosphosites on GAP-43 (Serine-86, Threonine-95, and Threonine-172) and BASP1 (Threonine-31, Serine-40, Serine-170) were found to be sensitive to CaN (Caraveo et al., 2017; **Figure 2**). The phosphorylation of GAP-43 and BASP1 at these other residues may be of functional significance. For example, JNK phosphorylates GAP-43 in growth cone membranes, and this modification is associated with axon growth and regeneration (Kawasaki et al., 2018).

# MECHANISMS OF ACTIN CYTOSKELETON REGULATION

Regulation of the actin cytoskeleton is important for axon guidance and growth (Gomez and Letourneau, 2014; Blanquie and Bradke, 2018), endocytosis (Smythe and Ayscough, 2006), and exocytosis (Eitzen, 2003). Therefore, understanding how GAP-43 and BASP1 modulate actin dynamics provides insight into the mechanisms through which they achieve their physiological functions. To test if GAP-43 and BASP1 perform their functions through identical pathways, knockin mice expressing GAP-43 in place of BASP1 was generated (Frey et al., 2000). While these mice exhibited no gross abnormality in the brain, they showed small morphological differences in axon sprouts (Frey et al., 2000). This indicates that GAP-43 and

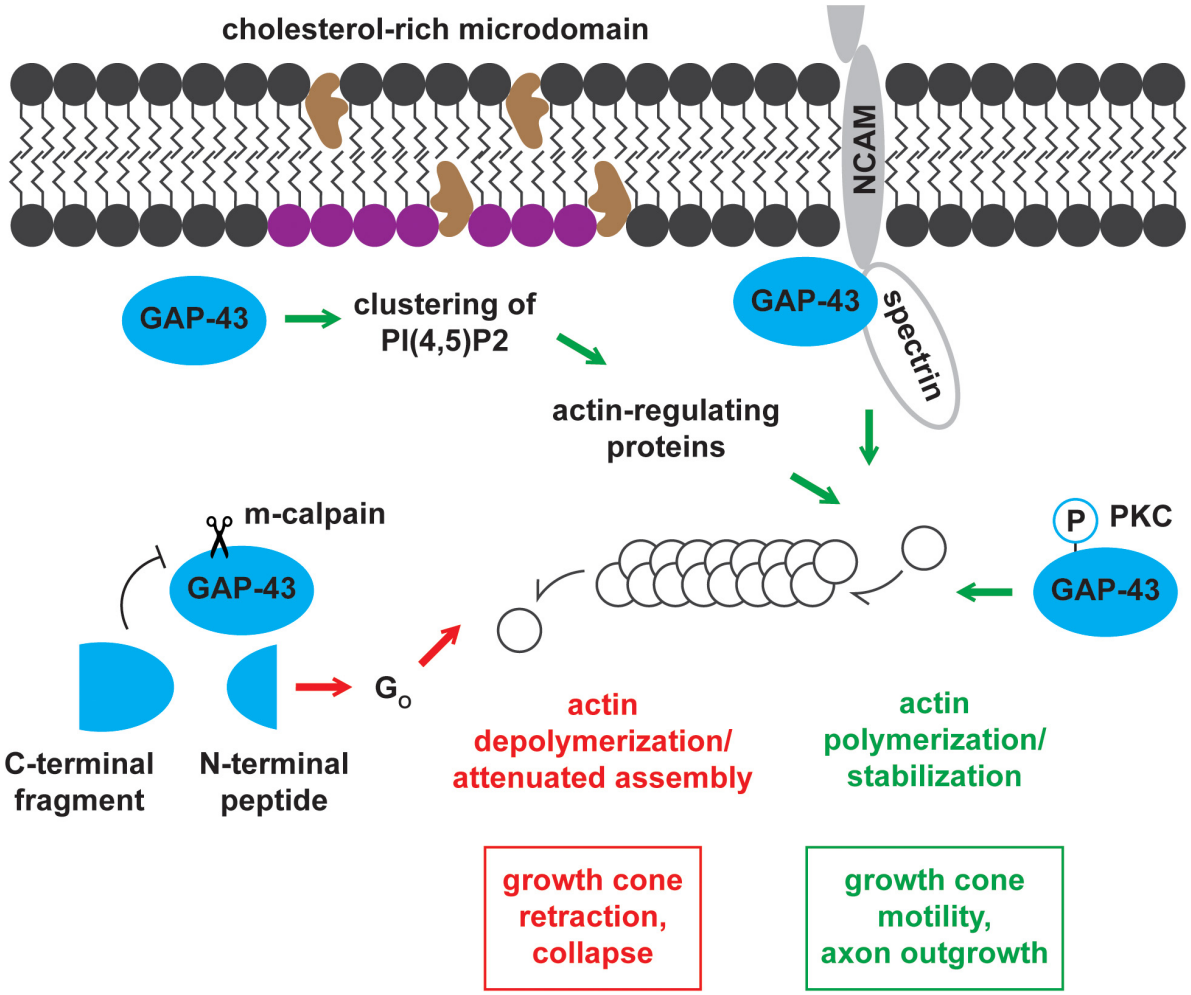


**FIGURE 3 |** Mechanisms of actin cytoskeleton regulation by GAP-43. GAP-43 positively and negatively regulates the actin cytoskeleton through multiple routes of action. GAP-43 promotes growth cone motility and axon outgrowth by (1) recruiting actin-regulating proteins by forming PI(4,5)P2 clusters, (2) interacting with NCAM and spectrin, and (3) stabilizing actin filaments in a PKC-dependent manner. Conversely, m-calpain cleavage product of GAP-43 drives growth cone retraction and collapse through the $G_o$ signaling pathway.

BASP1 act through partially redundant pathways, a concept that was reinforced by observations of phenotypic differences between GAP-43- and BASP1-induced neurite outgrowth and of synergistic axon sprouting with co-overexpression of GAP-43 and BASP1 (Caroni et al., 1997).

## Signaling Through PI(4,5)$P_2$ Clusters

Growth-associated protein-43 and BASP1 regulate actin dynamics through a shared pathway involving PI(4,5)$P_2$ (Laux et al., 2000; Caroni, 2001). In the intracellular surface of cholesterol-rich rafts, GAP-43 and BASP1 co-distribute with and promote the clustering of PI(4,5)$P_2$ (Laux et al., 2000). Concentrating PI(4,5)$P_2$ in local environments is thought to enhance the recruitment of actin-regulating proteins (Caroni, 2001). These proteins include WASP and ERM proteins known for their roles in actin polymerization and actin cytoskeleton-membrane crosslinking, respectively (Sechi and Wehland, 2000). The functions of WASP and ERM proteins contribute to growth cone motility and outgrowth (**Figure 3**).

## PKC-Dependent Modulation of Actin

Growth-associated protein-43 binds and directly regulates actin filaments in a PKC-dependent manner (He et al., 1997). Phosphorylated GAP-43 binds actin with higher affinity ($K_d$ = 161 nM) compared to the unphosphorylated form ($K_d$ = 1.2 uM) (He et al., 1997). In accordance with this enhanced binding, the cytoskeletal association of GAP-43 increases with phosphorylation (Tejero-Díez et al., 2000). Moreover, phosphorylated GAP-43 stabilizes actin filaments, thereby promoting growth cone extension and motility (He et al., 1997; **Figure 3**). On the other hand, unphosphorylated GAP-43 inhibits growth cone extension likely by serving as a barbed end-capping protein (He et al., 1997). Capping proteins significantly increase the concentration of actin monomers needed for

polymerization and attenuate actin assembly, which is critical for growth cone extension. While BASP1 may similarly regulate the actin cytoskeleton, this hypothesis remains to be tested.

## Functional Association With NCAM-180 and Spectrin

Growth-associated protein-43 has also been proposed to modulate actin dynamics through the functional association with the neural cell adhesion molecule-180 (NCAM-180) and the cytoskeletal protein spectrin (Korshunova et al., 2007; **Figure 3**). NCAMs engage in homophilic and heterophilic binding with components of other cells and the extracellular matrix (ECM) (Ditlevsen et al., 2008). These interactions, in addition to establishing cell-cell and cell-ECM adhesions, initiate intracellular signaling cascades important for neuronal development, synaptic plasticity, and regeneration (Ditlevsen et al., 2008). NCAMs directly associate with intracellular signaling molecules to activate these downstream cascades (Ditlevsen et al., 2008). NCAM-180 has been shown to mediate neurite outgrowth by interacting with spectrin (Leshchyns'ka et al., 2003), and spectrin was shown to bind GAP-43 (Riederer and Routtenberg, 1999). Based on these observations, NCAM-180, spectrin, and GAP-43 have been hypothesized to function in a complex to mediate neurite outgrowth. In support of this hypothesis, NCAM-mediated neurite outgrowth, in the presence of GAP-43, required functional NCAM-180 and spectrin (Korshunova et al., 2007). BASP1 was shown to function independently of this mechanism in PC12 cells and hippocampal neurons, where BASP1 failed to substitute the stimulation of NCAM-mediated neurite outgrowth by GAP-43 (Korshunova et al., 2008).

# PROPERTIES OF GAP-43 AND BASP1 AND THEIR LINK TO NEURODEGENERATIVE DISEASES

## Intrinsic Disorder and Phase Separation in Pathological Protein Aggregation

Growth-associated protein-43 and BASP1 are intrinsically disordered proteins (Zhang et al., 1994; Geist et al., 2013; Forsova and Zakharov, 2016). The functional significance of this property remains understudied in both physiological and pathological contexts. In many neurodegenerative diseases, intrinsically disordered proteins form soluble and fibril aggregates that are central to the pathogenesis (Chiti and Dobson, 2006). The recent discovery of liquid-liquid phase separation, which condensates disordered proteins, gained interest as a potential mechanism of pathological protein aggregation (Elbaum-Garfinkle, 2019). Furthermore, proteins forming aggregates in neurodegenerative diseases such as Tau (Wegmann et al., 2018) and Huntingtin (Peskett et al., 2018) were shown to undergo phase separation. The involvement of disordered proteins in neurodegenerative diseases questions whether GAP-43 and BASP1 also phase separate in this context, whether this process turns aberrant, and what the functional consequences are.

## Post-transcriptional Regulation in Neurodegenerative Diseases

Post-transcriptional regulation allows a rapid adjustment of the location and level of protein expression (Bronicki and Jasmin, 2013). This spatiotemporal regulation is particularly important in neurons because of their large and complex morphology (Bronicki and Jasmin, 2013). A key regulator of this process is the neuron-specific RNA-binding protein HuD (Bronicki and Jasmin, 2013). HuD post-transcriptionally regulates GAP-43 during neuritogenesis, regeneration, and learning (Anderson et al., 2001, 2003; Quattrone et al., 2001; Pascale et al., 2004). Interestingly, HuD is associated with various neurodegenerative disorders. The level of HuD was shown to be decreased in the hippocampus of Alzheimer's Disease patients (Amadio et al., 2009). This decrease correlated with diminished expression of ADAM10, a protein known to reduce the generation of pathogenic amyloid-β peptides (Amadio et al., 2009). From genetic studies, HuD was also identified as a susceptibility gene for Parkinson's Disease (Noureddine et al., 2005; DeStefano et al., 2008). Additionally, HuD was shown to aberrantly interact with FUS mutant that is causally linked to Amyotrophic Lateral Sclerosis (De Santis et al., 2019). In light of these findings, the post-transcriptional regulation of GAP-43 may be dysregulated in neurodegenerative disorders.

## PKC and CaM in Neurodegenerative Diseases

Growth-associated protein-43 and BASP1 engage in intracellular $Ca^{2+}$ signaling through PKC and CaM (Cimler et al., 1985; Apel et al., 1990; Maekawa et al., 1993). $Ca^{2+}$ signaling plays a central role in neuronal physiology, and $Ca^{2+}$ dyshomeostasis contributes to the pathogenesis of neurodegenerative disorders (Bezprozvanny, 2009). As part of $Ca^{2+}$ signaling cascades, PKC and CaM significantly impact the disease states.

Protein kinase C has a vital role in memory encoding and storage (Sun and Alkon, 2014); therefore, its involvement in Alzheimer's Disease – a major form of dementia – has been studied extensively. Few studies showed that the activity of PKC is decreased in the brains of Alzheimer's Disease patients (Wang et al., 1994; Matsushima et al., 1996), suggesting potential adverse effects of its diminished activity. In alignment with this finding, the PKC activator bryostatin reduced the production of amyloid-β peptides and premature mortality in mouse models of Alzheimer's Disease (Etcheberrigaray et al., 2004). On the other hand, whole genome-sequencing of late-onset Alzheimer's Disease patients identified gain-of-function mutations in PKC (Alfonso et al., 2016). This study demonstrated that enhanced PKC activity mediates synaptic depression induced by amyloid-β peptides (Alfonso et al., 2016). Other studies also linked PKC activation to synaptic changes such as reduced cell-surface expression of AMPA receptor (Liu et al., 2010) and dysregulated structural plasticity (Calabrese and Halpain, 2005). These findings point to the importance of balanced PKC activity in neuronal physiology. They also raise the possibility that PKC-dependent functions of GAP-43 and BASP1

affect cellular pathways whose dyshomeostasis contribute to neurodegenerative diseases.

Calmodulin connects $Ca^{2+}$ signals to cellular functions through various effector proteins (Chin and Means, 2000). These effectors include $Ca^{2+}$/CaM-dependent kinases and phosphatases like CaMKII and CaN. CaMKII and CaN critically regulate synaptic functions (Mulkey et al., 1994; Pang et al., 2010) and contribute to synaptopathy in neurodegenerative diseases (Kuchibhotla et al., 2008; Gu et al., 2009; Teravskis et al., 2018). CaM also affects pathogenic processes such as $Ca^{2+}$ dysregulation and pathogenic protein fibrillation by directly binding the plasma membrane $Ca^{2+}$ APTase (PCMA) and amyloid-β peptides (Berrocal et al., 2012; Corbacho et al., 2017). Likewise, CaM binding by GAP-43 and BASP1 may directly and indirectly affect processes involved in neurodegenerative disorders.

## FUNCTIONS OF GAP-43 AND BASP1 AND THEIR LINK TO NEURODEGENERATIVE DISEASES

Growth-associated protein-43 and BASP1 regulate the actin cytoskeleton, which in turn modulates axon outgrowth (Gomez and Letourneau, 2014; Blanquie and Bradke, 2018) and synaptic functions (Eitzen, 2003; Smythe and Ayscough, 2006). Actin dynamics are altered in neurodegenerative disorders, and this change culminates in structural defects and synaptic dysfunctions. Disruption of dendritic actin filaments were observed in *Drosophila* models of polyglutamine diseases (Lee et al., 2011). This disruption was associated with decreased dendritic complexity – an early deficit that may contribute to the pathogenesis (Lee et al., 2011). Similarly, decreased levels of synaptosomal actin filaments were detected in mouse models and patient brains of Alzheimer's Disease (Kommaddi et al., 2018). This reduction inversely correlated with dendritic spine density and behavioral performance (Kommaddi et al., 2018). Moreover, in *Drosophila*, pathogenic tau mutant and amyloid-β promoted abnormal accumulation and bundling of actin filaments, which correlated with neurotoxicity (Fulga et al., 2007).

In addition, actin binding proteins contribute to the pathogenesis of neurodegenerative disorders. For instance, the actin depolymerizing factor cofilin was found to be hyperactivated in Alzheimer's Disease (Bamburg et al., 2010). The accumulation of hyperactivated cofilin formed cofilin-actin rods that led to impaired synaptic functions and synapse loss (Bamburg et al., 2010; Cichon et al., 2012; Munsie and Truant, 2012). Conversely, the level of the actin stabilizing protein drebrin was dramatically reduced in Alzheimer's Disease (Harigaya et al., 1996; Hatanpää et al., 1999). A reduction in drebrin levels impaired neuritogenesis (Geraldo et al., 2008), resulted in synaptic dysfunctions (Kojima and Shirao, 2007), and correlated with cognitive impairment (Counts et al., 2006). These findings warrant examination of the actin regulators GAP-43 and BASP1 in neurodegenerative diseases.

## REGULATION OF GAP-43 AND BASP1 IN NEURODEGENERATIVE DISEASES

Growth-associated protein-43 and BASP1 were examined in many neurodegenerative diseases – Alzheimer's Disease (Masliah et al., 1991; De La Monte et al., 1995; Bogdanovic et al., 2000; Rekart et al., 2004; Musunuri et al., 2014; Tagawa et al., 2015), Parkinson's Disease (Caraveo et al., 2017; Saal et al., 2017; Wang et al., 2019b), Huntington's Disease (Apostol et al., 2006; Dong and Cong, 2018), Amyotrophic Lateral Sclerosis (Parhad et al., 1992; Ikemoto et al., 1999; Andrés-Benito et al., 2017), and Spinal Muscular Atrophy (Fallini et al., 2016) – through studies of human patients and cellular and animal models. Most of these studies present correlational changes in GAP-43 and BASP1 but do not address their functional implications. In the following sections, GAP-43 and BASP1 will be discussed in the context of Alzheimer's and Parkinson's Disease, two neurodegenerative diseases in which they have been studied the most.

### Alzheimer's Disease

Alzheimer's Disease (AD) is the most common neurodegenerative disorder causing dementia (Barker et al., 2002). AD is neuropathologically characterized by extracellular amyloid beta (Aβ) deposits termed amyloid plaques (Masters et al., 1985) and intracellular neurofibrillary tangles composed of the microtubule-binding protein tau (Goedert et al., 1988). While AD involves a widespread loss of neurons, it primarily affects cholinergic neurons in the basal forebrain (Whitehouse et al., 1982), noradrenergic neurons in the locus coeruleus (Bondareff et al., 1982), and pyramidal neurons in the entorhinal cortex, subiculum, and hippocampal CA1 (Hyman et al., 1984; Morrison and Hof, 2002). These vulnerable neurons have long and thin axons with sparse myelination (Braak and Del Trecidi, 2015). Such axonal properties increase the energetic demand and exposure to pathogenic species that contribute to the vulnerability in AD (Braak and Del Trecidi, 2015). Immunohistochemical studies found that GAP-43 levels were decreased in the neocortex but was preserved or even elevated in the hippocampus of AD patients (Masliah et al., 1991; De La Monte et al., 1995; Bogdanovic et al., 2000; Rekart et al., 2004). The reduction in cortical GAP-43 immunoreactivity likely reflects a profound neuron loss. The preservation or increase in hippocampal GAP-43 immunoreactivity raises the possibility that surviving neurons, by upregulating GAP-43, initiate axon outgrowth to compensate for the lost connections. Hippocampal GAP-43 immunoreactivity was observed in dystrophic neurites associated with plaques and correlated with aberrant sprouting (Masliah et al., 1991; Bogdanovic et al., 2000), which is characteristic of synaptic pathology in AD (Masliah, 1995). Based on this observation, GAP-43-associated axon outgrowth appears to be unsuccessful in establishing functional connections and seems to be contributing to the synaptic pathology instead. Examination of entorhinal fibers in amyloid precursor protein transgenic mice provides evidence that this aberrant sprouting is driven by amyloid deposition (Phinney et al., 1999). This finding highlights the importance of extrinsic

factors on the successful regenerative response and emphasizes the need for combined therapy that overcomes both extrinsic and intrinsic barriers to axon remodeling. In agreement with the immunohistochemical data, quantitative mass spectrometry detected a reduction of GAP-43 in the temporal neocortex of AD patients (Musunuri et al., 2014). The same study also measured decreased levels of BASP1 in AD patients (Musunuri et al., 2014). In addition to their changes in expression, the extent of their phosphorylation was altered in AD. The overall phosphorylation of both proteins decreased in the temporal lobe of AD patients compared to non-AD individuals (Tagawa et al., 2015). For a detailed analysis of the phosphoproteome over the course of disease progression, four mouse models of AD at early, middle, and late time points were examined with respect to control mice. This analysis identified 5 phosphosites in GAP-43 and 6 phosphosites in BASP1 (**Figure 2** shows equivalent sites in rat proteins based on sequence alignment in Clustal Omega; Tagawa et al., 2015). Phosphorylation at these sites generally increased in the middle stage of pathology and progressively decreased (Tagawa et al., 2015). Although the physiological relevance of these changes remains to be examined, this study prompts us to explore the possibility of modulating GAP-43 and BASP1 phosphorylation for therapeutic interventions in AD.

## Parkinson's Disease

Parkinson's Disease (PD) is the most common neurodegenerative movement disorder (Tysnes and Storstein, 2017). PD is neuropathologically characterized by the accumulation of α-synuclein inclusions termed Lewy bodies (Spillantini et al., 1997). In PD, dopaminergic neurons in the substantia nigra pars compacta (SNc) primarily degenerate, causing motor symptoms such as bradykinesia, rigidity, and tremor (Tysnes and Storstein, 2017). The axons of the SNc dopaminergic neurons are long, thin, and poorly myelinated (Braak et al., 2004). Additionally, they branch extensively in the striatum and form extraordinarily large numbers of synapses (Bolam and Pissadaki, 2012) with transmitter release sites numbering up to 300,000 (Matsuda et al., 2009). These axonal properties contribute to the selective vulnerability in PD (Braak et al., 2004). A transcriptome-based meta-analysis of multiple studies found that GAP-43 and BASP1 are downregulated in the brains of PD patients. This same study identified BASP1 as an important regulator of other differentially expressed genes associated with synaptic signaling. Immunoreactivity of tyrosine hydroxylase (TH), a marker for dopaminergic neurons, was reduced in the SNc and striatum of PD patients in reflection of a substantial neuron loss (Saal et al., 2017). However, in the remaining TH+ SNc dopaminergic neurons, GAP-43 protein and mRNA levels were likewise decreased. In agreement with these data, reduced GAP-43 expression has also been detected in the cerebral spinal fluid of PD patients (Sjogren et al., 2000). Further evidence implicates the involvement of GAP-43 and BASP1 in PD. In an *in vitro* scratch lesion model using α-syn mutations causing autosomal-dominant forms of PD, the study found reduced neurite regeneration and subsequent loss of dopaminergic neurons accompanied by a reduction of striatal expression of GAP-43 (Tonges et al., 2014). In one PD patient, infusion with glial cell-derived neurotrophic factor at the putamen provided benefits even after cessation of treatment (Patel et al., 2013). While these reports suggest that increasing GAP-43 expression and therefore the axonal tree would be beneficial, other groups suggest that reduction of the axonal tree, in fact, confers protection in models of PD (Pacelli et al., 2015). The apparent discrepancy between these studies can be addressed if taken into consideration that the effect in neuronal sprouting needs to be regulated. In support of this idea, one study found that modulation of the activity of GAP-43 and BASP1 through CaN can alter the degeneration of axonal trees and confer neuroprotection in a rat model of PD (Caraveo et al., 2017). This model displayed presynaptic and behavioral impairments along with hypophosphorylation at 3 CaN-sensitive sites each in GAP-43 and BASP1 (**Figure 2**; Caraveo et al., 2017). Treatment with low doses of Tacrolimus, which partially inhibits CaN, ameliorated the presynaptic and behavioral deficits in addition to rescuing phosphorylation at these sites (Caraveo et al., 2017). This correlation suggests a potential involvement of GAP-43 and BASP1 phosphorylation in PD pathogenesis. Interestingly, Tacrolimus is an FDA-approved drug currently in widespread clinical use at high doses to suppress the rejection of organs in transplant patients, a process in which CaN also plays a critical role (Tron et al., 2019). This opens the possibility that Tacrolimus could be repurposed as a potential therapy for the treatment of PD.

# CONCLUDING REMARKS

Growth-associated protein-43 and BASP1 are essential for developing axons to grow toward their correct targets and form synaptic connections during neuronal development and after neural injury. These axonal functions highly depend on their expression levels and phosphorylation status, which when modulated appropriately, can stimulate mature neurons to re-enter a growth state. This transition, which can protect and enable surviving neurons to re-establish functional connections, has been explored as a therapeutic avenue for neurodegenerative diseases. Specifically, the effects of delivering agents that upregulate GAP-43, such as BDNF, have been tested in animal models of PD (Gupta et al., 2009). BDNF treatment, although unable to revert neurodegeneration, demonstrated protective effects on remaining neurons and ameliorated behavioral impairments (Palasz et al., 2020). Several investigations into understanding the mechanism of potential therapies have identified GAP-43 as either upregulated or essential for its ameliorative effects. Levetiracetam for treatment of retinopathy (Mohammad et al., 2019) as well as for the repair of convulsant-induced cognitive impairment (Wang et al., 2019a) directly signals through the PKC/GAP-43 signaling pathway. Similarly, TGN-020 for treatment of spinal cord injury (Li et al., 2019b), and senegenin for the potential treatment for Aβ-induced neurotoxicity (Jesky and Chen, 2016), involve upregulation of GAP-43 protein levels for both neuroprotection and *in vitro* regeneration. Low GAP-43 levels in cerebrospinal fluid were associated with a poorer response to treatment of primary

progressive multiple sclerosis using fingolimod or alemtuzumab (Sandelius et al., 2019) suggesting that GAP-43 is important in mediating its therapeutic effects. In rat models of PD, treatments with Pilose antler extracts led to an increase in striatal GAP-43 protein expression and less dopaminergic SNc neuronal cell death (Li et al., 2019a). Despite the positive effects of neurotrophic factors in animal models, their short half-life, low bioavailability, and limited permeability through the blood-brain barrier (BBB) imposed challenges in their application to patients (Palasz et al., 2020). Such challenges associated with using neurotrophic factors to increase GAP-43 and BASP1 levels can be avoided by using other pharmacological agents that can cross the BBB and modulate their activities, for instance, via phosphorylation. A potential candidate is the FDA-approved CaN inhibitor Tacrolimus. In a rat model of PD, tacrolimus was shown to cross the BBB, alter phosphorylation of GAP-43 and BASP1, and confer neuroprotection at doses 10-fold lower than the standard immunosuppressive dose (Caraveo et al., 2017). At sub-immunosuppressive doses, the risk of secondary effects, such as opportunistic infections, posterior reversible leukoencephalopathy, and seizures typically achieved at clinical doses would be avoided. Moreover, these lower Tacrolimus doses would finely tune GAP-43 and BASP1 to drive sufficient, but not hyperactive, axonal sprouting in a spatially and temporally confined manner. This regulation is necessary to promote regeneration specifically in the affected neuronal populations at the right time window while preventing potential complications arising from hyperconnectivity. Additionally, external inhibitory factors in the central nervous system (Fournier and Strittmatter, 2001) and other disease-associated factors (Phinney et al., 1999) need to be prevented from blocking axon growth or driving the formation of aberrant connections. Moreover, determining the stages of pathogenesis at which regeneration of remaining axons can be protective will be important. Further exploration of these areas will facilitate the development of GAP-43- and BASP1-targeting therapies for neurodegenerative diseases.

## AUTHOR CONTRIBUTIONS

DC contributed by writing and revising the entire review, as well as generating figures. AS contributed to writing the section "Involvement in Neural Injury Response" and building **Figure 1**. GC conceived the review, contributed to the concluding remarks, and edited the review. All authors contributed to the article and approved the submitted version.

## FUNDING

This review manuscript was supported by the Parkinson's Foundation grant PF-JFA-1949 and the National Institute of Mental Health grant 2T32MH067564.

## ACKNOWLEDGMENTS

We would like to thank the members of the laboratory for constructive feedback.

## REFERENCES

Acarin, L., González, B., and Castellano, B. (2000). Neuronal, astroglial and microglial cytokine expression after an excitotoxic lesion in the immature rat brain. *Eur. J. Neurosci.* 12, 3505–3520. doi: 10.1046/j.1460-9568.2000.00226.x

Aigner, L., Arber, S., Kapfhammer, J. P., Laux, T., Schneider, C., Botteri, F., et al. (1995). Overexpression of the neural growth-associated protein GAP-43 induces nerve sprouting in the adult nervous system of transgenic mice. *Cell* 83, 269–278. doi: 10.1016/0092-8674(95)90168-x

Aigner, L., and Caroni, P. (1995). Absence of persistent spreading, branching, and adhesion in GAP-43-depleted growth cones. *J. Cell Biol.* 128, 647–660. doi: 10.1083/jcb.128.4.647

Alexander, K. A., Cimler, B. M., Meier, K. E., and Storm, D. R. (1987). Regulation of calmodulin binding to P-57. A neurospecific calmodulin binding protein. *J. Biol. Chem.* 262, 6108–6113.

Alfonso, S. I., Callender, J. A., Hooli, B., Antal, C. E., Mullin, K., Sherman, M. A., et al. (2016). Gain-of-function mutations in protein kinase Cα (PKCα) may promote synaptic defects in Alzheimer's disease. *Sci. Signal.* 9:ra47. doi: 10.1126/scisignal.aaf6209

Allegra Mascaro, A. L., Cesare, P., Sacconi, L., Grasselli, G., Mandolesi, G., Maco, B., et al. (2013). *In vivo* single branch axotomy induces GAP-43-dependent sprouting and synaptic remodeling in cerebellar cortex. *Proc. Natl. Acad. Sci. U.S.A.* 110, 10824–10829. doi: 10.1073/pnas.1219256110

Amadio, M., Pascale, A., Wang, J., Ho, L., Quattrone, A., Gandy, S., et al. (2009). nELAV proteins alteration in Alzheimer's disease brain: a novel putative target for amyloid-beta reverberating on AbetaPP processing. *J. Alzheimers Dis.* 16, 409–419. doi: 10.3233/jad-2009-0967

Anderson, K. D., Merhege, M. A., Morin, M., Bolognani, F., and Perrone-Bizzozero, N. I. (2003). Increased expression and localization of the RNA-binding protein HuD and GAP-43 mRNA to cytoplasmic granules in DRG neurons during nerve regeneration. *Exp. Neurol.* 183, 100–108. doi: 10.1016/s0014-4886(03)00103-1

Anderson, K. D., Sengupta, J., Morin, M., Neve, R. L., Valenzuela, C. F., and Perrone-Bizzozero, N. I. (2001). Overexpression of HuD accelerates neurite outgrowth and increases GAP-43 mRNA expression in cortical neurons and retinoic acid-induced embryonic stem cells *in vitro*. *Exp. Neurol.* 168, 250–258. doi: 10.1006/exnr.2000.7599

Andreasen, T. J., Luetje, C. W., Heideman, W., and Storm, D. R. (1983). Purification of a novel calmodulin binding protein from bovine cerebral cortex membranes. *Biochemistry* 22, 4615–4618. doi: 10.1021/bi00289a001

Andrés-Benito, P., Moreno, J., Aso, E., Povedano, M., and Ferrer, I. (2017). Amyotrophic lateral sclerosis, gene deregulation in the anterior horn of the spinal cord and frontal cortex area 8: implications in frontotemporal lobar degeneration. *Aging* 9, 823–851. doi: 10.18632/aging.101195

Apel, E. D., Byford, M. F., Au, D., Walsh, K. A., and Storm, D. R. (1990). Identification of the protein kinase C phosphorylation site in neuromodulin. *Biochemistry* 29, 2330–2335. doi: 10.1021/bi00461a017

Apel, E. D., Litchfield, D. W., Clark, R. H., Krebs, E. G., and Storm, D. R. (1991). Phosphorylation of neuromodulin (GAP-43) by casein kinase II. Identification of phosphorylation sites and regulation by calmodulin. *J. Biol. Chem.* 266, 10544–10551.

Apostol, B. L., Illes, K., Pallos, J., Bodai, L., Wu, J., Strand, A., et al. (2006). Mutant huntingtin alters MAPK signaling pathways in PC12 and striatal cells: ERK1/2 protects against mutant huntingtin-associated toxicity. *Hum. Mol. Genet.* 15, 273–285. doi: 10.1093/hmg/ddi443

Aumiller, W. M., and Keating, C. D. (2016). Phosphorylation-mediated RNA/peptide complex coacervation as a model for intracellular liquid organelles. *Nat. Chem.* 8, 129–137. doi: 10.1038/nchem.2414

Bähler, M., and Rhoads, A. (2002). Calmodulin signaling via the IQ motif. *FEBS Lett.* 513, 107–113. doi: 10.1016/s0014-5793(01)03239-2

Bamburg, J. R., Bernstein, B. W., Davis, R. C., Flynn, K. C., Goldsbury, C., Jensen, J. R., et al. (2010). ADF/Cofilin-actin rods in neurodegenerative diseases. *Curr. Alzheimer Res.* 7, 241–250. doi: 10.2174/156720510791050902

Barker, W. W., Luis, C. A., Kashuba, A., Luis, M., Harwood, D. G., Loewenstein, D., et al. (2002). Relative frequencies of Alzheimer disease, Lewy body, vascular and frontotemporal dementia, and hippocampal sclerosis in the State of Florida Brain Bank. *Alzheimer Dis. Assoc. Disord.* 16, 203–212. doi: 10.1097/00002093-200210000-00001

Barnes, J. A., and Gomes, A. V. (1995). PEST sequences in calmodulin-binding proteins. *Mol. Cell. Biochem.* 149-150, 17–27. doi: 10.1007/978-1-4615-2015-3_2

Benowitz, L. I., Apostolides, P. J., Perrone-Bizzozero, N., Finklestein, S. P., and Zwiers, H. (1988). Anatomical distribution of the growth-associated protein GAP-43/B-50 in the adult rat brain. *J. Neurosci.* 8, 339–352. doi: 10.1523/jneurosci.08-01-00339.1988

Berrocal, M., Sepulveda, M. R., Vazquez-Hernandez, M., and Mata, A. M. (2012). Calmodulin antagonizes amyloid-β peptides-mediated inhibition of brain plasma membrane Ca(2+)-ATPase. *Biochim. Biophys. Acta* 1822, 961–969. doi: 10.1016/j.bbadis.2012.02.013

Bezprozvanny, I. (2009). Calcium signaling and neurodegenerative diseases. *Trends Mol. Med.* 15, 89–100. doi: 10.1016/j.molmed.2009.01.001

Bird, C. W., Gardiner, A. S., Bolognani, F., Tanner, D. C., Chen, C.-Y., Lin, W.-J., et al. (2013). KSRP modulation of GAP-43 mRNA stability restricts axonal outgrowth in embryonic hippocampal neurons. *PLoS One* 8:e79255. doi: 10.1371/journal.pone.0079255

Blanquie, O., and Bradke, F. (2018). Cytoskeleton dynamics in axon regeneration. *Curr. Opin. Neurobiol.* 51, 60–69. doi: 10.1016/j.conb.2018.02.024

Bogdanovic, N., Davidsson, P., Volkmann, I., Winblad, B., and Blennow, K. (2000). Growth-associated protein GAP-43 in the frontal cortex and in the hippocampus in Alzheimer's disease: an immunohistochemical and quantitative study. *J. Neural Transm.* 107, 463–478. doi: 10.1007/s007020070088

Bolam, J. P., and Pissadaki, E. K. (2012). Living on the edge with too many mouths to feed: why dopamine neurons die. *Mov. Disord.* 27, 1478–1483. doi: 10.1002/mds.25135

Bolognani, F., Tanner, D. C., Merhege, M., Deschenes-Furry, J., Jasmin, B., and Perrone-Bizzozero, N. I. (2006). *In vivo* post-transcriptional regulation of GAP-43 mRNA by overexpression of the RNA-binding protein HuD. *J. Neurochem.* 96, 790–801. doi: 10.1111/j.1471-4159.2005.03607.x

Bomze, H. M., Bulsara, K. R., Iskandar, B. J., Caroni, P., and Skene, J. H. (2001). Spinal axon regeneration evoked by replacing two growth cone proteins in adult neurons. *Nat. Neurosci.* 4, 38–43. doi: 10.1038/82881

Bondareff, W., Mountjoy, C. Q., and Roth, M. (1982). Loss of neurons of origin of the adrenergic projection to cerebral cortex (nucleus locus ceruleus) in senile dementia. *Neurology* 32, 164–168. doi: 10.1212/wnl.32.2.164

Braak, H., and Del Tredici, K. (2015). Neuroanatomy and pathology of sporadic Alzheimer's disease. *Adv. Anat. Embryol. Cell Biol.* 215, 1–162. doi: 10.1007/978-3-540-79850-7_1

Braak, H., Ghebremedhin, E., Rüb, U., Bratzke, H., and Del Tredici, K. (2004). Stages in the development of Parkinson's disease-related pathology. *Cell Tissue Res.* 318, 121–134. doi: 10.1007/s00441-004-0956-9

Bronicki, L. M., and Jasmin, B. J. (2013). Emerging complexity of the HuD/ELAVl4 gene; implications for neuronal development, function, and dysfunction. *RNA* 19, 1019–1037. doi: 10.1261/rna.039164.113

Buffo, A., Holtmaat, A. J., Savio, T., Verbeek, J. S., Oberdick, J., Oestreicher, A. B., et al. (1997). Targeted overexpression of the neurite growth-associated protein B-50/GAP-43 in cerebellar Purkinje cells induces sprouting after axotomy but not axon regeneration into growth-permissive transplants. *J. Neurosci.* 17, 8778–8791. doi: 10.1523/jneurosci.17-22-08778.1997

Bullock, R., Zauner, A., Woodward, J. J., Myseros, J., Choi, S. C., Ward, J. D., et al. (1998). Factors affecting excitatory amino acid release following severe human head injury. *J. Neurosurg.* 89, 507–518. doi: 10.3171/jns.1998.89.4.0507

Calabrese, B., and Halpain, S. (2005). Essential role for the PKC target MARCKS in maintaining dendritic spine morphology. *Neuron* 48, 77–90. doi: 10.1016/j.neuron.2005.08.027

Caraveo, G., Soste, M., Cappelleti, V., Fanning, S., Van Rossum, D. B., Whitesell, L., et al. (2017). FKBP12 contributes to α-synuclein toxicity by regulating the calcineurin-dependent phosphoproteome. *Proc. Natl. Acad. Sci. U.S.A.* 114, E11313–E11322.

Carmichael, S. T., Archibeque, I., Luke, L., Nolan, T., Momiy, J., and Li, S. (2005). Growth-associated gene expression after stroke: evidence for a growth-promoting region in peri-infarct cortex. *Exp. Neurol.* 193, 291–311. doi: 10.1016/j.expneurol.2005.01.004

Caroni, P. (2001). New EMBO member's review: actin cytoskeleton regulation through modulation of PI(4,5)P(2) rafts. *EMBO J.* 20, 4332–4336. doi: 10.1093/emboj/20.16.4332

Caroni, P., Aigner, L., and Schneider, C. (1997). Intrinsic neuronal determinants locally regulate extrasynaptic and synaptic growth at the adult neuromuscular junction. *J. Cell Biol.* 136, 679–692. doi: 10.1083/jcb.136.3.679

Chen, H., Lin, W., Zhang, Y., Lin, L., Chen, J., Zeng, Y., et al. (2016). IL-10 promotes neurite outgrowth and synapse formation in cultured cortical neurons after the oxygen-glucose deprivation via JAK1/STAT3 pathway. *Sci. Rep.* 6, 30459–30416.

Cheng, M. Y., Wang, E. H., Woodson, W. J., Wang, S., Sun, G., Lee, A. G., et al. (2014). Optogenetic neuronal stimulation promotes functional recovery after stroke. *Proc. Natl. Acad. Sci. U.S.A.* 111, 12913–12918. doi: 10.1073/pnas.1404109111

Chiaramello, A., Neuman, T., Peavy, D. R., and Zuber, M. X. (1996). The GAP-43 gene is a direct downstream target of the basic helix-loop-helix transcription factors. *J. Biol. Chem.* 271, 22035–22043. doi: 10.1074/jbc.271.36.22035

Chiaretti, A., Barone, G., Riccardi, R., Antonelli, A., Pezzotti, P., Genovese, O., et al. (2009). NGF, DCX, and NSE upregulation correlates with severity and outcome of head trauma in children. *Neurology* 72, 609–616. doi: 10.1212/01.wnl.0000342462.51073.06

Chin, D., and Means, A. R. (2000). Calmodulin: a prototypical calcium sensor. *Trends Cell Biol.* 10, 322–328. doi: 10.1016/s0962-8924(00)01800-6

Chiti, F., and Dobson, C. M. (2006). Protein misfolding, functional amyloid, and human disease. *Annu. Rev. Biochem.* 75, 333–366. doi: 10.1146/annurev.biochem.75.101304.123901

Chung, S., Eckrich, M., Perrone-Bizzozero, N., Kohn, D. T., and Furneaux, H. (1997). The Elav-like proteins bind to a conserved regulatory element in the 3′-untranslated region of GAP-43 mRNA. *J. Biol. Chem.* 272, 6593–6598. doi: 10.1074/jbc.272.10.6593

Cichon, J., Sun, C., Chen, B., Jiang, M., Chen, X. A., Sun, Y., et al. (2012). Cofilin aggregation blocks intracellular trafficking and induces synaptic loss in hippocampal neurons. *J. Biol. Chem.* 287, 3919–3929. doi: 10.1074/jbc.m111.301911

Cimler, B. M., Andreasen, T. J., Andreasen, K. I., and Storm, D. R. (1985). P-57 is a neural specific calmodulin-binding protein. *J. Biol. Chem.* 260, 10784–10788.

Corbacho, I., Berrocal, M., Török, K., Mata, A. M., and Gutierrez-Merino, C. (2017). High affinity binding of amyloid β-peptide to calmodulin: structural and functional implications. *Biochem. Biophys. Res. Commun.* 486, 992–997. doi: 10.1016/j.bbrc.2017.03.151

Costigan, M., Befort, K., Karchewski, L., Griffin, R. S., D'urso, D., Allchorne, A., et al. (2002). Replicate high-density rat genome oligonucleotide microarrays reveal hundreds of regulated genes in the dorsal root ganglion after peripheral nerve injury. *BMC Neurosci.* 3:16. doi: 10.1186/1471-2202-3-16

Counts, S. E., Nadeem, M., Lad, S. P., Wuu, J., and Mufson, E. J. (2006). Differential expression of synaptic proteins in the frontal and temporal cortex of elderly subjects with mild cognitive impairment. *J. Neuropathol. Exp. Neurol.* 65, 592–601. doi: 10.1097/00005072-200606000-00007

Csuka, E., Morganti-Kossmann, M. C., Lenzlinger, P. M., Joller, H., Trentz, O., and Kossmann, T. (1999). IL-10 levels in cerebrospinal fluid and serum of patients with severe traumatic brain injury: relationship to IL-6, TNF-alpha, TGF-beta1 and blood-brain barrier function. *J. Neuroimmunol.* 101, 211–221. doi: 10.1016/s0165-5728(99)00148-4

de Groen, P. C., Eggen, B. J., Gispen, W. H., Schotman, P., and Schrama, L. H. (1995). Cloning and promoter analysis of the human B-50/GAP-43 gene. *J. Mol. Neurosci.* 6, 109–119. doi: 10.1007/bf02736770

De La Monte, S. M., Federoff, H. J., Ng, S. C., Grabczyk, E., and Fishman, M. C. (1989). GAP-43 gene expression during development: persistence in a distinctive set of neurons in the mature central nervous system. *Brain Res. Dev. Brain Res.* 46, 161–168. doi: 10.1016/0165-3806(89)90279-4

De La Monte, S. M., Ng, S. C., and Hsu, D. W. (1995). Aberrant GAP-43 gene expression in Alzheimer's disease. *Am. J. Pathol.* 147, 934–946.

De Santis, R., Alfano, V., De Turris, V., Colantoni, A., Santini, L., Garone, M. G., et al. (2019). Mutant FUS and ELAVL4 (HuD) aberrant crosstalk in

amyotrophic lateral sclerosis. *Cell Rep.* 27:3818. doi: 10.1016/j.celrep.2019.05.085

Dekker, L. V., De Graan, P. N., Oestreicher, A. B., Versteeg, D. H., and Gispen, W. H. (1989a). Inhibition of noradrenaline release by antibodies to B-50 (GAP-43). *Nature* 342, 74–76. doi: 10.1038/342074a0

Dekker, L. V., De Graan, P. N., Versteeg, D. H., Oestreicher, A. B., and Gispen, W. H. (1989b). Phosphorylation of B-50 (GAP43) is correlated with neurotransmitter release in rat hippocampal slices. *J. Neurochem.* 52, 24–30. doi: 10.1111/j.1471-4159.1989.tb10893.x

DeKosky, S. T., Goss, J. R., Miller, P. D., Styren, S. D., Kochanek, P. M., and Marion, D. (1994). Upregulation of nerve growth factor following cortical trauma. *Exp. Neurol.* 130, 173–177. doi: 10.1006/exnr.1994.1196

Dennis, D. J., Han, S., and Schuurmans, C. (2019). bHLH transcription factors in neural development, disease, and reprogramming. *Brain Res.* 1705, 48–65. doi: 10.1016/j.brainres.2018.03.013

Dent, E. W., and Meiri, K. F. (1998). Distribution of phosphorylated GAP-43 (neuromodulin) in growth cones directly reflects growth cone behavior. *J. Neurobiol.* 35, 287–299. doi: 10.1002/(sici)1097-4695(19980605)35:3<287::aid-neu6>3.0.co;2-v

DeStefano, A. L., Latourelle, J., Lew, M. F., Suchowersky, O., Klein, C., Golbe, L. I., et al. (2008). Replication of association between ELAVL4 and Parkinson disease: the GenePD study. *Hum. Genet.* 124, 95–99. doi: 10.1007/s00439-008-0526-4

Ditlevsen, D. K., Povlsen, G. K., Berezin, V., and Bock, E. (2008). NCAM-induced intracellular signaling revisited. *J. Neurosci. Res.* 86, 727–743. doi: 10.1002/jnr.21551

Dong, X., and Cong, S. (2018). Identification of differentially expressed genes and regulatory relationships in Huntington's disease by bioinformatics analysis. *Mol. Med. Rep.* 17, 4317–4326.

Edmonds, B. T., Moomaw, C. R., Hsu, J. T., Slaughter, C., and Ellis, L. (1990). The p38 and p34 polypeptides of growth cone particle membranes are the alpha- and beta-subunits of G proteins. *Brain Res. Dev. Brain Res.* 56, 131–136. doi: 10.1016/0165-3806(90)90172-u

Eggen, B. J., Nielander, H. B., Rensen-De Leeuw, M. G., Schotman, P., Gispen, W. H., and Schrama, L. H. (1994). Identification of two promoter regions in the rat B-50/GAP-43 gene. *Brain Res. Mol. Brain Res.* 23, 221–234. doi: 10.1016/0169-328x(94)90229-1

Eitzen, G. (2003). Actin remodeling to facilitate membrane fusion. *Biochim. Biophys. Acta* 1641, 175–181. doi: 10.1016/s0167-4889(03)00087-9

Elbaum-Garfinkle, S. (2019). Matter over mind: liquid phase separation and neurodegeneration. *J. Biol. Chem.* 294, 7160–7168. doi: 10.1074/jbc.rev118.001188

Etcheberrigaray, R., Tan, M., Dewachter, I., Kuipéri, C., Van Der Auwera, I., Wera, S., et al. (2004). Therapeutic effects of PKC activators in Alzheimer's disease transgenic mice. *Proc. Natl. Acad. Sci. U.S.A.* 101, 11141–11146. doi: 10.1073/pnas.0403921101

Fallini, C., Donlin-Asp, P. G., Rouanet, J. P., Bassell, G. J., and Rossoll, W. (2016). Deficiency of the survival of motor neuron protein impairs mRNA localization and local translation in the growth cone of motor neurons. *J. Neurosci.* 36, 3811–3820. doi: 10.1523/jneurosci.2396-15.2016

Filbin, M. T. (2003). Myelin-associated inhibitors of axonal regeneration in the adult mammalian CNS. *Nat. Rev. Neurosci.* 4, 703–713. doi: 10.1038/nrn1195

Forsova, O. S., and Zakharov, V. V. (2016). High-order oligomers of intrinsically disordered brain proteins BASP1 and GAP-43 preserve the structural disorder. *FEBS J.* 283, 1550–1569. doi: 10.1111/febs.13692

Fournier, A. E., and Strittmatter, S. M. (2001). Repulsive factors and axon regeneration in the CNS. *Curr. Opin. Neurobiol.* 11, 89–94. doi: 10.1016/s0959-4388(00)00178-1

Frey, D., Laux, T., Xu, L., Schneider, C., and Caroni, P. (2000). Shared and unique roles of CAP23 and GAP43 in actin regulation, neurite outgrowth, and anatomical plasticity. *J. Cell Biol.* 149, 1443–1454. doi: 10.1083/jcb.149.7.1443

Fulga, T. A., Elson-Schwab, I., Khurana, V., Steinhilb, M. L., Spires, T. L., Hyman, B. T., et al. (2007). Abnormal bundling and accumulation of F-actin mediates tau-induced neuronal degeneration *in vivo*. *Nat. Cell Biol.* 9, 139–148. doi: 10.1038/ncb1528

Gamby, C., Waage, M. C., Allen, R. G., and Baizer, L. (1996). Analysis of the role of calmodulin binding and sequestration in neuromodulin (GAP-43) function. *J. Biol. Chem.* 271, 26698–26705. doi: 10.1074/jbc.271.43.26698

Gauthier-Kemper, A., Igaev, M., Sündermann, F., Janning, D., Brühmann, J., Moschner, K., et al. (2014). Interplay between phosphorylation and palmitoylation mediates plasma membrane targeting and sorting of GAP43. *Mol. Biol. Cell* 25, 3284–3299. doi: 10.1091/mbc.e13-12-0737

Geist, L., Zawadzka-Kazimierczuk, A., Saxena, S., Żerko, S., Koźmiński, W., and Konrat, R. (2013). $^{1}$H,$^{13}$C and $^{15}$N resonance assignments of human BASP1. *Biomol. NMR Assign.* 7, 315–319.

Geraldo, S., Khanzada, U. K., Parsons, M., Chilton, J. K., and Gordon-Weeks, P. R. (2008). Targeting of the F-actin-binding protein drebrin by the microtubule plus-tip protein EB3 is required for neuritogenesis. *Nat. Cell Biol.* 10, 1181–1189. doi: 10.1038/ncb1778

Goedert, M., Wischik, C. M., Crowther, R. A., Walker, J. E., and Klug, A. (1988). Cloning and sequencing of the cDNA encoding a core protein of the paired helical filament of Alzheimer disease: identification as the microtubule-associated protein tau. *Proc. Natl. Acad. Sci. U.S.A.* 85, 4051–4055. doi: 10.1073/pnas.85.11.4051

Gomez, T. M., and Letourneau, P. C. (2014). Actin dynamics in growth cone motility and navigation. *J. Neurochem.* 129, 221–234. doi: 10.1111/jnc.12506

Grasselli, G., Mandolesi, G., Strata, P., and Cesare, P. (2011). Impaired sprouting and axonal atrophy in cerebellar climbing fibres following *in vivo* silencing of the growth-associated protein GAP-43. *PLoS One* 6:e20791. doi: 10.1371/journal.pone.0020791

Grasselli, G., and Strata, P. (2013). Structural plasticity of climbing fibers and the growth-associated protein GAP-43. *Front. Neural Circuits* 7:25. doi: 10.3389/fncir.2013.00025

Gu, Z., Liu, W., and Yan, Z. (2009). {beta}-Amyloid impairs AMPA receptor trafficking and function by reducing Ca2+/calmodulin-dependent protein kinase II synaptic distribution. *J. Biol. Chem.* 284, 10639–10649. doi: 10.1074/jbc.m806508200

Gudasheva, T. A., Povarnina, P. Y., Volkova, A. A., Kruglov, S. V., Antipova, T. A., and Seredenin, S. B. (2019). A nerve growth factor dipeptide mimetic stimulates neurogenesis and synaptogenesis in the hippocampus and striatum of adult rats with focal cerebral ischemia. *Acta Nat.* 11, 31–37. doi: 10.32607/20758251-2019-11-3-31-37

Gupta, S. K., Mishra, R., Kusum, S., Spedding, M., Meiri, K. F., Gressens, P., et al. (2009). GAP-43 is essential for the neurotrophic effects of BDNF and positive AMPA receptor modulator S18986. *Cell Death Differ.* 16, 624–637. doi: 10.1038/cdd.2008.188

Gwag, B. J., Sessler, F. M., Robine, V., and Springer, J. E. (1997). Endogenous glutamate levels regulate nerve growth factor mRNA expression in the rat dentate gyrus. *Mol. Cells* 7, 425–430.

Han, M.-H., Jiao, S., Jia, J.-M., Chen, Y., Chen, C. Y., Gucek, M., et al. (2013). The novel caspase-3 substrate Gap43 is involved in AMPA receptor endocytosis and long-term depression. *Mol. Cell. Proteomics* 12, 3719–3731. doi: 10.1074/mcp.m113.030676

Harigaya, Y., Shoji, M., Shirao, T., and Hirai, S. (1996). Disappearance of actin-binding protein, drebrin, from hippocampal synapses in Alzheimer's disease. *J. Neurosci. Res.* 43, 87–92. doi: 10.1002/jnr.490430111

Hartl, M., Nist, A., Khan, M. I., Valovka, T., and Bister, K. (2009). Inhibition of Myc-induced cell transformation by brain acid-soluble protein 1 (BASP1). *Proc. Natl. Acad. Sci. U.S.A.* 106, 5604–5609. doi: 10.1073/pnas.0812101106

Haruta, T., Takami, N., Ohmura, M., Misumi, Y., and Ikehara, Y. (1997). Ca2+-dependent interaction of the growth-associated protein GAP-43 with the synaptic core complex. *Biochem. J.* 325(Pt 2), 455–463. doi: 10.1042/bj3250455

Hatanpää, K., Isaacs, K. R., Shirao, T., Brady, D. R., and Rapoport, S. I. (1999). Loss of proteins regulating synaptic plasticity in normal aging of the human brain and in Alzheimer disease. *J. Neuropathol. Exp. Neurol.* 58, 637–643. doi: 10.1097/00005072-199906000-00008

Haynes, C., Oldfield, C. J., Ji, F., Klitgord, N., Cusick, M. E., Radivojac, P., et al. (2006). Intrinsic disorder is a common feature of hub proteins from four eukaryotic interactomes. *PLoS Comput. Biol.* 2:e100. doi: 10.1371/journal.pcbi.0020100

He, Q., Dent, E. W., and Meiri, K. F. (1997). Modulation of actin filament behavior by GAP-43 (neuromodulin) is dependent on the phosphorylation status of serine 41, the protein kinase C site. *J. Neurosci.* 17, 3515–3524. doi: 10.1523/jneurosci.17-10-03515.1997

Heemskerk, F. M., Schrama, L. H., Gianotti, C., Spierenburg, H., Versteeg, D. H., De Graan, P. N., et al. (1990). 4-Aminopyridine stimulates B-50 (GAP43)

phosphorylation and [3H]noradrenaline release in rat hippocampal slices. *J. Neurochem.* 54, 863–869. doi: 10.1111/j.1471-4159.1990.tb02331.x

Hens, J. J., Ghijsen, W. E., Weller, U., Spierenburg, H. A., Boomsma, F., Oestreicher, A. B., et al. (1998). Anti-B-50 (GAP-43) antibodies decrease exocytosis of glutamate in permeated synaptosomes. *Eur. J. Pharmacol.* 363, 229–240. doi: 10.1016/s0014-2999(98)00835-8

Hess, D. T., Patterson, S. I., Smith, D. S., and Skene, J. H. (1993). Neuronal growth cone collapse and inhibition of protein fatty acylation by nitric oxide. *Nature* 366, 562–565. doi: 10.1038/366562a0

Hulo, S., Alberi, S., Laux, T., Muller, D., and Caroni, P. (2002). A point mutant of GAP-43 induces enhanced short-term and long-term hippocampal plasticity. *Eur. J. Neurosci.* 15, 1976–1982. doi: 10.1046/j.1460-9568.2002.02026.x

Hyman, B. T., Van Hoesen, G. W., Damasio, A. R., and Barnes, C. L. (1984). Alzheimer's disease: cell-specific pathology isolates the hippocampal formation. *Science* 225, 1168–1170. doi: 10.1126/science.6474172

Ikemoto, A., Hirano, A., and Akiguchi, I. (1999). Increased expression of growth-associated protein 43 on the surface of the anterior horn cells in amyotrophic lateral sclerosis. *Acta Neuropathol.* 98, 367–373. doi: 10.1007/s004010051096

Jacobson, R. D., Virág, I., and Skene, J. H. (1986). A protein associated with axon growth, GAP-43, is widely distributed and developmentally regulated in rat CNS. *J. Neurosci.* 6, 1843–1855. doi: 10.1523/jneurosci.06-06-01843.1986

Jesky, R., and Chen, H. (2016). The neuritogenic and neuroprotective potential of senegenin against Aβ-induced neurotoxicity in PC 12 cells. *BMC Complement. Altern. Med.* 16:26. doi: 10.1186/s12906-016-1006-3

Karns, L. R., Ng, S. C., Freeman, J. A., and Fishman, M. C. (1987). Cloning of complementary DNA for GAP-43, a neuronal growth-related protein. *Science* 236, 597–600. doi: 10.1126/science.2437653

Kawamata, T., Ren, J., Cha, J. H., and Finklestein, S. P. (1999). Intracisternal antisense oligonucleotide to growth associated protein-43 blocks the recovery-promoting effects of basic fibroblast growth factor after focal stroke. *Exp. Neurol.* 158, 89–96. doi: 10.1006/exnr.1999.7101

Kawasaki, A., Okada, M., Tamada, A., Okuda, S., Nozumi, M., Ito, Y., et al. (2018). Growth cone phosphoproteomics reveals that GAP-43 Phosphorylated by JNK is a marker of axon growth and regeneration. *iScience* 4, 190–203. doi: 10.1016/j.isci.2018.05.019

Kohn, D. T., Tsai, K. C., Cansino, V. V., Neve, R. L., and Perrone-Bizzozero, N. I. (1996). Role of highly conserved pyrimidine-rich sequences in the 3′ untranslated region of the GAP-43 mRNA in mRNA stability and RNA-protein interactions. *Brain Res. Mol. Brain Res.* 36, 240–250. doi: 10.1016/0169-328x(95)00239-o

Kojima, N., and Shirao, T. (2007). Synaptic dysfunction and disruption of postsynaptic drebrin-actin complex: a study of neurological disorders accompanied by cognitive deficits. *Neurosci. Res.* 58, 1–5. doi: 10.1016/j.neures.2007.02.003

Kommaddi, R. P., Das, D., Karunakaran, S., Nanguneri, S., Bapat, D., Ray, A., et al. (2018). Aβ mediates F-actin disassembly in dendritic spines leading to cognitive deficits in Alzheimer's disease. *J. Neurosci.* 38, 1085–1099. doi: 10.1523/jneurosci.2127-17.2017

Korshunova, I., Caroni, P., Kolkova, K., Berezin, V., Bock, E., and Walmod, P. S. (2008). Characterization of BASP1-mediated neurite outgrowth. *J. Neurosci. Res.* 86, 2201–2213. doi: 10.1002/jnr.21678

Korshunova, I., Novitskaya, V., Kiryushko, D., Pedersen, N., Kolkova, K., Kropotova, E., et al. (2007). GAP-43 regulates NCAM-180-mediated neurite outgrowth. *J. Neurochem.* 100, 1599–1612.

Koseki, H., Donegá, M., Lam, B. Y., Petrova, V., Van Erp, S., Yeo, G. S., et al. (2017). Selective rab11 transport and the intrinsic regenerative ability of CNS axons. *eLife* 6:e26956.

Kossmann, T., Hans, V., Imhof, H. G., Trentz, O., and Morganti-Kossmann, M. C. (1996). Interleukin-6 released in human cerebrospinal fluid following traumatic brain injury may trigger nerve growth factor production in astrocytes. *Brain Res.* 713, 143–152. doi: 10.1016/0006-8993(95)01501-9

Kossmann, T., Hans, V. H., Imhof, H. G., Stocker, R., Grob, P., Trentz, O., et al. (1995). Intrathecal and serum interleukin-6 and the acute-phase response in patients with severe traumatic brain injuries. *Shock* 4, 311–317. doi: 10.1097/00024382-199511000-00001

Kuchibhotla, K. V., Goldman, S. T., Lattarulo, C. R., Wu, H.-Y., Hyman, B. T., and Bacskai, B. J. (2008). Abeta plaques lead to aberrant regulation of calcium homeostasis *in vivo* resulting in structural and functional disruption of neuronal networks. *Neuron* 59, 214–225. doi: 10.1016/j.neuron.2008.06.008

Laux, T., Fukami, K., Thelen, M., Golub, T., Frey, D., and Caroni, P. (2000). GAP43, MARCKS, and CAP23 modulate PI(4,5)P(2) at plasmalemmal rafts, and regulate cell cortex actin dynamics through a common mechanism. *J. Cell Biol.* 149, 1455–1472. doi: 10.1083/jcb.149.7.1455

Lee, S. B., Bagley, J. A., Lee, H. Y., Jan, L. Y., and Jan, Y.-N. (2011). Pathogenic polyglutamine proteins cause dendrite defects associated with specific actin cytoskeletal alterations in Drosophila. *Proc. Natl. Acad. Sci. U.S.A.* 108, 16795–16800. doi: 10.1073/pnas.1113573108

Leshchyns'ka, I., Sytnyk, V., Morrow, J. S., and Schachner, M. (2003). Neural cell adhesion molecule (NCAM) association with PKCbeta2 via betaI spectrin is implicated in NCAM-mediated neurite outgrowth. *J. Cell Biol.* 161, 625–639. doi: 10.1083/jcb.200303020

Li, C., Sun, Y., Yang, W., Ma, S., Zhang, L., Zhao, J., et al. (2019a). Pilose Antler Extracts (PAEs) protect against neurodegeneration in 6-OHDA-Induced Parkinson's Disease Rat Models. *Evid. Based. Complement. Altern. Med.* 2019:7276407.

Li, J., Jia, Z., Xu, W., Guo, W., Zhang, M., Bi, J., et al. (2019b). TGN-020 alleviates edema and inhibits astrocyte activation and glial scar formation after spinal cord compression injury in rats. *Life Sci.* 222, 148–157. doi: 10.1016/j.lfs.2019.03.007

Li, P., Banjade, S., Cheng, H.-C., Kim, S., Chen, B., Guo, L., et al. (2012). Phase transitions in the assembly of multivalent signalling proteins. *Nature* 483, 336–340. doi: 10.1038/nature10879

Liang, X., Lu, Y., Neubert, T. A., and Resh, M. D. (2002). Mass spectrometric analysis of GAP-43/neuromodulin reveals the presence of a variety of fatty acylated species. *J. Biol. Chem.* 277, 33032–33040. doi: 10.1074/jbc.m204607200

Lin, L., Chen, H., Zhang, Y., Lin, W., Liu, Y., Li, T., et al. (2015). IL-10 Protects neurites in oxygen-glucose-deprived cortical neurons through the PI3K/Akt Pathway. *PLoS One* 10:e0136959. doi: 10.1371/journal.pone.0136959

Liu, S.-J., Gasperini, R., Foa, L., and Small, D. H. (2010). Amyloid-beta decreases cell-surface AMPA receptors by increasing intracellular calcium and phosphorylation of GluR2. *J. Alzheimers Dis.* 21, 655–666. doi: 10.3233/jad-2010-091654

Liu, Y. C., and Storm, D. R. (1989). Dephosphorylation of neuromodulin by calcineurin. *J. Biol. Chem.* 264, 12800–12804.

Lovinger, D. M., Colley, P. A., Akers, R. F., Nelson, R. B., and Routtenberg, A. (1986). Direct relation of long-term synaptic potentiation to phosphorylation of membrane protein F1, a substrate for membrane protein kinase C. *Brain Res.* 399, 205–211. doi: 10.1016/0006-8993(86)91510-6

Maekawa, S., Maekawa, M., Hattori, S., and Nakamura, S. (1993). Purification and molecular cloning of a novel acidic calmodulin binding protein from rat brain. *J. Biol. Chem.* 268, 13703–13709.

Maekawa, S., Murofushi, H., and Nakamura, S. (1994). Inhibitory effect of calmodulin on phosphorylation of NAP-22 with protein kinase C. *J. Biol. Chem.* 269, 19462–19465.

Maier, D. L., Mani, S., Donovan, S. L., Soppet, D., Tessarollo, L., Mccasland, J. S., et al. (1999). Disrupted cortical map and absence of cortical barrels in growth-associated protein (GAP)-43 knockout mice. *Proc. Natl. Acad. Sci. U.S.A.* 96, 9397–9402. doi: 10.1073/pnas.96.16.9397

Masliah, E. (1995). Mechanisms of synaptic dysfunction in Alzheimer's disease. *Histol. Histopathol.* 10, 509–519.

Masliah, E., Mallory, M., Hansen, L., Alford, M., Albright, T., Deteresa, R., et al. (1991). Patterns of aberrant sprouting in Alzheimer's disease. *Neuron* 6, 729–739. doi: 10.1016/0896-6273(91)90170-5

Mason, M. (2002). Transcriptional upregulation of SCG10 and CAP-23 Is correlated with regeneration of the axons of peripheral and central neurons *in Vivo*. *Mol. Cell. Neurosci.* 20, 595–615. doi: 10.1006/mcne.2002.1140

Masters, C. L., Simms, G., Weinman, N. A., Multhaup, G., Mcdonald, B. L., and Beyreuther, K. (1985). Amyloid plaque core protein in Alzheimer disease and Down syndrome. *Proc. Natl. Acad. Sci. U.S.A.* 82, 4245–4249. doi: 10.1073/pnas.82.12.4245

Matsubara, M., Nakatsu, T., Kato, H., and Taniguchi, H. (2004). Crystal structure of a myristoylated CAP-23/NAP-22 N-terminal domain complexed with Ca2+/calmodulin. *EMBO J.* 23, 712–718. doi: 10.1038/sj.emboj.7600093

Matsuda, W., Furuta, T., Nakamura, K. C., Hioki, H., Fujiyama, F., Arai, R., et al. (2009). Single nigrostriatal dopaminergic neurons form widely spread and

highly dense axonal arborizations in the neostriatum. *J. Neurosci.* 29, 444–453. doi: 10.1523/jneurosci.4029-08.2009

Matsushima, H., Shimohama, S., Chachin, M., Taniguchi, T., and Kimura, J. (1996). Ca2+-dependent and Ca2+-independent protein kinase C changes in the brain of patients with Alzheimer's disease. *J. Neurochem.* 67, 317–323. doi: 10.1046/j.1471-4159.1996.67010317.x

McGuire, C. B., Snipes, G. J., and Norden, J. J. (1988). Light-microscopic immunolocalization of the growth- and plasticity-associated protein GAP-43 in the developing rat brain. *Brain Res.* 469, 277–291. doi: 10.1016/0165-3806(88)90189-7

McLaughlin, R. E., and Denny, J. B. (1999). Palmitoylation of GAP-43 by the ER-Golgi intermediate compartment and Golgi apparatus. *Biochim. Biophys. Acta* 1451, 82–92. doi: 10.1016/s0167-4889(99)00074-9

Meiri, K. F., Pfenninger, K. H., and Willard, M. B. (1986). Growth-associated protein, GAP-43, a polypeptide that is induced when neurons extend axons, is a component of growth cones and corresponds to pp46, a major polypeptide of a subcellular fraction enriched in growth cones. *Proc. Natl. Acad. Sci. U.S.A.* 83, 3537–3541. doi: 10.1073/pnas.83.10.3537

Metz, G. A., and Schwab, M. E. (2004). Behavioral characterization in a comprehensive mouse test battery reveals motor and sensory impairments in growth-associated protein-43 null mutant mice. *Neuroscience* 129, 563–574. doi: 10.1016/j.neuroscience.2004.07.053

Miao, Y., Tipakornsaowapak, T., Zheng, L., Mu, Y., and Lewellyn, E. (2018). Phospho-regulation of intrinsically disordered proteins for actin assembly and endocytosis. *FEBS J.* 285, 2762–2784. doi: 10.1111/febs.14493

Miyake, K., Yamamoto, W., Tadokoro, M., Takagi, N., Sasakawa, K., Nitta, A., et al. (2002). Alterations in hippocampal GAP-43, BDNF, and L1 following sustained cerebral ischemia. *Brain Res.* 935, 24–31. doi: 10.1016/s0006-8993(02)02420-4

Mohammad, H. M. F., Sami, M. M., Makary, S., Toraih, E. A., Mohamed, A. O., and El-Ghaiesh, S. H. (2019). Neuroprotective effect of levetiracetam in mouse diabetic retinopathy: effect on glucose transporter-1 and GAP43 expression. *Life Sci.* 232:116588. doi: 10.1016/j.lfs.2019.116588

Morganti-Kossman, M. C., Lenzlinger, P. M., Hans, V., Stahel, P., Csuka, E., Ammann, E., et al. (1997). Production of cytokines following brain injury: beneficial and deleterious for the damaged tissue. *Mol. Psychiatry* 2, 133–136. doi: 10.1038/sj.mp.4000227

Morrison, J. H., and Hof, P. R. (2002). Selective vulnerability of corticocortical and hippocampal circuits in aging and Alzheimer's disease. *Prog. Brain Res.* 136, 467–486. doi: 10.1016/s0079-6123(02)36039-4

Mosevitsky, M., and Silicheva, I. (2011). Subcellular and regional location of "brain" proteins BASP1 and MARCKS in kidney and testis. *Acta Histochem.* 113, 13–18. doi: 10.1016/j.acthis.2009.07.002

Mosevitsky, M. I. (2005). "Nerve ending "signal" proteins GAP-43, MARCKS, and BASP1. *Int. Rev. Cytol.* 245, 245–325. doi: 10.1016/s0074-7696(05)45007-x

Mosevitsky, M. I., Capony, J. P., Gyu, S., Novitskaya, V. A., Ayu, P., and Zakharov, V. V. (1997). The BASP1 family of myristoylated proteins abundant in axonal termini. Primary structure analysis and physico-chemical properties. *Biochimie* 79, 373–384. doi: 10.1016/s0300-9084(97)80032-6

Mosevitsky, M. I., Novitskaya, V. A., Ayu, P., and Gyu, S. (1994). Neuronal protein GAP-43 is a member of novel group of brain acid-soluble proteins (BASPs). *Neurosci. Res.* 19, 223–228. doi: 10.1016/0168-0102(94)90146-5

Mulkey, R. M., Endo, S., Shenolikar, S., and Malenka, R. C. (1994). Involvement of a calcineurin/inhibitor-1 phosphatase cascade in hippocampal long-term depression. *Nature* 369, 486–488. doi: 10.1038/369486a0

Munsie, L. N., and Truant, R. (2012). The role of the cofilin-actin rod stress response in neurodegenerative diseases uncovers potential new drug targets. *BioArchitecture* 2, 204–208. doi: 10.4161/bioa.22549

Musunuri, S., Wetterhall, M., Ingelsson, M., Lannfelt, L., Artemenko, K., Bergquist, J., et al. (2014). Quantification of the brain proteome in Alzheimer's disease using multiplexed mass spectrometry. *J. Proteome Res.* 13, 2056–2068. doi: 10.1021/pr401202d

Nedivi, E., Basi, G. S., Akey, I. V., and Skene, J. H. (1992). A neural-specific GAP-43 core promoter located between unusual DNA elements that interact to regulate its activity. *J. Neurosci.* 12, 691–704. doi: 10.1523/jneurosci.12-03-00691.1992

Neve, R. L., Coopersmith, R., Mcphie, D. L., Santeufemio, C., Pratt, K. G., Murphy, C. J., et al. (1998). The neuronal growth-associated protein GAP-43 interacts with rabaptin-5 and participates in endocytosis. *J. Neurosci.* 18, 7757–7767. doi: 10.1523/jneurosci.18-19-07757.1998

Neve, R. L., Finch, E. A., Bird, E. D., and Benowitz, L. I. (1988). Growth-associated protein GAP-43 is expressed selectively in associative regions of the adult human brain. *Proc. Natl. Acad. Sci. U.S.A.* 85, 3638–3642. doi: 10.1073/pnas.85.10.3638

Nguyen, T. L. X., Kim, C. K., Cho, J.-H., Lee, K.-H., and Ahn, J.-Y. (2010). Neuroprotection signaling pathway of nerve growth factor and brain-derived neurotrophic factor against staurosporine induced apoptosis in hippocampal H19-7/IGF-IR [corrected]. *Exp. Mol. Med.* 42, 583–595. doi: 10.3858/emm.2010.42.8.060

Noureddine, M. A., Qin, X.-J., Oliveira, S. A., Skelly, T. J., Van Der Walt, J., Hauser, M. A., et al. (2005). Association between the neuron-specific RNA-binding protein ELAVL4 and Parkinson disease. *Hum. Genet.* 117, 27–33. doi: 10.1007/s00439-005-1259-2

O'Neil, K. T., and DeGrado, W. F. (1990). How calmodulin binds its targets: sequence independent recognition of amphiphilic alpha-helices. *Trends Biochem. Sci.* 15, 59–64. doi: 10.1016/0968-0004(90)90177-d

Pacelli, C., Giguere, N., Bourque, M. J., Levesque, M., Slack, R. S., and Trudeau, L. E. (2015). Elevated mitochondrial bioenergetics and axonal arborization size are key contributors to the vulnerability of dopamine neurons. *Curr. Biol.* 25, 2349–2360. doi: 10.1016/j.cub.2015.07.050

Palasz, E., Wysocka, A., Gasiorowska, A., Chalimoniuk, M., Niewiadomski, W., and Niewiadomska, G. (2020). BDNF as a promising therapeutic agent in Parkinson's Disease. *Int. J. Mol. Sci.* 21:1170. doi: 10.3390/ijms21031170

Pang, Z. P., Cao, P., Xu, W., and Südhof, T. C. (2010). Calmodulin controls synaptic strength via presynaptic activation of calmodulin kinase II. *J. Neurosci.* 30, 4132–4142. doi: 10.1523/jneurosci.3129-09.2010

Parhad, I. M., Oishi, R., and Clark, A. W. (1992). GAP-43 gene expression is increased in anterior horn cells of amyotrophic lateral sclerosis. *Ann. Neurol.* 31, 593–597. doi: 10.1002/ana.410310605

Pascale, A., Gusev, P. A., Amadio, M., Dottorini, T., Govoni, S., Alkon, D. L., et al. (2004). Increase of the RNA-binding protein HuD and posttranscriptional up-regulation of the GAP-43 gene during spatial memory. *Proc. Natl. Acad. Sci. U.S.A.* 101, 1217–1222. doi: 10.1073/pnas.0307674100

Patel, N. K., Pavese, N., Javed, S., Hotton, G. R., Brooks, D. J., and Gill, S. S. (2013). Benefits of putaminal GDNF infusion in Parkinson disease are maintained after GDNF cessation. *Neurology* 81, 1176–1178. doi: 10.1212/wnl.0b013e3182a55ea5

Patterson, S. I., and Skene, J. H. (1999). A shift in protein S-palmitoylation, with persistence of growth-associated substrates, marks a critical period for synaptic plasticity in developing brain. *J. Neurobiol.* 39, 423–437. doi: 10.1002/(sici)1097-4695(19990605)39:3<423::aid-neu8>3.0.co;2-z

Perrone-Bizzozero, N. I., Cansino, V. V., and Kohn, D. T. (1993). Posttranscriptional regulation of GAP-43 gene expression in PC12 cells through protein kinase C-dependent stabilization of the mRNA. *J. Cell Biol.* 120, 1263–1270. doi: 10.1083/jcb.120.5.1263

Perrone-Bizzozero, N. I., Neve, R. L., Irwin, N., Lewis, S., Fischer, I., and Benowitz, L. I. (1991). Post-transcriptional regulation of GAP-43 mRNA levels during neuronal differentiation and nerve regeneration. *Mol. Cell. Neurosci.* 2, 402–409. doi: 10.1016/1044-7431(91)90027-l

Peskett, T. R., Rau, F., O'driscoll, J., Patani, R., Lowe, A. R., and Saibil, H. R. (2018). A liquid to solid phase transition underlying pathological huntingtin exon1 aggregation. *Mol. Cell* 70, 588–601.e6.

Phinney, A. L., Deller, T., Stalder, M., Calhoun, M. E., Frotscher, M., Sommer, B., et al. (1999). Cerebral amyloid induces aberrant axonal sprouting and ectopic terminal formation in amyloid precursor protein transgenic mice. *J. Neurosci.* 19, 8552–8559. doi: 10.1523/jneurosci.19-19-08552.1999

Qi, D., Ouyang, C., Wang, Y., Zhang, S., Ma, X., Song, Y., et al. (2014). HO-1 attenuates hippocampal neurons injury via the activation of BDNF-TrkB-PI3K/Akt signaling pathway in stroke. *Brain Res.* 1577, 69–76. doi: 10.1016/j.brainres.2014.06.031

Quattrone, A., Pascale, A., Nogues, X., Zhao, W., Gusev, P., Pacini, A., et al. (2001). Posttranscriptional regulation of gene expression in learning by the neuronal ELAV-like mRNA-stabilizing proteins. *Proc. Natl. Acad. Sci. U.S.A.* 98, 11668–11673. doi: 10.1073/pnas.191388398

Rechsteiner, M., and Rogers, S. W. (1996). PEST sequences and regulation by proteolysis. *Trends Biochem. Sci.* 21, 267–271. doi: 10.1016/s0968-0004(96)10031-1

Rekart, J. L., Meiri, K., and Routtenberg, A. (2005). Hippocampal-dependent memory is impaired in heterozygous GAP-43 knockout mice. *Hippocampus* 15, 1–7. doi: 10.1002/hipo.20045

Rekart, J. L., Quinn, B., Mesulam, M. M., and Routtenberg, A. (2004). Subfield-specific increase in brain growth protein in postmortem hippocampus of Alzheimer's patients. *Neuroscience* 126, 579–584. doi: 10.1016/j.neuroscience.2004.03.060

Riederer, B. M., and Routtenberg, A. (1999). Can GAP-43 interact with brain spectrin? *Brain Res. Mol. Brain Res.* 71, 345–348. doi: 10.1016/s0169-328x(99)00179-5

Rostami, E., Krueger, F., Plantman, S., Davidsson, J., Agoston, D., Grafman, J., et al. (2014). Alteration in BDNF and its receptors, full-length and truncated TrkB and p75(NTR) following penetrating traumatic brain injury. *Brain Res.* 1542, 195–205. doi: 10.1016/j.brainres.2013.10.047

Routtenberg, A., and Lovinger, D. M. (1985). Selective increase in phosphorylation of a 47-kDa protein (F1) directly related to long-term potentiation. *Behav. Neural Biol.* 43, 3–11. doi: 10.1016/s0163-1047(85)91426-8

Saal, K.-A., Galter, D., Roeber, S., Bähr, M., Tönges, L., and Lingor, P. (2017). Altered expression of growth associated protein-43 and Rho kinase in human patients with Parkinson's disease. *Brain Pathol.* 27, 13–25. doi: 10.1111/bpa.12346

Sandelius, Å, Sandgren, S., Axelsson, M., Malmeström, C., Novakova, L., Kostanjevecki, V., et al. (2019). Cerebrospinal fluid growth-associated protein 43 in multiple sclerosis. *Sci. Rep.* 9:17309.

Sanna, M. D., Quattrone, A., Ghelardini, C., and Galeotti, N. (2014). PKC-mediated HuD-GAP43 pathway activation in a mouse model of antiretroviral painful neuropathy. *Pharmacol. Res.* 81, 44–53. doi: 10.1016/j.phrs.2014.02.004

Sechi, A. S., and Wehland, J. (2000). The actin cytoskeleton and plasma membrane connection: PtdIns(4,5)P(2) influences cytoskeletal protein activity at the plasma membrane. *J. Cell Sci.* 113(Pt 21), 3685–3695.

Shen, Y., Mani, S., Donovan, S. L., Schwob, J. E., and Meiri, K. F. (2002). Growth-associated protein-43 is required for commissural axon guidance in the developing vertebrate nervous system. *J. Neurosci.* 22, 239–247. doi: 10.1523/jneurosci.22-01-00239.2002

Silver, J., and Miller, J. H. (2004). Regeneration beyond the glial scar. *Nat. Rev. Neurosci.* 5, 146–156. doi: 10.1038/nrn1326

Sjogren, M., Minthon, L., Davidsson, P., Granerus, A. K., Clarberg, A., Vanderstichele, H., et al. (2000). CSF levels of tau, beta-amyloid(1-42) and GAP-43 in frontotemporal dementia, other types of dementia and normal aging. *J. Neural Transm.* 107, 563–579. doi: 10.1007/s007020070079

Skene, J. H. (1989). Axonal growth-associated proteins. *Annu. Rev. Neurosci.* 12, 127–156. doi: 10.1146/annurev.ne.12.030189.001015

Skene, J. H., Jacobson, R. D., Snipes, G. J., Mcguire, C. B., Norden, J. J., and Freeman, J. A. (1986). A protein induced during nerve growth (GAP-43) is a major component of growth-cone membranes. *Science* 233, 783–786. doi: 10.1126/science.3738509

Skene, J. H., and Virág, I. (1989). Posttranslational membrane attachment and dynamic fatty acylation of a neuronal growth cone protein, GAP-43. *J. Cell Biol.* 108, 613–624. doi: 10.1083/jcb.108.2.613

Skene, J. H., and Willard, M. (1981). Changes in axonally transported proteins during axon regeneration in toad retinal ganglion cells. *J. Cell Biol.* 89, 86–95. doi: 10.1083/jcb.89.1.86

Smythe, E., and Ayscough, K. R. (2006). Actin regulation in endocytosis. *J. Cell Sci.* 119, 4589–4598. doi: 10.1242/jcs.03247

Spencer, S. A., Schuh, S. M., Liu, W. S., and Willard, M. B. (1992). GAP-43, a protein associated with axon growth, is phosphorylated at three sites in cultured neurons and rat brain. *J. Biol. Chem.* 267, 9059–9064.

Spillantini, M. G., Schmidt, M. L., Lee, V. M., Trojanowski, J. Q., Jakes, R., and Goedert, M. (1997). Alpha-synuclein in Lewy bodies. *Nature* 388, 839–840.

Strittmatter, S. M., Fankhauser, C., Huang, P. L., Mashimo, H., and Fishman, M. C. (1995). Neuronal pathfinding is abnormal in mice lacking the neuronal growth cone protein GAP-43. *Cell* 80, 445–452. doi: 10.1016/0092-8674(95)90495-6

Strittmatter, S. M., Igarashi, M., and Fishman, M. C. (1994). GAP-43 amino terminal peptides modulate growth cone morphology and neurite outgrowth. *J. Neurosci.* 14, 5503–5513. doi: 10.1523/jneurosci.14-09-05503.1994

Sudo, Y., Valenzuela, D., Beck-Sickinger, A. G., Fishman, M. C., and Strittmatter, S. M. (1992). Palmitoylation alters protein activity: blockade of G(o) stimulation by GAP-43. *EMBO J.* 11, 2095–2102. doi: 10.1002/j.1460-2075.1992.tb05268.x

Sun, M.-K., and Alkon, D. L. (2014). The "Memory Kinases": roles of pkc isoforms in signal processing and memory formation. *Prog. Mol. Biol. Transl. Sci.* 122, 31–59.

Sun, Y., Leong, N. T., Jiang, T., Tangara, A., Darzacq, X., and Drubin, D. G. (2017). Switch-like Arp2/3 activation upon WASP and WIP recruitment to an apparent threshold level by multivalent linker proteins *in vivo*. *eLife* 6:e29140.

Tagawa, K., Homma, H., Saito, A., Fujita, K., Chen, X., Imoto, S., et al. (2015). Comprehensive phosphoproteome analysis unravels the core signaling network that initiates the earliest synapse pathology in preclinical Alzheimer's disease brain. *Hum. Mol. Genet.* 24, 540–558. doi: 10.1093/hmg/ddu475

Takasaki, A., Hayashi, N., Matsubara, M., Yamauchi, E., and Taniguchi, H. (1999). Identification of the calmodulin-binding domain of neuron-specific protein kinase C substrate protein CAP-22/NAP-22. Direct involvement of protein myristoylation in calmodulin-target protein interaction. *J. Biol. Chem.* 274, 11848–11853. doi: 10.1074/jbc.274.17.11848

Tejero-Díez, P., Rodríguez-Sánchez, P., Martín-Cófreces, N. B., and Díez-Guerra, F. J. (2000). bFGF stimulates GAP-43 phosphorylation at ser41 and modifies its intracellular localization in cultured hippocampal neurons. *Mol. Cell. Neurosci.* 16, 766–780. doi: 10.1006/mcne.2000.0915

Teravskis, P. J., Covelo, A., Miller, E. C., Singh, B., Martell-Martínez, H. A., Benneyworth, M. A., et al. (2018). A53T mutant alpha-synuclein induces Tau-dependent postsynaptic impairment independently of neurodegenerative changes. *J. Neurosci.* 38, 9754–9767. doi: 10.1523/jneurosci.0344-18.2018

Tompa, P., and Fuxreiter, M. (2008). Fuzzy complexes: polymorphism and structural disorder in protein-protein interactions. *Trends Biochem. Sci.* 33, 2–8. doi: 10.1016/j.tibs.2007.10.003

Tonges, L., Szego, E. M., Hause, P., Saal, K. A., Tatenhorst, L., Koch, J. C., et al. (2014). Alpha-synuclein mutations impair axonal regeneration in models of Parkinson's disease. *Front. Aging Neurosci.* 6:239. doi: 10.3389/fnagi.2014.00239

Tron, C., Lemaitre, F., Verstuyft, C., Petitcollin, A., Verdier, M. C., and Bellissant, E. (2019). Pharmacogenetics of membrane transporters of tacrolimus in solid organ transplantation. *Clin. Pharmacokinet.* 58, 593–613. doi: 10.1007/s40262-018-0717-7

Tsai, K. C., Cansino, V. V., Kohn, D. T., Neve, R. L., and Perrone-Bizzozero, N. I. (1997). Post-transcriptional regulation of the GAP-43 gene by specific sequences in the 3′ untranslated region of the mRNA. *J. Neurosci.* 17, 1950–1958. doi: 10.1523/jneurosci.17-06-01950.1997

Tysnes, O.-B., and Storstein, A. (2017). Epidemiology of Parkinson's disease. *J. Neural Transm.* 124, 901–905.

Udvadia, A. J., Köster, R. W., and Skene, J. H. (2001). GAP-43 promoter elements in transgenic zebrafish reveal a difference in signals for axon growth during CNS development and regeneration. *Development* 128, 1175–1182.

Uzumcu, A., Candan, S., Toksoy, G., Uyguner, Z. O., Karaman, B., Eris, H., et al. (2009). Mutational screening of BASP1 and transcribed processed pseudogene TPPsig-BASP1 in patients with Möbius syndrome. *J. Genet. Genomics* 36, 251–256. doi: 10.1016/s1673-8527(08)60112-5

Wang, H. Y., Pisano, M. R., and Friedman, E. (1994). Attenuated protein kinase C activity and translocation in Alzheimer's disease brain. *Neurobiol. Aging* 15, 293–298. doi: 10.1016/0197-4580(94)90023-x

Wang, M. J., Jiang, L., Chen, H. S., and Cheng, L. (2019a). Levetiracetam protects against cognitive impairment of subthreshold convulsant discharge model rats by activating protein kinase C (PKC)-Growth-Associated Protein 43 (GAP-43)-Calmodulin-Dependent Protein Kinase (CaMK) Signal Transduction Pathway. *Med. Sci. Monit.* 25, 4627–4638. doi: 10.12659/msm.913542

Wang, Q., Zhang, Y., Wang, M., Song, W.-M., Shen, Q., Mckenzie, A., et al. (2019b). The landscape of multiscale transcriptomic networks and key regulators in Parkinson's disease. *Nat. Commun.* 10:5234.

Weber, J. R., and Skene, J. H. (1997). Identification of a novel repressive element that contributes to neuron-specific gene expression. *J. Neurosci.* 17, 7583–7593. doi: 10.1523/jneurosci.17-20-07583.1997

Wegmann, S., Eftekharzadeh, B., Tepper, K., Zoltowska, K. M., Bennett, R. E., Dujardin, S., et al. (2018). Tau protein liquid-liquid phase separation can initiate tau aggregation. *EMBO J.* 37:e98049.

Wetmore, C., Olson, L., and Bean, A. J. (1994). Regulation of brain-derived neurotrophic factor (BDNF) expression and release from hippocampal neurons is mediated by non-NMDA type glutamate receptors. *J. Neurosci.* 14, 1688–1700. doi: 10.1523/jneurosci.14-03-01688.1994

Whitehouse, P. J., Price, D. L., Struble, R. G., Clark, A. W., Coyle, J. T., and Delon, M. R. (1982). Alzheimer's disease and senile dementia: loss of neurons in the basal forebrain. *Science* 215, 1237–1239. doi: 10.1126/science.7058341

Widmer, F., and Caroni, P. (1990). Identification, localization, and primary structure of CAP-23, a particle-bound cytosolic protein of early development. *J. Cell Biol.* 111, 3035–3047. doi: 10.1083/jcb.111.6.3035

Wiederkehr, A., Staple, J., and Caroni, P. (1997). The motility-associated proteins GAP-43, MARCKS, and CAP-23 share unique targeting and surface activity-inducing properties. *Exp. Cell Res.* 236, 103–116. doi: 10.1006/excr.1997.3709

Wu, H., Lu, D., Jiang, H., Xiong, Y., Qu, C., Li, B., et al. (2008). Simvastatin-mediated upregulation of VEGF and BDNF, activation of the PI3K/Akt pathway, and increase of neurogenesis are associated with therapeutic improvement after traumatic brain injury. *J. Neurotrauma* 25, 130–139. doi: 10.1089/neu.2007.0369

Xiao, H.-S., Huang, Q.-H., Zhang, F.-X., Bao, L., Lu, Y.-J., Guo, C., et al. (2002). Identification of gene expression profile of dorsal root ganglion in the rat peripheral axotomy model of neuropathic pain. *Proc. Natl. Acad. Sci. U.S.A.* 99, 8360–8365.

Yamamoto, Y., Sokawa, Y., and Maekawa, S. (1997). Biochemical evidence for the presence of NAP-22, a novel acidic calmodulin binding protein, in the synaptic vesicles of rat brain. *Neurosci. Lett.* 224, 127–130. doi: 10.1016/s0304-3940(97)13482-6

Yang, P., Qin, Y., Bian, C., Zhao, Y., and Zhang, W. (2015). Intrathecal delivery of IL-6 reactivates the intrinsic growth capacity of pyramidal cells in the sensorimotor cortex after spinal cord injury. *PLoS One* 10:e0127772. doi: 10.1371/journal.pone.0127772

Yang, P., Wen, H., Ou, S., Cui, J., and Fan, D. (2012). IL-6 promotes regeneration and functional recovery after cortical spinal tract injury by reactivating intrinsic growth program of neurons and enhancing synapse formation. *Exp. Neurol.* 236, 19–27. doi: 10.1016/j.expneurol.2012.03.019

Zakharov, V. V., Capony, J.-P., Derancourt, J., Kropolova, E. S., Novitskaya, V. A., Bogdanova, M. N., et al. (2003). Natural N-terminal fragments of brain abundant myristoylated protein BASP1. *Biochim. Biophys. Acta* 1622, 14–19. doi: 10.1016/s0304-4165(03)00099-0

Zakharov, V. V., and Mosevitsky, M. I. (2007). M-calpain-mediated cleavage of GAP-43 near Ser41 is negatively regulated by protein kinase C, calmodulin and calpain-inhibiting fragment GAP-43-3. *J. Neurochem.* 101, 1539–1551. doi: 10.1111/j.1471-4159.2007.04452.x

Zakharov, V. V., and Mosevitsky, M. I. (2010). Oligomeric structure of brain abundant proteins GAP-43 and BASP1. *J. Struct. Biol.* 170, 470–483. doi: 10.1016/j.jsb.2010.01.010

Zhang, M., Vogel, H. J., and Zwiers, H. (1994). Nuclear magnetic resonance studies of the structure of B50/neuromodulin and its interaction with calmodulin. *Biochem. Cell Biol.* 72, 109–116. doi: 10.1139/o94-017

**Conflict of Interest:** The authors declare that the research was conducted in the absence of any commercial or financial relationships that could be construed as a potential conflict of interest.

frontiers in Cell and Developmental Biology

ORIGINAL RESEARCH
published: 16 September 2020
doi: 10.3389/fcell.2020.571258

# Erythropoietin Improves Atrophy, Bleeding and Cognition in the Newborn Intraventricular Hemorrhage

*Carmen Hierro-Bujalance[1,2], Carmen Infante-Garcia[1,2], Daniel Sanchez-Sotano[1], Angel del Marco[1,2], Ana Casado-Revuelta[1], Carmen Maria Mengual-Gonzalez[1], Carmen Lucena-Porras[1], Marcos Bernal-Martin[1], Isabel Benavente-Fernandez[2,3], Simon Lubian-Lopez[2,3]* and Monica Garcia-Alloza[1,2]**

[1] Division of Physiology, School of Medicine, Universidad de Cádiz, Cádiz, Spain, [2] Instituto de Investigacion e Innovacion en Ciencias Biomedicas de la Provincia de Cádiz (INiBICA), Cádiz, Spain, [3] Division of Paediatrics, Section of Neonatology, Hospital Universitario Puerta del Mar, Cádiz, Spain

OPEN ACCESS

**Edited by:**
Luis B. Tovar-y-Romo, National Autonomous University of Mexico, Mexico

**Reviewed by:**
Magnus Gram, Lund University, Sweden
Christoph Bührer, Charité – Universitätsmedizin Berlin, Germany

***Correspondence:**
Simon Lubian-Lopez
simonp.lubian.sspa@juntadeandalucia.es
Monica Garcia-Alloza
monica.garcia@uca.es

**Specialty section:**
This article was submitted to Molecular Medicine, a section of the journal Frontiers in Cell and Developmental Biology

**Received:** 10 June 2020
**Accepted:** 18 August 2020
**Published:** 16 September 2020

**Citation:**
Hierro-Bujalance C, Infante-Garcia C, Sanchez-Sotano D, del Marco A, Casado-Revuelta A, Mengual-Gonzalez CM, Lucena-Porras C, Bernal-Martin M, Benavente-Fernandez I, Lubian-Lopez S and Garcia-Alloza M (2020) Erythropoietin Improves Atrophy, Bleeding and Cognition in the Newborn Intraventricular Hemorrhage. Front. Cell Dev. Biol. 8:571258. doi: 10.3389/fcell.2020.571258

The germinal matrix-intraventricular hemorrhage (GM-IVH) is one of the most devastating complications of prematurity. The short- and long-term neurodevelopmental consequences after severe GM-IVH are a major concern for neonatologists. These kids are at high risk of psychomotor alterations and cerebral palsy; however, therapeutic approaches are limited. Erythropoietin (EPO) has been previously used to treat several central nervous system complications due to its role in angiogenesis, neurogenesis and as growth factor. In addition, EPO is regularly used to reduce the number of transfusions in the preterm infant. Moreover, EPO crosses the blood-brain barrier and EPO receptors are expressed in the human brain throughout development. To analyze the role of EPO in the GM-IVH, we have administered intraventricular collagenase (Col) to P7 mice, as a model of GM-IVH of the preterm infant. After EPO treatment, we have characterized our animals in the short (14 days) and the long (70 days) term. In our hands, EPO treatment significantly limited brain atrophy and ventricle enlargement. EPO also restored neuronal density and ameliorated dendritic spine loss. Likewise, inflammation and small vessel bleeding were also reduced, resulting in the preservation of learning and memory abilities. Moreover, plasma gelsolin levels, as a feasible peripheral marker of GM-IVH-induced damage, recovered after EPO treatment. Altogether, our data support the positive effect of EPO treatment in our preclinical model of GM-IVH, both in the short and the long term.

**Keywords: brain atrophy, neuronal loss, erythropoietin, gelsolin, germinal matrix-intraventricular hemorrhage, preterm infant**

## INTRODUCTION

Every year there are over 15 million preterm births and ~7% of these kids suffer long term neurodevelopmental impairment (Maxwell et al., 2017). The germinal matrix-intraventricular hemorrhage (GM-IVH) is one of the most common complications observed in the preterm infant (PTI) (Tan et al., 2018). While the incidence of GM-IVH has declined since the 1990s, due to improvements in neonatal care, the increased survival of extremely PTI has also contributed to

maintain the absolute number of GM-IVH very high (Mukerji et al., 2015). GM-IVH in premature infants arises from the germinal matrix (GM), which is a complex vascularized layer rich in immature vessels that surrounds the lateral ventricles, corresponding with the subventricular zone (SVZ), from where neurons and glial cells rise during fetal development. GM microvasculature is extremely fragile due to an abundance of angiogenic blood vessels that exhibit paucity of pericytes, immaturity of basal lamina and deficiency of glial fibrillary acidic protein in the ensheathing astrocytes endfeet (Ballabh, 2010). Therefore, PTI with very low weight birth are more susceptible to local hemorrhage (Perlman, 2009). The short- and long-term neurodevelopmental complications in the PTI with severe or even mild GM-IVH are a major concern, since these kids are at high risk of neurosensory impairment, developmental delay, cerebral palsy, deafness, psychomotor alterations or cerebral palsy (Ballabh, 2010; Mukerji et al., 2015; Benavente-Fernandez et al., 2018).

Therapeutic approaches focus on enhancing the stability of GM vasculature and regulating the cerebral blood flow (Ballabh, 2010). Following this idea, erythropoietin (EPO) promotes the survival, proliferation and differentiation of erythrocyte progenitors in bone marrow (Lombardero et al., 2011) and is regularly used in PTI to reduce the number of transfusions. EPO crosses the blood-brain barrier in a dose-dependent manner and EPO receptors are expressed in the human brain throughout development (Kollensperger et al., 2011). Previous studies have reported that EPO can play a potential role in angiogenesis and neurogenesis (Lombardero et al., 2011; Juul and Pet, 2015). Thus, EPO has been used to treat infants with hypoxic-ischemic encephalopathy (Razak and Hussain, 2019). EPO treatment to PTI has shown a significant decrease of white matter injury and it might improve neurodevelopmental outcome of extremely PTI (Neubauer et al., 2010), although other studies failed to detect significant benefits, as recent PENUT study has recently reported (Juul et al., 2020). At present, EpoRepair (Erythropoietin for the Repair of Cerebral Injury in Very Preterm Infants) trial (Ruegger et al., 2015) outcomes are also awaited soon. Therefore, the role of EPO in GM-IVH of the PTI remains unclear. To deepen at this level, we have induced a GM-IVH in mice by intraventricular administration of collagenase (Col). After EPO treatment, brain atrophy and ventricular dilatation were significantly reduced. Spine and neuronal loss were limited, and overspread small vessel damage and inflammation were reduced, resulting in the preservation of learning and memory abilities. Interestingly, plasma gelsolin levels, as a feasible peripheral marker of GM-IVH-induced damage, previously observed in other brain disorders (Xu et al., 2012; Peng et al., 2015; Benavente-Fernandez et al., 2018), recovered after EPO administration.

# MATERIALS AND METHODS

## Animals and Treatments

Germinal matrix-intraventricular hemorrhage was induced to male and female CD1 mice at P7 by intracerebroventricular (icv) infusion of Col VII-S (batch number: SLBG8830V Sigma, St Louis, MO) (Segado-Arenas et al., 2018). Mice were anesthetized with isoflurane and placed in a stereotaxic frame (David-Kopf, California, United States). 0.3 IU of Col in 1 μl of TESCA 50 mM (TES buffer, Sigma, ref. T1375, St. Louis, MO, United States) and calcium chloride anhydrous 0.36 mM (Sigma, ref. C1016, St. Louis, MO, United States), pH7.4 and 37°C, were injected with Hamilton syringe in the right ventricle at 0.2 μl/min (+ 5 more minutes to avoid the retraction of the liquid). Sham animals received 1 μl of TESCA. Control mice received no injection. EPO treatment (10.000 or 20.000 IU) (EPO10 and EPO20) was ip injected on 3 consecutive days: immediately after completing the lesions, as well as 24 and 48 h later (Kaindl et al., 2008; Fan et al., 2011; Zhang et al., 2020). A set of mice (10–12/group) were sacrificed at P14 to analyze the early effects of EPO and a second set (10–12/group) were aged up to P70 to assess the long-term effects of EPO treatment. Two weeks before sacrifice mice underwent behavioral assessment. Animals that died before the experiments were completed were not included in subsequent analyses. All animals were maintained in the Animal Facility of the University of Cadiz under 12 h light/dark cycles and controlled temperature (21 ± 2°C) with *ad libitum* access to food and water. All experimental procedures were approved by the University of Cadiz Bioethical Committee (Guidelines for Care and Use of Experimental Animals, European Commission Directive 2010/63/UE and Spanish Royal Decree 53/2013).

## Rotarod

Rotarod (Ugo Basile Srl; Varese, Italia) was used to evaluate motor skills as described (Segado-Arenas et al., 2018). Mice were placed in the cylinder 4 min at 4 rpm for habituation purposes. During the test speed was progressively increased from 4 to 60 rpm, in 1 min, and the time spent on the rotarod was recorded.

## Morris Water Maze

A round pool (0.95 m in diameter) was filled with water (21 ± 1°C) and four equal virtual quadrants were indicated with geometric cues located in the walls. Experiments were run as previously described (Infante-Garcia et al., 2017). Briefly, the scape platform was invisible, 2–3 cm below the surface. The acquisition started starting 12 days before sacrifice and consisted of 4 trials/day for 4 days with the submerged platform in the virtual quadrant number 2. Time limit to locate the platform was 60 s/trial with an intertrial interval of 10 min. When the animal did not find the platform it was manually placed on it for 10 s. Retention 1 commenced 24 h after the finalization of the acquisition phase, and retention 2 was run 72 h after the end of the acquisition phase. Retention phases consisted in a single trial with the platform removed. Time required to locate the platform (acquisition), percentage of time spent in quadrant 2 (retention) and swimming velocity were analyzed using Smart software, Panlab (Spain).

## Motor Activity and New Object Discrimination Task

Spontaneous motor activity was analyzed by measuring the distance traveled by mice for 30 min in a rectangular box

(22 × 44 × 40 cm), as described (Infante-Garcia et al., 2016). The next day mice were placed in the same box and exposed to two objects (not used afterward), for habituation purposes. On the third day mice were exposed to two sample trials and a test trial. On the first sample trial, mice were placed into the center of the box containing 3 copies of an object arranged in a triangle-shaped spatial configuration. Mice explored for 5 min and after 30 min delay they received a second sample trial with 4 novel objects, arranged in a quadratic-shaped spatial configuration, for another 5 min. Test trial was performed after 30 min delay and mice were exposed to 2 copies of the object from sample trial 2 ("recent" objects) placed at the same position, and 2 copies of the object from sample trial 1 ("familiar" objects) placed one of them at the same position ("familiar non-displaced" object) and the another in a new position ("familiar displaced" object). "What," "where" and "when" integrated episodic memories were analyzed as described (Infante-Garcia et al., 2016).

## Cresyl Violet Staining

We analyzed brain morphology in 6 sections 1 mm apart (from 1.5 to −3.5 mm from Bregma). Sections were dehydrated in 70% ethanol for 15 min. They were stained with cresyl violet (Sigma, St. Louis, MO, United States) solution (0.5% w/v) for 10 min, as previously described (Ramos-Rodriguez et al., 2017). Sections were then fixed sequentially in 0.25% acetic acid, 100% ethanol and xylene for 2 min. Sections were mounted with DPX (Sigma, St. Louis, MO, United States). Analysis was conducted blind to the experimental conditions. Images were acquired using an optical Olympus Bx60 microscope (Japan) with an attached Olympus DP71 camera and Cell F software (Olympus, Hamburg, Germany). Cortex and lateral ventricle sizes were measured using Adobe Photoshop and Image J software.

## NeuN and Microglia Immunostaining

NeuN and microglia immunohistochemistry was performed as described (Infante-Garcia et al., 2015). Anti-NeuN (Chemicon, CA, United States) (1:200) and anti-Iba1 (Wako, Osaka, Japan) (1:1000) were used as primary antibodies for neuron and microglia assessment and incubated overnight at 4°C. Alexa Fluor 594 or Alexa Fluor 488 (1:1000), respectively, were used as secondary antibodies. DAPI 1mg/ml (Sigma) (1:3000) counterstain was used after NeuN immunohistochemistry and the percentage of NeuN-positive cells (normalized by total cells stained with DAPI) was quantified in the cortex and the SVZ using Image J software (Ramos-Rodriguez et al., 2016). Analysis was conducted blind to the experimental conditions. Number of microglia cells, individual microglia size and burden were quantified in the cortex and the SVZ using Image J software (Infante-Garcia et al., 2016).

## Golgi-Cox Staining

Neuron architecture was further analyzed by Golgi-Cox staining, using Rapid Golgi Stain Kit (FD Neurotechnologies, United States. Ref: PK401) following manufacturer's indications with minor modifications. Brains were maintained in the kit solutions for 3 weeks, and in 3% agarose liquid solution afterward. Blocks were cut into 200 μm on a vibratome (Ted Pella, Inc., California, United States) Sections were stained as indicated by manufacturer. Sections were dehydrated with ethanol and mounted with DPX (Sigma, United States). Neurons were photographed with Olympus U-RFLT microscope (Olympus, Japan), using MMI Cell Tools software. Neuronal complexity was analyzed by sholl analysis in 10 μm concentric circles from neuronal soma. Analysis was conducted blind to the experimental conditions. Number of crossings every 10 μm were quantified. Spine density was calculated (spines/10 μm) (Infante-Garcia et al., 2015). Ratios of curvature were calculated by dividing the end-to-end distance of a dendrite segment by the total length between the two segment ends using Image J software (Ramos-Rodriguez et al., 2017).

## Prussian Blue Staining

Consecutive sections to those used for cresyl violet staining were used for Prussian blue iron staining and neutral red counterstaining to analyze the presence of hemorrhages (Infante-Garcia et al., 2015). Images were acquired using an optical Olympus Bx60 microscope (Japan) with an attached Olympus DP71 camera and Cell F software (Olympus, Hamburg, Germany). Analysis was conducted blind to the experimental conditions. Hemorrhage burden (% of area covered by hemorrhages) was analyzed in the SVZ (up to 20 μm from the lateral ventricles), the cortex and the hippocampus using ImageJ software.

## Western Blot for Tau and Akt

We quantified phopho-tau, total tau, phospo-Akt and total Akt levels in the striatum (including the SVZ), cortex and hippocampus from all animals under study. Samples were prepared as previously described (Infante-Garcia et al., 2016). Briefly, tissue was homogenized in lysis buffer (Cell Signaling, United States) with a protease/phosphatase inhibitor cocktail (Sigma, United States). After centrifugation for 5 min, at 15000 *g* and 4 °C Bradford (Bio-Rad, Germany) protein assay was used for protein concentration in supernatants. Proteins were separated on 10% acrylamide-bisacrylamide gels, followed by electrophoretic transfer to PVDF membranes (Schleicher & Schuell, Keene, NH). Antibodies used included: phospho-tau clone AT8 (1:1000, Fisher Scientific, MA, United States), phospho-Akt (Ser473) (1:1000) (Cell signaling, United States), anti-total Akt antibody (1:2000) (cell signaling, United States) and anti-total tau antibody (1:1000) (DAKO, Denmark). Optical density was semi-quantified after normalizing to β-actin (1:2,500,000) (Sigma, United States), using ImageJ software. Data were represented as percentage of Control values.

## Matrix Metalloproteinase 9 and Gelsolin Plasma Determinations

Plasma matrix metalloproteinase 9 (MMP9) and gelsolin levels were measured, as feasible markers of central damage, in the short (P14) and the long (P70) term. We used ELISA kits for MMP9 (R&D System Corp, MN, United States) and gelsolin (Cusabio Biotech Co., Wuhan, Hubei Province, China),

following manufacturer's indications as previously described (Segado-Arenas et al., 2018).

## Statistical Analysis

One-way ANOVA, followed by Tuckey b test or Tamhane tests as required, were used. No statistical differences were detected between Sham and Control groups, therefore all animals were combined in a single Control group. Two-way ANOVA was used to analyze the MWM test (groupXday) and neurites architecture (groupXradius). SPSS v.15 software was used for all statistical analysis.

# RESULTS

## EPO Significantly Restores Cognitive Impairment After Inducing a GM-IVH

The overall compromise in GM-IVH mice for "what," "where" and "when" paradigms in the new object discrimination test, was significant improvement after EPO treatment ("what" [$F_{(5,225)} = 11.30$, $^{**}p < 0.01$ vs. rest of the groups, $\#\#p < 0.01$ vs. Control and Control + EP20], "where" [$F_{(5,249)} = 8.36$, $^{**}p < 0.01$ vs. rest of the groups, $\#\#p < 0.01$ vs. Control], "when" [$F_{(5,258)} = 10.95$, $^{**}p < 0.01$ vs. rest of the groups, $\#\#p < 0.01$ vs. Control and Control + EP20]) (**Figure 1A**). Similar results were detected in the Morris water maze test. We did not detect a significant groupXday effect [$F_{(15,1335)} = 0.859$, $p = 0.611$], although further daily assessment revealed differences on individual acquisition days (day 1 [$F_{(5,371)} = 0.878$, $p = 0.496$], day 2 [$F_{(5,344)} = 0.969$, $p = 0.437$], day 3 [$F_{(5,351)} = 3.498$, $^{**}p = 0.004$ vs. rest of the groups], day 4 [$F_{(5,358)} = 2.59$, $\dagger p = 0.025$ vs. Control, Control + EPO10, Control + EPO20 and Col + EPO20]) (**Figure 1B**). Also in the retention phase, EPO10 and EPO20 significantly improved Col-induced impairment (24 h [$F_{(5,85)} = 4.29$, $\dagger\dagger p = 0.002$ vs. Control, Control + EPO10, Control + EPO20 and Col + EPO10]; 72 h [$F_{(5,89)} = 2.75$, $\ddagger p = 0.025$ vs. Control and Col + EPO20]) (**Figure 1C**). Time in rotarod ([$F_{(5,57)} = 0.611$, $p = 0.962$]), spontaneous motor activity ([$F_{(5,85)} = 0.289$, $p = 0.917$]) and swimming velocity ([$F_{(5,89)} = 0.781$, $p = 0.566$]) (**Figure 1D**) were not affected, suggesting that alterations in learning and memory were motor-independent. However, we cannot exclude that larger lesions may reproduce motor-related alterations, as commonly observed in patients (Hinojosa-Rodríguez et al., 2017).

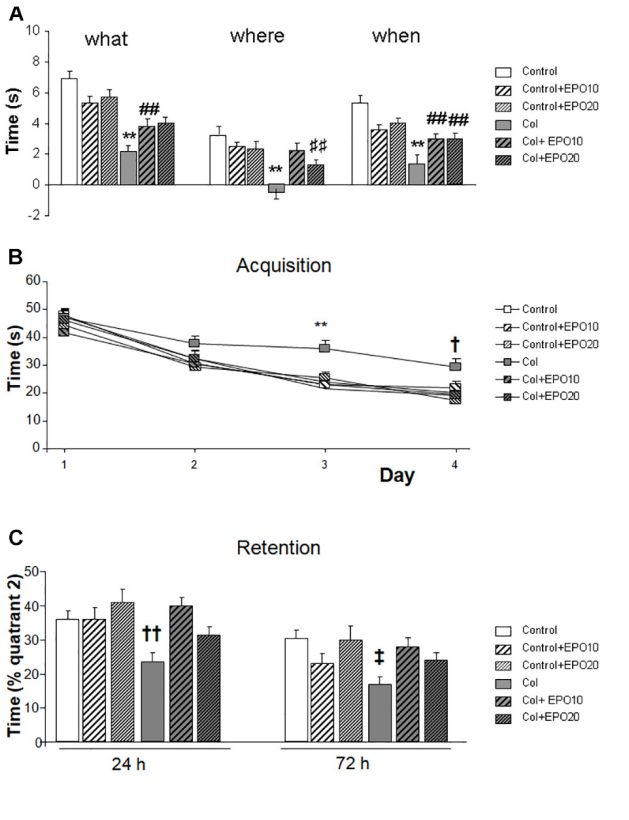


D

| Treatment | Distance (cm) | Swimming velocity (cm/s) | Rotarod time (s) |
|---|---|---|---|
| Control | 18170.94±1697.94 | 24.16±115 | 16.30±2.28 |
| Control+EPO10 | 19394.03±2210.70 | 23.10±1.05 | 17.40±2.02 |
| Control+EPO20 | 19605.08±1689.14 | 21.35±1.20 | 14.00±1.12 |
| Col | 17086.82±2285,.47 | 23.96±0.99 | 14.80±1.10 |
| Col+EPO10 | 18358.75±1239.07 | 22.29±1.51 | 17.00±1.94 |
| Col+EPO20 | 20036.82±2849.26 | 24.02±1.43 | 16.67±1.32 |

**FIGURE 1 |** EPO treatment significantly reduces GM-IVH cognitive impairment at P70. **(A)** Episodic memory is significantly impaired at P70 after inducing a GM-IVH, and EPO10 and EPO20 treatment counterbalances this limitation for "what" ($^{**}p < 0.01$ vs. rest of the groups, $\#\#p < 0.01$ vs. Control and Control + EPO20), "where" ($^{**}p < 0.01$ vs. rest of the groups, $\tau\tau p < 0.01$ vs. Control) and "when" ($^{**}p < 0.01$ vs. rest of the groups, $\#\#p < 0.01$ vs. Control and Control + EPO20) paradigms. **(B)** Spatial memory was also impaired after Col lesions, when analyzed in the acquisition phase of the Morris water maze, while EPO treatments significantly reversed this situation on individual days (day 1: $p = 0.496$, day 2: $p = 0.437$, day 3: $^{**}p = 0.004$ vs. rest of the groups, day 4: $\dagger p = 0.025$ vs. Control, Control + EPO10, Control + EPO20 and Col + EPO20). **(C)** A similar profile was observed in the retention phase and EPO10 and EPO20 treatment significantly improved the time spent where the platform used to be located, 24 ($\dagger\dagger p = 0.002$ vs. Control, Control + EPO10, Control + EPO20 and Col + EPO10) and 72 h ($\ddagger p = 0.025$ vs. Control and Col + EPO20) after completing the acquisition phase. **(D)** Motor skills were not affected in rotarod ($p = 0.962$), spontaneous motor activity ($p = 0.917$) and swimming velocity ($p = 0.566$).

## EPO Treatment Reduces Brain Atrophy and Neuronal Alterations After Inducing a GM-IVH

One week after Col lesions, the size of the ipsilateral hemispheres was reduced. EPO10 partially limited this effect, that was completely reversed by EPO20 treatment [$F_{(5,222)} = 3.775$, $\ddagger\ddagger p = 0.003$ vs. Control, Control + EPO10 and Control + EPO20, $\#\#p = 0.003$ vs. Control + 10]. The effect was still present at P70 [$F_{(5,174)} = 2.83$, $^{*}p = 0.017$ vs. rest of the groups] (**Figure 2A**). Reduced cortical size was slightly improved by EPO treatment, although differences did not reach statistical significance in the short term (P14) [$F_{(5,222)} = 1.107$, $p = 0.358$]. In the long term (P70) EPO treatment improved cortical atrophy [$F_{(5,175)} = 2.95$, $\ddagger p = 0.014$ vs. Control and Col + EPO10] (**Figure 2A**). Also, EPO

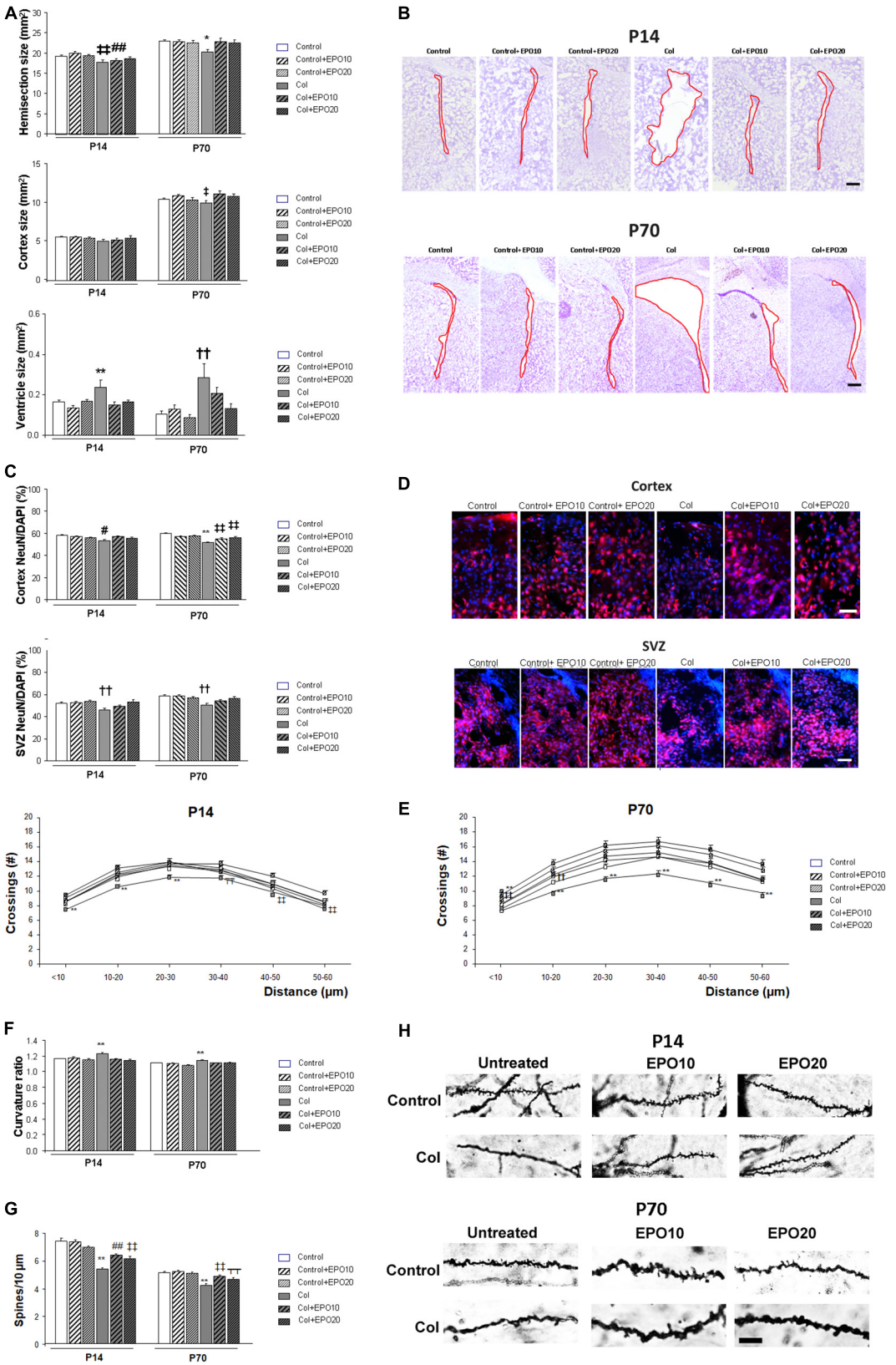


**FIGURE 2 |** Continued

**FIGURE 2 |** EPO treatment limits brain atrophy and neuronal alterations after induction of a GM-IVH with Col. **(A)** Ipsilateral hemisection size was reduced in P14 and P70 mice while EPO treatment limited this effect (P14: ‡‡$p$ = 0.003 vs. Control, Control + EPO10 and Control + EPO20, ##$p$ = 0.003 vs. Control + EPO10; P70: *$p$ = 0.017 vs. rest of the groups). Differences observed in the cortex did not reach statistical significance at P14 ($p$ = 0.358), although at P70 cortical compromise was ameliorated by EPO treatment (‡$p$ = 0.014 vs. Control and Col + EPO10). Significant ventricle enlargement was detected at P14 and EPO treatment reversed this effect (**$p$ = 0.001 vs. rest of the groups) and a similar profile was observed at P70 (††$p$ = 0.001 vs. Control, Control + EPO10, Control + EPO20, Col + EPO20). **(B)** Illustrative example of cresyl violet staining showing the ipsilateral ventricle enlargement at P14 and P70, after inducing a GM-IVH, while ventricle size is maintained in mice treated with EPO. Red line borders the ventricle. Scale bar = 250 μm. **(C)** At P14, NeuN/DAPI ratio was reduced in the ipsilateral cortex and EPO treatment improved this situation (#$p$ = 0.034 vs. Control, Control + EPO10 and Col + EPO10). A similar profile was observed at P70 (**$p$ < 0.001 vs. rest of the groups, ‡‡$p$ < 0.01 vs. Control, Control + EPO10 and Control + EPO20). The SVZ was also affected after Col lesions and EPO treatment significantly improved the NeuN/DAPI ratio both at P14 and P70 (P14: ††$p$ = 0.002 vs. Control, Control + EPO10, Control + EPO20 and Col + EPO20; P70: ††$p$ = 0.002 vs. Control, Control + EPO10, Control + EPO20 and Col + EPO20; P70). **(D)** Illustrative example of NeuN (red)/DAPI (blue) staining in the ipsilateral cortex and SVZ from mice with GM-IVH induced by Col, where a reduction in $NeuN^+$cells can be observed, while more $NeuN^+$cells are detected after EPO10 and EPO20 treatment. Scale 50 μm. **(E)** Neuronal complexity was affected by Col lesions and EPO treatment significantly improved this effect at P14 (**$p$ < 0.01 vs. rest of the groups; ‡$p$ = 0.017 vs. Cont + EPO20; ‡‡$p$ = 0.003 vs. Cont + EPO20; ∓∓$p$ < 0.01 vs. rest Control and Cont + EPO20) or P70 (**$p$ < 0.01 vs. rest of the groups, ‡‡$p$ < 0.01 vs. Control, Control + EPO20; ††$p$ < 0.01 vs. Control + EPO20, Col + EPO10 and Col + EPO20). **(F)** Neuron curvature ratio was also impaired after Col lesions and EPO treatment significantly ameliorated this situation both at P14 (**$p$ < 0.01 vs. rest of the groups) and P70 (**$p$ < 0.01 vs. rest of the groups). **(G)** Spine density compromise was also limited after EPO treatment in the ipsilateral hemispheres at P14 (**$p$ < 0.01 vs. rest of the groups, ‡‡$p$ < 0.01 vs. Control, Control + EPO10 and Control + EPO20, ##$p$ < 0.01 vs. Control and Control + EPO10) and at P70 (**$p$ < 0.01 vs. rest of the groups, ‡‡$p$ < 0.01 vs. Control, Control + EPO10 and Control + EPO20, ⊤⊤$p$ < 0.01 vs. Control + EPO10). **(H)** Illustrative example of spines labeled by Golgi-Cox staining. A reduction in spine density is observed in mice after lesions with Col and this effect is limited by EPO10 and EPO20 treatment at P14 and P70. Scale = 12.5 μm.

treatment completely reversed ventricle enlargement after Col lesions at P14 [$F_{(5,104)}$ = 4.48, **$p$ = 0.001 vs. rest of the groups] (**Figures 2A,B**). A similar profile was detected with EPO20 at P70 [$F_{(5,146)}$ = 4.21, ††$p$ = 0.001 vs. Control, Control + EPO10, Control + EPO20, Col + EPO20] (**Figure 2A**). No statistical differences were observed when EPO10 and EPO20 treatments were compared, and even though a slightly higher improvement was observed in the cortex from EPO10-treated animals at P70, an overall better response was observed after EPO20 treatments in all the other paradigms under study, including cortical size at P14, as well as hemisection and ventricle sizes at P14 and P70.

At P14 NeuN/DAPI ratio was reduced in the ipsilateral cortex after Col lesions, and EPO treatment improved this situation [$F_{(5,3428)}$ = 2.41, #$p$ = 0.034 vs. Control, Control + EPO10 and Col + EPO10] (**Figures 2C,D**). A similar outcome was observed at P70 [$F_{(5,2996)}$ = 14.35, **$p$ < 0.001 vs. rest of the groups, ‡‡$p$ < 0.01 vs. Control, Control + EPO10 and Control + EPO20] (**Figures 2C,D**). EPO20 treatment also improved NeuN/DAPI compromise in the SVZ at P14 [$F_{(5,987)}$ = 3.82, ††$p$ = 0.002 vs. Control, Control + EPO10, Control + EPO20 and Col + EPO20] and P70 [$F_{(5,977)}$ = 4.73, ††$p$ = 0.002 ‡vs. Control, Control + EPO10, Control + EPO20 and Col + EPO20] (**Figures 2C,D**).

Neuronal architecture was also altered after GM-IVH. Analysis of neurites intersections by sholl analysis after Golgi-Cox staining revealed a groupXradius distance effect by 2 way ANOVA in the ipsilateral hemisphere at P14 [$F_{(25,3997)}$ = 1.54, $p$ = 0.041]. Further assessment of individual distances revealed and overall improvement in mice treated with EPO10 and EPO20 (<10 μm [$F_{(5,670)}$ = 7.59, **$p$ < 0.01 vs. rest of the groups]; 10–20 μm [$F_{(5,669)}$ = 7.28, **$p$ < 0.01 vs. rest of the groups]; 20–30 μm [$F_{(5,658)}$ = 5.08, **$p$ < 0.01 vs. rest of the groups]; 30–40 μm [$F_{(5,656)}$ = 6.60, ∓∓$p$ < 0.01 vs. Control and Cont + EPO20]; 40–50 μm [$F_{(5,671)}$ = 3.60, ‡‡$p$ < 0.01 vs. Cont + EPO20]; 50–60μm [$F_{(5,673)}$ = 3.87, ‡‡$p$ = 0.002 vs. Cont + EPO20] (**Figure 2E**). At P70, we did not detect a significant groupXradius effect by 2 way ANOVA [$F_{(25,3779)}$ = 0.964, $p$ = 0.514]. Assessment of individual distances revealed that EPO treatment limited neuronal simplification (<10 μm [$F_{(5,456)}$ = 11.10, **$p$ < 0.01 vs. rest of the groups, ‡‡$p$ < 0.01 vs. Control, Control + EPO20]; 10–20 μm [$F_{(5,668)}$ = 10.48, **$p$ < 0.01 vs. rest of the groups; ††$p$ < 0.01 vs. Control + EPO20, Col + EPO10 and Col + EPO20]; 20–30 μm [$F_{(5,655)}$ = 8.77, **$p$ < 0.01 vs. rest of the groups]; 30–40 μm [$F_{(5,662)}$ = 6.60, **$p$ < 0.01 vs. rest of the groups]; 40–50 μm [$F_{(5,664)}$ = 8.42, **$p$ < 0.01 vs. rest of the groups]; 50–60 μm [$F_{(5,674)}$ = 6.51, **$p$ < 0.01 vs. rest of the groups]) (**Figure 2E**). Neuron curvature ratio was also impaired after Col lesions and EPO treatment significantly ameliorated this situation both at P14 ([$F_{(5,813)}$ = 5.78, **$p$ < 0.01 vs. rest of the groups]) and P70 ([$F_{(5,565)}$ = 5.901, **$p$ < 0.01 vs. rest of the groups]) (**Figure 2F**). Spine density (number of spines/10 μm) was also restored after EPO treatment in the short (P14 [$F_{(5,3985)}$ = 27.55, **$p$ < 0.01 vs. rest of the groups, ‡‡$p$ < 0.01 vs. Control, Control + EPO10 and Control + EPO20, ##$p$ < 0.01 vs. Control and Control + EPO10]) and the long term (P70 [$F_{(5,1091)}$ = 15.44, **$p$ < 0.01 vs. rest of the groups, ‡‡$p$ < 0.01 vs. Control, Control + EPO10 and Control + EPO20, –$p$ < 0.01 vs. Control + EPO10]) (**Figures 2G,H**).

## EPO Treatment Reduces Central Bleeding in a GM-IVH Model

Increased hemorrhage burden in the SVZ after Col lesions was completely reversed by EPO10 and EPO20 administration at P14 [$F_{(5,112)}$ = 11.089, *$p$ = 0.013 vs. rest of the groups] and P70 [$F_{(5,125)}$ = 11.089, **$p$ < 0.01 vs. rest of the groups], due to a reduction in the number of individual hemorrhages (P14: [$F_{(5,111)}$ = 2,76, *$p$ = 0.021 vs. rest of the groups]; P70: [$F_{(5,127)}$ = 15.36, **$p$ < 0.01 vs. rest of the groups], while individual hemorrhage size was not affected (P14: [$F_{(5,1111)}$ = 1.55, $p$ = 0.169] P70 [$F_{(5,149)}$ = 0.967, $p$ = 0.440]) (**Figure 3A**). A similar profile was observed in the cortex and increased hemorrhage burden was reduced by EPO (P14 [$F_{(5,271)}$ = 12.16, **$p$ < 0.01 vs. rest of the groups]; P70 [$F_{(5,277)}$ = 6.64, **$p$ < 0.01 vs. rest of the groups]),

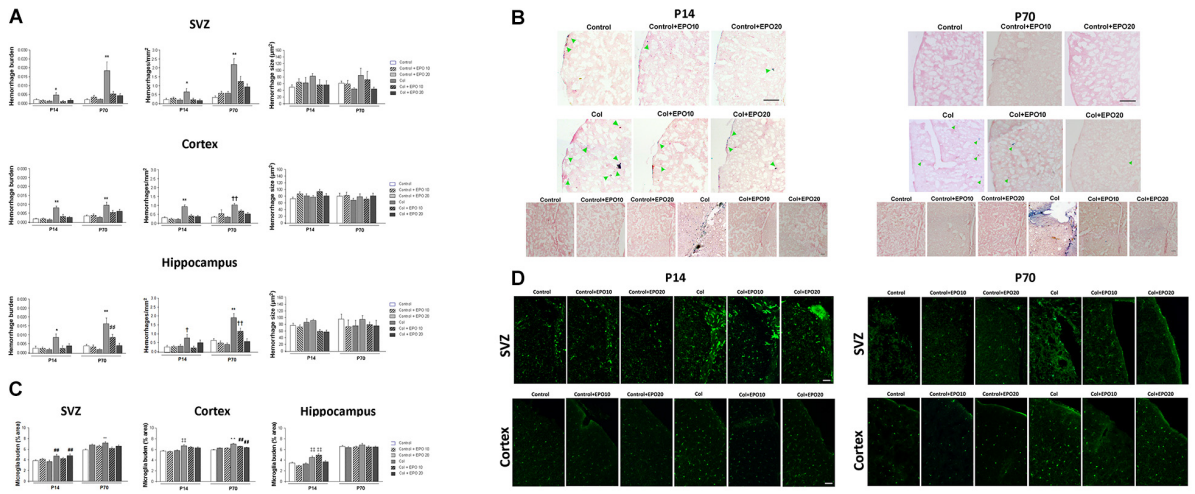


**FIGURE 3 |** EPO treatment reduces vascular damage and inflammation after inducing a GM-IVH. **(A)** Hemorrhage burden was significantly increased in the SVZ after Col lesions and EPO10 and EP20 treatments reversed this effect, both in the short (P14) and the long term (P70) (P14: $*p = 0.013$ vs. rest of the groups and P70: $**p < 0.01$ vs. rest of the groups). The number of individual hemorrhages was reduced after EPO treatment (P14: $*p = 0.021$ vs. rest of the groups; P70: $**p < 0.01$ vs. rest of the groups), while individual hemorrhage size was not affected (P14: $p = 0.169$]; P70: $p = 0.440$]. When we analyzed the cortex we observed a similar profile and increased hemorrhage burden, after Col lesions, was reduced by EPO treatment (P14: $**p < 0.01$ vs. rest of the groups; P70: $**p < 0.01$ vs. rest of the groups), due to a reduction in the number of individual hemorrhages after the treatment (P14: $**p < 0.01$ vs. rest of the groups; P70: $††p < 0.01$ vs. Control, Control + EPO10, Control + EPO20 and Col + EPO20), while hemorrhage size was not affected (P14: $p = 0.123$; P70: $p = 0.296$). In the hippocampus, increased hemorrhage burden in the ipsilateral side was reversed by EPO administration (P14: $*p = 0.02$ vs. rest of the groups; P70: $**p < 0.01$ vs. rest of the groups, $##p < 0.01$ vs. Control + EPO10 and Control + EPO20). The number of individual hemorrhages was reduced after the treatment (P14: $†p = 0.046$ vs. Control, Control + EPO10, Control + EPO20 and Col + EPO10; and P70: $**p < 0.01$ vs. rest of the groups, $††p < 0.01$ vs. Control, Control + EPO10, Control + EPO20, Col + EPO20) while hemorrhage size was not affected (P14: $p = 0.005$, no further differences detected; P70: $p = 0.270$). **(B)** Illustrative images of cortical Prussian blue staining and Congo red counterstain for hemorrhages. Increased bleeding after Col lesions was reduced by EPO treatment both at P14 and P70. Green arrow point at individual cortical hemorrhages. Scale bar = 250 μm. Bottom panels show increased hemorrhage burden in the SVZ from Col-lesioned animals, both at P14 and P70. Scale bar = 25 μm. **(C)** Microglia activation after Col lesions was reduced by EPO treatment at P14 and P70 in the SVZ (P14: $##p = 0.003$ vs. Control and Control + EPO20; P70: $**p < 0.01$ vs. rest of the groups), cortex (P14: $‡‡p < 0.01$; P70: $**p < 0.01$ vs. rest of the groups; $##p < 0.01$ vs. Control) and hippocampus (P14: $‡‡p < 0.01$ vs. Control, Control + EPO10 and Control + EPO20; P70: $p = 0.098$). **(D)** Illustrative example of microglia immunostaining for IBA-1 (green) in the SVZ and cortex from all groups under study. Increased microglia activation can be observed in Col-treated mice while EPO treatment significantly reduces this effect. Scale bar = 50 μm.

number of individual hemorrhages was reduced by EPO (P14 [$F_{(5,266)} = 20.75$, $**p < 0.01$ vs. rest of the groups]; P70 [$F_{(5,228)} = 10.01$, $††p < 0.01$ vs. Control, Control + EPO10, Control + EPO20 and Col + EPO20]) while hemorrhage size was not affected (P14 [$F_{(5,553)} = 1.74$, $p = 0.123$]; P70 [$F_{(5,690)} = 1.22$, $p = 0.296$]) (**Figures 3A,B**). The hippocampus showed a similar trend (hemorrhage burden: P14 [$F_{(5,124)} = 2.79$, $*p = 0.02$ vs. rest of the groups]; P70 [$F_{(5,103)} = 13.01$ $**p < 0.01$ vs. rest of the groups, $##p < 0.01$ vs. Control + EPO10 and Control + EPO20]; number of hemorrhages: P14 [$F_{(5,124)} = 2.33$, $†p = 0.046$ vs. Control, Control + EPO10, Control + EPO20 and Col + EPO10] and P70 [$F_{(5,116)} = 15.80$, $**p < 0.01$ vs. rest of the groups, $††p < 0.01$ vs. Control, Control + EPO10, Control + EPO20, Col + EPO20] and hemorrhage size: P14 [$F_{(5,285)} = 3.42$, $p = 0.005$, no further differences detected], P70 [$F_{(5,286)} = 1.28$, p = 0.270]).

## Inflammation Is Reduced in a GM-IVH After EPO Treatment

After Col lesions, microglia burden was analyzed in the SVZ, cortex and hippocampus at P14 and P70. Col-induced GM-IVH increased microglia burden, and EPO treatment limited this effect when we analyzed the SVZ at P14 [$F_{(5,817)} = 3.63$, $##p = 0.003$ vs. Control and Control + EPO20] and at P70 [$F_{(5,768)} = 4.71$, $**p < 0,01$ vs. rest of the groups] (**Figures 3C,D**). We observed a similar profile when we analyzed the cortex, and EPO treatment reduced microglia burden at P14 ([$F_{(5,3870)} = 12.66$, $‡‡p < 0,01$ vs. Control, Control + EPO10 and Control + EPO20]) and P70 ([$F_{(5,3521)} = 18.122$, $**p < 0,01$ vs. rest of the groups; $##p < 0.01$ vs. Control]) (**Figures 3C,D**). In the hippocampus, EPO treatment successfully reduced microglia burden at the highest dose (EPO20) at P14 [$F_{(5,775)} = 14.78$, $‡‡p < 0.01$ vs. Control, Control + EPO10 and Control + EPO20], whereas differences did not reach statistical significance at P70 [$F_{(5,687)} = 1.86$, $p = 0.098$]) (**Figure 3C**).

## EPO Treatment Reduces Tau Phosphorylation in a GM-IVH Murine Model

Increased tau phosphorylation after Col lesions was reduced by EPO treatment at P14, however, differences did not reach statistical significance (striatum [$F_{(5,25)} = 1.61$, $p = 0.193$]; cortex: [$F_{(5,25)} = 0.275$, $p = 0.922$] and hippocampus: [$F_{(5,24)} = 0.8889$, $p = 0.504$]) (**Figures 4A,B**). At P70 EPO

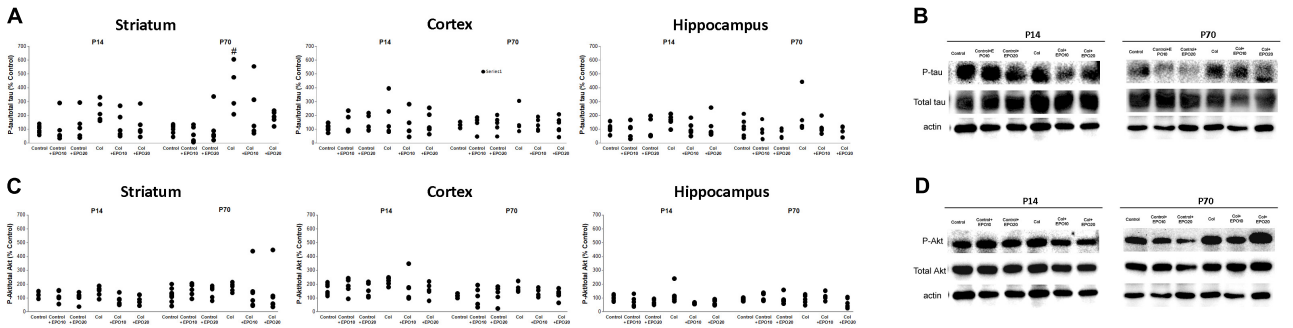


**FIGURE 4 |** EPO treatment reduces tau and Akt phosphorylation after Col lesions. **(A)** Increased tau phosphorylation after Col lesions was reduced after EPO treatment at P14 although differences did not reach statistical significance (striatum: $p = 0.193$; cortex: $p = 0.922$ and hippocampus: $p = 0.504$]). A similar profile was observed when we analyzed animals in the long term (P70) (striatum: #$p = 0.023$ vs Control + EPO20; cortex: $p = 0.658$ and hippocampus: $p = 0.522$). **(B)** Illustrative example of phospho-tau/total tau striatum westerns blots at P14 and P70, showing an increased phosphorylation after Col lesions at P70, that is reduced by EPO treatment. **(C)** Increased phosphor-Akt/total Akt ratios after Col lesions were reduced by EPO treatment in the ipsilateral hemisphere although differences did not reach statistical significance at P14 (striatum: $p = 0.127$; cortex: $p = 0.552$; hippocampus: $p = 0.055$) or at P70 (striatum: $p = 0.931$; cortex: $p = 0.425$; hippocampus: $p = 0.475$). **(D)** Illustrative example of striatum phosphor-Akt/total Akt western blots at P14 and P70, after EPO treatments.

limited tau hyperphosphorylation in the striatum [$F_{(5,26)} = 3.17$, #$p = 0.023$ vs. Control + EPO20]) and while a similar profile was observed in the hippocampus, differences did not reach statistical significance [$F_{(5,24)} = 0.860$, $p = 0.522$]. No differences were observed in the cortex at P70 [$F_{(5,24)} = 0.659$, $p = 0.658$] (**Figures 4A,B**).

## Effect of EPO Treatment on Akt Phosphorylation in a GM-IVH Murine Model

We detected a slight increase in phosphoAkt/total Akt ratios after inducing a GM-IVH. EPO treatment reduced this effect in the ipsilateral hemisphere although no differences were observed at P14 (striatum [$F_{(5,25)} = 1.91$, $p = 0.127$]; cortex [$F_{(5,25)} = 0{,}813$, $p = 0.552$], hippocampus [$F_{(5,24)} = 2.54$, $p = 0.055$]) (**Figures 4C,D**) or P70 (striatum P70 [$F_{(5,30)} = 0.260$, $p = 0.931$]; cortex [$F_{(5,22)} = 1.029$, $p = 0.425$]; hippocampus [$F_{(5,31)} = 0.930$, $p = 0.475$]) (**Figures 4C,D**).

## EPO Treatment Reduces Alterations in Plasma Markers After Col Lesions

MMP9 plasma levels were not significantly affected (P14 [$F_{(5,63)} = 0.689$, $p = 0.633$]; P70 [$F_{(5,63)} = 0.953$, $p = 0.453$]) (**Figure 5A**). On the other hand, gelsolin levels were reduced after Col lesions at P14, as described (Segado-Arenas et al., 2018), while EPO treatment counterbalanced this situation [$F_{(5,60)} = 4.372$, $^{**}p = 0.002$ vs. rest of the groups]. Differences were no longer significant in the long term (P70 [$F_{(5,60)} = 0.770$, $p = 0.575$]) (**Figure 5B**).

# DISCUSSION

Germinal matrix-intraventricular hemorrhage remains one of the most serious complications of the PTI (Mukerji et al., 2015) and has no successful treatment (Brouwer et al., 2014). Most of the current approaches have focused on strengthening the GM or stabilizing brain blood flow to prevent the GM-IVH (Ballabh, 2010). Prenatal glucocorticoids (Carson et al., 2016), indomethacin (Fowlie and Davis, 2003) or phenobarbital have been proposed as feasible treatments. On the other hand, it has also been suggested that stem cells therapy might provide an encouraging approach. Nevertheless, some limitations still exist, such as choosing the right cells, the appropriate patients or routes of administration. Also, safety issues remain to be solved and significantly limit the use of stem cells in the clinic (Chang et al., 2017).

Recombinant human EPO is regularly used to prevent or treat anemia of the PTI and studies in patients reveal that the early use of erythropoiesis-stimulating agents may reduce the incidence of GM-IVH and be neuroprotective (Neubauer et al., 2010). The doses of EPO used in our study are high when compared with those used in PTI patients (Juul et al., 2020). Dose conversion remains a relevant issue in experimental animal models (for review Nair and Jacob, 2016) and doses tend to be reduced as we ascend in the phylogenetic scale. The doses used in our study are in the range of those previously used in other neonate murine models (Kaindl et al., 2008; Fan et al., 2011; Hoeber et al., 2016; Zhang et al., 2020). Moreover, safety of EPO has been previously addressed with large doses of EPO, even in extremely low weight infants (McAdams et al., 2013). Erythropoiesis-stimulating agents may also have a positive effect on neurodevelopmental impairment of the PTI (for review see Ohlsson and Aher, 2017, 2020). Following this idea, and while results remain controversial, EPO may specifically provide beneficial effects on the neurodevelopment outcome in the PTI without severe adverse side effects (Wang et al., 2015). Nevertheless later updates on the beneficial effects of EPO remain controversial and the promising, but conflicting, results related to EPO as a neuroprotective agent require further study (Ohlsson and Aher, 2020). Moreover, several clinical trials have been in progress in the last few years assessing EPO in neonatal populations (Maxwell et al., 2017). The multicenter (19 sites,

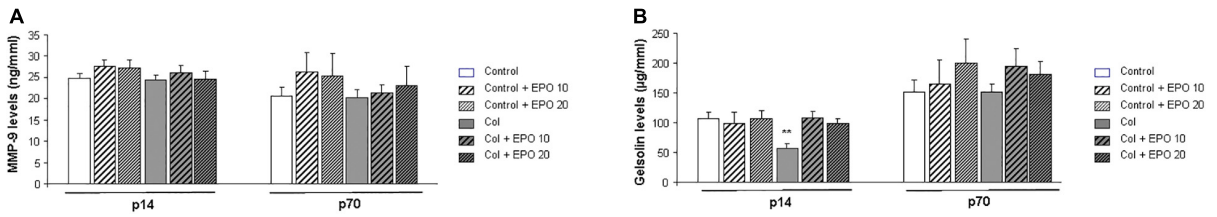


**FIGURE 5 |** Effect of EPO treatment on peripheral markers of GM-IVH. **(A)** EPO treatment does not affect MMP9 plasma levels at P14 ($p = 0.633$) or P70 ($p = 0.453$). **(B)** EPO treatment restores plasma gelsolin levels after inducing a GM-IVH in the short term, while differences are no longer detected in the long term (P70) (P14 $^{**}p = 0.002$ vs. rest of the groups, P70 $p = 0.575$).

30 hospitals), randomized, double-blind trial of EPO, PENUT (Preterm Epo Neuroprotection), has recently shown limited effects on very PTI after ≈2 years follow up. The PENUT study is an extremely relevant study on the field, however, individual groups were not analyzed and it remains possible that cognitive and physical problems might become evident later in life (Juul et al., 2020). Following this idea, Volpe (2020) has commented this aspect as a main limitation, also acknowledged in the study, since cognitive testing at 2 years of age is not as reliable as testing at later ages. In this sense, other studies comparing early assessments (before 3 years of age) with later cognitive tests at school age, showed a relatively low pooled sensitivity (55%) of early assessments to identify school-age cognitive deficits. Moreover, EPO is especially successful in protecting preoligodendrocytes. White matter development is an active process that continues well after infancy and it's closely related to specific cognitive functions that may be affected at later stages. Therefore Volpe suggests the necessity of testing longer duration of treatment, reaching full-term equivalent age or even longer (Volpe, 2020). A previous meta-analysis has also showed that that prophylactic EPO improves cognitive development (Fischer et al., 2017) and early EPO treatment may decrease the rates of necrotizing enterocolitis as well as brain complications, including IVH and periventricular leukomalacia (Ohlsson and Aher, 2017). Moreover, it seems that an early high dose of EPO has a weak but widespread effect on brain structural connectivity network in very PTI, supporting a trophic effect of EPO that increases network segregation, predominantly in local connections (Jakab et al., 2019). Nevertheless, recent updates report a limited success of EPO treatment (Ohlsson and Aher, 2020), supporting further studies given the controversial outcomes. Altogether, and given the present results, EPO administration is not currently recommended because the benefits are not fully established (Ohlsson and Aher, 2017; Fleiss and Gressens, 2019) and the underlying mechanisms and specific effects in the GM-IVH have not been studied in depth. At this point, as it has previously been stressed out there are no preclinical data showing the neuroprotective effects of EPO in a model of encephalopathy of prematurity, limiting the understanding of the best paradigm to deliver neuroprotection in this population (Fleiss and Gressens, 2019).

In order to help disentangle the effects of EPO treatment, we have treated with EPO a recently characterized murine model of GM-IVH of the preterm newborn, induced by Col administration (Segado-Arenas et al., 2018). While evident limitations persist, it is noteworthy that this model reproduces morphological, functional and neurodevelopmental alterations of the GM-IVH. Col administration in the lateral ventricle breaks the extracellular matrix that surrounds the GM capillaries, increases blood brain barrier permeability and induces bleeding (Segado-Arenas et al., 2018). Moreover Col administration to neonate (P7) CD1 mice results in brain atrophy, ventricle enlargement, increased inflammation, widespread small vessel damage and cognitive impairment that are still detected in the adulthood (Segado-Arenas et al., 2018), as observed in the clinic. EPO treatment, at 10.000 or 20.000 IU/Kg significantly ameliorated learning and memory alterations in the long term (P70). Although the fact that young P14 mice cannot be assessed at cognitive level is limiting, early histopathological complications at P14 match the functional outcomes at P70. In our hands, motor-related alterations are limited with this approach, and we cannot exclude that larger lesions could reproduce motor impairment as regularly observed in the clinic (Hinojosa-Rodríguez et al., 2017). While the studies on the effect of EPO in neonates with GM-IVH are limited (Ruegger et al., 2015), our data are in accordance with a seminal study by Neubauer et al. (2010) in which children with GM-IVH showed a remarkably strong benefit from EPO treatment at 5 years of age and later. While some controversy persists (Leuchter et al., 2014; Natalucci et al., 2016), these observations are also in line with studies showing that EPO improves cognitive outcomes in PTI both early in life (18–22 months) (Wang et al., 2015) and once the patients reach school (3.5–4 years old) (Ohls et al., 2016).

Morphopathological changes after Col lesions resemble those detected in PTI with GM-IVH, including complicated post-hemorrhagic ventricular dilatation (Brouwer et al., 2014). Moreover, these changes are directly associated with an overall brain atrophy and bad prognosis (Saliba et al., 1990). Also, the neuronal population is compromised around the ventricles (Georgiadis et al., 2008), as well as in areas located far from the lesion area, such as the cortex, supporting an overspread long-lasting damage, as previously described (Segado-Arenas et al., 2018). The mechanisms implicated have not been elucidated, and atrophy has been attributed to both loss of ischemic infracted tissue and defective development of the damaged areas (Semple et al., 2013). In our hands, curvature ratio, as an indicator of neuron wellness (Infante-Garcia et al., 2015), neuronal complexity and spine density were compromised

in mice after GM-IVH, while EPO treatment rescued these alterations, supporting its neurotrophic role (Juul and Pet, 2015) and neuroprotective effect at different levels. To our knowledge, the role of EPO in a model of GM-IVH of the PTI has not been previously assessed, however, in line with our observations, EPO protects against striatum atrophy, hippocampus injury, and white matter loss in a model of hypoxia-ischemia in neonatal mice (Fan et al., 2011).

We observed an increase of widespread hemorrhages after Col lesions, as previously described (Segado-Arenas et al., 2018). Hemorrhage density and burden seem to be higher in the SVZ at later ages (P70), suggesting that small vessel damage might be a long-term consequence of the GM-IVH. We never addressed age differences, since P14 brains are extremely immature (Semple et al., 2013) and can hardly be compared to fully developed P70 brains. The fact that EPO treatment successfully counterbalances this effect might be attributed to its role in erythropoiesis, that requires iron utilization, and therefore reduces the potential toxicity of free iron (Juul and Ferriero, 2014). Likewise, EPO promotes revascularization in hypoxic-ischemic neonatal models (Iwai et al., 2007). Previous studies have also shown that EPO induces angiogenesis through the production of vascular endothelial growth factor, protecting capillaries (Wang et al., 2008) and bood brain barrier integrity (Marti et al., 2000). Col lesions also provoked an inflammatory response that is commonly observed in PTI (Juul and Ferriero, 2014). The antioxidant and anti-inflammatory effects of EPO have been widely assessed in different models of brain insult (Wei et al., 2017) and in our hands EPO treatment significantly reduces microglia activation after GM-IVH induction. Iba-1 immunostatining is classically used to label microglia, however, we only analyzed microglia burden and it is possible that more complex inflammatory changes are not covered with our approach. Previous studies have shown that microglia express EPO receptors (Nagai et al., 2001) and that EPO may reduce motility, as an important feature of microglial pathological reaction to damage (Mitkovski et al., 2015), while promoting the polarization of microglia toward the protective M2 phenotype (Wei et al., 2017).

Hyperphosphorylated tau is a toxic pathological hallmark of neurodegenerative disorders, increased in this and other models with central hemorrhages (Infante-Garcia et al., 2016; Segado-Arenas et al., 2018). Col lesions increased tau phosphorylation in the striatum, as the closest area to the ventricle. EPO slightly reduced this situation in the striatum and no effect was detected in the cortex or the hippocampus. Previous studies have reported that EPO, alone or combined with other treatments, may reduce tau phosphorylation associated to different cognitive disorders (Kang et al., 2010; Vinothkumar et al., 2019). Even though glycogen synthase kinase-3β inhibition reduces tau phosphorylation (Maqbool et al., 2016), enhances myelination, improves clinical recovery in a model of GM-IVH (Dohare et al., 2018a) and restores altered neurogenesis in preterm patients with intraventricular hemorrhage (Dohare et al., 2018b), the narrow effect in our studies limits further conclusions at this level. Also, since Akt is implicated in cell cycle regulation, cell survival and apoptosis, it is feasible that the beneficial effects observed after EPO treatment could be Akt-mediated. Previous studies have shown that Akt phosphorylation is increased in subarachnoid hemorrhage models (Guo et al., 2018). It has also been pointed out that EPO, in combination with insulin-like growth factor-1, may contribute to increase Akt activation (Kang et al., 2010). However, we only observed a slight increase in phopho-Akt levels after inducing a GM-IVH.

MMP9 levels were not affected, in agreement with previous studies (Segado-Arenas et al., 2018). On the other hand, plasma gelsolin levels were significantly reduced in mice after GM-IVH, as previously reported (Segado-Arenas et al., 2018). Plasma gelsolin is a feasible peripheral marker of central complications and low plasma gelsolin levels have been associated with poor outcomes in adult brain hemorrhagic alterations (Chou et al., 2011), in premature infants (Kose et al., 2014) and other newborn complications (Benavente-Fernandez et al., 2018). EPO treatment significantly restores plasma gelsolin levels, suggesting that its positive effects at central level are also detected in the periphery and reinforcing further studies on the utility of plasma gelsolin as a prognostic tool.

## CONCLUSION

Erythropoietin is a safe, already approved drug to treat other complications of the PTI. Altogether, our data support further assessment of EPO (Volpe, 2020) as a feasible treatment to protect against central complications associated to GM-IVH in the short (P14) and the long term (P70). Moreover we provide evidence of gelsolin, as a feasible marker for a devastating disease. Ultimately, our study helps to further understand the pathophysiology underlying the IVH of the preterm newborn and the best paradigms to define new protection for PTI (Fleiss and Gressens, 2019).

## DATA AVAILABILITY STATEMENT

The raw data supporting the conclusions of this article will be made available by the authors, without undue reservation upon reasonable request.

## ETHICS STATEMENT

The animal study was reviewed and approved by Junta de Andalucia (Guidelines for Care and Use of Experimental Animals, European Commission Directive 2010/63/UE and Spanish Royal Decree 53/2013) and the University of Cádiz Bioethics Committee.

## AUTHOR CONTRIBUTIONS

CH-B, CI-G, DS-S, and AM: experiments design, data acquisition, analysis, and interpretation. AC-R, CM-G, CL-P, and MB-M: data acquisition and analysis. IB-F: study concept and design and critical revision of manuscript for intellectual content. SL-L and MG-A: study concept and design, drafting, and critical revision

of manuscript for intellectual content. All authors read and approved the final manuscript.

## FUNDING

CH-B Predoctoral Fellowship, Universidad de Cádiz. MG-A Programa Estatal de I+D+I Orientada a los Retos de la Sociedad (BFU 2016-75038-R), financed by the Agencia Estatal de Investigación (AEI) and Fondo Europeo de Desarrollo Regional (FEDER), Ministerio de Ciencia, Innovación y Universidades. I+D+i Programa operativo FEDER Andalucía 2014–2020 FEDER-UCA18-107189. MG-A and IB-F Proyectos de Investigación e Innovación para Grupos de Investigación INIBICA (LI19/11IN-CO34).

## REFERENCES

Ballabh, P. (2010). Intraventricular hemorrhage in premature infants: mechanism of disease. *Pediatr Res.* 67, 1–8. doi: 10.1203/pdr.0b013e3181c1b176

Benavente-Fernandez, I., Ramos-Rodriguez, J. J., Infante-Garcia, C., Jimenez-Gomez, G., Lechuga-Sancho, A., Lubian-Lopez, S., et al. (2018). Altered plasma-type gelsolin and amyloid-beta in neonates with hypoxic-ischaemic encephalopathy under therapeutic hypothermia. *J. Cereb. Blood Flow. Metab.* 39, 1349–1354. doi: 10.1177/0271678x18757419

Brouwer, A. J., Groenendaal, F., Benders, M. J., and de Vries, L. S. (2014). Early and late complications of germinal matrix-intraventricular haemorrhage in the preterm infant: what is new? *Neonatology* 106, 296–303. doi: 10.1159/000365127

Carson, R., Monaghan-Nichols, A. P., DeFranco, D. B., and Rudine, A. C. (2016). Effects of antenatal glucocorticoids on the developing brain. *Steroids* 114, 25–32. doi: 10.1016/j.steroids.2016.05.012

Chang, Y. S., Ahn, S. Y., Sung, S., and Park, W. S. (2017). Stem cell therapy for neonatal disorders: prospects and challenges. *Yonsei Med. J.* 58, 266–271. doi: 10.3349/ymj.2017.58.2.266

Chou, S. H., Lee, P. S., Konigsberg, R. G., Gallacci, D., Chiou, T., Arai, K., et al. (2011). Plasma-type gelsolin is decreased in human blood and cerebrospinal fluid after subarachnoid hemorrhage. *Stroke* 42, 3624–3627. doi: 10.1161/strokeaha.111.631135

Dohare, P., Cheng, B., Ahmed, E., Yadala, V., Singla, P., Thomas, S., et al. (2018a). Glycogen synthase kinase-3beta inhibition enhances myelination in preterm newborns with intraventricular hemorrhage, but not recombinant Wnt3A. *Neurobiol. Dis.* 118, 22–39. doi: 10.1016/j.nbd.2018.06.015

Dohare, P., Kidwai, A., Kaur, J., Singla, P., Krishna, S., Klebe, D., et al. (2018b). GSK3beta inhibition restores impaired neurogenesis in preterm neonates with intraventricular hemorrhage. *Cereb Cortex* 29, 3482–3495. doi: 10.1093/cercor/bhy217

Fan, X., Heijnen, C. J., van der, K. M., Groenendaal, F., and van Bel, F. (2011). Beneficial effect of erythropoietin on sensorimotor function and white matter after hypoxia-ischemia in neonatal mice. *Pediatr Res.* 69, 56–61. doi: 10.1203/pdr.0b013e3181fcbef3

Fischer, H. S., Reibel, N. J., Bührer, C., and Dame, C. (2017). Prophylactic early erythropoietin for neuroprotection in preterm infants: a meta-analysis. *Pediatrics* 139:e20164317. doi: 10.1542/peds.2016-4317

Fleiss, B., and Gressens, P. (2019). "Neuroprotection of the preterm brain," in *Handbook of Clinical Neurology, (3rd Series)*, Vol. 162, eds L. D. Vries and H. Glass (Amsterdam: Elsevier).

Fowlie, P. W., and Davis, P. G. (2003). Prophylactic indomethacin for preterm infants: a systematic review and meta-analysis. *Arch. Dis. Child Fetal. Neonatal Ed.* 88, F464–F466.

Georgiadis, P., Xu, H., Chua, C., Hu, F., Collins, L., Huynh, C., et al. (2008). Characterization of acute brain injuries and neurobehavioral profiles in a rabbit model of germinal matrix hemorrhage. *Stroke* 39, 3378–3388. doi: 10.1161/strokeaha.107.510883

Guo, D., Xie, J., Zhao, J., Huang, T., Guo, X., and Song, J. (2018). Resveratrol protects early brain injury after subarachnoid hemorrhage by activating autophagy and inhibiting apoptosis mediated by the Akt/mTOR pathway. *Neuroreport* 29, 368–379. doi: 10.1097/wnr.0000000000000975

Hinojosa-Rodríguez, M., Harmony, T., Carrillo-Prado, C., Van Horn, J. D., Irimia, A., Torgerson, C., et al. (2017). Clinical neuroimaging in the preterm infant: diagnosis and prognosis. *Neuroimage Clin.* 16, 355–368. doi: 10.1016/j.nicl.2017.08.015

Hoeber, D., Sifringer, M., van de Looij, Y., Herz, J., Sizonenko, S. V., Kempe, K., et al. (2016). Erythropoietin restores long-term neurocognitive function involving mechanisms of neuronal plasticity in a model of hyperoxia-induced preterm brain injury. *Oxid Med. Cell Longev.* 2016:9247493.

Infante-Garcia, C., Jose Ramos-Rodriguez, J., Delgado-Olmos, I., Gamero-Carrasco, C., Teresa Fernandez-Ponce, M., Casas, L., et al. (2017). Long-term mangiferin extract treatment improves central pathology and cognitive deficits in APP/PS1 mice. *Mol. Neurobiol.* 54, 4696–4704. doi: 10.1007/s12035-016-0015-z

Infante-Garcia, C., Jose Ramos-Rodriguez, J., Marin-Zambrana, Y., Teresa Fernandez-Ponce, M., Casas, L., Mantell, C., et al. (2016). Mango leaf extract improves central pathology and cognitive impairment in a type 2 diabetes mouse model. *Brain Pathol.* 27, 499–507. doi: 10.1111/bpa.12433

Infante-Garcia, C., Ramos-Rodriguez, J. J., Galindo-Gonzalez, L., and Garcia-Alloza, M. (2015). Long-term central pathology and cognitive impairment are exacerbated in a mixed model of Alzheimer's disease and type 2 diabetes. *Psychoneuroendocrinology* 65, 15–25. doi: 10.1016/j.psyneuen.2015.12.001

Iwai, M., Cao, G., Yin, W., Stetler, R. A., Liu, J., and Chen, J. (2007). Erythropoietin promotes neuronal replacement through revascularization and neurogenesis after neonatal hypoxia/ischemia in rats. *Stroke* 38, 2795–2803. doi: 10.1161/strokeaha.107.483008

Jakab, A., Ruegger, C., Bucher, H. U., Makki, M., Huppi, P. S., Tuura, R., et al. (2019). Network based statistics reveals trophic and neuroprotective effect of early high dose erythropoetin on brain connectivity in very preterm infants. *Neuroimage Clin.* 22:101806. doi: 10.1016/j.nicl.2019.101806

Juul, S. E., Comstock, B. A., Wadhawan, R., Mayock, D. E., Courtney, S. E., Robinson, T., et al. (2020). A randomized trial of erythropoietin for neuroprotection in preterm infants. *N. Engl. J. Med.* 382, 233–243.

Juul, S. E., and Ferriero, D. M. (2014). Pharmacologic neuroprotective strategies in neonatal brain injury. *Clin. Perinatol.* 41, 119–131. doi: 10.1016/j.clp.2013.09.004

Juul, S. E., and Pet, G. C. (2015). Erythropoietin and neonatal neuroprotection. *Clin. Perinatol.* 42, 469–481. doi: 10.1016/j.clp.2015.04.004

Kaindl, A. M., Sifringer, M., Koppelstaetter, A., Genz, K., Loeber, R., Boerner, C., et al. (2008). Erythropoietin protects the developing brain from hyperoxia-induced cell death and proteome changes. *Ann. Neurol.* 64, 523–534. doi: 10.1002/ana.21471

Kang, Y. J., Digicaylioglu, M., Russo, R., Kaul, M., Achim, C. L., Fletcher, L., et al. (2010). Erythropoietin plus insulin-like growth factor-I protects against neuronal damage in a murine model of human immunodeficiency virus-associated neurocognitive disorders. *Ann. Neurol.* 68, 342–352. doi: 10.1002/ana.22070

Kollensperger, M., Krismer, F., Pallua, A., Stefanova, N., Poewe, W., and Wenning, G. K. (2011). Erythropoietin is neuroprotective in a transgenic mouse model of multiple system atrophy. *Mov. Disord.* 26, 507–515. doi: 10.1002/mds.23474

Kose, M., Elmas, T., Gokahmetoglu, S., Ozturk, M. A., Ekinci, D., Elmali, F., et al. (2014). Predictive value of gelsolin for the outcomes of preterm neonates: a pilot study. *Pediatr Int.* 56, 856–859. doi: 10.1111/ped.12391

Leuchter, R. H., Gui, L., Poncet, A., Hagmann, C., Lodygensky, G. A., Martin, E., et al. (2014). Association between early administration of high-dose erythropoietin in preterm infants and brain MRI abnormality at term-equivalent age. *JAMA.* 312, 817–824. doi: 10.1001/jama.2014.9645

Lombardero, M., Kovacs, K., and Scheithauer, B. W. (2011). Erythropoietin: a hormone with multiple functions. *Pathobiology* 78, 41–53. doi: 10.1159/000322975

Maqbool, M., Mobashir, M., and Hoda, N. (2016). Pivotal role of glycogen synthase kinase-3: a therapeutic target for Alzheimer's disease. *Eur. J. Med. Chem.* 107, 63–81. doi: 10.1016/j.ejmech.2015.10.018

Marti, H. H., Bernaudin, M., Petit, E., and Bauer, C. (2000). Neuroprotection and angiogenesis: dual role of erythropoietin in brain ischemia. *News Physiol. Sci.* 15, 225–229. doi: 10.1152/physiologyonline.2000.15.5.225

Maxwell, J. R., Yellowhair, T. R., Oppong, A. Y., Camacho, J. E., Lowe, J. R., Jantzie, L. L., et al. (2017). Cognitive development in preterm infants: multifaceted deficits reflect vulnerability of rigorous neurodevelopmental pathways. *Minerva Pediatr.* 69, 298–313.

McAdams, R. M., McPherson, R. J., Mayock, D. E., and Juul, S. E. (2013). Outcomes of extremely low birth weight infants given early high-dose erythropoietin. *J. Perinatol.* 33, 226–230. doi: 10.1038/jp.2012.78

Mitkovski, M., Dahm, L., Heinrich, R., Monnheimer, M., Gerhart, S., Stegmuller, J., et al. (2015). Erythropoietin dampens injury-induced microglial motility. *J. Cereb. Blood Flow. Metab.* 35, 1233–1236. doi: 10.1038/jcbfm.2015.100

Mukerji, A., Shah, V., and Shah, P. S. (2015). Periventricular/intraventricular hemorrhage and neurodevelopmental outcomes: a meta-analysis. *Pediatrics* 136, 1132–1143. doi: 10.1542/peds.2015-0944

Nagai, A., Nakagawa, E., Choi, H. B., Hatori, K., Kobayashi, S., and Kim, S. U. (2001). Erythropoietin and erythropoietin receptors in human CNS neurons, astrocytes, microglia, and oligodendrocytes grown in culture. *J. Neuropathol. Exp. Neurol.* 60, 386–392. doi: 10.1093/jnen/60.4.386

Nair, A. B., and Jacob, S. (2016). A simple practice guide for dose conversion between animals and human. *J. Basic Clin. Pharm.* 7, 27–31. doi: 10.4103/0976-0105.177703

Natalucci, G., Latal, B., Koller, B., Rüegger, C., Sick, B., Held, L., et al. (2016). Effect of Early prophylactic high-dose recombinant human erythropoietin in very preterm infants on neurodevelopmental outcome at 2 years: a randomized clinical trial. *JAMA* 315, 2079–2085. doi: 10.1001/jama.2016.5504

Neubauer, A. P., Voss, W., Wachtendorf, M., and Jungmann, T. (2010). Erythropoietin improves neurodevelopmental outcome of extremely preterm infants. *Ann. Neurol.* 67, 657–666.

Ohls, R. K., Cannon, D. C., Phillips, J., Caprihan, A., Patel, S., Winter, S., et al. (2016). Preschool assessment of preterm infants treated with darbepoetin and erythropoietin. *Pediatrics.* 137:e20153859. doi: 10.1542/peds.2015-3859

Ohlsson, A., and Aher, S. M. (2017). Early erythropoiesis-stimulating agents in preterm or low birth weight infants. *Cochrane Database Syst. Rev.* 11:CD004863.

Ohlsson, A., and Aher, S. M. (2020). Early erythropoiesis-stimulating agents in preterm or low birth weight infants. *Cochrane Database Syst Rev.* 2:CD004863.

Peng, M., Jia, J., and Qin, W. (2015). Plasma gelsolin and matrix metalloproteinase 3 as potential biomarkers for Alzheimer disease. *Neurosci Lett.* 595, 116–121. doi: 10.1016/j.neulet.2015.04.014

Perlman, J. M. (2009). The relationship between systemic hemodynamic perturbations and periventricular-intraventricular hemorrhage–a historical perspective. *Semin. Pediatr. Neurol.* 16, 191–199. doi: 10.1016/j.spen.2009.09.006

Ramos-Rodriguez, J. J., Sanchez-Sotano, D., Doblas-Marquez, A., Infante-Garcia, C., Lubian-Lopez, S., and Garcia-Alloza, M. (2017). Intranasal insulin reverts central pathology and cognitive impairment in diabetic mother offspring. *Mol. Neurodegener.* 12:57.

Ramos-Rodriguez, J. J., Spires-Jones, T., Pooler, A. M., Lechuga-Sancho, A. M., Bacskai, B. J., and Garcia-Alloza, M. (2016). Progressive neuronal pathology and synaptic loss induced by prediabetes and type 2 diabetes in a mouse model of Alzheimer's disease. *Mol. Neurobiol.* 54, 3428–3438. doi: 10.1007/s12035-016-9921-3

Razak, A., and Hussain, A. (2019). Erythropoietin in perinatal hypoxic-ischemic encephalopathy: a systematic review and meta-analysis. *J. Perinat. Med.* 47, 478–489. doi: 10.1515/jpm-2018-0360

Ruegger, C. M., Hagmann, C. F., Buhrer, C., Held, L., Bucher, H. U., and Wellmann, S. (2015). Erythropoietin for the repair of cerebral injury in very preterm infants (EpoRepair). *Neonatology* 108, 198–204. doi: 10.1159/000437248

Saliba, E., Bertrand, P., Gold, F., Marchand, S., and Laugier, J. (1990). Area of lateral ventricles measured on cranial ultrasonography in preterm infants: association with outcome. *Arch. Dis. Child* 65, 1033–1037. doi: 10.1136/adc.65.10_spec_no.1033

Segado-Arenas, A., Infante-Garcia, C., Benavente-Fernandez, I., Sanchez-Sotano, D., Ramos-Rodriguez, J. J., Alonso-Ojembarrena, A., et al. (2018). Cognitive impairment and brain and peripheral alterations in a murine model of intraventricular hemorrhage in the preterm newborn. *Mol. Neurobiol.* 55, 4896–4910. doi: 10.1007/s12035-017-0693-1

Semple, B. D., Blomgren, K., Gimlin, K., Ferriero, D. M., and Noble-Haeusslein, L. J. (2013). Brain development in rodents and humans: identifying benchmarks of maturation and vulnerability to injury across species. *Prog. Neurobiol.* 10, 1–16. doi: 10.1016/j.pneurobio.2013.04.001

Tan, A. P., Svrckova, P., Cowan, F., Chong, W. K., and Mankad, K. (2018). Intracranial hemorrhage in neonates: a review of etiologies, patterns and predicted clinical outcomes. *Eur. J. Paediatric Neurol.* 22, 690–717. doi: 10.1016/j.ejpn.2018.04.008

Vinothkumar, G., Krishnakumar, S., and Riya, V. P. (2019). Correlation between abnormal GSK3β, β Amyloid, total Tau, p-Tau 181 levels and neuropsychological assessment total scores in CKD patients with cognitive dysfunction: impact of rHuEPO therapy. *J. Clin. Neurosci.* 69, 38–42. doi: 10.1016/j.jocn.2019.08.073

Volpe, J. J. (2020). Commentary–Do the negative results of the PENUT trial close the book on erythropoietin for premature infant brain? *J. Neonatal. Perinatal. Med.* 13, 149–152. doi: 10.3233/npm-200444

Wang, H., Zhang, L., and Jin, Y. (2015). A meta-analysis of the protective effect of recombinant human erythropoietin (rhEPO) for neurodevelopment in preterm infants. *Cell Biochem. Biophys.* 71, 795–802. doi: 10.1007/s12013-014-0265-1

Wang, L., Chopp, M., Gregg, S. R., Zhang, R. L., Teng, H., Jiang, A., et al. (2008). Neural progenitor cells treated with EPO induce angiogenesis through the production of VEGF. *J. Cereb. Blood Flow Metab.* 28, 1361–1368. doi: 10.1038/jcbfm.2008.32

Wei, S., Luo, C., Yu, S., Gao, J., Liu, C., Wei, Z., et al. (2017). Erythropoietin ameliorates early brain injury after subarachnoid haemorrhage by modulating microglia polarization via the EPOR/JAK2-STAT3 pathway. *Exp. Cell Res.* 361, 342–352. doi: 10.1016/j.yexcr.2017.11.002

Xu, J. F., Liu, W. G., Dong, X. Q., Yang, S. B., and Fan, J. (2012). Change in plasma gelsolin level after traumatic brain injury. *J. Trauma Acute Care Surg.* 72, 491–496. doi: 10.1097/ta.0b013e318226ec39

Zhang, J., Luo, X., Huang, C., Pei, Z., Xiao, H., Huang, S., et al. (2020). Erythropoietin prevents LPS-induced preterm birth and increases offspring survival. *Am. J. Reprod. Immunol.* 84:e13283.

**Conflict of Interest:** The authors declare that the research was conducted in the absence of any commercial or financial relationships that could be construed as a potential conflict of interest.

frontiers in Cellular Neuroscience

ORIGINAL RESEARCH
published: 23 September 2020
doi: 10.3389/fncel.2020.547215

# Effect of β-Hydroxybutyrate on Autophagy Dynamics During Severe Hypoglycemia and the Hypoglycemic Coma

*Carmen Torres-Esquivel, Teresa Montiel, Marco Flores-Méndez† and Lourdes Massieu**

*Departamento de Neuropatología Molecular, División de Neurociencias, Instituto de Fisiología Celular, Universidad Nacional Autónoma de México, Ciudad de México, Mexico*

OPEN ACCESS

**Edited by:**
*João M. N. Duarte, Lund University, Sweden*

**Reviewed by:**
*Patricia Fernanda Schuck, Federal University of Rio de Janeiro, Brazil*
*Karin Borges, The University of Queensland, Australia*

***Correspondence:**
*Lourdes Massieu*
*lmassieu@ifc.unam.mx*

**†Present address:**
*Marco Flores-Méndez, Perelman Center for Cellular and Molecular Therapeutics, Children's Hospital of Philadelphia, Philadelphia, PA, United States*

**Specialty section:**
*This article was submitted to Cellular Neuropathology, a section of the journal Frontiers in Cellular Neuroscience*

**Received:** *30 March 2020*
**Accepted:** *31 August 2020*
**Published:** *23 September 2020*

**Citation:**
*Torres-Esquivel C, Montiel T, Flores-Méndez M and Massieu L (2020) Effect of β-Hydroxybutyrate on Autophagy Dynamics During Severe Hypoglycemia and the Hypoglycemic Coma. Front. Cell. Neurosci. 14:547215. doi: 10.3389/fncel.2020.547215*

Glucose supply from blood is mandatory for brain functioning and its interruption during acute hypoglycemia or cerebral ischemia leads to brain injury. Alternative substrates to glucose such as the ketone bodies (KB), acetoacetate (AcAc), and β-hydroxybutyrate (BHB), can be used as energy fuels in the brain during hypoglycemia and prevent neuronal death, but the mechanisms involved are still not well understood. During glucose deprivation adaptive cell responses can be activated such as autophagy, a lysosomal-dependent degradation process, to support cell survival. However, impaired or excessive autophagy can lead to cell dysfunction. We have previously shown that impaired autophagy contributes to neuronal death induced by glucose deprivation in cortical neurons and that D isomer of BHB (D-BHB) reestablishes the autophagic flux increasing viability. Here, we aimed to investigate autophagy dynamics in the brain of rats subjected to severe hypoglycemia (SH) without glucose infusion (GI), severe hypoglycemia followed by GI (SH + GI), and a brief period of hypoglycemic coma followed by GI (Coma). The effect of D-BHB administration after the coma was also tested (Coma + BHB). The transformation of LC3-I to LC3-II and the abundance of autophagy proteins, Beclin 1 (BECN1), ATG7, and ATG12–ATG5 conjugate, were analyzed as an index of autophagosome formation, and the levels of sequestrosome1/p62 (SQSTM1/p62) were determined as a hallmark of autophagic degradation. Data suggest that autophagosomes accumulate in the cortex and the hippocampus of rats after SH, likely due to impaired autophagic degradation. In the cortex, autophagosome accumulation persisted at 6 h after GI in animals exposed to SH but recovered basal levels at 24 h, while in the hippocampus no significant effect was observed. In animals subjected to coma, autophagosome accumulation was observed at 24 h after GI in both regions. D-BHB treatment reduced LC3-II and SQSTM1/p62 content and reduced ULK1 phosphorylation by AMPK, suggesting it stimulates the autophagic flux and decreases AMPK activity

reducing autophagy initiation. D-BHB also reduced the number of degenerating cells. Together, data suggest different autophagy dynamics after GI in rats subjected to SH or the hypoglycemic coma and support that D-BHB treatment can modulate autophagy dynamics favoring the autophagic flux.

**Keywords: hypoglycemia, ketone bodies, neuronal death, autophagy, AMPK**

## INTRODUCTION

The brain is a highly dynamic and energy-demanding organ that depends on the continuous glucose supply from blood, thereby disturbed glucose metabolism can lead to brain dysfunction and even brain injury (Mergenthaler et al., 2013). Reduced cerebral glucose delivery occurs during hypoglycemia, a condition considered as a major complication of insulin treatment in type 1 diabetes mellitus (DMT1) patients (Cryer, 2005). Patients can suffer two events of moderate hypoglycemia (60–40 mg/dl blood glucose) per week and one of severe hypoglycemia (SH, >35 mg/dl) per year. The presence of repeated episodes of moderate hypoglycemia increases the risk for SH, which can culminate in the state of coma resulting in irreversible brain damage in vulnerable brain regions, such as the cortex and hippocampus (Auer et al., 1984). Under conditions of limited glucose availability, such as ischemia, hypoxia, hypoglycemia, and cerebral trauma, alternative energy substrates to glucose, such as the ketone bodies (KB), acetoacetate (AcAc), and β-hydroxybutyrate (BHB), can be used by the brain (Melø et al., 2006) and prevent brain injury (Suzuki et al., 2002; Masuda et al., 2005; Puchowicz et al., 2008; Haces et al., 2008; Julio-Amilpas et al., 2015). KB are metabolized through the tricarboxylic acid cycle (TCA) and their protective effect has been attributed to enhanced cellular energy metabolism, improved mitochondrial activity, and decreased production of mitochondrial reactive oxygen species (ROS; Maalouf et al., 2007; Marosi et al., 2016). Other actions have been described for KB including epigenetic, antioxidant, anti-inflammatory, and the up-regulation of brain-derived neurotrophic factor; they activate ATP-sensitive potassium channels and have been described as signaling molecules (Newman and Verdin, 2014; Camberos-Luna and Massieu, 2020). In addition, we have recently reported that the D isomer of BHB (D-BHB) stimulates the autophagic flux during glucose deprivation and prevents neuronal death in cortical cultures (Camberos-Luna et al., 2016).

Macro-autophagy (here referred to as autophagy) can be activated during nutrient deprivation and is characterized by the formation of a double-membrane structure named autophagosome that subsequently fuses with a lysosome leading to the degradation of damaged proteins and organelles for the restoration of cell homeostasis (Klionsky and Emr, 2000; Yin et al., 2016). During nutrient deprivation, mTOR inhibition by AMPK leads to ULK1 S317 phosphorylation, which in turn phosphorylates Beclin-1 (BECN1) promoting the activity of class III PtdIns3K complex, initiating the formation of the nucleation site. On the contrary, during nutrient abundance mTOR activity phosphorylates ULK1 S757, preventing its activation by AMPK and autophagy initiation. Also, AMPK can directly phosphorylate ULK1 at S317 and initiate autophagy (Egan et al., 2011; Kim et al., 2011). The autophagy-related proteins (ATG) are key players in autophagosome formation and membrane expansion. Microtubule-associated light chain-3 (LC3) is cleaved by ATG4 and conjugated with phosphatidylethanolamine (PE) to produce LC3-II. LC3-II is associated with autophagosomes where it functions as a docking site of adaptor proteins such as SQSTM1/p62, which delivers polyubiquitinated proteins to the autophagosome for degradation. SQSTM1/p62 is degraded together with cargo by lysosome hydrolytic enzymes. ATG7 and ATG3 form the conjugation system involved in the relocation of LC3-I to the phagophore membrane and ATG5 covalently binds to ATG12 forming the ATG12–ATG5-ATG16 conjugate essential for autophagosome membrane elongation. Mature autophagosomes fuse with a lysosome leading to cargo degradation (Sou et al., 2008; Wirawan et al., 2012). Enhanced conversion of LC3-I to LC3-II and a reduction in SQSTM1/p62 abundance is taken as an index of autophagic flux.

Deficient autophagy in the central nervous system leads to the accumulation of ubiquitinated proteins, axonal degeneration, and neuronal death. Loss of cortical and cerebellar neurons has been observed in ATG7-deficient animals (Komatsu et al., 2005, 2006) and animals lacking ATG5 do not survive (Kuma et al., 2004). Also, excessive autophagy can lead to cell death, and its inhibition can prevent acute ischemic brain injury (Carloni et al., 2008; Fu et al., 2016; Wang et al., 2018). Autophagy dynamics during severe hypoglycemia *in vivo* has not been investigated, neither its role in selective neuronal death. Hence, we have studied the changes in autophagy markers during severe hypoglycemia (SH) without glucose infusion (GI), and during GI after SH or a brief period of coma. We also investigated whether D-BHB treatment in animals subjected to coma is associated with the preservation of functional autophagy, as we have previously observed *in vitro* (Camberos-Luna et al., 2016). We have evaluated the changes in the abundance of proteins involved in autophagosome formation and maturation, Beclin1 (BECN1), p-ULK1, ATG7, ATG12–ATG5, and LC3-II, and in SQSTM1/p62 as a marker of autophagy degradation. The role of AMPK and mTOR in autophagy activation was also investigated. Results suggest that in the cerebral cortex SH induced the accumulation of autophagosomes, which persisted 6 h after GI likely due to deficient autophagy degradation, and recovered at 24 h. In contrast, in the hippocampus, autophagosomes accumulated after SH but no change was observed after GI.

In animals exposed to the hypoglycemic coma, significant autophagosome accumulation was observed at 24 h after GI in both brain regions. Besides, AMPK-dependent phosphorylation of ULK1 S317 was observed at this time in animals subjected to coma, suggesting autophagy activation. When D-BHB was administered after the coma, SQSTM1/p62 degradation was enhanced and ULK1 S317 phosphorylation was reduced, increasing cell survival. Data suggest that D-BHB attenuates autophagy activation and restores the autophagic flux promoting cell survival.

## MATERIALS AND METHODS

Three-month-old male Wistar rats (280–320 g) were used throughout the study. They were obtained from the Instituto de Fisiología Celular (IFC) animal house, at the Universidad Nacional Autónoma de México (UNAM). The guide for the Care and Use of Laboratory Animals (NIH publications No. 80-23 Revised 1996) of the National Institute of Health was followed and animals were handled accordingly and with the approval of the Animal Care Committee (CICUAL) of the IFC (protocol number LMT160-20). The number of animals used was optimized and all efforts were made to minimize their suffering. Experiments are reported according to the ARRIVE guidelines (Animal Research: Reporting *in vivo* Experiments). Animals were kept with food and water *ad libitum* and under standard dark/light cycle and temperature conditions and housed in individual cages. A sample size of three to seven animals per group was used. Animals were randomly distributed among the different groups and at least one animal from each experimental group was included per experiment. Seventy-three animals were used for western blot, 28 for histology and immunocytochemistry determinations, and 21 for BHB blood determinations, as indicated in figure legends.

### Induction of Severe Hypoglycemia Without Glucose Infusion (SH)

Severe hypoglycemia (SH) was induced in the home cage in non-anesthetized animals partially fasted overnight (food restricted to four pellets) and during the experimental period. They received a single intraperitoneal injection of 32 U/kg human insulin (Lilly, Humulin 70/30, Indianapolis, IN, USA). Blood glucose was monitored from a blood sample obtained from the tail vein before (basal levels) and at 0.5, 1, 2, and 3 h after insulin injection using a standard glucometer (Abbott Laboratories, Bedford, MA, USA). One-hour after insulin administration, animals reached SH (<40–30 mg/dl) and were euthanized 2 h later (**Figure 1A**). Brains were extracted and prepared for western blotting.

### Induction of Severe Hypoglycemia With Glucose Infusion (SH + GI)

Animals were subjected to SH and rescued with GI. They were partially fasted overnight and during the whole experimental period. To monitor electrical brain activity through electroencephalogram (EEG) recording, 1 week before hypoglycemia animals were implanted with epidural electrodes under 2.0 to 3.0% isoflurane anesthesia. Meloxicam (1 mg/kg i.p.) was administered post-surgery as an anti-inflammatory. Animals were intraperitoneally (i.p.) injected (between 9:00 and 11:00 am) with 32 U/kg insulin to induce hypoglycemia. Blood glucose was monitored before (time 0) and at 0.5, 1, 2, 3, 6, 7, and 27 h after insulin. To determine basal brain electrical activity, EEG recording started 30 min before insulin administration and continued during the whole hypoglycemic and GI periods until the normal electrical activity was completely recovered (**Figure 1B**). Animals were rescued with glucose after the loss of the righting reflex (RR), which precedes the coma state (Haces et al., 2010) by an intraperitoneal (i.p.) bolus of 0.3 ml of 25% glucose in Krebs–Henseleit buffer. Immediately after, an intravenous (i.v.) infusion (25% glucose at 1.5 ml/h during 3 h) was administered through the tail vein using a perfusion pump (Harvard Apparatus 22, South Natick, MA, USA). None of the animals from this group showed EEG isoelectricity (indicative of the hypoglycemic coma). From these animals, one subgroup was euthanized at 6 h after GI (9 h after an insulin injection) and a second subgroup at 24 h after GI (27 h after an insulin injection; **Figure 1B**). Brains were extracted and prepared for western blotting.

### Induction of Hypoglycemic Coma With Glucose Infusion (Coma)

Animals subjected to coma (Coma), were equally treated as those from the SH + GI group, but after the loss of the RR, hypoglycemia was left to progress to the state of coma (EEG isoelectricity). After 5 min of isoelectricity animals received an i.p. bolus of 0.3 ml of 25% glucose as described for the SH + GI group, and 12 min afterward an intravenous (i.v.) infusion (25% glucose at 1.5 ml/h during 3 h) was administered through the tail vein as described above. The coma period ranged from 6 to 12 min (mean = 8.9 $\pm$ 0.34). A minimum period of 6 min coma was chosen because according to our previous studies, shorter coma periods produce very limited neuronal death or none. Therefore, animals showing coma periods of 5 min or less were discarded. Conversely, a maximum period of 12 min coma was selected because respiratory failure can be observed in animals showing longer coma periods. From these animals, one subgroup was euthanized at 6 h and a second subgroup at 24 h after GI (**Figure 1C**). Brains were extracted and prepared for western blot analysis (6 and 24 h) and histology (24 h). Animals showing seizures were also discarded.

Control animals were treated in parallel with the rest of the experimental groups. They were partially fasted overnight and during the duration of the experimental period and received vehicle solution (0.1% acetic acid) instead of insulin. Glucose was measured at different times after vehicle injection.

### Treatment With D-BHB (Coma + BHB)

Animals exposed to coma were either treated (Coma + BHB) or non-treated (Coma) with 250 or 500 mg/kg total dose of D-BHB (Cat. 298360, Sigma–Aldrich, St. Louis, MO, USA) divided into two intraperitoneal (i.p.) administrations. The first administration of D-BHB (125 or 250 mg/kg) was given 10 min

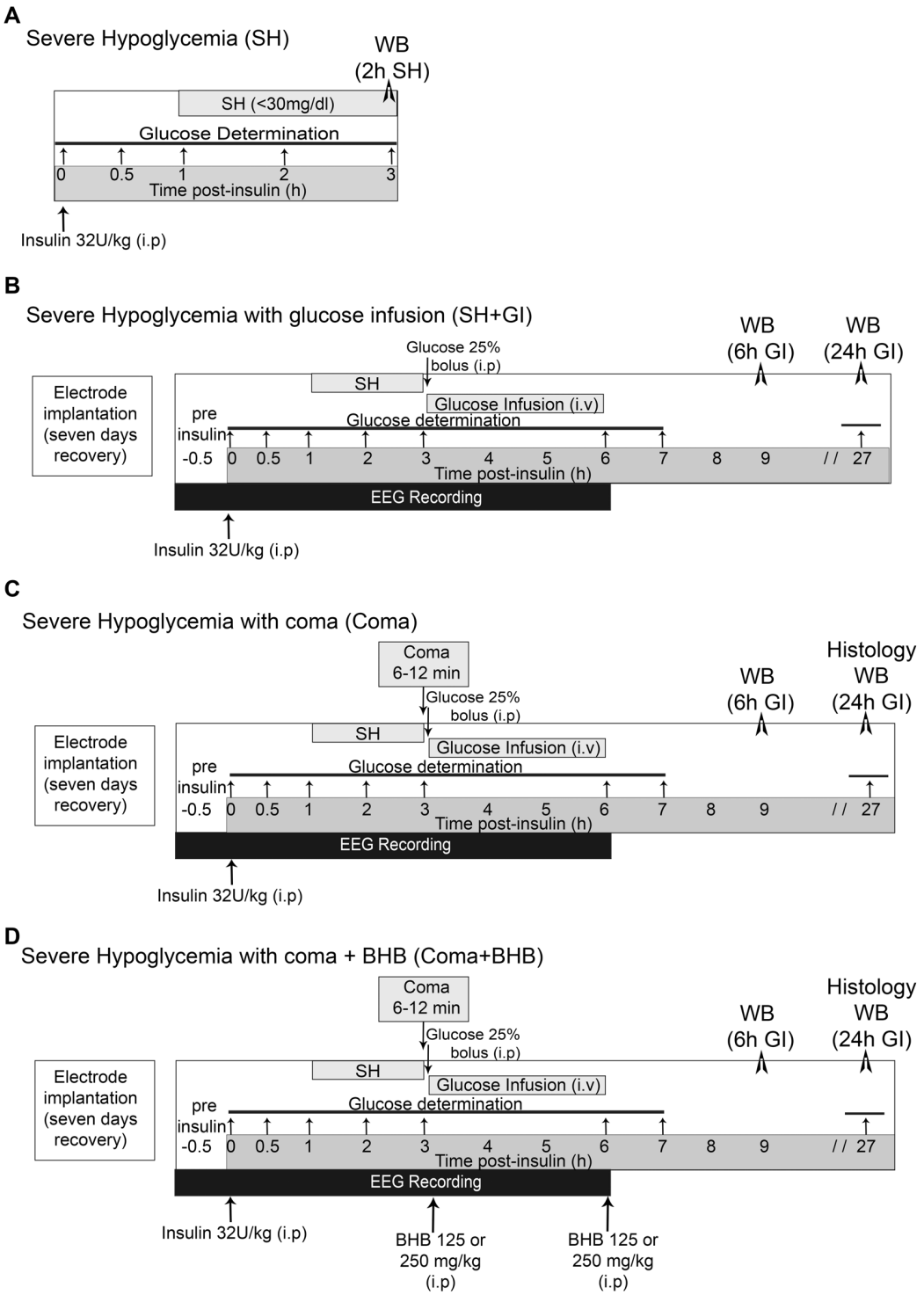


**FIGURE 1 |** Induction severe hypoglycemia and the hypoglycemic coma. **(A)** Severe hypoglycemia (SH) group. SH was induced by the intraperitoneal (i.p.) injection of insulin (32 U/kg) and animals were euthanized 2 h after they reached 30 mg/dl blood glucose. **(B)** SH + GI group. Animals were implanted with electrodes 1 week before the induction of hypoglycemia for electroencephalogram (EEG) recording and were subjected to SH with glucose infusion (GI). Insulin was injected (i.p) and 2 h after animals reached SH, they were rescued with glucose before they fell into the coma state. **(C)** Coma group. Animals were treated identically as those from the SH + GI, but SH was left to progress to the coma state for 6–12 min and immediately after they were rescued with glucose. **(D)** Coma + BHB group. Animals were treated identically as the Coma group, but they received two doses of either 125 or 250 mg/kg D isomer of β-hydroxybutyrate (D-BHB; i.p.), the first 10 min after the onset of glucose infusion after the coma and the second at the end of glucose infusion glucose infusion. Animals were euthanized 6 or 24 h after GI in groups **(B–D)**.

after glucose i.v. the infusion was started and the second at the end of the glucose infusion (3 h after the coma). Animals were euthanized at 6 or 24 h GI as indicated in **Figure 1D**. Brains were extracted and prepared for western blotting (6 and 24 h) and histology (24 h).

## Determination of D-BHB in Blood

Blood samples were obtained from the tail vein (seven animals per group) and D-BHB was measured using blood glucose and ketone monitoring system (FreeStyle Optium Neo, Abbott Diabetes Care, Limited, Witney, Oxon, UK) and keto strips (FreeStyle Optium β-ketone). Samples were obtained from intact control and fasted animals at different times throughout the experimental period. D-BHB was also determined in blood samples from animals of the Coma and the Coma + BHB groups, before (time 0) and at different times after insulin injection (1 and 2 h), at the time the animals reached the coma, at different times after recovery with glucose or glucose + D-BHB (250 mg/kg), and after the second administration of D-BHB (250 mg/kg), as indicated in **Figure 2C**. Animals from these groups were identically treated during the hypoglycemia period before recovery and were randomly assigned to each one of the treatments.

## SDS–PAGE and Western Blots

The hippocampus and parietal cortex were dissected and homogenized in 1:10 weight/volume lysis buffer containing: Tris-HCl 50 mM, NaCl 150 mM, SDS 1%, Triton X-100 1%, Sodium deoxycholate 0.5%, PMSF 1 mM, NaPPi 5 mM, $Na_3VO_4$ 2 mM and Complete protease inhibitor cocktail (Roche complete, 1162600, USA), pH 7.5. Proteins were determined by the Lowry method and samples were denaturized in Laemmli buffer. Thirty to forty micrograms of protein was resolved in 10–16% SDS–PAGE and then electroblotted to PVDF membranes. Membranes were blocked in TBS/milk 5% for 1 h and incubated overnight at 4°C with specific primary antibodies: LC3 (1:5,000, Cat. PD014, MBL International Woburn, USA); ATG5 (1:1,000, Cat. S6133158, Santa Cruz Biotechnology, Dallas, TX, USA), p-ULK1 S317 (1:500, MB59600629, My BioSource, San Diego, CA, USA); BECN1 (1:2,000, Cat. 3738), ATG7 (1:1,000, Cat. 2631S), ULK1 (1:6,000, Cat. 8054), p-ULK1 S757 (1:6,000, Cat. 14202), mTOR (1:1,000, Cat. 2983S), p-mTOR S2448 (1:1,000, Cat.

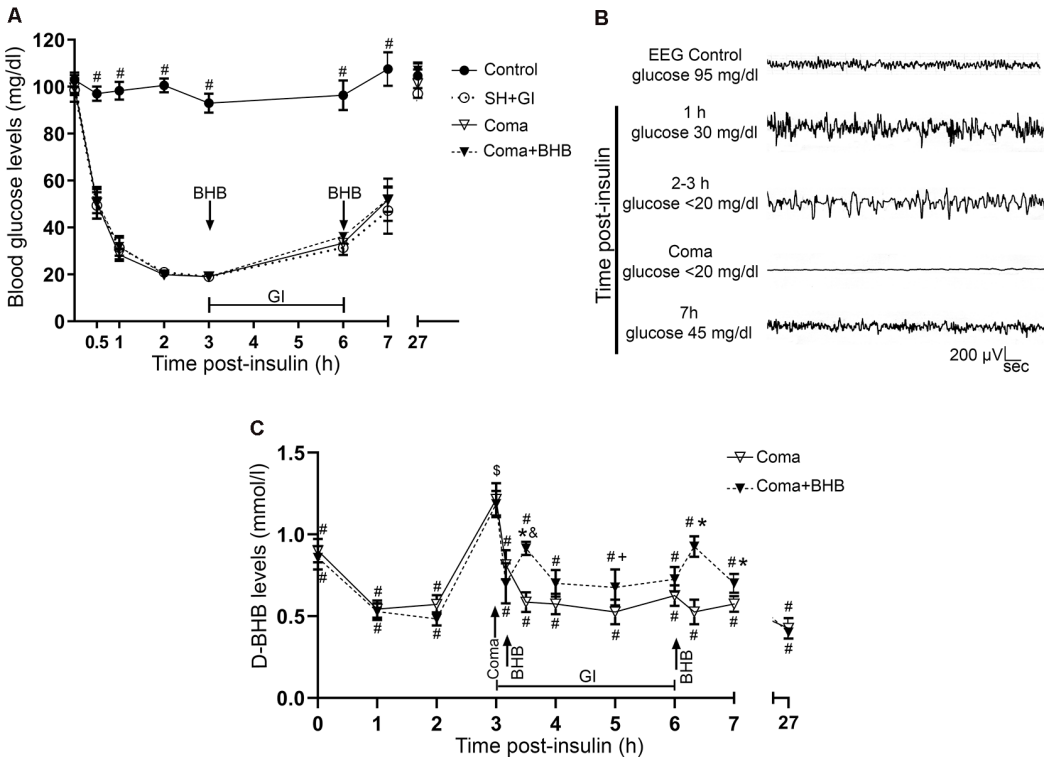


**FIGURE 2 |** Glucose and D-BHB concentration in blood and EEG recording. **(A)** Blood glucose concentration in control and hypoglycemic animals rescued with glucose (SH + GI), and in animals subjected to coma treated (Coma + BHB) and non-treated (Coma) with D-BHB. Data represent mean ± SEM and were analyzed by one-way ANOVA followed by a Fisher's *post hoc* test for multiple comparisons. $^{\#}p \leq 0.05$ relative to the hypoglycemia groups, $n = 6$–10. **(B)** Representative EEG recording showing the changes in brain electrical activity in one representative insulin-injected animal before insulin administration (control), during SH (1–3 h after insulin), during the coma, and after GI. **(C)** D-BHB blood levels were determined at different times after insulin injection and GI in rats subjected to coma treated and non-treated with D-BHB. Data represent mean ± SEM and were analyzed by one-way or two-way ANOVA followed by a Fisher's *post hoc* test for multiple comparisons, for intragroup and intergroup comparisons, respectively. $^{*}p \leq 0.05$ vs. the Coma group, $^{\$}p \leq 0.05$ vs. the corresponding 2 h post-insulin value, $^{\#}p \leq 0.05$ vs. the corresponding 3 h value (coma state), $^{\&}p \leq 0.05$ vs. the corresponding 3.1 h value (before D-BHB administration), $^{+}p \leq 0.05$ vs. the corresponding 3.5 h value (20 min post D-BHB administration), $n = 7$ for each experimental group.

2971), AMPK (1:1,000, Cat. 2532), SQSTM1/p62 (1:2,500, Cat. 5114), were from Cell Signaling Technology (Danvers, MA, USA); Actin (1:7,000, Cat. MAB1501 Chemicon Merck Millipore, Darmstadt, Germany) was used as loading control. The reactions of primary antibodies were detected using the respective horseradish peroxidase, goat anti-rabbit, or goat anti-mouse secondary antibody (Cat. 115035-003 and 115035-062 respectively, Jackson Immunoresearch Laboratories, West Grove, PA, USA). Immunoreactivity was detected by chemiluminescent HRP substrate (Luminata$^{TM}$ Forte, Cat. WBLUF0100, Merck Millipore), using a C-Digit Blot Scanner (LI-COR Biosciences, UK). The optical density of the bands of interest was measured using the ImageJ program. Data were calculated as the protein/actin ratio.

## Histology

Twenty-four hours after the treatments, animals from each group ($n$ = 4–7) were anesthetized with an overdose of pentobarbital and intracardially perfused with 0.9% saline solution followed by 4% paraformaldehyde in 0.1 mM phosphate buffer; brains were extracted and transferred to a 20–30% sucrose gradient (24 and 72 h, respectively). Coronal brain sections of 20 and 40 μm were obtained in a cryostat (LEICA CM1510S) for histological analysis.

## Fluoro-Jade B Staining

Slides were covered for 5 and 2 min with 80 and 70% ethanol respectively, they were washed and covered with 0.06% potassium permanganate for 10 min. Sections were incubated for 20 min with 0.0004% FJB (Cat. AB310, Chemicon), dried at 50°C, rinsed with xylol, and covered with permount (Julio-Amilpas et al., 2015). They were observed under an epifluorescence microscope Nikon Eclipse Ci (using AT-EGFP/F filter) and FJB-positive cells were counted in both hemispheres. In the parietal cortex total FJB-positive cells were counted bilaterally in 15 sections separated by 200 μm. In the case of the hippocampus, six sections were used and cells were counted in a 200 $\mu m^2$ area of the crest and the inferior blade of the dentate gyrus using the ImageJ program. Data are reported as the total number of positive cells in both subregions. Cell damage was confirmed by the presence of pyknotic cells after Nissl staining of adjacent sections.

## Immunohistochemistry

Brain sections were permeabilized by 30 min (PBS/Triton-X100 0.9%), washed for 10 min in PBS, and incubated with citrates buffer 0.1% at 58°C for 20 min. They were incubated in PBS/glycine 0.1% for 15 min and then blocked 1 h in PBS/BSA 5%/goat serum 2%/Tween 0.5%/Triton 0.9% at room temperature. Afterward, sections were incubated in primary antibodies against LC3 (1:300) or SQSTM1/p62 (1:200, Cat. ab56416, Abcam, Cambridge, UK) in PBS/BSA 1%/Triton X-100 0.3%/Tween-20 0.05%, for 48 h at 4°C. The slides were washed in PBS and incubated for 2 h with secondary antibody Alexa 488 anti-rabbit and Dry-Light 488 anti-mouse (1:300 Cat. 111-545-144 and 115-485-166 respectively, Jackson Immunoresearch Laboratories, West Grove, PA, USA). Subsequently, cell nuclei were stained with Hoechst 0.001% (Cat. 33258, Sigma–Aldrich). Slides were incubated in Sudan Black B (Cat. 199664, Sigma–Aldrich) for 3 min to decrease background fluorescence. Images were obtained using a confocal microscope ZEISS LSM800 for LC3, SQSTM1/p62, and Hoechst. Images were acquired and processed using the ZEN 3.1 program from Zeiss. Confocal stacks composed from 28 to 35 slices (0.3 μm) were acquired and the maximum projection was obtained from each image ($x$-$y$, $x$-$z$, and $y$-$z$ orientations) from three independent experiments.

## Statistical Analysis

All data are expressed as mean ± SEM and were analyzed by the Student's $t$-test when a comparison between two groups was made, or one-way ANOVA followed by Fisher's LSD test for multiple comparisons when more than two groups were compared. The time-course in D-BHB blood levels in the Coma and the Coma + BHB groups was compared by two-way ANOVA followed by a Fisher's LSD multiple comparison test, and the intragroup comparisons were made by one-way ANOVA followed by Fisher's LSD test for multiple comparisons.

# RESULTS

## Glucose Concentration and Electroencephalogram Recording

Blood glucose levels were measured and electrical brain activity was recorded at different times after insulin injection and GI. Results show a mean basal blood glucose concentration close to 100 mg/dl in all groups. In control animals, glucose concentration was constant during the experimental period (**Figure 2A**). In hypoglycemic animals (SH + GI, Coma, and Coma + BHB) glucose concentration declined close to 30 mg/dl after 1 h insulin administration and decreased further to 20 mg/dl during the next 2 h before GI. At the end of the GI, glucose levels reached 30 mg/dl and 1 h later they raised to 55 mg/ml; control values were recovered at 24 h. No significant differences were found in blood glucose concentration between the experimental groups (**Figure 2A**). **Figure 2B** shows a representative EEG recording obtained before, during, and after the hypoglycemic coma. After 2–3 h insulin administration, electrical brain activity declined to show the high amplitude and low-frequency waves as previously reported (Julio-Amilpas et al., 2015). At this time glucose concentration declined below 20 mg/dl; animals were drowsy and lost their RR. In animals exposed to coma, electrical brain activity was completely suppressed and recovered 1 h after GI. Animals rescued with glucose plus D-BHB (either 250 or 500 mg/kg) showed similar changes in brain electrical activity (not shown).

## Autophagy Dynamics During Hypoglycemia and Glucose Infusion in Animals Subjected to Severe Hypoglycemia or the Hypoglycemic Coma

The changes in the content of LC3-II and SQSTM1/p62 were determined 2 h after the induction of hypoglycemia and 6 and

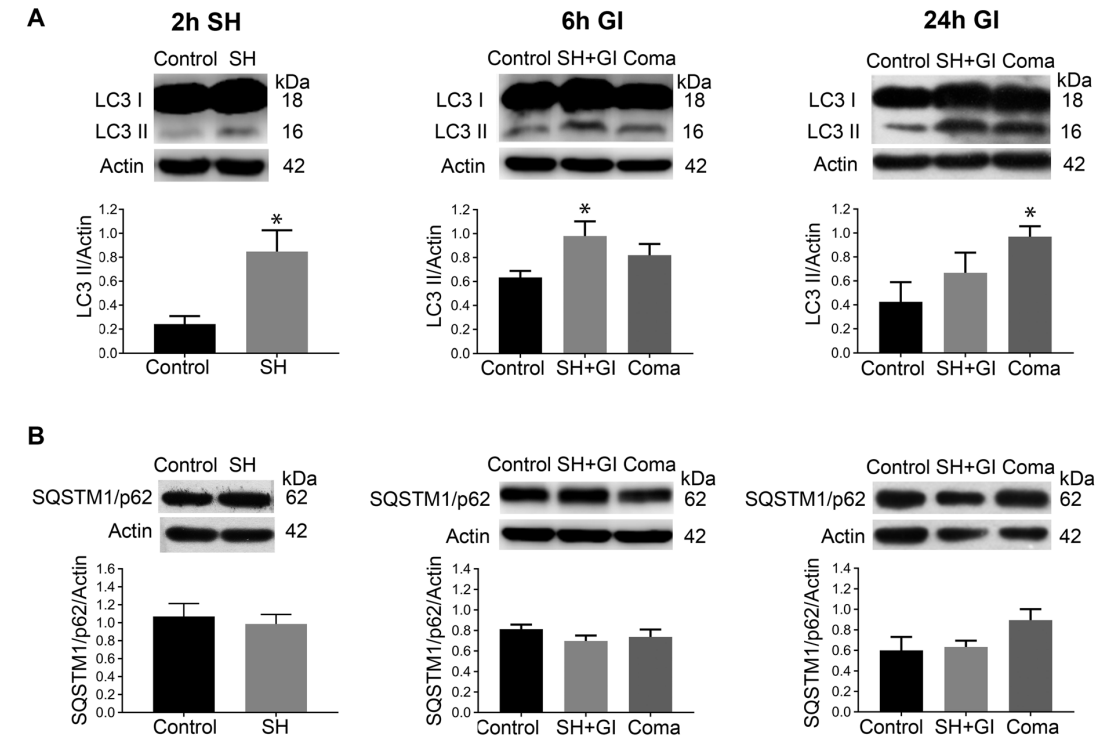


**FIGURE 3 |** Autophagy dynamics in the parietal cortex induced by severe hypoglycemia and the hypoglycemic coma at different times. Changes in **(A)** LC3-II/Actin and **(B)** SQSTM1/p62/Actin 2 h after SH (2 h SH) and 6 and 24 h after glucose infusion (6 h GI and 24 h GI). Bars represent mean ± SEM. Data were analyzed by one-way ANOVA followed by a Fisher's *post hoc* test for multiple comparisons. For the 2 h group, a Student's *t*-test was used for statistical analysis. $^*p \leq 0.05$ vs. control, $n = 4$–6 for the 2 and 24 h groups and $n = 3$ for the 6 h groups.

24 h after GI in rats exposed to SH + GI or the hypoglycemic coma. In the parietal cortex 2 h after SH, the transformation of LC3-I to LC3-II notably increased, while no change in SQSTM1/p62 was observed. At 6 h after GI, LC3-II remained significantly elevated and returned to control levels at 24 h in the SH + GI group (**Figure 3A**). As the increase in LC3-II was not accompanied by a decrease in SQSTM1/p62 (**Figure 3B**), results suggest that the autophagic flux is blocked and that increased LC3-II results from autophagosome accumulation. In animals subjected to coma, LC3-II showed a moderate non-significant increase at 6 h after GI, but it increased notably at 24 h. As in the case of SH + GI, augmented LC3-II was not accompanied by a decline in SQSTM1/p62, suggesting autophagic flux impairment at 24 h after GI (**Figures 3A,B**). In agreement with these observations, LC3 immunoreactivity increased 24 h after GI in the Coma group (**Figure 5C**).

Similar to the parietal cortex in the hippocampus LC3-II significantly increased 2 h after hypoglycemia, while no significant change in SQSTM1/p62 was found (**Figures 4A,B**). In rats subjected to SH + GI, no significant change in LC3-II or SQSTM1/p62 was observed at 6 h and 24 h (**Figure 4B**). In contrast, in the Coma group, a significant increase in LC3-II was found at 24 h after GI, while SQSTM1/p62 content showed no reduction suggesting deficient autophagic degradation. In agreement with these observations, augmented immunoreactivity against LC3 was observed in brain sections from animals exposed to coma, in the inferior blade (not shown) and the crest of the dentate gyrus at 24 h after GI (**Figure 6C**).

Altogether, these data suggest that autophagosomes accumulate during the hypoglycemic period due to deficient autophagic degradation. After GI the autophagic flux is restored in the SH + GI group, while in rats experiencing a period of coma autophagosomes accumulate at 24 h, likely due to impaired autophagic flux. No changes in the LC3-I band were observed at 2 h or 6 h in the SH + GI and Coma groups (data not shown), while at 24 h there was a slight significant increase in the LC3-I band in the hippocampus of rats experiencing coma but not in the cortex (**Supplementary Figure S2**).

## D-BHB Administration After the Hypoglycemic Coma Stimulates the Autophagic Flux and Increases Cell Survival

In a previous study, we have reported that D-BHB stimulates the autophagic flux and prevents neuronal death in cortical cultured neurons exposed to glucose deprivation and glucose

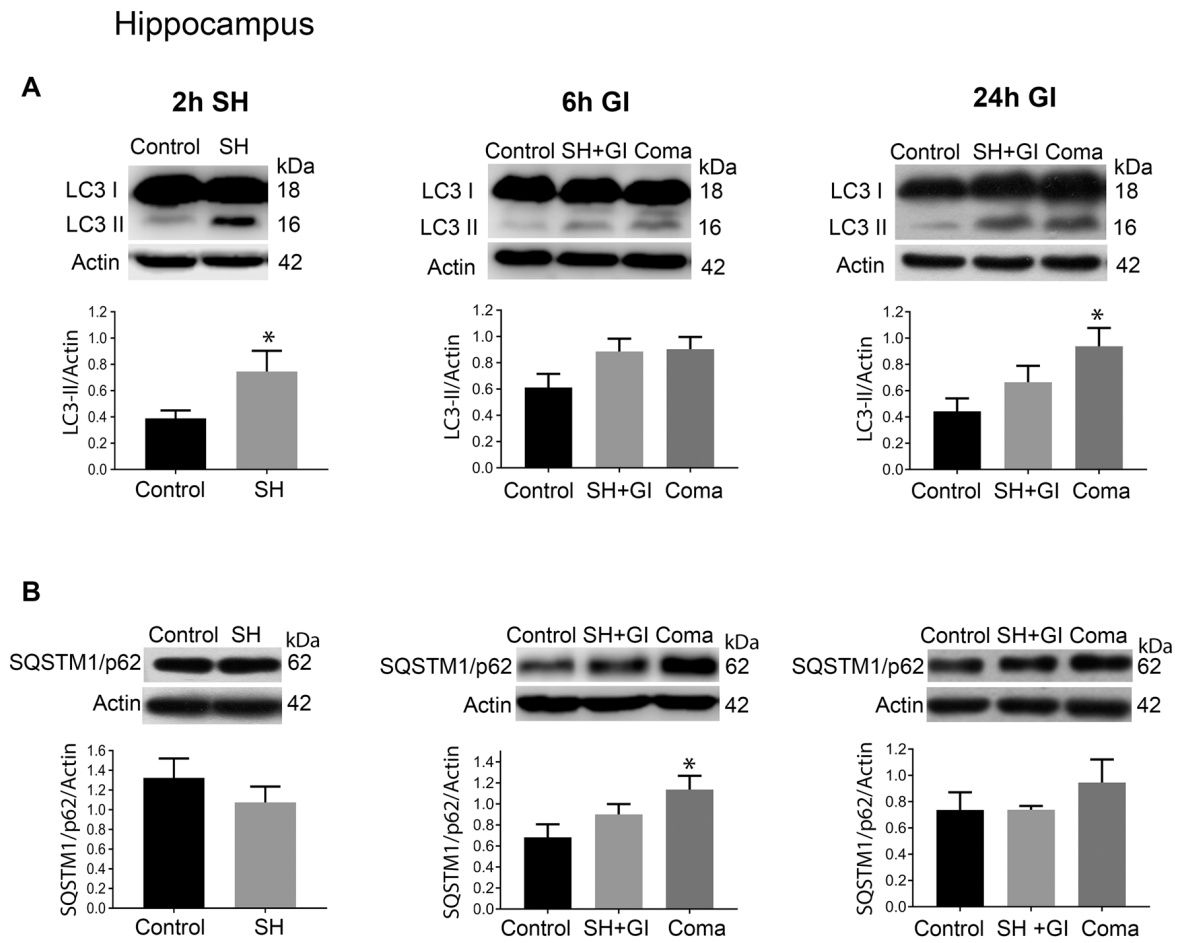


**FIGURE 4 |** Autophagy dynamics in the hippocampus induced by severe hypoglycemia and the hypoglycemic coma at different times. Changes in **(A)** LC3-II/Actin and **(B)** SQSTM1/p62/Actin 2 h after SH (2 h SH) and 6 and 24 h after glucose infusion (6 h GI and 24 h GI). Bars represent mean ± SEM. Data were analyzed by one-way ANOVA followed by a Fisher's *post hoc* test for multiple comparisons. For the 2 h group, a Student's *t*-test was used for statistical analysis. $^*p \leq 0.05$ vs. control, $n = 4$–6 for the 2 and 24 h groups and $n = 3$ for the 6 h groups.

reintroduction (Camberos-Luna et al., 2016). Hence, we aimed to test whether the KB exerts the same effect in the hypoglycemia model. Rats exposed to the hypoglycemic coma were recovered with glucose and D-BHB 250 mg/kg (two doses of 125 mg/kg) and were analyzed at 6 and 24 h. D-BHB treatment did not affect 6 h on LC3-II or SQSTM1/p62 in the cortex or the hippocampus (data not shown). However, at 24 h D-BHB reduced the increase in LC3-II induced by coma in both brain regions, while no change in SQSTM1/p62 was found (**Supplementary Figures S1A,B**). These results are consistent with immunohistochemistry data, showing reduced LC3 immunoreactivity in rats treated with D-BHB (**Supplementary Figures S1A,B**). When 500 mg/kg D-BHB (two administrations of 250 mg/kg each) was administered, the transformation of LC3-I to LC3-II significantly diminished relative to animals exposed to coma in both the cortex and the hippocampus (**Figures 5A**, **6A**). Also, a significant reduction of SQSTM1/p62 was observed in D-BHB-treated rats (**Figures 5B**, **6B**), suggesting that at higher doses D-BHB stimulates the autophagic flux in both regions. In agreement with these results, immunohistochemistry analysis showed reduced immunoreactivity to LC3 and SQSTM1/p62 in the parietal cortex and the dentate gyrus of animals treated with 500 mg/kg of D-BHB (**Figures 5C**, **6C**). Confocal *Z*-stacks images show that LC3 and SQSTM1/p62 are present in the cytoplasm surrounding the nucleus and also in neurites. In animals subjected to coma LC3 and SQSTM1/p62 immunoreactivity augment, while in D-BHB-treated animals, immunofluorescence is less intense and more diffuse. Orthogonal images from the *x-z* and *y-z* orientations confirm that LC3 and SQSTM1/p62 are located in the cytoplasm.

D-BHB treatment did not affect LC3-I in the cortex relative to the control and Coma groups and did not reduce the increase in LC3-I induced by the coma in the hippocampus (**Supplementary Figure S2**).

Then we tested the effect of D-BHB administration on cell survival. In previous studies, we have reported that a short period of coma induces neuronal death in the cerebral

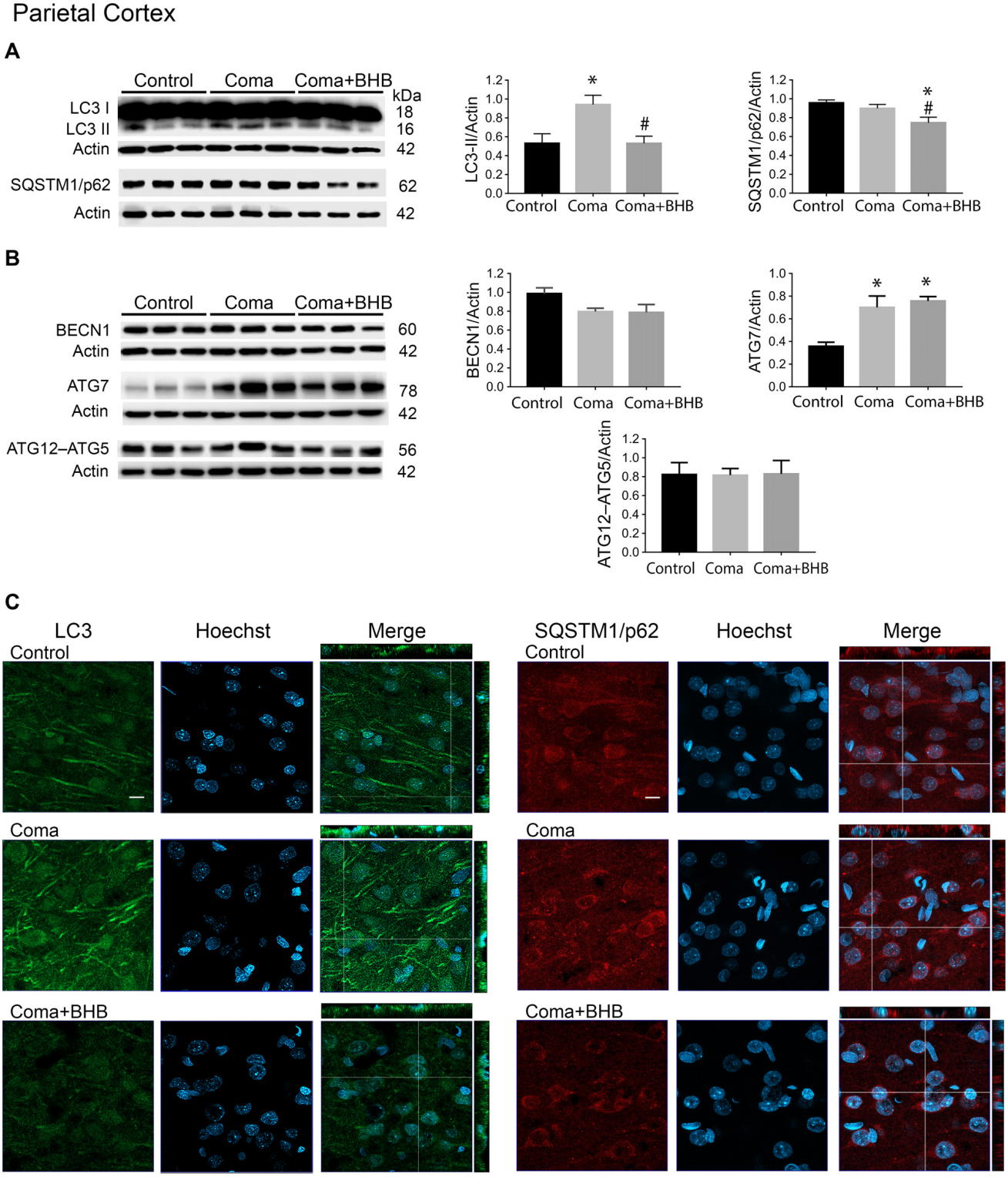


**FIGURE 5 |** Effect of D-BHB on autophagy-related proteins in the parietal cortex 24 h after the hypoglycemic coma. Changes in **(A)** LC3-II/Actin and SQSTM1/p62/Actin, **(B)** BECN1/Actin, ATG7/Actin, and ATG12–ATG5/Actin. **(C)** Confocal representative images of immunoreactivity to LC3 and SQSTM1/p62 in animals treated and non-treated with D-BHB (500 mg/kg). Orthogonal images (x-z upper) and y-z (right) orientations are shown. Data are expressed as mean ± SEM. Statistical analysis was performed by one-way ANOVA followed by the Fisher *post hoc* test for multiple comparisons. $^{*}p \leq 0.05$ vs. control, $^{\#}p < 0.05$ vs. coma, $n$ = 4–5 control, $n$ = 5–6 Coma, $n$ = 5 Coma + BHB. Scale bar = 10 μm.

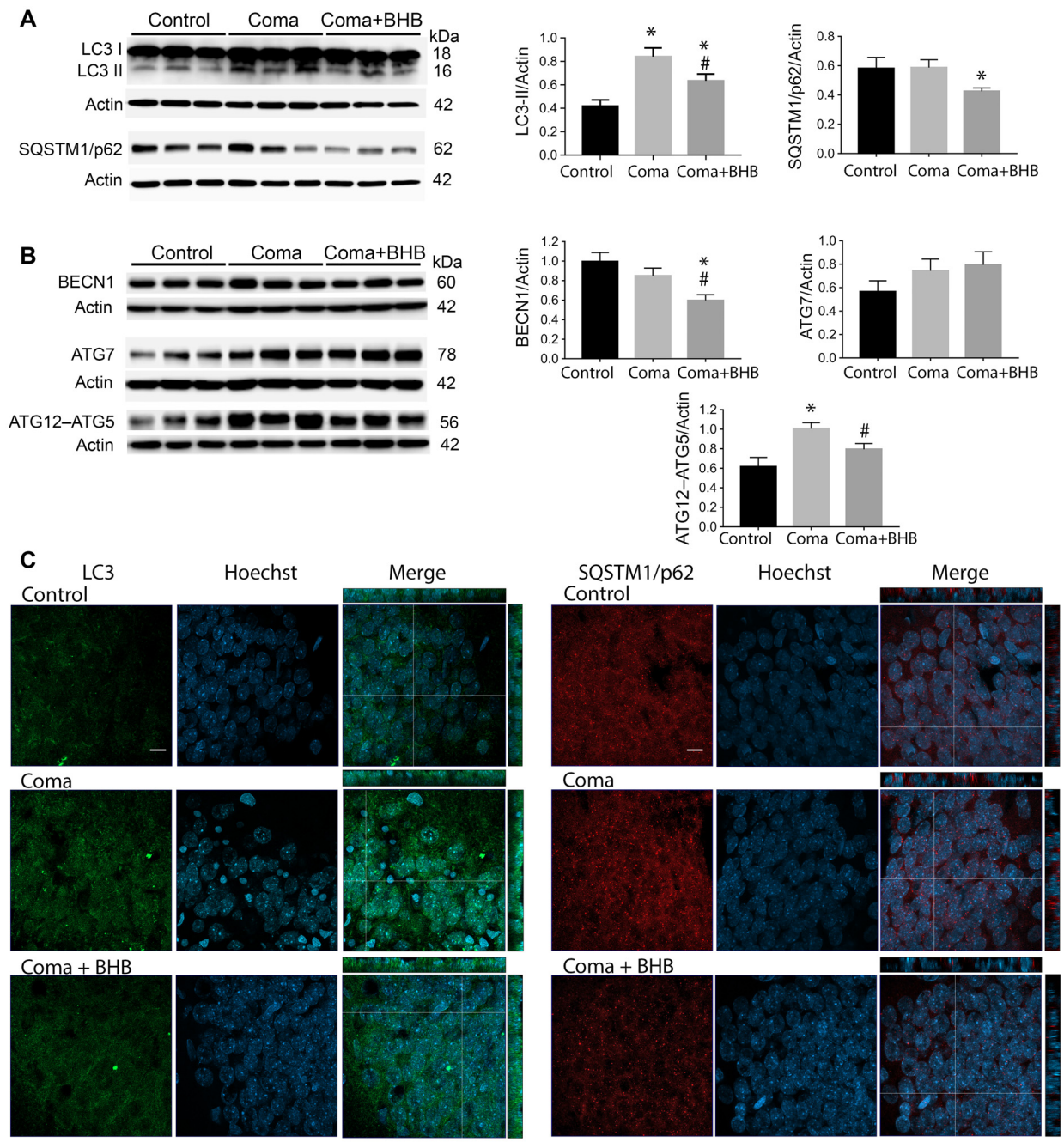


**FIGURE 6 |** Effect of D-BHB on autophagy-related proteins in the hippocampus 24 h after the hypoglycemic coma. **(A)** Changes in LC3-II/Actin and SQSTM1/p62/Actin, **(B)** BECN1/Actin, ATG7/Actin, and ATG12–ATG5. **(C)** Confocal representative images of immunoreactivity to LC3 and SQSTM1/p62 in animals treated and non-treated with D-BHB (500 mg/kg). Orthogonal images (x-z upper) and y-z (right) orientations are shown. Data are expressed as mean ± SEM. Statistical analysis was performed by one-way ANOVA followed by the Fisher *post hoc* test for multiple comparisons. $^{*}p \leq 0.05$ relative to control, $^{\#}p < 0.05$ relative to coma, $n$ = 4–5 control, $n$ = 5–6 Coma, $n$ = 5 Coma + BHB. Scale bar = 10 μm.

cortex and the dentate gyrus (Languren et al., 2019). FJB and cresyl violet staining were used to evidence neuronal damage. At 24 h after glucose infusion, degenerating cells labeled with FJB were observed in the parietal cortex, mainly in the superficial and medium layers (II–IV), and in the hippocampus, primarily in the crest and the inferior blade of the dentate gyrus (**Figure 7A**). Adjacent cresyl violet-stained sections showed dark shrunk cells with pyknotic

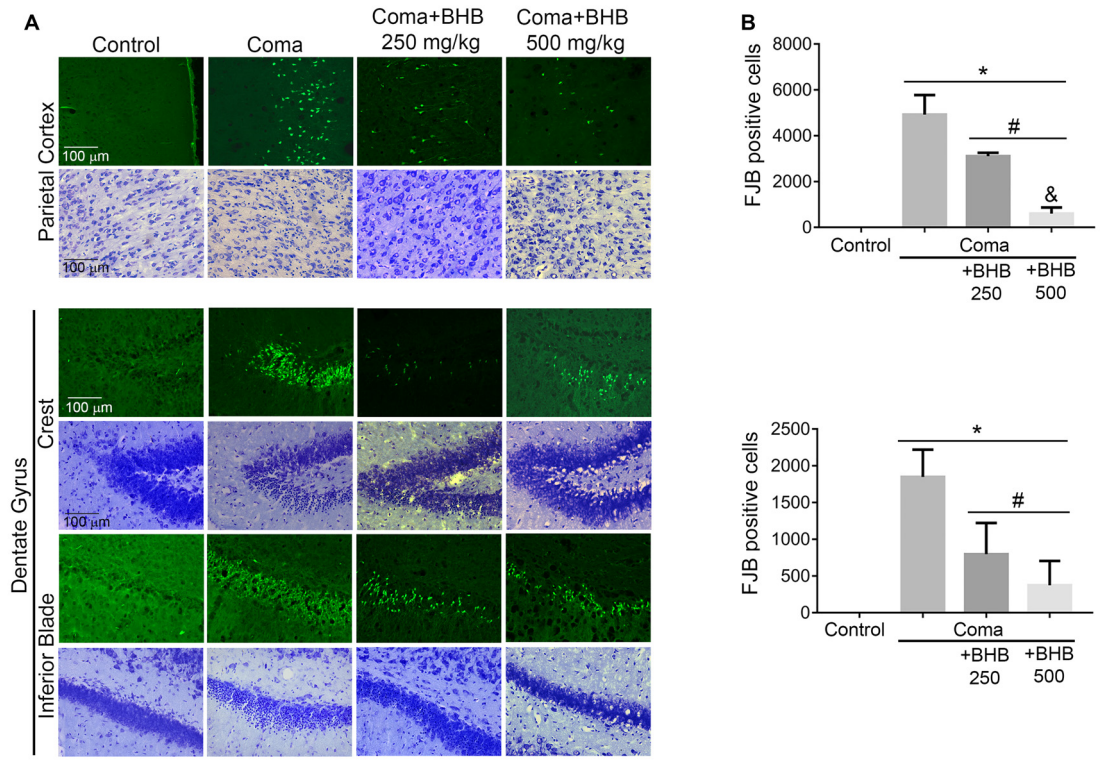


**FIGURE 7 |** Effect of D-BHB treatment on cell survival in the cortex and the hippocampus of rats exposed to the hypoglycemic coma. **(A)** Representative micrographs of FJB-positive cells and cresyl violet-stained sections of the parietal cortex and dentate gyrus. **(B)** The number of FJB-positive cells in control and hypoglycemic animals treated and non-treated with 250 or 500 mg/kg D-BHB in the parietal cortex and the dentate gyrus of the hippocampus. Data are expressed as mean ± SEM and were analyzed by one-way ANOVA followed by Fisher *post hoc* test for multiple comparisons. $^{*}p \leq 0.05$ vs. control, $^{\#}p \leq 0.05$ vs. coma, $^{\&}p \leq 0.05$ vs. 250 mg/kg, $n = 6$ control, $n = 7$ coma, $n = 4$ Coma + BHB.

nuclei in the same location where FJB-positive cells were present (**Figure 7A**).

D-BHB treatment reduced the number of FJB-positive cells in both cerebral regions (**Figure 7B**). In the parietal cortex, protection by D-BHB was dose-dependent. A 36% reduction in the number of FJB-labelled cells was observed when animals were treated with two doses of 250 mg/kg D-BHB after the hypoglycemic coma. When 500 mg/kg D-BHB was used, the number of FJB-positive cells was reduced by 87% (**Figure 7B**). Accordingly, cresyl violet-stained sections of animals treated with D-BHB showed cells with a light cytoplasm and morphologically similar to those in control animals. In the hippocampus, the number of degenerating cells was reduced by 57 and 80%, when animals were treated with 250 or 500 mg/kg of D-BHB, respectively, although no significant difference was found between the two doses (**Figure 7B**). These results demonstrate that D-BHB can reduce neurodegeneration when administered post the hypoglycemic coma and that a 500 mg/kg total dose is more effective.

D-BHB blood levels were determined at different times in intact control animals, fasted animals, and animals subjected to coma treated and non-treated with D-BHB. As expected, fasting-induced a significant increase in D-BHB blood levels to 0.9 ± 0.075 mM relative to intact controls (0.6 ± 0.057), and these levels were maintained throughout the whole experimental period, recovering control values 27 h later (0.56 ± 0.13; not shown). One-hour after insulin administration, when glucose blood levels decreased close to 30 mg/dl, D-BHB decayed to 0.5 mM (**Figure 2C**). When glucose further decreased below 20 mg/dl and animals reached the coma state, D-BHB blood concentration significantly increased up to 1.2 mM but declined soon after the coma to 0.8–0.7 mM (**Figure 2C**). To this stage, both animal groups showed a similar behavior suggesting they similarly reacted to insulin. During recovery, 30 min after animals were rescued with glucose alone, D-BHB decreased further (0.58 ± 0.059) and its levels remained low and statistically different from the coma value during the whole glucose infusion period. In contrast, in animals rescued with glucose and D-BHB (250 mg/kg), KB levels did not decline but significantly increased to 0.91 ± 0.040 after 20 min, and progressively declined to 0.7 mM during the glucose infusion period (**Figure 2C**). Twenty minutes after the second administration of D-BHB its blood levels increased again but rapidly declined after 30 min. Twenty-four hours after glucose infusion, D-BHB levels declined close to control values in both groups (**Figure 2C**). Altogether, these results suggest that D-BHB

endogenous production is stimulated during the coma state, but is rapidly consumed during GI. Under these conditions, the exogenous administration D-BHB during the recovery period significantly increases its blood levels relative to animals rescued with glucose alone.

## Autophagy Initiation After the Hypoglycemic Coma

To investigate whether the elevation of LC3-II induced by the hypoglycemic coma is associated with autophagy induction, the changes in autophagy initiation proteins were determined. In the parietal cortex, no significant changes in BECN1 were observed. The antibody used against ATG5, detects a 56 kDa band corresponding to the ATG12–ATG5 conjugate and a 32 kDa band corresponding to ATG5 alone. In the present conditions, the 32 kDa band showed a very low intensity and is not shown. No changes were detected in the ATG12–ATG5 conjugate relative to control rats, suggesting no activation of autophagy at this time (**Figure 5B**). However, a significant increase in ATG7 was found. In the hippocampus no changes in BECN1 were observed, ATG7 showed a trend to increase and ATG12–ATG5 conjugate was significantly elevated, suggesting increased autophagosome formation (**Figure 6B**).

Then we tested the effect of D-BHB on autophagy initiation proteins and observed no change in BECN1, ATG7, and ATG12–ATG5 conjugate in the parietal cortex relative to the Coma group (**Figure 5B**), while in the hippocampus D-BHB treatment induced no change in ATG7 content, but produced a significant decrease in BECN1 and ATG12–ATG5 conjugate compared to the Coma group (**Figure 6B**). These results suggest that D-BHB inhibits autophagy initiation in the hippocampus.

## Role of mTOR and AMPK Activation on Autophagy Initiation After the Hypoglycemic Coma

Activation of AMPK and inhibition of the mTOR complex leads to autophagy initiation. Therefore, the levels of phosphorylation of the downstream target of these two kinases, ULK1 were determined 24 h after the coma as an index as of their activity. No significant changes in total mTOR, p-mTOR S2448, total ULK1, and p-ULK1 S757 were found in the cortex (**Figures 8A,B**), suggesting that mTOR activity is not inhibited at this time. Total AMPK showed no change and p-ULK1 S317 tended to increase (**Figures 8A,B**). In the hippocampus no changes in total mTOR, p-mTOR S2448 and p-ULK S757 were present, but a significant increase in total ULK1 was found (**Figures 9A,B**). In contrast, total AMPK and p-ULK1 S317 significantly increased after the coma (**Figures 9A,B**). Overall, these results agree with those of ATG proteins and suggest that at 24 h autophagy is initiated mainly in the hippocampus in an AMPK activity-dependent manner.

## Effect of D-BHB on mTOR and AMPK Activation After the Hypoglycemic Coma

The effect of 500 mg/kg of D-BHB was tested in mTOR and ULK1 phosphorylation. No changes in p-mTOR S2448 and

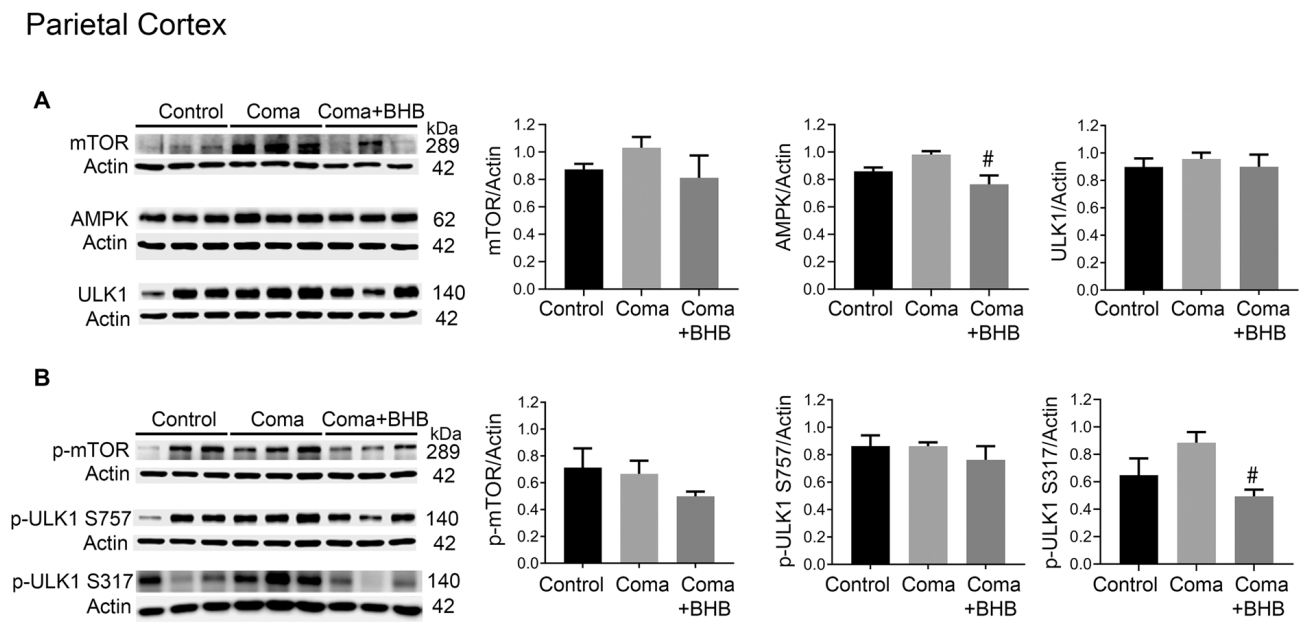


**FIGURE 8 |** mTOR and AMPK activity in the parietal cortex of animals treated and non-treated with D-BHB 24 h after the hypoglycemic coma. **(A)** Total levels of mTOR, AMPK, and ULK1. **(B)** Phosphorylation levels of mTOR S2448, ULK1 S757, and ULK1 S317. Data are expressed as mean ± SEM. Statistical analysis was performed by one-way ANOVA followed by the Fisher *post hoc* test for multiple comparisons. $^{\#}p \leq 0.05$ vs. coma. $n$ = 4–5 control, $n$ = 5–6 coma, $n$ = 4–5 Coma + BHB.

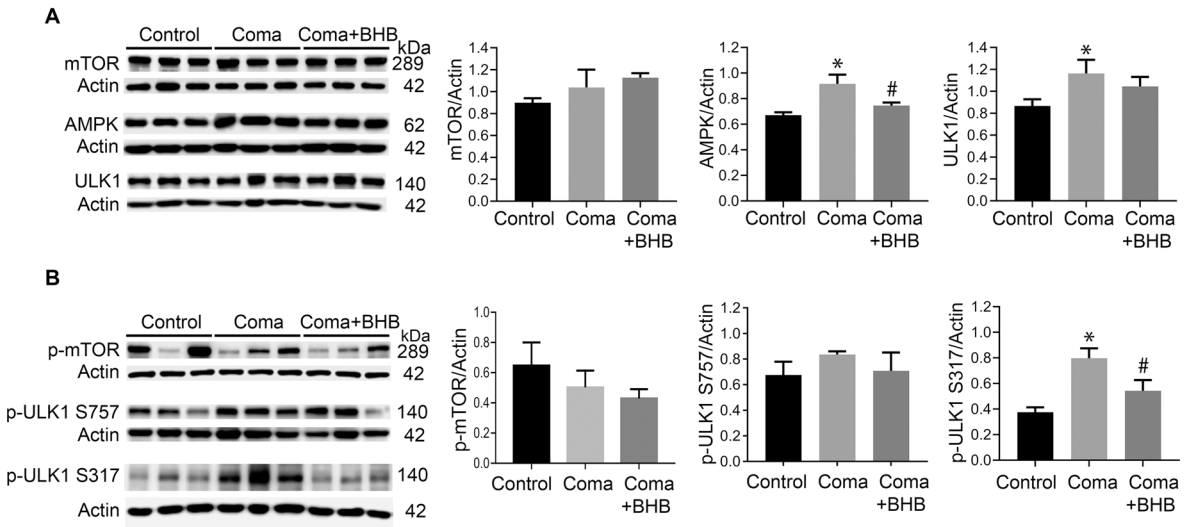


**FIGURE 9 |** mTOR and AMPK activity in the parietal cortex of animals treated and non-treated with D-BHB 24 h after the hypoglycemic coma. **(A)** Total levels of mTOR, AMPK, and ULK1. **(B)** Phosphorylation levels of mTOR S2448 and ULK1 S757 and ULK1 S317. Data are expressed as mean ± SEM. Statistical analysis was performed by one-way ANOVA followed by the Fisher *post hoc* test for multiple comparisons. $^{*}p \leq 0.05$ vs. control, $^{\#}p \leq 0.05$ vs. to coma. $n$ = 4–5 control, $n$ = 5–6 coma, $n$ = 4–5 Coma + BHB.

p-ULK1 S757 were found neither in the cortex nor the hippocampus of D-BHB-treated animals as compared to the Coma group (**Figures 8B**, **9B**). D-BHB treatment decreased total AMPK and prevented the increase in p-ULK1 S317 induced by the hypoglycemic coma in both brain regions, suggesting that in D-BHB-treated rats AMPK is less activated (**Figures 8A,B**, **9A,B**). Altogether, these results suggest that D-BHB treatment attenuates autophagy activation.

## DISCUSSION

Under nutrient-limiting conditions, cells activate autophagy to restore cell homeostasis (Mizushima et al., 2010). However, during conditions of severe energy failure such as ischemia, hypoxia, and cerebral trauma, neuronal death can result from dysfunctional (Carloni et al., 2008; Sarkar et al., 2014) or excessive autophagy (Shi et al., 2012). In contrast, it has been reported that during mild hypoxia and ischemic preconditioning, autophagy is activated to protect cells by removing damaged organelles and proteins (Sheng et al., 2012; Sun et al., 2018). We have previously reported that glucose depletion in cortical cultured neurons activates autophagy, but after glucose reintroduction deficient autophagic degradation is triggered due to calpain-mediated lysosomal dysfunction contributing to neuronal death (Geronimo-Olvera et al., 2017).

Evidence about autophagy dynamics in an *in vivo* model of severe hypoglycemia is still lacking. We have addressed this question and the present findings suggest for the first time, that autophagosomes accumulate during a period of SH relative to control animals, likely due to deficient autophagic degradation in the parietal cortex and the hippocampus. When glucose was infused after SH a significant increase in autophagosome formation relative to controls animals was observed at 6 h, but it was statistically significant only in the parietal cortex. This increase was transient and returned to control values at 24 h, suggesting that basal levels of autophagy were restored at this time. In contrast, animals experiencing a period of coma showed a non-significant elevation in LC3-II at 6 h relative to control values, but at 24 h LC3-II further and significantly increased. The increase in LC3-II was not different from the SH group but it was different to control rats in both brain regions, suggesting that autophagy does not recover basal values when rats experience a period of coma. As no decrease in SQTSM1/p62 was observed, it is suggested that autophagosome accumulation results from deficient autophagic flux. On the other hand, it was observed that LC3-I abundance significantly increased in the hippocampus but not in the cortex, suggesting the up-regulation of this protein after GI or its deficient degradation, possibly due to impaired proteasomal activity (Gao et al., 2010). Further experiments are needed to identify the mechanism involved.

The differential autophagy dynamics observed after SH and the hypoglycemic coma might be related to the duration and the intensity of energy failure. Early studies revealed that the levels of phosphocreatine and ATP are not altered during non-coma hypoglycemia, while isoelectricity triggers a severe unbalance of the energy state leading to energy depletion (Ferrendelli and Chang, 1973; Lewis et al., 1974). On the other hand, previous studies have shown that GI after non-coma SH increases ROS production and 3-nitrotyrosine protein residues, but neuronal death is limited to a few scattered cells in the cerebral cortex (Haces et al., 2010; Amador-Alvarado et al., 2014; Julio-Amilpas et al., 2015). In contrast, it is well known that GI after the

coma induces oxidative stress and severe oxidative damage, which is highly involved in neuronal death in the cortex and the hippocampus (Suh et al., 2003, 2007). Thus, it is feasible that non-coma hypoglycemia transiently activates autophagy to remove damaged organelles and other cellular components to reestablish cell homeostasis and prevent neuronal death, while the excessive accumulation of oxidatively damaged molecules after the coma, will exacerbate autophagosome formation and impair the autophagic flux.

On the other hand, the present results indicate that autophagy is activated in the hippocampus 24 h after GI in an AMPK-dependent mTOR-independent manner in rats exposed to coma. A moderate increase in ATG7 and a significant elevation in the ATG12–ATG5 conjugate relative to the control group were found. As these proteins are essential for autophagosome formation and elongation, respectively, these results suggest that autophagy is activated in the hippocampus 24 after GI. In agreement with these results, a significant increase in p-ULK1 S317 was found relative to control animals suggesting that autophagy is initiated by AMPK activation. In the cortex, autophagy initiation was not so evident. A significant elevation of ATG7 was found but neither in ATG12–ATG5 conjugate nor in p-ULK1 S317, although a trend to augment was observed. The differences observed in autophagy activation in the cortex and the hippocampus, might be related to the high energy demand of the latter, due to its role in synaptic plasticity and its high vulnerability to hypoglycemic injury (Auer et al., 1984).

The mechanisms leading to AMPK activation in the present conditions were not explored and need further investigation. The stimulation of calcium-calmodulin kinase β (CAMKKβ) by increased intracellular calcium might be involved, as calcium homeostasis is lost during severe energy deprivation (Sun et al., 2016). Also, liver kinase B1 (LKB1), an upstream AMP kinase, might have a role as its levels of phosphorylation increase after brain ischemia (Li et al., 2007). Also, AMPK activity can be stimulated by reactive oxygen and nitrogen species, and CAMKKβ and LKB1 can be activated by nitric oxide and peroxynitrite, respectively (Cardaci et al., 2012; Li et al., 2013; Xia et al., 2018).

It is well known that during glucose limiting conditions other energy substrates can be used by the brain, such as the KB. Increasing evidence supports the protective effect of KB exogenous intake or ketosis induction against acute brain injury (Camberos-Luna and Massieu, 2020). We have previously shown that D-BHB administration during hypoglycemia prevents ROS production in the cortex and the hippocampus and diminishes neuronal death (Julio-Amilpas et al., 2015). Here, we investigated whether the administration of D-BHB post-hypoglycemic coma reduces neuronal damage and improves autophagic flux, as previously observed in cortical cultured neurons (Camberos-Luna et al., 2016). According to the results, a total dose of 250 mg/kg D-BHB reduced the increase in LC3-II but was unable to stimulate the degradation of SQSTM1/p62. In contrast, 500 mg/kg of D-BHB significantly reduced LC3-II and SQSTM1/p62 in the parietal cortex and the hippocampus, suggesting the improvement of autophagic cargo degradation. These observations correlated with a reduced number of FJB-positive cells in both brain regions, suggesting that the protective effect of D-BHB is associated at least in part, with the re-establishment of the autophagic flux, as previously reported (Camberos-Luna et al., 2016; Montiel et al., 2020). Importantly, results also show that D-BHB treatment attenuates autophagosome formation in the hippocampus at late stages after GI, supporting the idea that dysfunctional and/or excessive autophagy contributes to neuronal death.

The decrease in LC3-II and SQSTM1/p62 induced by D-BHB treatment can also result from diminished autophagy activation. According to the results, D-BHB did not affect BECN1, ATG7, and ATG12–ATG5 conjugate in the parietal cortex, thus it mainly improved autophagic degradation in this cerebral region. However, in the hippocampus, D-BHB prevented the phosphorylation of ULK1 S317 by AMPK suggesting less AMPK activation. This result correlated with diminished BECN1 and ATG12–ATG5 conjugate supporting that D-BHB attenuates the initiation of autophagy in this region. These results agree with recent findings in the rat striatum after NMDA-induced excitotoxicity (Montiel et al., 2020). Decreased activation of AMPK by D-BHB treatment is possibly related to improved mitochondrial metabolism and ATP synthesis and decreased ROS production (Maalouf et al., 2007; Julio-Amilpas et al., 2015; Marosi et al., 2016).

According to the determination of D-BHB blood levels, fasting-induced mild ketosis as it increased D-BHB up to 0.9 mM. However, it rapidly declined after insulin administration suggesting it is consumed by the brain during hypoglycemia. Results also indicate that during severe hypoglycemia, when animals reach the coma, the endogenous KB production is stimulated but declines soon after the coma. Animals from both groups behaved similarly during the hypoglycemia period before glucose recovery suggesting the similarly reacted to insulin. However, it remains to be determined whether a differential response to insulin affects neuronal survival and autophagy. According to the present data, the exogenous administration of D-BHB immediately after the coma, was able to increase its levels close to fasting values. Notably, D-BHB concentration declined 30 min after its first and second administration, suggesting its utilization during the recovery period. These results agree with a previous study showing that D-BHB administration during hypoglycemia before the coma, increases its levels close to fasting values providing the brain with an alternative substrate to glucose (Julio-Amilpas et al., 2015).

The contribution to neuronal survival of the endogenous D-BHB production and utilization, resulting from insulin administration, cannot be disregarded. In the present experimental conditions, it possibly contributes to the limited neuronal death associated with a brief period of coma (Haces et al., 2010; Languren et al., 2019), as compared to longer periods (30–60 min), where neuronal death is extensive and distributed in the cortex and all layers of the hippocampal formation (Auer et al., 1984; Suh et al., 2007). Nonetheless, according to the present data, additional D-BHB exogenous supplementation during GI, associates with improved cell survival, as a lower number of degenerating cells were observed in D-BHB-treated rats, and this effect was dose-dependent.

The protective effect of exogenous KB administration against acute brain injury has been demonstrated in several *in vivo* models (Suzuki et al., 2001, 2002; Haces et al., 2008; Julio-Amilpas et al., 2015; Montiel et al., 2020), and this study adds new knowledge about the role of autophagy as a possible mechanism involved. Protection protocols using ketosis induction by diet approaches as the ketogenic diet or medium-chain triglycerides supplementation, relay on the up-regulation of monocarboxylate transporters to favor KB oxidation by the brain. In contrast, the exogenous administration of KB or KB derivatives rapidly increases their blood concentration but require repetitive or continuous administration to sustain elevated KB blood levels (Camberos-Luna and Massieu, 2020). It remains to be determined whether there is an up-regulation of MCT transporters in the present conditions, which can facilitate KB uptake in the brain, as it has been reported after ischemia and cerebral trauma (Tseng et al., 2003; Prins et al., 2004; Zhang et al., 2005; Prins and Giza, 2006; Prins, 2008; Moreira et al., 2009), and recently after severe hypoglycemia in female rats (Uddin et al., 2020).

In conclusion, the present study reports for the first time, that autophagy follows different dynamics during glucose recovery in animals experiencing SH or hypoglycemic coma, and that it is differentially activated in the cortex and the hippocampus as a response to the initial energy failure and recovery. Also, results support that D-BHB treatment is associated with the stimulation of the autophagic flux in the cortex and the hippocampus and with the attenuation of autophagy in the latter. These effects might be involved in the protective effect exerted by D-BHB against hypoglycemic neuronal death. These data increase our knowledge about the adaptive brain responses to severe hypoglycemia, and the role of D-BHB as alternative energy fuel to glucose in the modulation of these responses.

## DATA AVAILABILITY STATEMENT

The raw data supporting the conclusions of this article will be made available by the authors, without undue reservation.

## ETHICS STATEMENT

The animal study was reviewed and approved by Comité Interno para el Cuidado y Uso de Animales de Laboratorio (CICUAL) from Instituto de Fisiología Celular (protocol number IFC LMT16020).

## AUTHOR CONTRIBUTIONS

CT-E, TM, and MF-M performed all the experiments. CT-E performed all western blot, histology, and immunohistochemistry analysis. CT-E and LM analyzed all data and wrote the article. CT-E, TM, and LM conceived the study, designed the experiments, and participated in all discussions.

## FUNDING

The present work was supported by PAPIIT-UNAM grant IN204919 and CONACyT grant A1S-17357 to LM. CT-E is a doctoral student from the Programa de Doctorado en Ciencias Biomédicas, at the Universidad Nacional Autónoma de México (UNAM) and she was a recipient of CONACyT fellowship (573885).

## ACKNOWLEDGMENTS

We thank Ruth Rincón Heredia for her assistance in confocal imaging analysis, Claudia Rivero Cerecedo for animal care at the Bioterium of IFC, and Ana Maria Escalante and Francisco Pérez for Computer facilities.

## SUPPLEMENTARY MATERIAL

The Supplementary Material for this article can be found online at: https://www.frontiersin.org/articles/10.3389/fncel.2020.547215/full#supplementary-material.

## REFERENCES

Amador-Alvarado, L., Montiel, T., and Massieu, L. (2014). Differential production of reactive oxygen species in distinct brain regions of hypoglycemic mice. *Metab. Brain Dis.* 29, 711–719. doi: 10.1007/s11011-014-9508-5

Auer, R. N., Wieloch, T., Olsson, Y., and Siesjo, B. K. (1984). The distribution of hypoglycemic brain damage. *Acta Neuropathol.* 64, 177–191. doi: 10.1007/BF00688108

Camberos-Luna, L., and Massieu, L. (2020). Therapeutic strategies for ketosis induction and their potential efficacy for the treatment of acute brain injury and neurodegenerative diseases. *Neurochem. Int.* 133:104614. doi: 10.1016/j.neuint.2019.104614

Camberos-Luna, L., Gerónimo-Olvera, C., Montiel, T., Rincon-Heredia, R., and Massieu, L. (2016). The ketone body, β-hydroxybutyrate stimulates the autophagic flux and prevents neuronal death induced by glucose deprivation in cortical cultured neurons. *Neurochem. Res.* 41, 600–609. doi: 10.1007/s11064-015-1700-4

Cardaci, S., Filomeni, G., and Ciriolo, M. R. (2012). Redox implications of AMPK-mediated signal transduction beyond energetic clues. *J. Cell Sci.* 125, 2115–2125. doi: 10.1242/jcs.095216

Carloni, S., Buonocore, G., and Balduini, W. (2008). Protective role of autophagy in neonatal hypoxia-ischemia induced brain injury. *Neurobiol. Dis.* 32, 329–339. doi: 10.1016/j.nbd.2008.07.022

Cryer, P. E. (2005). Mechanisms of hypoglycemia-associated autonomic failure and its component syndromes in diabetes. *Diabetes* 54, 3592–3601. doi: 10.2337/diabetes.54.12.3592

Egan, D., Kim, J., Shaw, R. J., and Guan, K. L. (2011). The autophagy initiating kinase ULK1 is regulated *via* opposing phosphorylation by AMPK and mTOR. *Autophagy* 7, 643–644. doi: 10.4161/auto.7.6.15123

Ferrendelli, J. A., and Chang, M. M. (1973). Brain metabolism during hypoglycemia. Effect of insulin on regional central nervous system glucose and energy reserves in mice. *Arch. Neurol.* 28, 173–177. doi: 10.1001/archneur.1973.00490210053006

Fu, L., Huang, L., Cao, C., Yin, Q., and Liu, J. (2016). Inhibition of AMP-activated protein kinase alleviates focal cerebral ischemia injury in mice: Interference with mTOR and autophagy. *Brain Res.* 1650, 103–111. doi: 10.1016/j.brainres.2016.08.035

Gao, Z., Gammoh, N., Wong, P.-M., Erdjument-Bromage, H., Tempst, P., and Jiang, X. (2010). Processing of autophagic protein LC3 by the 20S proteasome. *Autophagy* 6, 126–137. doi: 10.4161/auto.6.1.10928

Geronimo-Olvera, C., Montiel, T., Rincon-Heredia, R., Castro-Obregon, S., and Massieu, L. (2017). Autophagy fails to prevent glucose deprivation/glucose reintroduction-induced neuronal death due to calpain-mediated lysosomal dysfunction in cortical neurons. *Cell Death Dis.* 8:e2911. doi: 10.1038/cddis.2017.299

Haces, M. L., Hernández-Fonseca, K., Medina-Campos, O. N., Montiel, T., Pedraza-Chaverri, J., and Massieu, L. (2008). Antioxidant capacity contributes to protection of ketone bodies against oxidative damage induced during hypoglycemic conditions. *Exp. Neurol.* 211, 85–96. doi: 10.1016/j.expneurol.2007.12.029

Haces, M. L., Montiel, T., and Massieu, L. (2010). Selective vulnerability of brain regions to oxidative stress in a non-coma model of insulin-induced hypoglycemia. *Neuroscience* 165, 28–38. doi: 10.1016/j.neuroscience.2009.10.003

Julio-Amilpas, A., Montiel, T., Soto-Tinoco, E., Geronimo-Olvera, C., and Massieu, L. (2015). Protection of hypoglycemia-induced neuronal death by β-hydroxybutyrate involves the preservation of energy levels and decreased production of reactive oxygen species. *J. Cereb. Blood Flow Metab.* 35, 851–860. doi: 10.1038/jcbfm.2015.1

Kim, J., Kundu, M., Viollet, B., and Guan, K. L. (2011). AMPK and mTOR regulate autophagy through direct phosphorylation of Ulk1. *Nat. Cell Biol.* 13, 132–141. doi: 10.1038/ncb2152

Klionsky, D. J., and Emr, S. D. (2000). Autophagy as a regulated pathway of cellular degradation. *Science* 290, 1717–1721. doi: 10.1126/science.290.5497.1717

Komatsu, M., Waguri, S., Chiba, T., Murata, S., Iwata, J., Tanida, I., et al. (2006). Loss of autophagy in the central nervous system causes neurodegeneration in mice. *Nature* 441, 880–884. doi: 10.1038/nature04723

Komatsu, M., Waguri, S., Ueno, T., Iwata, J., Murata, S., Tanida, I., et al. (2005). Impairment of starvation-induced and constitutive autophagy in Atg7-deficient mice. *J. Cell Biol.* 169, 425–434. doi: 10.1083/jcb.200412022

Kuma, A., Hatano, M., Matsui, M., Yamamoto, A., Nakaya, H., Yoshimori, T., et al. (2004). The role of autophagy during the early neonatal starvation period. *Nature* 432, 1032–1036. doi: 10.1038/nature03029

Languren, G., Montiel, T., Ramirez-Lugo, L., Balderas, I., Sanchez-Chavez, G., Sotres-Bayon, F., et al. (2019). Recurrent moderate hypoglycemia exacerbates oxidative damage and neuronal death leading to cognitive dysfunction after the hypoglycemic coma. *J. Cereb. Blood Flow Metab.* 39, 808–821. doi: 10.1177/0271678X17733640

Lewis, L. D., Ljunggren, B., Ratcheson, R. A., and Siesjo, B. K. (1974). Cerebral energy state in insulin-induced hypoglycemia, related to blood glucose and to EEG. *J. Neurochem.* 23, 673–679. doi: 10.1111/j.1471-4159.1974.tb04390.x

Li, J., Zeng, Z., Viollet, B., Ronnett, G. V., and McCullough, L. D. (2007). Neuroprotective effects of adenosine monophosphate-activated protein kinase inhibition and gene deletion in stroke. *Stroke* 38, 2992–2999. doi: 10.1161/STROKEAHA.107.490904

Li, L., Chen, Y., and Gibson, S. B. (2013). Starvation-induced autophagy is regulated by mitochondrial reactive oxygen species leading to AMPK activation. *Cell. Signal.* 25, 50–65. doi: 10.1016/j.cellsig.2012.09.020

Maalouf, M., Sullivan, P. G., Davis, L., Kim, D. Y., and Rho, J. M. (2007). Ketones inhibit mitochondrial production of reactive oxygen species production following glutamate excitotoxicity by increasing NADH oxidation. *Neuroscience* 145, 256–264. doi: 10.1016/j.neuroscience.2006.11.065

Marosi, K., Kim, S. W., Moehl, K., Scheibye-Knudsen, M., Cheng, A., Cutler, R., et al. (2016). 3-hydroxybutyrate regulates energy metabolism and induces BDNF expression in cerebral cortical neurons. *J. Neurochem.* 139, 769–781. doi: 10.1111/jnc.13868

Masuda, R., Monahan, J. W., and Kashiwaya, Y. (2005). D-beta-hydroxybutyrate is neuroprotective against hypoxia in serum-free hippocampal primary cultures. *J. Neurosci. Res.* 80, 501–509. doi: 10.1002/jnr.20464

Melø, T. M., Nehlig, A., and Sonnewald, U. (2006). Neuronal-glial interactions in rats fed a ketogenic diet. *Neurochem. Int.* 48, 498–507. doi: 10.1016/j.neuint.2005.12.037

Mergenthaler, P., Lindauer, U., Dienel, G. A., and Meisel, A. (2013). Sugar for the brain: the role of glucose in physiological and pathological brain function. *Trends Neurosci.* 36, 587–597. doi: 10.1016/j.tins.2013.07.001

Mizushima, N., Yoshimori, T., and Levine, B. (2010). Methods in mammalian autophagy research. *Cell* 140, 313–326. doi: 10.1016/j.cell.2010.01.028

Montiel, T., Montes-Ortega, L. A., Flores-Yáñez, S., and Massieu, L. (2020). Treatment with the ketone body D-β-hydroxybutyrate attenuates autophagy activated by NMDA and reduces excitotoxic neuronal damage in the rat striatum *in vivo*. *Curr. Pharm. Des.* 26, 1377–1387. doi: 10.2174/1381612826666200115103646

Moreira, T. J., Pierre, K., Maekawa, F., Repond, C., Cebere, A., Liljequist, S., et al. (2009). Enhanced cerebral expression of MCT1 and MCT2 in a rat ischemia model occurs in activated microglial cells. *J. Cereb. Blood Flow Metab.* 29, 1273–1283. doi: 10.1038/jcbfm.2009.50

Newman, J. C., and Verdin, E. (2014). Ketone bodies as signaling metabolites. *Trends Endocrino. Metab.* 25, 42–52. doi: 10.1016/j.tem.2013.09.002

Prins, M. L. (2008). Cerebral metabolic adaptation and ketone metabolism after brain injury. *J. Cereb. Blood Flow Metab.* 28, 1–16. doi: 10.1038/sj.jcbfm.9600543

Prins, M. L., and Giza, C. C. (2006). Induction of monocarboxylate transporter 2 expression and ketone transport following traumatic brain injury in juvenile and adult rats. *Dev. Neurosci.* 28, 447–456. doi: 10.1159/000094170

Prins, M. L., Lee, S. M., Fujima, L. S., and Hovda, D. A. (2004). Increased cerebral uptake and oxidation of exogenous betaHB improves ATP following traumatic brain injury in adult rats. *J. Neurochem.* 90, 666–672. doi: 10.1111/j.1471-4159.2004.02542.x

Puchowicz, M. A., Zechel, J. L., Valerio, J., Emancipator, D. S., Xu, K., Pundik, S., et al. (2008). Neuroprotection in diet-induced ketotic rat brain after focal ischemia. *J. Cereb. Blood Flow Metab.* 28, 1907–1916. doi: 10.1038/jcbfm.2008.79

Sarkar, C., Zhao, Z., Aungst, S., Sabirzhanov, B., Faden, A. I., and Lipinski, M. M. (2014). Impaired autophagy flux is associated with neuronal cell death after traumatic brain injury. *Autophagy* 10, 2208–2222. doi: 10.4161/15548627.2014.981787

Sheng, R., Liu, X.-Q., Zhang, L.-S., Gao, B., Han, R., Wu, Y.-Q., et al. (2012). Autophagy regulates endoplasmic reticulum stress in ischemic preconditioning. *Autophagy* 8, 310–325. doi: 10.4161/auto.18673

Shi, R., Weng, J., Zhao, L., Li, X.-M., Gao, T.-M., and Kong, J. (2012). Excessive autophagy contributes to neuron death in cerebral ischemia. *CNS Neurosci. Ther.* 18, 250–260. doi: 10.1111/j.1755-5949.2012.00295.x

Sou, Y. S., Waguri, S., Iwata, J., Ueno, T., Fujimura, T., Hara, T., et al. (2008). The Atg8 conjugation system is indispensable for proper development of autophagic isolation membranes in mice. *Mol. Biol. Cell* 19, 4762–4775. doi: 10.1091/mbc.E08-03-0309

Suh, S. W., Aoyama, K., Chen, Y., Garnier, P., Matsumori, Y., Gum, E., et al. (2003). Hypoglycemic neuronal death and cognitive impairment are prevented by poly(ADP-ribose) polymerase inhibitors administered after hypoglycemia. *J. Neurosci.* 23, 10681–10690. doi: 10.1523/JNEUROSCI.23-33-10681.2003

Suh, S. W., Gum, E. T., Hamby, A. M., Chan, P. H., and Swanson, R. A. (2007). Hypoglycemic neuronal death is triggered by glucose reperfusion and activation of neuronal NADPH oxidase. *J. Clin. Invest.* 117, 910–918. doi: 10.1172/JCI30077

Sun, F., Xu, X., Wang, X., and Zhang, B. (2016). Regulation of autophagy by $Ca^2$. *Tumour Biol.* 37, 15467–15476. doi: 10.1007/s13277-016-5353-y

Sun, Y., Zhu, Y., Zhong, X., Chen, X., Wang, J., and Ying, G. (2018). Crosstalk between autophagy and cerebral ischemia. *Front. Neurosci.* 12:1022. doi: 10.3389/fnins.2018.01022

Suzuki, M., Suzuki, M., Kitamura, Y., Mori, S., Sato, K., Dohi, S., et al. (2002). Beta-hydroxybutyrate, a cerebral function improving agent, protects rat brain against ischemic damage caused by permanent and transient focal cerebral ischemia. *Jpn. J. Pharmacol.* 89, 36–43. doi: 10.1254/jjp.89.36

Suzuki, M., Suzuki, M., Sato, K., Dohi, S., Sato, T., Matsuura, A., et al. (2001). Effect of beta-hydroxybutyrate, a cerebral function improving agent, on cerebral hypoxia, anoxia and ischemia in mice and rats. *Jpn. J. Pharmacol.* 87, 143–150. doi: 10.1254/jjp.87.143

Tseng, M. T., Chan, S. A., and Schurr, A. (2003). Ischemia-induced changes in monocarboxylate transporter 1 reactive cells in rat hippocampus. *Neurol. Res.* 25, 83–86. doi: 10.1179/016164103101200978

Uddin, M. M., Ibrahim, M. M. H., Aryal, D., and Briski, K. P. (2020). Sex-dimorphic moderate hypoglycemia preconditioning effects on hippocampal

CA1 neuron bio-energetic and anti-oxidant function. *Mol. Cell. Biochem*. 473, 39–50. doi: 10.1007/s11010-020-03806-7

Wang, J. F., Mei, Z. G., Fu, Y., Yang, S. B., Zhang, S. Z., Huang, W. F., et al. (2018). Puerarin protects rat brain against ischemia/reperfusion injury by suppressing autophagy *via* the AMPK-mTOR-ULK1 signaling pathway. *Neural Regen. Res.* 13, 989–998. doi: 10.4103/1673-5374.233441

Wirawan, E., Vanden Berghe, T., Lippens, S., Agostinis, P., and Vandenabeele, P. (2012). Autophagy: for better or for worse. *Cell Res.* 22, 43–61. doi: 10.1038/cr.2011.152

Xia, G., Zhu, T., Li, X., Jin, Y., Zhou, J., and Xiao, J. (2018). ROS-mediated autophagy through the AMPK signaling pathway protects INS-1 cells from human islet amyloid polypeptide-induced cytotoxicity. *Mol. Med. Rep*. 18, 2744–2752. doi: 10.3892/mmr.2018.9248

Yin, Z., Pascual, C., and Klionsky, D. J. (2016). Autophagy: machinery and regulation. *Microb. Cell* 3, 588–596. doi: 10.15698/mic2016.12.546

Zhang, F., Vannucci, S. J., Philp, N. J., and Simpson, I. A. (2005). Monocarboxylate transporter expression in the spontaneous hypertensive rat: effect of stroke. *J. Neurosci. Res.* 79, 139–145. doi: 10.1002/jnr.20312

**Conflict of Interest**: The authors declare that the research was conducted in the absence of any commercial or financial relationships that could be construed as a potential conflict of interest.

frontiers in Cell and Developmental Biology

ORIGINAL RESEARCH
published: 09 October 2020
doi: 10.3389/fcell.2020.584604

# Comparative Transcriptome Analysis of the Regenerating Zebrafish Telencephalon Unravels a Resource With Key Pathways During Two Early Stages and Activation of Wnt/β-Catenin Signaling at the Early Wound Healing Stage

*Yeliz Demirci[1,2,3†], Gokhan Cucun[1,2†], Yusuf Kaan Poyraz[1,2], Suhaib Mohammed[3], Guillaume Heger[4], Irene Papatheodorou[3] and Gunes Ozhan[1,2*]*

[1] İzmir Biomedicine and Genome Center (IBG), Dokuz Eylül University Health Campus, İzmir, Turkey, [2] İzmir International Biomedicine and Genome Institute (IBG-İzmir), Dokuz Eylül University, İzmir, Turkey, [3] European Molecular Biology Laboratory – European Bioinformatics Institute (EMBL-EBI), Cambridge, United Kingdom, [4] École Centrale de Nantes, Nantes, France

Owing to its pronounced regenerative capacity in many tissues and organs, the zebrafish brain represents an ideal platform to understand the endogenous regeneration mechanisms that restore tissue integrity and function upon injury or disease. Although radial glial and neuronal cell populations have been characterized with respect to specific marker genes, comprehensive transcriptomic profiling of the regenerating telencephalon has not been conducted so far. Here, by processing the lesioned and unlesioned hemispheres of the telencephalon separately, we reveal the differentially expressed genes (DEGs) at the early wound healing and early proliferative stages of regeneration, i.e., 20 h post-lesion (hpl) and 3 days post-lesion (dpl), respectively. At 20 hpl, we detect a far higher number of DEGs in the lesioned hemisphere than in the unlesioned half and only 7% of all DEGs in both halves. However, this difference disappears at 3 dpl, where the lesioned and unlesioned hemispheres share 40% of all DEGs. By performing an extensive comparison of the gene expression profiles in these stages, we unravel that the lesioned hemispheres at 20 hpl and 3 dpl exhibit distinct transcriptional profiles. We further unveil a prominent activation of Wnt/β-catenin signaling at 20 hpl, returning to control level in the lesioned site at 3 dpl. Wnt/β-catenin signaling indeed appears to control a large number of genes associated primarily with the p53, apoptosis, forkhead box O (FoxO), mitogen-activated protein kinase (MAPK), and mammalian target of rapamycin (mTOR) signaling pathways specifically at 20 hpl. Based on these results, we propose that the lesioned and unlesioned hemispheres react to injury dynamically during telencephalon regeneration and that the activation of Wnt/β-catenin signaling at the early wound healing stage plays a key role in the regulation of cellular and molecular events.

**Keywords: brain regeneration, telencephalon, comparative transcriptome analysis, zebrafish, Wnt/β-catenin pathway, wound healing**

OPEN ACCESS

***Edited by:***
*Alicia Guemez-Gamboa, Northwestern University, United States*

***Reviewed by:***
*Sepand Rastegar, Karlsruhe Institute of Technology (KIT), Germany*
*Jan Kaslin, Australian Regenerative Medicine Institute (ARMI), Australia*
*Shawn M. Burgess, National Human Genome Research Institute (NHGRI), United States*

***Correspondence:**
*Gunes Ozhan*
*gunes.ozhan@ibg.edu.tr*

*† These authors have contributed equally to this work*

***Specialty section:***
*This article was submitted to Molecular Medicine, a section of the journal Frontiers in Cell and Developmental Biology*

***Received:*** *17 July 2020*
***Accepted:*** *11 September 2020*
***Published:*** *09 October 2020*

***Citation:***
*Demirci Y, Cucun G, Poyraz YK, Mohammed S, Heger G, Papatheodorou I and Ozhan G (2020) Comparative Transcriptome Analysis of the Regenerating Zebrafish Telencephalon Unravels a Resource With Key Pathways During Two Early Stages and Activation of Wnt/β-Catenin Signaling at the Early Wound Healing Stage. Front. Cell Dev. Biol. 8:584604. doi: 10.3389/fcell.2020.584604*

## INTRODUCTION

All vertebrate brains studied so far undergo adult neurogenesis, where they generate functional new neurons and integrate them into the existing brain circuitry after fetal and early postnatal development. Adult neurogenesis is achieved *via* stem or progenitor cells, in particular zones that exhibit varying degrees of abundance and neurogenic capacity among vertebrate species, and correlates with the capacity to regenerate upon damage to neuronal networks caused by injury (Doetsch and Scharff, 2001; Chapouton et al., 2007; Kaslin et al., 2008; Bonfanti and Peretto, 2011; Alunni and Bally-Cuif, 2016). Radial glia or glia-like cells (RGCs) have the characteristics of astrocytes, the star-shaped glial cells of the central nervous system (CNS), and act as primary neural stem cells (NSCs) that generate new neurons in the adult brain (Doetsch et al., 1999; Noctor et al., 2001; Seri et al., 2001; Dhaliwal and Lagace, 2011; Ming and Song, 2011).

Mammalian adult neurogenesis takes place predominantly *via* the NSCs confined to two distinct parts of the forebrain, i.e., the subventricular zone (SVZ) of the lateral ventricles in the telencephalon and the subgranular zone (SGZ) of the dentate gyrus in the hippocampus (Alvarez-Buylla et al., 2001; Kriegstein and Alvarez-Buylla, 2009; Bonfanti and Peretto, 2011). The restricted capacity of the neurogenic niches is explained partially by the reduction of constitutively active adult proliferation zones in mammalian brain during evolution (Rakic, 2002; Lindsey and Tropepe, 2006; Tanaka and Ferretti, 2009), a specific or general resistance against cell proliferation due to the evolution of tight control mechanisms against tumorigenesis (Pearson and Sanchez Alvarado, 2008), resistance to integrate new cells into a mature neural network (Kempermann et al., 2004; Kaslin et al., 2008), an altered cellular plasticity that affects stem or progenitor cell characteristics (Shihabuddin et al., 2000; Peng et al., 2002; Kizil et al., 2012b), or a non-permissive environment related to scar formation at the wound site after injury (Ekdahl et al., 2003; Fitch and Silver, 2008; Rolls et al., 2009). Low neurogenecity is paralleled by a limited potential in the integration of the newborn neurons in most regions of the mammalian brain, necessitating the use of another platform free of these constraints for the development of new therapeutic approaches (Bhardwaj et al., 2006; Ernst and Frisen, 2015; Alunni and Bally-Cuif, 2016).

In contrast to mammals, adult neurogenesis in zebrafish is robust and widespread, with 16 distinct constitutively proliferative zones that are mostly located along the ventricular surface but also deeper in the brain parenchyma (Kaslin et al., 2008). These zones are detected along the entire rostro-caudal axis of the zebrafish brain and contain ventricularly positioned self-renewing neural progenitors (Grandel et al., 2006; Kaslin et al., 2008; Kizil et al., 2012b; Grandel and Brand, 2013). Zebrafish CNS regenerates *via* the proliferation and differentiation of the radial glial cells (RGCs), also referred to as ependymoglia due to their functional orthology to the mammalian ependymal cells, and the neuroepithelial-like progenitor cells (Grandel et al., 2006; Ganz et al., 2010; Fleisch et al., 2011; Kizil et al., 2012b; Kaslin et al., 2017; Lindsey et al., 2017; Zambusi and Ninkovic, 2020). The permissive environment, which is necessary for these progenitors—upon injury—to become activated and differentiate into functional neurons, results most likely from the fact that zebrafish does not form any obvious scar tissue after injury in the CNS, thus granting zebrafish a regeneration potential higher than that of mammals (Becker and Becker, 2002; Kroehne et al., 2011).

Being one of the best-characterized regions of the adult zebrafish brain, the telencephalon harbors at least two distinct neurogenic zones, the dorsal and the medio-ventral neurogenic niches, with ependymoglial cells that differ in their proliferation and progeny characteristics (Marz et al., 2010; Zambusi and Ninkovic, 2020). Accordingly, these cells express different markers including glial fibrillary acidic protein (Gfap), S100β, nestin, brain lipid-binding protein (Blbp), aromatase, and SRY-box 2 (Sox2), confirming their radial glia-like nature (Adolf et al., 2006; Pellegrini et al., 2007; Lam et al., 2009; Ganz et al., 2010; Marz et al., 2010; Kroehne et al., 2011). A recent study on transcriptome analysis has identified novel markers for radial glia, newborn neurons, and mature neurons (Lange et al., 2020). Several inflammation-related programs including the chemokine receptor Cxcr5, the zinc finger transcription factor Gata3, and cysteinyl leukotriene signaling have been shown to promote the proliferation and generation of newborn neurons, thus enhancing neuronal regeneration in response to injury (Kizil et al., 2012a,b; Kyritsis et al., 2012). Fibroblast growth factor (Fgf) signaling and aryl hydrocarbon receptor (AhR) signaling have also been reported to directly regulate ependymoglial cell proliferation in the adult zebrafish telencephalon (Ganz et al., 2010; Di Giaimo et al., 2018). Yet, little is known about the neural signaling pathways and the molecular interaction networks that are involved in zebrafish brain regeneration. This is particularly in question for the early stages of brain regeneration, where a deeper knowledge of the contributory pathways with a special focus on their crosstalk is necessary to understand the underlying mechanisms.

To address these questions, we have set out to identify the genes that are differentially expressed in the zebrafish telencephalon during early regeneration in response to stab wound injury and focused on two early stages: (1) the early wound healing stage at 20 h post-lesion (hpl) and (2) the early proliferative stage at 3 days post-lesion (dpl). To this end, we have performed whole transcriptome analyses of the telencephalon by comparing (a) the lesioned and unlesioned hemispheres at two regenerative stages separately and (b) the lesioned hemispheres of the two stages to each other. Upon comparing the injury responses of the hemispheres at the early wound healing stage, we have found that the number of differentially expressed genes (DEGs) in the lesioned hemisphere is by far higher than that of the unlesioned hemisphere. In the early proliferative stage, however, the difference between the responses of the hemispheres declined noticeably and more than 40% of all DEGs are shared. Our comparative transcriptome analyses of the lesioned hemispheres at the wound healing and proliferative stages have revealed a considerably large pool of DEGs that are not shared, reflecting a discrepancy in the transcriptional profiles of these stages. Using Gene Ontology (GO) term and Kyoto Encyclopedia of Genes and Genomes (KEGG) pathway analysis,

we have deciphered an enrichment of the gene sets related to the Wnt/β-catenin signaling pathway predominantly at 20 hpl and confirmed this experimentally at the messenger RNA (mRNA) and protein levels. To further investigate how Wnt/β-catenin signaling regulates regeneration at the molecular level, we have unveiled the Wnt targetome by analyzing the transcriptomes of the lesioned hemispheres where Wnt signaling is suppressed from the time of injury to 20 hpl or 3 dpl. Our data have demonstrated that the Wnt targetome at 20 hpl is considerably larger than that at 3 dpl and that Wnt/β-catenin signaling controls a variety of key signaling pathways including p53, apoptosis, forkhead box O (FoxO), mitogen-activated protein kinase (MAPK), and mammalian target of rapamycin (mTOR) at the early wound healing stage of brain regeneration. Overall, by using a prominent combination of bioinformatics and experimental validation of the bioinformatics data, we unravel the whole transcriptomes of the lesioned and unlesioned hemispheres at the early wound healing and proliferative stages of brain regeneration and highlight the significance of Wnt/β-catenin signaling in the regulation of cellular and molecular events taking place during early regeneration.

# MATERIALS AND METHODS

## Stab Wound Assay

A transgenic reporter of Tcf/Lef-mediated transcription 6xTCF/Lef-miniP:2dGFP [Tg(6XTCF:dGFP)] (Shimizu et al., 2012) was used for RNA isolation and transcriptome analysis. Wild-type (wt) AB zebrafish were used for immunofluorescence staining. Before surgery, fish were anesthetized with 0.02% of Tricaine (MS-222, Sigma-Aldrich). Stab injury was performed in 6–9-months-old male fish as previously described (Kroehne et al., 2011; Baumgart et al., 2012). A 30-gauge needle was inserted through the left nostril until the end of the telencephalon. Afterward, the fish were transferred into a tank with freshwater. Animal experiments were approved by the Animal Experiments Local Ethics Committee of İzmir Biomedicine and Genome Center (IBG-AELEC).

## Drug Treatment

To inhibit Wnt/β-catenin signaling during regeneration, zebrafish that are exposed to stab wound injury of the brain were immersed in fish water containing 20 μM IWR-1 (Sigma-Aldrich, MO, United States) dissolved in dimethyl sulfoxide (DMSO). Inhibitor of Wnt response (IWR) treatment was initiated directly after stab injury and terminated at either 20 hpl or 3 dpl. IWR-1 containing fish water was refreshed daily.

## Tissue Preparation

After performing stab wound injury in the telencephalon, the fish were euthanized and severed heads were fixed in 4% paraformaldehyde (PFA) overnight at 4°C. Next, the heads were transferred into 20% sucrose–20% EDTA for 2 days at 4°C and 30% sucrose–20% EDTA overnight at 4°C. The heads were embedded in 20% sucrose–7.5% gelatin solution kept in a box filled with dry ice. Brain sections of 14 μm were cut at −20°C using a cryostat (CM1850, Leica, Wetzlar, Germany) and stored at -20°C until further use.

## Immunohistochemistry and Imaging

The brain sections on slides were dried at room temperature (RT) for 20 min. The slides were washed twice with PBSTX (1× PBS/0.3% Triton X-100) for 10 min. After incubation with 10 mM sodium citrate for 15 min at 85°C, they were washed with 1 × PBS twice for 5 min and incubated with diluted primary antibody in PBSTX at 4°C overnight. The next day, the slides were washed three times with PBSTX for 10 min at RT, incubated with secondary antibody, and washed three times with 1× PBS for 5 min at RT. Images were obtained using an LSM 880 laser scanning confocal microscope (Carl Zeiss AG, Oberkochen, Germany). The primary antibodies are as follows: mouse anti-GFAP (1:500, ab154474, Abcam, Cambridge, United Kingdom), mouse anti-PCNA (1:500, M0879, Dako, Agilent, CA, United States), rabbit anti-S100β (1:500, Z0311, Dako, Agilent), mouse anti-acetylated tubulin (1:250, T6793, Sigma-Aldrich, MO, United States), and rabbit anti-phospho-β-catenin (1:100, D2F1, Cell Signaling Technology, MA, United States). The secondary antibodies are as follows: rhodamine (TRITC) AffiniPure donkey anti-rabbit IgG (1:200, 711-025-152, Jackson Immunoresearch Laboratories, PA, United States) and Cy5 AffiniPure donkey anti-rat IgG (H+L) (1:400, 712-175-150, Jackson Immunoresearch Laboratories). Nuclear staining was performed with 4′,6-diamidino-2-phenylindole (DAPI; 4083S, Cell Signaling Technology).

## RNA Isolation and cDNA Preparation

After stab wound injury was performed, zebrafish were anesthetized using 0.02% Tricaine-S solution and sacrificed at either 20 h post-lesion (hpl) or 3 days post-lesion (dpl). Firstly, the heads were separated from the fish and then the lesioned (left) and unlesioned (right) hemispheres were dissected individually to examine the influence of the injury between them (**Figures 1A,B**). The left and right hemispheres of healthy zebrafish telencephalon were used as control samples. The experiments were carried out in triplicate for each group. All brain samples were transferred into an RNAprotect tissue reagent (Qiagen, Hilden, Germany) immediately to prevent RNA degradation. Total RNA was extracted using the RNeasy Plus Micro Kit (Qiagen) according to the manufacturer's instructions. RNA samples were quantified by using a NanoDrop 2000 spectrophotometer (Thermo Scientific, MA, United States). RNA integrity was assessed using an Agilent RNA 6000 Pico with the Agilent 2100 Bioanalyzer (Agilent Technologies, CA, United States). The samples were sent to the Genomics Core Facility (GeneCore, EMBL Heidelberg, Germany) for library preparation and RNA sequencing.

## Library Preparation and RNA Sequencing

Libraries were prepared using an Illumina TruSeq RNA Library Preparation Kit v2 (Illumina, San Diego, CA, United States) according to the manufacturer's recommendations by using 500 ng complementary DNA (cDNA) as input. For size selection, 300

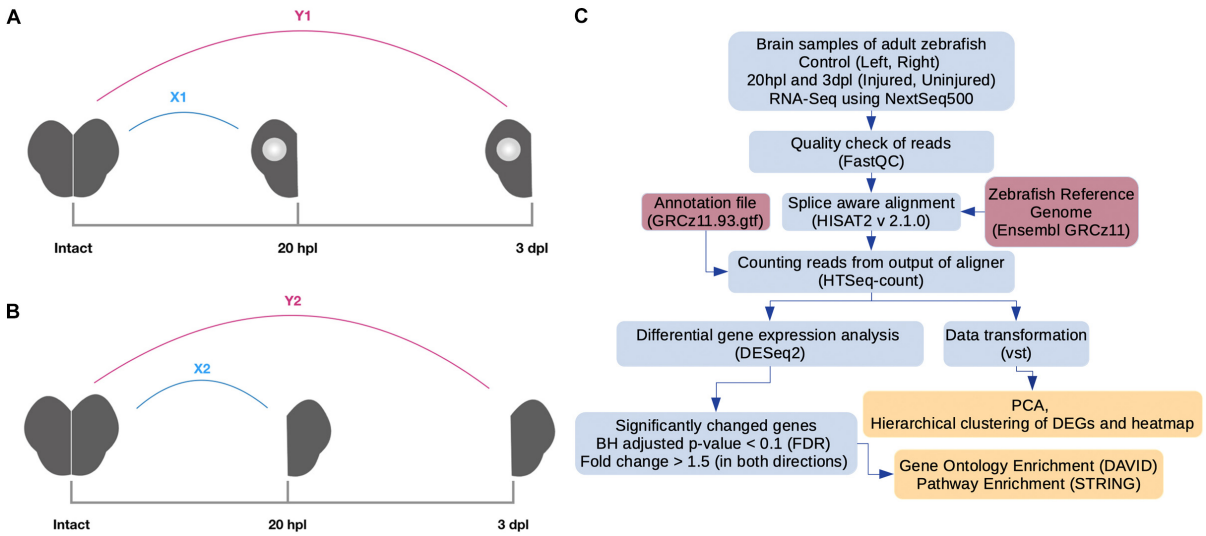


**FIGURE 1 |** Pipeline for RNA preparation and analysis of RNA sequencing (RNA-seq) data. **(A)** Preparation of RNA samples from the lesioned hemispheres at 20 hpl or 3 dpl. *X1*: comparison of the lesioned hemisphere at 20 hpl with the intact brain; *Y1*: comparison of the lesioned hemisphere at 3 dpl with the intact brain. **(B)** Preparation of RNA samples from the unlesioned hemispheres at 20 hpl or 3 dpl. *X2*: comparison of the unlesioned hemisphere at 20 hpl with the intact brain; *Y2*: comparison of the unlesioned hemisphere at 3 dpl with the intact brain. **(C)** RNA-seq reads were generated using Illumina NextSeq 500. The quality of reads was checked by the FastQC tool. Next, alignment and counting of reads were performed by using a zebrafish reference genome (Ensembl, GRCz11) and the annotation file (Ensembl, GRCz11.93) by HISAT2 and HTSeq-count tools, respectively. Counts were transformed with variance stabilizing transformation (vst) to perform principal component analysis and hierarchical clustering. To select genes as differentially expressed, we used the DESeq2 package with the following criteria: fold change > 1.5 (in both directions) and Benjamini–Hochberg adjusted *p*-value (FDR) < 0.1. Gene Ontology and pathway enrichment analyses were performed by using DAVID and the STRING tool of Cytoscape, respectively. *hpl*, hours post-lesion; *dpl*, days post-lesion.

bp cDNAs were selected. Paired-end, strand-specific sequencing for total RNA was performed on Illumina NextSeq 500 with 75 bp read lengths.

## Bioinformatics Analysis

For each sample, quality control of the reads was inspected by using the FastQC tool; low-quality reads and adapter sequences were removed by using Trimmomatic (Bolger et al., 2014). RNA sequencing (RNA-seq) reads were aligned to the zebrafish reference genome (Ensembl, GRCz11) using HISAT2 (2.1.0) (Kim et al., 2015). After alignment, the transcripts were assembled and counted by HTSeq (Anders et al., 2015) by using the annotation file from the Ensembl website (Danio_rerio.GRCz11.93.gtf) (**Figure 1C**). The DESeq2 package (Love et al., 2014) of Bioconductor (Gentleman et al., 2004) was used to carry out normalization of read counts, their transformation (vst), and differential expression analysis. Principal component analysis (PCA) was performed to check the vst-transformed read counts and visualized with ggplot2 (Wickham, 2016; **Supplementary Figure S1**). To find DEGs, we performed Wald tests for the following comparisons using DESeq2: 20 hpl lesioned hemisphere vs. control (X1); 20 hpl unlesioned hemisphere vs. control (X2); 20 hpl lesioned hemisphere after IWR treatment vs. 20 hpl lesioned hemisphere (X3); 20 hpl lesioned hemisphere after IWR treatment vs. control (X4); 3 dpl lesioned hemisphere vs. control (Y1); 3 dpl unlesioned hemisphere vs. control (Y2); 3 dpl lesioned hemisphere after IWR treatment vs. 3-dpl lesioned hemisphere (Y3); and 3 dpl lesioned hemisphere after IWR treatment vs. control (Y4) (**Figures 1A,B**, **6B**). For all eight groups, we selected a gene as upregulated if the fold change > 1.5 and downregulated if the fold change < 0.67 ( = 1/1.5), which we will simply refer to as "FC > 1.5 in both directions" hereafter (**Supplementary Table S1**). The lists of the significantly downregulated and upregulated genes obtained from individual comparisons were used as inputs for statistical enrichment analyses with regard to GO terms by using the Database for Annotation, Visualization and Integrated Discovery (DAVID) 6.8 bioinformatics functional annotation tool (Huang da et al., 2009). Functional enrichment was performed in three categories of GO terms: biological process (BP), molecular function (MF), and cellular component (CC). The EASE score, a modified one-tailed Fisher's exact test, was used to identify the GO terms by means of a user-defined gene list for each defined DAVID GO term. KEGG pathway (Kanehisa and Goto, 2000) and Reactome pathway (Fabregat et al., 2018) analyses were performed using all significantly changed genes with the StringApp tool of Cytoscape 3.7.2 (Shannon et al., 2003; Doncheva et al., 2019). Gene lists related to the selected GO terms and KEGG pathways were obtained from the KEGG and AmiGO databases and plotted using the GOplot package (Walter et al., 2015).

## qPCR and Statistical Analysis

All samples with RIN ≥ 7.0 (our samples ranged from 8.1 to 10) were converted to cDNA using ProtoScript II First Strand cDNA Synthesis Kit (New England BioLabs, MA, United States)

according to the manufacturer's instructions. Zebrafish *rpl13a* (*ribosomal protein L13a*) was used as the reference gene for normalization to determine the relative gene expression levels. Quantitative PCR (qPCR) was performed in triplicate using GoTaq qPCR Master Mix (Promega, Madison, WI, United States) at an Applied Biosystems 7500 Fast Real Time PCR machine (Foster City, CA, United States). The data were analyzed using the GraphPad Prism 8 software (Graphpad Software Inc., CA, United States). The values are the mean ± SEM (standard error of mean) of three samples. Primer sequences for the following zebrafish genes are listed in **Supplementary Table S2**: *adam8a*, *c1qc*, *capgb*, *cd74b*, *cdk2*, *csf1ra*, *ctgfa*, *egfp*, *epha2a*, *foxo1a*, *fsta*, *gadd45ga*, *gfap*, *grem1b*, *il6st*, *inhbab*, *isl1*, *klf11b*, *lef1*, *mCherry*, *mpeg1.1*, *pappaa*, *pcna*, *prg4b*, *rpl13a*, *sgk2b*, *tbx2a*, and *tfa*.

# RESULTS

## Transcriptome Profiling of the Telencephalon During the Early Wound Healing Stage of Regeneration

While the later stages of brain regeneration have been relatively better understood, little is known about the early stages especially at the level of differential gene expression. To determine the changes in gene expression that control the molecular mechanisms underlying early brain regeneration, we aimed to identify and compare the entire transcriptomes of the zebrafish telencephalon at two early regenerative stages, i.e., 20 hpl and 3 dpl. Several telencephalon genes have been found to be significantly upregulated in the lesioned and unlesioned hemispheres (Kroehne et al., 2011; Kizil et al., 2012b). However, their injury responses have not been compared at the transcriptome level before. Thus, to distinguish between the responses of the lesioned and unlesioned hemispheres and avoid the dilution of genes that are differentially expressed mainly in the lesioned hemisphere, we decided to dissect the telencephalic hemispheres and have their transcriptome sequenced separately (**Figure 1**). Before sequencing, we validated the injury response by measuring the expression levels of *gfap* and *gata3* that are known to be strongly upregulated in the lesioned hemisphere upon injury (**Supplementary Figure S1**) (Kroehne et al., 2011). We found that 1,472 genes [829 upregulated (Up) and 643 downregulated (Down)] were significantly differentially expressed in the lesioned hemisphere at 20 hpl (X1) as compared to the equivalent hemisphere of the unlesioned brain, and 1,356 (785 Up and 571 Down) of them were unique to X1 (**Figure 2A** and **Supplementary Table S3**). *en1a*, *abhd2b*, and *lyrm5b* were in the top 10 Down genes while *mthfd1l*, *tbx2a*, and *entpd2b* were in the top 10 Up genes in X1 (**Figure 2B**). In the unlesioned hemisphere at 20 hpl (X2), we detected 211 DEGs (76 Up and 135 Down) with lower fold changes in both the Up and Down genes as compared to X1, and 95 genes (32 Up and 63 Down) were unique to X2 (**Figure 2A** and **Supplementary Table S3**). *igfbp1a*, *cd74a*, and *nt5c2l1* were the top three Down genes while *stat3*, *anxa2a*, and *mid1ip1b* were the top three Up genes in X2 (**Figure 2C**). Only 7% of all DEGs, i.e., 116 genes (44 Up and 72 Down), including those encoding for several heat shock proteins, leucine-rich repeat-containing proteins, and phosphatases were shared between X1 and X2 (**Figure 2A** and **Supplementary Table S3**). The top GO terms in X1 and X2 showed no overlap, parallel to the low number of genes shared between them (**Figures 2D,E**). We also determined altered GO terms and Reactome pathways by comparing the X1 and X2 groups (**Supplementary Figures S2, S3** and **Supplementary Tables S4, S5**). While there were 20 KEGG pathways significantly enriched in X1, only four pathways were enriched in X2 (**Figure 2F** and **Supplementary Table S5**). To confirm the results of the bioinformatics analyses, we quantified the expressions of several genes related to tissue regeneration (Kroehne et al., 2011; Tsujioka et al., 2017; Galvao et al., 2018; Yu et al., 2019). *prg4a* and *klf11* were indeed upregulated only in the lesioned hemisphere (**Figure 2G**), while *gfap* and *il6st* were so in both hemispheres (**Figure 2H**). Several tubulin genes (*tubb6*, *tuba1b*, *tuba8l*, *tub*, and *tubb4b*) were upregulated not only in X1 but also in X2 (*tuba8l4*) (**Supplementary Table S1**). We confirmed this by immunofluorescence staining for acetylated tubulin, a neuronal microtubule marker that mainly labeled the parenchyma cells in the control and became strongly upregulated in the cells lining the ventricle after injury (**Figures 2I,J**). These data collectively indicate that, at the early wound healing stage, remarkably, i.e., seven times, higher numbers of genes are differentially expressed in the lesioned hemisphere as compared to the unlesioned hemisphere.

## Transcriptome Profiling of the Telencephalon During the Early Proliferative Stage of Regeneration

The telencephalon is known to react to injury by a strong induction of proliferation that peaks at 3 dpl mainly in the ventricular zone of the lesioned hemisphere (Kroehne et al., 2011; Marz et al., 2011; Lindsey et al., 2017). By analyzing the transcriptomics data at 3 dpl, we identified 1,707 genes (924 Up and 783 Down) to be significantly differentially expressed in the lesioned hemisphere at 3 dpl (Y1) as compared to the corresponding hemisphere of the unlesioned brain, and 861 (589 Up and 272 Down) of them were unique to Y1 (**Figure 3A** and **Supplementary Tables S1, S3**). In contrast to 20 hpl, most DEGs were shared between Y1 and Y2 (unlesioned hemisphere at 3 dpl), where we identified a total of 1,215 DEGs (530 Up and 685 Down), only 369 (195 Up and 174 Down) of which were unique to Y2 (**Figure 3A** and **Supplementary Tables S1, S3**). *en1a*, *mhc1uba*, and *mhc2dab* were in the top 10 Down genes in both Y1 and Y2, while *capgb*, *c1qb*, and *entpd2b* were in the top 10 Up genes in Y1 (**Figure 3B**) and *isl1*, *msh4*, and *tfa* were in the top 11 Up genes in Y2 (**Figure 3C**). Eight hundred forty-six genes (335 Up and 511 Down) were shared between Y1 and Y2 and harbored many members of gene families encoding for solute carriers, calcium channels, ring finger proteins, and protocadherins (**Figure 3A** and **Supplementary Table S3**). The top 40 GO terms in Y1 and Y2 overlapped by 25% (**Figures 3D,E**). We also defined altered GO terms and Reactome pathways by comparing the Y1 and Y2 groups (**Supplementary Figures S4, S5** and

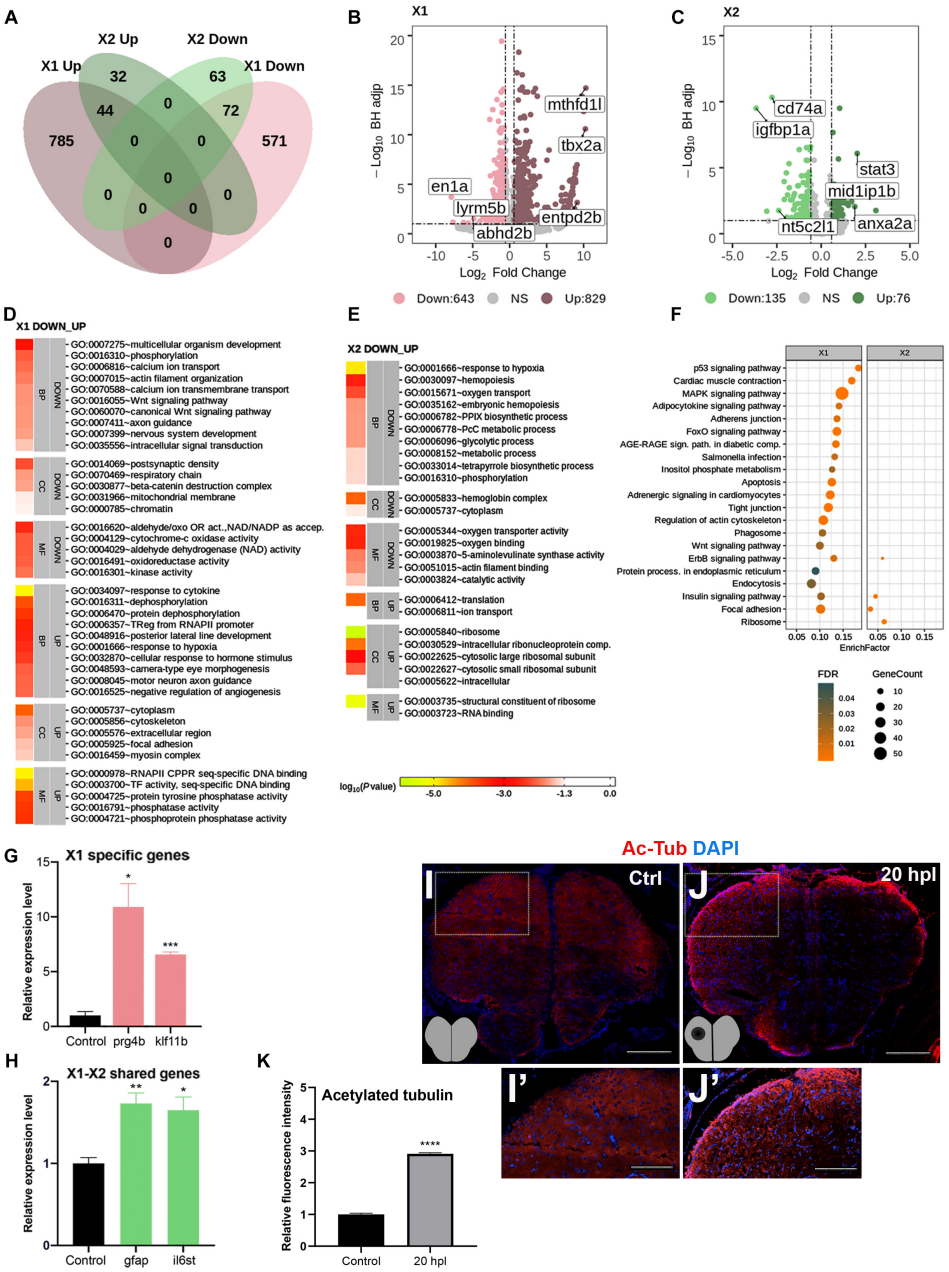


**FIGURE 2 |** Transcriptome profiling of the telencephalon during the early wound healing stage of regeneration. **(A)** The Venn diagram shows the number of upregulated (*Up*) or downregulated (*Down*) differentially expressed genes (DEGs) in the lesioned (*X1*, *pink*) and unlesioned (*X2*, *green*) hemispheres and the overlap between each set of DEGs at 20 hpl. A total of 1,472 and 211 genes were significantly changed in X1 and X2, respectively. There were 116 genes shared between X1 and X2. **(B,C)** Volcano plots representing changes in the gene expression levels in X1 and X2. *Each point* represents a gene. The *X*-axis shows $\log_2$ of fold change in the condition compared to control and the *vertical dashed lines* indicate the fold change cutoffs. The *Y*-axis represents -$\log_{10}$ of the Benjamini–Hochberg adjusted *p*-value, where the significance threshold is indicated by the *dashed horizontal line*. Number of upregulated genes in X1 and X2: 829 and 76, respectively, and downregulated genes in X1 and X2: 643 and 135, respectively. *Darker* and *lighter shades* in **(A–C)** indicate upregulation and downregulation, respectively. **(D,E)** DAVID bioinformatics tool was used to show the most significantly enriched GO terms based on the transcriptional changes in X1 and X2 comparisons. The heatmap scale shows $\log_{10}$ of the EASE *p*-value for the most significantly enriched GO terms. **(F)** STRING bioinformatics tool was used to show the most significantly enriched KEGG pathways based on the transcriptional changes in X1 and X2. The *dot plot* represents KEGG pathways enriched in X1 and X2 by using all significantly changed genes in these comparisons based on FDR and EnrichFactor. **(G,H)** Relative expression levels of X1-specific genes (*prg4b* and *klf11b*) and the genes shared between X1 and X2 (*gfap* and *il6st*). Statistical significance was evaluated using unpaired *t*-test. $^*p < 0.05$, $^{**}p < 0.01$, and $^{***}p < 0.001$. *Error bars* represent ± standard error of the mean (SEM, $n = 3$). **(I–I',J–J')** Anti-acetylated tubulin staining of the control and 20 hpl brain sections with *boxed* areas magnified. Sections are counterstained for DAPI. *Scale bars*, 200 μm in **(I,J)**; 100 μm in **(I')** and **(J')**. **(K)** Relative fluorescence intensity in brain sections stained for anti-acetylated tubulin. *DAVID*, Database for Annotation, Visualization and Integrated Discovery; *GO*, Gene Ontology; *BP*, biological process; *CC*, cellular component; *MF*, molecular function; *STRING*, Search Tool for the Retrieval of Interacting Genes/Proteins; *KEGG*, Kyoto Encyclopedia of Genes and Genomes; *FDR*, false discovery rate; *hpl*, hours post-lesion. See section "Materials and Methods" for the definition of DEGs covered in X and Y comparisons. $^*p < 0.05$, $^{**}p < 0.01$, $^{***}p < 0.001$, and $^{****}p < 0.0001$.

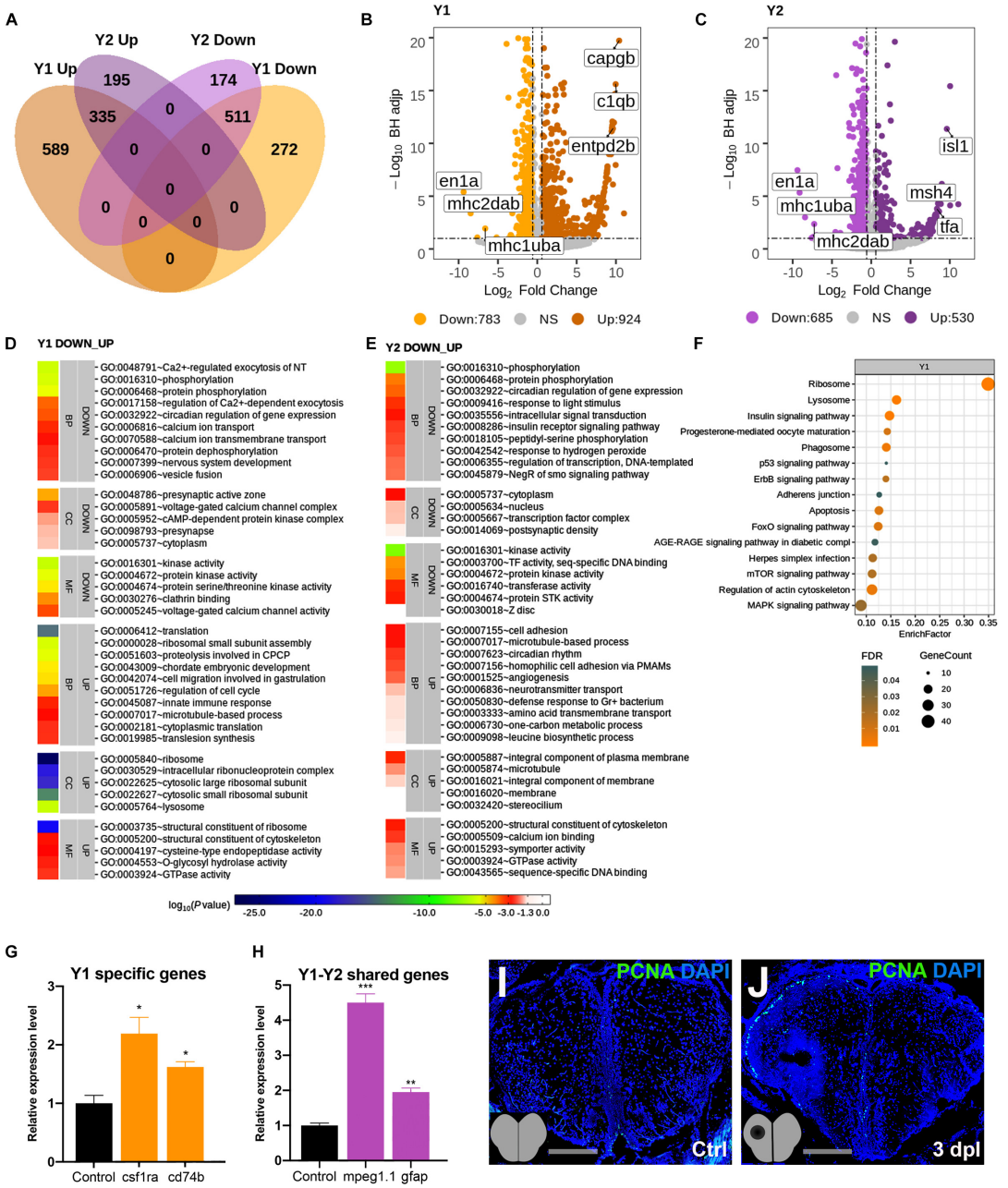


**FIGURE 3 |** Transcriptome profiling of the telencephalon during the early proliferative stage of regeneration. **(A)** The Venn diagram shows the number of upregulated (*Up*) or downregulated (*Down*) differentially expressed genes (DEGs) in the lesioned (*Y1*, *orange*) and unlesioned (*Y2*, *purple*) hemispheres and the overlap between each set of DEGs at 3 dpl. A total of 1,707 and 1,215 genes were significantly changed in Y1 and Y2, respectively. There were 846 genes shared between Y1 and Y2. **(B,C)** Volcano plots representing changes in the gene expression levels in Y1 and Y2. *Each point* represents a gene. The *X*-axis shows $\log_2$ of fold change in the condition compared to the control and *dashed vertical lines* indicate the fold change cutoff. The *Y*-axis represents $-\log_{10}$ of the Benjamini–Hochberg adjusted *p*-value, where the significance threshold is indicated by the *dashed horizontal line*. Number of upregulated genes in Y1 and Y2: 924 and 530, respectively, and downregulated genes in Y1 and Y2: 783 and 685, respectively. *Darker* and *lighter shades* in **(A–C)** indicate upregulation and downregulation, respectively. **(D,E)** DAVID bioinformatics tool was used to show the most significantly enriched GO terms based on the transcriptional changes in Y1 and Y2 comparisons. The heatmap scale shows $\log_{10}$ of the EASE *p*-value for the most significantly enriched GO terms. **(F)** STRING bioinformatics tool was used to show the most significantly enriched KEGG pathways based on the transcriptional changes in X1 and X2. The *dot plot* represents KEGG pathways enriched in X1 and X2 by using all significantly changed genes in these comparisons based on FDR and EnrichFactor. **(G,H)** Relative expression levels of Y1-specific genes (*csf1ra* and *cd74b*) and the genes shared between Y1 and Y2 (*mpeg1.1* and *gfap*). Statistical significance was evaluated using unpaired *t*-test. $^*p < 0.05$, $^{**}p < 0.01$, and $^{***}p < 0.001$. *Error bars* represent ± standard error of the mean (SEM, $n = 3$). **(I,J)** Anti-PCNA staining of the control and 3 dpl brain sections. Sections are counterstained for DAPI. *DAVID*, Database for Annotation, Visualization and Integrated Discovery; *GO*, Gene Ontology; *BP*, biological process; *CC*, cellular component; *MF*, molecular function; *STRING*, Search Tool for the Retrieval of Interacting Genes/Proteins; *KEGG*, Kyoto Encyclopedia of Genes and Genomes; *FDR*, false discovery rate; *dpl*, days post-lesion. See section "Materials and Methods" for the definition of DEGs covered in X and Y comparisons.

**Supplementary Tables S4, S5**). There were 15 KEGG pathways significantly enriched in Y1 (**Figure 3F** and **Supplementary Table S5**). The qPCR results confirmed that the regeneration-related DEGs *csf1ra* and *cd74b* (Chitu et al., 2016; Hwang et al., 2017) were upregulated in the lesioned hemisphere (**Figure 3G**) and *mpeg1.1* and *gfap* (Kroehne et al., 2011; Paredes et al., 2015) in both hemispheres (**Figure 3H**). Moreover, we observed a remarkable increase in the number of proliferating cells at the ventricular zone of the telencephalon in the lesioned hemisphere, detected by proliferating cell nuclear antigen (PCNA) antibody staining (**Figures 3I,J**). Thus, we conclude that the number of DEGs is higher in both hemispheres during the proliferative stage in comparison to the early wound healing stage and that 41% of all DEGs are shared between the lesioned and unlesioned hemispheres at this stage.

## The Early Wound Healing and Proliferative Stages of Brain Regeneration Are More Different Than Similar

Next, to compare the molecular and cellular events that occur in the lesioned hemisphere of the telencephalon at its early wound healing and proliferative stages, we compared the transcriptome profiles of the X1 and Y1 groups in detail. There were 1,015 DEGs (566 Up and 449 Down) that were unique to X1 and 1,250 DEGs (705 Up and 545 Down) were unique to Y1 (**Figure 4A** and **Supplementary Table S6**). We found that 457 genes (27% of X1 DEGs and 31% of Y1 DEGs) were shared between X1 and Y1 (**Figure 4A** and **Supplementary Table S6**). Among them, 395 genes were regulated in the same way, i.e., Up in both or Down in both, while 62 were regulated inversely. We next intersected the DEGs in X1 and Y1 to reveal genes differentially expressed at both time points. The heatmap displayed four groups of shared genes: group 1 with nine genes (e.g., *caspb* and *notch3*) Down in X1 and Up in Y1; group 2 with 185 genes (e.g., *hif1an*) Down in both X1 and Y1; group 3 with 53 genes (e.g., *mapk6*) Up in X1 and Down in Y1; and group 4 with 210 genes (e.g., *stat3*, *il6st*, *slc7a11*, and *s100b*) Up in both X1 and Y1 (**Figures 4B,C** and **Supplementary Table S6**). To compare the molecular data obtained from 20 hpl and 3 dpl using GO term enrichment, we used three groups of DEGs: (1) DEGs unique to X1; (2) DEGs unique to Y1; and (3) DEGs shared between X1 and Y1. GO term and KEGG pathway analyses showed enrichment of the Wnt signaling pathway exclusively in X1, whereas several other signaling pathways including p53, ErbB, FoxO, apoptosis, insulin, and MAPK were shared between X1 and Y1; mTOR signaling was uniquely enriched in Y1 (**Figure 4D**, **Supplementary Figure S6**, and **Supplementary Table S5**). To validate differential gene expression, we selected DEGs that are unique to X1 (*tbx2a* and *grem1b*), unique to Y1 (*cdk2* and *c1qc*), or shared between X1 and Y1 (*adam8a* and *capgb*), which are all known to be involved in tissue regeneration (Schlomann et al., 2000; Garnier et al., 2009; Satoh and Makanae, 2014; Peterson et al., 2015; Wang et al., 2015; Tang et al., 2017). All selected DEGs became upregulated after injury in the corresponding hemisphere, as detected by qPCR (**Figures 4E–H**). Furthermore, immunofluorescence staining for the glial cell markers S100β and glial fibrillary acidic protein (GFAP) confirmed upregulation at both 20 hpl and 3 dpl (**Figures 4I–N**). Overall, the early wound healing and proliferative stages of brain regeneration share less than a third of their individual pools of DEGs, strongly suggesting that the molecular and cellular mechanisms of regeneration substantially differ at these stages.

## Wnt/β-Catenin Signaling Is Activated During the Early Wound Healing Stage in the Regenerating Brain

Comparative analyses of the GO terms and KEGG pathways for the genes that are differentially expressed at 20 hpl and 3 dpl have disclosed a strong and specific enrichment of gene sets related to Wnt signaling at 20 hpl: "Wnt signaling pathway," "canonical Wnt signaling pathway," "β-catenin destruction complex," and "negative regulation of canonical Wnt signaling pathway" (**Figure 4D**, **Supplementary Figure S6**, and **Supplementary Tables S4, S5**). Thus, we next aimed to address the role and molecular targets of Wnt/β-catenin signaling, the so-called canonical Wnt pathway, during the early wound healing stage of brain regeneration. Wnt/β-catenin signaling is one of the most common intracellular signal transduction pathways activated in response to injury of virtually all tissues/organs (Ozhan and Weidinger, 2014). While Wnt signaling has been revealed to promote regeneration of the optic tectum, the spinal cord, and the tectum of the midbrain in zebrafish (Shimizu et al., 2012, 2018; Strand et al., 2016; Wehner et al., 2017; Lindsey et al., 2019), it has not yet been associated with the regeneration of the telencephalon. We have used the Tg(6XTCF:dGFP) transgenic zebrafish reporter of Tcf/Lef-mediated transcription, which has been shown to sensitively detect Wnt/β-catenin pathway activity in several cellular contexts (Shimizu et al., 2012). GFP expression in the reporter line is difficult to detect because of the unstable nature of GFP, leading to a low level of fluorescence in the adult zebrafish. We have performed immunofluorescence staining for anti-GFP at 20 hpl and detected Wnt activity in the lesioned area, most likely in the brain endothelial and blood cells (**Supplementary Figure S7**). Quantification of pathway activity by qPCR in the reporter line indeed showed an upregulation of Wnt signaling in both the lesioned and unlesioned hemispheres at 20 hpl (**Figure 5A**). Interestingly, signaling became downregulated in the lesioned hemisphere at 3 dpl while staying elevated in the unlesioned hemisphere, suggesting that it is specifically suppressed in the lesioned hemisphere after the wound healing stage. We also verified the significant activation of Wnt/β-catenin signaling at 20 hpl in the lesioned telencephalic hemispheres of the samples that were sent for RNA sequencing (**Figure 5B**). The Wnt/β-catenin target genes *lef1* and *egr2a* were likewise upregulated at 20 hpl in the lesioned hemispheres (**Figure 5C**). Immunofluorescence staining of brain sections showed an elevation of phospho-β-catenin (Ser675) levels in the lesioned hemisphere, especially in the vicinity of the lesion, indicating an increased transcriptional activity of β-catenin (**Figures 5D–I**). Considering the high levels of Wnt/β-catenin activity in the

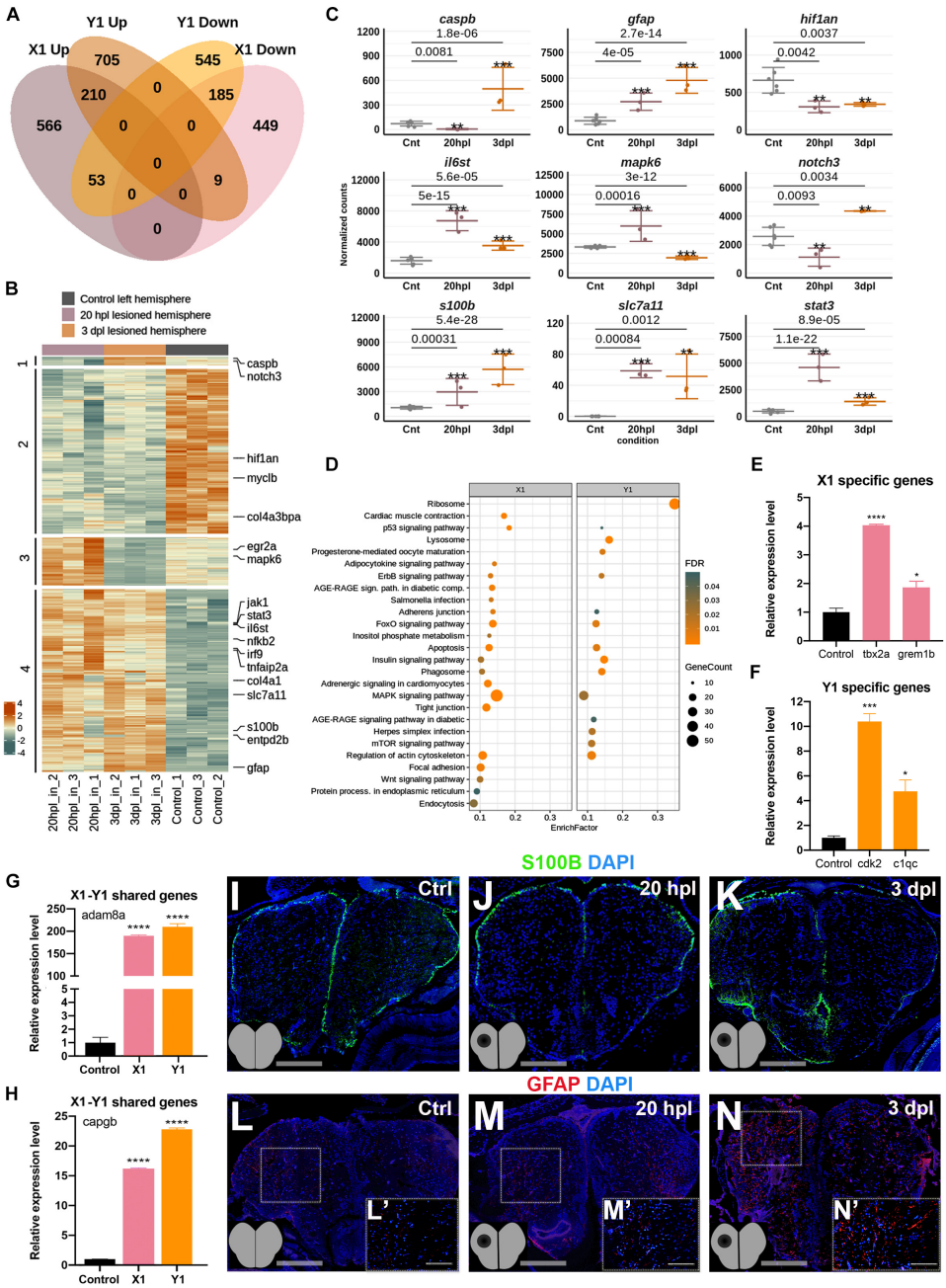


**FIGURE 4 |** Early wound healing and proliferative stages of brain regeneration are more different than similar. **(A)** The Venn diagram shows the number of upregulated (*Up*) or downregulated (*Down*) differentially expressed genes (DEGs) in the lesioned 20-hpl (*X1*, *pink*) and lesioned 3-dpl (*Y1*, *orange*) hemispheres and the overlap between each set of DEGs. Out of 1,472 genes, 1,015 were significantly changed only in X1, while 1,250 out of 1,707 genes were so in Y1. There were 457 genes shared between X1 and Y1. *Darker* and *lighter shades* indicate upregulation and downregulation, respectively. **(B)** The heatmap shows the expressions of genes shared between X1 and Y1. Each *column* represents a single hemisphere from a single telencephalon and each *row* shows a single gene. The *scale bar* shows counts *Z*-scores from high to low expression, represented by a color gradient from *orange* to *green*, respectively. **(C)** Dot plot representation of normalized transformed read counts of a representative set of genes shared between X1 and Y1 (*gray*: control samples; *pink*: 20-hpl lesioned hemisphere; *orange*: 3 dpl lesioned hemisphere). The mean ± standard deviations (SD) of three independent experiments are plotted. **(D)** STRING bioinformatics tool was used to show the most significantly enriched KEGG pathways based on the transcriptional changes in X1 and X2. The *dot plot* represents KEGG pathways enriched in X1 and Y1 by using all significantly changed genes in these comparisons based on FDR and EnrichFactor. **(E,F)** Relative expression levels of DEGs that are unique to X1 (*tbx2a* and *grem1b*) or unique to Y1 (*cdk2* and *c1qc*). **(G,H)** Relative expression levels of DEGs shared between X1 and Y1 (*adam8a* and *capgb*). Statistical significance was evaluated using unpaired *t*-test. ****$p < 0.0001$. *Error bars* represent ± standard error of the mean (SEM, $n = 3$). **(I–K)** Anti-S100β staining of the control, 20 hpl, and 3 dpl brain sections. **(L–N,L′–N′)** Anti-GFAP staining of the control, 20 hpl, and 3 dpl brain sections with *boxed* areas magnified. Sections are counterstained for DAPI. *Scale bars*, 200 μm in **(L–N)**; 100 μm in **(L′–N′)**. *STRING*, Search Tool for the Retrieval of Interacting Genes/Proteins; *KEGG*, Kyoto Encyclopedia of Genes and Genomes; *FDR*, false discovery rate; *hpl*, hours post-lesion; *dpl*, days post-lesion. See section "Materials and Methods" for the definition of DEGs covered in X and Y comparisons. *$p < 0.05$, **$p < 0.01$, ***$p < 0.001$, and ****$p < 0.0001$.

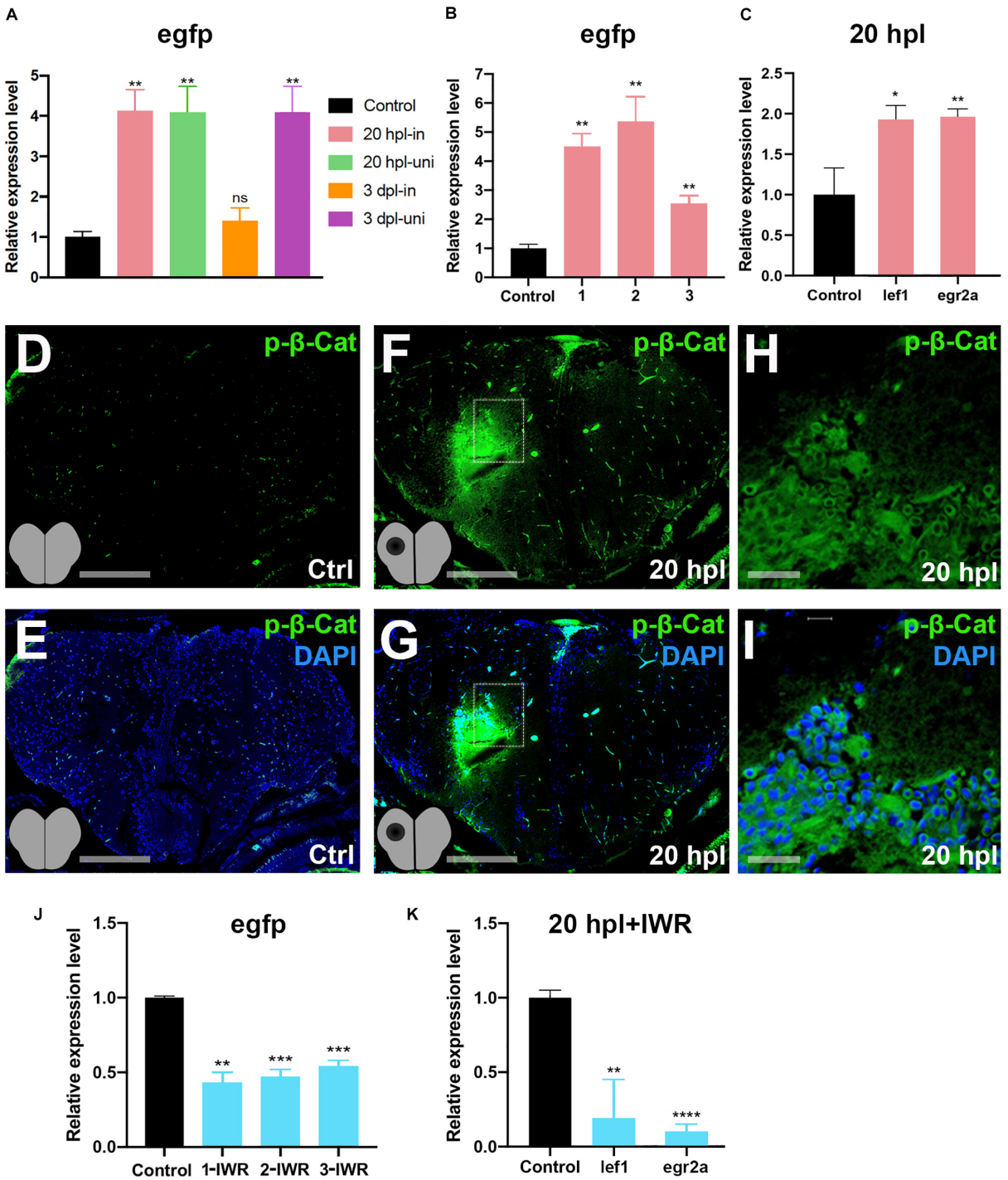


**FIGURE 5 |** Wnt/β-catenin signaling is activated during the early wound healing stage in the regenerating brain. **(A)** Relative expression levels of *egfp* as a reporter of Wnt/β-catenin signaling activity in the lesioned and unlesioned hemispheres of the telencephalon during the early wound healing and proliferative stages of regeneration. Three hemispheres were pooled for each sample. **(B)** Relative expression levels of *EGFP* as a reporter of Wnt/β-catenin signaling activity in the lesioned hemispheres of three independent telencephalon samples used for RNA sequencing during the early wound healing stage. **(C)** Relative expression levels of the known Wnt target genes *lef1* and *egr2a* in the lesioned hemisphere of the telencephalon during the early wound healing stage. **(D,E)** Anti-phospho-β-catenin staining of control brain sections. **(F,G)** Anti-phospho-β-catenin staining of 20-hpl brain sections. The lesioned area is *boxed* and shown in **(H,I)**. Sections are counterstained for DAPI. *Scale bars*, 200 μm in **(D–G)**; 25 μm in **(H,I)**. **(J)** Relative expression levels of *egfp* as a reporter of Wnt/β-catenin signaling activity in lesioned + IWR-1-treated hemispheres of three independent telencephalon samples collected at 20 hpl. **(K)** Relative expression levels of the Wnt target genes *lef-1* and *egr2a* in the pooled three lesioned + IWR-1-treated hemispheres at 20 hpl. Statistical significance was evaluated using unpaired *t*-test. $^{**}p < 0.01$ and $^{***}p < 0.001$. *Error bars* represent ± standard error of the mean (SEM, $n = 3$). *hpl*, hours post-lesion. $^{*}p < 0.05$, $^{**}p < 0.01$, $^{***}p < 0.001$, and $^{****}p < 0.0001$.

endothelial compartment of the zebrafish and mouse brains (Moro et al., 2012; Martowicz et al., 2019), it is likely that these Wnt-positive cells are non-CNS cells. To unravel how Wnt/β-catenin signaling regulates brain regeneration at the molecular level, we set out to identify its target genes in the early stage where signaling was significantly enhanced. To this purpose, we initially confirmed that Wnt/β-catenin signaling could be efficiently inhibited by the Wnt antagonist IWR-1, as evidenced by the significant reduction in the expressions of *egfp* in the Tg(6XTCF:dGFP) Wnt reporter and the canonical Wnt target genes *lef1* and *egr2a* in the lesioned hemisphere at 20 hpl (**Figures 5J,K**). Thus, we conclude that Wnt/β-catenin signaling is activated in the early wound healing stage of brain regeneration and returns to control level in the lesioned site at the early proliferative phase.

## Inhibition of Wnt/β-Catenin Signaling During the Early Wound Healing Stage Identifies 119 Target Genes That Are Positively Regulated by the Pathway

Next, to identify the Wnt targetome at the early wound healing and proliferative stages of brain regeneration, we suppressed Wnt/β-catenin signaling starting from the time of injury to 20 hpl or to 3 dpl by treating the zebrafish with the Wnt antagonist IWR-1 and had the transcriptome of the lesioned hemispheres sequenced at 20 hpl or 3 dpl. There were 293 genes (64 Up and 229 Down) in X3 and 103 genes (70 Up and 33 Down) in Y3 comparisons (**Figure 6A** and **Supplementary Table S1**). We termed DEGs that are Up in X1 and Down in X3 as the positively regulated Wnt targetome at 20 hpl and the genes that are Up in Y1 and Down in Y3 as the positively regulated Wnt targetome at 3 dpl (**Figures 1A**, **6B**). The Wnt targetome that was composed of 119 genes at 20 hpl (**Figures 6C,D** and **Supplementary Table S7**) sharply narrowed down to nine genes at 3 dpl (**Supplementary Figure S9** and **Supplementary Table S7**). Next, to validate the Wnt targetome at 20 hpl, we measured the expression levels of some genes selected from the targetome by qPCR. All selected genes were significantly upregulated in the lesioned hemisphere following injury and became downregulated when Wnt signaling was inhibited by IWR-1 from the time of injury until 20 hpl (**Figures 6E,F**). These results strongly suggest a key role for Wnt/β-catenin signaling in the early wound healing stage of regeneration.

## Inhibition of Wnt/β-Catenin Signaling During the Early Wound Stage Results in a Marked Alteration of the Gene Expression Profiles Represented in KEGG Pathway Enrichment

Among the KEGG pathways that were significantly enriched in the lesioned hemisphere at 20 hpl (X1) or 3 dpl (Y1), several of them, including the p53 signaling pathway, apoptosis, MAPK signaling pathway, and FoxO signaling pathway, were shared between X1 and Y1, whereas the Wnt and mTOR signaling pathways were unique to X1 and Y1, respectively (**Figures 2F**, **3F**, **4D**). Thus, we set out to compare how these KEGG pathways are altered in the lesioned hemisphere at 20 hpl and 3 dpl in response to inhibition of Wnt/β-catenin signaling. We termed the comparison of the 20 hpl lesioned hemisphere + IWR treatment to control as X4 and the comparison of the 3 dpl lesioned hemisphere + IWR treatment to control as Y4 (**Figure 6B**). There were 868 genes (387 Up and 481 Down) differentially expressed in X4 and 1,977 (1,179 Up and 798 Down) were so in Y4 (**Supplementary Table S1**). The genes we obtained from the KEGG and AmiGO databases included substantial numbers of genes involved in the Wnt, MAPK, apoptosis, mTOR, p53, and FoxO signaling pathways (**Supplementary Table S8**). To compare the alterations in the gene expression profiles related with these pathways during two regenerative stages, we intersected these genes with DEGs in X1, X4, Y1, and Y4. Strikingly, the number of significantly altered genes in X1 decreased dramatically after IWR treatment in X4 for all pathways (**Figures 7A–D** and **Supplementary Figure S10** compare the total number of brown and blue shaded boxes in X1 and X4; **Supplementary Table S8**). Among the Wnt signaling pathway genes that were detected in the two KEGG pathways, "WNT signaling pathway" (**Figure 7A**) and "WNT_GO signaling pathway" (**Supplementary Figure S10A**), 12 of the 14 genes that were Up in X1 (*csnk2a4*, *wnt5b*, *fosl1a*, *jun*, *mycb*, *dkk1a*, *gskip*, *ppm1ab*, *tnksa*, *fermt2*, *tmem198b*, and *tle3b*) did not significantly change any more after IWR treatment in X4, indicating that these 12 genes are positively regulated Wnt targets (**Figure 7A** and **Supplementary Figure S10A** compare the number of brown shaded boxes in X1 and X4). 18 of the 24 genes that were Down in X1 (*lrp6*, *ctbp1*, *fzd3b*, *apc*, *ctnnd2b*, *fzd3a*, *camk2d2*, *daam1b*, *ppp3r1a*, *fzd9b*, *tcf7l2*, *ccnd2a*, *rac3b*, *ndrg2*, *fto*, *reck*, *ankrd6b*, and *ccdc136b*) did not change any more in X4, suggesting that these 18 genes are negatively regulated Wnt targets (**Figure 7A** and **Supplementary Figure S10A** compare the number of blue shaded boxes in X1 and X4). On the contrary, the number of altered genes in Y1 did not change much either in Y4 (**Figure 7A** and **Supplementary Figure S10** compare the total number of brown and blue shaded boxes in Y1 and Y4; **Supplementary Table S8**). Accordingly, 20 out of 30 DEGs determined in the Wnt pathway-related genes that were differentially regulated in Y1 were likewise regulated after IWR treatment in Y4 (**Figure 7A** and **Supplementary Figure S10A**). Finally, we were able to validate some selected genes, i.e., *epha2a* as a MAPK pathway-related gene, *sgk2b* and *foxo1a* as FoxO signaling-related genes, and *gadd45ga* as a p53 pathway-related gene at 20 hpl (**Figure 7B**). Taken together, these data indicate that Wnt/β-catenin signaling controls the expression of a wide range of genes related to various signaling pathways, including p53, apoptosis, FoxO, MAPK, and mTOR, at the early wound healing stage of brain regeneration.

# DISCUSSION

Although the zebrafish telencephalon has been carefully explored for its neurogenic niches that harbor stem or progenitor cells

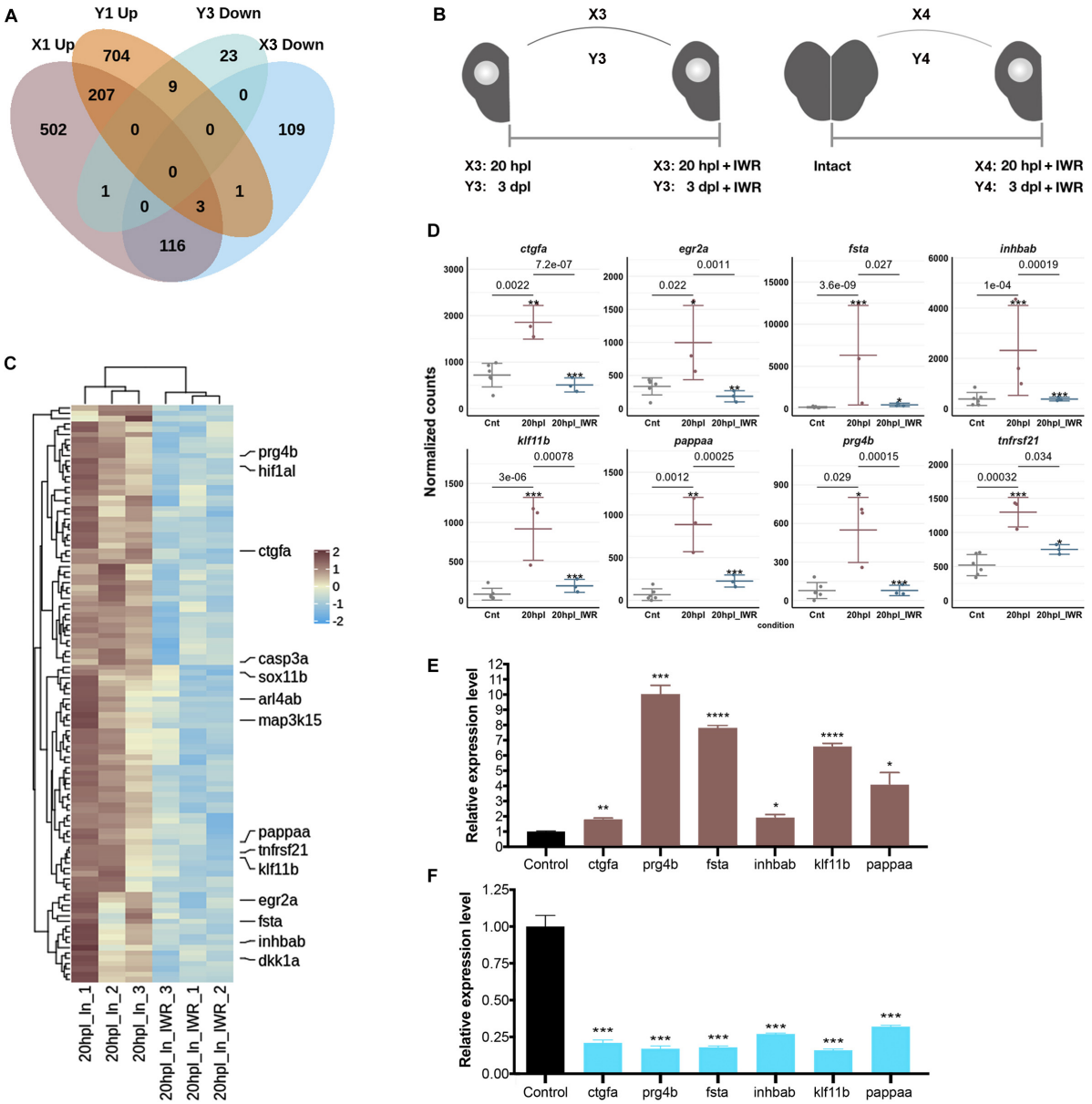


**FIGURE 6 |** Inhibition of Wnt/β-catenin signaling during the early wound healing stage identifies 119 target genes that are positively regulated by the pathway. **(A)** The Venn diagram shows the number of differentially expressed genes (DEGs) that are upregulated (*Up*) in the lesioned 20-hpl (*X1*, *dark pink*), downregulated (*Down*) in the lesioned + IWR-1-treated 20-hpl (*X3*, *light blue*), Up in the lesioned 3-dpl (*Y1*, *dark orange*), or Down in the lesioned + IWR-1-treated 3-dpl (*Y3*, *turquoise*) hemispheres and the overlap between each set of DEGs. There were 119 genes Up in X1 and Down in X3, while only nine genes were Up in Y1 and Down in Y3. **(B)** Preparation of RNA samples from the lesioned hemisphere at 20 hpl or 3 dpl. *X3*: 20-hpl lesioned hemisphere after IWR treatment vs. 20-hpl lesioned hemisphere; *Y3*: 3-dpl lesioned hemisphere after IWR treatment vs. 3-dpl lesioned hemisphere; *X4*: 20-hpl lesioned hemisphere after IWR treatment vs. control; *Y4*: 3-dpl lesioned hemisphere after IWR treatment vs. control. **(C)** The heatmap shows the Wnt target genes that are Up in X1 and Down in X3. Each *column* represents a single hemisphere from a single telencephalon and each *row* shows a single gene. The *scale bar* shows counts *Z*-scores from high to low expression, represented by a color gradient from *orange* to *green*, respectively. **(D)** Dot plot representation of normalized transformed read counts of a representative set of Wnt target genes that are Up in X1 and Down in X3 (*brown*: 20-hpl lesioned hemispheres; *blue*: 20-hpl lesioned + IWR-1-treated hemispheres). The mean ± standard deviations (SD) of three independent experiments are plotted. **(E,F)** Relative expression levels of the Wnt target genes that are Up in X1 and Down in X3 (*ctgfa*, *prg4b*, *fsta*, *inhbab*, *klf11b*, and *pappaa*). Statistical significance was evaluated using unpaired *t*-test. $^{*}p < 0.05$, $^{**}p < 0.01$, $^{***}p < 0.001$, and $^{****}p < 0.0001$. *Error bars* represent ± standard error of the mean (SEM, $n = 3$). See section "Materials and Methods" for the definition of DEGs covered in X and Y comparisons.

expressing different marker genes, comparative analysis of the transcriptome profiles at the early stages of telencephalon regeneration has not been performed yet. This is the first study that uncovers the global gene expression profiles of the regenerating zebrafish telencephalon in the lesioned and unlesioned hemispheres at two early stages of regeneration,

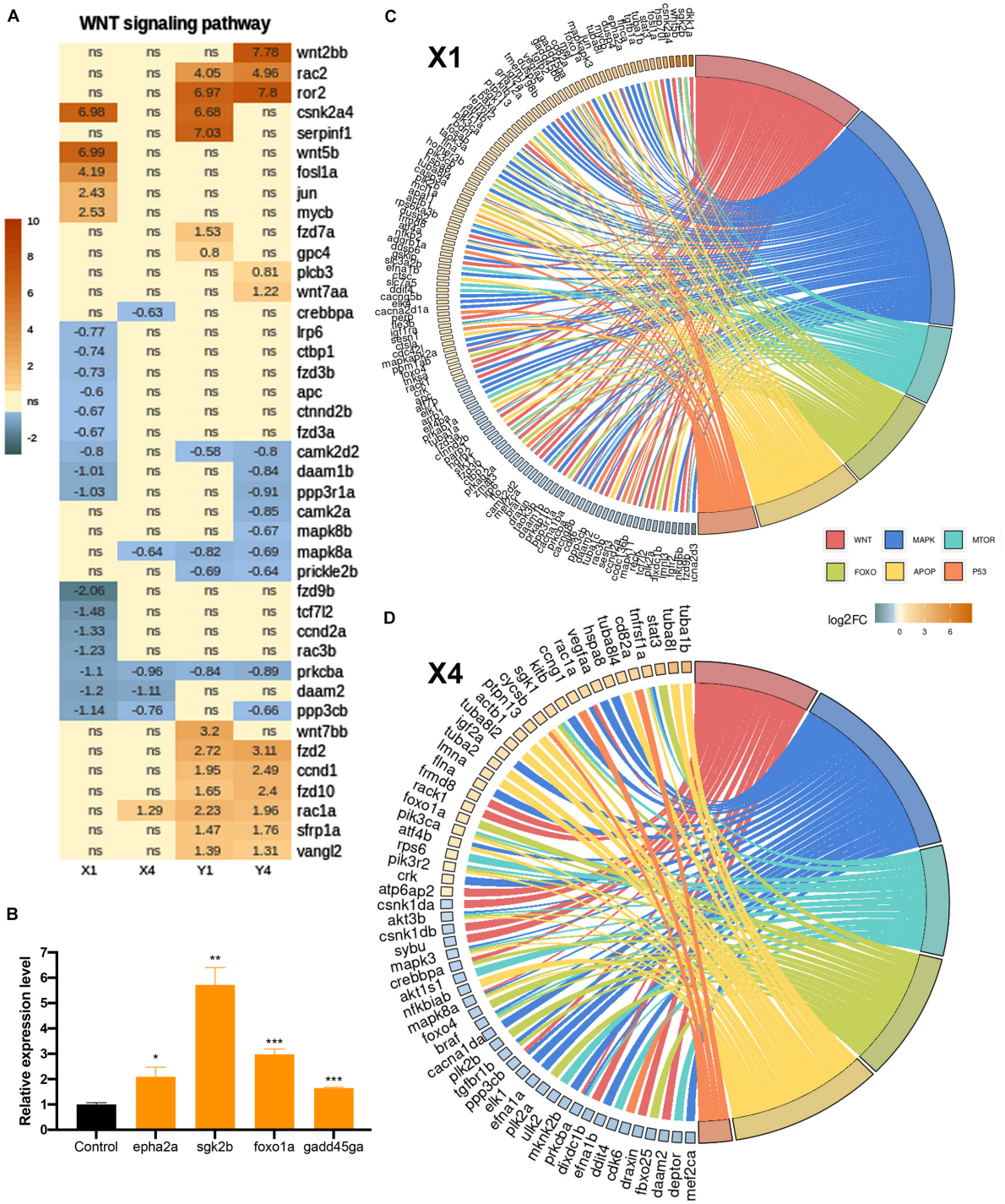


**FIGURE 7 |** Inhibition of Wnt/β-catenin signaling during the early wound stage results in a marked alteration of the gene expression profiles represented in Kyoto Encyclopedia of Genes and Genomes (KEGG) pathway enrichment. Heatmap representation of the uniquely changed genes in **(A)** the Wnt signaling pathway in X1, X4, Y1, and Y4 comparisons. Each *column* represents a comparison according to the DESeq2 results and each *row* shows a single gene. The *scale bar* shows $\log_2$ of the fold change values (when statistically significant) from high to low fold change, represented by a color gradient from *orange* to *blue*, respectively. Statistical significance was evaluated using Wald test. *ns*, non-significant. **(B,C)** GOChord plot of selected GO terms belonging to the biological process (BP) sub-ontology and KEGG pathways for X1 and X4 comparisons, respectively. The genes related to the Wnt-KEGG pathway and Wnt-Gene Ontology BP are intersected and represented as one group. The genes are linked to their assigned pathways by *ribbons* and ordered according to their $\log_2$ of the fold change values from high to low fold change, represented by a color gradient from *orange* to *blue*, respectively. **(D)** Relative expression levels of pathway-related genes (*epha2a*, *sgk2b*, *foxo1a*, and *gadd45ga*). Statistical significance was evaluated using unpaired *t*-test. $^{*}p < 0.05$, $^{**}p < 0.01$, and $^{***}p < 0.001$. *Error bars* represent ± standard error of the mean (SEM, $n = 3$). See section "Materials and Methods" for the definition of DEGs covered in X and Y comparisons.

which we defined as 20 hpl, corresponding to the early wound healing stage, and 3 dpl, to the early proliferative stage. Using comparative gene expression profiling, we describe for the first time that: (i) the total number of DEGs in the lesioned hemisphere is substantially higher than that in the unlesioned one at 20 hpl; (ii) the number of DEGs in 3 dpl is elevated as compared to 20 hpl and that 40% of all DEGs at 3 dpl are shared between the lesioned and unlesioned hemispheres; (iii) transcriptomes at 20 hpl and 3 dpl share less than a third of their DEGs; (iv) Wnt/β-catenin signaling is activated at 20 hpl, controlling the transcription of a large pool of target genes, 119 of which are positively regulated by the pathway; and (v) Wnt/β-catenin signaling results in a marked alteration of the gene expression profiles represented as enrichment of the KEGG pathways, including p53, apoptosis, MAPK, mTOR, and FoxO, at the early wound healing stage of brain regeneration.

Injury-induced proliferative response has been proposed to be primarily confined to the lesioned hemisphere of the telencephalon (Marz et al., 2011). Nevertheless, several genes are upregulated both in the lesioned and unlesioned hemispheres, though not to the same degree (Kroehne et al., 2011; Kizil et al., 2012b). The difference in the responses of the two hemispheres to injury could be due to differences in the methods used to induce a telencephalic injury. Nevertheless, whether the unlesioned part could be used as an effective internal control is a matter of debate. Strikingly, studies of hemispherectomy, where one cerebral hemisphere is completely removed or functionally disconnected, have demonstrated that the contralesional hemisphere is able to undertake various functions of the lesioned side, most likely due to a strong interaction between the lesioned and the intact halves in brain injuries (Sebastianelli et al., 2017). Such an interplay would be inevitably reflected as differential gene expression after injury not only in the lesioned but also in the unlesioned site of the telencephalon. Our results show that, at both 20 hpl and 3 dpl, many DEGs were shared between the lesioned (X1 or Y1) and the unlesioned (X2 or Y2) hemispheres and that the number of shared DEGs at 3 dpl was far higher than that at 20 hpl (see **Figures 2A**, **3A**). Thus, the lesioned and unlesioned hemispheres indeed appear to interact during telencephalon regeneration, and the level of this interaction increases from the early wound healing to the proliferative stage. The injury response appears to be most intense and peculiar at the wound site during the early wound healing stage and extends outside as the proliferative stage starts, leading to a considerable difference between the transcriptional programs activated at these two stages.

Cytokines released from innate immune cells play key roles in the regulation of the acute inflammatory response that is required for functional regeneration of the zebrafish CNS after injury (Kyritsis et al., 2012; Elsaeidi et al., 2014; Fuller-Carter et al., 2015; Tsarouchas et al., 2018). Our data showed prominent upregulation of the anti-inflammatory cytokine genes *il11a*, *il21*, and *il6st*, cytokine receptor encoding *il17ra1a*, the tumor necrosis factor receptor superfamily (TNFRSF) genes *tnfrsf18*, *tnfrsf21*, and the genes related to cytokine response *junba*, *jun*, *rel*, and *timp2a* at 20 hpl, suggesting that signaling through these early response cytokines is essential to orchestrate innate immune response (Opal and DePalo, 2000; Placke et al., 2010). Apoptosis is also activated in the early regenerative phase of various tissues including *Xenopus* tail, mouse liver, and cornea and is indispensable for effective wound healing (Tseng et al., 2007; Wilson et al., 2007; Li et al., 2010). Remarkably, we observed a significant upregulation of the apoptosis-related genes including *apaf1*, *baxa*, *traf4b*, *tgfb2*, *sgk1*, and *casp3a* selectively in the lesioned hemisphere at 20 hpl (Elmore, 2007; Gilbert et al., 2016; Liu et al., 2017; Kreckel et al., 2019). Strikingly, many of them were downregulated when Wnt/β-catenin signaling was suppressed, pointing out a positive regulatory role for Wnt signaling in apoptosis during early brain regeneration. Dual-specific phosphatase (DUSP) genes were also upregulated in the lesioned hemisphere. Among these, *dusp6* has been shown to promote cell death in different contexts (Domercq et al., 2011; Piya et al., 2012). Apoptosis has been proposed as a key factor to resolve inflammation by driving the conversion of immune response into a wound healing response in the early phases of tissue repair (Brown et al., 1997; Wu and Chen, 2014). Thus, parallel elevations in the expression levels of genes related to cytokine signaling and apoptosis at 20 hpl could underlie the capacity of zebrafish telencephalon to convert the early inflammatory response into a healing ability and consolidate this time point as a representative of the early wound healing stage during telencephalon regeneration.

Angiogenic sprouting into the injured area has been described as another prominent event that takes place as early as 15 h after injury during heart regeneration in zebrafish (Marin-Juez et al., 2016). Significantly upregulated *vascular endothelial growth factor a-a* (*vegfaa*), a key regulator of angiogenesis, is essential for cardiomyocyte proliferation and heart regeneration (Marin-Juez et al., 2016). Likewise, the neuropilin genes *nrp1a*, *nrp1b*, and *nrp2a*, which encode for transmembrane receptors of vascular endothelial growth factors (VEGFs), are upregulated in injured hearts at 1 dpl and the glucose transporter gene *slc2a1b* upregulated in vascular endothelial cells in response to hypoxia (Delcourt et al., 2015; Guo and Vander Kooi, 2015; Lowe et al., 2019). CNS regeneration also involves an intense crosstalk between neurons and vascular niches that mediates angiogenesis mainly through the activation of VEGF and contributes to neuroprotection (Ruiz de Almodovar et al., 2009). We noted a significant upregulation of *vegfaa*, *nrp1a*, *nrp1b*, and *slc2a1b* genes specifically in the lesioned hemisphere at 20 hpl, arguing that injury activates a fast angiogenic sprouting mechanism during telencephalon regeneration.

Optic nerve injury in adult zebrafish induces the expression of the axon growth inhibitor suppressor of cytokine signaling 3 (*socs3*) in retinal ganglion cells, ultimately attenuating regeneration (Smith et al., 2009; Elsaeidi et al., 2014). We found that while upregulated at 20 hpl, *socs3a* was strongly downregulated at 3 dpl. *socs3b*, *sox11b*, and *klf6a*, which are associated with optic nerve regeneration (Veldman et al., 2007), were likewise induced at 20 hpl, with *sox11b* becoming downregulated at 3 dpl. More axon guidance genes including *robo1*, *tnc*, and *boc* (Lee et al., 2001; Connor et al., 2005; Schweitzer et al., 2005) were downregulated primarily in the

lesioned hemisphere at 20 hpl. Such biphasic expression of axon growth inhibitors during brain regeneration suggests a stage-specific regulation of axon growth.

The proliferative response of the injured zebrafish telencephalon is driven by the RGCs and reaches a peak at the lesioned site around 3 dpl (Marz et al., 2011; Kizil et al., 2012c). At this stage, we observed that some quiescent RGC genes such as *fabp7a*, *mt-atp8*, *hipk1a*, *s100b*, and *mgll* were upregulated in both hemispheres, while *ptn*, *luzp2*, *psap*, *hepacama*, and *anxa11b* were only upregulated in the lesioned side (Kaslin et al., 2017; Lange et al., 2020). On the other hand, proliferating RGC genes including *tmsb4x*, *hmgb2a*, *hmga1a*, *rps23*, and *ran* were exclusively upregulated in the lesioned half, whereas the general proliferation marker *ccnd1* was upregulated in both halves (Lange et al., 2020). Besides, we found that many cell cycle-associated genes such as *pcna*, *mki67*, *rpl35*, *mdka*, *ccna2*, and *cdk1* were upregulated predominantly in the lesioned hemisphere (Sobecki et al., 2017). Together, these results validate 3 dpl as a highly proliferative phase dominated by RGC activities and reveal that this proliferative response is clearly more pronounced in the lesioned hemisphere.

As the resident macrophages of the CNS, microglia have been shown to engulf dead cells after brain injury in zebrafish (Herzog et al., 2019). Previous studies have identified various microglia- and/or macrophage-specific markers that are differentially regulated during regeneration of the retina and olfactory bulb (Oosterhof et al., 2017; Mitchell et al., 2019). At 3 dpl, a considerable number of microglial genes including *mhc1zba*, *marco*, *spi1b*, *csf1ra*, and *mfap4* were upregulated exclusively in the lesioned hemisphere, while a few including *mpeg1.1* and *sall3a* were upregulated in both hemispheres. This prominent emanation of microglial signature at 3 dpl correlates with the extensive proliferation of microglia induced by neuronal cell death (Oosterhof et al., 2017). Furthermore, we found 18 innate immune response genes (see **Supplementary Table S4**) to be upregulated at 3 dpl. Among them, *nfkb2* and *csf1ra* are involved in the activation of innate immune response during heart and tail fin regeneration (Petrie et al., 2014; Karra et al., 2015; Morales and Allende, 2019). Activation of the immune response thus needs to be analyzed together with the related signaling pathways to understand the mechanisms of proper tissue healing.

Wnt/β-catenin signaling appears to play a positive, regeneration-promoting role in most systems, from invertebrates that display whole-body regeneration to organs that mammals can completely or partially regenerate, such as the liver, skeletal muscle, and kidney (Whyte et al., 2012; Ozhan and Weidinger, 2014). Wnt signaling is also essential for the organs that regenerate completely only in the lower vertebrates, such as the appendages (Stoick-Cooper et al., 2007; Singh et al., 2018) and the eye (Hayashi et al., 2008; Patel et al., 2017). In the adult zebrafish, Wnt/β-catenin signaling is involved in the proliferation and differentiation of neural stem or progenitor cells in the hypothalamus, optic tectum, and spinal cord (Wang et al., 2009; Shi et al., 2015; Shitasako et al., 2017; Wehner et al., 2017). Our results further support the role of canonical Wnt signaling in regeneration by providing the first evidence of active signaling in the zebrafish telencephalon at a very early stage of regeneration, i.e., 20 hpl. Wnt/β-catenin signaling activity has been identified around the necrotic lesions in mouse liver and hair follicle regeneration models (Ito et al., 2007; Whyte et al., 2012; Zhao et al., 2019). Likewise, we have demonstrated the early activation of Wnt/β-catenin signaling near the lesioned area of the telencephalon. At 1 dpl, the telencephalic lesion is known to be filled with blood cells and is surrounded by macrophages/microglial cells, indicating an early infiltration of these cells into the site of tissue damage (Ayari et al., 2010). Therefore, identification of the types of blood and immune cells with active Wnt/β-catenin signaling at 20 hpl would unravel its role in the early wound healing process of brain regeneration. Interestingly, signaling becomes downregulated to control levels in the lesioned hemisphere at 3 dpl. Wnt/β-catenin signaling has been reported to have biphasic roles during heart, muscle, and liver development, where early and late signaling activities have diverse roles (Monga et al., 2001; Naito et al., 2006; Klaus et al., 2007; Ueno et al., 2007; Brack et al., 2008; Gessert and Kuhl, 2010). Thus, it is likely that Wnt signaling is regulated at least in a biphasic manner in the course of adult brain response to injury.

Several of the Wnt target genes we identified, including *sox11b*, *casp3a*, *klf11*, and *egr2a*, are known to be involved in the regulation of Wnt/β-catenin activity (Spittau and Krieglstein, 2012; Zaman et al., 2012; Zimmerman et al., 2013; Liu et al., 2019). Moreover, a wide range of genes related to the p53, apoptosis, MAPK, mTOR, and FoxO pathways are regulated by Wnt/β-catenin signaling during early wound healing, but become far less responsive to Wnt later at the proliferative stage. Wnt/β-catenin signaling has been implicated in the regulation of proliferation and differentiation of various progenitor cells during tissue regeneration *via* controlling the p53, mTOR, and FoxO pathways (Hirose et al., 2014; Peng et al., 2014; Maiese, 2015; Lund-Ricard et al., 2020). Besides, an intense crosstalk between the MAPK and Wnt signaling pathways has been deciphered in development, cancer, and regeneration (Caverzasio and Manen, 2007; Bikkavilli et al., 2008; Zhang et al., 2014). Our results reveal for the first time that these signaling pathways are activated in response to canonical Wnt pathway early after the telencephalon injury. Further functional studies will clarify how Wnt signaling interacts with these pathways to regulate the early regenerative response in brain regeneration.

In conclusion, our comparative transcriptome analyses of the regenerating zebrafish telencephalon at the early wound healing and proliferative stages reveal differentially expressed genes and altered biological pathways that control the cellular and molecular mechanisms of regeneration. The great burden caused by traumatic brain injuries and neurodegenerative diseases to humanity necessitates the development of therapeutic interventions, which is tightly dependent on unraveling these mechanisms that render possible effective brain regeneration.

## DATA AVAILABILITY STATEMENT

All datasets have been deposited in ArrayExpress under the link: https://www.ebi.ac.uk/arrayexpress/experiments/E-MTAB-9321/ with the accession number "E-MTAB-9321".

## ETHICS STATEMENT

The animal study was reviewed and approved by the Animal Experiments Local Ethics Committee of İzmir Biomedicine and Genome Center (IBG AELEC/IBG-HADYEK).

## AUTHOR CONTRIBUTIONS

GO, YD, and GC designed the experiments. GC and YP performed the molecular and cell biology experiments. YD, SM, GH, and IP conducted the bioinformatics analyses. GO, YD, and GC wrote the manuscript. All authors contributed to the discussion.

## FUNDING

This work was supported by the Scientific and Technological Research Council of Turkey (TUBITAK, grant number 215Z365). GO Lab is funded by EMBO Installation Grant (IG 3024). YD was supported by an EMBO Short-Term Fellowship (#7783) and a FEBS Short-Term Fellowship. GH was supported by an EMBL-EBI/Embassy of France in London Fellowship.

## ACKNOWLEDGMENTS

We thank İzmir Biomedicine and Genome Center Vivarium-Zebrafish Core Facility, Optical Imaging Core Facility, and Histopathology Core Facility for providing zebrafish care, microscope facility support, and histopathology service support, respectively. We also would like to thank the Genomics Core Facility (GeneCore) of EMBL, Heidelberg.

## SUPPLEMENTARY MATERIAL

The Supplementary Material for this article can be found online at: https://www.frontiersin.org/articles/10.3389/fcell.2020.584604/full#supplementary-material

## REFERENCES

Adolf, B., Chapouton, P., Lam, C. S., Topp, S., Tannhauser, B., Strahle, U., et al. (2006). Conserved and acquired features of adult neurogenesis in the zebrafish telencephalon. *Dev. Biol.* 295, 278–293. doi: 10.1016/j.ydbio.2006.03.023

Alunni, A., and Bally-Cuif, L. (2016). A comparative view of regenerative neurogenesis in vertebrates. *Development* 143, 741–753. doi: 10.1242/dev.122796

Alvarez-Buylla, A., Garcia-Verdugo, J. M., and Tramontin, A. D. (2001). A unified hypothesis on the lineage of neural stem cells. *Nat. Rev. Neurosci.* 2, 287–293. doi: 10.1038/35067582

Anders, S., Pyl, P. T., and Huber, W. (2015). HTSeq–a python framework to work with high-throughput sequencing data. *Bioinformatics* 31, 166–169. doi: 10.1093/bioinformatics/btu638

Ayari, B., El Hachimi, K. H., Yanicostas, C., Landoulsi, A., and Soussi-Yanicostas, N. (2010). Prokineticin 2 expression is associated with neural repair of injured adult zebrafish telencephalon. *J. Neurotrauma* 27, 959–972. doi: 10.1089/neu.2009.0972

Baumgart, E. V., Barbosa, J. S., Bally-Cuif, L., Gotz, M., and Ninkovic, J. (2012). Stab wound injury of the zebrafish telencephalon: a model for comparative analysis of reactive gliosis. *Glia* 60, 343–357. doi: 10.1002/glia.22269

Becker, C. G., and Becker, T. (2002). Repellent guidance of regenerating optic axons by chondroitin sulfate glycosaminoglycans in zebrafish. *J. Neurosci.* 22, 842–853. doi: 10.1523/jneurosci.22-03-00842.2002

Bhardwaj, R. D., Curtis, M. A., Spalding, K. L., Buchholz, B. A., Fink, D., Bjork-Eriksson, T., et al. (2006). Neocortical neurogenesis in humans is restricted to development. *Proc. Natl. Acad. Sci. U.S.A.* 103, 12564–12568. doi: 10.1073/pnas.0605177103

Bikkavilli, R. K., Feigin, M. E., and Malbon, C. C. (2008). p38 mitogen-activated protein kinase regulates canonical Wnt-beta-catenin signaling by inactivation of GSK3beta. *J. Cell Sci.* 121(Pt 21), 3598–3607. doi: 10.1242/jcs.032854

Bolger, A. M., Lohse, M., and Usadel, B. (2014). Trimmomatic: a flexible trimmer for Illumina sequence data. *Bioinformatics* 30, 2114–2120. doi: 10.1093/bioinformatics/btu170

Bonfanti, L., and Peretto, P. (2011). Adult neurogenesis in mammals–a theme with many variations. *Eur. J. Neurosci.* 34, 930–950. doi: 10.1111/j.1460-9568.2011.07832.x

Brack, A. S., Conboy, I. M., Conboy, M. J., Shen, J., and Rando, T. A. (2008). A temporal switch from notch to Wnt signaling in muscle stem cells is necessary for normal adult myogenesis. *Cell Stem Cell* 2, 50–59. doi: 10.1016/j.stem.2007.10.006

Brown, D. L., Kao, W. W., and Greenhalgh, D. G. (1997). Apoptosis down-regulates inflammation under the advancing epithelial wound edge: delayed patterns in diabetes and improvement with topical growth factors. *Surgery* 121, 372–380. doi: 10.1016/s0039-6060(97)90306-8

Caverzasio, J., and Manen, D. (2007). Essential role of Wnt3a-mediated activation of mitogen-activated protein kinase p38 for the stimulation of alkaline phosphatase activity and matrix mineralization in C3H10T1/2 mesenchymal cells. *Endocrinology* 148, 5323–5330. doi: 10.1210/en.2007-0520

Chapouton, P., Jagasia, R., and Bally-Cuif, L. (2007). Adult neurogenesis in non-mammalian vertebrates. *Bioessays* 29, 745–757. doi: 10.1002/bies.20615

Chitu, V., Gokhan, S., Nandi, S., Mehler, M. F., and Stanley, E. R. (2016). Emerging roles for CSF-1 receptor and its ligands in the nervous system. *Trends Neurosci.* 39, 378–393. doi: 10.1016/j.tins.2016.03.005

Connor, R. M., Allen, C. L., Devine, C. A., Claxton, C., and Key, B. (2005). BOC, brother of CDO, is a dorsoventral axon-guidance molecule in the embryonic vertebrate brain. *J. Comp. Neurol.* 485, 32–42. doi: 10.1002/cne.20503

Delcourt, N., Quevedo, C., Nonne, C., Fons, P., O'Brien, D., Loyaux, D., et al. (2015). Targeted identification of sialoglycoproteins in hypoxic endothelial cells and validation in zebrafish reveal roles for proteins in angiogenesis. *J. Biol. Chem.* 290, 3405–3417. doi: 10.1074/jbc.M114.618611

Dhaliwal, J., and Lagace, D. C. (2011). Visualization and genetic manipulation of adult neurogenesis using transgenic mice. *Eur. J. Neurosci.* 33, 1025–1036. doi: 10.1111/j.1460-9568.2011.07600.x

Di Giaimo, R., Durovic, T., Barquin, P., Kociaj, A., Lepko, T., Aschenbroich, S., et al. (2018). The aryl hydrocarbon receptor pathway defines the time frame for restorative neurogenesis. *Cell Rep.* 25, 3241–3251.e5. doi: 10.1016/j.celrep.2018.11.055

Doetsch, F., Caille, I., Lim, D. A., Garcia-Verdugo, J. M., and Alvarez-Buylla, A. (1999). Subventricular zone astrocytes are neural stem cells in the adult mammalian brain. *Cell* 97, 703–716. doi: 10.1016/s0092-8674(00)80783-7

Doetsch, F., and Scharff, C. (2001). Challenges for brain repair: insights from adult neurogenesis in birds and mammals. *Brain Behav. Evol.* 58, 306–322. doi: 10.1159/000057572

Domercq, M., Alberdi, E., Sanchez-Gomez, M. V., Ariz, U., Perez-Samartin, A., and Matute, C. (2011). Dual-specific phosphatase-6 (Dusp6) and ERK mediate AMPA receptor-induced oligodendrocyte death. *J. Biol. Chem.* 286, 11825–11836. doi: 10.1074/jbc.M110.153049

Doncheva, N. T., Morris, J. H., Gorodkin, J., and Jensen, L. J. (2019). Cytoscape stringapp: network analysis and visualization of proteomics data. *J. Proteome Res.* 18, 623–632. doi: 10.1021/acs.jproteome.8b00702

Ekdahl, C. T., Claasen, J. H., Bonde, S., Kokaia, Z., and Lindvall, O. (2003). Inflammation is detrimental for neurogenesis in adult brain. *Proc. Natl. Acad. Sci. U.S.A.* 100, 13632–13637. doi: 10.1073/pnas.2234031100

Elmore, S. (2007). Apoptosis: a review of programmed cell death. *Toxicol. Pathol.* 35, 495–516. doi: 10.1080/01926230701320337

Elsaeidi, F., Bemben, M. A., Zhao, X. F., and Goldman, D. (2014). Jak/Stat signaling stimulates zebrafish optic nerve regeneration and overcomes the inhibitory actions of Socs3 and Sfpq. *J. Neurosci.* 34, 2632–2644. doi: 10.1523/JNEUROSCI.3898-13.2014

Ernst, A., and Frisen, J. (2015). Adult neurogenesis in humans- common and unique traits in mammals. *PLoS Biol.* 13:e1002045. doi: 10.1371/journal.pbio.1002045

Fabregat, A., Jupe, S., Matthews, L., Sidiropoulos, K., Gillespie, M., Garapati, P., et al. (2018). The reactome pathway knowledgebase. *Nucleic Acids Res.* 46, D649–D655. doi: 10.1093/nar/gkx1132

Fitch, M. T., and Silver, J. (2008). CNS injury, glial scars, and inflammation: inhibitory extracellular matrices and regeneration failure. *Exp. Neurol.* 209, 294–301. doi: 10.1016/j.expneurol.2007.05.014

Fleisch, V. C., Fraser, B., and Allison, W. T. (2011). Investigating regeneration and functional integration of CNS neurons: lessons from zebrafish genetics and other fish species. *Biochim. Biophys. Acta* 1812, 364–380. doi: 10.1016/j.bbadis.2010.10.012

Fuller-Carter, P. I., Carter, K. W., Anderson, D., Harvey, A. R., Giles, K. M., and Rodger, J. (2015). Integrated analyses of zebrafish miRNA and mRNA expression profiles identify miR-29b and miR-223 as potential regulators of optic nerve regeneration. *BMC Genomics* 16:591. doi: 10.1186/s12864-015-1772-1

Galvao, J., Iwao, K., Apara, A., Wang, Y., Ashouri, M., Shah, T. N., et al. (2018). The kruppel-like factor gene target dusp14 regulates axon growth and regeneration. *Invest. Ophthalmol. Vis. Sci.* 59, 2736–2747. doi: 10.1167/iovs.17-23319

Ganz, J., Kaslin, J., Hochmann, S., Freudenreich, D., and Brand, M. (2010). Heterogeneity and Fgf dependence of adult neural progenitors in the zebrafish telencephalon. *Glia* 58, 1345–1363. doi: 10.1002/glia.21012

Garnier, D., Loyer, P., Ribault, C., Guguen-Guillouzo, C., and Corlu, A. (2009). Cyclin-dependent kinase 1 plays a critical role in DNA replication control during rat liver regeneration. *Hepatology* 50, 1946–1956. doi: 10.1002/hep.23225

Gentleman, R. C., Carey, V. J., Bates, D. M., Bolstad, B., Dettling, M., Dudoit, S., et al. (2004). Bioconductor: open software development for computational biology and bioinformatics. *Genome Biol.* 5:R80. doi: 10.1186/gb-2004-5-10-r80

Gessert, S., and Kuhl, M. (2010). The multiple phases and faces of wnt signaling during cardiac differentiation and development. *Circ. Res.* 107, 186–199. doi: 10.1161/circresaha.110.221531

Gilbert, R. W. D., Vickaryous, M. K., and Viloria-Petit, A. M. (2016). Signalling by transforming growth factor beta isoforms in wound healing and tissue regeneration. *J. Dev. Biol.* 4:21. doi: 10.3390/jdb4020021

Grandel, H., and Brand, M. (2013). Comparative aspects of adult neural stem cell activity in vertebrates. *Dev. Genes Evol.* 223, 131–147. doi: 10.1007/s00427-012-0425-5

Grandel, H., Kaslin, J., Ganz, J., Wenzel, I., and Brand, M. (2006). Neural stem cells and neurogenesis in the adult zebrafish brain: origin, proliferation dynamics, migration and cell fate. *Dev. Biol.* 295, 263–277. doi: 10.1016/j.ydbio.2006.03.040

Guo, H. F., and Vander Kooi, C. W. (2015). Neuropilin functions as an essential cell surface receptor. *J. Biol. Chem.* 290, 29120–29126. doi: 10.1074/jbc.R115.687327

Hayashi, T., Mizuno, N., and Kondoh, H. (2008). Determinative roles of FGF and Wnt signals in iris-derived lens regeneration in newt eye. *Dev. Growth Differ.* 50, 279–287. doi: 10.1111/j.1440-169X.2008.01005.x

Herzog, C., Pons Garcia, L., Keatinge, M., Greenald, D., Moritz, C., Peri, F., et al. (2019). Rapid clearance of cellular debris by microglia limits secondary neuronal cell death after brain injury in vivo. *Development* 146:dev174698. doi: 10.1242/dev.174698

Hirose, K., Shiomi, T., Hozumi, S., and Kikuchi, Y. (2014). Mechanistic target of rapamycin complex 1 signaling regulates cell proliferation, cell survival, and differentiation in regenerating zebrafish fins. *BMC Dev. Biol.* 14:42. doi: 10.1186/s12861-014-0042-9

Huang da, W., Sherman, B. T., and Lempicki, R. A. (2009). Systematic and integrative analysis of large gene lists using DAVID bioinformatics resources. *Nat. Protoc.* 4, 44–57. doi: 10.1038/nprot.2008.211

Hwang, I. K., Park, J. H., Lee, T. K., Kim, D. W., Yoo, K. Y., Ahn, J. H., et al. (2017). CD74-immunoreactive activated M1 microglia are shown late in the gerbil hippocampal CA1 region following transient cerebral ischemia. *Mol. Med. Rep.* 15, 4148–4154. doi: 10.3892/mmr.2017.6525

Ito, M., Yang, Z., Andl, T., Cui, C., Kim, N., Millar, S. E., et al. (2007). Wnt-dependent de novo hair follicle regeneration in adult mouse skin after wounding. *Nature* 447, 316–320. doi: 10.1038/nature05766

Kanehisa, M., and Goto, S. (2000). KEGG: kyoto encyclopedia of genes and genomes. *Nucleic Acids Res.* 28, 27–30. doi: 10.1093/nar/28.1.27

Karra, R., Knecht, A. K., Kikuchi, K., and Poss, K. D. (2015). Myocardial NF-kappaB activation is essential for zebrafish heart regeneration. *Proc. Natl. Acad. Sci. U.S.A.* 112, 13255–13260. doi: 10.1073/pnas.1511209112

Kaslin, J., Ganz, J., and Brand, M. (2008). Proliferation, neurogenesis and regeneration in the non-mammalian vertebrate brain. *Philos. Trans. R. Soc. Lond. B Biol. Sci.* 363, 101–122. doi: 10.1098/rstb.2006.2015

Kaslin, J., Kroehne, V., Ganz, J., Hans, S., and Brand, M. (2017). Distinct roles of neuroepithelial-like and radial glia-like progenitor cells in cerebellar regeneration. *Development* 144, 1462–1471. doi: 10.1242/dev.144907

Kempermann, G., Wiskott, L., and Gage, F. H. (2004). Functional significance of adult neurogenesis. *Curr. Opin. Neurobiol.* 14, 186–191. doi: 10.1016/j.conb.2004.03.001

Kim, D., Langmead, B., and Salzberg, S. L. (2015). HISAT: a fast spliced aligner with low memory requirements. *Nat. Methods* 12, 357–360. doi: 10.1038/nmeth.3317

Kizil, C., Dudczig, S., Kyritsis, N., Machate, A., Blaesche, J., Kroehne, V., et al. (2012a). The chemokine receptor cxcr5 regulates the regenerative neurogenesis response in the adult zebrafish brain. *Neural Dev.* 7:27. doi: 10.1186/1749-8104-7-27

Kizil, C., Kaslin, J., Kroehne, V., and Brand, M. (2012b). Adult neurogenesis and brain regeneration in zebrafish. *Dev. Neurobiol.* 72, 429–461. doi: 10.1002/dneu.20918

Kizil, C., Kyritsis, N., Dudczig, S., Kroehne, V., Freudenreich, D., Kaslin, J., et al. (2012c). Regenerative neurogenesis from neural progenitor cells requires injury-induced expression of Gata3. *Dev. Cell* 23, 1230–1237. doi: 10.1016/j.devcel.2012.10.014

Klaus, A., Saga, Y., Taketo, M. M., Tzahor, E., and Birchmeier, W. (2007). Distinct roles of Wnt/beta-catenin and Bmp signaling during early cardiogenesis. *Proc. Natl. Acad. Sci. U.S.A.* 104, 18531–18536. doi: 10.1073/pnas.0703113104

Kreckel, J., Anany, M. A., Siegmund, D., and Wajant, H. (2019). TRAF2 controls death receptor-induced caspase-8 processing and facilitates proinflammatory signaling. *Front. Immunol.* 10:2024. doi: 10.3389/fimmu.2019.02024

Kriegstein, A., and Alvarez-Buylla, A. (2009). The glial nature of embryonic and adult neural stem cells. *Annu. Rev. Neurosci.* 32, 149–184. doi: 10.1146/annurev.neuro.051508.135600

Kroehne, V., Freudenreich, D., Hans, S., Kaslin, J., and Brand, M. (2011). Regeneration of the adult zebrafish brain from neurogenic radial glia-type progenitors. *Development* 138, 4831–4841. doi: 10.1242/dev.072587

Kyritsis, N., Kizil, C., Zocher, S., Kroehne, V., Kaslin, J., Freudenreich, D., et al. (2012). Acute inflammation initiates the regenerative response in the adult zebrafish brain. *Science* 338, 1353–1356. doi: 10.1126/science.1228773

Lam, C. S., Marz, M., and Strahle, U. (2009). gfap and nestin reporter lines reveal characteristics of neural progenitors in the adult zebrafish brain. *Dev. Dyn.* 238, 475–486. doi: 10.1002/dvdy.21853

Lange, C., Rost, F., Machate, A., Reinhardt, S., Lesche, M., Weber, A., et al. (2020). Single cell sequencing of radial glia progeny reveals the diversity of newborn neurons in the adult zebrafish brain. *Development* 147:dev185595. doi: 10.1242/dev.185595

Lee, J. S., Ray, R., and Chien, C. B. (2001). Cloning and expression of three zebrafish roundabout homologs suggest roles in axon guidance and cell migration. *Dev. Dyn.* 221, 216–230. doi: 10.1002/dvdy.1136

Li, F., Huang, Q., Chen, J., Peng, Y., Roop, D. R., Bedford, J. S., et al. (2010). Apoptotic cells activate the "phoenix rising" pathway to promote wound healing and tissue regeneration. *Sci. Signal.* 3:ra13. doi: 10.1126/scisignal.2000634

Lindsey, B. W., Aitken, G. E., Tang, J. K., Khabooshan, M., Douek, A. M., Vandestadt, C., et al. (2019). Midbrain tectal stem cells display diverse regenerative capacities in zebrafish. *Sci. Rep.* 9:4420. doi: 10.1038/s41598-019-40734-z

Lindsey, B. W., Douek, A. M., Loosli, F., and Kaslin, J. (2017). A whole brain staining, embedding, and clearing pipeline for adult zebrafish to visualize cell proliferation and morphology in 3-dimensions. *Front. Neurosci.* 11:750. doi: 10.3389/fnins.2017.00750

Lindsey, B. W., and Tropepe, V. (2006). A comparative framework for understanding the biological principles of adult neurogenesis. *Prog. Neurobiol.* 80, 281–307. doi: 10.1016/j.pneurobio.2006.11.007

Liu, W., Wang, X., Liu, Z., Wang, Y., Yin, B., Yu, P., et al. (2017). SGK1 inhibition induces autophagy-dependent apoptosis via the mTOR-Foxo3a pathway. *Br. J. Cancer* 117, 1139–1153. doi: 10.1038/bjc.2017.293

Liu, Z., Zhong, Y., Chen, Y. J., and Chen, H. (2019). SOX11 regulates apoptosis and cell cycle in hepatocellular carcinoma via Wnt/beta-catenin signaling pathway. *Biotechnol. Appl. Biochem.* 66, 240–246. doi: 10.1002/bab.1718

Love, M. I., Huber, W., and Anders, S. (2014). Moderated estimation of fold change and dispersion for RNA-seq data with DESeq2. *Genome Biol.* 15:550. doi: 10.1186/s13059-014-0550-8

Lowe, V., Wisniewski, L., Sayers, J., Evans, I., Frankel, P., Mercader-Huber, N., et al. (2019). Neuropilin 1 mediates epicardial activation and revascularization in the regenerating zebrafish heart. *Development* 146:dev174482. doi: 10.1242/dev.174482

Lund-Ricard, Y., Cormier, P., Morales, J., and Boutet, A. (2020). mTOR signaling at the crossroad between metazoan regeneration and human diseases. *Int. J. Mol. Sci.* 21:2718. doi: 10.3390/ijms21082718

Maiese, K. (2015). FoxO transcription factors and regenerative pathways in diabetes mellitus. *Curr. Neurovasc. Res.* 12, 404–413. doi: 10.2174/1567202612666150807112524

Marin-Juez, R., Marass, M., Gauvrit, S., Rossi, A., Lai, S. L., Materna, S. C., et al. (2016). Fast revascularization of the injured area is essential to support zebrafish heart regeneration. *Proc. Natl. Acad. Sci. U.S.A.* 113, 11237–11242. doi: 10.1073/pnas.1605431113

Martowicz, A., Trusohamn, M., Jensen, N., Wisniewska-Kruk, J., Corada, M., Ning, F. C., et al. (2019). Endothelial beta-catenin signaling supports postnatal brain and retinal angiogenesis by promoting sprouting, tip cell formation, and VEGFR (vascular endothelial growth factor receptor) 2 expression. *Arterioscler. Thromb. Vasc. Biol.* 39, 2273–2288. doi: 10.1161/ATVBAHA.119.312749

Marz, M., Chapouton, P., Diotel, N., Vaillant, C., Hesl, B., Takamiya, M., et al. (2010). Heterogeneity in progenitor cell subtypes in the ventricular zone of the zebrafish adult telencephalon. *Glia* 58, 870–888. doi: 10.1002/glia.20971

Marz, M., Schmidt, R., Rastegar, S., and Strahle, U. (2011). Regenerative response following stab injury in the adult zebrafish telencephalon. *Dev. Dyn.* 240, 2221–2231. doi: 10.1002/dvdy.22710

Ming, G. L., and Song, H. (2011). Adult neurogenesis in the mammalian brain: significant answers and significant questions. *Neuron* 70, 687–702. doi: 10.1016/j.neuron.2011.05.001

Mitchell, D. M., Sun, C., Hunter, S. S., New, D. D., and Stenkamp, D. L. (2019). Regeneration associated transcriptional signature of retinal microglia and macrophages. *Sci. Rep.* 9:4768. doi: 10.1038/s41598-019-41298-8

Monga, S. P., Pediaditakis, P., Mule, K., Stolz, D. B., and Michalopoulos, G. K. (2001). Changes in WNT/beta-catenin pathway during regulated growth in rat liver regeneration. *Hepatology* 33, 1098–1109. doi: 10.1053/jhep.2001.23786

Morales, R. A., and Allende, M. L. (2019). Peripheral macrophages promote tissue regeneration in zebrafish by fine-tuning the inflammatory response. *Front. Immunol.* 10:253. doi: 10.3389/fimmu.2019.00253

Moro, E., Ozhan-Kizil, G., Mongera, A., Beis, D., Wierzbicki, C., Young, R. M., et al. (2012). In vivo Wnt signaling tracing through a transgenic biosensor fish reveals novel activity domains. *Dev. Biol.* 366, 327–340. doi: 10.1016/j.ydbio.2012.03.023

Naito, A. T., Shiojima, I., Akazawa, H., Hidaka, K., Morisaki, T., Kikuchi, A., et al. (2006). Developmental stage-specific biphasic roles of Wnt/beta-catenin signaling in cardiomyogenesis and hematopoiesis. *Proc. Natl. Acad. Sci. U.S.A.* 103, 19812–19817. doi: 10.1073/pnas.0605768103

Noctor, S. C., Flint, A. C., Weissman, T. A., Dammerman, R. S., and Kriegstein, A. R. (2001). Neurons derived from radial glial cells establish radial units in neocortex. *Nature* 409, 714–720. doi: 10.1038/35055553

Oosterhof, N., Holtman, I. R., Kuil, L. E., van der Linde, H. C., Boddeke, E. W., Eggen, B. J., et al. (2017). Identification of a conserved and acute neurodegeneration-specific microglial transcriptome in the zebrafish. *Glia* 65, 138–149. doi: 10.1002/glia.23083

Opal, S. M., and DePalo, V. A. (2000). Anti-inflammatory cytokines. *Chest* 117, 1162–1172. doi: 10.1378/chest.117.4.1162

Ozhan, G., and Weidinger, G. (2014). "Restoring tissue homeostasis: wnt signaling in tissue regeneration after acute injury," in *Wnt Signalling in Development and Disease: Molecular Mechanisms and Biological Functions*, eds S. P. Hoppler, and R. T. Moon (Hoboken, NJ: Wiley-Blackwell), 339–356.

Paredes, R., Ishibashi, S., Borrill, R., Robert, J., and Amaya, E. (2015). Xenopus: an in vivo model for imaging the inflammatory response following injury and bacterial infection. *Dev. Biol.* 408, 213–228. doi: 10.1016/j.ydbio.2015.03.008

Patel, A. K., Park, K. K., and Hackam, A. S. (2017). Wnt signaling promotes axonal regeneration following optic nerve injury in the mouse. *Neuroscience* 343, 372–383. doi: 10.1016/j.neuroscience.2016.12.020

Pearson, B. J., and Sanchez Alvarado, A. (2008). Regeneration, stem cells, and the evolution of tumor suppression. *Cold Spring Harb. Symp. Quant. Biol.* 73, 565–572. doi: 10.1101/sqb.2008.73.045

Pellegrini, E., Mouriec, K., Anglade, I., Menuet, A., Le Page, Y., Gueguen, M. M., et al. (2007). Identification of aromatase-positive radial glial cells as progenitor cells in the ventricular layer of the forebrain in zebrafish. *J. Comp. Neurol.* 501, 150–167. doi: 10.1002/cne.21222

Peng, W. M., Yu, L. L., Bao, C. Y., Liao, F., Li, X. S., and Zuo, M. X. (2002). Transplanted neuronal precursors migrate and differentiate in the developing mouse brain. *Cell Res.* 12, 223–228. doi: 10.1038/sj.cr.7290128

Peng, X., Yang, L., Chang, H., Dai, G., Wang, F., Duan, X., et al. (2014). Wnt/beta-catenin signaling regulates the proliferation and differentiation of mesenchymal progenitor cells through the p53 pathway. *PLoS One* 9:e97283. doi: 10.1371/journal.pone.0097283

Peterson, S. L., Nguyen, H. X., Mendez, O. A., and Anderson, A. J. (2015). Complement protein C1q modulates neurite outgrowth in vitro and spinal cord axon regeneration in vivo. *J. Neurosci.* 35, 4332–4349. doi: 10.1523/JNEUROSCI.4473-12.2015

Petrie, T. A., Strand, N. S., Yang, C. T., Rabinowitz, J. S., and Moon, R. T. (2014). Macrophages modulate adult zebrafish tail fin regeneration. *Development* 141, 2581–2591. doi: 10.1242/dev.098459

Piya, S., Kim, J. Y., Bae, J., Seol, D. W., Moon, A. R., and Kim, T. H. (2012). DUSP6 is a novel transcriptional target of p53 and regulates p53-mediated apoptosis by modulating expression levels of Bcl-2 family proteins. *FEBS Lett.* 586, 4233–4240. doi: 10.1016/j.febslet.2012.10.031

Placke, T., Kopp, H. G., and Salih, H. R. (2010). Glucocorticoid-induced TNFR-related (GITR) protein and its ligand in antitumor immunity: functional role and therapeutic modulation. *Clin. Dev. Immunol.* 2010:239083. doi: 10.1155/2010/239083

Rakic, P. (2002). Neurogenesis in adult primate neocortex: an evaluation of the evidence. *Nat. Rev. Neurosci.* 3, 65–71. doi: 10.1038/nrn700

Rolls, A., Shechter, R., and Schwartz, M. (2009). The bright side of the glial scar in CNS repair. *Nat. Rev. Neurosci.* 10, 235–241. doi: 10.1038/nrn2591

Ruiz de Almodovar, C., Lambrechts, D., Mazzone, M., and Carmeliet, P. (2009). Role and therapeutic potential of VEGF in the nervous system. *Physiol. Rev.* 89, 607–648. doi: 10.1152/physrev.00031.2008

Satoh, A., and Makanae, A. (2014). Conservation of position-specific gene expression in axolotl limb skin. *Zoolog. Sci.* 31, 6–13. doi: 10.2108/zsj.31.6

Schlomann, U., Rathke-Hartlieb, S., Yamamoto, S., Jockusch, H., and Bartsch, J. W. (2000). Tumor necrosis factor alpha induces a metalloprotease-disintegrin, ADAM8 (CD 156): implications for neuron-glia interactions during neurodegeneration. *J. Neurosci.* 20, 7964–7971. doi: 10.1523/jneurosci.20-21-07964.2000

Schweitzer, J., Becker, T., Lefebvre, J., Granato, M., Schachner, M., and Becker, C. G. (2005). Tenascin-C is involved in motor axon outgrowth in the trunk of developing zebrafish. *Dev. Dyn.* 234, 550–566. doi: 10.1002/dvdy.20525

Sebastianelli, L., Saltuari, L., and Nardone, R. (2017). How the brain can rewire itself after an injury: the lesson from hemispherectomy. *Neural Regen. Res.* 12, 1426–1427. doi: 10.4103/1673-5374.215247

Seri, B., Garcia-Verdugo, J. M., McEwen, B. S., and Alvarez-Buylla, A. (2001). Astrocytes give rise to new neurons in the adult mammalian hippocampus. *J. Neurosci.* 21, 7153–7160. doi: 10.1523/jneurosci.21-18-07153.2001

Shannon, P., Markiel, A., Ozier, O., Baliga, N. S., Wang, J. T., Ramage, D., et al. (2003). Cytoscape: a software environment for integrated models of biomolecular interaction networks. *Genome Res.* 13, 2498–2504. doi: 10.1101/gr.1239303

Shi, W., Fang, Z., Li, L., and Luo, L. (2015). Using zebrafish as the model organism to understand organ regeneration. *Sci. China Life Sci.* 58, 343–351. doi: 10.1007/s11427-015-4838-z

Shihabuddin, L. S., Horner, P. J., Ray, J., and Gage, F. H. (2000). Adult spinal cord stem cells generate neurons after transplantation in the adult dentate gyrus. *J. Neurosci.* 20, 8727–8735. doi: 10.1523/jneurosci.20-23-08727.2000

Shimizu, N., Kawakami, K., and Ishitani, T. (2012). Visualization and exploration of Tcf/Lef function using a highly responsive Wnt/beta-catenin signaling-reporter transgenic zebrafish. *Dev. Biol.* 370, 71–85. doi: 10.1016/j.ydbio.2012.07.016

Shimizu, Y., Ueda, Y., and Ohshima, T. (2018). Wnt signaling regulates proliferation and differentiation of radial glia in regenerative processes after stab injury in the optic tectum of adult zebrafish. *Glia* 66, 1382–1394. doi: 10.1002/glia.23311

Shitasako, S., Ito, Y., Ito, R., Ueda, Y., Shimizu, Y., and Ohshima, T. (2017). Wnt and Shh signals regulate neural stem cell proliferation and differentiation in the optic tectum of adult zebrafish. *Dev. Neurobiol.* 77, 1206–1220. doi: 10.1002/dneu.22509

Singh, B. N., Weaver, C. V., Garry, M. G., and Garry, D. J. (2018). Hedgehog and Wnt signaling pathways regulate tail regeneration. *Stem Cells Dev.* 27, 1426–1437. doi: 10.1089/scd.2018.0049

Smith, P. D., Sun, F., Park, K. K., Cai, B., Wang, C., Kuwako, K., et al. (2009). SOCS3 deletion promotes optic nerve regeneration in vivo. *Neuron* 64, 617–623. doi: 10.1016/j.neuron.2009.11.021

Sobecki, M., Mrouj, K., Colinge, J., Gerbe, F., Jay, P., Krasinska, L., et al. (2017). Cell-cycle regulation accounts for variability in Ki-67 expression levels. *Cancer Res.* 77, 2722–2734. doi: 10.1158/0008-5472.CAN-16-0707

Spittau, B., and Krieglstein, K. (2012). Klf10 and Klf11 as mediators of TGF-beta superfamily signaling. *Cell Tissue Res.* 347, 65–72. doi: 10.1007/s00441-011-1186-6

Stoick-Cooper, C. L., Weidinger, G., Riehle, K. J., Hubbert, C., Major, M. B., Fausto, N., et al. (2007). Distinct Wnt signaling pathways have opposing roles in appendage regeneration. *Development* 134, 479–489. doi: 10.1242/dev.001123

Strand, N. S., Hoi, K. K., Phan, T. M. T., Ray, C. A., Berndt, J. D., and Moon, R. T. (2016). Wnt/beta-catenin signaling promotes regeneration after adult zebrafish spinal cord injury. *Biochem. Biophys. Res. Commun.* 477, 952–956. doi: 10.1016/j.bbrc.2016.07.006

Tanaka, E. M., and Ferretti, P. (2009). Considering the evolution of regeneration in the central nervous system. *Nat. Rev. Neurosci.* 10, 713–723. doi: 10.1038/nrn2707

Tang, J., Yu, Y., Zheng, H., Yin, L., Sun, M., Wang, W., et al. (2017). ITRAQ-based quantitative proteomic analysis of *Cynops orientalis* limb regeneration. *BMC Genomics* 18:750. doi: 10.1186/s12864-017-4125-4

Tsarouchas, T. M., Wehner, D., Cavone, L., Munir, T., Keatinge, M., Lambertus, M., et al. (2018). Dynamic control of proinflammatory cytokines Il-1beta and Tnf-alpha by macrophages in zebrafish spinal cord regeneration. *Nat. Commun.* 9:4670. doi: 10.1038/s41467-018-07036-w

Tseng, A. S., Adams, D. S., Qiu, D., Koustubhan, P., and Levin, M. (2007). Apoptosis is required during early stages of tail regeneration in *Xenopus laevis*. *Dev. Biol.* 301, 62–69. doi: 10.1016/j.ydbio.2006.10.048

Tsujioka, H., Kunieda, T., Katou, Y., Shirahige, K., Fukazawa, T., and Kubo, T. (2017). *interleukin-11* induces and maintains progenitors of different cell lineages during *Xenopus* tadpole tail regeneration. *Nat. Commun.* 8:495. doi: 10.1038/s41467-017-00594-5

Ueno, S., Weidinger, G., Osugi, T., Kohn, A. D., Golob, J. L., Pabon, L., et al. (2007). Biphasic role for Wnt/beta-catenin signaling in cardiac specification in zebrafish and embryonic stem cells. *Proc. Natl. Acad. Sci. U.S.A.* 104, 9685–9690. doi: 10.1073/pnas.0702859104

Veldman, M. B., Bemben, M. A., Thompson, R. C., and Goldman, D. (2007). Gene expression analysis of zebrafish retinal ganglion cells during optic nerve regeneration identifies KLF6a and KLF7a as important regulators of axon regeneration. *Dev. Biol.* 312, 596–612. doi: 10.1016/j.ydbio.2007.09.019

Walter, W., Sanchez-Cabo, F., and Ricote, M. (2015). GOplot: an R package for visually combining expression data with functional analysis. *Bioinformatics* 31, 2912–2914. doi: 10.1093/bioinformatics/btv300

Wang, Y. H., Keenan, S. R., Lynn, J., McEwan, J. C., and Beck, C. W. (2015). Gremlin1 induces anterior-posterior limb bifurcations in developing Xenopus limbs but does not enhance limb regeneration. *Mech. Dev.* 138(Pt 3), 256–267. doi: 10.1016/j.mod.2015.10.003

Wang, Z., Gerstein, M., and Snyder, M. (2009). RNA-Seq: a revolutionary tool for transcriptomics. *Nat. Rev. Genet.* 10, 57–63. doi: 10.1038/nrg2484

Wehner, D., Tsarouchas, T. M., Michael, A., Haase, C., Weidinger, G., Reimer, M. M., et al. (2017). Wnt signaling controls pro-regenerative collagen XII in functional spinal cord regeneration in zebrafish. *Nat. Commun.* 8:126. doi: 10.1038/s41467-017-00143-0

Whyte, J. L., Smith, A. A., and Helms, J. A. (2012). Wnt signaling and injury repair. *Cold Spring Harb. Perspect. Biol.* 4:a008078. doi: 10.1101/cshperspect.a008078

Wickham, H. (2016). *Ggplot2: Elegant Graphics for Data Analysis*. New York, NY: Springer-Verlag.

Wilson, S. E., Chaurasia, S. S., and Medeiros, F. W. (2007). Apoptosis in the initiation, modulation and termination of the corneal wound healing response. *Exp. Eye Res.* 85, 305–311. doi: 10.1016/j.exer.2007.06.009

Wu, Y. S., and Chen, S. N. (2014). Apoptotic cell: linkage of inflammation and wound healing. *Front. Pharmacol.* 5:1. doi: 10.3389/fphar.2014.00001

Yu, L., Dawson, L. A., Yan, M., Zimmel, K., Lin, Y. L., Dolan, C. P., et al. (2019). BMP9 stimulates joint regeneration at digit amputation wounds in mice. *Nat. Commun.* 10:424. doi: 10.1038/s41467-018-08278-4

Zaman, G., Sunters, A., Galea, G. L., Javaheri, B., Saxon, L. K., Moustafa, A., et al. (2012). Loading-related regulation of transcription factor EGR2/Krox-20 in bone cells is ERK1/2 protein-mediated and prostaglandin, Wnt signaling pathway-, and insulin-like growth factor-I axis-dependent. *J. Biol. Chem.* 287, 3946–3962. doi: 10.1074/jbc.M111.252742

Zambusi, A., and Ninkovic, J. (2020). Regeneration of the central nervous system-principles from brain regeneration in adult zebrafish. *World J. Stem Cells* 12, 8–24. doi: 10.4252/wjsc.v12.i1.8

Zhang, Y., Pizzute, T., and Pei, M. (2014). A review of crosstalk between MAPK and Wnt signals and its impact on cartilage regeneration. *Cell Tissue Res.* 358, 633–649. doi: 10.1007/s00441-014-2010-x

Zhao, L., Jin, Y., Donahue, K., Tsui, M., Fish, M., Logan, C. Y., et al. (2019). Tissue repair in the mouse liver following acute carbon tetrachloride depends on injury-induced Wnt/beta-Catenin signaling. *Hepatology* 69, 2623–2635. doi: 10.1002/hep.30563

Zimmerman, Z. F., Kulikauskas, R. M., Bomsztyk, K., Moon, R. T., and Chien, A. J. (2013). Activation of Wnt/beta-catenin signaling increases apoptosis in melanoma cells treated with trail. *PLoS One* 8:e69593. doi: 10.1371/journal.pone.0069593

**Conflict of Interest:** The authors declare that the research was conducted in the absence of any commercial or financial relationships that could be construed as a potential conflict of interest.

frontiers in Cellular Neuroscience

ORIGINAL RESEARCH
published: 28 October 2020
doi: 10.3389/fncel.2020.573208

# MiR34a Regulates Neuronal MHC Class I Molecules and Promotes Primary Hippocampal Neuron Dendritic Growth and Branching

*Yue Hu[1], Wenqin Pei[1], Ying Hu[1], Ping Li[1], Chen Sun[1], Jiawei Du[1], Ying Zhang[1], Fengqin Miao[1], Aifeng Zhang[2], Yuqing Shen[1]* and Jianqiong Zhang[1,3]**

[1]Department of Microbiology and Immunology, Key Laboratory of Developmental Genes and Human Disease, Ministry of Education, Medical School, Southeast University, Nanjing, China, [2]Department of Pathology, Medical School, Southeast University, Nanjing, China, [3]Jiangsu Key Laboratory of Molecular and Functional Imaging, Zhongda Hospital, Medical School, Southeast University, Nanjing, China

OPEN ACCESS

**Edited by:**
*Alicia Guemez-Gamboa, Northwestern University, United States*

**Reviewed by:**
*Francesca Ruberti, Institute of Biochemistry and Cell Biology, Italy*
*Michael Chopp, Henry Ford Health System, United States*
*Sivakumar Sambandan, Max Planck Institute for Biophysical Chemistry, Germany*

***Correspondence:**
*Jianqiong Zhang*
*zhjq@seu.edu.cn*
*Yuqing Shen*
*yuqingshenseu@hotmail.com*

**Specialty section:**
*This article was submitted to Cellular Neurophysiology, a section of the journal Frontiers in Cellular Neuroscience*

**Received:** *16 June 2020*
**Accepted:** *07 September 2020*
**Published:** *28 October 2020*

**Citation:**
*Hu Y, Pei W, Hu Y, Li P, Sun C, Du J, Zhang Y, Miao F, Zhang A, Shen Y and Zhang J (2020) MiR34a Regulates Neuronal MHC Class I Molecules and Promotes Primary Hippocampal Neuron Dendritic Growth and Branching. Front. Cell. Neurosci. 14:573208. doi: 10.3389/fncel.2020.573208*

In the immune system, Major Histocompatibility Complex class I (MHC-I) molecules are located on the surface of most nucleated cells in vertebrates where they mediate immune responses. Accumulating evidence indicates that MHC-I molecules are also expressed in the central nervous system (CNS) where they play important roles that are significantly different from their immune functions. Classical MHC-I molecules are temporally and spatially expressed in the developing and adult CNS, where they participate in the synaptic formation, remodeling and plasticity. Therefore, clarifying the regulation of MHC-I expression is necessary to develop an accurate understanding of its function in the CNS. Here, we show that microRNA 34a (miR34a), a brain enriched noncoding RNA, is temporally expressed in developing hippocampal neurons, and its expression is significantly increased after MHC-I protein abundance is decreased in the hippocampus. Computational algorithms identify putative miR34a target sites in the 3′UTR of MHC-I mRNA, and here we demonstrate direct targeting of miR34a to MHC-I mRNA using a dual-luciferase reporter assay system. MiR34a targeting can decrease constitutive MHC-I expression in both Neuro-2a neuroblastoma cells and primary hippocampal neurons. Finally, miR34a mediated reduction of MHC-I results in increased dendritic growth and branching in cultured hippocampal neurons. Taken together, our findings identify miR34a as a novel regulator of MHC-I for shaping neural morphology in developing hippocampal neurons.

**Keywords: hippocampal development, dendritic growth and branching, primary hippocampal neurons, miR-34a, MHC class I**

## INTRODUCTION

For a long time, the central nervous system (CNS) has been considered to be "immune-privileged." This view, however, has changed following the identification of classical immune molecules such as cytokines, complement, and major histocompatibility complex (MHC) proteins in the healthy, uninfected CNS (Joly et al., 1991). Several studies have demonstrated that these immune proteins impart pleiotropic effects on neurons (Boulanger et al., 2001).

In the immune system, classical MHC-I proteins are located on the surface of most nucleated cells where they regulate T cell and NK cell-mediated immune responses. In the vertebrate CNS, MHC-I proteins are constitutively expressed on the surface of axons and dendrites of some neurons over discrete developmental and adult stages (Elmer and Mcallister, 2012). Decades of research has now definitively shown that classical MHC-I molecules play extremely important and diverse roles in the CNS including regulation of synapse formation, remodeling, and plasticity and that these roles are distinct from their originally identified immune functions (Corriveau et al., 1998; Boulanger, 2009; Elmer and Mcallister, 2012).

Our previous studies reported on the specific spatial and temporal expression pattern of classical MHC-I molecules in developing C57BL/6 mouse brains. In the developing cerebellum and hippocampus, levels of MHC-I protein gradually increase from postnatal day 0 (P0) to a peak value at P15, a crucial period for synaptic remodeling and plasticity. After completing their functions, protein abundance becomes significantly reduced with age until neuronal MHC-I proteins can no longer be detected after P60. In contrast, mRNA expression is gradually increased from P0 to P60 after which it remains relatively stable (Liu et al., 2013; Li et al., 2020). A similar expression pattern of MHC-I proteins is observed during human CNS development (Zhang et al., 2013a,b). This evidence suggests that the expression of MHC-I proteins is tightly regulated in the developing CNS due to their role in important neurodevelopmental events. Due to this discrepancy between protein abundance and mRNA levels during development, the complex regulation of MHC-I expression at the transcriptional and post-transcriptional level needs to be further investigated.

We recently found that NLRC5 is a critical transcriptional factor of MHC-I during development from P0 to P15 in hippocampal neurons (Li et al., 2020). All previous studies on the post-transcriptional regulation of MHC-I expression have only detailed regulation in the immune system. MEX-3C acts as a novel ubiquitin E3 ligase, binding to the 3′UTR of HLA-A2 mRNA and degrading it to fine-tune regulation of HLA-A protein abundance (Cano et al., 2012). RNA-binding protein HNRNPR positively regulates the expression of both classical and nonclassical MHC-I proteins through binding to the 3′UTR of HLA-A, -B, -C, and -G mRNA and enhancing protein stability (Reches et al., 2016). MicroRNA hsa-miR148 is increased in HIV infected cells to decrease HLA-C expression and evade host immune recognition (Kulkarni et al., 2011, 2013). Although we know some transcriptional factors can regulate MHC-I expression at the level of transcription in the developing CNS, whether it is regulated post-transcriptionally remains poorly understood.

MicroRNAs (miRNAs) are small non-coding RNAs. They function as post-transcriptional regulators and target the 3′UTR of messenger RNA transcripts (mRNAs). MiRNA binding can either result in the degradation of genetic transcripts or can result in silencing mRNA translation indirectly (Bartel, 2009). Accumulating evidence demonstrates microRNAs play a non-negligible role in modulating neuronal activities and maintaining homeostasis of the CNS (Davis et al., 2015; Yu et al., 2015; Evgenia and De Strooper, 2017). Our study reveals miR34a functions as a negative regulator of classical MHC-I molecules in both Neuro-2a cells and in primary cultured mouse hippocampal neurons. In mice, miR34a is especially abundant in brain tissue and participates in neuronal morphology and function by modulating the expression of synaptic targets (Agostini et al., 2011a,b; Morgado et al., 2015). However, its relationship with MHC-I has not yet been reported. We find that the expression of miR34a is negatively correlated with that of MHC-I protein levels in the developing hippocampus. We also demonstrate that the putative miR34a target sites are located in MHC-I mRNA 3′UTR. By binding to the 3′UTR region of MHC-I mRNA, miRNA-34a decreases the level of MHC-I mRNA and proteins. Inhibition of miR34a decreases dendritic growth and branching in cultured hippocampal neurons due to enhanced MHC-I protein expression. All these findings provide the first evidence that miRNA-34a acts as a novel regulator in modulating neuronal MHC-I.

# MATERIALS AND METHODS

## Animals

Experimental animals were C57BL/6J mice (Cat# n000013c57, RRID: MGI:5657312) purchased from GemPharmatech Company, Limited (China) in this study. The animals were housed in polypropylene cages under pathogen-free conditions of constant temperature and humidity, maintained on a 12–12 h day-night cycle, with food and water provided *ad libitum* in the standard animal facility. Animal experiments were conducted according to the protocols evaluated and approved by the Institutional Animal Care and Use Committee (IACUC) of the Medical School of Southeast University (approval ID: SYXK-2010.4987). Postnatal day P0 was designated as the day of birth. P0, P8, P15, P30, and P60 male mice were used for experiments. Fresh tissues, RNA, protein, or others extracted from mice were stored in liquid nitrogen.

## Cell Lines

Mouse neuroblastoma N2a cells, also known as Neuro-2a cells (RRID: CVCL_0470), are murine neuroblastoma cells obtained from the cell bank of the Type Culture Collection of the Chinese Academy of Science (China). Cell lines employed in our laboratory were authenticated in 2019 using short tandem repeat (STR) analysis at Shanghai Biowing Biotechnology Company, Limited. Neuro-2a cells were seeded in 25-$cm^2$ cell culture flasks in modified Eagle's medium (MEM; Gibco, USA) with an additional 10% FBS (Gibco-BRL, USA) and 1% penicillin-streptomycin antibiotics (Gibco-BRL, USA). The growth medium was changed every 2–3 days. Before each experiment, monolayers of cells were trypsinized and diluted in MEM, then transferred to new culture plates. Neuro-2a cells were transfected with miR34a mimic or miR34a inhibitor (Ribo Life Science, China). The following microRNA mimics and inhibitors were used: miR34a mimic upstream sequence: 5′-UGGCAG UGUCUUAGCUGGUUGU-3′, and downstream sequence:

5′-AACCAGCUAAGACACUGCCAUU-3′; miR34a inhibitor: 5′-ACAACCAGCUAAGACACUGCCA-3′; mimic negative control upstream sequence: 5′-UUCUUCGAACGUGUCACGU TT-3′, and downstream sequence: 5′-ACGUGACACGUUCGG AGAATT-3′; inhibitor negative control upstream sequence: 5′-CAGUACUUUUGUGUAGUACAA-3′. To ensure the characteristics of Neuro-2a cells, cells used in all the experiments were not passaged for more than 10 times.

## Primary Neuron Culture

Hippocampal neuronal cells were isolated from E16.5 to 18.5 fetus as previously described (Kaech and Banker, 2006). Primary hippocampal neurons were seeded in 6-well plates, or on glass coverslips (coated with 100 μg/ml poly-d-lysine, Sigma–Aldrich, USA) placed in 24-well plates. Cells were cultured in Neurobasal media (Gibco, USA) supplemented with GlutaMAX (Invitrogen, USA) and glucose (Sigma–Aldrich, USA). An optimized serum-free supplement B27 (Invitrogen, USA) was added to the Neurobasal Medium. The growth medium was changed after 3 DIV by half volume. The lentivirus used in this study were synthesized by Shanghai Genechem Company, Limited. Gene sequences inserted in lentivirus are shown in **Supplementary Material and Methods**.

## Luciferase Reporter Assay

The full length of H-2D$^b$ and H-2K$^b$ 3′UTR containing the putative miRNA target sites and the mutated sequence was chemically synthesized and cloned into pmiRGLO vector (Genewiz, China). The sequences of H-2D$^b$ and H-2K$^b$ 3′UTR are shown in **Supplementary Material and Methods**. HET293T cells were transfected with the H-2D$^b$/H-2K$^b$ 3′UTR pmiRGLO vector, or mutated H-2D$^b$/H-2K$^b$ 3′UTR pmiRGLO vector and microRNA mimics (Ribo Life Science, China). The following microRNA mimics were used in this study: miR34a mimic upstream sequence: 5′-UGGCAGUGUCUU AGCUGGUUGU-3′, and downstream sequence: 5′-AACCAG CUAAGACACUGCCAUU-3′; miR146b mimic upstream sequence: 5′-UGAGAACUGAAUUCCAUAGGCU-3′, and downstream sequence: 5′-CCUAUGGAAUUCAGUUCUCA UU-3′; miR148a mimic upstream sequence: 5′-UCAGUGCAC UACAGAACUUUGU-3′, and downstream sequence: 5′-AAA GUUCUGUAGUGCACUGAUU; miR181a mimic upstream sequence: 5′-AACAUUCAACGCUGUCGGUGAGU-3′, and downstream sequence: 5′-UCACCGACAGCGUUGAAUGUU UU-3′; miR181c mimic upstream sequence: 5′-AACAUUCAA CCUGUCGGUGAGU-3′, and downstream sequence: 5′-UCA CCGACAGGUUGAAUGUUUU-3′. Luciferase activity was determined 48 h post-transfection, using the Dual-Luciferase Reporter assay kit (Promega, USA) and measured by using a TD 20/20n luminometer (Turner Biosystems, USA). These data represented the average of three independent experiments, performed in three wells each time, and were shown with the standard error.

## Real-Time Quantitative PCR

Total RNA was isolated from Neuro-2a cells or mouse hippocampus by TRIzol reagent (Invitrogen, USA). The RNA was subjected to reverse transcription using the HiScript II 1st Strand cDNA Synthesis Kit (+gDNA wiper) (Vazyme Biotech, China). Real-time PCR analysis was performed using the following primers (Ribo Life Science, China): H-2D$^b$ (forward primer: 5′-GGCGAGTGCGTGGAGTG-3′; reverse primer: 5′-CATCACAAAAGCCACCACAGC-3′), H-2K$^b$ (forward primer: 5′-GACGAGAGACTCAGGGCCTAC-3′; reverse primer: 5′-AACGGTCGCCATGTTGGAGAC-3′), GAPDH (forward primer: 5′-AGGTCGGTGTGAACGGAT TTG-3′; reverse primer: 5′-TGTAGACCATGTAGTTGAGGT CA-3′), miR34a (forward primer: 5′-TGGCAGTGTCTTAGC TGGTTGT; reverse primer: 5′-CGAATTCTAGAGCTCGAG GCAG), U6 (forward primer: 5′-CGCAAATTCGTGAAGCGT TCC; reverse primer: 5′-CGAATTCTAGAGCTCGAGGCAG). Relative quantification was performed following the instruction for ChamQ SYBR qPCR Master Mix (Vazyme Biotech, China) with a Real-Time PCR system (Applied Biosystems, USA). U6 snRNA was used as the endogenous control for miRNA Real-time PCR analyses, GAPDH was used as a housekeeping gene for normalization. All reactions were run in triplicate. Results were represented as fold expression of the control.

## Western Blotting Analysis

The whole-cell lysates were lysed by RIPA lysis buffer (Sangon Biotech, China) with protease inhibitors. Protein extracted from cells was quantified by the BCA protein assay kit (Thermo, USA). Equal amounts of protein (35–45 μg) in a protein sample buffer were denatured at 100°C for 10 min. The protein samples were loaded into the SDS-PAGE gel sample well. To observe the electrophoresis process, and to determine the molecular weight of proteins, pre-stained protein ladders were added into the gel as well. Proteins were transferred to a polyvinylidene fluoride (PVDF) membrane (Millipore, USA) after SDS-PAGE was finished. PVDF membrane was incubated in 5% BSA (AMRESCO, USA) in Tris-buffered saline at 37°C for 2 h to block nonspecific binding, and then probed with primary antibodies at 4°C for 12–16 h (anti-GAPDH, 1:1,000, Cell Signaling, USA; anti-classical MHC-I, 1:1,000, Bioworld, USA; anti-Flag, 1:2,000, Bioworld, China). After washed with TBST, the membrane was incubated with a peroxidase-conjugated secondary antibody for 1.5 h at room temperature. The Immunodetection of the PVDF membrane was performed with an enhanced chemiluminescent (ECL) substrate (Pierce, USA). Detection was performed using a Luminoimage analyzer (Tanon, China) and quantification was analyzed by densitometry using ImageJ software (USA).

## Immunofluorescence Staining

Mouse anti-microtubule-associated protein2 (MAP2, 1:200, Abcam, USA), Flag (1:100, Bioworld, China), DAPI (1:1,000, Sigma–Aldrich, USA), and secondary antibodies conjugated with Alexa Fluor 546 (1:500, Invitrogen, USA) were used in immunofluorescence experiments. Coverslips were rinsed in PBS to remove medium before fixed by 4% paraformaldehyde (Sigma Aldrich, USA) in 0.01 M PBS for 20 min. Then coverslips were rinsed three times in PBS. Cells were permeabilized with 0.25% Triton X-100 (Sigma Aldrich, USA) for 15 min and washed three times again. Cells were

blocked with BSA for 2 h before incubated with primary antibodies overnight at 4°C in a humid chamber. After that, cells were rinsed and incubated with secondary antibodies for 2 h at room temperature in the dark. After washed three times, the coverslips were sealed with glycerin and observed with a fluorescence microscope (Olympus Fluoview FV 1000, Japan).

## Sholl Analysis

Sholl Analysis is a method for quantitative analysis of neuron axons and dendrites. For the Sholl analysis, a group of concentric circles is superimposed on the cell body and the branch patterns of neuron dendrites and axons in different regions are obtained by calculating the number of branches that intersect each circle, thereby quantitatively characterizing the imaged nerve metamorphic characteristics.

## Statistical Analysis

All *in vitro* experiments were repeated at least three times. All statistical analyses were performed with one-way ANOVA or Student's *t*-test using GraphPad Prism 8.0.1 (GraphPad Software, USA). The numerical data are expressed as the mean ± standard error of the mean (SEM). A value of $P < 0.05$ was considered to be statistically significant. No data points were excluded.

# RESULTS

## MiR34a Targets MHC-I Molecules

We previously reported on the expression of H-2K$^b$ and H-2D$^b$ mRNA and protein from P0 to P60 in the hippocampus of C57BL/6 mice (Li et al., 2020). There was an increase of H-2K$^b$ and H-2D$^b$ proteins from P0 to P15 before it decreased to a relatively low level, despite a sustained increased H-2K$^b$ and H-2D$^b$ mRNA from P0 to P60, suggesting post-transcriptional regulation mechanisms such as miRNAs might be involved after P15. According to TargetScan and miRanda analysis, several miRNAs such as miR146b, miR148a, miR181a, miR181c, and miR34a were predicted to target H-2K$^b$ and H-2D$^b$ (**Figure 1A**). To confirm if H-2D$^b$ and H-2K$^b$ expression was regulated by those miRNAs, the wild type sequence of H-2D$^b$ or H-2K$^b$ 3′UTR was cloned into pmirGLO dual-luciferase reporter vectors and co-transfected with miRNA mimics in HEK293T cells. MicroRNA mimics were chemically synthesized to enhance the function of endogenous miRNAs. Of all the miRNAs investigated, only miR34a mimics manifested attenuated luciferase signal compared to the non-targeting Ctrl (**Figures 1B,C**). This downregulation was aborted when transfected with mutated plasmids and miR34a mimics (**Figure 2A**, upper panel). The mutated sequence was designed according to TargetScan where the estimated binding site of miR34a to H-2D$^b$ or H-2K$^b$ was changed (**Figure 2B**). The same effect was also shown in H-2K$^b$ 3′UTR-luciferase plasmid with miR34a mimics (**Figure 2A**, lower panel). In summary, these results showed that the binding of miR34a to MHC-I mRNA was dependent on the 3′UTR sequence of H-2D$^b$ or H-2K$^b$ and miR34a could decrease MHC-I expression.

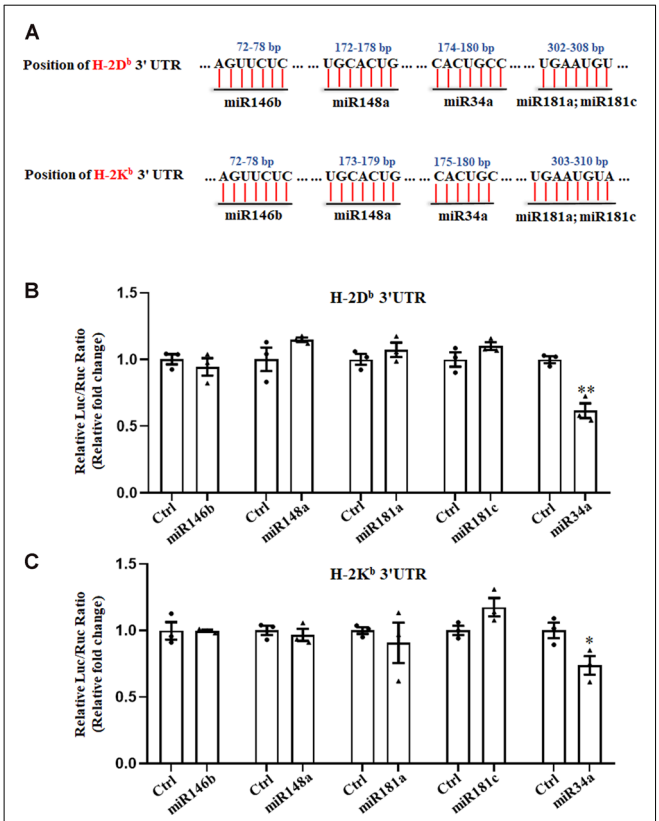


**FIGURE 1** | Searching for miRNAs that target H-2K$^b$ and H-2D$^b$. **(A)** A schematic drawing of the H-2K$^b$ and H-2D$^b$ 3′UTR with indication of miR146b, miR148a, miR34a, miR181a and miR181c putative binding sites within the 3′UTR. **(B,C)** HEK293T cells were cotransfected with a dual luciferase reporter containing the wild-type H-2D$^b$ 3′UTR **(B)** or H-2K$^b$ 3′UTR **(C)** and different miRNA mimics with their controls for 48 h. All data are presented as the means ± SEM of three individual experiments. Values indicated the Firefly luciferase activity normalized to Renilla luciferase activity. $^*P < 0.05$; $^{**}P < 0.01$ vs. negative control.

It is worth noting that miR34a was expressed over different periods of C57BL/6 mouse hippocampal development. MiR34a was expressed at a low level postnatally, while expression increased dramatically after P15 (**Figure 2C**). Since H-2K$^b$ and H-2D$^b$ proteins were dramatically decreased after P15 in the hippocampus, miR34a might contribute to the regulation of MHC-I expression during this developmental stage.

## MiR34a Regulates MHC-I Expression in Neuro-2a Cell Lines

To further verify the regulation of MHC-I by miR34a, we investigated its effect on Neuro-2a cell lines using miR34a mimics and inhibitors. Neuro-2a cells were previously reported to express H-2D$^b$ but not H-2K$^b$ (Li et al., 2020), so only the expression of H-2D$^b$ was investigated here. In contrast to miRNA mimics, the miRNA inhibitors could effectively inhibit mature miRNA function without degrading it (the endogenous miRNA levels remained unchanged). After transfecting miRNA mimics into Neuro-2a cells, miR34a expression was significantly upregulated as examined by real-time PCR (**Figure 3A**). As

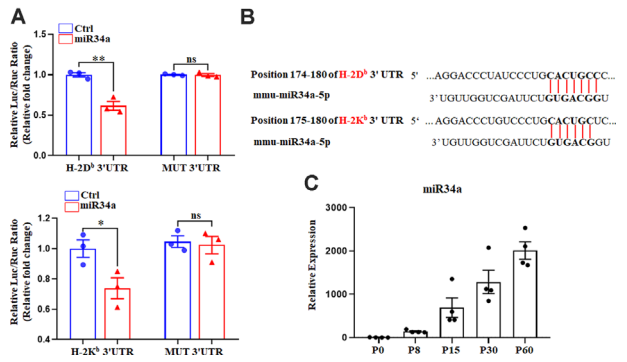


**FIGURE 2 |** MiR34a participates in the regulation of H-2D$^b$ and H-2K$^b$. **(A)** HEK293T cells were cotransfected with a dual luciferase reporter containing the wild-type or mutant constructs of H-2D$^b$ 3′ UTR (upper panel) or H-2K$^b$ 3′ UTR (lower panel) for 48 h. All data are presented as the means ± SEM of three individual experiments. Values indicated the Firefly luciferase activity normalized to Renilla luciferase activity. *$P < 0.05$; **$P < 0.01$ vs. negative control; ns: non-significant. **(B)** Putative miR34a binding sites in the 3′ UTR of H-2K$^b$ and H-2D$^b$, The potential complementary residues are shown in bold. **(C)** miR34a expression in different periods of mice hippocampus. Data are presented as the means ± SEM of four individual experiments.

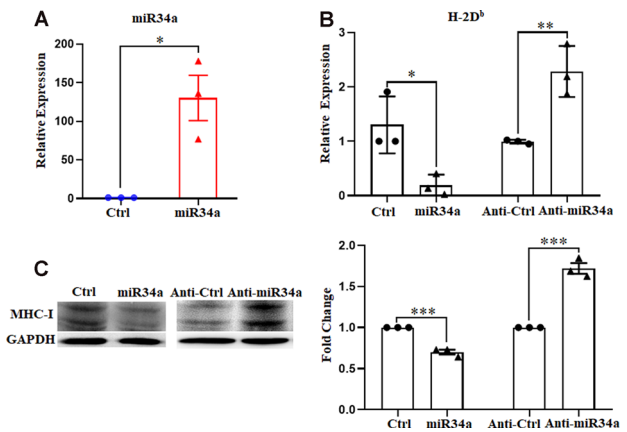


**FIGURE 3 |** MiR34a has a negative impact on classical MHC-I expression in Neuro-2a cells. **(A)** Increased expression of miRNA-34a in neuro-2a cells transfected with miR34a mimic for 24 h was detected by RT-qPCR. *$P < 0.05$ vs. negative control. **(B)** Neuro-2a cells were transfected with 50 nM miR34a mimic or 100 nM miR34a inhibitor for 24 h followed by measurement of H-2D$^b$ expression with RT-qPCR analysis. *$P < 0.05$; **$P < 0.01$ vs. negative control. **(C)** Expression of the classical MHC-I protein in neuro-2a cells transfected with miR control, miR34a mimic, inhibitor control or miR34a inhibitor for 48 h was detected by western blotting. GAPDH was probed as an internal control for experiments. Densitometric analysis of the classical MHC-I expression using ImageJ is presented. ***$P < 0.001$ vs. negative control. All data are presented as the means ± SEM of three independent experiments.

shown in **Figure 3B**, overexpressing miR34a mimics alleviated H-2D$^b$ expression in Neuro-2a cells. At the same time, the transfection of miR34a inhibitors increased H-2D$^b$ expression. Consistent with these findings, the change of MHC-I protein was identical with MHC-I mRNA when treated with miR34a mimics or inhibitors (**Figure 3C**). Taken together, these results suggested

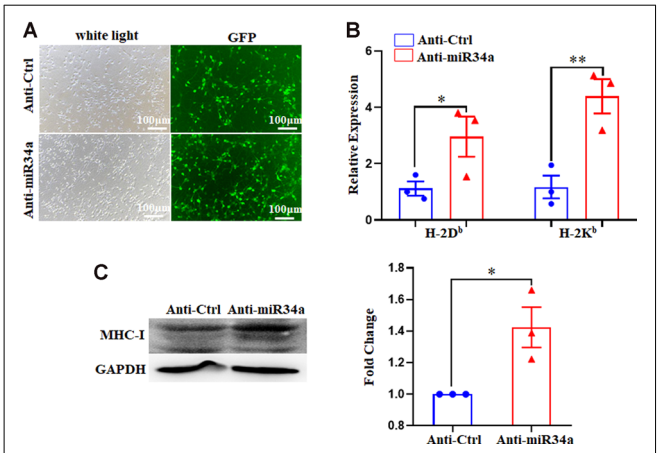


**FIGURE 4 |** MiR34a blockade induces classical MHC-I expression in primary hippocampal neurons. **(A)** Representative images of transfection efficiency with anti-Ctrl-GFP lentivirus or anti-miR34a-GFP lentivirus infection in primary hippocampal neurons. Cells were infected with lentivirus at DIV 1 and observed at DIV 5 with a fluorescence microscope. Bars: 100 μm. **(B)** Increased levels of H-2D$^b$ and H-2K$^b$ in primary hippocampal neurons infected with anti-miR34a-GFP lentivirus for 4 days compared to those infected with anti-Ctrl-GFP lentivirus. The level of indicated mRNA was determined by RT-qPCR. *$P < 0.05$; **$P < 0.01$ vs. negative control. **(C)** Expression of the classical MHC-I protein in mouse primary hippocampal neurons infected with anti-Ctrl-GFP lentivirus or anti-miR34a-GFP lentivirus for 4 days as determined by western blotting. Densitometric data of the classical MHC-I protein expression using ImageJ are presented as the means ± SEM of three independent experiments. *$P < 0.05$ vs. negative control. All data are presented as the means ± SEM of three independent experiments.

that the expression of MHC-I mRNA and proteins was regulated by miR34a in Neuro-2a cell lines.

## Manipulated miR34a Expression Changes MHC-I Levels in Primary Mouse Hippocampal Neurons

Since Neuro-2a is a murine neuroblastoma cell line, whether regulation of MHC-I by miR34a also applied to neurons required additional investigation. We dissected primary hippocampal neurons from embryonic E16.5–18.5 C57BL/6 mice. The cultured neurons were infected with anti-miR34a-GFP lentivirus which expressed miR34a specific sponge at DIV (days *in vitro*) 1. The sponge contains a series of antisense sequences of miR34a that can bind to miR34a through complementary base pairing, thereby preventing miR34a from binding to its target sequence. Transfection efficiency was estimated at approximately 80% after 4 days post lentivirus infection as observed by fluorescence microscopy (**Figure 4A**). As compared to neurons infected with a control virus, both H-2D$^b$ and H-2K$^b$ mRNA and protein expression were upregulated in neurons infected with anti-miR34a-GFP lentivirus (**Figures 4B,C**). In concordance with this, infection of miR34a-GFP lentivirus (**Figure 5A**), which increased the endogenous level of miR34a (**Figure 5B**), inhibited both MHC-I mRNA and protein expression in cultured hippocampal neurons (**Figures 5C,D**). In general, we confirmed that MHC-I expression was regulated by miR34a in primary cultured mouse hippocampal neurons.

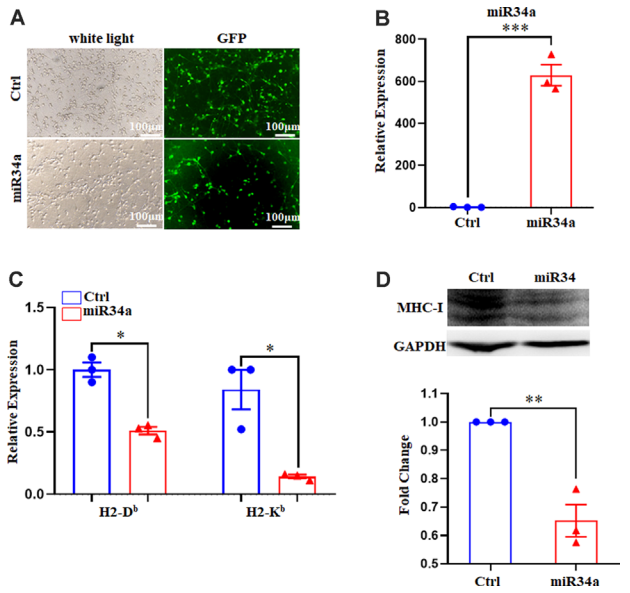


**FIGURE 5 |** Increased miR34a inhibits classical MHC-I expression in primary hippocampal neurons. **(A)** Representative images of transfection efficiency with Ctrl-GFP lentivirus or miR34a-GFP lentivirus infection in primary hippocampal neurons. Cells were infected with lentivirus at DIV 1 and observed at DIV 5 with a fluorescence microscope. Bars: 100 μm. **(B)** Cells were assessed for miRNA-34a expression at the mRNA levels after lentivirus infection. ***$P < 0.001$ vs. negative control. **(C)** Decreased H-2D$^b$ and H-2K$^b$ in primary hippocampal neurons infected with miR34a-GFP lentivirus compared to those infected with Ctrl-GFP lentivirus for 4 days. The level of indicated mRNA was determined by RT-qPCR. *$P < 0.05$ vs. negative control. **(D)** Expression of the classical MHC-I protein in mouse primary hippocampal neurons infected with Ctrl-GFP lentivirus or miR34a-GFP lentivirus for 4 days as determined by western blotting. Densitometric data of the classical MHC-I protein expression using ImageJ are presented as the means ± SEM of three independent experiments. **$P < 0.01$ vs. negative control. All data are presented as the means ± SEM of three independent experiments.

## Dendritic Growth and Branching Varies According to Changes of miR34a Expression in Hippocampal Neurons, Which is Mediated by MHC-I Molecules

One of the established roles of MHC-I in neuronal development is to inhibit axon and dendrite outgrowth in hippocampal and cortical neurons both *in vitro* and *in vivo* (Washburn et al., 2011). We explored whether changes in the expression of MHC-I by miR34a would affect the shape of neurites in cultured hippocampal neurons. Neurons were infected with anti-miR34a-GFP lentivirus or anti-Ctrl-GFP lentivirus at DIV 1. After cultured for several days, they were fixed and immunostained for MAP2 at DIV 5. Compared to the anti-Ctrl-treated neurons, a significant decrease of total dendrite length in anti-miR34a-GFP-treated neurons was observed (**Figures 6A,B**). We also detected a dramatic decrease in dendritic complexity in anti-miR34a-GFP-treated neurons (**Figures 6C,D**) as revealed by Sholl analysis. To confirm that this effect is mediated by increased MHC-I expression upon anti-miR34a-GFP lentivirus infection, blockade of MHC-I was achieved by adding a monoclonal MHC class I antibody OX18 to the culture medium at DIV 3 and neurons was fixed and immunostained for MAP2 at DIV 5. Neurons treated with the MHC class I antibody exhibited a marked increase in dendritic length and complexity, and the antibody successfully rescued decreased neurite outgrowth of anti-miR34a-GFP-treated neurons (**Figures 6A–D**).

In concordance with this, miR34a-GFP lentivirus treated neurons showed dramatically increased total dendritic length compared to Ctrl-GFP neurons (**Figures 7A,B**), as well as dendritic branching (**Figures 7C,D**). Increased expression of H-2D$^b$ in HEK293T cells and cultured hippocampus neurons was achieved by infection with an H-2D$^b$-Flag-lentivirus for 96 h and stained with Flag antibody (**Supplementary Figure 1**; **Figure 7E**). In our previous research, overexpression of H-2D$^b$ in neurons induced enhanced expression of MHC class I molecules could decrease neurite growth and branching (Shen et al., 2019). We further demonstrated miR34a-mediated enhancement of total dendritic length was thoroughly blocked by overexpression of H-2D$^b$ (**Figures 7E,F**), and miR34a-mediated increment of the average number of intersections was slightly reduced by overexpression of H-2D$^b$ in hippocampus neurons (**Figures 7G,H**). This phenomenon indicated that miR34a shaped neurite neuron morphology in cultured hippocampal neurons by modulation of MHC-I molecules.

## DISCUSSION

In the immune system, MHC-I molecules are constitutively expressed on almost all nucleated cells, binding and presenting peptides from processed cellular antigens to cytotoxic T cells. Apart from that, MHC-I proteins can be induced upon cytokine stimulation. Both constitutive and inducible expression of MHC-I molecules is mainly dependent on the binding of transcriptional factors to conserved promoter elements: enhancer A (EnhA), IFN-stimulated response element (ISRE), and the SXY module in the MHC-I promoter. NLRC5 cooperates with transcription factors that bind to the SXY module to drive MHC-I expression (Meissner et al., 2012; Neerincx et al., 2013).

Since people find MHC-I molecules are expressed throughout the healthy CNS, accumulating evidence validates their critical roles in neural development. They regulate activity-dependent refinement of synaptic plasticity (Huh et al., 2000; Glynn et al., 2011; Datwani et al., 2009; Lee et al., 2014), limit the establishment of synaptic connections and the degree of dendrite arborization (Bilousova et al., 2012; Shen et al., 2019), as well as inhibit NMDAR function and hippocampal-dependent memory formation (Fourgeaud et al., 2010; Wu et al., 2011). Even though regulation of MHC-I expression has been extensively investigated in the immune system for many years now, a multitude of basic questions about the mechanism(s) governing neuronal MHC-I expression remains poorly understood. We previously reported that calcium-dependent protein kinase C (PKC) was important in relaying intracranial kainic acid (KA) stimulation signals to up-regulate MHC-I expression in hippocampal neurons and that this

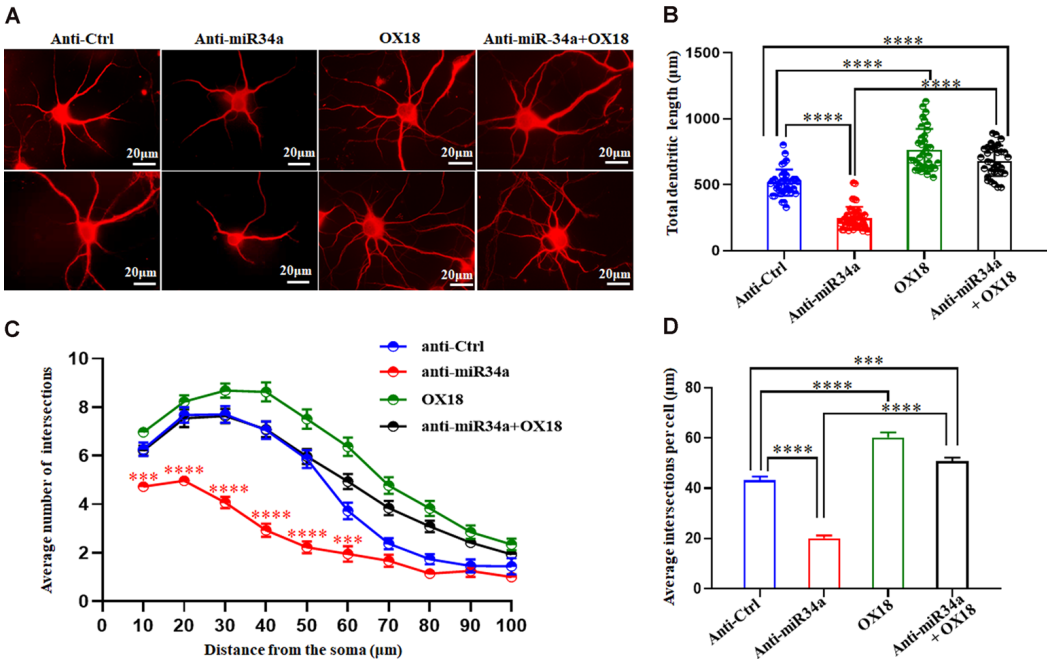


**FIGURE 6 |** MiR34a deficiency in hippocampal neurons decreases dendritic growth and branching. **(A)** Primary hippocampal neurons infected with anti-Ctrl-GFP lentivirus or anti-miR34a-GFP lentivirus were fixed and immunostained for MAP2 at DIV 5 to confirm shape of neurites. MHC class I antibody OX18 was added into the culture medium at DIV 3 to block MHC class I expression. A combination of anti-miR34a-GFP lentivirus treatment and antibody blockade was applied to neurons and it's morphology was monitored by MAP2 at DIV 5. Bars: 20 μm. **(B)** Quantification of neurite length. $^{****}P < 0.0001$ vs. negative control. **(C,D)** Sholl analysis was performed on these neurons. Sholl profile and the average total numbers of intersections per cell were shown ($n = 37$ anti-Ctrl group, $n = 43$ anti-miR34a group, $n = 36$ OX18 blockade group, $n = 33$ anti-miR34a + OX18 group, $^{***}P < 0.001$; $^{****}P < 0.0001$).

signaling cascade relied on activation of the MAPK pathway (Lv et al., 2015). We also confirmed that NLRC5, but not CIITA, was broadly expressed in the mouse brain and promoted MHC-I expression in hippocampal neurons (Li et al., 2020). In this study, we analyze the regulation of MHC-I expression from a new perspective: regulation by miRNAs in hippocampal neurons, adding new information regarding the tight and complex regulatory system that controls classical MHC-I molecule levels during the development of the hippocampus.

MicroRNAs are endogenously expressed non-coding RNAs that regulate complementary mRNA expression. In vertebrates, microRNAs are ubiquitously expressed in the brain with a growing body of evidence showing their functions in neural development and their contributions to neurodevelopmental diseases (Fineberg et al., 2009). To exert their regulatory function, miRNAs silence gene expression at the post-transcription level by guiding Argonaute (AGO) family proteins to constitute miRNA-induced silencing complexes (miRISCs), finally degrading gene transcripts if mRNA is fully complementary to the miRNA seed region (Jonas and Izaurralde, 2015). In this way, the sequence of mRNAs can be used for the prediction of possible binding miRNAs by matching their sequence with the seed region of miRNA. To begin our work, computational algorithms identify several candidate miRNAs by searching for the presence of conserved miRNA seed sequences that match H-2K$^b$ and H-2D$^b$ mRNA. MiR146b, miR148a, miR181a, miR181c, and miR34a are further tested by luciferase activity assay in HEK293T cells for their ability to regulate H-2K$^b$ and H-2D$^b$ expression. MiR34a, which is perfectly complementary to the seed sequence of H-2D$^b$ and partially complementary to the seed sequence of H-2K$^b$, is the only miRNA among all candidates that effectively decrease H-2K$^b$ and H-2D$^b$ 3′UTR-luciferase activity in HEK293T cells. In cases when the mRNA target is only partially complementary to the miRNA, additional protein partners are recruited by AGO proteins to mediate mRNA silencing in the absence of direct cleavage by AGO protein. Other post-transcriptional regulation mechanisms such as translation inhibition can also be used by miRNA to regulate protein expression of the target gene. In our study, manipulating miR34a expression can change both H-2K$^b$ mRNA level and MHC-I protein expression in neuro-2a cells and cultured mouse hippocampal neurons, implying that both translational repression and mRNA degradation contribute to miR34a regulated MHC-I expression. Further experiments are required to dissect the detailed pathway(s) used by miR34a to regulate MHC-I expression in hippocampal neurons.

Although we confirm the regulation of MHC-I expression by miR34a in cultured hippocampal neurons, whether it can repress MHC-I expression in the developing hippocampus *in vivo* is still unknown. So far, miR34a is shown to be expressed in the CNS. It influences terminal neuronal differentiation,

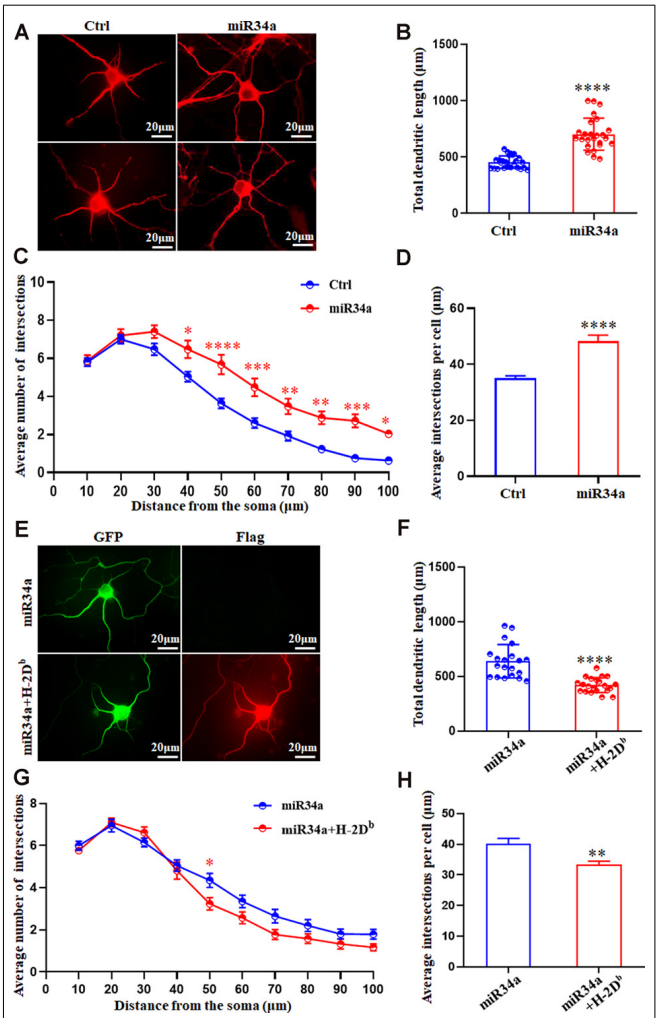


**FIGURE 7 |** MiR34a overexpression in hippocampal neurons increases dendritic growth and branching. **(A)**Primary hippocampal neurons were infected with miR34a-GFP lentivirus for 4 days. Neurons were fixed and immunostained for MAP2 at DIV 5. Bars: 20 μm. **(B)** Quantification of neurite length. ****$P < 0.0001$ vs. negative control. **(C,D)** Sholl analysis was performed on these neurons. Sholl profiles and the average total numbers of intersections per cell were shown ($n = 25$ Ctrl group, $n = 25$ miR34a group. *$P < 0.05$; **$P < 0.01$; ***$P < 0.001$; ****$P < 0.0001$ vs. negative control). **(E)** Primary hippocampal neurons were infected with miR34a-GFP lentivirus with/without H-2D$^b$-Flag-lentivirus at DIV 1. Neurons were immunostained by anti-Flag antibody at DIV 5. The expression of GFP and Flag was observed with a fluorescence microscope. Bars: 20 μm. **(F)** Quantification of neurite length was shown. ****$P < 0.0001$ vs. miR34a-GFP. **(G,H)** Sholl analysis was performed on these neurons. Sholl profiles and the average total numbers of intersections per cell were shown ($n = 20$ miR34a group, $n = 21$ miR34a + H-2D$^b$ group. *$P < 0.05$; **$P < 0.01$ vs. miR34a-GFP).

regulates neurite outgrowth, and mediates dendritic spine morphology and function (Agostini et al., 2011a,b). As a brain-enriched microRNA, miR34a upregulates with brain age (Li et al., 2011; Jauhari et al., 2018). It can modulate mitochondrial activity by regulating mitochondrial protein abundance in aging cells, eventually leading to age-related diseases (Rippo et al., 2014). During the development of the mouse hippocampus, it was reported that P15 was a critical period for refinement of neuronal connections (Hashimoto and Kano, 2003) when MHC-I is expressed. Inappropriate neuronal MHC-I expression after this critical period in the hippocampus could be deleterious, thus shutting down MHC-I expression after p15 is necessary. We previously demonstrated that the MHC-I protein level was dramatically decreased after P15 while MHC-I mRNA was kept at in high level (Li et al., 2020). In this study, we find that miR34a is expressed at a low level in early postnatal mice, while it increases dramatically after P15, following the peak of MHC-I protein expression at P15. As we find that miR34a can decrease MHC-I expression in primary cultured hippocampus neurons, expression of miR34a at this stage could be one of the mechanisms for decreasing MHC-I expression. However, our *in vitro* experiment shows decreased both MHC-I mRNA and protein expression following increased miR34a, which is not in concordance with *in vivo* findings that only MHC-I protein is decreased. Other transcriptional and post-transcriptional regulation mechanisms may contribute to divergent expression of MHC-I mRNA and protein expression after P15. Thus, the regulation of MHC-I by miR34a in the hippocampal neuron *in vivo* still needs to be investigated.

Our findings also indicate that decreased miR34a inhibits neurite outgrowth and branching in cultured hippocampal neurons, which recapitulates our previous finding that upregulated MHC-I expression can decrease neurite outgrowth (Shen et al., 2019). We also confirm the causal relationship between miR34a mediated modulation of MHC-I and hippocampal dendritic growth by successfully rescuing the decreased length and branching of anti-miR34a-GFP lentivirus treated neurons by blocking with MHC class I antibody. On the other hand, the miR34a-GFP lentivirus-mediated increase of dendritic complexity can be blocked by overexpression of H-2D$^b$. However, a study from Agostini et al. (2011b) reports that miR34a negatively affects dendritic outgrowth of cortical and hippocampus neurons, which is different from our results. There are several possible reasons for this discrepancy. First, in their report, hippocampal neurons are co-transfected with a GFP expression and a miR34a overexpression plasmids (PremiR34a) with siPORT NeoFX transfection agent. While in our study, primary mouse hippocampal neurons are infected with lentivirus to inhibit or overexpress miR34a expression. With high transfection efficiency shown by immunofluorescence in neurons, we can confirm the expression of miR34a after virus infection by Real-time quantitative PCR. We find that inhibition of miR34a decreases dendritic growth and branching and at the same time, overexpression of miR34a increases dendritic growth and branching in cultured hippocampal neurons. Secondary, they transfect neurons at DIV 4, and cells are analyzed 72 h later while in our study neurons are infected at DIV 1 and analyzed 96 h later. We suppose that different transfection methods and different time points to treat the neurons cause inconsistent results in neuron morphology. In conclusion, all these results will help us to better understand the tight regulation of MHC-I expression in the developing hippocampus, which is also helpful towards elucidating its role in aging and degenerative diseases.

## DATA AVAILABILITY STATEMENT

All datasets presented in this study are included in the article/**Supplementary Material**.

## ETHICS STATEMENT

The animal study was reviewed and approved by Institutional Animal Care and Use Committee (IACUC) of the Medical School of Southeast University (approval ID: SYXK-2010.4987).

## AUTHOR CONTRIBUTIONS

YH conceived of the presented idea and carried out the experiments, YH wrote the manuscript with support from YS and PL. All authors discussed the results and contributed to the final manuscript. JZ helped supervise the project. All authors contributed to the article and approved the submitted version.

## FUNDING

This work was supported by the National Natural Science Foundation of China (Grant No. 81571615) and the Postgraduate Research and Practice Innovation Program of Jiangsu Province, China (KYCX19_0058).

## SUPPLEMENTARY MATERIAL

The Supplementary Material for this article can be found online at: https://www.frontiersin.org/articles/10.3389/fncel.2020.573208/full#supplementary-material.

**SUPPLEMENTARY FIGURE 1 |** Overexpression of H-2D$^b$ in HEK293T cells was achieved using lentivirus delivery. Cell lysates were immunoblotted with Flag and GAPDH antibodies to confirm the expression of H-2D$^b$.

**SUPPLEMENTARY TABLE 1 |** Sequences of H-2D$^b$ and H-2K$^b$ 3′UTR are listed, and lentivirus-mediated gene sequences are shown.

## REFERENCES


Agostini, M., Tucci, P., Killick, R., Candi, E., Sayan, B. S., Rivetti di Val Cervo, P., et al. (2011a). Neuronal differentiation by TAp73 is mediated by microRNA-34a regulation of synaptic protein targets. *Proc. Natl. Acad. Sci. U S A* 108, 21093–21098. doi: 10.1073/pnas.1112061109

Agostini, M., Tucci, P., Steinert, J. R., Shalom-Feuerstein, R., Rouleau, M., Aberdam, D., et al. (2011b). microRNA-34a regulates neurite outgrowth, spinal morphology and function. *Proc. Natl. Acad. Sci. U S A* 108, 21099–21104. doi: 10.1073/pnas.1112063108

Bartel, D. P. (2009). MicroRNAs: target recognition and regulatory functions. *Cell* 136, 215–233. doi: 10.1016/j.cell.2009.01.002

Bilousova, T., Dang, H., Xu, W., Gustafson, S., Jin, Y., Wickramasinghe, L., et al. (2012). Major histocompatibility complex class I molecules modulate embryonic neuritogenesis and neuronal polarization. *J. Neuroimmunol.* 247, 1–8. doi: 10.1016/j.jneuroim.2012.03.008

Boulanger, L. M. (2009). Immune proteins in brain development and synaptic plasticity. *Neuron* 64, 93–109. doi: 10.1016/j.neuron.2009.09.001

Boulanger, L. M., Huh, G. S., and Shatz, C. J. (2001). Neuronal plasticity and cellular immunity: shared molecular mechanisms. *Curr. Opin. Neurobiol.* 11, 568–578. doi: 10.1016/s0959-4388(00)00251-8

Cano, F., Bye, H., Duncan, L. M., Buchet-Poyau, K., Billaud, M., Wills, M. R., et al. (2012). The RNA-binding E3 ubiquitin ligase MEX-3C links ubiquitination with MHC-I mRNA degradation. *EMBO J.* 31, 3596–3606. doi: 10.1038/emboj.2012.218

Corriveau, R. A., Huh, G. S., and Shatz, C. J. (1998). Regulation of class I MHC gene expression in the developing and mature CNS by neural activity. *Neuron* 21, 505–520. doi: 10.1016/s0896-6273(00)80562-0

Datwani, A., McConnell, M. J., Kanold, P. O., Micheva, K. D., Busse, B., Shamloo, M., et al. (2009). Classical MHC I molecules regulate retinogeniculate refinement and limit ocular dominance plasticity. *Neuron* 64, 463–470. doi: 10.1016/j.neuron.2009.10.015

Davis, G. M., Haas, M. A., and Pocock, R. (2015). MicroRNAs: not "fine-tuners" but key regulators of neuronal development and function. *Front. Neurol.* 6:245. doi: 10.3389/fneur.2015.00245

Elmer, B. M., and Mcallister, A. K. (2012). Major histocompatibility complex class I proteins in brain development and plasticity. *Trends Neurosci.* 35, 660–670. doi: 10.1016/j.tins.2012.08.001

Evgenia, S., and De Strooper, B. (2017). Noncoding RNAs in neurodegeneration. *Nature* 18, 627–640. doi: 10.1038/nrn.2017.90

Fineberg, S. K., Kosik, K. S., and Davidson, B. L. (2009). MicroRNAs potentiate neural development. *Neuron* 64, 303–309. doi: 10.1016/j.neuron.2009.10.020

Fourgeaud, L., Davenport, C. M., Tyler, C. M., Cheng, T. T., Spencer, M. B., and Huganir, B. R. L. (2010). MHC class I modulates NMDA receptor function and AMPA receptor trafficking. *Proc. Natl. Acad. Sci. U S A* 107, 22278–22283. doi: 10.1073/pnas.0914064107

Glynn, M. W., Elmer, B. M., Garay, P. A., Liu, X. B., Needleman, L. A., El-Sabeawy, F., et al. (2011). MHC class I negatively regulates synapse density during the establishment of cortical connections. *Nat. Neurosci.* 14, 442–451. doi: 10.1038/nn.2764

Hashimoto, K., and Kano, M. (2003). Functional differentiation of multiple climbing fiber inputs during synapse elimination in the developing cerebellum. *Neuron* 38, 785–796. doi: 10.1016/s0896-6273(03)00298-8

Huh, G. S., Boulanger, L. M., Du, H., Riquelme, P. A., Brotz, T. M., and Shatz, C. J. (2000). Functional requirement for class I MHC in CNS development and plasticity. *Science* 290, 2155–2159. doi: 10.1126/science.290.5499.2155

Jauhari, A., Singh, T., Singh, P., Parmar, D., and Yadav, S. (2018). Regulation of miR-34 family in neuronal development. *Mol. Neurobiol.* 55, 936–945. doi: 10.1007/s12035-016-0359-4

Joly, E., Mucke, L., and Oldstone, M. (1991). Viral persistence in neurons explained by lack of major histocompatibility class I expression. *Science* 253, 1283–1285. doi: 10.1126/science.1891717

Jonas, S., and Izaurralde, E. (2015). Towards a molecular understanding of microRNA-mediated gene silencing. *Nat. Rev. Genet.* 16, 421–433. doi: 10.1038/nrg3965

Kaech, S., and Banker, G. (2006). Culturing hippocampal neurons. *Nat. Protoc.* 1, 2406–2415. doi: 10.1038/nprot.2006.356

Kulkarni, S., Qi, Y., O'hUigin, C., Pereyra, F., Ramsuran, V., McLaren, P., et al. (2013). Genetic interplay between HLA-C and MIR148A in HIV control and Crohn disease. *Proc. Natl. Acad. Sci. U S A* 110, 20705–20710. doi: 10.1073/pnas.1312237110

Kulkarni, S., Savan, R., Qi, Y., Gao, X., Yuki, Y., Bass, S. E., et al. (2011). Differential microRNA regulation of HLA-C expression and its association with HIV control. *Nature* 472, 495–498. doi: 10.1038/nature09914

Lee, H., Brott, B. K., Kirkby, L. A., Adelson, J. D., Cheng, S., Feller, M. B., et al. (2014). Synapse elimination and learning rules co-regulated by MHC class I H2-Db. *Nature* 509, 195–200. doi: 10.1038/nature13154

Li, X., Khanna, A., Li, N., and Wang, E. (2011). Circulatory miR34a as an RNA-based, noninvasive biomarker for brain aging. *Aging* 3, 985–1002. doi: 10.18632/aging.100371

Li, P., Shen, Y., Cui, P., Hu, Y., Zhang, Y., Miao, F., et al. (2020). Neuronal NLRC5 regulates MHC class I expression in Neuro cells and also during hippocampal development. *J. Neurochem.* 152, 182–194. doi: 10.1111/jnc.14876

Liu, J., Shen, Y., Li, M., Shi, Q., Zhang, A., Miao, F., et al. (2013). The expression pattern of classical MHC class I molecules in the development of mouse central nervous system. *Neurochem. Res.* 38, 290–299. doi: 10.1007/s11064-012-0920-0

Lv, D., Shen, Y. Q., Peng, Y. Q., Liu, J. E., Miao, F. Q., and Zhang, J. Q. (2015). Neuronal MHC class I expression is regulated by activity driven calcium signaling. *PLoS One* 10:e0135223. doi: 10.1371/journal.pone.0135223

Meissner, T. B., Liu, Y. J., Lee, K. H., Li, A., Biswas, A., van Eggermond, M. C., et al. (2012). NLRC5 cooperates with the RFX transcription factor complex to induce MHC class I gene expression. *J. Immunol.* 188, 4951–4958. doi: 10.4049/jimmunol.1103160

Morgado, A. L., Xavier, J. M., Dionísio, P. A., Ribeiro, M. F., Dias, R. B., Sebastião, A. M., et al. (2015). MicroRNA-34a modulates neural stem cell differentiation by regulating expression of synaptic and autophagic proteins. *Mol. Neurobiol.* 51, 1168–1183. doi: 10.1007/s12035-014-8794-6

Neerincx, A., Castro, W., Guarda, G., and Kufer, T. A. (2013). NLRC5, at the heart of antigen presentation. *Front. Immunol.* 4:397. doi: 10.3389/fimmu.2013.00397

Reches, A., Nachmani, D., Berhani, O., Duev-Cohen, A., Shreibman, D., Ophir, Y., et al. (2016). HNRNPR regulates the expression of classical and nonclassical MHC class I proteins. *J. Immunol.* 196, 4967–4976. doi: 10.4049/jimmunol.1501550

Rippo, M. R., Olivieri, F., Monsurrò, V., Prattichizzo, F., Albertini, M. C., and Procopio, A. D. (2014). MitomiRs in human inflamm-aging: a hypothesis involving miR-181a, miR34a and miR-146a. *Exp. Gerontol.* 56, 154–163. doi: 10.1016/j.exger.2014.03.002

Shen, Y. Q., Zhao, H. H., Li, P., Peng, Y. Q., Cui, P. F., Miao, F. Q., et al. (2019). MHC class I molecules and pirb shape neuronal morphology by affecting the dendritic arborization of cortical neurons. *Neurochem. Res.* 44, 312–322. doi: 10.1007/s11064-018-2676-7

Washburn, L. R., Zekzer, D., Eitan, S., Lu, Y., Dang, H., Middleton, B., et al. (2011). A potential role for shed soluble major histocompatibility class I molecules as modulators of neurite outgrowth. *PLoS One* 6:e18439. doi: 10.1371/journal.pone.0018439

Wu, Z. P., Washburn, L., Bilousova, T. V., Boudzinskaia, M., Escande-Beillard, N., Querubin, J., et al. (2011). Enhanced neuronal expression of major histocompatibility complex class I leads to aberrations in neurodevelopment and neurorepair. *J. Neuroimmunol.* 232, 8–16. doi: 10.1016/j.jneuroim.2010.09.009

Yu, B., Zhou, S., Yi, S., and Gu, X. (2015). The regulatory roles of non-coding RNAs in nerve injury and regeneration. *Prog. Neurobiol.* 134, 122–139. doi: 10.1016/j.pneurobio.2015.09.006

Zhang, A., Yu, H., He, Y., Shen, Y., Pan, N., Liu, J., et al. (2013a). The spatio-temporal expression of MHC class I molecules during human hippocampal formation development. *Brain Res.* 1529, 26–38. doi: 10.1016/j.brainres.2013.07.001

Zhang, A., Yu, H., Shen, Y., Liu, J., He, Y., Shi, Q., et al. (2013b). The expression patterns of MHC class I molecules in the developmental human visual system. *Neurochem. Res.* 38, 273–281. doi: 10.1007/s11064-012-0916-9

**Conflict of Interest**: The authors declare that the research was conducted in the absence of any commercial or financial relationships that could be construed as a potential conflict of interest.

frontiers in Cell and Developmental Biology

ORIGINAL RESEARCH
published: 30 April 2021
doi: 10.3389/fcell.2021.668408

# Transcriptome Analyses Reveal IL6/Stat3 Signaling Involvement in Radial Glia Proliferation After Stab Wound Injury in the Adult Zebrafish Optic Tectum

*Yuki Shimizu*[1,2]*, *Mariko Kiyooka*[3] and *Toshio Ohshima*[3,4]

[1] Functional Biomolecular Research Group, Biomedical Research Institute, National Institute of Advanced Industrial Science and Technology, Osaka, Japan, [2] DBT-AIST International Laboratory for Advanced Biomedicine, National Institute of Advanced Industrial Science and Technology, Osaka, Japan, [3] Department of Life Science and Medical Bio-Science, Waseda University, Tokyo, Japan, [4] Graduate School of Advanced Science and Engineering, Institute for Advanced Research of Biosystem Dynamics, Waseda Research Institute for Science and Engineering, Waseda University, Tokyo, Japan

OPEN ACCESS

**Edited by:**
Luis B. Tovar-y-Romo, National Autonomous University of Mexico, Mexico

**Reviewed by:**
Erika Calvo-Ochoa, Hope College, United States
Sepand Rastegar, Karlsruhe Institute of Technology (KIT), Germany

***Correspondence:**
Yuki Shimizu
yuki.shimizu@aist.go.jp

**Specialty section:**
This article was submitted to Molecular Medicine, a section of the journal Frontiers in Cell and Developmental Biology

**Received:** 16 February 2021
**Accepted:** 30 March 2021
**Published:** 30 April 2021

**Citation:**
Shimizu Y, Kiyooka M and Ohshima T (2021) Transcriptome Analyses Reveal IL6/Stat3 Signaling Involvement in Radial Glia Proliferation After Stab Wound Injury in the Adult Zebrafish Optic Tectum. Front. Cell Dev. Biol. 9:668408. doi: 10.3389/fcell.2021.668408

Adult zebrafish have many neurogenic niches and a high capacity for central nervous system regeneration compared to mammals, including humans and rodents. The majority of radial glia (RG) in the zebrafish optic tectum are quiescent under physiological conditions; however, stab wound injury induces their proliferation and differentiation into newborn neurons. Although previous studies have functionally analyzed the molecular mechanisms of RG proliferation and differentiation and have performed single-cell transcriptomic analyses around the peak of RG proliferation, the cellular response and changes in global gene expression during the early stages of tectum regeneration remain poorly understood. In this study, we performed histological analyses which revealed an increase in isolectin B4+ macrophages prior to the induction of RG proliferation. Moreover, transcriptome and pathway analyses based on differentially expressed genes identified various enriched pathways, including apoptosis, the innate immune system, cell proliferation, cytokine signaling, p53 signaling, and IL6/Jak-Stat signaling. In particular, we found that Stat3 inhibition suppressed RG proliferation after stab wound injury and that IL6 administration into cerebroventricular fluid activates RG proliferation without causing injury. Together, the findings of these transcriptomic and functional analyses reveal that IL6/Stat3 signaling is an initial trigger of RG activation during optic tectum regeneration.

**Keywords: zebrafish, brain regeneration, optic tectum, radial glia, STAT3 signaling, transcriptome analysis**

## INTRODUCTION

Neural stem cells (NSCs) have been observed in the adult brains of all vertebrates and can continuously generate new neurons (Kizil et al., 2012; Balthazart and Ball, 2014; Berninger and Jessberger, 2016; Kempermann et al., 2018; Joven and Simon, 2018; McDonald and Vickaryous, 2018). The adult mammalian brain has two neurogenic regions, the subventricular zone (SVZ) and

the subgranular zone in the hippocampus (Altman and Das, 1965; Eriksson et al., 1998), whereas the neurogenic regions of birds and reptiles are mainly located in the telencephalon (Balthazart and Ball, 2014; McDonald and Vickaryous, 2018). Conversely, the adult brains of teleosts contain many neurogenic niches (Zupanc and Horschke, 1995; Adolf et al., 2006; Grandel et al., 2006; Alunni et al., 2010); for instance, zebrafish have 16 different proliferative niches (Grandel et al., 2006) while medaka has 10 (Alunni et al., 2010). Moreover, mammals and birds display a limited central nervous system (CNS) regenerative capacity compared to amphibians and teleosts (Alunni and Bally-Cuif, 2016). In mammals, stroke activates neural progenitors in the SVZ which then migrate toward injured areas; however, functional recovery remains limited despite the presence of some newborn neurons (Yamashita et al., 2006; Kaneko et al., 2018). In contrast, urodele amphibians and teleosts have a high capacity for brain regeneration (Urata et al., 2018) and adult zebrafish have many neurogenic niches and display a high regenerative capacity in the CNS, including the brain, retina, and spinal cord (Becker et al., 1997; Adolf et al., 2006; Grandel et al., 2006; Raymond et al., 2006; März et al., 2011). Therefore, zebrafish are a well-studied model organism in CNS regeneration due to their high neurogenic potential, easy genetic manipulation, and the availability of genomic and transcriptomic data. In particular, various injury models in the brain, retina, and spinal cord of adult zebrafish have been developed to elucidate and analyze the molecular mechanisms that enable CNS regeneration (Ramachandran et al., 2010; Dias et al., 2012; Kishimoto et al., 2012).

Radial glia (RG), or ependymoglia (neurepithelial-like stem cells), have been reported to function as NSCs in the neurogenic niches of adult zebrafish (Than-Trong and Bally-Cuif, 2015). In the telencephalon, which is a well-studied region of the adult zebrafish brain, RG mainly function as active NSCs that continuously proliferate and generate newborn neurons under both physiological and regenerative conditions (März et al., 2010; Kroehne et al., 2011; Rothenaigner et al., 2011). The molecular mechanisms that regulate adult and regenerative neurogenesis by RG in the telencephalon have been investigated comprehensively using pharmacological inhibitors, transgenic strains, and transcriptome analyses (Kizil et al., 2012; Cosacak et al., 2019; Demirci et al., 2020; Lange et al., 2020). On the other hand, most of RG are quiescent, while neuroepithelial-like stem cells contribute to adult neurogenesis in the adult optic tectum (Ito et al., 2010). Previous studies have shown that stab wound injury in the optic tectum induces RG proliferation and differentiation into neurons in young adult zebrafish (2–4 months old) under regenerative conditions (Shimizu et al., 2018; Ueda et al., 2018; Yu and He, 2019), but induces RG proliferation without neurogenesis in elderly adult zebrafish (6–12 months old) (Lindsey et al., 2019). Moreover, Yu and He found that only a few neurons were generated from RG using long-term EdU labeling and Cre-loxP-based clonal analysis. The analysis of gene expression changes in RG using single-cell RNA-sequencing (RNA-seq) at 3 days post-injury (dpi) showed that Notch signaling inhibition promotes RG proliferation and differentiation. However, few studies have investigated gene expression changes that trigger RG proliferation during the early stages of tectum regeneration compared to the retina and telencephalon (Sifuentes et al., 2016; Demirci et al., 2020).

During the early stages after CNS damage, inflammatory responses commonly occur in both mammals and teleosts (Kizil et al., 2015; Buscemi et al., 2019; Lambertsen et al., 2019). In the mouse CNS, both the negative and positive effects of inflammatory responses on tissue regeneration, have been well studied in order to improve tissue damage and neurodegenerative disorders (Shichita et al., 2014; Rajkovic et al., 2018; Otani and Shichita, 2020). In zebrafish, inflammatory responses are required during brain regeneration to induce RG cell proliferation and differentiation (Kyritsis et al., 2012; Ueda et al., 2018), and the acute inflammation induced by zymosan A injection is sufficient to induce RG proliferation without injury (Kyritsis et al., 2012). Although multiple studies have analyzed the function of inflammatory mediators, such as cytokines and leukotriene, in the zebrafish telencephalon and retina (Kyritsis et al., 2012; Zhao et al., 2014; Bhattarai et al., 2016), the molecular mechanisms related to inflammatory signaling that trigger RG proliferation following optic tectum injury remain poorly understood.

In this study, we analyzed the cellular and transcriptomic changes and molecular mechanisms regulating RG proliferation during the early stages of tectum regeneration. Together, the findings of these transcriptomic and functional analyses revealed that IL6/Stat3 signaling is an initial trigger of RG activation during optic tectum regeneration. Therefore, components of molecular mechanisms that cooperate with IL6/Stat3 signaling during tissue regeneration could be promising molecular targets to enhance the regenerative capacity of the human CNS.

# MATERIALS AND METHODS

## Zebrafish Strains

Zebrafish (*Danio rerio*) were maintained according to standard procedures (Westerfield, 2007). All experiments were performed according to protocols approved by the Institutional Animal Care and Use Committee of the National Institute of Advanced Industrial Science and Technology and Waseda University. The RIKEN Wako (RW) wild-type strain was obtained from the Zebrafish National BioResource Center of Japan[1]. The *Tg(gfap:GFP)*$^{mi2001}$ strain with RG-specific GFP expression (Bernardos and Raymond, 2006) was obtained from the Zebrafish International Resource Center (ZIRC). Three-to-four-month-old RW and *Tg*(*gfap:GFP*) fish were used for all experiments.

## Stab Wound Injury

Zebrafish were anesthetized using 0.02% tricaine (pH 7.0; Nacalai Tesque, Kyoto, Japan) and a 30-gauge (30G) needle (Terumo, Tokyo, Japan) was inserted vertically into the right hemisphere of the optic tectum through the boundary of two bones on the right optic tectum, as described previously (Shimizu et al., 2018). The uninjured left hemisphere was considered an internal control. The 30G needle was inserted to a depth of approximately

[1]http://www.shigen.nig.ac.jp/zebra/

0.75 mm, almost equal to half the length of the 30G bevel. For gene expression analyses, such as RNA-seq and quantitative real-time PCR, both hemispheres of the optic tectum were injured and fixed at each time point.

## Histology and Immunohistochemistry

For immunohistochemistry (IHC), zebrafish were anesthetized using 0.02% tricaine and perfused intracardially with Ringer's solution, followed by 4% paraformaldehyde (PFA; FUJIFILM Wako, Osaka, Japan) solution. After the brains had been dissected, they were fixed in 4% PFA overnight at 4°C, transferred into 20% sucrose overnight at 4°C for cryopreservation, and then embedded in a 2:1 mixture of 20% sucrose and O.C.T. compound (Tissue-Tek, Torrance, CA, United States). The brain tissues were then cut into 14 μm thick sections using a cryostat (CM1850, Leica, Wetzlar, Germany) and IHC was performed as described previously (Shimizu et al., 2018) with the following For primary antibodies: mouse anti-proliferating cell nuclear antigen (PCNA, 1:200, sc-56, Santa Cruz Biotechnology, Dallas, TX, United States), rabbit anti-brain lipid binding protein (BLBP, 1:500, ABN14, Millipore, Burlington, MA, United States), and Dylight 594-conjugated isolectin B4 (IB4, 1:200, Vector Laboratories, Burlingame, CA, United States). Alexa Fluor 488- and 568-conjugated subclass-specific secondary antibodies (1:500, Invitrogen, Carlsbad, CA, United States) were used. For PCNA immunodetection, antigen retrieval was performed by incubating slides in 10 mM sodium citrate for 30 min at 85°C before treatment with the primary antibody. For nuclear staining, the samples were incubated in Hoechst 33258 (1:500, FUJIFILM Wako) for 30 min after IHC. Sections were embedded in PermaFluor (Thermo Fisher Scientific, Waltham, MA, United States).

## RNA Sequencing

Zebrafish with or without stab wound injuries were anesthetized using 0.02% tricaine and both hemispheres of the optic tectum were dissected. For RNA-seq, total RNA was extracted from three pooled individuals using TRIzol reagent (Invitrogen) and purified using a Directo-zol RNA Miniprep kit (Zymo Research, Irvine, CA, United States) for each biological replicate. All RNA samples were sent to Macrogen Japan (Tokyo, Japan) and libraries were prepared from samples with RIN > 7.0 using NovaSeq6000. RNA-seq was performed in triplicate for each group using NovaSeq6000 (Illumina, CA, United States) with 2 × 100 bp paired ends. Sequencing data from the intact optic tectum was used as a control for the injured tectum at 6, 12, and 24 h post-injury (hpi).

## Bioinformatics Analysis

The quality of the raw data produced from each sample was checked using FastQC (v0.11.5) and low-quality reads (<Q20) and adapter sequences were removed using Trimmomatic-0.33 (Bolger et al., 2014). Trimmed and filtered reads were aligned to the zebrafish reference genome (Ensembl, GRCz11) using HISAT2 (v2.0.5) (Kim et al., 2015) before being assembled and counted using FeatureCounts (v1.6.3) (Liao et al., 2014). The iDEP.82 pipeline (Ge et al., 2018) was used to normalize read counts and DESeq2 (Love et al., 2014) was used to identify differentially expressed genes (DEGs) with fold change >2 in both directions and a Benjamini-Hochberg adjusted *p*-value (FDR) < 0.05 between intact and injured tectum at 6, 12, and 24 hpi. The Matascape pipeline (Zhou et al., 2019) (min overlap: 3, *p*-value cutoff: 0.01, min enrichment: 1.5) was used to perform enrichment analyses based on the DEGs using Gene Ontology (GO) terms, Kyoto Encyclopedia of Genes and Genomes (KEGG) pathways (Kanehisa and Goto, 2000), and Reactome pathways (Fabregat et al., 2018).

## Quantitative Real-Time PCR

Zebrafish with or without stab wound injuries were anesthetized using 0.02% tricaine and both hemispheres of the optic tectum were dissected. Total RNA from each fish was purified using a Directo-zol RNA Miniprep kit and cDNA was synthesized using ReverTra Ace with gDNA remover (Toyobo, Osaka, Japan). Quantitative real-time PCR (qRT-PCR) was performed using gene-specific primers for *actb2*, *gfap*, *il6*, *il11a*, *il11b*, *jak1*, and *stat3*, as listed in **Supplementary Table 5**.

## Flow Cytometory and Cell Sorting

Zebrafish were anesthetized using 0.02% tricaine and both hemispheres of the injured optic tectum were dissected. The samples dissected from three zebrafish were pooled in HBSS (FUJIFILM Wako) which was subsequently replaced with PBS containing 0.4% glucose, 0.04% BSA (Sigma-Aldrich, St. Louis, MO, United States), and 0.04% L-cysteine with 0.5% DNase and 0.5% papain. After incubation at 37°C for 5 min, the pooled sample was washed three times with DMEM (Sigma-Aldrich) containing 10% horse serum (Vector Laboratories), 20 μM L-glutamine, and 10 μM sodium pyruvate. After dissociation by pipetting and centrifugation at 300 × *g*, the pellets were resuspended in PBS and filtered through a 25 μm cell strainer. Cell sorting was performed using a FACSAria™ III (BD): 450,000 of the $GFP^{high}$ population and $GFP^{neg}$ population in *Tg(gfap:GFP)* were sorted separately into PBS with 3% FBS. For qRT-PCR, RNA was extracted from sorted cells and synthesized into cDNA using CellAmpTM Direct Lysis and RT kits (Takara Bio, Shiga, Japan). To obtain sufficient RNA for cDNA synthesis, extracted RNA was concentrated by precipitation with a Gene-Packman Coprecipitant (Nacalai Tesque).

## Drug Administration and Cerebroventricular Microinjection

To inhibit Stat3 signaling, injured zebrafish were maintained in water containing 10 or 100 μM S3I-201 (Selleck, Houston, TX, United States) (Liang et al., 2012) dissolved in 1% dimethyl sulfoxide (DMSO, FUJIFILM Wako) for 24 h. To activate Stat3 signaling without injuring the tectum, 100 ng/μL human IL6 (PeproTech, Cranbury, NJ, United States) was injected into the cerebrospinal fluid as described previously (Kizil and Brand, 2011).

## Cell Quantification

To quantify proliferative RG in the adult optic tectum, we counted the number of BLBP+ PCNA+ cells imaged using a confocal microscope C1 plus (Nikon) with UPlanSApo 20 × (NA 0.70) and 40 × (NA 0.95) objectives. To quantify proliferated RG after stab injury, we counted the number of BLBP+/PCNA+ cells in 3–5 serial sections (every other section) around the center of the injury and also in the uninjured hemisphere as an internal control. To quantify RG proliferation in the intact tectum or tectum treated with PBS or IL6 microinjection, we counted the number of BLBP+ PCNA+ cells in 5–10 serial sections (every other section) in a similar area to the injured tectum.

## Statistical Analysis

All experimental data were expressed as the mean ± standard error of the mean (SEM). Sample numbers are provided in the figure legends. Statistical analysis between two groups was performed using paired or unpaired Student's *t*-tests. When comparing three or more groups, one-way analysis of variance (ANOVA) was performed followed by Tukey's *post hoc* test. *P*-values were calculated using GraphPad Prism and were presented as follows: $^{***}p < 0.001$; $^{**}p < 0.01$; and $^{*}p < 0.05$.

# RESULTS

## Stab Wound Injury Induced Macrophage Migration and RG Proliferation in the Adult Optic Tectum Within 24 h

Previously, we found that RG proliferation was induced by stab wound injury in the adult optic tectum (Shimizu et al., 2018) while other studies have shown that immune responses during the early stages after stab wound injury are required for RG proliferation in the adult telencephalon and optic tectum (Kyritsis et al., 2012; Ueda et al., 2018). Although molecular pathways that work in RG after the tectum injury have been well investigated by pharmacological experiments, transgenic lines and single cell RNA-seq (Shimizu et al., 2018; Ueda et al., 2018; Lindsey et al., 2019; Yu and He, 2019; Kiyooka et al., 2020), the global changes in gene expression related to immune activation and RG proliferation during the early stages of optic tectum regeneration had not yet been investigated. In this study, we first determined the time points for RNA-seq by evaluating RG and macrophage responses at 6, 12, and 24 hpi. After immunostaining for BLBP, an RG marker, and PCNA, a proliferative cell marker at 6, 12, and 24 hpi (**Figures 1A–D** and **Supplementary Figure 1**), we quantified BLBP+ PCNA+ cells in intact (control) and injured optic tectum (injured hemisphere and contralateral uninjured hemisphere; **Figure 1E**). At 6 hpi, the number of proliferative RG cells in the two hemispheres of the optic tectum did not significantly differ (**Figure 1E**); however, significant RG proliferation was observed on the injured side at 12 hpi in comparison to the contralateral uninjured hemisphere. Furthermore, the number of BLBP-PCNA+ cells, which likely include immune cells such as microglia and macrophages (Lindsey et al., 2019; Yu and He, 2019), also significantly increased from 12 to 24 hpi (**Figure 1F**). To examine macrophage responses after injury, we performed immunostaining using an IB4 antibody conjugated with Dylight 594 (Lai et al., 2017) in the intact and injured optic tectum at 6, 12, and 24 hpi (**Figures 2A–D** and **Supplementary Figure 2**). Few IB4-positive cells were observed in the intact optic tectum (**Figures 2A,E**), suggesting that IB4-positive cells were not microglia as there were fewer of these cells in the intact optic tectum than GFP-positive cells in *Tg*(*mpeg1:GFP*) (Lindsey et al., 2019; Yu and He, 2019). Interestingly, we found that there were significantly more IB4-positive cells in the injured hemisphere than in the uninjured hemisphere at 6, 12, and 24 hpi. Together, these results indicate that during the early stages of tectum regeneration, innate immune activation such as macrophage migration is induced at 6 hpi, followed by the activation of RG proliferation at 12 and 24 hpi.

## Comprehensive Transcriptomic Analyses During the Early Stages of Optic Tectum Regeneration

Since macrophage migration into the injured tectum was observed at 6 hpi and RG proliferation was induced at 12 hpi (**Figures 1E**, **2E**), we investigated changes in gene expression related to macrophage migration and the induction of RG proliferation during the early stages of tectum regeneration. Comprehensive transcriptome analysis was performed between the intact and injured optic tectum at 6, 12, and 24 hpi and DEGs were quantified at each time point (fold change >2 in both directions and FDR < 0.05) to identify the major responses during early tectum regeneration. We identified a total of 1,087 DEGs [777 upregulated (UP), 310 downregulated (DOWN)] at 6 hpi, 1,121 DEGs (986 UP, 135 DOWN) at 12 hpi, and 1,711 DEGs (1,565 UP, 146 DOWN) at 24 hpi (**Figures 3A,B**). The top 100 up- or downregulated DEGs at each time point are shown in **Supplementary Table 1**. Next, we analyzed pathways enriched for up- or downregulated DEGs at 6, 12, and 24 hpi using Metascape enrichment analysis for GO terms, KEGG pathways, and Reactome pathways (**Supplementary Figures 3–5** and **Supplementary Tables 2–4**). The enriched GO terms for biological processes (BP) based on the upregulated DEGs at 6, 12, and 24 hpi (**Figure 3C**, GO_UP) included "response to wounding," "cell proliferation," "JAK-STAT cascade," "hemostasis" and some GO terms related to cytokines and the immune system. In addition, KEGG pathway analyses based on the upregulated DEGs (**Figure 3D**, KEGG_UP) included "cell cycle," "p53 signaling pathway," "AGE-RAGE signaling pathway in diabetic complication," "apoptosis" and cytokine-related pathways such as "adipocytokine signaling pathway" and "cytokine-cytokine receptor interaction." Reactome analyses of the upregulated DEGs (**Figure 3E**, Reactome_UP) also included "interleukin-6 (IL6) family signaling," "caspase activation," "hemostasis," and some pathways related to the immune system and cytokine signaling. When the same analyses were performed based on downregulated DEGs, amino acid metabolism was the only enriched pathway shared between

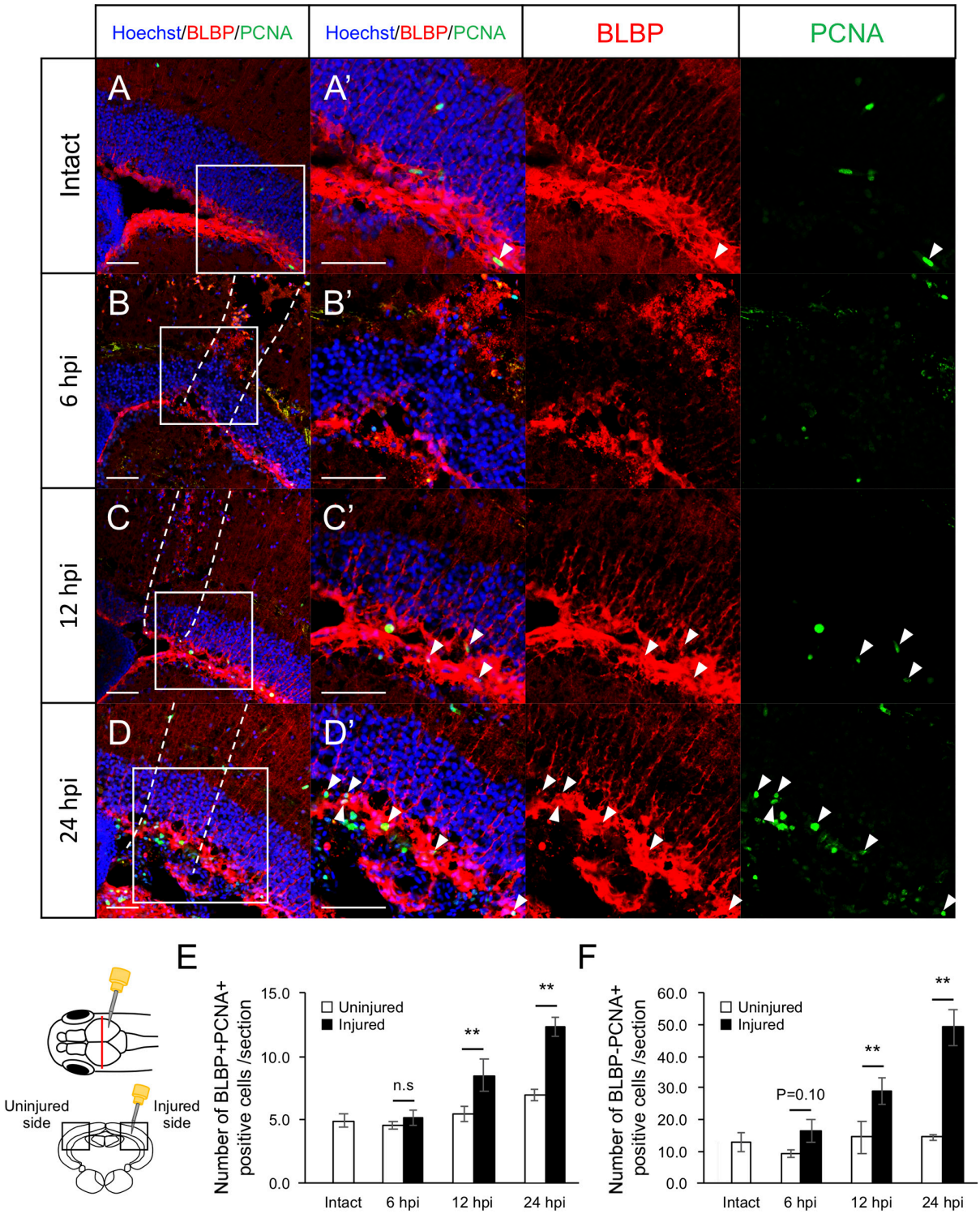


**FIGURE 1 |** Induction of RG proliferation during the early stages after stab wound injury. **(A–D)** Representative images of proliferative RG (BLBP+ PCNA+) in intact fish **(A)** and injured fish during the early stages of regeneration, 6, 12, and 24 hpi **(B–D)**. **(A'–D')** Magnified images of the boxed area in each image. White arrowheads indicate BLBP+ PCNA+ cells and dashed lines **(B–D)** indicate area injured by needle insertion. Scale bar: 100 μm in **(A–D)**, 50 μm in **(A'–D')**. **(E)** Quantification of proliferative RG in intact fish ($n$ = 4) and on the uninjured and injured hemispheres of injured fish at 6, 12, and 24 hpi. Statistical analyses between uninjured and injured hemispheres at each time point were evaluated using paired Student's $t$-tests. **(F)** Quantification of proliferative cells except RG (BLBP-PCNA+) in intact fish ($n$ = 4) and the uninjured and injured hemispheres of injured fish at 6, 12, and 24 hpi. Statistical analyses between uninjured and injured hemispheres at each time point were evaluated using paired Student's $t$-tests.

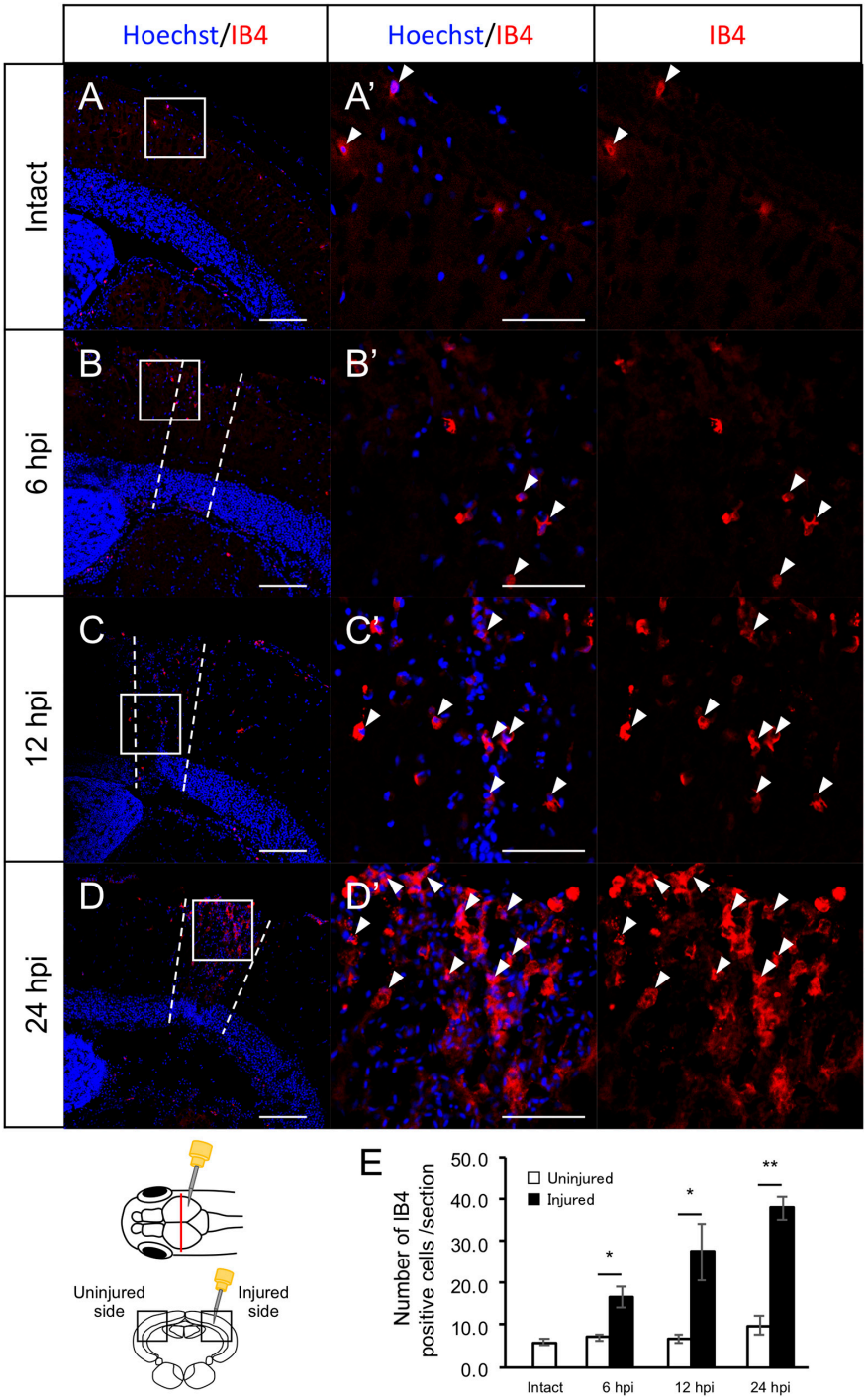


**FIGURE 2 |** Induction of IB4+ macrophage migration during the early stages after stab wound injury. **(A–D)** Representative images of IB4-positive macrophages in intact fish **(A)** and the injured hemisphere of injured fish during the early stages of regeneration, 6, 12, and 24 hpi **(B–D)**. **(A'–D')** Magnified images of the boxed area in each image. White arrowheads indicate BLBP+ PCNA+ cells and dashed lines **(B–D)** indicate the area injured by needle insertion. Scale bar: 100 μm in **(A–D)**, 50 μm in **(A'–D')**. **(E)** Quantification of IB4-positive cells in intact fish ($n$ = 4) and the uninjured and injured hemispheres of injured fish at 6, 12, and 24 hpi. Statistical analyses between uninjured and injured hemispheres at each time point were evaluated using paired Student's $t$-tests.

GO BP, KEGG, and Reactome analysis. Therefore, these pathway analyses based on DEGs within 24 h after optic tectum injury suggest that immune activation, cell proliferation, apoptosis, and cytokine signaling, including the IL6/Jak-Stat pathway, are major responses during the early stages of tectum regeneration.

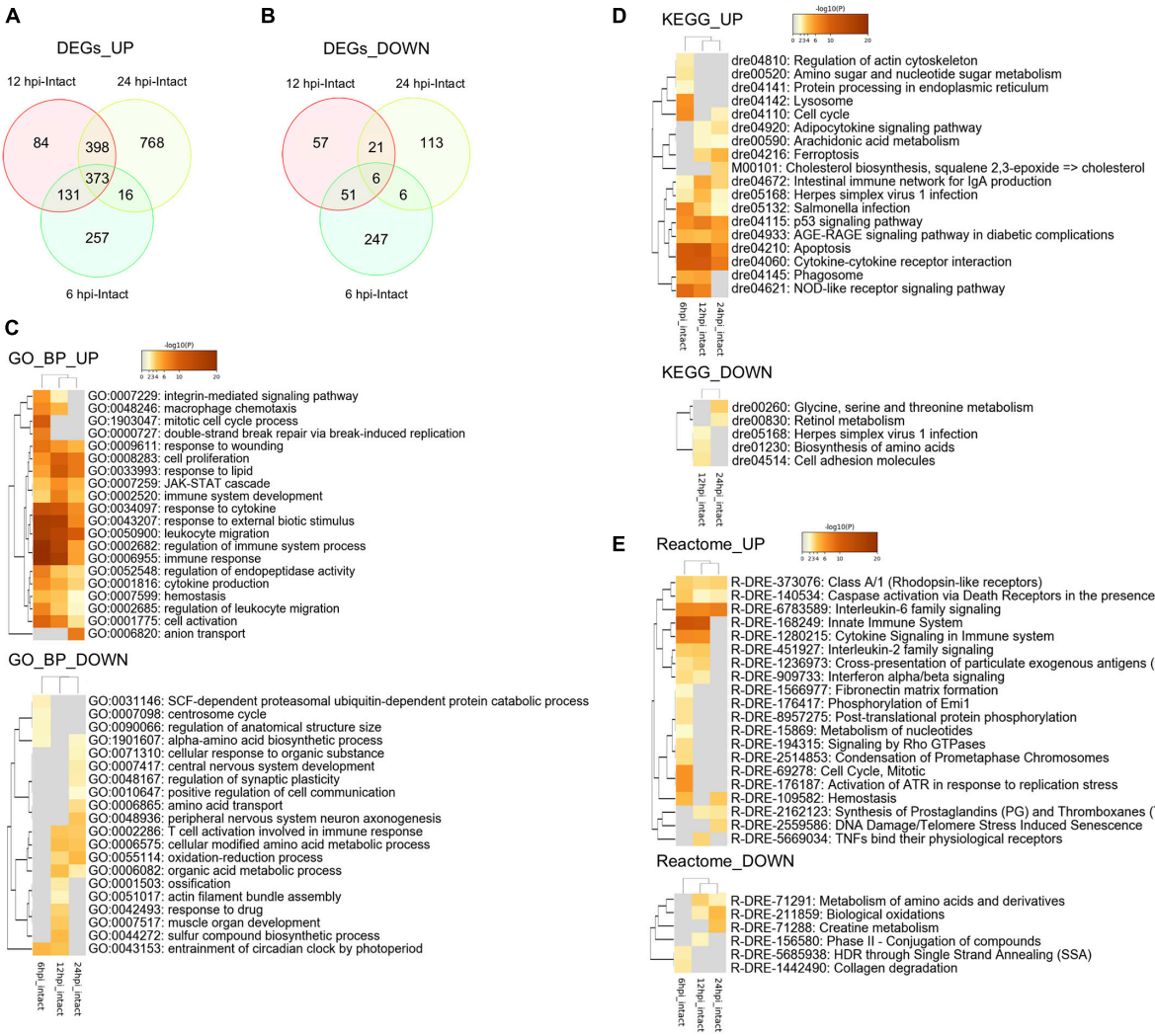


**FIGURE 3 |** Transcriptomic and enrichment analyses during the early stages of optic tectum regeneration. **(A,B)** Venn diagram indicating upregulated **(A)** and downregulated **(B)** differentially expressed genes (DEGs) identified by DEseq2 between injured (6, 12, and 24 hpi) and intact optic tectum. Fold change >2 in both directions and FDR < 0.05. **(C–E)** Heatmaps indicating clusters of significantly enriched GO biological process (BP) **(C)**, KEGG pathway **(D)**, and Reactome pathway **(E)** terms based on DEGs between the injured and intact tectum (6, 12, and 24 hpi) using Metascape enrichment analysis. UP and DOWN indicate enrichment analyses based on up- and downregulated DEGs, respectively.

## IL6/Jak1-Stat3 Signaling Is Activated During the Early Stages of Optic Tectum Regeneration

Previous studies have shown that *stat3* is upregulated in Müller glia during the early stages (8 and 16 hpi) of retinal regeneration (Sifuentes et al., 2016) and that injection with *stat3* morpholino antisense oligonucleotides can suppress the proliferation of Müller glia after retinal injury (Nelson et al., 2012). However, the functions of IL6/Jak1-Stat3 signaling during optic tectum regeneration have not yet been studied. Since the upregulated DEGs during the early stages of tectum regeneration were enriched for IL6 family cytokines and Jak-Stat signaling (**Figures 3C,E**), we quantified changes in the expression of *il6*, *il11a*, and *il11b* (IL6 family cytokines in the top 100 upregulated DEGs at 6, 12, or 24 hpi) and *stat3*, *jak1*, and *gfap* (Jak-Stat signaling) at different time points from 1 to 7 dpi (**Figures 4A–F**). Changes in *il6*, *il11a*, *il11b*, and *stat3* expression peaked around 6 hpi, after which *jak1* and *gfap* were upregulated. To further examine the changes in *stat3* expression in RG during the early stages of optic tectum injury, we isolated RG from *Tg*(*gfap:GFP*), which display RG-specific GFP expression (**Figures 4G,H** and **Supplementary Figure 6**). Notably, *stat3* expression was significantly higher in $GFP^{high}$-positive cells than in the intact reporter fish at 24 hpi (**Figure 4I**). Moreover, we confirmed that the IL6 receptors *il6r* and *il6st* were expressed in $GFP^{high-}$positive cells using RT-PCR (data not shown). Taken together, these results suggest that the upregulation of IL6 family cytokines stimulates Stat3 signaling in RG during the early stages of optic tectum regeneration.

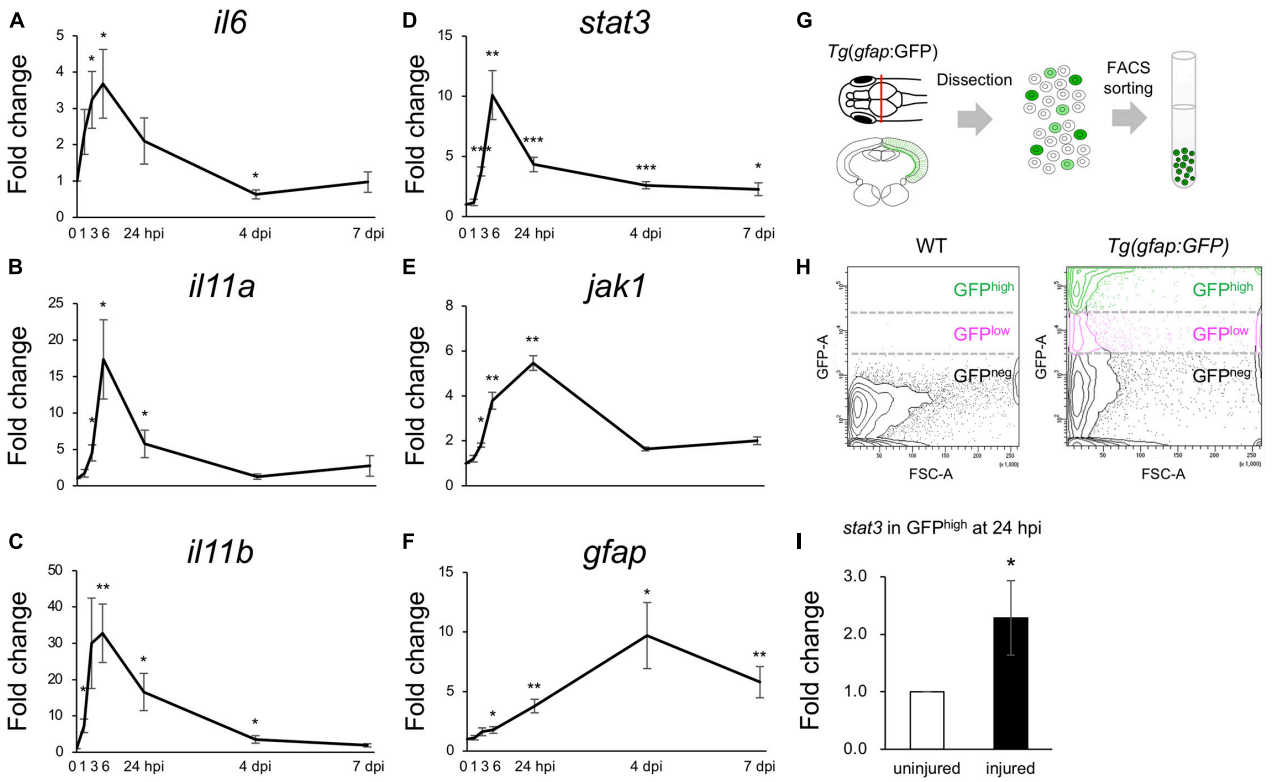


**FIGURE 4 |** Activation of IL6/Stat3 signaling during the early stages of optic tectum regeneration. **(A–F)** Quantitative real-time (qRT-) PCR analyses of IL6 superfamily cytokines *il6* **(A)**, *il11a* **(B)**, and *il11b* **(C)**, and Jak/Stat signaling components *stat3* **(D)**, *jak1* **(E)**, and *gfap* **(F)**. Each graph indicates relative gene expression in the injured tectum from 1 to 7 dpi compared to intact optic tectum ($n$ = 4 per gene per time point). Statistical analyses between intact and injured hemispheres at each time point were evaluated using unpaired Student's $t$-tests. **(G)** Schematic diagram of the cell sorting workflow using the RG-specific reporter line, *Tg(gfap:GFP)*. **(H)** Representative images of FACS plots for GFP-positive cells from the optic tectum of wild-type (left) or *Tg(gfap:GFP)* (right) fish. **(I)** Quantification of *stat3* expression in $GFP^{high}$-positive cells from uninjured and injured optic tectum at 24 hpi using qPCR. The graph shows relative *stat3* expression in $GFP^{high}$-positive cells from injured tectum at 24 hpi compared to uninjured tectum ($n$ = 11). Statistical analyses between uninjured and injured hemispheres was evaluated using unpaired Student's $t$-tests.

## Stat3 Inhibitors Suppress RG Proliferation After Stab Wound Injury

To examine whether Stat3 signaling activation is required for RG proliferation after tectum injury, we maintained injured zebrafish in water containing the Stat3 inhibitor S3I-201 (10 or 100 μM) or 1% DMSO for 1 day and performed immunostaining for BLBP and PCNA at 24 hpi to quantify cell proliferation (**Figures 5A–D**). The number of proliferative RG (BLBP+ PCNA+)was significantly lower in fish treated with 100 μM S3I-201 than in those treated with 1% DMSO or 10 μM S3I-201 (**Figure 5E**), suggesting that S3I-201 inhibited RG proliferation after tectum injury in a dose-dependent manner. However, the number of BLBP-PCNA+ cells, likely including immune cells, was not significantly changed by S3I-201 treatment (**Figure 5F**). Moreover, we confirmed that Stat3 inhibitor does not significantly affect NE proliferation in the intact zebrafish (**Supplementary Figure 7**). Taken together, these results suggest that Stat3 inhibitor specifically suppressed RG proliferation and that Stat3 signaling is required to induce RG proliferation after stab wound injury in the optic tectum.

## Cerebroventricular Microinjection of IL6 Recombinant Protein Induces RG Proliferation Without Stab Wound Injury

To determine whether IL6 was sufficient to induce RG proliferation under physiological conditions, we injected human IL6 recombinant protein (100 ng/μL) or PBS into the cerebrospinal fluid (**Figure 6C**) and performed immunostaining on fixed samples using anti-BLBP and anti-PCNA antibodies to quantify proliferating RG. We respectively counted the number of BLBP+ PCNA+ cells in the injected and contralateral hemispheres and found that the IL6 injection significantly increased the number of proliferating RG in the contralateral hemisphere compared to that with PBS injection (**Figures 6A,B,D**). We also counted the number of BLBP-PCNA+ cells and confirmed that the number of BLBP− PCNA+ cells except NE was not significantly increased in the contralateral hemisphere (**Figure 6E**) and that IL6 injection had no significant effect in the NE proliferation (data not shown). In the injected hemisphere, we found the small incision by glass capillary compared to that by the 30G needle (data not shown). The stab wound injury by the 30G needle did not significantly increase

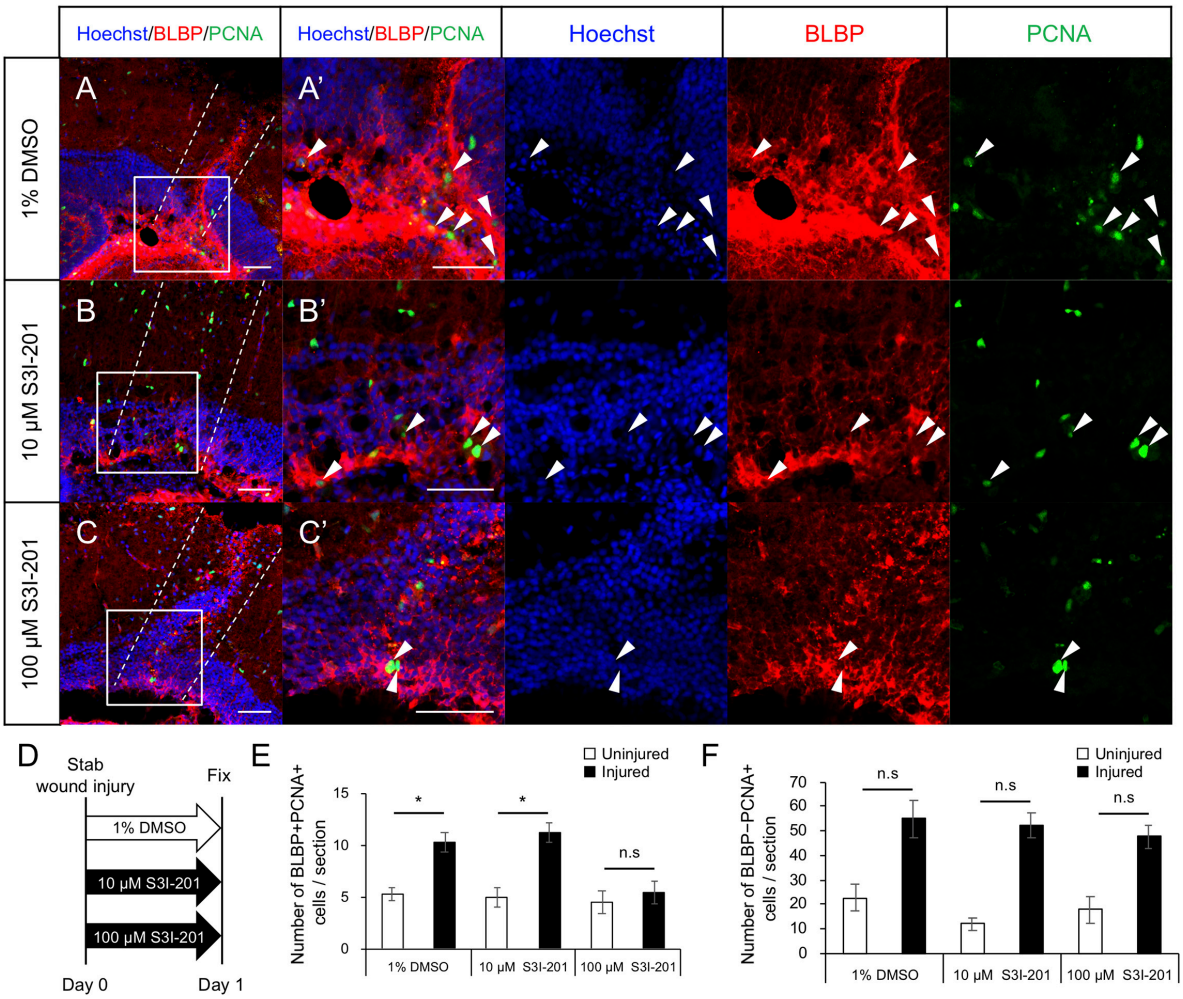


**FIGURE 5 |** Stat3 inhibitor S3I-201 suppresses RG proliferation after stab wound injury in adult optic tectum. **(A–C)** Representative images of proliferative RG (BLBP+ PCNA+) in injured optic tectum treated with 1% DMSO **(A)**, 10 μM S3I-201 **(B)**, or 100 μM S3I-201 **(C)** at 1 dpi. **(A'–C')** Magnified images of the boxed area in each image. White arrowheads indicate BLBP+ PCNA+ cells and dashed lines indicate the area injured by needle insertion. Scale bar: 50 μm in **(A–C)** and **(A'–C')**. **(D)** Schematic diagram of drug administration. **(E)** Quantification of proliferative RG (BLBP+ PCNA+) treated with 1% DMSO, 10 μM S3I-201 ($n$ = 4), or 100 μM S3I-201 ($n$ = 5) at 1 dpi. Statistical analyses were performed using one-way ANOVA with Tukey's *post hoc* test. **(F)** Quantification of proliferative cells except RG (BLBP-PCNA+) treated with 1% DMSO, 10 μM S3I-201 ($n$ = 4), or 100 μM S3I-201 ($n$ = 5) at 1 dpi. Statistical analyses were performed using one-way ANOVA with Tukey's *post hoc* test.

both BLBP+ PCNA+ and BLBP-PCNA+ cells in the contralateral hemisphere (**Figures 1E,F**), suggesting that the smaller incision in the injected hemisphere also have no significant effects on cell proliferation in the contralateral side. Taken together, these results suggest that IL6 is sufficient to induce RG proliferation in the adult zebrafish optic tectum without stab wound injury. Transcriptomic analyses and functional analyses reveal that IL6/Stat3 signaling is an important initial trigger of RG proliferation at the early stages of tectum regeneration.

## DISCUSSION

Zebrafish display a superior capacity for neuronal regeneration in the CNS and the molecular mechanisms that regulate regenerative neurogenesis in the telencephalon and optic tectum have been well studied; however, few comprehensive transcriptomic analyses have been performed to study regenerating optic tectum. In this study, we attempted to elucidate the triggers that stimulate RG proliferation in response to optic tectum injury, with a particular focus on the early stages of tectum regeneration. First, we confirmed that the levels of IB4+ macrophages increased at 6 hpi, followed by the induction of RG proliferation, while transcriptomic analyses based on DEGs revealed that apoptosis, the immune system, cytokine signaling, cell proliferation, and IL6/Jak-Stat signaling were upregulated during the early stages of tectum regeneration. After validating that *il6* and *stat3* expression peaked at 6 hpi and that *jak1* expression peaked at 24 hpi, we revealed that Stat3 inhibition suppressed RG proliferation at 1 dpi and that

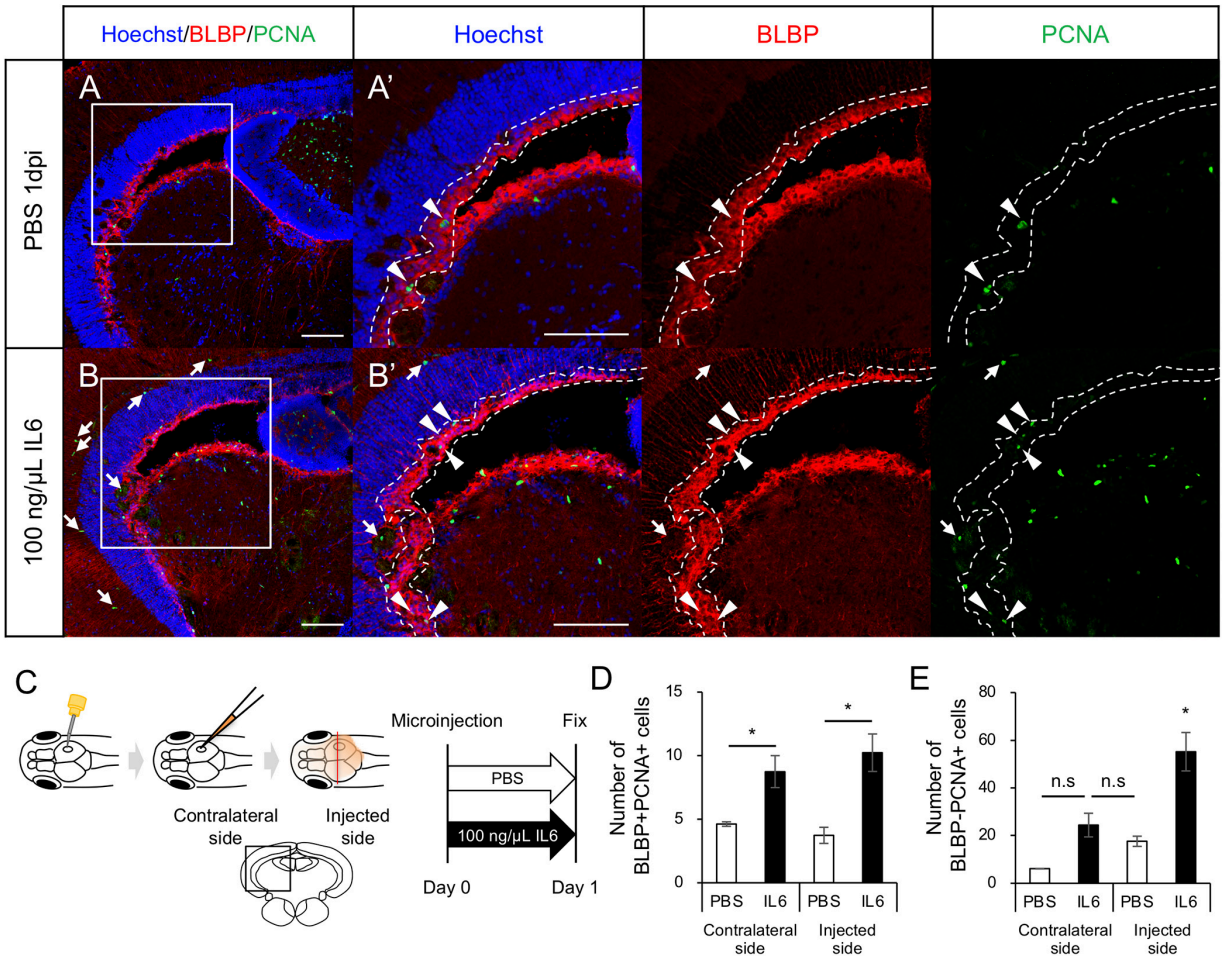


**FIGURE 6 |** IL6 induces RG proliferation without stab wound injury in adult optic tectum. **(A,B)** Representative images of proliferative RG (BLBP+ PCNA+) in the contralateral side with PBS or 100 ng/μL IL6 at 1 dpi. Allow heads indicate BLBP+ PCNA+ cells and arrows indicate BLBP- PCNA+ cells. Scale bar: 100 μm in **(A–D)** and **(A',B')**. **(C)** Schematic diagram of cerebroventricular microinjection. A small hole was made in the center of the skull above the right hemisphere of the optic tectum using a 30G needle. The injected solution spread through the corticospinal fluid. **(D)** Quantification of proliferative RG (BLBP+ PCNA+) in the injected and contralateral hemisphere with PBS ($n$ = 4) or 100 ng/μL IL6 ($n$ = 3) at 1 dpi. **(E)** Quantification of BLBP- PCNA+ cells in the injected and contralateral hemisphere with PBS or IL6 at 1 dpi. Statistical analyses were performed using one-way ANOVA with Tukey's *post hoc* test.

microinjecting human recombinant IL6 into cerebroventricular fluid induced RG proliferation without injury. Together, our findings demonstrate that IL6/Stat3 signaling is an initial trigger of RG activation during optic tectum regeneration and that transcriptome analyses are powerful tools for investigating molecular mechanisms.

## Macrophage Migration Prior to RG Proliferation After Optic Tectum Injury

Previous studies have shown that the activation of innate immune responses is required for tissue regeneration in both the CNS and other tissues, such as the heart and fin (Kyritsis et al., 2012; Petrie et al., 2014; Lai et al., 2017). In the optic tectum, dexamethasone-induced immunosuppression also suppresses RG cell proliferation after stab wound injury (Ueda et al., 2018). Here, we labeled macrophages using IB4 antibody (Lai et al., 2017), although *Tg*(*mpeg1:GFP*)$^{gl22}$ (Ellett et al., 2011) and antibodies such as L-plastin and 4C4 have also been utilized to examine microglia and macrophage responses (Baumgart et al., 2012; Kyritsis et al., 2012; Oosterhof et al., 2017). Previously, Lai et al. found that IB4 staining colocalized with GFP-positive cells in *Tg(mpeg1:EGFP)* but not with GFP-positive cells in the neutrophil reporter fish, *TgBAC(mpx:GFP)*$^{i114}$ (Renshaw et al., 2006), while Zou et al. (2013) showed that IB4 staining colocalized with GFP-positive cells in other macrophage reporter line, *Tg(cora1a:eGFP)* (Li et al., 2012) and not with endothelial cell reporter line, *Tg(flk:GFP)* (Choi et al., 2007). Together, these findings suggest that IB4 labels macrophages but not neutrophils and vascular endothelial cells. In this study, we noted an increase in the number of IB4-positive cells from 6 h after tectum injury, followed by RG proliferation. This is consistent with the increase in 4C4 positive cells and mpeg1:GFP+ cells followed by RG proliferation previously reported in the

injured telencephalon (Baumgart et al., 2012; Kanagaraj et al., 2020). These things suggest that macrophage/microglia activation triggers RG reprogramming during brain regeneration though each role of infiltrating macrophage and resident microglia still remains little known. M1 and M2 macrophage polarization and their functions have been well studied in mammals and macrophage polarization is considered a promising therapeutic target for chronic inflammation, tissue regeneration, and cancer (Noy and Pollard, 2014; Hu et al., 2015). However, improved characterization of M1/M2 macrophages/microglia in zebrafish is necessary to fully understand their contribution toward tissue regeneration in zebrafish.

## Global Gene Expression Changes and Enriched Pathways at the Early Stages of Tectum Regeneration

Our transcriptome and pathway analyses during the early stages of optic tectum regeneration suggested the upregulation of genes related to the innate immune system, apoptosis, cell proliferation, cytokine signaling, and the IL6/Jak-Stat pathway. The zebrafish innate immune system includes macrophages, neutrophils, dendritic cells, and natural killer cells and our transcriptome analyses demonstrated the upregulation of macrophage markers (*mpeg1* and *mfap4*), neutrophil markers (*lyz*, *mpx*, and *nccrp1*), and a dendritic cell marker (*spi1b*) during early tectum regeneration, suggesting innate immune system activation. Moreover, T cell markers such as *cd4-1*, *cd8a*, and *foxp3a* were not upregulated at 24 hpi, suggesting that the adaptive immune system was not activated within 24 h after the injury. Studies have shown that regulatory T (T-reg) cells expressing *foxp3a* are required for tissue regeneration in the heart, retina, and spinal cord (Hui et al., 2017), with T-reg cell depletion in the mouse brain adversely affecting neurological recovery from stroke (Ito et al., 2019). Therefore, functional analyses of innate immune cells and T-reg cells are important for understanding the high tissue regeneration capacity of zebrafish.

We also found that many genes related to cytokine signaling were upregulated at 24 hpi, including pro-inflammatory molecules such as *il1b* and *il6*, and anti-inflammatory molecules such as *il4*, *il13,* and *il10*. Although both the IL6/Stat3 and IL4/Stat6 pathways induce NSC proliferation in the retina or telencephalon (Zhao et al., 2014; Bhattarai et al., 2016), we focused on IL6/Stat3 signaling as *il6* and *stat3* expression were upregulated earlier than *il4* and *stat6* after tectum injury. Thus, these secreted molecules are promising therapeutic targets for damaged tissue regeneration and should be investigated further in future functional and translational studies.

Previous studies have shown that the reprogramming of the transcription factor *ascl1a* and related genes, such as *lin28a*, *sox2*, *stat3,* and *her4*, play important functions in the retina (Ramachandran et al., 2010; Gorsuch et al., 2017; Elsaeidi et al., 2018). Therefore, we detected *lin28a* and *stat3* in upregulated DEGs and *her4.1* and *her4.2* in downregulated DEGs, while we found that *ascl1a* (log2FC = 0.63, FDR = 0.091) and *sox2* (log2FC = 0.75, FDR < 0.001) upregulation peaked at 12 hpi. These findings suggest that *stat3*, *ascl1a*, *lin28*a, *sox2*, and *her4* play important roles in RG activation during tectum regeneration. The regulation of adult and regenerative neurogenesis by *her* family genes and Notch signaling have been well studied in the optic tectum (Dozawa et al., 2014; Ueda et al., 2018; Yu and He, 2019; Kiyooka et al., 2020); however, further studies are required to investigate the regulation of adult NSCs by *ascl1a*, *lin28a*, and *sox2* during brain regeneration.

Compared to transcriptome analyses during the early stages of telencephalon regeneration (Demirci et al., 2020), many enriched pathways, including apoptosis, the innate immune system, cell proliferation, cytokine signaling, p53 signaling, and AGE-RAGE signaling, are shared between the telencephalon and optic tectum within 24 h after stab wound injury. In the zebrafish CNS, the roles of RG and neuroepithelial-like stem cells are thought to differ in different neurogenic regions. In particular, the neurogenic potential of RG during optic tectum regeneration has been controversial. RG-specific RNA-seq or single cell RNA-seq in different regions or conditions are promising for understanding the functions of RG in the adult zebrafish CNS and further transcriptomic data may allow comparative analysis between different brain regions or different species.

## Functions of Stat3 Signaling in the Activation of NSCs During Tissue Regeneration

Based on the enrichment analyses of upregulated DEGs during the early stages of tectum regeneration, we attempted to elucidate the function of IL6 and Stat3 in RG proliferation. We found that Stat3 inhibition after tectum injury suppressed RG proliferation, while injecting recombinant human IL6 induced RG proliferation without stab wound injury, consistent with previous analyses of IL6/Stat3 signaling in the zebrafish retina (Nelson et al., 2012; Zhao et al., 2014). We confirmed the *stat3* upregulation and expression of IL6 receptors in RG using FACS sorting. Moreover, microglia specific RNA-seq (Oosterhof et al., 2017; Zambusi et al., 2020) has shown that *il6* is highly expressed in the *mpeg1*+ cells including microglia and macrophages compared to the other types of cells. These findings suggest that IL6 secreted from microglia/macrophages in the injured tectum stimulates the RG proliferation through the activation of stat3 signaling. In addition, Gorsuch et al. showed that Stat3 interacts with Ascl1a, Lin28a, and Sox2 during the retinal regeneration, while Sifuentes et al. found that *stat3* expression is upregulated in Müller glia prior to *ascl1a*, *lin28a*, and *sox2* expression using Müller glia-specific RNA-seq during the early stages of retinal regeneration (8 and 16 hpi). Consistently, we confirmed *stat3* upregulation before *ascl1a* and *sox2*, suggesting that Stat3 signaling activation is an upstream trigger for the regenerative program of NSCs. Furthermore, Stat3 signaling is known to be required for the regeneration of other tissues in zebrafish, such as the heart, hair cells, and fins (Liang et al., 2012; Fang et al., 2013; Miskolci et al., 2019), suggesting that Stat3 regulates different target genes in different tissue regeneration. In mammals, Stat3 also plays important roles in neuronal regeneration from Müller glia in retina (Jorstad et al., 2020) and embryonic stem cell pluripotency (Raz et al., 1999). During the retina regeneration

in mice and chickens, inhibition of Stat3 signaling promotes neuronal differentiation of Müller glia (Todd et al., 2016; Jorstad et al., 2020), while the functions of Stat3 signaling in the neuronal differentiation of NSCs during regeneration have not been well investigated in zebrafish compared to the involvement of Stat3 signaling in the proliferation of NSCs (Nelson et al., 2012; Wan et al., 2014; Zhao et al., 2014). Therefore, it is important to investigate the molecular mechanisms that cooperate with Stat3 signaling during tissue regeneration in mammals and zebrafish in order to investigate promising molecular targets to enhance the regenerative capacity of the human CNS.

## DATA AVAILABILITY STATEMENT

Raw RNA-seq data are available in the NCBI Sequenced Read Archive under link: https://dataview.ncbi.nlm.nih.gov/object/PRJNA668620 with the accession numbers SRR13370844–SRR13370855.

## ETHICS STATEMENT

The animal study was reviewed and approved by the Institutional Animal Care and Use Committee of the National Institute of Advanced Industrial Science and Technology and Waseda University.

## AUTHOR CONTRIBUTIONS

YS and TO designed the experiments. YS performed histological and molecular experiments and bioinformatics analyses. MK performed FACS based analysis. YS, MK, and TO wrote and revised the manuscript. All authors approved the submitted version manuscript.

## FUNDING

This study was supported by JSPS KAKENHI, Grant-in-Aid for Early-Career Scientists Grant No. 18K14824. The study was partially supported by DAICENTER project grant from the DBT (Govt. of India) to Renu Wadhwa and special strategic grant from AIST (Japan).

## ACKNOWLEDGMENTS

We thank Drs. Takeyama and Hosokawa in Waseda University for giving insightful advices in the bioinformatic analyses.

## SUPPLEMENTARY MATERIAL

The Supplementary Material for this article can be found online at: https://www.frontiersin.org/articles/10.3389/fcell.2021.668408/full#supplementary-material

## REFERENCES

Adolf, B., Chapouton, P., Lam, C. S., Topp, S., Tannhauser, B., Strahle, U., et al. (2006). Conserved and acquired features of adult neurogenesis in the zebrafish telencephalon. *Dev. Biol.* 295, 278–293. doi: 10.1016/j.ydbio.2006.03.023

Altman, J., and Das, G. D. (1965). Autoradiographic and histological evidence of postnatal hippocampal neurogenesis in rats. *J. Comp. Neurol.* 124, 319–335. doi: 10.1002/cne.901240303

Alunni, A., and Bally-Cuif, L. (2016). A comparative view of regenerative neurogenesis in vertebrates. *Development* 143, 741–753. doi: 10.1242/dev.122796

Alunni, A., Hermel, J. M., Heuzé, A., Bourrat, F., Jamen, F., and Joly, J. S. (2010). Evidence for neural stem cells in the medaka optic tectum proliferation zones. *Dev. Neurobiol.* 70, 693–713. doi: 10.1002/dneu.20799

Balthazart, J., and Ball, G. F. (2014). Endogenous versus exogenous markers of adult neurogenesis in canaries and other birds: advantages and disadvantages. *J. Comp. Neurol.* 522, 4100–4120. doi: 10.1002/cne.23661

Baumgart, E. V., Barbosa, J. S., Bally-Cuif, L., Götz, M., and Ninkovic, J. (2012). Stab wound injury of the zebrafish telencephalon: a model for comparative analysis of reactive gliosis. *Glia* 60, 343–357. doi: 10.1002/glia.22269

Becker, T., Wullimann, M. F., Becker, C. G., Bernhardt, R. R., and Schachner, M. (1997). Axonal regrowth after spinal cord transection in adult zebrafish. *J. Comp. Neurol.* 377, 577–595. doi: 10.1002/(sici)1096-9861(19970127)377:4<577::aid-cne8>3.0.co;2-#

Bernardos, R. L., and Raymond, P. A. (2006). GFAP transgenic zebrafish. *Gene Exp. Patterns* 6, 1007–1013. doi: 10.1016/j.modgep.2006.04.006

Berninger, B., and Jessberger, S. (2016). Engineering of adult neurogenesis and gliogenesis. *Cold Spring Harb. Perspect. Biol.* 8:a018861. doi: 10.1101/cshperspect.a018861

Bhattarai, P., Thomas, A. K., Cosacak, M. I., Papadimitriou, C., Mashkaryan, V., Froc, C., et al. (2016). IL4/STAT6 signaling activates neural stem cell proliferation and neurogenesis upon amyloid-β42 aggregation in Adult Zebrafish brain. *Cell Rep.* 17, 941–948. doi: 10.1016/j.celrep.2016.09.075

Bolger, A. M., Lohse, M., and Usadel, B. (2014). Trimmomatic: a flexible trimmer for Illumina sequence data. *Bioinformatics* 30, 2114–2120. doi: 10.1093/bioinformatics/btu170

Buscemi, L., Price, M., Bezzi, P., and Hirt, L. (2019). Spatio-temporal overview of neuroinflammation in an experimental mouse stroke model. *Sci. Rep.* 9:507. doi: 10.1038/s41598-018-36598-4

Choi, J., Dong, L., Ahn, J., Dao, D., Hammerschmidt, M., and Chen, J. N. (2007). FoxH1 negatively modulates flk1 gene expression and vascular formation in zebrafish. *Dev. Biol.* 304, 735–744. doi: 10.1016/j.ydbio.2007.01.023

Cosacak, M. I., Bhattarai, P., Reinhardt, S., Petzold, A., Dahl, A., Zhang, Y., et al. (2019). Single-cell transcriptomics analyses of neural stem cell heterogeneity and contextual plasticity in a Zebrafish brain model of amyloid toxicity. *Cell Rep.* 27, 1307–1318. doi: 10.1016/j.celrep.2019.03.090

Demirci, Y., Cucun, G., Poyraz, Y. K., Mohammed, S., Heger, G., Papatheodorou, I., et al. (2020). Comparative transcriptome analysis of the regenerating zebrafish telencephalon unravels a resource with key pathways during two early stages and activation of wnt/β-catenin signaling at the early wound healing stage. *Front. Cell Dev. Biol.* 8:584604. doi: 10.3389/fcell.2020.584604

Dias, T. B., Yang, Y. J., Ogai, K., Becker, T., and Becker, C. G. (2012). Notch signaling controls generation of motor neurons in the lesioned spinal cord of adult zebrafish. *J. Neurosci.* 32, 3245–3252. doi: 10.1523/JNEUROSCI.6398-11.2012

Dozawa, M., Kono, H., Sato, Y., Ito, Y., Tanaka, H., and Ohshima, T. (2014). Valproic acid, a histone deacetylase inhibitor, regulates cell proliferation in the adult zebrafish optic tectum. *Dev. Dyn.* 243, 1401–1415. doi: 10.1002/dvdy.24173

Ellett, F., Pase, L., Hayman, J. W., Andrianopoulos, A., and Lieschke, G. J. (2011). mpeg1 promoter transgenes direct macrophage-lineage expression in zebrafish. *Blood* 117, e49–e56. doi: 10.1182/blood-2010-10-314120

Elsaeidi, F., Macpherson, P., Mills, E. A., Jui, J., Flannery, J. G., and Goldman, D. (2018). Notch suppression collaborates with ascl1 and Lin28 to unleash a regenerative response in fish retina, but not in mice. *J. Neurosci.* 38, 2246–2261. doi: 10.1523/JNEUROSCI.2126-17.2018

Eriksson, P. S., Perfilieva, E., Björk-Eriksson, T., Alborn, A. M., Nordborg, C., Peterson, D. A., et al. (1998). Neurogenesis in the adult human hippocampus. *Nat. Med.* 4, 1313–1317. doi: 10.1038/3305

Fabregat, A., Jupe, S., Matthews, L., Sidiropoulos, K., Gillespie, M., Garapati, P., et al. (2018). The reactome pathway knowledgebase. *Nucleic Acids Res.* 46, 649–655. doi: 10.1093/nar/gkx1132

Fang, Y., Gupta, V., Karra, R., Holdway, J. E., Kikuchi, K., and Poss, K. D. (2013). Translational profiling of cardiomyocytes identifies an early Jak1/Stat3 injury response required for zebrafish heart regeneration. *Proc. Natl. Acad. Sci. U.S.A.* 110, 13416–13421. doi: 10.1073/pnas.1309810110

Ge, S. X., Son, E. W., and Yao, R. (2018). DEP: an integrated web application for differential expression and pathway analysis of RNA-Seq data. *BMC Bioinformatics* 19:534. doi: 10.1186/s12859-018-2486-6

Gorsuch, R. A., Lahne, M., Yarka, C. E., Petravick, M. E., Li, J., and Hyde, D. R. (2017). Sox2 regulates Muller glia reprogramming and proliferation in the regenerating zebrafish retina via Lin28 and Ascl1a. *Exp. Eye Res.* 161, 174–192. doi: 10.1016/j.exer.2017.05.012

Grandel, H., Kaslin, J., Ganz, J., Wenzel, I., and Brand, M. (2006). Neural stem cells and neurogenesis in the adult zebrafish brain: origin, proliferation dynamics, migration and cell fate. *Dev. Biol.* 295, 263–277. doi: 10.1016/j.ydbio.2006.03.040

Hu, X., Leak, R. K., Shi, Y., Suenaga, J., Gao, Y., Zheng, P., et al. (2015). Microglial and macrophage polarization—new prospects for brain repair. *Nat. Rev. Neurol.* 11, 56–64. doi: 10.1038/nrneurol.2014.207

Hui, S. P., Sheng, D. Z., Sugimoto, K., Gonzalez-Rajal, A., Nakagawa, S., Hesselson, D., et al. (2017). Zebrafish regulatory T cells mediate organ-specific regenerative programs. *Dev. Cell* 4, 659–672. doi: 10.1016/j.devcel.2017.11.010

Ito, M., Komai, K., Mise-Omata, S., Iizuka-Koga, M., Noguchi, Y., Kondo, T., et al. (2019). Brain regulatory T cells suppress astrogliosis and potentiate neurological recovery. *Nature* 565, 246–250. doi: 10.1038/s41586-018-0824-5

Ito, Y., Tanaka, H., Okamoto, H., and Ohshima, T. (2010). Characterization of neural stem cells and their progeny in the adult zebrafish optic tectum. *Dev. Biol.* 342, 26–38. doi: 10.1016/j.ydbio.2010.03.008

Jorstad, N. L., Wilken, M. S., Todd, L., Finkbeiner, C., Nakamura, P., Radulovich, N., et al. (2020). STAT signaling modifies ascl1 chromatin binding and limits neural regeneration from muller glia in adult mouse retina. *Cell Rep.* 30, 2195–2208. doi: 10.1016/j.celrep.2020.01.075

Joven, A., and Simon, A. (2018). Homeostatic and regenerative neurogenesis in salamanders. *Prog. Neurobiol.* 170, 81–98. doi: 10.1016/j.pneurobio.2018.04.006

Kanagaraj, P., Chen, J. Y., Skaggs, K., Qadeer, Y., Conner, M., Cutler, N., et al. (2020). Microglia stimulate zebrafish brain repair via a specific inflammatory cascade. *bioRxiv* [Preprint]. doi: 10.1101/2020.10.08.330662

Kanehisa, M., and Goto, S. (2000). KEGG: kyoto encyclopedia of genes and genomes. *Nucleic Acids Res.* 28, 27–30. doi: 10.1093/nar/28.1.27

Kaneko, N., Herranz-Pérez, V., Otsuka, T., Sano, H., Ohno, N., Omata, T., et al. (2018). New neurons use Slit-Robo signaling to migrate through the glial meshwork and approach a lesion for functional regeneration. *Sci. Adv.* 4:eaav0618. doi: 10.1126/sciadv.aav0618

Kempermann, G., Gage, F. H., Aigner, L., Song, H., Curtis, M. A., Thuret, S., et al. (2018). Human adult neurogenesis: evidence and remaining questions. *Cell Stem Cell* 23, 25–30. doi: 10.1016/j.stem.2018.04.004

Kim, D., Langmead, B., and Salzberg, S. L. (2015). HISAT: a fast spliced aligner with low memory requirements. *Nat. Methods* 12, 357–360. doi: 10.1038/nmeth.3317

Kishimoto, N., Shimizu, K., and Sawamoto, K. (2012). Neuronal regeneration in a zebrafish model of adult brain injury. *Dis. Model. Mech.* 5, 200–209. doi: 10.1242/dmm.007336

Kiyooka, M., Shimizu, Y., and Ohshima, T. (2020). Histone deacetylase inhibition promotes regenerative neurogenesis after stab wound injury in the adult zebrafish optic tectum. *Biochem. Biophys. Res. Commun.* 529, 366–371. doi: 10.1016/j.bbrc.2020.06.025

Kizil, C., and Brand, M. (2011). Cerebroventricular microinjection (CVMI) into adult zebrafish brain is an efficient misexpression method for forebrain ventricular cells. *PLoS One* 6:e27395. doi: 10.1371/journal.pone.0027395

Kizil, C., Kaslin, J., Kroehne, V., and Brand, M. (2012). Adult neurogenesis and brain regeneration in zebrafish. *Dev. Neurobiol.* 72, 429–461. doi: 10.1002/dneu.20918

Kizil, C., Kyritsis, N., and Brand, M. (2015). Effects of inflammation on stem cells: together they strive? *EMBO Rep.* 16, 416–426. doi: 10.15252/embr.201439702

Kroehne, V., Freudenreich, D., Hans, S., Kaslin, J., and Brand, M. (2011). Regeneration of the adult zebrafish brain from neurogenic radial glia-type progenitors. *Development* 138, 4831–4841. doi: 10.1242/dev.072587

Kyritsis, N., Kizil, C., Zocher, S., Kroehne, V., Kaslin, J., Freudenreich, D., et al. (2012). Acute inflammation initiates the regenerative response in the adult zebrafish brain. *Science* 338, 1353–1356. doi: 10.1126/science.1228773

Lai, S. L., Marín-Juez, R., Moura, P. L., Kuenne, C., Lai, J. K. H., Tsedeke, A. T., et al. (2017). Reciprocal analyses in zebrafish and medaka reveal that harnessing the immune response promotes cardiac regeneration. *eLife* 6:e25605. doi: 10.7554/eLife.25605

Lambertsen, K. L., Finsen, B., and Clausen, B. H. (2019). Post-stroke inflammation-target or tool for therapy? *Acta Neuropathol.* 137, 693–714. doi: 10.1007/s00401-018-1930-z

Lange, C., Rost, F., Machate, A., Reinhardt, S., Lesche, M., Weber, A., et al. (2020). Single cell sequencing of radial glia progeny reveals the diversity of newborn neurons in the adult zebrafish brain. *Development* 147:dev185595. doi: 10.1242/dev.185595

Li, L., Yan, B., Shi, Y. Q., Zhang, W. Q., and Wen, Z. L. (2012). Live imaging reveals differing roles of macrophages and neutrophils during zebrafish tail fin regeneration. *J. Biol. Chem.* 287, 25353–25360. doi: 10.1074/jbc.M112.349126

Liang, J., Wang, D., Renaud, G., Wolfsberg, T. G., Wilson, A. F., and Burgess, S. M. (2012). The stat3/socs3a pathway is a key regulator of hair cell regeneration in zebrafish. *J. Neurosci.* 32, 10662–10673. doi: 10.1523/JNEUROSCI.5785-10.2012

Liao, Y., Smyth, K. G., and Shi, W. (2014). featureCounts: an efficient general purpose program for assigning sequence reads to genomic features. *Bioinformatics* 30, 923–930. doi: 10.1093/bioinformatics/btt656

Lindsey, B. W., Aitken, G. E., Tang, J. K., Khabooshan, M., Douek, A. M., Vandestadt, C., et al. (2019). Midbrain tectal stem cells display diverse regenerative capacities in zebrafish. *Sci. Rep.* 9:4420. doi: 10.1038/s41598-019-40734-z

Love, M. I., Huber, W., and Anders, S. (2014). Moderated estimation of fold change and dispersion for RNA-seq data with DESeq2. *Genome Biol.* 15:550. doi: 10.1186/s13059-014-0550-8

März, M., Chapouton, P., Diotel, N., Vaillant, C., Hesl, B., Takamiya, M., et al. (2010). Heterogeneity in progenitor cell subtypes in the ventricular zone of the zebrafish adult telencephalon. *Glia* 58, 870–888. doi: 10.1002/glia.20971

März, M., Schmidt, R., Rastegar, S., and Strähle, U. (2011). Regenerative response following stab injury in the adult zebrafish telencephalon. *Dev. Dyn.* 240, 2221–2231. doi: 10.1002/dvdy.22710

McDonald, R. P., and Vickaryous, M. K. (2018). Evidence for neurogenesis in the medial cortex of the leopard gecko, *Eublepharis macularius*. *Sci. Rep.* 8:9648. doi: 10.1038/s41598-018-27880-6

Miskolci, V., Squirrell, J., Rindy, J., Vincent, W., Sauer, J. D., Gibson, A., et al. (2019). Distinct inflammatory and wound healing responses to complex caudal fin injuries of larval zebrafish. *eLife* 8:e45976. doi: 10.7554/eLife.45976

Nelson, C. M., Gorsuch, R. A., Bailey, T. J., Ackerman, K. M., Kassen, S. C., and Hyde, D. R. (2012). Stat3 defines three populations of Muller glia and is required for initiating maximal muller glia proliferation in the regenerating zebrafish retina. *J. Comp. Neurol.* 520, 4294–4311. doi: 10.1002/cne.23213

Noy, R., and Pollard, J. W. (2014). Tumor-associated macrophages: from mechanisms to therapy. *Immunity* 41, 49–61. doi: 10.1016/j.immuni.2014.06.010

Oosterhof, N., Holtman, I. R., Kuil, L. E., van der Linde, H. C., Boddeke, E. W., Eggen, B. J., et al. (2017). Identification of a conserved and acute neurodegeneration-specific microglial transcriptome in the zebrafish. *Glia* 65, 138–149. doi: 10.1002/glia.23083

Otani, K., and Shichita, T. (2020). Cerebral sterile inflammation in neurodegenerative diseases. *Inflamm Regen.* 40:28. doi: 10.1186/s41232-020-00137-4

Petrie, T. A., Strand, N. S., Yang, C. T., Rabinowitz, J. S., and Moon, R. T. (2014). Macrophages modulate adult zebrafish tail fin regeneration. *Development* 141, 2581–2591. doi: 10.1242/dev.098459

Rajkovic, O., Potjewyd, G., and Pinteaux, E. (2018). Regenerative medicine therapies for targeting neuroinflammation after stroke. *Front. Neurol.* 9:734. doi: 10.3389/fneur.2018.00734

Ramachandran, R., Fausett, B. V., and Goldman, D. (2010). Ascl1a regulates Müller glia dedifferentiation and retinal regeneration through a Lin-28-dependent, let-7 microRNA signalling pathway. *Nat. Cell Biol.* 12, 1101–1107. doi: 10.1038/ncb2115

Raymond, P. A., Barthel, L. K., Bernardos, R. L., and Perkowski, J. J. (2006). Molecular characterization of retinal stem cells and their niches in adult zebrafish. *BMC Dev. Biol.* 6:36. doi: 10.1186/1471-213X-6-36

Raz, R., Lee, C. K., Cannizzaro, L. A., d'Eustachio, P., and Levy, D. E. (1999). Essential role of STAT3 for embryonic stem cell pluripotency. *Proc. Natl. Acad. Sci. U.S.A.* 96, 2846–2851. doi: 10.1073/pnas.96.6.2846

Renshaw, S. A., Loynes, C. A., Trushell, D. M., Elworthy, S., Ingham, P. W., and Whyte, M. K. (2006). A transgenic zebrafish model of neutrophilic inflammation. *Blood* 108, 3976–3978. doi: 10.1182/blood-2006-05-024075

Rothenaigner, I., Krecsmarik, M., Hayes, J. A., Bahn, B., Lepier, A., Fortin, G., et al. (2011). Clonal analysis by distinct viral vectors identifies bona fide neural stem cells in the adult zebrafish telencephalon and characterizes their division properties and fate. *Development* 38, 1459–1469. doi: 10.1242/dev.058156

Shichita, T., Ito, M., and Yoshimura, A. (2014). Post-ischemic inflammation regulates neural damage and protection. *Front. Cell Neurosci.* 8:319. doi: 10.3389/fncel.2014.00319

Shimizu, Y., Ueda, Y., and Ohshima, T. (2018). Wnt signaling regulates proliferation and differentiation of radial glia in regenerative processes after stab injury in the optic tectum of adult zebrafish. *Glia* 66, 1382–1394. doi: 10.1002/glia.23311

Sifuentes, C. J., Kim, J. W., Swaroop, A., and Raymond, P. A. (2016). Rapid, dynamic activation of muller glial stem cell responses in zebrafish. *Invest. Ophthalmol. Vis. Sci.* 57, 5148–5160. doi: 10.1167/iovs.16-19973

Than-Trong, E., and Bally-Cuif, L. (2015). Radial glia and neural progenitors in the adult zebrafish central nervous system. *Glia* 63, 1406–1428. doi: 10.1002/glia.22856

Todd, L., Squires, N., Suarez, L., and Fischer, A. J. (2016). Jak/Stat signaling regulates the proliferation and neurogenic potential of Muller glia-derived progenitor cells in the avian retina. *Sci. Rep.* 6:35703. doi: 10.1038/srep35703

Ueda, Y., Shimizu, Y., Shimizu, N., Ishitani, T., and Ohshima, T. (2018). Involvement of sonic hedgehog and notch signaling in regenerative neurogenesis in adult zebrafish optic tectum after stab injury. *J. Comp. Neurol.* 526, 2360–2372. doi: 10.1002/cne.24489

Urata, Y., Yamashita, W., Inoue, T., and Agata, K. (2018). Spatio-temporal neural stem cell behavior leads to both perfect and imperfect structural brain regeneration in adult newts. *Biol. Open* 7:bio033142. doi: 10.1242/bio.033142

Wan, J., Zhao, X. F., Vojtek, A., and Goldman, D. (2014). Retinal injury, growth factors, and cytokines converge on beta-catenin and pStat3 signaling to stimulate retina regeneration. *Cell Rep.* 9, 285–297. doi: 10.1016/j.celrep.2014.08.048

Westerfield, M. (2007). *The Zebrafish Book. A Guide for the Laboratory use of Zebrafish (Danio rerio)*, 5th Edn. Esugene: University of Oregon Press.

Yamashita, T., Ninomiya, M., Hernández Acosta, P., García-Verdugo, J. M., Sunabori, T., Sakaguchi, M., et al. (2006). Subventricular zone-derived neuroblasts migrate and differentiate into mature neurons in the post-stroke adult striatum. *J. Neurosci.* 26, 6627–6636. doi: 10.1523/JNEUROSCI.0149-06.2006

Yu, S., and He, J. (2019). Stochastic cell-cycle entry and cell-state-dependent fate outputs of injury-reactivated tectal radial glia in zebrafish. *eLife* 8:e48660. doi: 10.7554/eLife.48660

Zambusi, A., Pelin Burhan, Ö, Di Giaimo, R., Schmid, B., and Ninkovic, J. (2020). Granulins regulate aging kinetics in the adult zebrafish telencephalon. *Cells* 9:350. doi: 10.3390/cells9020350

Zhao, X. F., Wan, J., Powell, C., Ramachandran, R., Myers, M. G. Jr., and Goldman, D. (2014). Leptin and IL-6 family cytokines synergize to stimulate Muller glia reprogramming and retina regeneration. *Cell Rep.* 9, 272–284. doi: 10.1016/j.celrep.2014.08.047

Zhou, Y., Zhou, B., Pache, L., Chang, M., Khodabakhshi, A. H., Tanaseichuk, O., et al. (2019). Metascape provides a biologist-oriented resource for the analysis of systems-level datasets. *Nat. Commun.* 10:1523. doi: 10.1038/s41467-019-09234-6

Zou, S., Tian, C., Ge, S., and Hu, B. (2013). Neurogenesis of retinal ganglion cells is not essential to visual functional recovery after optic nerve injury in adult zebrafish. *PLoS One* 8:e57280. doi: 10.1371/journal.pone.0057280

Zupanc, G. K., and Horschke, I. (1995). Proliferation zones in the brain of adult gymnotiform fish: a quantitative mapping study. *J. Comp. Neurol.* 353, 213–233. doi: 10.1002/cne.903530205

**Conflict of Interest:** The authors declare that the research was conducted in the absence of any commercial or financial relationships that could be construed as a potential conflict of interest.

# Advantages of publishing in Frontiers

**OPEN ACCESS**
Articles are free to read for greatest visibility and readership

**FAST PUBLICATION**
Around 90 days from submission to decision

**HIGH QUALITY PEER-REVIEW**
Rigorous, collaborative, and constructive peer-review

**TRANSPARENT PEER-REVIEW**
Editors and reviewers acknowledged by name on published articles

**Frontiers**
Avenue du Tribunal-Fédéral 34
1005 Lausanne | Switzerland

**Visit us:** www.frontiersin.org
**Contact us:** frontiersin.org/about/contact

**REPRODUCIBILITY OF RESEARCH**
Support open data and methods to enhance research reproducibility

**DIGITAL PUBLISHING**
Articles designed for optimal readership across devices

**FOLLOW US**
@frontiersin

**IMPACT METRICS**
Advanced article metrics track visibility across digital media

**EXTENSIVE PROMOTION**
Marketing and promotion of impactful research

**LOOP RESEARCH NETWORK**
Our network increases your article's readership